N62-14468

PROCEEDINGS OF THE
NATIONAL MEETING ON

MANNED SPACE FLIGHT

REPRODUCED BY
U.S. DEPARTMENT OF COMMERCE
NATIONAL TECHNICAL INFORMATION SERVICE
SPRINGFIELD, VA. 22161

PROCEEDINGS

of the

NATIONAL MEETING ON MANNED SPACE FLIGHT
(Unclassified Portion)

St. Louis, Missouri

April 30 - May 2, 1962

Cosponsored by the
Institute of the Aerospace Sciences
and
National Aeronautics and Space Administration

Published by the

Institute of the Aerospace Sciences
2 East 64th Street New York 21, N.Y.

Cover by Bob Van Steinberg
Commercial Artist
General Electric Company
Light Military Electronics Dept.
Utica, New York

1962
INSTITUTE OFFICERS AND COUNCIL

PRESIDENT
L. Eugene Root

VICE PRESIDENTS
Raymond C. Blaylock (C)
Harold Luskin (W)
Charles Tilgner, Jr. (E)

TREASURER
Charles H. Colvin

COUNSEL
Allan D. Emil

STAFF

DIRECTOR
S. Paul Johnston

SECRETARY
Robert R. Dexter

CONTROLLER
Joseph J. Maitan

TECHNICAL SERVICES DIRECTOR
Paul J. Burr

NATIONAL MEETINGS DIRECTOR
E. W. Robischon

PUBLICATIONS DIRECTOR
Welman A. Shrader

COUNCIL

Frederick L. Bagby
J. E. Barfoot
William B. Bergen
C. H. Christenson
L. C. Craigie
Preston E. Dickson
William C. Fortune
Martin Goland
Ephraim M. Howard
Willson H. Hunter
Paul M. Leland
Axel T. Mattson
George R. Mellinger
Vernon Outman
C. D. Perkins
Alan Pope
Orson B. Randell
L. B. Richardson
Ira G. Ross
Abe Silverstein
R. Dixon Speas
H. Guyford Stever
T. F. Walkowicz

ST. LOUIS SECTION OFFICERS

CHAIRMAN
Harold H Ostroff

CORRESPONDING SECRETARY
June Watson

RECORDING SECRETARY
Ervin T. Kisselburg

TREASURER
Roger W. Lahman

NATIONAL MEETING ON MANNED SPACE FLIGHT COMMITTEE

GENERAL CHAIRMEN
G. M. Low G. S. Graff

ACTIVITIES CHAIRMAN
F. H. Roever

T. M. Bellan
Margaret Bernard
H. E. Colbert
H. H. Cole
L. A. Goran
E. A. Jeude
H. H. Ostroff
C. H. Perisho
N. J. Pierce
H. C. Rechtien
C. E. Sadler
June Watson
T. L. Yount

TECHNICAL SESSIONS CHAIRMEN

W. J. Burke
K. A. Ehricke
E. M. Flesh
L. P. Greene
H. Luskin
W. J. North
J. P. Taylor
J. M. Vanderplas
W. C. Williams

TECHNICAL SESSIONS COORDINATORS

W. F. Boldt
R. V. Glowczuski
R. R. Jenny
J. M. Kolb
R. H. Mathews
W. McGough
J. F. Reilly
G. R. Waymon
N. Zimmerman

CONTENTS

Introduction of Congressman George Miller -- L. E. Root ____ 5

The New Era of Exploration -- George Miller ____ 6

Organizing for the Conquest of Space -- D. B. Holmes ____ 9

The Military Contribution to Space Exploration -- B. A. Schriever ____ 13

Design for Manned Space Flight -- Robert R. Gilruth ____ 15

The X-15 Program -- Joseph A. Walker ____ 17

Experience with Mercury Spacecraft Systems -- J. F. Yardley ____ 23

Mercury Operational Experience -- C. C. Kraft, Jr. ____ 30

Life Sciences Activities Associated with Project Mercury -- S. C. White and C. P. Laughlin ____ 42

Dyna-Soar Bioastronautics -- Robert Y. Walker ____ 47

Regenerative Environmental Control Systems for Manned Earth-Lunar Spacecraft -- M. G. Del Duca, R. G. Huebscher and A. E. Robertson ____ 53

Advanced Environmental Systems -- J. L. Mason and W. L. Burriss ____ 72

Thermal Balance of a Manned Space Station -- George B. Patterson and Arthur J. Katz ____ 86

Lift Control During Atmosphere Entry from Super-circular Velocity -- R. C. Wingrove and R. E. Coate ____ 95

Rendezvous Guidance Technology -- Robert S. Swanson and Peter W. Soule ____ 106

The Restricted Three-Body-Problem as a Perturbation of Euler's Problem of Two Fixed Centers and its Application to Lunar Trajectories -- R. Schulz-Arenstorff, M. C. Davidson, Jr., and H. J. Sperling ____ 130

Design Comparison of Lunar Return Configurations -- E. Offenhartz, C. F. Berninger, W. Zeh and M. C. Adams ____ 134

Self Erecting Manned Space Laboratory -- R. Berglund and E. A. Weber ____ 144

Progress Report on the Development of Protected Construction for Hypersonic Vehicles -- W. H. Dukes ____ 150

Re-Entry Materials -- D. L. Kummer and H. J. Siegel ____ 158

Some Abort Techniques and Procedures for Manned Spacecraft -- John M. Eggleston ____ 167

Human Control Performance and Tolerance Under Severe Complex Wave Form Vibration, with a Preliminary Historical Review of Flight Simulation -- C. Clark ____ 176

Crew Safety and Survival Aspects of the Lunar-Landing Mission -- Hubert M. Drake ____ 195

Effects of High G Conditions on Pilot Performance -- R. M. Chambers and L. Hitchcock ____ 204

The Mercury Capsule Attitude Control System -- J. W. Twombly ____ 228

Simulation Equipment Used in the Training of Astronauts and Flight Control Crews in Project Mercury -- Stanley Faber ____ 232

Paraglider Recovery Systems -- F. M. Rogallo ____ 237

Impact Attenuation Methods for Manned Spacecraft -- Harold W. Bixby ____ 241

Effect of Sterilization in Spacecraft Design -- Albin M. Nowitzky ____ 250

Liquid Propellant Launch Vehicles for Manned Space Flight -- Wilson B. Schramm ____ 259

Solid Propellant Boosters for Manned Space Flight -- Langdon F. Ayres ____ 266

The Potential for Nuclear Propulsion for Manned Spaceflights -- Maxwell W. Hunter, Jr. ____ 276

Manned Lunar Landing via Rendezvous -- F. Digesu ____ 288

Pilot's Flight Report -- John H. Glenn, Jr. ____ 296

Meteoroid Effects on Space Exploration -- M. Dubin ____ 310

INTRODUCTION OF CONGRESSMAN GEORGE MILLER

L. E. Root
President
Institute of the Aerospace Sciences

Tonight's main speaker is one of the key men in the U. S. space effort. There is almost no one of us here tonight, whose professional activities will not be affected in some way by the work of Congressman George Miller, Chairman of the Standing Committee on Science and Astronautics of the U. S. House of Representatives.

I think it can be said without exaggeration that we are fortunate to have "one of our own" profession in this key spot in the national legislative branch. Congressman Miller is one of the few engineers in Congress. In fact, he is credited with needling his fellow Congressmen, most of them lawyers, with the comment: "You people all think in circles. I am one of the few guys around here who has been trained to think in straight lines." And it seems clear enough that a technical background is very useful in framing legislation for the space effort.

Our speaker also has a long standing interest in science and technical subjects. He has long served on the House Armed Services Committee. And with the creation of the Science and Astronautics Committee, one of the major committees of the lower house, he switched over to that body. On the death of Overton Brooks of Louisiana last September, he took over as chairman.

However, perhaps equally significant was his earlier Chairmanship of the House Subcommittee on Oceanography. I suppose most of us are aware that, like space, the oceans covering 71 per cent of the earth's surface offer another frontier and that growth of oceanography as a new science and base of national power is inevitable.

One observer comments that George Miller has done more for oceanography than any man in Congress and this says a good deal about his scientific awareness. Our speaker has also broken the sound barrier seven years ago in a navy fighter when frankly he has damn well old enough to know better. Personally, he is characterized by an easy-going, story-telling manner and a quick, perceptive analytical mind. The book Californians in Congress says of him that he makes no effort to obtain personal publicity, that he is highly regarded in his District of Alameda County, as attested by a long series of sweeping electoral victories. The same book adds that he is esteemed as a practical politician and a hard worker.

According to a good many people, George Miller seems best characterized by the law of conservation of energy, or the most results for the least expenditure of resources. In election campaigns, he employs no election headquarters, no large bill boards. He does call on a large cadre of friends, including people from both parties. He has a deadly efficient post card system, and relies on the long memories of a great many constituents, of good personal efforts in their behalf by their man in Washington. He displays similar quiet efficiency in other areas.

Our speaker was born in San Francisco, son of the captain of a Sacramento river dredger. He has a civil engineering degree from the San Francisco Bay Area's St. Mary's College. He has been a civil engineer, travel agent, fish and game official. He was a First Lieutenant of Artillery in World War I, and in the great depression of the 30's was forced onto the WPA and put in some time as a street sweeper--a job which put him in contact with a lot of people in his home county, and also into politics where he was elected to the State Legislature in 1937. He has served 18 years in Congress and has pursued a moderate liberal line with a continuing strong interest in committee work. He is the senior member from Northern California. He likes to take jaunts in the Washington countryside and to hike in the wilderness areas of our Sierra Nevada Range.

In 1927, he married the former Esther Perkins, who had come from Nebraska to head personnel operations in a San Francisco department store. He likes to say jokingly of her that she's the "real sizer-up of people" and politician in the family. Though the facts suggest that Congressman Miller personally swings a highly effective if not obvious political stick. He has one daughter and two grandchildren.

Finally, Space Committee Chairman Miller is on record as accepting the race to the moon as inevitable and necessary. But he feels the scientific results are at least as important as the race itself, a view that I believe will find little quarrel in this audience. He stresses he chairs the Science and Astronautics Committee, in that order, and so he strongly supports the Bureau of Standards and the National Science Foundation, as both directly sustain the total national scientific capability. In back-home speeches, he stresses quality scientific education and equally hard the gap in production of engineers, and the critical role of the engineering professions in over-all national power.

I believe it can be said that as a Congressman, George Miller has represented the engineering field, as well as his constituents, in the way we would most of us expect to see it represented by a competent professional.

It is said that one of the axioms of the advertising business is that "a smart dime can never beat a dumb dollar." In the space business, I think, we have been proving this axiom wrong a good part of the time. Our smart, cleverly-instrumented, small-payload dimes have often made a good showing. They have frequently won out over the bigger, relatively dumber payloads of the competition in the U.S.S.R.

Nonetheless, in general, it seems that the rule holds good. It is still better to get there first with "the mostest."

And our guest tonight is a man who has a key part in seeing that in space we do---here is tonight's Speaker, The Honorable Chairman George P. Miller.

Banquet Speech

THE NEW ERA OF EXPLORATION

by

The Honorable George Miller

The Congress of the United States of America

Today you have heard reviews of all of our manned space programs - the X-15, Project Mercury, Project DynaSoar, Project Gemini, and Project Apollo. You have also heard the carefully chosen remarks of Mr. D. Brainerd Holmes, Director of the National Aeronautics and Space Administration's Manned Space Flight Program. You have heard a detailed report on Project Mercury which reveals the enormous progress this remarkable program has made in the 3½ years since its inception.

I am sure that, like myself, you are impressed with the scope of these programs and the progress which is being made. I am proud to have had a close association with these programs as a member and Chairman of the House Committee on Science and Astronautics. I am sure you will agree with me that the Committee has been one of the most faithful supporters of the Manned Space Flight Programs.

However great the progress we have made to date, it is a mere first step in the journey we have before us. Man is going to explore space just as surely as we meet here tonight.

The observation has been made that nations are either dynamic and grow, or they stagnate and fade away. I am proud that this nation has made the decision to push its frontiers forward. We are taking steps to grow and to lead the world by the example of our vigor. If we, the wealthiest nation on earth, had failed to accept the challenge of space exploration, and allowed this initiative to fall, by default, to a more vigorous nation, our stagnation as a nation would have begun.

I am proud that this nation has committed itself so strongly to the task. We are privileged to be part of this effort. But we, both as a nation and as individuals, must give of our best to accomplish the formidable tasks we have undertaken.

Consider our space programs against the historical background of the period of about 1500 AD. At that time, Europeans knew only dimly of the vast land area of Asia and absolutely nothing of the American continents. It was the age of great adventure and exploration, Columbus and Magellan had the foresight to conceive plans for voyages which, in a brief period of years, literally changed world history.

The voyages of Columbus and Magellan extended man's vision as few voyages in history have - before or since. The world was never the same again. Man raised his eyes above the horizon and was fascinated and drawn toward what he envisioned. I am convinced that Space Flight has again raised man's eyes. We are embarked on a series of voyages across distances incomparably far.

Many sciences will contribute to this new exploration. Most of you are well aware of the magnitude of the number of sciences which must be utilized. Nevertheless, I would emphasize that all scientific disciplines available today must be harnessed and make their contributions in order to successfully conclude the voyages which we have planned. This is truly a monumental task and will call for the best efforts not only from all of us, but also from the free world.

The United States has found that scientists all over the world are eager to associate themselves with American space efforts. This overseas effort among countries allied with the Western world will become more and more important as Europe (and Asia to a lesser degree) masses its own resources in the tremendous endeavor which is now underway to probe space.

Western Europe took a decisive step early in 1962 to become an active participant on its own in space development and exploration. It established the European Space Research Organization, ESRO. Twelve nations will be included in the organization and each will contribute to the space research budget according to its participation and capacity. ESRO's plans call for a first year budget of around $15 million, increasing to a minimum of $50 million within five years. It is expected that ESRO will emphasize purely scientific research, beginning first with sounding rockets. Within four years, it is anticipated that it will supplement this program with earth satellites, space probes, astronomical satellites, and lunar satellites. Approximately 800 people will be involved, plus an additional 150 for tracking, telemetry, data reduction, etc.

Four nations--the United Kingdom, Italy, West Germany and France--have also signed an agreement formally establishing the European Space Launcher Development Organization. The agreement will remain open until April 30 for the signature of other nations and it is expected that Australia, Denmark, Belgium, the Netherlands, Spain, and perhaps Sweden, Switzerland and Norway, will join.

This organization, known as ELDO, will seek to develop a three-stage satellite booster. The launching vehicle will be composed, according to present plans, of the British Blue Streak rocket for the first stage, the French Veronique as the second stage, and the West German third stage. The goal is the development of the launcher in time to boost a satellite into orbit from Woomera in 1965. It is estimated that the program will cost approximately $200 million over the next five years, with England furnishing a third.

Besides this cooperative effort on the part of Western Europe and Australia, various European nations are going into sizeable space programs of their own. The United Kingdom, for one, has established a National Committee for Space Research, which has been placed in charge of the program.

The UK program involves payload work being done at the, Edinburgh Royal Observatory, the University of London, and the Royal Aircraft Establishment at Farnborough. In addition, there will be launchings at Woomera and at Aberporth, England.

In France, a National Center for Space Studies has been created, to function directly under the Prime Minister, but to be administered by Civilian Scientists. Western Germany is reported also to be launching its own space research program.

European space research experts, both on a collective and individual nation basis, appear anxious to keep in touch with the American space program in order to avoid duplication of work as well as keep up to date on the results of our programs.

The international aspects of the program are strong from the United States' point of view. Existing agreements which call for the launching of joint satellites and for mutual aid in tracking, communications and otherfacets of the space effort, will probably have to be widened and implemented. Simple geography is likely to demand this in the more sophisticated future space programs. A good example is the use of the Jodrell Bank radio-telescope in Britain, which both American and Russian Scientists have used from time to time.

No discussion of the International aspects of space cooperation would be complete without mention of the various educational programs in which NASA is engaged. In the case of distinguished foreign scientists, it is clear that they can made immediate contributions to experimental space research. Indeed, the leading research in a number of fields was initiated abroad. But there is also a need to train younger scientists, since space research by means of instrumented satellites is only now beginning in most countries abroad.

For carefully selected, recognized senior scientists, the United States has established a postdoctoral associateship program that provides opportunities to work on either theory or experiments at NASA centers. Twenty-nine foreign nationals from 13 countries have participated in this program to date. Consistent with their senior status, liberal one-year stipends are provided participants by NASA through the National Academy of Science, which administers the program.

For younger scientists, NASA conducts three training programs. Foreign graduate students sponsored by their space committees or national research councils may be nominated for fellowships for periods of one to two years in American University laboratories carrying out space-related projects. The sponsoring agency abroad provides transocean travel and subsistence in this country while NASA, through the National Academy of Sciences, provides university costs and domestic travel. This program is expected to accommodate up to 100 graduate students per year at 25 to 30 universities beginning this coming fall. It may also be utilized to support extended visits by American university professors to lecture to appropriate groups of graduate students abroad.

On-the-job orientation and instruction of foreign technicians and scientists are also provided for varying periods at NASA laboratories and at the launching station at Wallops Island, Virginia, on a non-funded basis. Finally, increased participation in the operation of NASA's global network is encouraged through a training program under the direction of NASA's Goddard Space Flight Center at Greenbelt, Maryland.

NASA believes that these programs have stimulated strong interest abroad in space research and development. National space committees have been organized in nearly two dozen countries. The prospect of United States assistance for space research has been of great importance to nations in the early stages.

Every effort is being made so that the civilian space program of the United States reduces rather than increases the technological gap in the Western world. This has the greatest long-range implications for the economic well-being and the security of the free nations.

What will be the tangible benefits to mankind from these space programs we have undertaken? The exact benefits are hard to determine at the start of the voyage. Will the earth establish colonies on other planets? It obviously is too early to answer this question; however, I can visualize with some clarity some of the benefits which are typical of those we reasonably can expect.

As a first example, I point to the developments in the field of utilizing algae as an inexpensive and rapid method of providing a constant supply of very nutritious food. The developments, aimed at providing food for space crews on long trips, appear adaptable to use in providing food for the over-populated and under-developed nations of the earth. It might be that the algae tank could become as important to a family as the garden plot is today.

As a second example, I point out that today, in order to manufacture some of the components which are used in spacecraft, rooms of extreme cleanliness (or "white rooms") must be used. The same techniques of removing dust and dirt from these rooms are adaptable to the removable of germs as well. Thus, it is reasonable that our hospital operating rooms, and other rooms as well, could be made almost completely germless. Thus, the chances of infection during surgery would be decreased and recovery from illnesses would be increased.

All of you who followed John Glenn's flight are aware that his pulse rate, heart condition, respiration rate and blood pressure were constantly telemetered back to earth. Variations of this technique are already in use for more routine medical purposes today.

It is possible that, in the future, persons suspected of heart trouble or key personnel of the nation will carry with them micro-miniaturized instrumentation which will radio back to a central medical facility constant information on their physical condition. Automatic equipment at the central facility would constantly monitor the readings coming in and sound an alarm at the first sign of an abnormality. Thus, the first sign of a "bad" heart would be instantly detected, and medical attention provided.

The development of space suits, with provisions for not only countering the extremes of the high and low temperatures which will be

encountered on the moon, but which will provide constant communications, is proceeding on schedule. This development could lead to the availability of lightweight and comfortable "air-conditioned" clothing suitable for year-round use here on earth. Constant communications could be maintained with one's office, although this is looked upon as a mixed blessing.

One of the most perplexing problems of space flight is that of waste disposal. However, developments to date indicate that this problem will not be too difficult to solve. The solution shows promise of being adaptable to the drastic reduction of the pollution of our rivers and streams, and may eventually lead to the elimination of costly community sewage disposal systems.

All of us are thoroughly familiar with the evolution of the aircraft seat belt or safety belt, and its adaption to automobile use. The contour couches being used today for acceleration and vibration attenuating devices appear equally useful and adaptable for use for both military and civilian purposes in a number of modes of transportation.

This list could go on and on - new fuels, new metal fabrication techniques, fuel cells, high-temperature glasses, all of these developments will be accelerated. As has been wisely said - the funds we will expend for our space exploration programs will be spent here on earth, and not in space. The entire nation will benefit in a material manner.

To receive these rewards as we push our frontiers beyond what we had literally not conceived several years ago will require a maximum degree of cooperation. All Government agencies must share their technical developments and information learned in tests and flights. I am very gratified at the efforts which have been made to distribute the information gathered in Project Mercury.

I am equally pleased to see the cooperation of NASA and the Department of Defense. This free interchange of plans, developments, and test results will allow each Agency to carry out its individually assigned responsibilities, utilizing what has been learned by both.

Because of the extremely high cost of space activity, particular attention must be paid to the elimination of unnecessary duplication. However, because the program is of such significance to the nation, it must be pushed vigorously.

In conclusion, let me say that I see the world on the verge of an extension of our frontiers which will match or succeed any expansion ever experienced before. We must proceed vigorously with our space programs both as a hallmark of the vigor of our nation and to accelerate our national growth. We must reap the benefits from these programs and the technology which made them possible and distribute these benefits throughout the Free World. As our great President has so well stated, "We have a long way to go in this space race. We started late. But this is the new ocean, and I believe the United States must sail on it and be in a position second to none."

Luncheon Speech

ORGANIZING FOR THE CONQUEST OF SPACE

Delivered for

D. Brainerd Holmes
Director, Office of Manned Space Flight
National Aeronautics and Space Administration

By

George M. Low
Director, Spacecraft and Flight Missions
Office of Manned Space Flight, NASA

Mr. Holmes has asked me to express his sincere regrets for being unable to be with you today to deliver this address. Unfortunately, there was a last minute change in the schedule for our Congressional Hearings and Mr. Holmes had to stay in Washington to testify before the House Appropriations Committee.

Today I will not talk about our manned space flight program, about Projects Mercury, Gemini and Apollo, since these subjects are thoroughly covered in the technical presentations to this Conference. Instead, I will discuss the organizational structure we are creating in mustering the efforts of this Nation for the great task which lies ahead.

It is unfortunate that some seem to regard our current lunar program and the programs beyond as stunts. Nothing could be farther from the truth; on the contrary, we are firmly convinced that we are embarked upon a venture which holds very deep significance for the future of this Country in man's endless search for knowledge.

We can ill-afford to allow any misconceptions as to our program, or any thoughts that the program smacks of the theatrical, to persist. It is up to all of us to help dispel any such erroneous views since we need the wholehearted support of the entire country if we are to accomplish our mission.

The need for this support is, I believe, completely understandable since NASA is faced with one of the most complex engineering tasks ever undertaken by man. The number of Americans who will be directly involved in this program will be measured in the hundreds of thousands, and the number of industrial organizations in the many thousands. In addition, there will be participation by countless universities and research organizations. If we do not execute this effort with efficiency, it can cost our country dearly. At worst, it might cost us the mission's success, along with a serious set-back in national prestige, a loss of knowledge, and a loss of international leadership. At the least, it would cost us thousands of man-years of the Nation's best technical talent and literally billions of dollars in this decade.

Why do we want to go to the moon? I've tried to suggest an answer to that question. A program designed to land a man on the moon and bring him back to earth, will focus our scientific and technical talents on a task that is exceedingly broad in scope and high in complexity. By its very nature, it will lead to a general advancement in technology that has heretofore seldom been equalled. This advancement will, of course, lead to progress in all fields. The manned lunar landing program is thus providing the catalyst and the tonic for new advantures of the mind and spirit. Our Nation squarely faced this great technological challenge last May when the President said, "I believe that the Nation should commit itself to achieving the goal, before the decade is out, of landing a man on the moon and returning him safely to earth."

I will, for the remainder of my time, discuss the organization of NASA and, more particularly, the organization of the office of Manned Space Flight, which has been established to direct our efforts to establish man's proficiency in operating in space, including a round trip to the moon within this decade.

First, then, let me outline very briefly the thinking behind NASA's over-all organization as it relates to the Office of Manned Space Flight.

No new department or agency in the recent history of the Executive Branch of the Federal Government was created through the transfer of as many units from other departments and agencies as in the case of NASA. Three and one-half years ago, NASA did not exist. Today NASA comprises approximately 20,500 employees, ten major field centers, and a proposed budget for FY 1963 of nearly $3.8 billion.

From a purely organizational and managerial point of view, it might have been much easier to create an entirely new department or agency to handle the Nation's civilian space program. This possibility, I understand, was explored and rejected because of the time required to recruit and organize the technical and scientific talent required.

Instead, therefore, NASA has been organized by melding together a number of existing agencies and parts thereof. The research centers of the NACA formed the nucleus of the new organization. They were soon joined by a group from the Naval Research Center, and later on by the Jet Propulsion laboratory and by the Marshall Space Flight Center in Huntsville.

Our current concept of organization and management within NASA is based upon the establishment of Program Offices charged with the responsibility of program direction utilizing the skills and efforts of the various NASA Centers. The entire effort is then pulled together by a central general management organization. Such an arrangement permits top level focus on the "program problems" while retaining the continuity of reporting, growth, and control of the skill centers.

The primary responsibility for each of NASA's four major programs - Manned Space Flight, Space Sciences, Applications, and Advanced Research and Technology - is assigned to a specific Program Office. The director of a program office is the principal advisor to the Associate Administrator in regard to his program area. He is also the principal operating official in regard to management of his assigned program. His office directs the program by working directly with the Center directors and their project and systems managers. In addition to handling such matters as budgeting and programming of funds and establishing and issuing technical guidelines and schedules, each program director is also responsible for providing continuing leadership in external and interagency relationships related to his assigned program.

The Center directors are responsible to the Associate Administrator for their skill centers, but to the Program directors for their efforts performed on the various programs they are undertaking.

Now I would like to turn from the over-all NASA organization to the management channels and techniques we have established within the Office of Manned Space Flight.

We are firmly convinced that the unprecedented challenge we are facing in the management of all of the diverse elements required for the success of our mission calls for meticulous planning, careful organization, and immediate responsiveness.

I am not suggesting that management problems of this kind have never been faced before. They have. They are faced frequently by Government and industry, but on a scale not usually so sweeping. Neither am I suggesting that the organization we have developed to meet the problems is unique. On the contrary, we have borrowed liberally from our knowledge of Government and industry organizations.

It was in the light of this background and experience, and after considerable discussion and soul-searching within NASA, that the Program Office of Manned Space Flight was organized. This organization has been designed so that each of the important functional operating areas, particularly at the Manned Spacecraft Center in Houston, the Marshall Space Flight Center in Huntsville, and the Launch Operations Center at Cape Canaveral, has a corresponding home in the Program Office.

As a part of this Program Office, a basic Systems Engineering organization has been created and is being staffed. This organization will be composed of scientists and highly-skilled engineers, physicists, and mathematicians who will analyze the various missions, systems, and equipments which are being considered for the manned space flight endeavor.

It is our firm conviction that such a Systems office is vital. We are also convinced that the basic systems engineering decisions related to the mission approach must be retained within NASA, and exercised by employees of NASA. It would be desirable if we were able to find the total number of scientific and engineering personnel to support these key people, and employ them directly within the organization. This prospect, however, was carefully considered, and it was concluded that it could not possibly be achieved within the required time scale. Consequently, we have recently entered into a contractual arrangement under which the necessary personnel can be supplied and their knowledge and assistance used by the key people within the Systems Engineering organization in formulating their decisions and recommendations.

The contractor selected for this task is called BELLCOMM, a corporation owned jointly by AT&T and Western Electric Corporation.

BELLCOMM will provide an organization which can lend adequate support in developing the factual basis required to make the wide range of Systems Engineering decisions necessary. For example, we will draw upon this group for such things as studies of mission objectives and methods by which they can be achieved; and for trade-off studies to provide data required to reach management decisions on technical problems.

I have gone into some detail with regard to the concept under which we will draw upon contractor support in this instance. I think it is important to do this since this facet of our Systems Engineering operation is illustrative not only of our approach to the specific problems, but also of our basic management philosophy; that is, final broad management control and decision-making to be exercised by Government personnel.

In addition to the Systems Engineering organization, the Office of Manned Space Flight has a project management directorate for each major area of endeavor, including Aerospace Medicine, Spacecraft and Flight Missions, Launch Vehicles and Propulsion, Integration and Checkout, and Program Review and Resources Management.

The directorates of Spacecraft and Flight Missions and of Launch Vehicles and Propulsion are most closely associated with the two field centers responsible for the spacecraft and launch vehicle development: The Manned Spacecraft Center in Houston, Texas, and the Marshall Space Flight Center in Huntsville, Alabama.

The directorate of Aerospace Medicine will concentrate its efforts on the knowledge required for manned space flight missions; it has no responsibility for bioastronautics research that is not directly in support of the manned space flight program.

The Integration and Checkout directorate will have the over-all responsibility for the integrated check-out of the spacecraft-launch vehicle combination. Responsibility for check-out equipment for the spacecraft by itself, and for the launch vehicle by itself, will rest with our spacecraft and launch vehicle contractors. However, in order to

meet our mission objectives without undue delay, we will require a major effort at the launch site; there we will have to utilize new techniques, different from those in current practice. For example, we plan to assemble the spacecraft and launch vehicle in a building remote from the launch pad. There, under controlled atmosphere conditions, several complete space vehicles can be assembled, checked and tested. The entire vehicle will then be moved, vertically, to the launch pad. The actual time spent on the pad should be quite small.

During the time in the vertical assembly building, on the way to the pad, and on the pad, the space vehicle will undergo a continuous high speed check-out. The plans for this integrated check-out, and the provision of the check-out equipment, will be the responsibility of the directorate of Integration and Checkout, assisted by its contractor, the General Electric Company.

The sixth directorate, Program Review and Resources Management, is the administrative arm of the Office of Manned Space Flight.

Most of the contracting for the Manned Space Flight Program is being carried on by two major centers of the NASA organization. These are the Manned Spacecraft Center and the Marshall Space Flight Center. These centers will contract with many industrial organizations and will serve to integrate the efforts of these companies. The third NASA center, which provides very major support to the Office of Manned Space Flight, is the Launch Operations Center at Cape Canaveral. The integration of all center efforts will be done by close coordination with the program directorates of the Office of Manned Space Flight.

The general management of the Manned Space Flight Program is carried out by the Manned Space Flight Management Council. This Council is chaired by Mr. Holmes, the Director of Manned Space Flight. Its members are the Systems Engineering and Program Directors, Drs. Shea and Roadman and Messrs. Rosen, Sloan, Lilly and myself; the Director and Deputy Director of the Manned Spacecraft Center,Mr.Gilruth and Mr. Williams; the Director and Deputy Director of the Marshall Space Flight Center, Dr. von Braun and Dr. Rees; and the Director of the Launch Operations Center at Cape Canaveral, Dr. Debus. Here, then, are the men within Government who bear the specific responsibilities for carrying out this Nation's effort in manned space exploration. It is they who establish the detailed policies and technical approaches to carry out our program. Together, they comprise the "Board of Directors" for the manned space flight effort.

The organization I have described is now in being; and the Management Council last week held its fourth monthly meeting. Here are some of the other recent accomplishments:

We have acquired a 1600 acre site in Houston, Texas, and have started construction on the Manned Spacecraft Center.

We have initiated the Gemini program as a prelude to Apollo, by awarding a contract for the two-man Gemini spacecraft to McDonnell Aircraft Corporation; and by working out detailed arrangements for the Titan II and the Atlas-Agena launch vehicles for Gemini with the Air Force.

We have contracted with North American Aviation, Inc., to design, develop and construct the three-man Apollo spacecraft which is to land men on the moon.

We have acquired the giant Michoud Plant at New Orleans, Louisiana, and are converting its 1.8 million square feet of manufacturing space into the largest vehicle assembly area in the United States. The Saturn, Advanced Saturn and Nova vehicles will be assembled at Michoud.

Forty miles from Michoud, on the Pearl River in Mississippi, we are obtaining rights to 140,000 acres of land which will be called the Mississippi Test Facility. In this sparsely settled area we plan to construct captive tests stands where we will test-fire stages of Saturn, Advanced Saturn and Nova.

The Chrysler Corporation is now under contract to NASA for the production of Saturn first stages at Michoud.

The second stage of Saturn has been in development for over a year at the Douglas Aircraft Company, which will also produce the third stage of the Advanced Saturn.

We are negotiating a contract with the Boeing Company to produce at Michoud the first stage of the Advanced Saturn launch vehicle.

A contract for the second stage of Advanced Saturn is being negotiated with North American Aviation, Inc.

The giant F-1 engine for the Nova first stage has been under contract for several years. A contract for the Nova second stage engine, the M-1 hydrogen-oxygen engine is now being negotiated.

Through our agent, the U. S. Army Corps of Engineers, we are acquiring 73,000 acres along the Florida coast and adjacent to existing Cape Canaveral launching facilities. On this vast area, five times the present size of Cape Canaveral, construction will soon start on the largest launch sites in the free world.

We are also establishing close ties with the Air Force, the Navy, and the Army, whose assistance is vital to the accomplishment of our mission. A formal means for coordinating our efforts with the Air Force is currently being established with the Air Force Systems Command. Our mutual interests involve a number of important areas including procurement and contractor relationships; construction; technical support of the manned space flight efforts of NASA by the Air Force, and vice versa; the Atlantic Missile Range Operations; global communications and instrumentation; and, perhaps the most important item of all, the continuous interchange of information concerning our space efforts and studies. These matters have become sufficiently numerous and important to require more formalized working relationships than previously were needed if we are to proceed to work together in the most effective manner.

Let me conclude by reiterating a few of our basic concepts. We believe that we must obtain the very best efforts of the very best people we can find, both in Government and industry, if we are to achieve our National goal. We believe that our

organizational concepts and management techniques must be no less excellent than our technical efforts. We believe that with constant attention to these concepts, and with the hard work and dedication of the people involved, we will be able to carry out our responsibility to our Country to be second to none in man's conquest of space.

Luncheon Speech

THE MILITARY CONTRIBUTION TO SPACE EXPLORATION

General B. A. Schriever
Commander, Air Force Systems Command

It is a real pleasure to be with you today. I think it is very significant that the IAS and NASA are holding a national meeting on manned space flight. Only a few years ago, such a meeting would have been a highly theoretical gathering. It would have attracted very little public attention--except perhaps some ridicule. The fact that the situation is different today, is a sign not only of increased interest in space, but of concrete scientific and technical progress.

Recently I was reminded again of the startling progress that has been made. Winners from a high school science fair were invited to show their displays in my headquarters at Andrews. Two of our officers watched spellbound as one of the students put his gadget through its paces. The student's explanation grew more and more complex, till one of the officers turned to the other and whispered: "Very impressive--but what's he talking about?"

In science and technology we have come so far and so fast that our children today are familiar with concepts that we could not imagine when we were their age--or even just a few years ago. There is even a tendency to take for granted much of man's progress in space. But that progress, as this audience well knows, has not been automatic; it has been the product of imagination, teamwork, and sustained effort.

This afternoon I want to discuss with you the military contribution toward man's progress in the conquest of space. In looking at the nature and extent of the military contribution, we may be able to make a few useful predictions about the course of future space developments. At the same time we may notice interesting facts about the American attitude toward technology.

We have long taken pride in being a very practical people. Until comparatively recent years, this attitude was responsible for a marked neglect of basic scientific research. On the other hand, it has stimulated a fantastic rate of technical and industrial growth. Our basic preoccupation has been with the application of knowledge, rather than knowledge for its own sake.

This concentration on the immediate benefits of research and invention has paid off well. It has given us the highest standard of living in the world, built on a powerful industrial base. But there is another side to the coin. In our concentration on our interests we have often forgotten to look at what other nations were doing.

The result has been a curious paradox: Americans discovered two of the most outstanding inventions of this century--the airplane and the liquid-fueled rocket. Yet in neither case did we realize their significance to our national security until after other nations had turned them to military purposes and directed them against us and our allies.

During World War I, American airmen flew gallantly in combat--but the planes they flew were designed in Europe.

After World War II we made detailed studies of captured V-2 rockets--but the basic principles had been demonstrated by Robert Goddard in the 1920's. Goddard's work was largely neglected in this country, but during the 1920's and 1930's both the Germans and the Russians took his writings seriously. Both Nazi Germany and Soviet Russia saw the possibility that the rocket might give them a decisive breakthrough in weapons development.

Hitler nearly achieved this breakthrough. If the V-2 rocket--which was officially designated the "A-4"--had been developed a bit earlier, it might have led to more powerful and more accurate weapons that could have inflicted direct damage on this country. At the time of Germany's collapse the "A-9" and "A-10" vehicles--which were designed to reach New York--were already on the drawing boards.

There is much evidence to suggest that the Soviet Union has similar hopes in regard to space. This is a new medium for potential military operations, and it offers the chance to achieve significant technical breakthroughs. In addition to their possible military application, space achievements are dramatic indications of a nation's prestige and scientific capabilities.

The Soviets have long been aware of both the power and the propaganda aspects of space exploration. Much of their scientific and engineering effort is devoted to this area, and their space shots have been used as arguments for the alleged superiority of the Communist system. For the Soviet leaders, obviously, the conquest of space appears to have great practical value.

However, from a strictly scientific or commercial point of view, space does not appear to the general public to have much immediate practical value. The man in the street finds it hard to visualize the tangible benefits of space exploration--even though there have already been many.

In this country the real public support for a vigorous space program did not begin until after the first Sputnik. As the Soviets continued to demonstrate their space capabilities, our national attitude toward space underwent a change. The nation began to acquire the sense of urgency that is reflected in the decision to achieve a manned lunar landing before 1970.

It was an earlier sense of urgency that laid the foundation for many of the aspects of our national space program. This came from the realization that the Soviets were making an all-out effort to develop the intercontinental ballistic missile. To meet this challenge, the Air Force was assigned the mission of developing the ICBM--a task that was given top national priority.

Today ballistic missiles form an important and growing portion of the nation's deterrent strength.

In addition, ballistic missile technology has made and is continuing to make essential contributions to the national space program. Basically, it has provided a pool of knowledge and experience that can be drawn on as needed.

In addition, a number of specific contributions can be identified. Space boosters are modified versions of military rockets, and they are launched from military facilities. The Air Force is assigned responsibility for range management, and in addition 102 Air Force research and development officers are now assigned to duty with NASA.

This does not mean that military and civilian technological needs are identical in space, any more than they are in other realms. Military systems have a number of unique requirements, such as quick reaction time, the ability to operate in a hostile environment, and the high degree of maneuverability needed to intercept or avoid noncooperative objects.

In space development, we will undoubtedly find the same relationship that has proved true throughout the history of technology. This is the fact that military systems often demand more urgent development and higher performance requirements than their commercial or scientific equivalents.

This relationship has been quite evident in the evolution of modern aircraft. A passenger airliner is developed from a bomber or tanker aircraft--not the other way around. Many of the advances in civilian aviation have stemmed directly or indirectly from developments that were first required for military aircraft.

I think we can find the same pattern when we compare two programs for manned orbital flight. Mercury, which is a NASA responsibility, has received and continues to receive full military support. It is clearly a civilian scientific program, and the ballistic re-entry technique would be highly impractical for repeated, routine military operations.

Dyna Soar, by contrast, is an Air Force program and it receives support from NASA. Its chief aim is achievement of flexibility in re-entry, which is primarily a military requirement. Undoubtedly the knowledge gained from Dyna Soar may have future applications for civilian purposes, but the real reason for the program is to test concepts and sub-systems that may be needed for national security.

In today's world we cannot afford to lose sight of the intimate relationship between technical advancement and national security. Our opponents in world affairs seem clearly convinced that science and technology will be decisive factors in the contest between their system and ours.

If the Soviets should attain a really significant breakthrough in space technology, they may be able to deny other nations access to space--even for purposes of scientific research. Soviet attainment of this capability would pose a grave threat to our national security.

In the face of the possibility that the Soviets might try to pre-empt the use of space, our military capabilities in this realm are of utmost importance. We must have the necessary strength to insure that space is free to be used for peaceful purposes.

This is an essential military contribution to the progress of space exploration. In order to achieve success in our scientific endeavors, we must insure that access to space is guaranteed and that peace and freedom are preserved. Both the military and civilian aspects of our space program are vital, and both must be pursued with urgency. They share a common aim--the security and well-being of the United States.

DESIGN FOR MANNED SPACE FLIGHT

Robert R. Gilruth
Director, Manned Spacecraft Center
National Aeronautics and Space Administration

In approaching the task of talking to you about the subject, Design for Manned Space Flight, I asked myself - just what is different between manned flight in space and manned flight in airplanes?

Based on experience to date in the Mercury program and the beginnings of Gemini and Apollo, weighed against almost twenty years of airplane and missile projects, I am convinced that these are significant differences both in the design itself and in the environment the designer finds himself in.

Manned flight with airplanes developed during over half a century of time. In most of this period, the research laboratories were far ahead of the operational vehicles. Design rules and flight procedures have been highly developed. The role and risk of the test pilot is well understood. Flight programs can progress in phases - usually without publicity and public pressure and usually under military classification.

In manned space programs there is intense public interest. The exploration of the unknown, the cold war situation, the spending of large sums of public funds, combined with our completely open policy, keep the manned space program under full public attention at all times. The designer must learn to work and work well under this environment.

Unmanned space flight lacks one great element - namely the man - a chief factor in the public interest. Much more liberty can be taken with reliability rules. Finally, the cost and scope of unmanned programs have not approached those of manned programs and, therefore, they do not impose the massive system and integration requirements such as we find in Apollo.

The National program, of course, determines the type and scope of designs for manned space flight. In May 1961, President Kennedy established manned lunar landing as a National goal. During the months that have passed since his statement, that program has moved forward on a broad front in support of this objective:

a. The Saturn space booster has been placed under contract by the Marshall Space Flight Center, and initial flight tests have been accomplished.

b. Large booster development and test facilities have been sited and are being acquired.

c. The Manned Spacecraft Center has been established. A vigorous program is continuing on the Mercury project. The Gemini and Apollo spacecraft are under contract.

d. The national range at Cape Canaveral is being expanded.

e. A vigorous research and development program in support of the lunar landing mission is continuing.

Viewed from any angle, this is the beginning of a gigantic technical program. What are the problems of designing for this mission? How can an effort of this complexity be managed successfully? What have we learned from Project Mercury that will help us know what to expect and what to do about the problems?

Those of us who have worked on Mercury well realize the size of that task, its complexity, the painstaking system tests after assembly, the checkout time at the Cape, the ground complex, and the network problems. Many of us feel that in Mercury we were approaching a limit of sorts in checkout time and procedures for obtaining total complex readiness under the rules set down for manned flight with this system.

Yet the Mercury spacecraft is basically a very simple vehicle, the booster has had a long period of development, and the launch window is simply dictated by weather and daylight landing considerations.

By contrast, Apollo will have an enormous 3-stage booster, a spacecraft with a navigation system, mid-course propulsion and steering, a lunar landing and takeoff system, in addition to other basic Mercury systems expanded in scope. It also may have to rendezvous with another booster before it can even leave Earth orbit for the Moon. Judging on the basis of either of several criteria Apollo will be at least a full order of magnitude more complex than Mercury.

These criteria are shown in the slide (Figure 1), where the relative mission times, total energy of the systems, and the costs are compared. These are crude yardsticks but they indicate the size of the step being made in all phases of technology in this program. The mission time reflects the differences between a one-day Mercury flight and a voyage of exploration. The energy comparison shows the advance required in propulsion technology. The cost comparison may also be interpreted in terms of the people on the job - the size of the team - the management - coordination and integration problems.

What can be done to bring the task into reasonable bounds? I think all of us feel that the technical problems can be solved. Such factors as propulsion technology, guidance, reentry from escape speeds, lunar landing, crew systems and human factors will yield to intense research and development efforts.

Other more intangible problems lie in the integration of all these items into an operational system. As in all things, know-how comes from experience. We therefore need all the flight experience we can get to help in these areas. For this reason we are pursuing additional Mercury flights. We expect Project Gemini to provide direct support for the lunar effort by exploring rendezvous - long duration - and to provide for extensive space flight experience with two-man crews before the lunar voyage is attempted.

In Gemini we are also exploring advanced concepts in system engineering for space vehicles based on Mercury experience. Every effort is being made to reduce system interfaces - to package systems to facilitate their development - access - and checkout - and to minimize problems of final assembly and maintenance. This experience should have a direct influence in Apollo design.

We are also exploring the preferred role of man in the system. Properly used, man can contribute greatly to the simplicity of system interfaces. He has no equal as a mode selector - for commanding events in nontime critical operations, and as a sensor - operator in discriminating tasks such as lunar landing and takeoff operations and in rendezvous.

One other factor of great importance is the margin of performance. Certainly a tradeoff exists between performance - reliability - and schedule. Too many of our space systems have had to be optimized for absolute minimum weight regardless of assembly - checkout - and maintenance difficulties. In Apollo we have our first chance to use a booster designed for the mission instead of a mission designed for the booster.

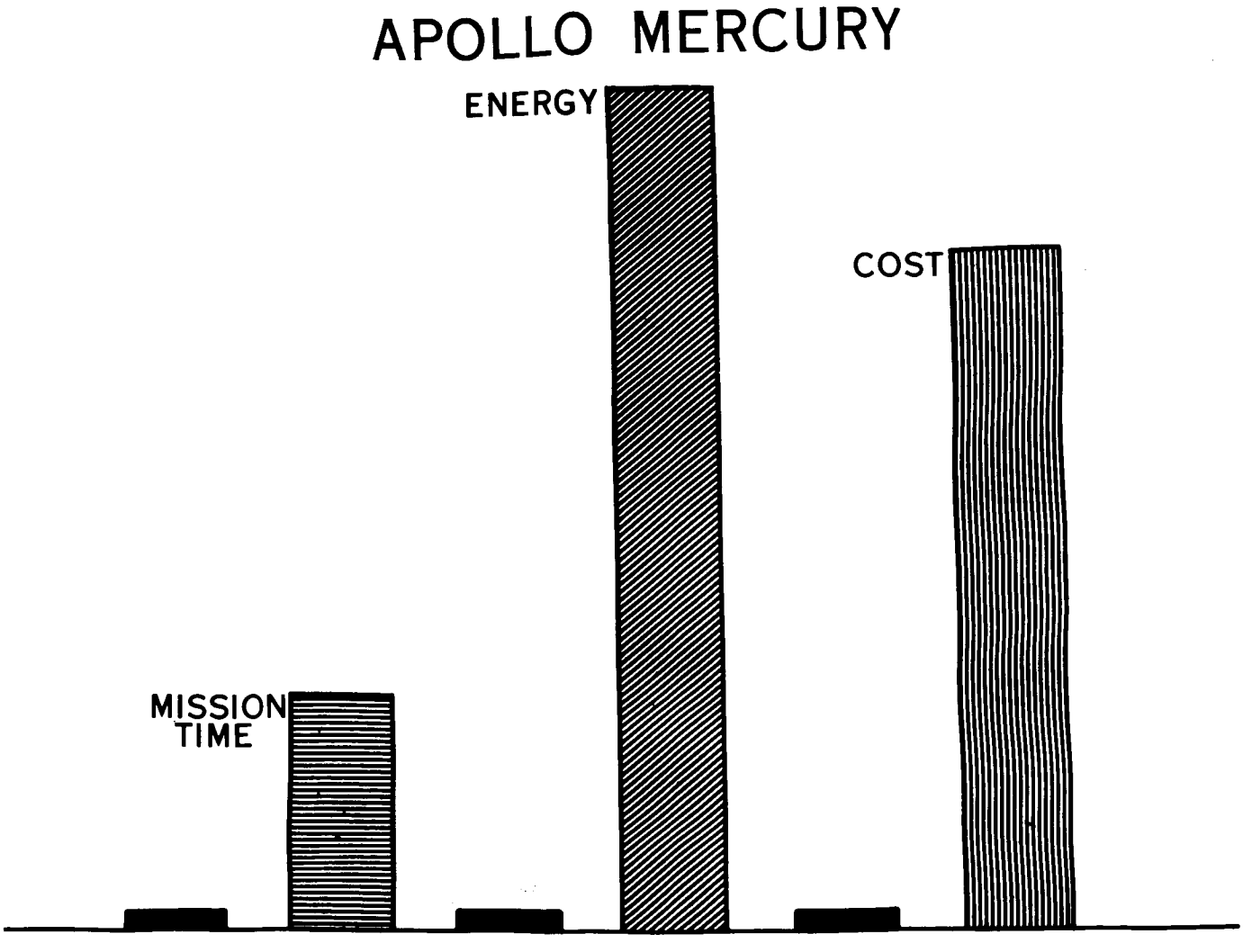

THE X-15 PROGRAM

Joseph A. Walker
Chief of Research Pilots Branch
NASA Flight Research Center
Edwards, California

Abstract

The X-15 has essentially attained its design performance in the flight research program accomplished to date.

The high-temperature structural design approach utilized for the X-15 configuration has been successful; no major design deficiencies were encountered nor major modifications required. With but few exceptions, the local thermal problems encountered have not affected primary structural areas.

In general, the aerodynamic derivatives extracted from flight-test data have confirmed the estimated derivatives obtained from wind-tunnel tests and thereby provided increased confidence in wind-tunnel evaluations at hypersonic speeds.

The aerodynamic flight control system and the simple stability augmentation system of the X-15 airplane have proved to be good technical designs. The airplane can be flown with satisfactory handling qualities through the range of dynamic pressures from about 1,500 lb/sq ft to below 100 lb/sq ft through the range of Mach numbers from about 6.0 to subsonic landing conditions.

Although only limited flight experience has been gained with the reaction-control system, its basic design appears to be completely adequate. This type of system apparently provides an adequate means of attitude control for future space vehicles. Pilot transition from aerodynamic controls to reaction controls has been accomplished without problems.

Reports from the X-15 pilots indicate that there are no piloting problems peculiar to the X-15 flight regime other than conventional pilot workload tasks.

Introduction

Since the first government flight in March 1960, the X-15 research program has been conducted in accordance with requirements for determining answers to the problems which the airplane was primarily built to study--aerodynamic and structural heating, hypersonic stability and control, control at low dynamic pressure, and piloting aspects. In addition, significant information, which was not considered to be of primary importance initially, has been derived relating to landing, aeromedical studies, simulation, and flight control systems. Other valuable data have been obtained on panel flutter, structural deformation, landing loads, structural effects on the stability augmentation system, engine nozzle erosion, and aerodynamic noise. This information was derived from several sources, including instrumentation of the X-15 airplane itself, postflight inspection of the X-15, medical data and commentary from the X-15 pilots, launch-airplane instrumentation and comments of the launch-airplane crew, comment of the escort-aircraft pilot and photography from the escort aircraft, and, on the ground, tracking, photography, and telemetry.

Flight Test Program

The X-15 was built with the objective of achieving a maximum velocity of at least 6,000 feet a second, an altitude of 250,000 feet, and a structural temperature of 1,200° F. Also, the airplane was constructed to be flown from launch through landing under direct control of the pilot. The validity of this approach has been verified by the successful progress of the research program. The maximum speed performance of the X-15 has been achieved at a Mach number of 6.04 (4,093 mph); an altitude of 246,000 feet has been exceeded; and a maximum temperature of 1,160° F has been obtained.

Shown in figure 1 is the performance capability of the X-15, including a shaded area which indicates the portion of the profile covered by flight test as of April 4, 1962. In addition, this performance envelope shows the relationship of dynamic pressure to altitude and velocity. As is apparent from the figure, the flight test dynamic-pressure has been intentionally limited to 1,500 lb/sq ft, thus allowing a margin for inadvertent overshoot.

Aerodynamic and Structural Heating

Heat-transfer data have been obtained on the X-15 in flight at speeds near free-stream Mach numbers of 3, 4, and 5, and at relatively low angles of attack. Turbulent heat-transfer methods were utilized and the results compared with X-15 flight data. The level of heat transfer predicted by reference-temperature methods is from 15 percent to 60 percent higher than the measured data, depending upon the assumed total-pressure level. Closer agreement with measured data has been obtained when the effective heating rate was neglected and attached-shock total-pressure levels were used.

Surface pressure and heat transfer which have been measured on the lower wing surface about mid-semispan and on the lower fuselage centerline are shown in figure 2. In the upper part of the figure, measured pressures are compared with calculated pressures for the lower wing and lower fuselage. In the lower part of the figure, measured heat-transfer data are compared with calculated values. For the wing, the surface pressures are closely estimated by assuming an attached shock and expanded flow over the wing. Similarly good agreement is shown for the lower-fuselage centerline where a tangent-cone approximation has been used to calculate the local-pressure levels. Whether the approach shown by the solid line in this figure can be generalized depends largely on measurements of the actual total-pressure levels in flight over a range of skin heating rates.

Some evidence of the manner in which boundary-layer transition takes place on the airplane in flight has been determined by utilizing temperature-

sensitive paint. In figure 3 a plot of wing boundary-layer transition for a selected midsemi-span station on the wing is shown with a postflight temperature-sensitive-paint pattern. The correlation between the paint and calculated laminar and turbulent flow is illustrated on the plot. Illustrated also is the critical nature of the shift between laminar and turbulent flow. Results suggest the advisability of continuing to use conservative estimates for the transition location.

Maximum temperatures measured on the X-15 show that speeds in excess of a Mach number of 6 have been accomplished without extreme structural temperatures. Comparison of calculated and measured internal temperatures has shown that satisfactory thermal gradients through the structure can be predicted from known heat input to the exposed surfaces, as illustrated in figure 4. In general, the hot-structure concept used for the primary structure of the X-15 has proved to be quite satisfactory. Structural problems have developed during the flight program as a result of local hot spots and discontinuities in the structural elements. Many of these problems pertain to the X-15 only; however, thermal problems with windshield glass, airflow through openings in the external structure, and structural discontinuities can be expected to appear on all hypersonic vehicles until adequate design information is available in these problem areas.

Landing

Landings with the X-15 airplane have shown that the main-gear loads measured during the second reaction after nose-gear contact are several times larger than the loads experienced during the initial phase of the landing, as illustrated in figure 5. The large loads during the second main-gear reaction are attributed to the main-gear location as well as to the large tail loads, the negative wing lift, and the airplane inertial loads after nose-gear touchdown. The high nose-gear contact velocities caused by the airplane pitching down result in high nose-gear loads and, consequently, high accelerations on the pilot during this phase of the landing. Calculated results show that the main-gear reaction can be reduced by proper control of the elevator angle during touchdown. Theoretical results show that increasing the skid coefficient of friction reduces the main-gear reaction slightly, but increases the nose-gear reaction. The present gear system of the X-15 has proved to be adequate in general and has required very little attention.

Lift and Drag

Generally good agreement has been obtained between flight and wind-tunnel measurements of aerodynamic forces on the X-15 for the low angle-of-attack range covered. In the future, flights will be extended to higher angles of attack where interference and nonlinear effects are the predominant flow characteristics. Throughout the Mach number range considered, up to a Mach number of about 5, and in the low angle-of-attack range, wind-tunnel trim lift and drag obtained on models showed excellent agreement with flight results in the X-15. Furthermore, at least up to a Mach number of 3 and for the Reynolds number range greater than 5 million, flight data indicate that reasonable values of the full-scale minimum drag can be obtained from extrapolations of the wind-tunnel results to flight Reynolds numbers, provided the condition of the boundary layer is known and a representative wind-tunnel model is tested, even to the extent of including all of the protuberances found on a full-scale airplane. Existing theoretical methods were adequate for estimating the X-15 minimum drag. These theories, however, underestimate the drag due to lift and overestimate the maximum lift-drag ratio, primarily because of the inability of the theories to predict the control-surface deflections for trim. The two-dimensional theory which has been known to predict base pressure on relatively thin wings with blunt trailing edges also predicts satisfactorily the base pressure behind the extremely blunt vertical surface of the X-15.

Stability and Control

The X-15 flight program has established fairly well-defined derivative trends for Mach numbers approaching the design limit. With few exceptions, these trends have agreed well with the wind-tunnel predictions (fig. 6). Also, many of the basic stability and control design parameters have been confirmed as a substantial portion of the overall flight envelope. A gradual development of these basic trends from one flight to the next has, in fact, generated a high level of confidence in proceeding to the more critical flight areas during the past several months.

No serious flight control problems have been encountered in the longitudinal mode. However, one serious deficiency in the lateral-directional mode has been observed in the form of an adverse dihedral effect at high Mach numbers and angle of attack with the lower rudder on and the roll damper off. This problem was not revealed until the inputs of the pilot were used with the airplane stability to determine closed-loop stability. The serious implications of the lateral-directional control problem are illustrated in figure 7, which shows the range of angles of attack and Mach number in which the controllability problem is expected with the lower rudder on and the roll damper off. Flight trim limits of angle of attack plotted against Mach number and the uncontrollable or extremely difficult control areas are designated. Recovery from high-altitude flight will require penetration of this uncontrollable region and, thus, loss of roll damper during the critical portion of reentry would be a significant problem. Two means are available for improving the X-15 controllability with the roll damper off: reduction of angle of attack, which for an altitude reentry results in higher dynamic pressure and higher structural temperatures, or a special technique referred to as the $\dot{\beta}$-technique. This technique involves the use of manual aileron input to counteract the sideslip as indicated to the pilot. Although these special control techniques have not completely alleviated the problem, they have provided sufficient improvement, when the side stick is used, to allow flight in the fringes of the uncontrollable region. Removal of the lower rudder appears to be a promising means of alleviating the lateral-directional instability at high angles of attack. Finally, additional reliability has been obtained by dualization of certain components in the stability augmentation system. Further studies and tests are planned for the high Mach number and angle-of-attack ranges to reveal any further flight control problems that exist in these more critical areas and to fill out the remainder of the flight

envelope. In general, with the stability augmentation system functioning, the X-15 handles very well (much the same as century series fighters) and verifies that the established handling-qualities criteria for aerodynamic stability and control serve as good guidelines. Further quantitative information must be obtained on the performance of the attitude control rockets.

The third X-15 is equipped with a self-adaptive flight control system built by Minneapolis-Honeywell Regulator Co. A self-adaptive flight control system, as the name implies, monitors its own performance and adjusts its gains to provide essentially constant aircraft dynamics throughout the aircraft's flight envelope without benefit of air-data sensing or scheduling. Additional features of the system include integration of aerodynamic and reaction controls and autopilot hold modes in attitude and angle of attack.

It was found during development that the X-15 adaptive system was more sensitive to structural feedbacks than had been anticipated. Notch filters were installed to reduce system gain at primary structural frequencies. This modification, and other minor development changes, have resulted in average gain levels somewhat lower than had been anticipated. The flight demonstration is continuing satisfactorily, with the current objectives of decreasing reaction-control fuel consumption and increasing the usable angle-of-attack range.

Simulation

Pilot training procedures have proved to be adequate for a program of the X-15 type. The use of the analog simulator to establish pilot cues and timing and to allow the pilot to practice until the techniques become routine has considerably eased the total piloting task, thereby improving the pilot's ability to obtain precise flight data in the time available. Predictable emergency conditions or off-design missions have been encountered during the program and, in each instance, simulator training has contributed greatly to the pilot's ability to complete the mission. The two most valuable training devices have been a fixed-base six-degree-of-freedom analog simulator and the F-104 in-flight landing-pattern simulator. Other training devices such as the centrifuge and the variable-stability airplane have contributed to the overall pilot-experience level; however, they are not considered necessary for continuous use on a flight-by-flight basis. Expected problems, primarily in the area of aerodynamic heating, have also been encountered, but neither pilot nor flight vehicle safety has been compromised by the incremental-performance philosophy of envelope-expansion testing.

Operational Experience

Figure 8 presents a tabulation of the X-15 mission success as of November 1, 1961. In every instance, failures to achieve the planned performance were the result of powerplant and propellant system problems and pilot presentation deficiencies; stability augmentation and cabin pressure/pressure-suit systems problems contributed to the failures in achieving the prime mission objectives. Alternative modes of operation were available with which to obtain increased probability of mission success. For example, if the flow-direction-sensor ball nose failed after launch, a 2g pull-up could be performed until specified pitch angle was achieved. Reentry could be accomplished by reference to pitch on the attitude indicator, setting predetermined stabilizer angle, or reference to the horizon. However, all of these alternative procedures resulted in comparatively inaccurate flight profiles. Generous tolerances were allowed in performance when considering achievement of prime objectives. Even on several successful flights, there were problems similar to those noted.

A comprehensive evaluation of the X-15 flight operations, performed by Mr. R. G. Nagel of the AFFTC, has indicated that the program benefited greatly from inclusion of a pilot in the control loop and from redundant systems (figs. 9 and 10). These figures indicate the effects of pilot and redundancy upon the prelaunch and postlaunch phases of the X-15 operation. In figure 9 the total number of launches or attempts is shown for pilot plus redundancy in the actual case as compared to a hypothetical case for an unmanned vehicle with no redundancy, while for the postlaunch phase, the comparison in figure 10 includes the actual case of pilot plus redundancy and hypothetical cases of pilot only, redundancy only, and an unmanned vehicle with no redundancy. Note that the impact of pilot plus redundancy is more marked for free-flight operations than for prelaunch operations because of the prelaunch checkout procedure for detecting troubles.

A comparison with an independent evaluation of the Bomarc missile by the Boeing Co. is shown in figure 11. Whereas the unmanned X-15 is hypothetical, the manned Bomarc is hypothetical. The similarity of success and failure percentages is striking and serves to place further emphasis upon the value of the pilot in the system and of redundancy for increased success in other aerospace programs. It is significant that the pilot has been able to do the job, if not prevented by factors beyond his control, and recovered the airplane in all cases. Of course, the flights were planned for pilot operation, but the tasks were challenging, even so. The planning and execution of flights was generally successful and indicates that the initial concepts were correct. It is believed that even increased utilization of the pilot will be possible in advanced vehicles.

Physiological Data

To date, recorded physiological data from X-15 pilots have indicated only reasonably expected responses. Heart rates during flight have usually been from 140 to 150 beats per minute, about double the pilot's resting preflight heart rate. These levels have been confirmed by measurement of heart rates of 150 beats per minute during operational fighter landings. The data are useful, therefore, in establishing physiological baselines for pilots of high-performance vehicles.

Figure 12 presents flight time histories of altitude, velocity, normal and longitudinal acceleration, breathing rate, and heart rate as measured during an X-15 flight. One can see the general parallel response of breathing and heart rate to greater or reduced physical loading caused by maneuvering and thrust and drag. The heart rate is believed to be the more accurate indicator of work load, since breathing can be intentionally varied somewhat (by holding one's breath at high g, for example). Note that the last 4 minutes (time

400 sec to 630 sec) have the highest continuous heart rate, coincident with a steep descending turn with speed brakes extended, followed by pull-out and landing-pattern maneuvering. The anticipatory "spin-up" surges before launch and before descent, followed by decrease to required load, can also be seen.

Future X-15 Program

The X-15 program for the immediate future will be oriented toward continuing research investigations in the following primary areas: flight characteristics at high angle of attack; aerodynamic heating; reaction controls, including rate damping; adaptive control system; performance; displays; energy management; and bioastronautics. As these programs are completed, follow-on programs will explore some interesting new experiments such as ultraviolet stellar photography, infrared exhaust signature, landing computer, detachable high-temperature leading edges, horizon definition, and hypersonic propulsion.

Concluding Remarks

In reviewing the broad aspects of the accomplishments of the X-15 program, the following conclusions may be made:

The exploratory flight studies have indicated that hypersonic aerodynamic heating effects can be predicted with sufficient accuracy to support the design of a hot-structure vehicle such as the X-15 airplane. The high-temperature structural design approach utilized for this configuration has been successful; no major design deficiencies were encountered nor major modifications required. With but few exceptions, the local thermal problems encountered have not affected primary structural areas.

In general, the aerodynamic derivatives extracted from flight-test data have confirmed the estimated derivatives obtained from wind-tunnel tests and thereby provided increased confidence in wind-tunnel evaluations at hypersonic speeds.

The aerodynamic flight control system and the simple stability augmentation system of the X-15 airplane have proved to be good technical designs. The airplane can be flown with satisfactory handling qualities through the range of dynamic pressures from above 1,500 lb/sq ft to below 100 lb/sq ft through the range of Mach numbers from about 6.0 to subsonic landing conditions.

Although only limited flight experience has been gained with the reaction-control system, its basic design appears to be completely adequate. This type of system apparently provides an adequate means of attitude control for future space vehicles. Pilot transition from aerodynamic controls to reaction controls has been accomplished without problems.

Reports from the X-15 pilots indicate that there are no piloting problems peculiar to the X-15 flight regime other than conventional pilot workload tasks.

Symbols

a_n normal acceleration, g units

a_x longitudinal acceleration, g units

C_{l_β} effective dihedral derivative

C_{m_α} longitudinal stability derivative

C_{N_α} slope of airplane normal-force-coefficient curve

C_{n_β} directional stability derivative

g acceleration due to gravity, ft/sec^2

H altitude, ft

h heat-transfer coefficient, $\frac{Btu}{ft^2\text{-}°F\text{-}sec}$

M Mach number

N_{Pr} Prandtl number

p pressure

$p_{t,A}$ attached-shock total pressure

$p_{t,N}$ total pressure behind normal shock

$p_{t,\infty}$ free-stream total pressure

q dynamic pressure, psf

T_R boundary-layer recovery temperature, $T_R = T_l\left(1 + \frac{\gamma - 1}{2}\eta M_l^2\right)$

T^* reference temperature, $T^* = T_l + 0.5\left(T_W - T_l\right) + 0.22\left(T_R - T_l\right)$

$(T^*)_{aw}$ adiabatic-wall reference temperature, $(T^*)_{aw} = T_l + 0.72\left(T_R - T_l\right)$

V velocity, ft/sec

V_{v_0} airplane sinking speed at initial touchdown, ft/sec

W airplane landing weight, lb

x_f length from fuselage nose, ft

x_w length from wing leading edge, ft

α angle of attack, deg

α_0 initial angle of attack at touchdown, deg

γ ratio of specific heats

δ_h horizontal-stabilizer position, deg

η recovery of factor $\left(\sqrt{N_{Pr}}\right.$ for laminar flow, $\left.\sqrt[3]{N_{Pr}}\right)$ for turbulent flow

Subscripts:

l local

W wall or skin

X-15 PERFORMANCE ENVELOPE

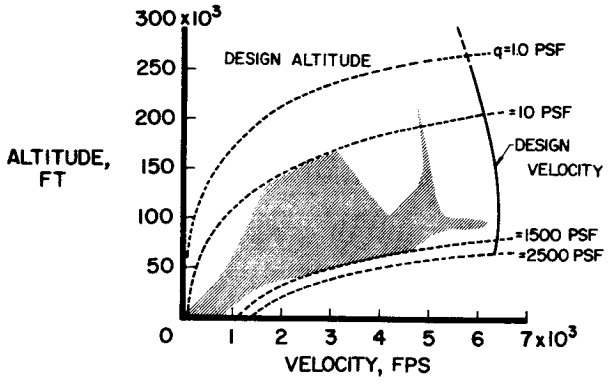

Figure 1

SURFACE PRESSURES AND HEAT TRANSFER

$\alpha \approx 4$

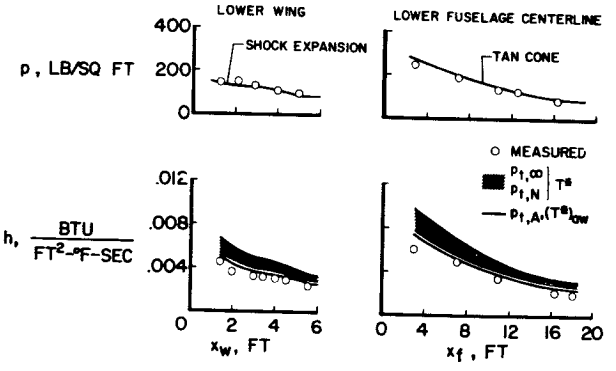

Figure 2

WING BOUNDARY-LAYER TRANSITION

$\alpha \approx 4$

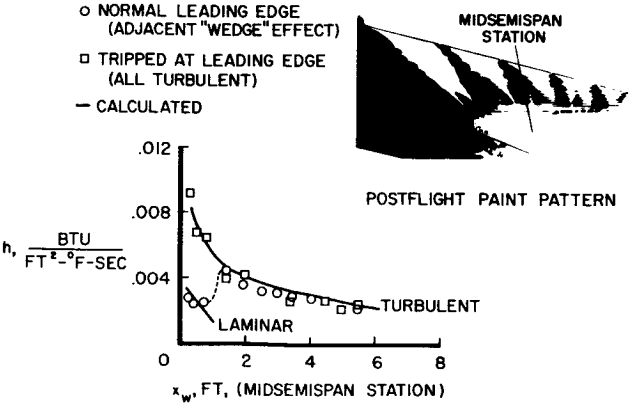

Figure 3

CALCULATED SPAR TEMPERATURES AT TIME = 225 SECONDS

FLIGHT TO MACH NUMBER OF 5.28

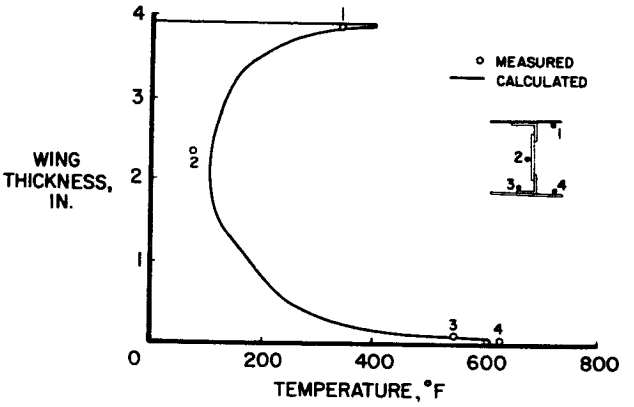

Figure 4

MAIN-GEAR-SKID VERTICAL REACTION

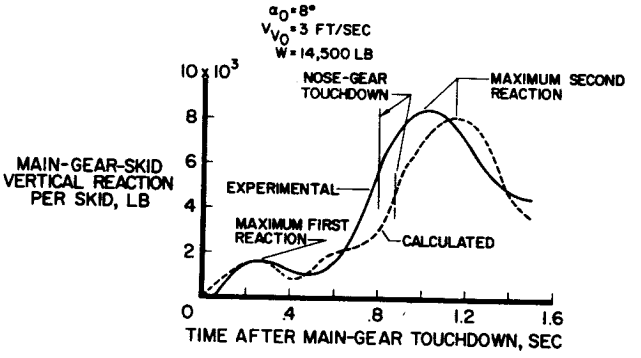

Figure 5

X-15 STABILITY DERIVATIVES

$2° < \alpha < 6°$

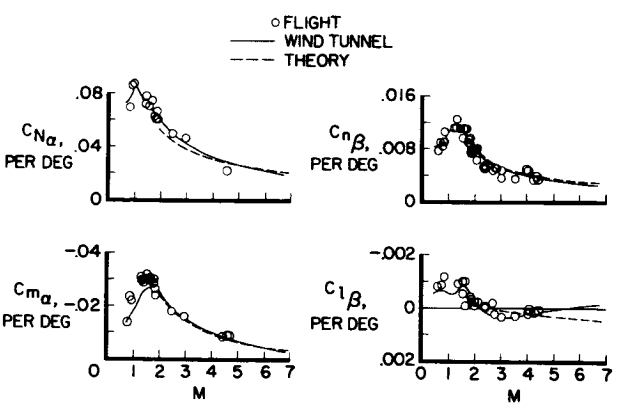

Figure 6

SUMMARY OF PREDICTED STABILITY AND CONTROL

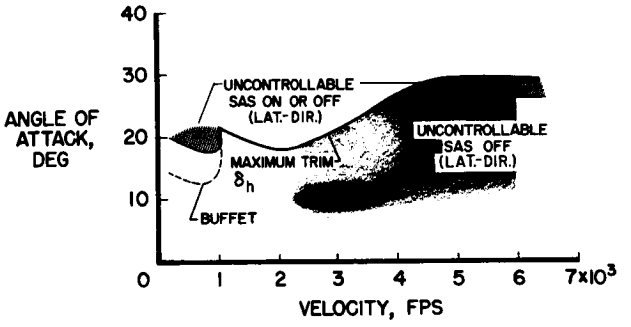

Figure 7

X-15 FLIGHT SUMMARY

AS OF NOVEMBER 1, 1961

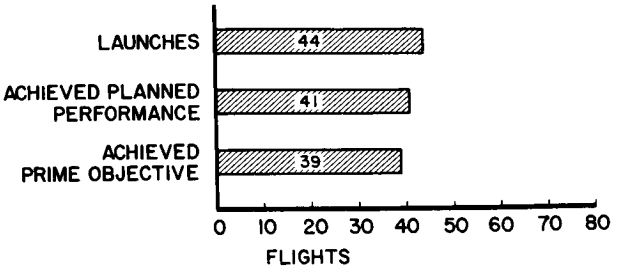

Figure 8

OVERALL PILOT-IN-THE-LOOP AND REDUNDANCY BENEFITS

PRE-LAUNCH + POST-LAUNCH

(THROUGH NOV. 1, 1961)

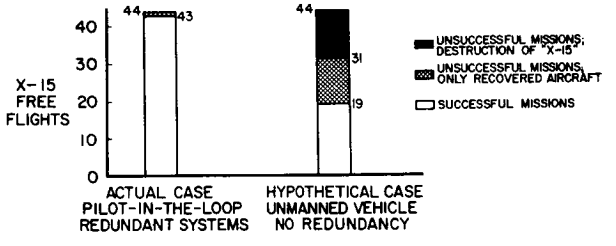

Figure 9

QUANTITATIVE SUMMARY OF X-15 FREE FLIGHTS

POST-LAUNCH PHASE

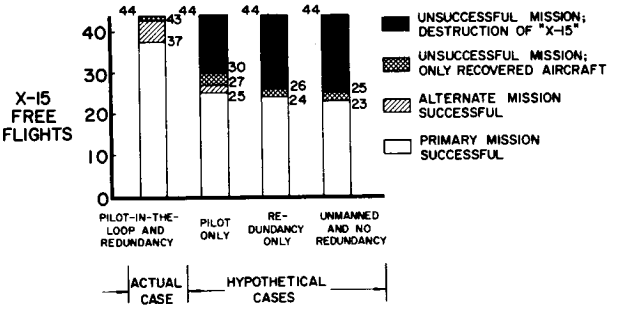

Figure 10

COMPARISON OF X-15 AND BOMARC PILOT AND REDUNDANCY ASPECTS

MISSION SUCCESS ON OVERALL FLIGHT BASIS

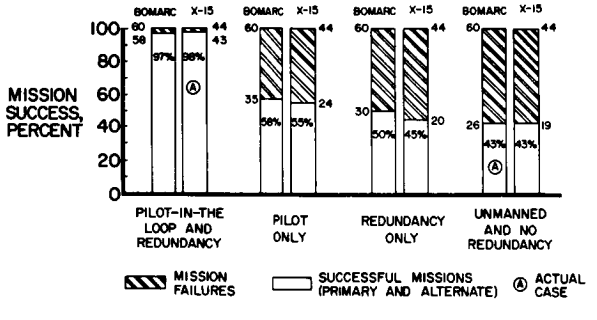

Figure 11

FLIGHT TIME HISTORY

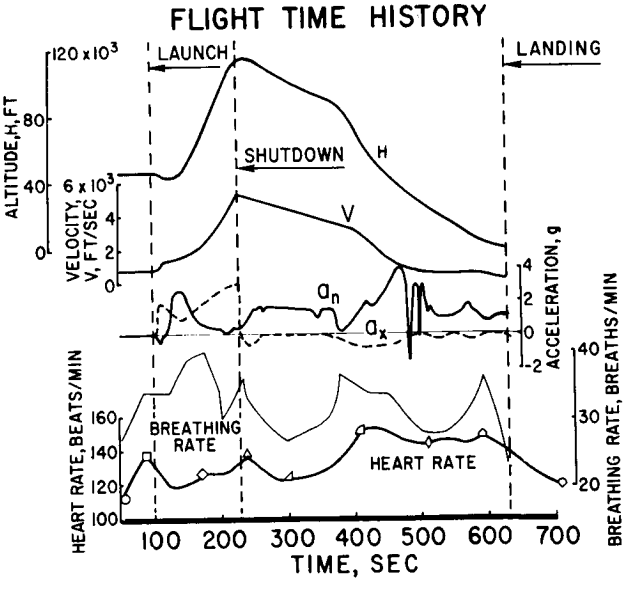

Figure 12

EXPERIENCE WITH MERCURY SPACECRAFT SYSTEMS

J. F. Yardley
Base Manager
McDonnell Aircraft Corporation

1. Introduction

Design of a manned spacecraft in 1958 and 1959 required that many decisions be made with no background of direct experience with similar vehicles and very little background of experience on vehicles of any type which had been exposed to the rigors of space. Under such circumstances, it was necessary to establish certain fundamental design principles which were believed to represent the proper balance between the conservatism required by the unknowns, the desired development schedule, and the extreme necessity to conserve weight.

One of the foremost of the program objectives was, of course, safety. Broadly speaking, the design principles chosen to achieve the level of safety desired in such an unknown venture were very similar to those used for manned aircraft design. Summarized in simplified form:

a. Flight safety should not be jeopardized by single failures of functional components in probable failure modes.

b. System requirements should be met wherever possible through the use of component designs already tried and proven, so that added risks of "state of the art" developments would be minimized.

c. Structural design should be kept simple and straightforward. Materials should be chosen for their reliability of performance and tolerance for extended environments insofar as possible.

d. Vehicle design should be such that the entire mission could be completed without an active pilot.

This paper will discuss actual experience with some of the Mercury spacecraft systems and relate this experience to these original design principles. The concluding remarks will suggest, in retrospect, how these principles should now be modified in the light of present Mercury experience.

2. Structure and Heat Protection

The basic primary structure chosen was a simple conventional semi-monocoque shell of titanium. Figure 1 shows an external view of the primary titanium structure. Welding was used as much as possible to avoid leakage. The primary structure was designed to operate "cool", but the materials chosen had considerable tolerance for elevated temperatures in the event that the heat protection failed locally. The decision to insulate the load carrying structure eliminated many thermal expansion problems which are difficult to predict analytically. The experience to date with this type of structure has been excellent. The only significant problem to date was an interface flexibility problem with the Atlas missile which resulted in stiffening both the Atlas and the adapter structure between the missile and the spacecraft.

The structural separation devices are a good example of the redundant design philosophy employed. All separation devices are designed to operate satisfactorily in spite of any single failure. For example, the main joint between the spacecraft and the adapter uses a three-segment clamp ring joined by three explosive bolts. If any one of these bolts fire, the joint will release. Each bolt has two separate firing means, and in one case, mechanical firing is possible. The electrical umbilicals between the spacecraft and the adapter must also positively release for satisfactory mission safety. Each of these wire bundles has a pyrotechnic disconnect and a mechanical disconnect in series. Figure 2 illustrates a typical joint. In three separate flights, this redundancy was needed to satisfactorily separate the umbilicals. The failures of the pyrotechnic disconnects were caused by the main clamp ring fairing which struck the disconnect during abort separations, thus jamming it. The fairing was redesigned to eliminate the possibility of aft motion during separation. This case is a good illustration of the value of this redundant design philosophy. Had no redundancy been employed in this joint, it is quite possible that these missions would have been complete failures.

Redundancy, however, can also cause added problems. For example, if two components are provided, either of which can perform the desired function at the desired time, then there is twice the probability that a random actuation of the component at the wrong time will occur. An example of this occurred on a flight test from Wallop's Island. The escape rocket was fired prematurely by a malfunctioning limit switch. In this particular case, there were three switches in parallel to fire the rocket when desired. The basic problem turned out to be a vibration of the switch and surrounding structure at extremely high dynamic pressures, but if these switches had been interlocked, the failure could not have occurred. Thus, it is important that the designer consider carefully the problem of "negative" redundancy as well as the problem of "positive" redundancy.

Heat protection of the spacecraft requires a considerable weight so complete redundancy was not feasible. To compensate for this, more conservative design criteria were selected. For example, the ablative heat shield is designed to absorb the additional heat produced during a re-entry where only two of the three retrorockets fire. In addition, the backup structure of the heat shield uses material with some ablative capabilities so that an extra margin of safety is obtained without added weight. Experience with the heat shield indicates consistent, reliable performance which correlates very well with analytical predictions. The only problems encountered have been in obtaining sound structure during the manufacturing process. Stringent process control coupled with certain design changes have remedied these fabrication problems. Figure 3 shows the MA-4 capsule illustrating the heat shield condition after orbital re-entry.

The afterbody heat protection largely consists of "shingles" of .016 inch thick beaded Rene 41 material which dissipate the heat by radiation. Exhaustive ground tests were made on these shingles using conservative combinations of heat, dynamic pressure, and noise. These shingles have performed admirably in all flight tests; in no instance have any of these shingles buckled, cracked or torn in any way. The heat protection on the small cylindrical afterbody is provided by .25 inch thick beryllium shingles. In this area radiation cooled shingles are not sufficient for the case of a completely uncontrolled re-entry, so a heat sink approach was necessary to allow for control system failure. Figure 4 illustrates the condition of these afterbody shingles subsequent to orbital re-entry.

In the case of the window, redundancy was employed. Protection from failure of the outer window is provided by an inner heat resistant window. The pressurization loads are also carried by redundant windows. No problems have been encountered with the window design.

3. Electrical System

Basic direct current electrical power is furnished by six silver-zinc batteries arranged to provide a main bus, a standby bus, and an isolated bus. Suitable switching provisions are available to isolate or parallel these batteries and buses in a variety of ways, so that maximum use can be made of this inherent redundancy. The batteries themselves have proven very reliable in service, as has the entire main power distribution system.

Alternating current electrical power is provided by static inverters arranged into two separate A.C. buses. A standby inverter is provided that automatically switches to the appropriate bus in the event of an inverter failure. Some trouble was experienced on early models of these inverters in the areas of starting reliability and overheating. Later model inverters have significantly improved these characteristics. Flight experience has illustrated again the value of the AC redundancy provided. On the MA-4 flight, one of the primary inverters failed during launch. Without a backup, the flight would have been aborted. In the actual case, however, automatic switchover was satisfactorily accomplished and the flight was successfully completed.

The sequential system consists of a number of sensors, relays, timers, etc., and actually is the "brain" of the automatic system. System design was complicated by the necessity to allow manual or ground command override capability. A high degree of redundancy was provided in this system, and experience has shown this to be desirable for the unmanned flights. In a system of this nature, the designer must give extremely careful consideration to the matter of "negative" redundancy. The first Mercury-Redstone

launch illustrates the type of thing that can happen. The Redstone received an erroneous cut-off command as it was lifting off. It shut down and settled back on the pad after rising one inch; this cut-off signal was sent to the spacecraft which automatically initiated the normal sequence as though the powered flight had been completed. The first sequential event was to jettison the escape tower. In an emergency situation of this nature, it might have been catastrophic to lose the escape tower at that moment. The design was changed to provide suitable interlocks so that this signal from the Redstone could not be sent until a certain velocity had been achieved.

The general experience with the sequential system has been quite satisfactory with failures usually confined to isolated timer circuits or sensors of a non-critical nature. During the recent MA-6 flight, however, a malfunctioning limit switch required that a grave decision be made during flight to re-enter without jettisoning the retro package. Here again is an example of insufficient negative redundancy. The heat shield release mechanism has two limit switches which are actuated when the mechanism is unlocked. These switches were wired in parallel giving good "positive" redundancy, but poor "negative" redundancy. In this particular case, it is far more important to know the mechanism is safely locked before re-entry than to know it has properly unlocked after parachute deployment, since landing without the impact system is perfectly acceptable. For future flights, it is planned to wire these switches in series so that a double failure is required before a false indication is given.

4. Automatic Stabilization System

The automatic stabilization system consists of attitude reference components, rate sensors, logic electronics, and suitable displays. It is designed to sense spacecraft attitudes and rates, and send signals to the control jets thus maintaining the desired attitude or changing from one attitude to another. Mode switching signals are provided to this system from the sequential system. It was not considered necessary to duplicate this automatic stabilization equipment since the astronaut provides an excellent backup for all of its functions. The detail design of the system, however, provides a certain amount of desirable redundancy. For example, the basic attitude reference system consists of attitude gyroscopes which are slaved to horizon scanners. Consideration was initially given to using the horizon scanners directly as the attitude reference and thus eliminating some components. This idea was discarded primarily because of the lack of experience with horizon scanners compared with attitude gyros. Flight tests to date show that this was a wise decision. While the horizon scanners have performed reliably, they sometimes provide an erroneous attitude reference due to certain atmospheric phenomena. For example, they sometimes mistake high altitude clouds and hurricanes for deep space. Figure 5 illustrates this effect on the MA-4 flight when the spacecraft passed over hurricane Debbie. These effects are not serious when the gyros are slowly torqued to the scanner reference, but could be quite disconcerting if these erroneous signals were used directly for control logic information. These effects have been reduced in magnitude and frequency of occurrence by certain internal circuitry changes to the horizon scanners.

The digital nature of the control logic also provides a degree of redundancy. The orbit attitude is maintained within desired limits by a series of five sector switches for each axis. Each switch backs up the previous one so that failures of any single switch will result in only minor variations from the normal limit cycle. The various modes of operation are also arranged to back up other modes. Thus, if for any reason orbit mode cannot be maintained, the system switches into orientation mode. This has actually happened on several flights because of malfunctions of some of the small jets used for orbit mode control.

Reliability of the automatic stabilization system has been exceptionally good on all flights. The only malfunction experienced to date was the failure of a 2 deg/sec signal from one of the rate gyros. This trouble was later traced to a broken wire in one of the spacecraft harnesses. These have been cases where it was initially suspected that this system was malfunctioning; subsequent investigation has always revealed that the system was working perfectly, and that the unusual indications were the

results of unusual maneuvers. For example, during the flight of MA-6 it was reported that the attitude indicator was giving erroneous attitudes when compared to the visual horizon reference. Later analysis verified that this was a normal situation resulting from manually yawing the spacecraft without interrupting the open loop orbital precession of the gyros while the scanners were not slaving. Thus the gyros were being precessed assuming the spacecraft was traveling blunt end forward while it was actually traveling small end forward. This naturally led to a discrepancy between actual attitude and indicated attitude.

5. Reaction Control System

Spacecraft attitude control is achieved through the use of small Hydrogen Peroxide jets. Two completely independent systems are provided. Each system has its own pressurant system, tankage, control valves, and thruster assemblies. One system, called the Automatic System, is energized solely by electrical signals. These signals can be received from either the automatic stabilization system (automatic mode) or from direct switches on the hand controller ("fly-by-wire" mode). This system has a set of low thrust jets (one lb. thrust) and a set of high thrust jets (twenty-four lbs. for pitch and yaw; six lbs. for roll). The other system, called the Manual System, can be energized entirely manually through the use of mechanically actuated throttling valves (manual direct mode), or can be energized electrically by hand controller motion (rate command mode). The manual system has only a set of the high thrust jets, but lower thrust can be obtained by proper use of the proportional throttling valves.

Experience to date with these systems clearly illustrates the value of redundancy.

Development problems have not yet been entirely eliminated; this results in less than the desired component reliability and would probably necessitate lengthy program delays if it were not for the fact that sufficient redundancy exists to achieve the necessary reliability for continued flight development Ground test development is difficult and time consuming because of the laboratory problems of proper simulation of altitude, internal heat generation, external heat balance, etc. Of course, zero "g" effects cannot be duplicated in the laboratory. Thus it is highly desirable to utilize actual flights for this development process.

Problems encountered to date include corrosion, temperature control, system cleanliness, and internal deterioration of thrust chamber assemblies. Internal corrosion products have resulted in sufficient foreign matter to plug some of the smaller orifices. Corrosion has also caused solenoid valve malfunctions and in one case the corrosion was so severe that an actual leak occurred in a plumbing line. This problem has been brought under reasonable control by special vacuum drying techniques, purging techniques, changes to materials and protective finishes, and by the addition of suitable filters in the systems.

Achieving satisfactory temperatures for the hydrogen peroxide in the tanks and lines has also presented problems. At present, the temperatures are controlled passively by means of insulation, conducting straps, etc. This passive method has proven satisfactory in all cases except for the lines and valves close to the roll thrusters. Temperatures in the area of the roll thrusters have been adequately controlled for the short missions by heat sinks; testing is currently underway to develop methods of adequate temperature control for longer periods of time.

Any foreign particles of even minute size can plug up some of the tiny orifices in the thrusters. For example, the MA-5 flight was terminated after two orbits because of a malfunction in one of the small thrusters. Post flight inspection revealed that the stoppage was caused by a small metal chip plugging an orifice. A filter had been provided about two inches upstream of the orifice which would have stopped this particle had it been introduced into the system upstream of this filter. Subsequent analysis indicated that this chip was torn from the threads immediately upstream of the orifice plate during assembly. It is probable that a slight burr existed on the threads and was overlooked during inspection. This machined thread has since been replaced with a rolled thread. Figure 6 shows a one pound thrust chamber and solenoid valve

disassembled. Foreign particles are minimized by system flushing, careful procedures during assembly and servicing of the system, strategic filter placement and stringent quality control.

Another problem which has caused malfunctions of the small jets is the disintegration of an internal screen inside the thruster assembly immediately downstream of the orifice plate. The combination of heat, errosive forces, and corrosive environment destroy this stainless steel screen. In some cases, these small pieces of wire work their way upstream through the orifice and subsequently block the orifice; this is believed to be the cause of the intermittent operation of one of the small jets on the recent MA-6 flight. These stainless steel screens are being replaced with screens of platinum wire which are further protected by a stainless steel diffuser plate. This configuration is currently being tested.

6. Environmental Control System

Spacecraft and pressure suit temperature, gas composition, and pressure are regulated by this equipment. The cabin and suit circuits are independent and designed so that either will provide a backup for the other. Pure oxygen, stored at 7500 psi, is supplied to replenish the oxygen used by breathing and leakage. Water evaporation is the basic cooling method. Carbon dioxide is removed chemically with lithium hydroxide. Water is removed with a periodically squeezed sponge. High speed compressors provide the ventilating flow. Pressure is automatically regulated to a differential value of 5.5 psi. The system has many modes of operation and has internal redundancy in many areas. Experience has demonstrated the adequacy and gross reliability of the system; it has also shown that many checkout problems encountered because of the many automatic backup features which require close operating tolerances for proper performance. Flight experience has been quite satisfactory. Problems encountered to date include cabin decompression, heat exchanger freezing, excessive use of oxygen, and high cabin temperatures.

During the MR-2 flight, a post-landing ventilation valve inadvertently opened due to launch vibration resulting in decompression of the cabin. A check valve protected the suit circuit so the flight was successfully completed, again illustrating the value of the fail safe design philosophy. The inflow valve operating linkage was modified and has given satisfactory service since that time.

Some troubles have been experienced in the past with freezing at the heat exchanger steam exhaust outlets. This is due to water flow in excess of the amount required to remove the internally generated heat. Freezing can be easily avoided by the astronaut if he is given steam exhaust duct temperature indications; this was demonstrated during the MA-6 flight.

Excessive oxygen usage occurred on some of the early flights due to vibration of the emergency rate valve linkage. Redesign corrected this deficiency. Some trouble has been experienced with obtaining perfect dynamic seals on the 7500 psi portion of the system, but such leaks have been of minute proportions. Prelaunch testing has uncovered other subtle means for using excessive oxygen. For example, the MA-6 ground testing indicated excessive oxygen use, although normal system pressure testing revealed no leaks. The trouble was finally traced to the wrist seals on the pressure suit which had no leakage at 5 psi differential pressure, but leaked badly at very low pressures of 2 to 4 inches of water. Once located, this trouble was quickly eliminated by improved seals.

7. Other Systems

The Mercury Spacecraft has a number of other systems (i. e., communications, instrumentation, rockets, etc.) which have not been discussed in detail. In general, most of these systems have given satisfactory service in spite of development difficulties, because of the general fail safe design philosophy.

8. Conclusions

Experience with Mercury Spacecraft systems has been briefly discussed and related to certain initial design criteria. In retrospect, these criteria can now be examined for their applicability to future manned spacecraft design.

The "fail safe" design criteria has definitely been demonstrated as a highly important rule to follow which permits safe flight testing in unexplored environments. This rule must be applied with considerable judgment to obtain the proper balance between positive redundancy, negative redundancy, and complexity.

The use of component designs which have been previously proven has definitely been beneficial. In many Mercury cases, this was not possible and experience has shown that more development troubles and failures were encountered in these cases.

Simple structural design has worked well, but no information has been gained to determine the degree of trouble which would be encountered with a more complicated structural approach. It is felt that manned spacecraft of the future could compromise in this area to obtain benefits in other areas without seriously jeopardizing the end results.

Fully automatic operation was originally required for two reasons. Firstly, because of the necessity for a number of unmanned development flights, and secondly, because of the uncertainty surrounding man's ability to function properly in the new environment. In retrospect, it is felt that the number of unmanned flights can be reduced in the future, but some will still be required to eliminate the development problems which cannot be solved without flight test. Manned flights to date indicate that human performance will be excellent in the new environment, and full automation on future spacecraft will not be required to back up the pilot. Thus the experience to date suggests that future manned spacecraft need not be designed so that the entire mission can be completed without an active pilot. The design must, however, be such that simple modifications will permit unmanned flight testing of some phases of the total mission.

MA-4 SPACECRAFT STRUCTURE

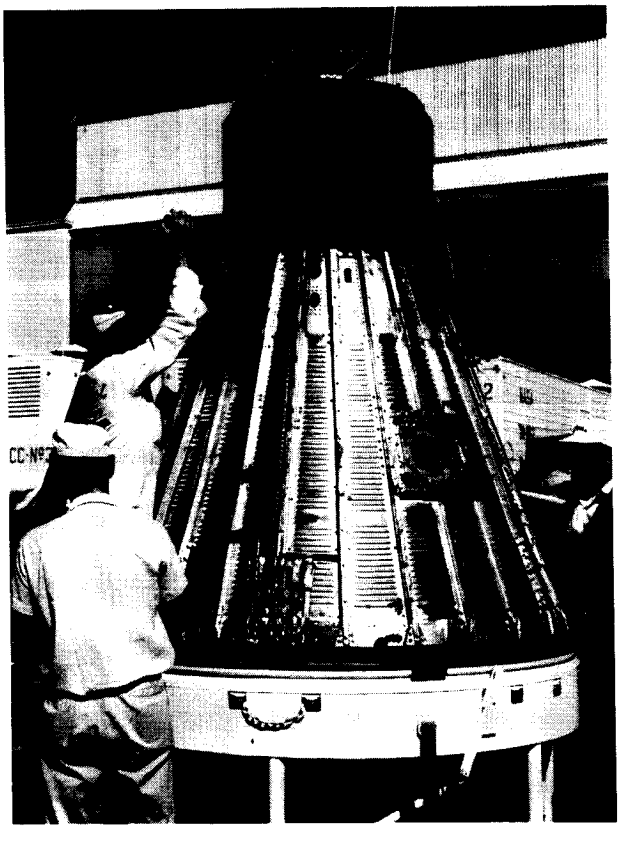

Figure 1

TYPICAL MERCURY CLAMP RING AND UMBILICAL JOINT

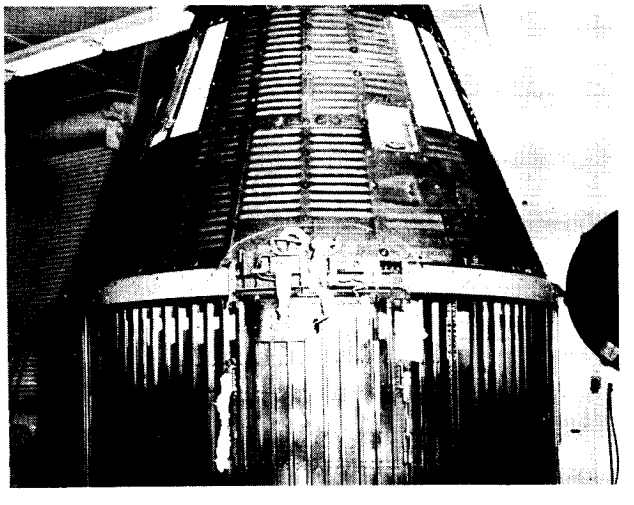

Figure 2

This page is reproduced again at the back of this report by a different reproduction method so as to furnish the best possible detail to the user.

MA-4 HEAT SHIELD AFTER RECOVERY

Figure 3

MA-4 HORIZON SCANNER ERROR DUE TO HURRICANE DEBBIE

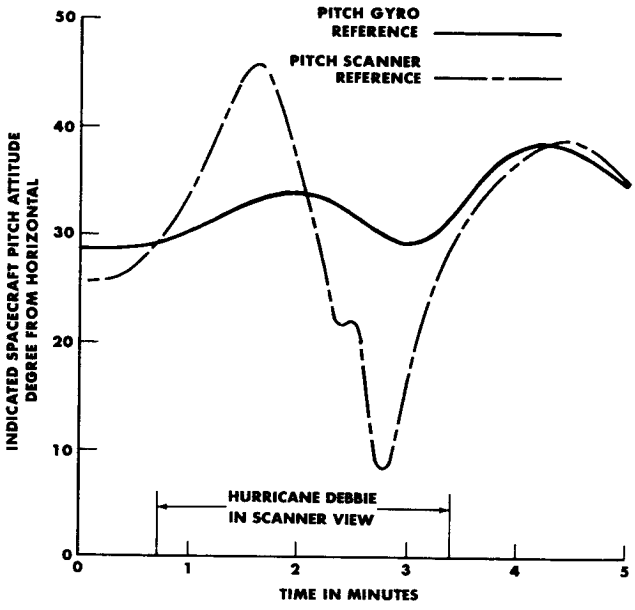

Figure 5

MA-6 AFTERBODY SHINGLES AFTER RE-ENTRY

Figure 4

MA-5 DISASSEMBLED ONE LB. YAW THRUST CHAMBER AND SOLENOID VALVE

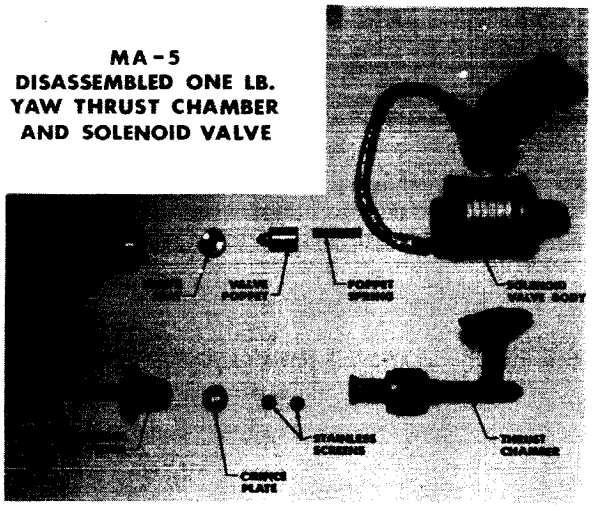

Figure 6

This page is reproduced again at the back of this report by a different reproduction method so as to furnish the best possible detail to the user.

MERCURY OPERATIONAL EXPERIENCE

Christopher C. Kraft, Jr.
Chief, Flight Operations Division
NASA Manned Spacecraft Center

Introduction

A number of papers have been given previously, both to the IAS and other scientific organizations, which deal with the operational planning for Project Mercury[1,2]. This paper deals with the operational experience gained from the development of facilities to perform real-time flight control and the experience gained from using these facilities. The discussion of this experience is primarily limited to the Mercury-Atlas orbital flights leading up to and including the flight of Astronaut John H. Glenn, Jr. In addition, the over-all recovery operation is discussed.

Network Stations

The orbital track flown in the three-orbit Mercury flight and the location of the network tracking stations established around the world to maintain contact with the spacecraft are presented in figure 1. This orbit and the supporting network were chosen for a number of reasons but primarily on the basis of the following:

(1) The desire to use the tracking facilities already available in the southern United States and the instrumentation on the Atlantic Missile Range

(2) The desire to obtain continuous tracking and voice contact with the astronaut throughout the powered flight and the insertion into orbit and during the reentry and landing phases

(3) The belief that radar tracking data should be available from a number of strategic locations around the world to establish the orbit properly

(4) The desire to maintain voice contact with the astronaut as often as possible during the early phases of the flight and on the order of every 15 to 20 minutes thereafter

(5) The need to remain within the temperate zones of the earth so that the design requirements on the spacecraft and the dangers of cold weather to the astronaut after landing could be reduced

All of these sites had voice and telemetry capabilities with the spacecraft. A large number of the sites had either C- or S-band radar tracking capability with teletype data facilities back to the Central Computing Center at Washington, D. C. The sites at Cape Canaveral; Bermuda; Muchea, Australia; Hawaii; Guaymas, Mexico; and California had facilities for radio command to the spacecraft. Teletype to and from the Control Center at Cape Canaveral was available to all the sites, and the capability of voice was provided from Hawaii through Bermuda and to the two sites in Australia. In addition, during John Glenn's flight, voice was provided to the Canary Islands and by single-sideband radio to the ships in the Indian Ocean and off the west coast of Africa.

The Communications and Computing Center is located at the NASA Goddard Space Flight Center, Greenbelt, Md., and high-speed data lines and voice and teletype lines were provided from this center to the Mercury Control Center at Cape Canaveral. All of these facilities were provided with the background of previous flight-test experience and on the basis of the safest operational concepts so that the safe recovery of the astronaut could be assured and to provide sufficient capability for controlling both unmanned and manned orbital flights. A great deal of experience has now been obtained from operating this complex network and should prove beneficial to future space-flight programs.

Based on the knowledge gained from the three Mercury-Atlas orbital flights flown to date, the following conclusions can be drawn:

The facilities provided by this network are, in most cases, more than adequate to provide both orbital information and data for performing flight control for unmanned and manned flights. Experience has shown that with the tracking and computing complex at Cape Canaveral and Washington, D. C., the orbital elements can be determined within a very few seconds after launch-vehicle cutoff with sufficient precision to assure control of the space vehicle should some abort condition present itself. Additional tracking obtained during the first half of the first orbit refines these computations to some extent and, together with the cutoff conditions, provides extremely accurate spacecraft positions for at least a three-orbit mission.

The computer program provided essentially real-time spacecraft position and, although complex, it has shown the capability of handling almost any trajectory problem which could exist. The radar tracking system has shown that low-altitude orbits can be acquired and tracked with a high degree of accuracy provided proper acquisition data and systems are available.

In all cases, horizon-to-horizon coverage on UHF, which provided excellent telemetry and voice contact with the spacecraft, was possible. The use of HF extended the contact times by about 2 minutes at each site and is considered an important adjunct to the spacecraft communications system. The command capabilities to the spacecraft proved to be adequate and useful and, of course, a necessity for unmanned operations. In this case, the coverage from a given site was more dependent upon antenna patterns than the other UHF systems, but with minor design changes horizon-to-horizon coverage is also believed to be possible with this system. As noted previously, either teletype or voice, or both, were available to all of the sites. However, experience has shown that voice facilities to all sites are highly desirable. The use of voice has proven to be very useful in providing real-time flight control, as evidenced by the rapid decisions required in the last two orbital flights. In conclusion, except for the voice requirements, the network facilities provided in

past flights appear to be in most cases more than adequate to support manned orbital flights.

In order to perform real-time flight control, the computing program and the computing complex provides the heart of this capability. Experience has shown that programs can be developed such that rapid decisions can be made within a few seconds of almost any foreseeable emergency situation. However, careful attention must be given to the data displays and the method in which these data are presented. The displays must be simple and the actual numbers of displays must be minimized. The point to be made here is that only the final decision-making processes should be displayed for human judgment, and that any processes involving arithmetic should be left for automatic computer decision. One of the most significant lessons to be gained from our experience is the need to bring the flight control personnel together with the computer programers and the computing complex. These engineers and mathematicians must work together intimately to provide proper flight control. Also, the development and checkout of the programs and displays require that all of these elements be together in one location on a continuous basis. It might be pointed out that the computers were used in Project Mercury for making only those computations associated with trajectory information. Future space programs will require computer programs and equipment to aid in making decisions regarding spacecraft systems performance and other tasks which may require rapid decision-making processes.

Flight Simulation

The most powerful tool developed in conjunction with the Mercury network was the capability of simulating all phases of the flight. The simulation provided training for both the astronaut and the flight control team in all aspects of the flight operation. In addition to training, the simulation facilities provided an excellent means of checking all of the network facilities and allowed development of operating procedures well in advance of an actual flight test. This flight simulation proved to be an important adjunct to the training of the maintenance and operating people at all of the sites in that it provided realistic problems in many phases of network operations.

The flight simulation was accomplished with the use of two facilities, both of which were provided with a Mercury spacecraft procedures trainer. One of these facilities utilized a complete simulation of a remote-site flight-control facility. The second and most beneficial facility was the one developed in conjunction with the Mercury Control Center. With this facility, not only could the astronaut and the procedures trainer be realistically tied in with the control center to simulate the powered phase of the flight, but a complete trajectory simulation was possible by using the actual launch and orbit computer programers. Also, by using taped procedures trainer outputs, each of the sites around the network was able to simulate in the proper sequence an entire three-orbit flight. A complete description of this system is not presented in this paper, but the importance of this equipment to the success of the mission cannot be too strongly emphasized. Although the flight-control procedures and ground rules were thoroughly thought out through paper studies, the simulation facilities provided the best means of proving and improving these procedures and rules. In fact, a great deal of the success of the Mercury flights can be directly attributed to these simulations.

As previously mentioned, mission rules for all phases of the operation beginning with the countdown and ending with recovery were established previous to each operation. The development of these rules and of the flight-control concepts began at the same time, which was a considerable length of time before any of the Mercury flight operations. The mission rules were established in an effort to provide for every conceivable situation which could occur onboard the spacecraft; that is, consideration of both the astronaut and the spacecraft systems and all of the conceivable ground equipment failures which could have a direct bearing on the flight operation. In addition, rules were established in an effort to handle a large number of launch-vehicle malfunctions. These rules of course, dealt primarily with the effects of a sudden cutoff condition and its effect on the spacecraft flight thereafter. As pointed out, these rules were established for the prelaunch, powered flight, and orbital flight phases of the mission.

Because of the complexity of the entire operation and the critical time element of powered flight, it was felt and borne out by flight experience that such a set of rules was an absolute necessity. Of course, it is impossible to think of everything that can happen; but if most of the contingencies have been anticipated, the rest of the time can be used to concentrate on the unexpected. Also, the simulated flights were an excellent test bed for all of these rules and many changes came about as a result of these tests. Furthermore, through simulations of the malfunctions covered by the mission rules, a much better understanding of all of the operating problems and spacecraft systems was achieved, and a number of problem areas was uncovered. Because of the many operating problems, the need for this type of operations analysis cannot be overemphasized. As a matter of fact, such a set of mission rules would be extremely useful to the conceptual design of any space flight program, and it would be beneficial to have these rules during the initial phases of the program as a set of design guidelines.

Flight Control

The organizational setup to perform control of the flight is presented in figure 2. This organization is limited to that group performing direct flight control from lift-off to landing. Within the Mercury Control Center the Operations Director was, of course, the over-all director of the entire flight operation with a Network Commander and a Recovery Commander supplying the necessary command-level support to the operation. The Flight Director had detailed flight-control responsibility for the flight following lift-off of the space vehicle. The organization used to perform the flight control activities is as shown by the block diagram. There was a Support Control Coordinator responsible for managing and operating the systems support to the Control Center. The Assistant Flight Directors, normally several people, provided necessary administrative and procedural support during both prelaunch

and the flight operation. The Network Status Monitor was responsible for the entire Mercury network during operating periods and for conducting the network countdown. The Launch-Vehicle Monitor was responsible for monitoring primarily the operation of the automatic abort system in the launch vehicle. In the bottom row of the diagram are the main flight-control elements who supported the Flight Director and actually performed the detailed control of the flight. The Flight Surgeon was responsible for all of the aeromedical aspects of the mission. The Environmental Control Monitor was responsible for the life-support system within the spacecraft. The Capsule Communicator maintained voice communications with the astronaut during the powered phase of the flight and when the spacecraft was over the Mercury Control Center. The Capsule Systems Monitor observed all of the spacecraft systems, such as, the reaction control system, attitude control system, and electrical control system. The Retrofire Controller was responsible for all of the times of retrofire associated with both the normal and aborted flights. The Flight Dynamics Officer had over-all control of the computing complex supporting the operation, monitored the various trajectory displays indicating launch-vehicle performance, and with the computer made the "go-no-go" decision at orbital insertion. All of these primary flight controllers had responsibility over their respective areas, not only during powered flight but during all of the orbital flight and reentry, and made recommendations to the Flight Director on their particular systems.

Figure 3 shows the organization of a typical remote site. The Capsule Communicator at the site acted as the Flight Director for a particular location and was responsible by voice and teletype to the Mercury Control Center. He was the engineer responsible for communicating with the astronaut and for making any decisions affecting the flight operation. He had a maintenance operations supervisor responsible for the detailed systems support at the site, a systems monitor who observed all of the major spacecraft systems, and, again, an aeromedical monitor responsible for the aeromedical aspects of the astronaut and the spacecraft.

Figures 4 and 5 present photographs of the Mercury Control Center and a typical remote site. The Mercury flight experience has shown that this size organization is about as big as can be coped with and still perform the flight control task. In the future, every effort must be made to automate as many of the systems outputs as possible so that only the final systems performance parameters are presented to the flight controllers and thereby limit the number of engineers required to analyze the flight performance.

Recovery Operations

The recovery operations for Project Mercury were, of course, one of the largest and more complex aspects of all of the operating plans required for the test. The following discussion is given as a description of the forces set up for the orbital flight of John Glenn. The recovery areas setup for this operation can be considered in two broad categories: Planned recovery areas in which the probability of landing was considered sufficiently high to require the positioning of location and retrieval units to assume recovery within a specific time; and contingency recovery areas in which the probability of landing was considered sufficiently low to require only the utilization of specialized search and rescue procedures.

The planned recovery areas were all located in the North Atlantic Ocean as shown in figure 6, and table I is a summary of the support positioned in these areas at launch time for the MA-6 flight.

Special recovery teams utilizing helicopters, amphibious vehicles, and salvage ships were located at the launch site to provide rapid access to the spacecraft for landings resulting from possible aborts during the late countdown and the early phase of powered flight. Winds at the launch site were measured and the locus of probable landing positions for various abort times were computed to facilitate positioning of these recovery forces.

Areas A to E supported all probable landings in the event an abort was necessitated at any time during powered flight. Area A would contain landings for abort velocities up to about 24,000 feet per second, and Areas B, C, D, and E would support higher abort velocities where programed use of the retrorockets become effective in localizing the landing area. Forces as shown in table I were positioned in these areas to provide for location and retrieval within a maximum of 3 hours in the areas of higher landing probability and 6 hours in the area where the probability of landing was somewhat lower.

Once the spacecraft was in orbital flight, Areas F, G, and H were available for landing at the end of the first, second, or third orbits, respectively. Forces as shown in table I were available to assure location and retrieval within a maximum of 3 hours for most probable landing situations.

Thus, to assure short-time recovery for all probable aborts that could occur during powered flight and for landings at the end of each of the three orbits, a total of 21 ships, 12 helicopters, and 16 search aircraft were on station in the deep-water landing areas at the time of the MA-6 launch. Backup search aircraft were available at several staging locations to assure maintaining the airborne aircraft listed in table I. These forces in the planned recovery areas were all linked by communications with the recovery control center located within the Mercury Control Center at Cape Canaveral.

Since it was recognized that certain low probability situations could lead to a spacecraft landing at essentially any point along the ground track over which the spacecraft flies, suitable recovery plans and support forces were provided to cover this unlikely contingency. In keeping with the low probabilities associated with remote landings, a minimum of support was planned for contingency recovery; however, a large force is required because of the extensive areas covered in three orbits around the earth. The location of contingency recovery units for the MA-6 flight is shown in figure 7. A typical unit consists basically of two search aircraft specially equipped for UHF/DF homing on spacecraft beacons, point-to-point and ground-to-air communications, and pararescue personnel equipped to provide on-scene assistance on both land and water. No retrieval forces were deployed in support of contingency landings;

however, procedures were available for retrieval support after the fact. These search and rescue units were stationed at the 16 locations shown in figure 7 and were all linked by communications with the recovery control center at Cape Canaveral. Throughout the MA-6 flight, the astronaut was continually provided with retrofiring times for landing in favorable contingency recovery areas. However, the contingency forces deployed had the capability of flying to any point along the orbital track if required.

Weather

As the whole world now knows, one of the most difficult operating problems encountered was the weather. Early in the project the NASA solicited the aid of the U.S. Weather Bureau in setting up an organization to supply pertinent weather information. This group developed means for obtaining fairly detailed weather data along the entire three-orbit track of the Mercury mission. This information was analyzed in many different ways to provide useful operational information. For instance, detailed analysis of the weather over the Atlantic Ocean for various periods of the year was made to provide a basis of planning the flight and to provide a background knowledge as to what could be expected to develop from day to day once a given weather pattern had been determined. As a guideline, weather ground rules were established on the basis of spacecraft structural limitations and recovery operating capabilities. These included such details as wind velocity, wave height, cloud cover, and visibility. During the days previous to and on the day of the operation, the U.S. Weather Bureau meteorologists provided weather information for all of the preselected recovery areas and the launching site. The other weather limitation was the result of the desire to obtain engineering photographic coverage in the launch area.

Flight Control and Recovery Operations for MA-6

In order to illustrate how the over-all operation is conducted, the MA-6 flight of John Glenn and the flight control and recovery operations utilized will be described starting with the initial countdown and ending with the final recovery operation.

The countdown for launching the Mercury-Atlas vehicle is conducted in two parts. The first part is conducted on the day before the launch and lasts approximately 4 hours. During this period detailed tests of all of the spacecraft systems are performed and those interface connections important to these systems are verified. This part of the countdown was conducted with no major problems or holds resulting. Approximately 17 1/2 hours separated the end of this count and the beginning of the final countdown, and during this period the spacecraft pyrotechnics were installed and connected and certain expendables such as fuel and oxygen were loaded.

At T-390 minutes the countdown was resumed and progressed without any unusual instance until T-120 minutes. During this period additional spacecraft systems checkouts were performed and the major portion of the launch vehicle countdown was begun. At T-120 minutes a built-in hold of 90 minutes had been scheduled to assure that all systems had been given sufficient time for checkout before astronaut insertion. During this period a problem developed with the guidance system rate beacon in the launch vehicle causing an additional 45 minute hold, and an additional 10 minutes was required to repair a broken microphone bracket in the astronaut's helmet after the astronaut insertion procedure had been started. The countdown proceeded to T-60 minutes when a 40 minute hold was required to replace a broken bolt because of misalinement on the spacecraft's hatch attachment. At T-45 minutes, a 15 minute hold was required to add fuel to the launch vehicle; and at T-22 minutes an additional 25 minutes was required for filling the liquid-oxygen tanks as a result of a minor malfunction in the ground support equipment used to pump liquid oxygen into the launch vehicle. At T-6 minutes and 30 seconds, a 2 minute hold was required to make a quick check of the network computer at Bermuda. In general, the countdown was very smooth and extremely well executed. A feeling of confidence was noted in all concerned, including the astronaut, and it is probably more than significant that this feeling has existed on the last three Mercury-Atlas launches.

The launch occurred at 9:47:39 a.m. e.s.t. on February 20, 1962. The powered portion of the flight which lasted 5 minutes and 1 second was completely normal and the astronaut was able to make all of the planned communications and observations throughout this period. Throughout this portion of the flight no abnormalities were noted in either the spacecraft systems or in the astronaut's physical condition. The launch-vehicle guidance system performed almost perfectly, and 10 seconds after cutoff the computer gave a "go" recommendation. The cutoff conditions obtained were excellent.

Table II presents the actual cutoff conditions that were obtained. The altitude achieved was 528,381 feet and the spacecraft velocity achieved was 25,730 feet per second. The other significant quantity, flight-path angle, was -0.047° at cutoff. The other quantities shown in the table give more information on the flight parameters. These values include a perigee of 86.92 nautical miles, an apogee of 140.92 nautical miles, an orbit period of 88 minutes and 29 seconds, and an inclination angle of 32.54°. Also shown are the maximum accelerations achieved during exit from and entry into the earth's atmosphere, both of these values being 7.7g. All of these values were within the expected tolerances for the launch vehicle and its guidance system. The Mercury network computing system performed flawlessly throughout both the powered and orbital phases of the flight and provided complete information on the orbit, spacecraft position, and retrofire times necessary for all of the recovery areas. A comparison of the planned and actual times at which the major events occurred are given in table III and the times at which all of the network sites acquired and lost contact with the spacecraft are presented in table IV.

The flight test experience which had been achieved on the previous Mercury-Atlas orbital flights, that is, the MA-4 and MA-5, had given the flight control team an excellent opportunity to exercise control over the mission. These flights

were, of course, much more difficult to control and complete successfully because of the lack of an astronaut within the spacecraft. All of the analyses and decisions had to be made on the basis of telemetered information from the spacecraft. The presence of an astronaut made the flight test much more simple to complete, primarily on the basis of astronaut observations and his capability of systems management. A manned flight, however, makes the job of monitoring spacecraft performance more complex because of the large number of backup and alternate systems from which the astronaut could choose.

After separation of the spacecraft from the launch vehicle, the astronaut was given all the pertinent data involved with orbit parameters and the retrofire times necessary had immediate reentry been required. Following these transmissions, which were primarily from the Bermuda site, the astronaut made the planned checks of all of the spacecraft control modes using both the automatic and manual proportional systems. These checks indicated that all of the control systems were operating satisfactorily. Also, the astronaut reported that he felt no ill effects as a result of going from high accelerations to weightlessness, that he felt he was in excellent condition, and, as the two previous astronauts had commented, that he was greatly impressed with the view from this altitude.

The first orbit went exactly as planned and both the astronaut and the spacecraft performed perfectly. Over the Canary Islands' site, the astronaut's air-to-ground transmissions were patched to the voice network and in turn to the Mercury Control Center and provided the control center and all other voice sites the capability of monitoring the transmissions to and from the spacecraft in real-time. This condition existed throughout all three orbits from all sites having voice to the control center and provided the best tool for maintaining surveillance of the flight.

Except for the control systems checks which were made periodically, the astronaut remained on the automatic system with brief periods on the fly-by-wire system which utilizes the automatic control jets. This procedure was as planned so that a fixed attitude would be provided for radar tracking and so that the astronaut could make the necessary reports and observations during the first orbit. During the first orbit, it was obvious from the astronaut's reports that he could establish the pitch and yaw attitude of the spacecraft with precision by using the horizon on both the light and dark sides of the earth, and that he could also achieve a reasonable yaw reference. Aside from the xylose tablet taken over Kano, he had his first and only food (a tube of applesauce) over Canton Island during this orbit and reported no problems with eating nor any noticeable discomforts following the intake of this food.

During the first orbit, the network radar systems were able to obtain excellent tracking data and these data, together with the data obtained at cutoff, provided very accurate information on the spacecraft position and orbit. As an example, between the time the spacecraft was inserted into orbit and the data were received from the Australian sites, the retrosequence times changed a total of only 7 seconds for retrofire at the end of 3 orbits. This indicated the accuracy of the orbit parameters. From this point to the end of the 3-orbit flight, using all of the available radar data, these times changed only 2 seconds. The final retrosequence time was 04:32:38 as compared with the time initially computed at cutoff of 04:32:47 and the time initially set into the clock on the ground before lift-off of 04:32:28. All of the network sites received data from the spacecraft and maintained communications with the astronaut from horizon to horizon, and everything progressed in a completely normal fashion. Because of the excellent condition of the astronaut and the spacecraft, there was no question about continuing into the second orbit, and a "go" decision was made among personnel at Guaymas, Mexico, and the Mercury Control Center and "foremost" the astronaut himself.

Shortly after the time that the "go" decision was made at Guaymas, the spacecraft began to drift in right yaw. After allowing the spacecraft to go through several cycles of drifting in yaw attitude and then being returned by the high thrust jets, the astronaut reported that he had no 1-pound jet action in left yaw. With an astronaut aboard the spacecraft, this malfunction was considered a minor problem, especially since he still had control over the spacecraft with a number of other available control systems. It should be pointed out, however, that without an astronaut aboard the spacecraft, this problem would have been very serious in that excessive amounts of fuel would have been used; and it may have been necessary to reenter the spacecraft in some contingency recovery area because of this high fuel-usage rate. From this point on the astronaut controlled the spacecraft attitude manually except for periodic checks of the automatic control system.

During the pass over the control center on the second orbit, it was noticed that the telemetry channel used to indicate that the landing bag was deployed was showing a read-out which, if true, indicated that the landing-bag deployment mechanism had been actuated. However, because there was no indication to the astronaut and he had not reported hearing any unusual noises or noticing any motions of the heat shield, it was felt that this signal, although a proper telemetry output, was false and probably had resulted from the failure of the sensing switch. Of course, this event caused a great deal of analysis to result and later required the most important decision of the mission to be made.

The flight continued with no further serious problems and the astronaut performed the planned 180° yaw maneuver over Africa to observe the earth and horizon while traveling in this direction and to determine his ability to control. Following this maneuver, the astronaut began to have what appeared to be trouble with the gyro reference system, that is, the attitudes as indicated by the spacecraft's instruments did not agree with the visual reference of the astronaut. However, the astronaut reported he had no trouble in maintaining the proper attitude of the spacecraft when he desired to do so by using the visual reference. Because of the problems with the automatic control system, previously mentioned, and the apparent gyro reference problem, the astronaut was forced to deviate from the flight plan to some extent, but he was able to continue all of the necessary control systems tasks and checks and to make a number of other prescribed tests which

allowed both the astronaut and the ground to evaluate his performance and the performance of the spacecraft systems. As observed by the ground and the astronaut, the horizon scanners appeared to deteriorate when on the dark side of the earth; but when the spacecraft again came into daylight, the reference system appeared to improve. However, analyses of the data subsequent to the flight proved that the horizon scanner system was functioning properly but the changes in spacecraft attitudes that resulted from the maneuvers performed by the astronaut caused the erroneous outputs which he noticed on the attitude instruments. It has been known that spurious attitude outputs would result if the gyro reference system were allowed to remain in effect during large deviations from the normal orbit attitude of 0° yaw, 0° roll, and -34° pitch, and this was apparently the case during the 180° yaw maneuver which was conducted over Africa. This condition will be alleviated in future flights by allowing the astronaut to disconnect the horizon scanner slaving system and the programed precession of the gyros which preserves the local horizon while he is maintaining attitudes other than the normal spacecraft orbit attitude.

As the "go-no-go" point at the end of the second and beginning of the third orbit approached, it was determined that although some spacecraft malfunctions had occurred, the astronaut continued to be in excellent condition and had complete control of the spacecraft. He was told by the Hawaiian site that the Mercury Control Center had made the decision to continue into the third orbit. The astronaut concurred, and the decision was made to complete the three-orbit mission.

One other problem which caused some minor concern was the increase in inverter temperatures to values somewhat above those desired. It appeared, and the flight test results confirmed, that the cooling system for these inverters was not functioning. However, recent tests made previous to the flight had shown that the inverters could withstand these and higher operating temperatures. The results of these tests caused the flight control people to minimize this problem, and it was decided that this minor malfunction was not of sufficient magnitude to terminate the flight after the second orbit. Furthermore, a backup inverter was still available for use had one of the main inverters failed during the third orbit.

During the third orbit, the apparent problems with the gyro reference system continued and the automatic stabilization and control system (ASCS) malfunctions in the yaw axis were still evident. However, these problems were not major and both the ground and the astronaut considered that the entire situation was well under control. This was primarily because of the excellent condition of the astronaut and his ability to use visual references on both the dark and light sides of the earth, and the fact that most of the control systems were still performing perfectly. The one problem which remained outstanding and unresolved was the determination of whether the heat-shield deployment mechanism had been actuated or whether the telemetry signal was false due to a sensing switch failure. During the pass over Hawaii on the third orbit, the astronaut was asked to perform some additional checks on the landing-bag deployment system. Although the test results were negative and further indicated that the signal was false, they were not conclusive. There were still other possible malfunctions and the decision was made at the control center that the safest path to take was to leave the retropackage on following retrofire. This decision was made on the basis that the retropackage straps attached to the spacecraft and the spacecraft heat shield would maintain the heat shield in the closed position until sufficient aerodynamic force was exerted to keep the shield on the spacecraft. In addition, based on studies made in the past, it was felt that the retention of the package would not cause any serious damage to the heat shield or the spacecraft during the reentry and would burn off during the reentry heat pulse.

Also over the Hawaiian site, the astronaut went over his retrosequence checklist and prepared for the retrofire maneuver. It was agreed that the flight plan would be followed and that the retrofire maneuver would take place using the automatic control system, with the astronaut prepared to take over manually should a malfunction occur. Additional time checks were also made over Hawaii to make sure that the retrofire clock was properly set and synchronized to provide retrofire at the proper moment. The astronaut himself continued to be in excellent condition and showed complete confidence in his ability to control any situation which might develop.

The retrofire maneuver took place at precisely the right time over the California site and, as a precautionary measure, the astronaut performed manual control along with the automatic control during this maneuver. The attitudes during retrofire were held within about 3° of the nominal attitudes as a result of this procedure, but large amounts of fuel were expended. Following this maneuver, the astronaut was instructed to retain the retropackage during reentry and was notified that he would have to retract the periscope manually and initiate the return to reentry attitude and the planned roll rate because of this interruption to the normal spacecraft sequence of events.

Following the firing of the retrorockets and with subsequent radar track, the real-time computers gave a predicted landing point. The predictions were within a small distance of where the spacecraft and astronaut were finally retrieved. As far as the ground was concerned, the reentry into the earth's atmosphere was entirely normal. The ionization blackout occurred within a few seconds of the expected time and although voice communications with the astronaut were lost for approximately 4 minutes and 20 seconds, the C-band radar units continued to track throughout this period and provided some confidence that all was well throughout the high heating period. As it might be expected, voice communications received from the astronaut following the ionization blackout period resulted in a great sigh of relief within the Mercury Control Center. The astronaut continued to report that he was in excellent condition after this time, and the reentry sequence from this point on was entirely normal.

A number of spacecraft control problems were experienced following peak reentry acceleration, primarily because of the method of control used during this period. In addition, large amounts of fuel from both the manual and automatic systems had been used and finally resulted in fuel depletion of

both systems just previous to the time that the drogue chute was deployed. The results of these flight tests have indicated that somewhat different control procedures be used during this period for the next flight.

The communications with the astronaut during the latter stages of descent on both the drogue and main parachutes were excellent and allowed communications with either the astronaut or the recovery forces throughout this entire descent phase and the recovery operations which took place following the landing. The landing occurred at 2:43 p.m. e.s.t. after 4 hours, 55 minutes, and 23 seconds of flight.

Recovery forces in all areas were notified of mission progress by the recovery control center. Based on mission progress, units located at the end of the third orbit knew they were to become involved, and figure 8 presents recovery details in the MA-6 landing area. An aircraft carrier with retrieval helicopters was located in the center of the planned landing area, one destroyer was located about 40 nautical miles downrange, and a second destroyer was located about 40 nautical miles uprange. Telemetry and search aircraft were airborne in the areas as shown. After the retrorocket maneuver and about 15 minutes prior to the estimated time of landing, the recovery control center notified the recovery forces that according to calculations, the landing was predicted to occur near the uprange destroyer as shown in figure 8. The astronaut was also provided with this information by the Mercury Control Center as soon as communications were reestablished after the spacecraft emerged from the ionization blackout. Lookouts aboard the USS Noa, the destroyer in the uprange position, sighted the main parachute of the spacecraft as it descended below a broken cloud layer at an altitude of about 5,000 feet from a range of approximately 5 nautical miles. Communications were established between the spacecraft and the destroyer, and a continuous flow of information was passed throughout the remainder of the recovery operation.

In this case, location was very straightforward in that a retrieval ship gained visual contact during spacecraft landing. However, as a matter of interest for future operations since visual sightings are probably the exception rather than the rule, other spacecraft location information available soon after landing is also plotted in figure 8. The SOFAR fix was approximately 4 nautical miles from the landing point, and the first two HF/DF fixes were within approximately 25 miles of the actual spacecraft position. This landing information, along with the calculated landing position provided by the Mercury network, would have assured bringing search aircraft within UHF/DF range. In fact, the airborne search aircraft in the landing areas obtained UHF/DF contact with the spacecraft shortly after beacon activation at main parachute opening; however, it was the Noa's day and she was on her way to retrieve.

The Noa had the spacecraft aboard 20 minutes after landing. Figure 9 shows the spacecraft as it is being lowered to the deck. Astronaut Glenn remained in the spacecraft during pickup; and after it was positioned on the ship's deck, he egressed from the spacecraft through the side hatch. Original plans had called for egress through the top at this time; however, the astronaut was becoming uncomfortably warm and decided to leave by the easier egress path.

In making the pickup, the Noa maneuvered alongside the spacecraft and engaged a hook into the spacecraft lifting loop. The hook is rigged on the end of a detachable pole to facilitate this engagement and the lifting line is rigged over one of the ship's regular boat davits as shown in figure 9. A deck winch is used for inhauling the lifting line, and when the spacecraft is properly positioned vertically, the davit is rotated inboard to position the spacecraft on deck. A brace attached to the davit is lowered over the top of the spacecraft to prevent swinging once the spacecraft is clear of the water.

Each ship in the recovery force had embarked a special medical team consisting of two doctors and one technician to provide medical care and/or initial postflight medical debriefing. For the MA-6 mission, postflight medical debriefing was the only requirement and was completed onboard the Noa in about 2 hours after pickup. The astronaut was then transferred to the aircraft carrier for further transfer to Grand Turk Island, and he arrived there approximately 5 hours after landing. Additional engineering and medical debriefings were conducted at Grand Turk.

References

1. Kraft, Christopher C., Jr.: Some Operational Aspects of Project Mercury. Presented at the Annual Meeting of Soc. of Experimental Test Pilots, Los Angeles, Calif., Oct. 9, 1959.

2. Mathews, Charles W.: Review of the Operational Plans for Mercury Orbital Mission. Presented at the Twenty-Eighth Annual Meeting of the Inst. of Aero. Sci., New York, N. Y., Jan. 25, 1960.

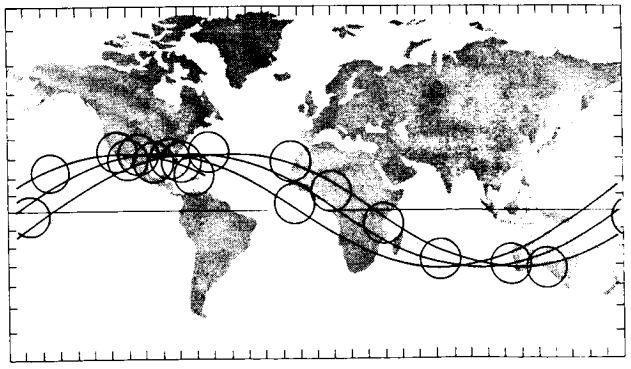

Figure 1.- Network station distribution.

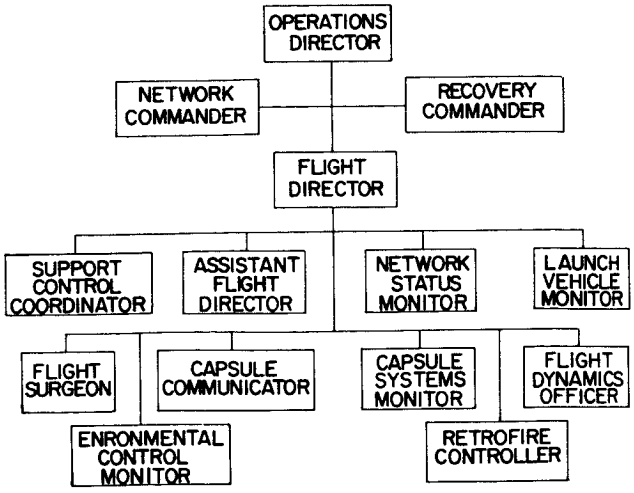

Figure 2.- Mercury Control Center organization.

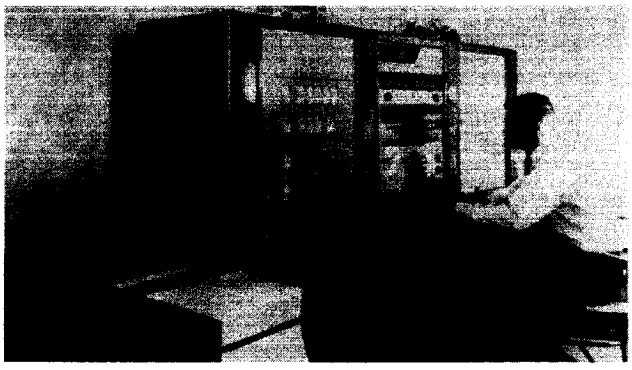

Figure 5.- Photograph of a typical remote site.

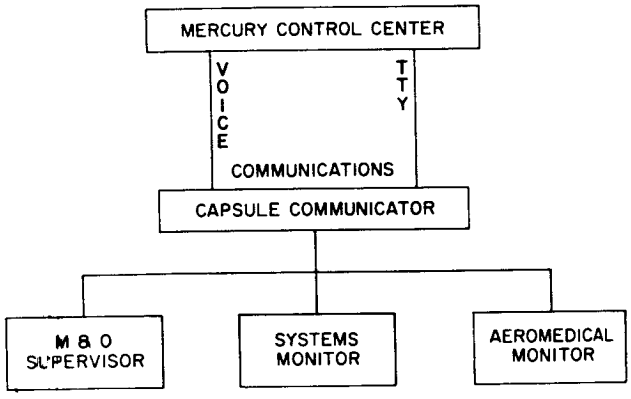

Figure 3.- Remote site organization.

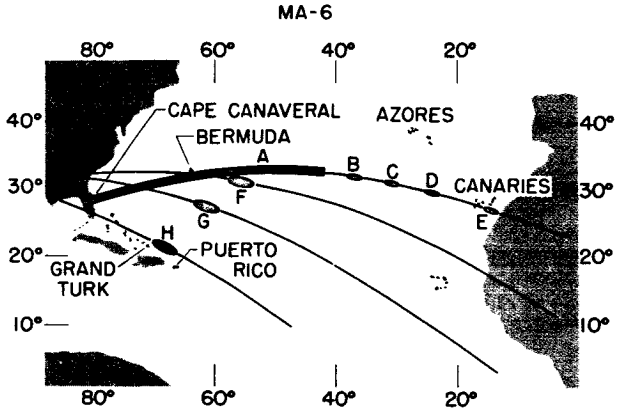

Figure 6.- Planned recovery areas.

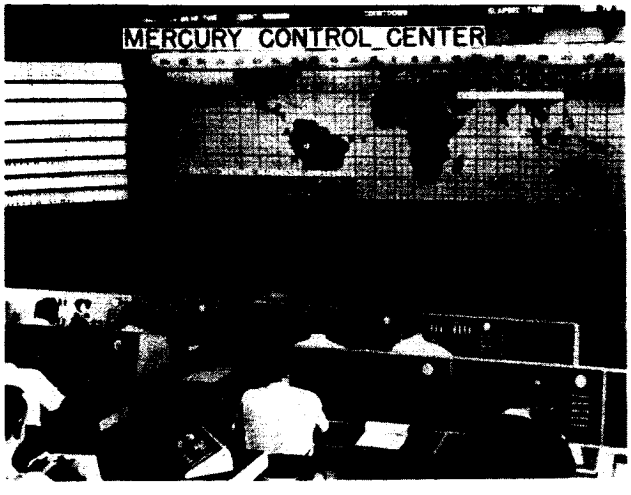

Figure 4.- Photograph of the Mercury Control Center.

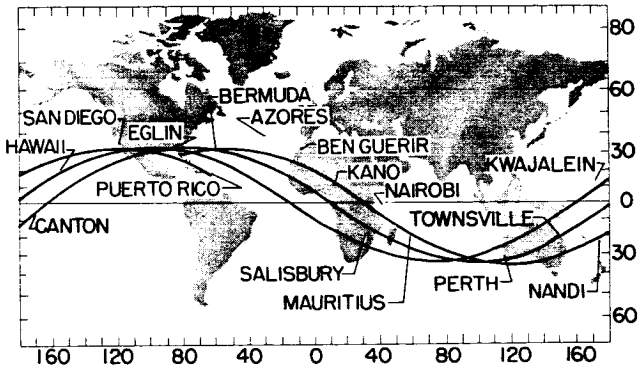

Figure 7.- MA-6 staging locations for contingency recovery.

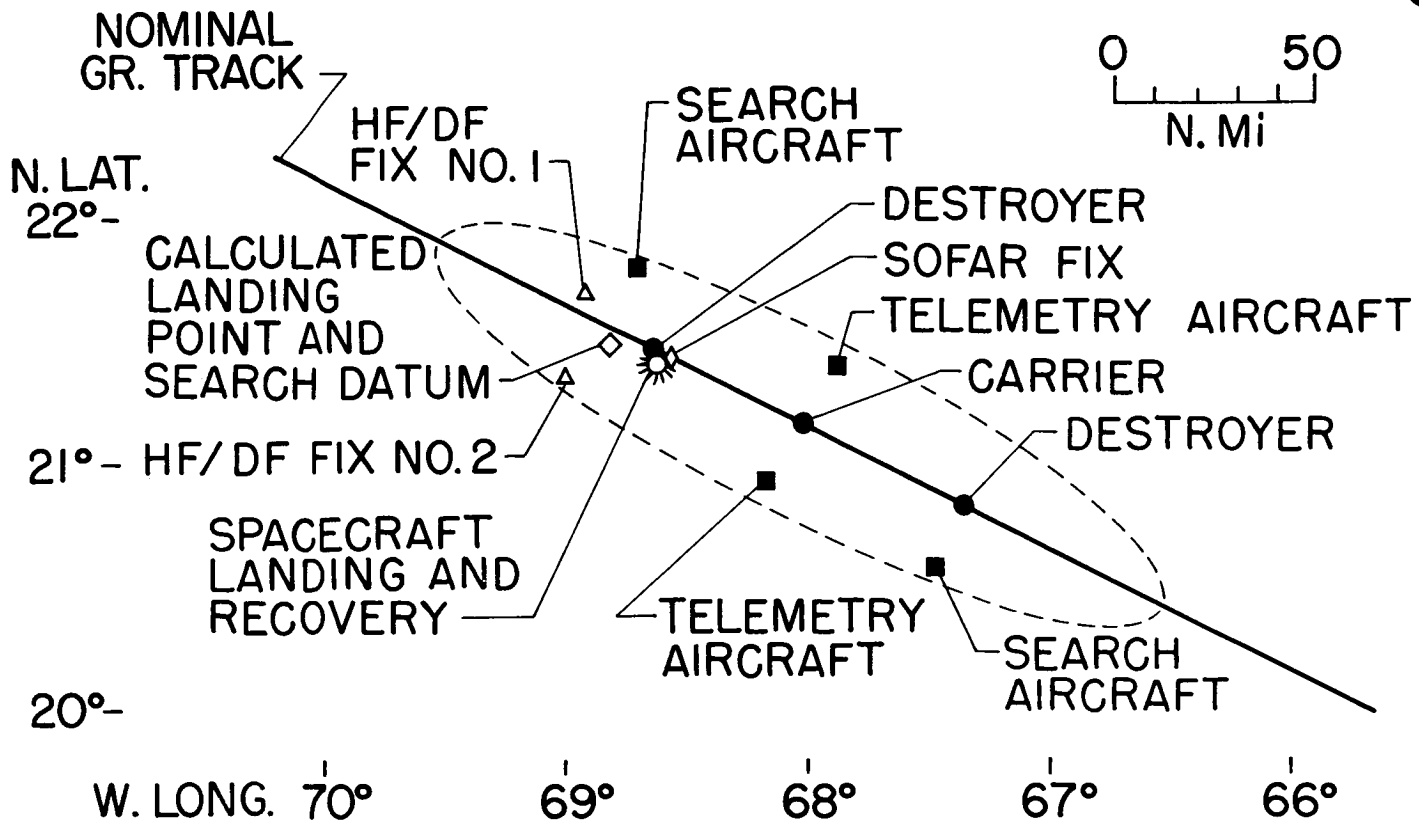

Figure 8.- MA-6 Landing area.

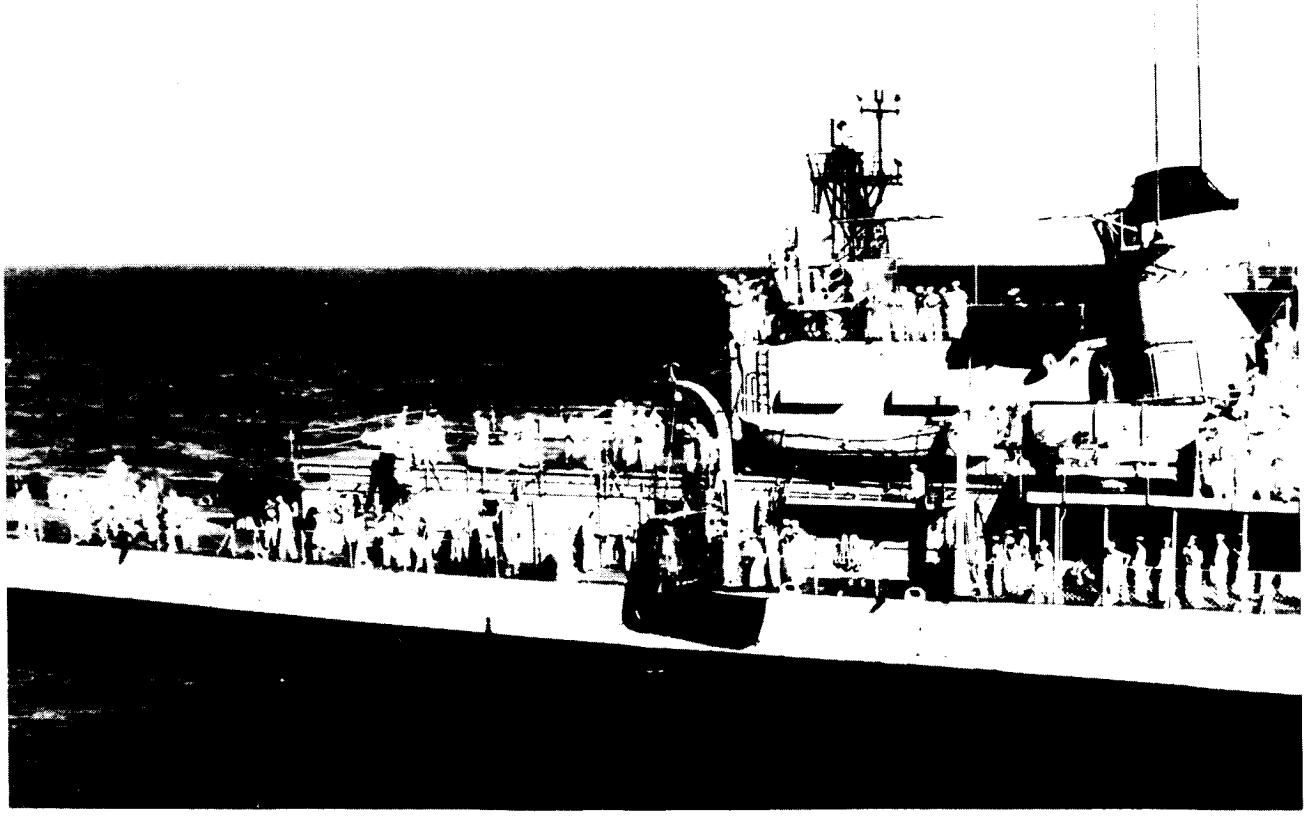

Figure 9.- MA-6 retrieval by destroyer Noa.

TABLE I. - MA-6 RECOVERY FORCES FOR THE PLANNED RECOVERY AREAS

Area	Number of search aircraft	Number of helicopters	Number of ships	Maximum recovery time, hr
Launch site	---	3	---	short
A	6	---	8 destroyers	3 to 6
B,C,D,E	1 each	---	1 destroyer each	3 to 6
F,G,H	2 each	3 each.	1 carrier each 2 destroyers each	3
Total	16	12	21	---

TABLE II. - FLIGHT CONDITIONS

Cutoff conditions:	
Altitude, ft	528,381
Velocity, ft/sec	25,730
Flight-path angle, deg	-0.047
Orbit parameters:	
Perigee altitude, nautical miles	86.92
Apogee altitude, nautical miles	140.92
Period, min:sec	88:29
Inclination angle, deg	32.54
Maximum conditions:	
Exit acceleration, g units	7.7
Exit dynamic pressure, lb/sq ft	982
Entry acceleration, g units	7.7
Entry dynamic pressure, lb/sq ft	472

TABLE III.- SEQUENCE OF EVENTS DURING MA-6 FLIGHT

Event	Planned Time[a], hr:min:sec	Actual Time, hr:min:sec
Booster-engine cutoff	00:02:11.4	00:02:09.6
Tower release	00:02:34.2	00.02:33.3
Escape rocket firing	00:02:34.2	00:02:33.4
Sustainer-engine cutoff (SECO)		00:05:01.4
Tail-off complete	00:05:03.8	00:05:02
Spacecraft separation	00:05:03.8	00:05:03.6
Retrofire initiation	04:32:58	04:33:08
Retro (left) No. 1	04:32:58	04:33:08
Retro (bottom) No. 2	04:33:03	04:33:13
Retro (right) No. 3	04:33:08	04:33:18
Retro assembly jettison	04:33:58	(b)
0.05g relay	04:43:53	[c]04:43:31
Drogue parachute deployment	04:50:00	04:49:17.2
Main parachute deployment	04:50:36	04:50:11
Main parachute jettison (water impact)	04:55:22	04:55:23

[a]Preflight calculated, based on nominal Atlas performance.

[b]Retro assembly kept on during reentry.

[c]The 0.05g relay was actuated manually by astronaut when he was in a "small g field."

TABLE IV.- NETWORK ACQUISITION TIMES FOR MA-6 FLIGHT

Station	Telemetry Signal		Voice Reception	
	Acquisition, hr:min:sec	Loss, hr:min:sec	Frequency	Duration, hr:min:sec
Canaveral	00:00:00	00:06:20	UHF	00:00:00 to 00:05:30
Bermuda	00:03:02	00:10:26	UHF	00:03:30 to 00:09:30
			HF	00:11:00 to few sec
Canary Islands	00:14:15	00:21:23	UHF	00:15:00 to 00:23:00
			HF	00:12:00 to 00:14:00
Atlantic Ship	Not in range			
Kano	00:21:13	00:28:21	UHF	00:22:00 to 00:29:00
Zanzibar	00:29:51	00:37:51	UHF	00:29:00 to 00:38:00
Indian Ocean Ship	00:40:02	00:48:31	UHF	00:41:00 to 00:48:00
Muchea	00:49:21	00:57:55	UHF	00:50:00 to 00:58:30
Woomera	00:54:00	01:02:41	UHF	00:56:00 to 01:03:00
Canton	01:09:19	01:17:42	UHF	01:09:00 to 01:15:30
			HF	01:03:30 to 01:04:00
Hawaii	Not in range			
California	01:26:41	01:31:23	UHF	01:27:30 to 01:30:00
			HF	01:19:00 to 01:25:30
Guaymas	01:26:47	01:33:25	UHF	01:26:00 to 01:33:30
			HF	01:20:30 to 01:26:00
Texas	01:29:24	01:36:18	UHF	01:28:30 to 01:36:30
Eglin	01:32:00	01:37:05		
Canaveral	01:33:20	01:40:03	UHF	01:33:30 to 01:40:00
Bermuda	01:36:38	01:43:53	UHF	01:37:30 to 01:42:00
Canary Islands	01:47:55	01:53:58	UHF	01:48:00 to 01:55:30
Atlantic Ship	01:51:54	01:58:31	UHF	01:53:00 to 01:58:00
Kano	01:54:47	02:01:21	UHF	01:55:00 to 02:01:00
Zanzibar	02:04:05	02:10:51	UHF	02:04:00 to 02:11:00
Indian Ocean Ship	02:12:17	02:22:09	UHF	02:13:00 to 02:22:00
Muchea	02:22:51	02:31:23	UHF	02:25:00 to 02:32:30
			HF	02:23:30 to 02:24:30
Woomera	02:27:36	02:35:45	UHF	02:28:00 to 02:37:00
Canton	02:42:51	02:49:45	UHF	02:42:30 to 02:49:00
Hawaii	02:49:01	02:55:19	UHF	02:49:00 to 02:55:30
California	02:58:11	03:04:48	UHF	02:58:30 to 03:04:30
Guaymas	02:59:59	03:06:44	UHF	03:00:30 to 03:06:30
Texas	03:03:14	03:09:39	UHF	03:03:30 to 03:10:30
Eglin	03:05:35	03:12:07	UHF	03:07:30 to 03:12:30
Canaveral	03:06:51	03:13:46	UHF	03:07:00 to 03:14:00
Bermuda	03:09:56	03:17:03	UHF	03:09:00 to 03:16:30
			HF	03:16:30 to 03:18:00
Canary Islands	Not in range		HF	03:20:00 to 03:25:00
Atlantic Ship	03:24:44	03:32:25	UHF	03:26:30 to 03:30:00
			HF	03:25:00 to 03:26:30
			HF	03:30:30 to 03:32:30
Kano	Not in range			
Zanzibar	Not in range		HF	03:30:00 to 03:32:30
			HF	03:40:00 to 03:41:30
			HF	03:44:00 to 03:44:30
Indian Ocean Ship	03:46:55	03:56:49	HF	03:47:00 to 03:55:00
Muchea	03:56:31	04:04:12	UHF	03:58:30 to 04:04:00
			HF	03:57:00 to 03:58:00
Woomera	04:03:16	04:06:19	UHF	04:03:00 to 04:07:00
Canton	Not in range		HF	04:15:30 to 04:21:00
Hawaii	04:21:49	04:28:49	UHF	04:20:30 to 04:30:30
California	04:31:17	04:37:57	UHF	04:31:30 to 04:38:30
Guaymas	04:33:44	04:39:49	UHF	04:33:30 to 04:40:30
Texas	04:36:53	04:42:32	UHF	04:38:00 to 04:39:30
Eglin	04:39:00	04:42:52	UHF	04:39:00 to 04:43:30
Canaveral (Canton)	04:40:52	04:42:55	UHF	04:40:30 to 04:43:30

N62-14471

LIFE SCIENCES ACTIVITIES ASSOCIATED WITH PROJECT MERCURY

Stanley C. White, M.D.
Chief, Life Systems Division
NASA Manned Spacecraft Center

C. Patrick Laughlin, M.D.
Assistant Resident in Internal Medicine
University Hospitals of Cleveland, Cleveland, Ohio
(Formerly with NASA Manned Spacecraft Center)

Introduction

Fifteen years of speculation and study concerning the problems of placing man into space flight produced a mass of reports which contemplated the hurdles and suggested solutions needed to permit safe flight. The accumulation of problems occurred in all disciplines. This could have been expected because the area of study was in the unknown, and speculation and calculation were the only methods of attack until flight data could be obtained.

The Life Sciences community was as prolific in the identification of potential problem areas as the other scientific disciplines. The arrival of the era of manned space flight offers the opportunity to assess the problems directly and to define what is speculation and what is problem.

This paper will discuss two areas of life sciences activities during the Project Mercury program. The first area will review the life-support activities associated with the spacecraft development and the provisions for the astronaut. The second area will present a summarization of the data concerning man's ability to live and work in this new environment and will attempt to present an analysis of the significance of the findings in light of future flights.

Life-Support Activities on the Spacecraft

Early in the development program of Project Mercury, the decision which established the astronaut as a vital and functioning segment of the spacecraft systems and flight plan was made. This decision affected the entire life support effort more than any other single event. The required provisions within the spacecraft were able to be defined. All systems which had the astronaut as an integral link were designed and tested to provide a reliable astronaut in the system. The crew station was provisioned to complement the expected capabilities of the astronaut. A full display of cockpit instruments was incorporated. The concept of using a full cockpit of instruments was considered to be a better procedure than one which called for refitting the spacecraft after the capability of man was demonstrated. If flight experience demonstrated that instruments were not needed or could not be used dependably by the astronaut, they would be easily removed or inactivated. The associated controls to permit the astronaut to backup the systems manually or to select an alternate system were provided. Their orientation was such that the relationship of one to another allowed natural operation by the astronaut while he was restrained within his couch and harness. Additional study was made to assure normal function of the pilot while wearing the full pressure suit. Logical grouping of the instruments and their placement in the panel were determined through repeated operational flight simulations. These test simulations used the most up-to-date flight procedures to represent the data needed and astronaut action required during each phase of flight. Controls were moved when more positive availability for operation was shown to be needed. Sizing of the switches, spacing of one control from the other, color coding of the groups of instruments, and selection of the calibration on the face of the instruments were studied to permit efficient action by the astronaut while using the pressure suit in both uninflated and inflated states. Couch, suit, and crew station were treated as an integral problem. One or all were modified as necessary to provide a more efficient astronaut.

The design criteria for the life-support systems aboard the spacecraft provided a sea-level equivalent man, as far as function was concerned, under normal flight operations. The environmental system provided an atmosphere of 5 psia consisting of nearly 100 percent oxygen partial pressure. The proposal to use this atmosphere raised the question of man's tolerance to such an oxygen-rich atmosphere. Earlier studies had been made which demonstrated that oxygen toxicity would not produce difficulty for the durations of flight proposed in the Mercury program.[1] However, the problem of atelectasis associated with prolonged 100 percent oxygen exposure was found in early test programs. This problem was due to the lack of the normal atmospheric nitrogen within the small alveoli of the lung and was aggravated by the position of the astronaut in the couch and the compression of the chest associated with launch and entry acceleration. During the early studies on a centrifuge, the lung areas affected were visualized through chest X-rays and the methods of resolving this problem were studied. It was found that scheduled deep inhalations and periodic voluntary coughs were adequate for the prevention of alveolar collapse and would permit reinflation after collapse. This easy solution for the problem permitted the continued use of a 100 percent oxygen system. Therefore, the most simple and reliable closed environmental system could be used in the Mercury spacecraft.

The acceleration-protection system, through the development of the contoured couch and the extension of the astronaut's tolerance to the levels of the anticipated emergency accelerations, permitted the safe removal of the astronaut from a failing booster under all flight emergencies. The advances in the couch and tolerance data did more to make manned flight possible, during the early phases of the Mercury program, than any other area of work. Early studies had shown that emergency acceleration profiles would double the known acceleration tolerance levels. The contoured couch permitted manned centrifuge flights to reach acceleration of 21g.[2] Even though physiological changes were seen during the high levels of exposures, the

changes were reversible and no residual damage could be found. With this new level of demonstrated tolerance, man could accept all normal and emergency flight accelerations. The solution of this part of the problem left only the landing-impact forces to be studied. The impact tolerance of man was established through the data from the rapid deceleration tests performed by Colonel John P. Stapp. His final series of tests[3] gave the upper limits for injury with the ability for full recovery. The design of the crushable structure for use under the couch kept the emergency landing loads imposed upon the astronaut to within these tolerance levels. However, the anticipated rate of onset of the landing accelerations exceeded the known tolerance data. Programs were carried out to demonstrate that these rates of onset were acceptable for water landings.[4] The required provisions for land landings dictated the need for the addition of the impact skirt in order that the multidirectional lateral loads could be kept within the known data limits. The test programs and measured landing loads from flight vehicles have been assessed by Mr. Peter Armitage at the Manned Spacecraft Center and the results have demonstrated that the acceleration protection system is safe for water and land.

The prime requirement established for the biomedical data-gathering system was the provision of instruments for the assessment of the astronaut status as part of the flight safety program. After this requirement had been met, the remainder of data collection was directed toward answering the many biomedical questions which had been raised concerning man in the new environment. The data indicating the adequacy of the operation of the environmental system were invaluable because it complemented the information gathered from the astronaut directly. The correlation of system information and information provided by the man was possible through the provision of a normal sea-level functioning man. The data collected plus the astronaut's voice reports have given an excellent profile of the astronaut's status throughout the flights. The clear, concise, and accurate reports have confirmed that man and his spacecraft did well while operating in the new environment.

The astronauts assigned the responsibility for surveillance of the life-support areas were valuable in providing the technical and operational transition needed to assure that the systems were adequate for flight. Their experience in aircraft was made available to the bioscientist and engineers working on the life systems area. They frequently participated in the testing of equipment and offered guidance on further improvements. As the specific astronaut was chosen for a flight, the relationship on the flight readiness of the life-support system became more personalized and minor changes were incorporated in the equipment which would aid the accomplishment of the flight plan. Postflight critiques of the life-support systems were made, and new changes such as the addition of wrist bearings and the fingertip lights on the gloves of the full pressure suit were incorporated after the astronaut had recommended their incorporation. New ideas and the prototype units were discussed and demonstrated to the astronauts. Their representative solicited the group astronaut opinion and then worked toward the integration of the desired changes into the system.

Each decision concerning the addition of support for man was based upon comprehensive discussions before it was implemented. Where conflict between further automatic or manual equipment was encountered, the functioning man won. As the program progressed, more backup devices became manual. Through the combined effort of all of the disciplines required for the development of the spacecraft, man has been placed into the space vehicle, and the vehicle has been ready to receive him.

Summary of Mercury Manned Flight Medical Data and Implications for Future Flight

Detailed medical data resulting from the manned flights in Project Mercury have been presented in Government technical documents and conferences following each of the flights.[5,6,7,8] The purpose of this discussion is to review the medical information and, more importantly, to discuss the implications of this experience on life-science planning and future activities.

As a matter of convenience the medical data have been divided into two source areas: (1) the preflight and postflight physical and laboratory examinations, and (2) the physiological information from the countdown and flight, which includes the astronauts' voice reports and the spacecraft bioinstrumentation. Comparative control data were obtained from prior clinical examinations, centrifuge training sessions, procedure trainers and launch countdown practices.

Physical Examination Data

Extensive clinical examinations were accomplished on the flight astronauts by a medical specialty group during the final days prior to launch. A preflight physical evaluation was made by the astronauts' Flight Surgeon on launch morning just prior to suiting. The postflight examination consisted of two parts, a cursory checkout on the recovery ship as soon as the astronaut was aboard and a detailed appraisal at a down-range debriefing site (either Grand Bahama or Grand Turk Island) by the initial medical specialty group. All of these examinations included the collection of blood and urine samples.

MR-3 Flight.- Astronaut Alan B. Shepard, who made the MR-3 flight, had a preflight physical examination at Cape Canaveral approximately T-8 hours. (T represents launch time.) His postflight examinations were at T+45 minutes (shipboard) and T+3 hours (Grand Bahama Island). Positive findings were limited to a 3-pound weight loss, and a few rales heard at the base of both lungs which cleared with coughing. His general condition was excellent. The physical findings and laboratory studies were all within the control clinical observations made in association with Astronaut Shepard's centrifuge training.

MR-4 Flight.- Astronaut Virgil I. Grissom was examined for the MR-4 flight at approximately T-7 hours (Cape Canaveral), T+30 minutes (shipboard) and T+2 hours (Grand Bahama Island). A 3-pound weight loss was recorded. The sinking of the

spacecraft and his subsequent exertion in the sea during recovery were reflected in the fatigue and elevated pulse and respiration rates observed aboard the recovery vessel. All vital signs had returned to normal at the Grand Bahama debriefing site examination. No other significant physical findings were observed.

MA-6 Flight.- Astronaut John Glenn's final preflight physical examination for the MA-6 flight was completed at approximately T-6 hours, 30 minutes (Cape Canaveral). Postflight examinations were at approximately T+6 hours (shipboard) and T+12 hours (Grand Turk Island). The recovery physicians reported a clinical impression of mild dehydration and fatigue. An approximate 5-pound weight loss was recorded. Vital signs (temperature, blood pressure, pulse, and respiration rates) were all within prelaunch values. There were superficial abrasions on the second and third fingers of the right hand caused by recoil of the explosive hatch actuator plunger. The remainder of the physical examination was unremarkable.

In summary, the preflight clinical examinations revealed no abnormalities. The postflight examinations all disclosed a healthy astronaut with no findings that could be specifically attributed to space flight. Certain of the comparative preflight and postflight blood and urine data were interpreted as consistent with the occurrence of stress while other values were believed to be normal fluctuations.

Physiological Data

Physiological data were available from the time of astronaut insertion into the spacecraft until he disconnected the biosensor plug from the suit as part of the landing procedure. Bioinstrumentation utilized in all flights consisted of two electrocardiograph leads, a respiration rate thermistor, and a rectal temperature thermistor. A blood pressure measuring system, similar to the clinical (indirect auscultatory) method, was added to the MA-6 spacecraft. The countdown and flight records were generally of excellent quality with the exception of the respiration rate trace. In addition to the biosensor data, the pilot's subjective evaluation of body sensations and the film from the pilot-observer camera provided important sources of information.

MR-3 Flight.- In the MR-3 suborbital mission, the total biosensor monitoring time was approximately 4 hours and 30 minutes. The actual flight duration from lift-off to water landing was 15 minutes and 22 seconds.

Pulse rates during countdown were well within expected ranges. A high of 138 beats per minute was recorded at spacecraft separation and a downward trend ensued during the following 5 minute zero-gravity interval. Pulse rate rose to a high of 132 beats per minute during reentry and was 111 beats per minute at loss of telemetry signal. The electrocardiogram waveform showed no significant variation during the countdown and flight. Body temperature remained near 99° F for the entire countdown and flight. Respiration rate during the countdown and flight was similar to rates noted at centrifuge training runs.

Astronaut Shepard reported no disturbing sensations with zero-gravity and both launch and reentry accelerations were well tolerated.

MR-4 Flight.- Physiological data for the MR-4 suborbital flight were recorded for approximately 3 hours and 35 minutes; 15 minutes of which was flight time. Pulse rates averaged 80 beats per minute during countdown, 138 beats per minute at lift-off, and increased to 162 beats per minute at spacecraft separation. A high of 171 beats per minute was recorded at retrofire, declining gradually through reentry to 137 beats per minute at loss of telemetry signal. The electrocardiogram revealed only sinus tachycardia. Rectal temperature did not fluctuate significantly during the flight. Respiration rates varied from 12 to 24 breaths per minute during countdown, but because of poor trace quality in-flight data were not obtained.

Astronaut Grissom reported no umpleasant feelings while weightless. A brief tumbling sensation was felt at booster engine cutoff which lasted only a few seconds. Hearing and visual acuity remained undisturbed.

MA-6 Flight.- The total monitoring time for the MA-6 orbital flight was 8 hours and 15 minutes, of which 4 hours and 53 minutes was actual flight time. Pulse rate during countdown varied from 56 to 86 beats per minute with a mean of 68 beats per minute. At lift-off, the pulse rate was 110 beats per minute, rising to 114 beats per minute at spacecraft separation, then apparently stabilized through weightlessness with a mean of 86 beats per minute. The highest pulse rate, 134 beats per minute, occurred during reentry at the time of maximum spacecraft oscillation.

Analysis of the electrocardiogram showed some variation in the origin of the heartbeat during the countdown which was not present during flight. These findings were believed to be within the range of normal physiological stress responses. Respiration rates were within expected values throughout the countdown and flight. Body temperature declined during the countdown as a result of external cooling of the suit circuit. There was a gradual rise after lift-off, increasing about 2° F for the entire flight, reflecting normal body temperature regulation.

Astronaut Glenn's in-flight commentary and postflight debriefing remarks indicated that vision, hearing, food chewing, swallowing, and urination were normal during flight. Deliberate attempts to stimulate the vestibular system did not produce any disturbing symptoms.

As pointed out in prior reports, the Mercury Redstone suborbital flights did not provide enough time to establish physiological trends, and no observed medical data could be specifically attributed to weightlessness. However, the Mercury Atlas orbital flight of Astronaut Glenn provided sufficient time for physiological responses to apparently stabilize, and trend information was obtained. Perhaps the most valuable medical observation made from each of the manned flights was that all the physiological and clinical examination data were consistent with normal function. This finding was supported by the competent performance displayed by each of the astronauts during space flight.

Discussion

As observed from the United States flights to date, no specific medical problems peculiar to weightlessness have been defined. No difficulty has been experienced by the astronauts in tolerating the acceleration associated with launch and reentry. Available Russian cosmonaut data[9] indicate similar observations with the exception of the symptomatology reported by Titov after about 6 hours of weightlessness. Although not definite, the Russian reports suggest that some disturbance in vestibular function did occur. This disturbance apparently did not interfere with operational performance of the spacecraft. Whether this disturbance is a consequence of extended exposure to weightlessness or represents an idiosyncratic response of Titov is not known. There are several possibilities which might explain the relative lack of physiological changes during weightlessness as observed in our flights. These include:

(1) Physiologic response mechanisms adapt quickly and no functional disturbances are produced.

(2) The bioinstrumentation utilized and the astronaut's subjective evaluation are not sufficient to detect subtle transient changes associated with short exposures.

(3) The exposure durations have been too brief to elicit physiologic changes.

(4) The combination of brief exposure and the restrained position are sufficient to curtail the appearance of adverse effects.

Additional space flight experiences will determine eventually which of the above explanations or combinations thereof are correct.

The effects of weightlessness on human physiology will continue to be a primary objective in early space flight programs. Planning and direction of ground-based and in-flight medical research relating to zero-gravity will be influenced by observations obtained from longer missions in the Mercury spacecraft. Plans for the two-man Gemini spacecraft are to provide an increased flight time, and thus to permit extended investigations. This exposure to increased space flight (up to 2 weeks) will be approached with essentially the same bioinstrumentation and technique as used in the Mercury program. Should physiologic problems arise which result in crew performance decrement, then detailed in-flight medical investigations, including the use of animals, might become necessary. If function abnormalities appear when the crew is unrestrained, then the Apollo earth-orbiting spacecraft or an earth-orbiting laboratory might be required for more detailed experiments. This approach then would utilize the flexibility inherent in the Gemini and Apollo designs, with the capability of earth-orbital flights carrying medical research equipment. Whenever valid, ground-based medical investigations would be applied to the solution of weightlessness problems.

Summary

The integration of the crew station with the man and his equipment was a continuous program requiring many compromises. The goal of this effort was the provision of equipment within the crew station which would permit flight control by the astronaut. The experience gained by flights to date have indicated that the provisions are adequate for the task.

The biomedical assessment program associated with flights on Project Mercury to date has produced no significant medical problems. The Russian experience with Cosmonaut Gherman Titov has shown some disturbance of the vestibular apparatus, however, symptoms were not severe enough to be incapacitating. The extension of knowledge, primarily in the prolongation of exposure to the weightless environment, is essential if the discrepancy between the United States and Soviet data is to be resolved. Presently planned programs of manned flight will yield further data in this area. The following factors will be active in the design of the medical portion of these programs:

(1) Investigation of in-flight medical responses will be extended as a function of time in zero-gravity, utilizing the Mercury, Gemini, and Apollo spacecrafts and existing techniques.

(2) Capability will continue to exist for the recognition of physiologic effects that might result in compromised crew performance. Performance must be maintained of sufficient quality to assure a safe reentry to earth from earth orbit.

(3) The design of on-going in-flight medical studies will be dependent on the interpretation of accumulated physiologic data.

(4) Ground-based medical studies will be utilized whenever possible in examining biologic responses to weightlessness.

References

1. Comroe, J. H., Jr., et. al.: Oxygen Toxicity, Jour. Amer. Med. Assoc. 128:710, 1945

2. Shepler, Herbert C.: Pilot Performance and Tolerance Studies of Orbital Reentry Accelerations Rep. #11; Letter Rep. concerning Bur. Aero. TED ADC AE-1412. Aviation Medical Acceleration Lab., U.S. Naval Air Development Center, Johnsville, Pennsylvania, September 16, 1959.

3. Stapp, J. P.: Tolerance to Abrupt Deceleration. Collected Papers on Aviation Medicine, AGARDograph No. 6, North Atlantic Treaty Organization (Paris), 1955, pp. 122-169.

4. Brinkley, James W.: Man Protection During Landing Impact of Aerospace Vehicles. Ballistic Missile and Space Tech. vol. 1, Academic Press, Inc. (New York) c. 1960, pp. 91-105.

5. Augerson, William S., and Laughlin, C. Patrick: Physiological Responses of the Astronaut in the MR-3 Flight. Proc. Conf. on Results of the First U.S. Manned Suborbital Space Flight, NASA, Nat. Inst. Health, and Nat. Acad. Sci., June 6, 1961, pp. 45-50.

6. Laughlin, C. Patrick and Augerson, William S.: Physiological Responses of the Astronaut in the MR-4 Space Flight. Results of the Second

U.S. Manned Suborbital Space Flight July 21, 1961. Manned Spacecraft Center, NASA, pp. 15-21.

7. Laughlin, C. Patrick, McCutcheon, Ernest P., Rapp, Rita M., Morris, David P., Jr., and Augerson, William S.: Physiological Responses of the Astronaut. Results of the First United States Manned Orbital Space Flight February 20, 1962. Manned Spacecraft Center, NASA, pp. 93-103.

8. Minners, Howard A., Douglas, William K., Knoblock, Edward C., Graybiel, Ashton, and Hawkins, Willard R.: Aeromedical Preparation and Results of Postflight Medical Examinations. Results of the First United States Manned Orbital Space Flight February 20, 1962. Manned Spacecraft Center, NASA, pp. 83-92.

9. Gazenko, O. G., and Yazdovsky, V. I.: Some Results of Physiological Reactions to Space Flight Conditions. Presented at Am. Rocket Society Meeting, December 1961.

DYNA-SOAR BIOASTRONAUTICS

Robert Y. Walker, Ph.D.
Staff Assistant, Human Engineering
The Boeing Company
Seattle, Washington

Dyna-Soar is a manned boost-orbit-glide vehicle. Conventional booster and guidance systems will place the glider on a course at the proper altitude and velocity with the resultant energy to accomplish the planned mission. After boost termination, the pilot verifies the course during orbit and controls the flight path during re-entry, approach, and landing.

The flight profiles and over-all flight regime for the Dyna-Soar's single-orbit mission will impose no new or extreme environmental hazards on the pilot. The environmental parameters of a normal space flight will not expose the pilot to stress magnitudes as great as pilots have experienced in the Mercury flights. Under presently planned flights, the pilot should be in an environment that is well within known human tolerances.

We will present the calculated environmental stress to be imposed on the pilot in both normal and emergency conditions and the design techniques developed to provide a cockpit that will keep the pilot well within his tolerance limits. The various primary environmental parameters will be discussed separately. The solution for each parameter will be discussed in a concurrent manner. No significance is attached to the order in which the specific parameters of the environment are considered. These seven primary factors are:

1. Acceleration;
2. Zero g;
3. Mechanical vibration;
4. Acoustic vibration;
5. Pilot's atmosphere;
6. Heat;
7. Humidity.

The first parameter - acceleration - receives most consideration. The flight profiles have been analyzed to determine the physiological stresses to be imposed on the pilot for each phase of the mission. Acceleration time histories have been developed for the boost, glide, and terminal phase, and emergency conditions. Emergency conditions would be abort from the pad, abort during boost, and ejection escape from the glider. The magnitude, duration, rate of onset, and the direction of acceleration were studied for these conditions.

To determine the proper magnitude and direction of the accelerations that determine the resultant external force acting on the pilot, we have used the Resultant Physiological Acceleration that would be significant in defining pilot performance and tolerance limits. The resultant physiological acceleration (or RPA) is the vectorial sum of all the g-normalized forces to which the pilot is exposed. This is the g load he actually feels.

Figure 1 indicates the g forces to which the pilot will be exposed during boost. The maximum RPA never reaches 5 g's and is above 4 g's prior to second-stage burnout for less than 15 seconds. The g prior to first-stage burnout is of much lower magnitude, while third-stage g just attains 4 g's. These forces act on the restrained pilot seated in the boost position in the transverse or $+g_x$ (chest-to-back) direction.

Figure 2 is a schematic illustration of an abort-off-the-pad recovery maneuver. The RPA for this maneuver never reaches 4 g's and is transmitted to the restrained pilot in a transverse $+g_x$ direction during the boost period. At termination of abort-rocket boost, the pilot must pitch the glider over from the vertical to the horizontal, subjecting him to an RPA under 4 g's for approximately 30 seconds in the positive $+g_z$ longitudinal (head-to-feet) direction. Following this, the pilot performs a roll-out and completes the prescribed landing maneuver.

For an abort due to a premature burnout of the first stage, the pilot could be subjected to a maximum peak RPA of about 7 g's in the $+g_z$ or longitudinal direction during the recovery maneuver. Abort recoveries in succeeding stages due to premature boost burnout would not be as severe.

The design objective of the Dyna-Soar glider is to accomplish a controlled rate of re-entry into the atmosphere. Re-entry profiles are slightly in excess of 1 g. This acceleration is transmitted to the pilot in a combination of positive longitudinal $+g_z$ (head-to-feet) and a negative transverse $-g_x$ (back-to-chest) directions.

The design performance requirements for the subsonic escape system are well within the dynamic pressure, Mach number, and altitude performance envelope of present escape systems. The Dyna-Soar pilot will actually be subjected to a less severe acceleration profile during escape than during an ejection from present fighters at supersonic speeds. Figure 3 shows a typical performance envelope for an ejection-seat rocket catapult. There is well-established data demonstrating the capability of pilots to withstand these forces.

The terminal phase and landing stress of the flight profile is very similar in acceleration forces to that of the present Century series of fighter planes.

Human acceleration experience for the RPA's computed for the Dyna-Soar profile fall well within demonstrated human tolerances. Tolerance to g is contingent upon peak g, the direction of g, the duration, the rate of onset, the seat-back position, and body restraint. By shifting the seat-back position, it is possible to obtain quite a range of human tolerance limits, all of which are well above the computed g values and durations that have been mentioned. It is particularly significant that, while I have mentioned durations of g's in seconds, research has demonstrated that man can tolerate these same g's for minutes under

particular seat-back positions or with anti-g suits.

In the Dyna-Soar, the pilot must be in an adequate physiological condition to monitor, to over-ride automatic controls, and to control the vehicle manually. Even the limited g's computed for this profile might impose problems on his sensing of instruments or proper manipulation of controls. Consequently, provision has been made to ensure the pilot's capability even with these limited g's. Figure 4 illustrates the two positions of the seat back. During boost the pilot's seat back will be in a position more vertical than in a normal seat, with his feet on the rudder pedals.

Research on the AML centrifuge at Wright-Patterson Air Force Base with human volunteers had indicated potentially dangerous vascular pressure levels in the subjects with angles aft of the vertical. AML recommended slightly forward angles during boost. The Air Force Dyna-Soar Pilot Consultant Group served as subjects in subsequent centrifuge tests under the anticipated boost accelerations in both slightly forward and aft angles with no evidence of degradation of performance in spite of the apparent high right heart pressure. These and other investigations, however, initiated re-design consideration of the seat-back angle for the boost phase of the flight profile. A forward angle, not as yet fixed will be selected to provide physiological protection and adequate operational capability. This is an example of the excellent coordination and interdisciplinary team work in the USAF system development program.

The upper arms are provided with rests (adjusted to the pilot's forearm length) so the thrust forces will not pull the arms back from either the side-arm controller for the right hand or the abort-control handle for the left hand.

A side-arm controller has been developed because a center-type stick cannot be controlled adequately when the pilot is subjected to high transverse g. The mere acceleration imposed on the arm and hand holding the stick could impart undesirable control actions.

The pressure suit does not have to be pressurized unless there is an emergency loss of air pressure in the cabin. The restraint system shown in Figure 5 is an integrated portion of this pressure suit. Shoulder straps come over the shoulder and attach to the suit on the right and left front chest. The belt straps are attached over the pressure suit at the lower abdomen. I would also like to point out at this time the connection for the atmosphere servicing system to the pilot. The helmet can have the face plate opened, although for reasons to be explained later, it will probably be kept closed with an air-tight seal until in orbit.

Following termination of boost, the pilot may shift the seat to 13° aft of the vertical if he wishes. This will allow him to sit in a more normal position, although he can control the vehicle from a more forward position without discomfort.

Before ejection, the seat back will be placed automatically in the 13° aft position and the feet must be withdrawn against the leading edge of the seat to ensure adequate clearance. Since the pilot initiates ejection, there is no reason to believe he will not have his seat back and his feet in the proper positions prior to pulling the D ring. The shock impact of ejection is well within human tolerance limits and constitutes no problem.

There is indication from recent research that a man undergoing stress from g in one axis has a lowered tolerance to combinations of acceleration. Such a combination could occur if the vehicle were to start a roll around the longitudinal axis during boost. In the Dyna-Soar, the Malfunction Detection System will initiate automatic abort before the spin or roll rate reaches a velocity that would affect the pilot.

Weightlessness or zero gravity is not expected to be a problem on these single-orbit missions, insofar as known from flights to date. The restraint system mentioned earlier will hold the pilot in the proper position to conduct all of his pilot functions under either normal or weightless conditions.

The next environmental parameter of significance is vibration of both the crew station and the pilot. Again the Malfunction Detection System will be activated before any vibration or oscillation of the air vehicle can damage the pilot.

The vibration present in the crew compartment is a random mechanical vibration rather than sinusoidal. The glider is designed to operate within the vibration parameters shown in Figure 6. Present design ground rules require any subsequent changes in the system to be designed to stay within this present profile. The intensities are not considered severe and are of relatively short duration. The low-frequency portion of the vibration envelope has its maximum intensity lasting about 10 seconds during the period of high dynamic pressure. The high-frequency portion of the spectrum occurs for about 5 seconds at lift-off and for about 15 seconds during the period of high dynamic pressure.

The low-frequency vibration band is made up of from 1 to 20 cycles per second. The high frequency band is from 5 to 2000 cycles per second. The low-frequency vibrations (occurring largely during the period of high dynamic pressure) are attributed to air turbulence while the high frequencies are caused by engine-induced vibration, aerodynamic vibration, and other miscellaneous sources including operating equipment aboard the vehicle.

The limited experience on human tolerance to random vibration is indicated by the dotted line in Figure 6. If these random vibrations are considered to have the same effect on the human as sinusoidal vibration, they are well within known human tolerance limits. It is questionable, however, to interpret random vibration effects in the same manner as sinusoidal vibration. Intensities are known to peak and could affect the pilot's operation. For these reasons, the

Air Force is undertaking research to provide data for comparing the effect of sinusoidal and random vibration of pilot performance. The first manned Mercury flight subjected the pilot to such vibration during the period of high dynamic pressure, but the vibration had no significant effect. Subsequent change in a structural fairing reduced this vibration significantly.

Closely related and interacting with mechanical vibration is the acoustic environment. High noise levels will be produced around the vehicle from the propulsion system, glider subsystem equipment, and aerodynamic interactions. The highest noise levels are external to the crew compartment. Consequently, the compartment walls attenuate the sound pressure to considerably lower levels within the crew compartment. Figure 7 shows the acoustic environment during the boost phase when the highest intensities occur inside the crew compartment. It is doubtful if the maximum values will be reached. It will be noted from the tolerance curves superimposed on these levels that there is only a 25-second period when the noise level is above human tolerance with no protection. There is a period of possibly 20 seconds at this same time when, if a maximum noise level did occur, there could be a slight degradation in performance with the helmet in place. The helmet keeps the noise level well below the human tolerance level.

The acoustic envelope within the crew compartment then, is attenuated significantly with the helmet. With the earphones in place there will be negligible communication interference, permitting more than 98% comprehension of speech heard through the earphones during the period of highest intensity. Outgoing communication received on the ground will have less disruption from the same noise profile because of filtering in the communication system.

Orbital or glide-phase noise levels are considerably lower than those experienced during boost, and hence, no interference is expected.

The pilot's atmosphere and thermal environment constitute the last major consideration requiring special development. The atmospheric control also regulates the heat and humidity, which may be stresses on the pilot. Consequently, they will be considered as interacting stresses. The atmosphere of the crew compartment can undergo pre-designed variations in pressure, temperature, and composition. Variation in operating temperature of different subsystems within the crew compartment will influence the temperature of the compartment, which calls for the ability of the system to compensate for these changes.

The design of the crew station calls for a cabin capable of maintaining pressure at 7.35 PSIA (or approximately that of 18,000 feet). The atmosphere will be 40% O_2 - 60% N_2 by weight with 100% O_2 for emergency operation. Controlled cabin leakage will be 0.25 pound per minute.

Under normal operations the pilot will be suited and his suit and physiological sensing equipment checked out about two hours before launch. The pilot will also be kept in a controlled temperature and transported in a van to the launch site. During this period and until the pilot is connected to the glider's atmosphere system, the suit will be ventilated by forced circulation. The helmet face plate will be closed before the crew-station hatch is closed.

The glider's atmosphere is supplied from liquid O_2 and N_2 tanks through a metering system that provides the correct ratio of O_2 and N_2. The liquid is fed through heat exchangers that use the low temperature of the liquid gases for cooling the various glider subsystems. The cool gases now mixed are fed into the suit through the service connection on the right side of the suit. The suit contains a distribution system to cover the entire body with the atmosphere exhausted in the area of the head. This distribution of cool air cools the body and removes moisture. All suit air is vented from the helmet to the cabin. The cabin air is vented when cabin pressure is above 7.35 PSIA. All cabin gases enter the cabin via the pilot's suit until the glider is again below 15,000 feet, at which time a reflief valve permits entrance of ambient air.

The circulation of cooled air keeps the cabin temperature down to operating limits for the subsystems within the crew compartment. The pilot may control his suit temperature and indirectly the cabin temperature by regulating the temperature of air flowing through the system.

Up to altitudes of 18,000 feet, the cabin is open to the external atmosphere. The cabin air valves automatically seal at 18,000 feet to hold the cabin pressure at 7.35 PSIA. In normal operations the pilot's full-pressure suit operates essentially at cabin pressure. The suit pressure, however, is regulated so that the pilot will not be automatically exposed to less than 5 PSIA. The crew compartment is provided positive pressure relief at 8 PSIG and negative relief at -1 PSIG.

Pilot tolerance and performance at the normal compartment pressure is not considered a problem as this pressure is a common operational level in modern high-performance aircraft. Under emergency conditions, if the compartment pressure drops from 7.35 PSIA, the pilot is automatically put on 100% O_2 at 5 PSIA. Cabin pressure may slowly fall off from a leak, but no explosive decompression is anticipated. Actually, if leakage occurs, normal flow may keep the compartment pressure somewhere between 7.35 and ambient PSIA.

In case of total loss of cabin pressure and with only partial denitrogenation, there is some possibility of a pilot experiencing bends. However, crew selection has been made from experienced pilots who have been indoctrinated and are experienced with this problem. With a suit pressure of 5 PSIA under emergency conditions with 100% O_2, there should be no bends problem, but the suit may be a little stiff for proper operation of controls. If control is difficult due to the pressurized suit, the pilot may elect to go on full automatic glider control during periods of high control requirement or may reduce suit pressure to 3.5 PSIA.

There are two sources of heat in this vehicle. One would be the normal heat generated by

equipment operating within the crew compartment which, as stated earlier, is controlled by the normal air flow through the pilot's suit into the crew compartment and then vented to the outside through a controlled leakage rate. The second major source of heat arises during the later stages of orbital flight and the re-entry of the vehicle. Surface heat generated during boost will not significantly affect the crew station.

The wall surfaces are designed with a water wall that absorbs heat from the outer skin and dissipates it by evaporation of the water, which is vented to the outside. The highest wall temperature could occur after depletion of the water sometime after landing (the pilot will normally be out of the cockpit). The forward windows will be covered with a heat shield until after re-entry to protect them from reaching high temperatures. The heat shield will be jettisoned after re-entry. The side windows, which are not cooled, will attain a maximum temperature of 320°F due to their location and small surface area. The pilot will be able--through his ventilated suit and subsequent ventilation of the crew station-- to maintain a cabin air temperature between 60° and 90°F at his choice.

Figure 8 shows the temperature tolerance and performance limits established by the Air Force for design of crew stations. These are the maximum temperatures and durations to which the crew may be subjected with a ventilated suit meeting the Dyna-Soar ventilation conditions.

With a ventilated suit, Air Force design requirements permit a maximum allowance of 195°F external suit temperature for 130 minutes. The crew-compartment thermal environment is shown in Figure 9. The estimated Dyna-Soar maximum heat profile will start building up after 70 minutes from 80°F to a maximum cabin temperature of 140°F. Again this build-up occurs during the re-entry period, with the maximum temperature occuring after landing. The maximum estimated cabin temperature is 55°F below the maximum allowable temperature for 130 minutes of exposure. Here the pilot will be exposed to the maximum temperature for less than 30 minutes.

Coupled with thermal control is the problem of humidity, which is controlled by the temperature, saturation, and flow rate of ventilating air within the suit. Under the moderate work load and environmental temperature calculated for these flights, the pilot will rarely exceed a water-production rate of one pound per hour which will be removed by the ventilation of the suit. The designed ventilation flow rates permit a mass flow rate of 0.25 pound per minute and an emergency of 0.17 pound per minute. The volume flow rate will vary with suit pressure and temperature.

The low-orbit mission profile of this vehicle is such that no known radiation problems from outer space are anticipated.

Experimentation has been employed to evaluate pilot capabilities under the calculated environmental stresses. Since it is not possible now to expose a man to combined simulation of all these stresses simultaneously, design for control of the individual stresses has been such that there is a wide margin of safety for each parameter. On this basis, it is assumed that the pilot will be able to operate during the relatively short periods of combined stresses with no degradation of his required performance level.

As I stated in the introduction, the Dyna-Soar flight missions impose no new environmental stresses on the Dyna-Soar pilot. Engineering design has been able to provide adequate protection for all of the seven major environmental stresses. The design engineers have been faced with a real challenge to provide this protection and keep the vehicle configuration within other mandatory design parameters with a limited budget.

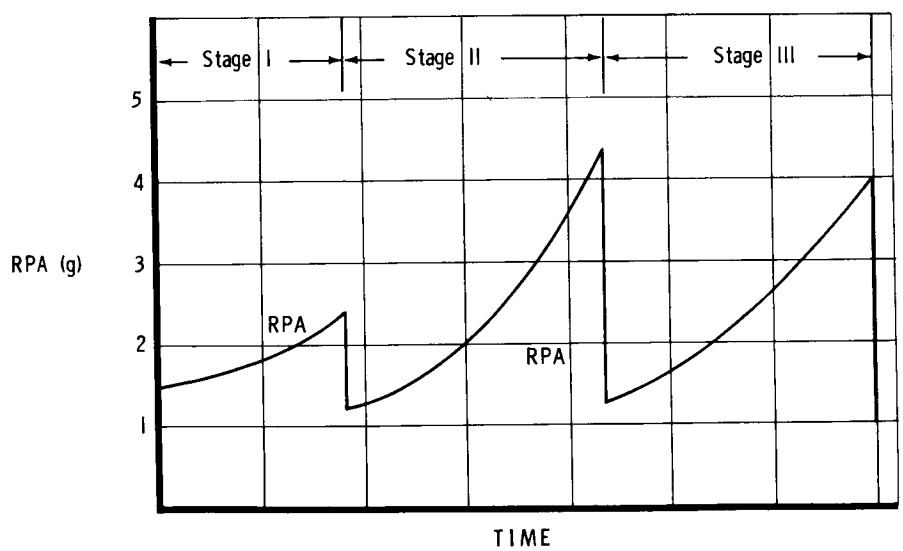

Figure 1 RESULTANT PHYSIOLOGICAL ACCELERATION BOOST FLIGHT PHASE

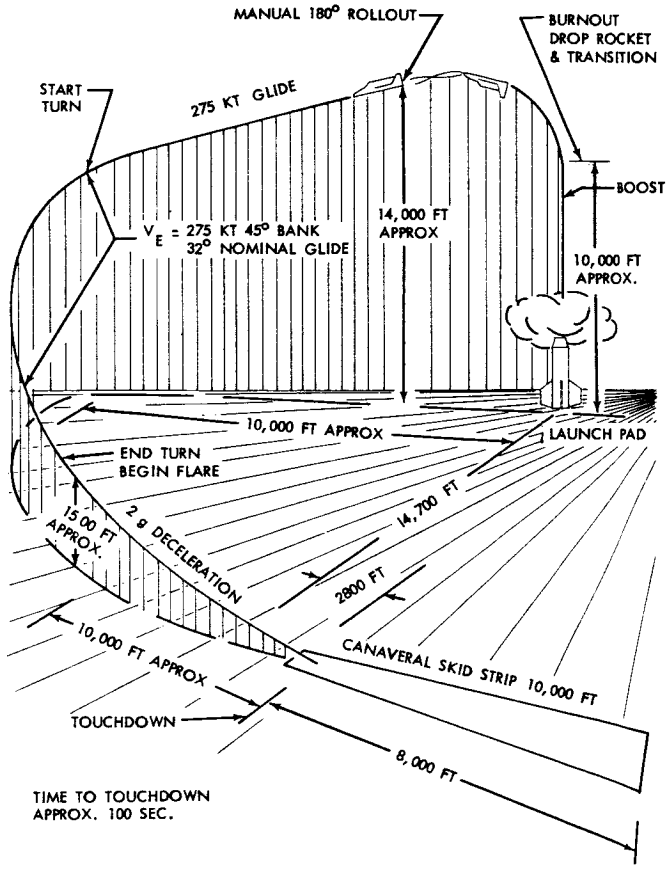

Figure 2 PAD ESCAPE RECOVERY MANEUVER

2B20649-2

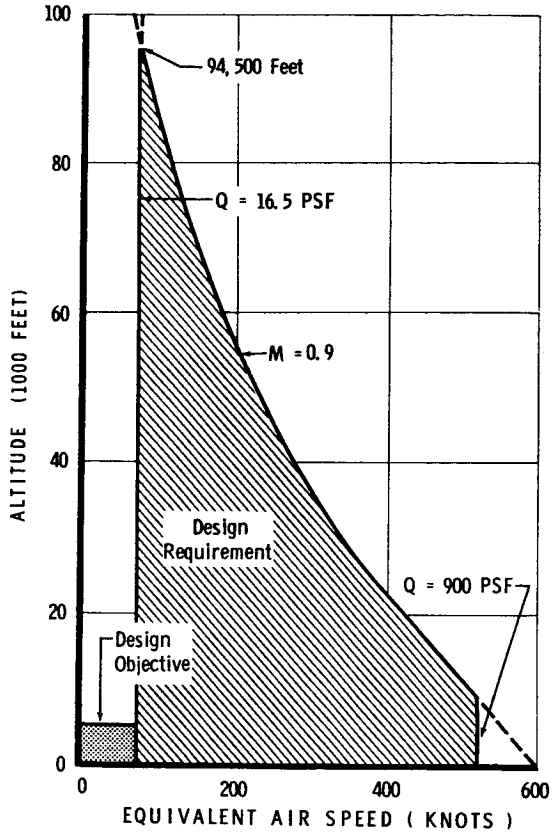

Figure 3 PILOT EJECTION ESCAPE SYSTEM PERFORMANCE ENVELOPE

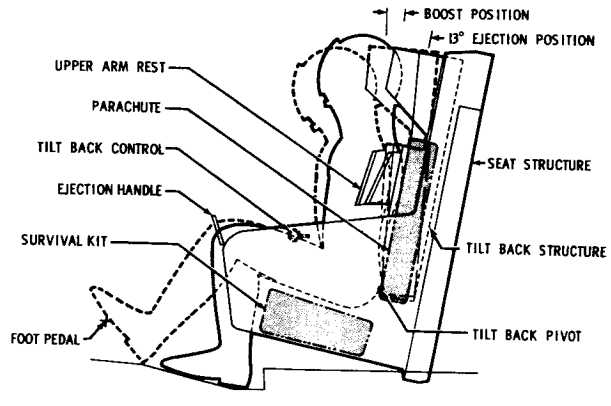

Figure 4 2 POSITION EJECTION SEAT

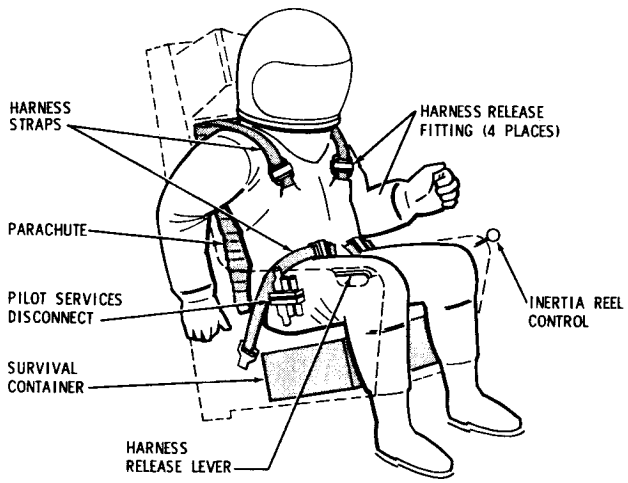

Figure 5 RESTRAINT SYSTEM
MAN-SEAT ATTACHMENT POINTS

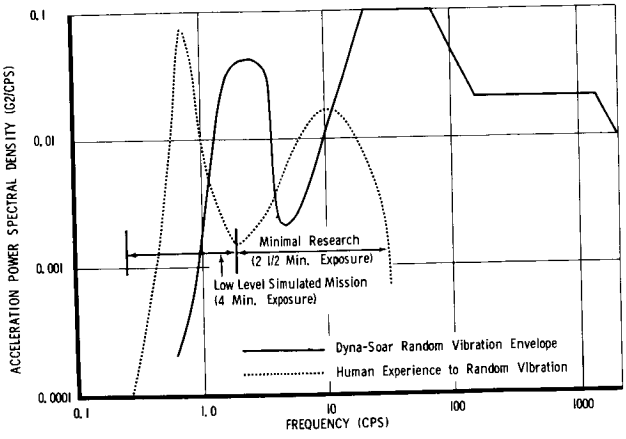

Figure 6 ACOUSTIC ENVIRONMENT INSIDE CREW COMPARTMENT

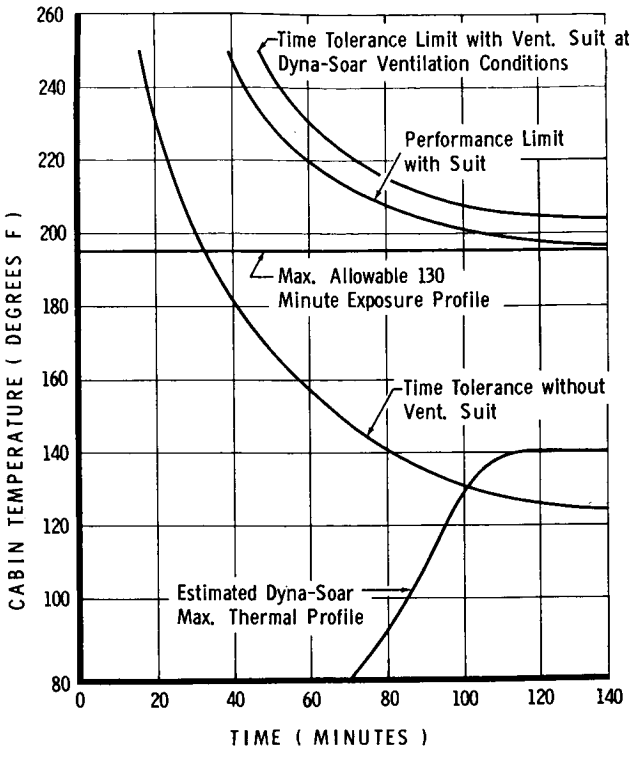

Figure 8 CREW COMPARTMENT THERMAL ENVIRONMENT

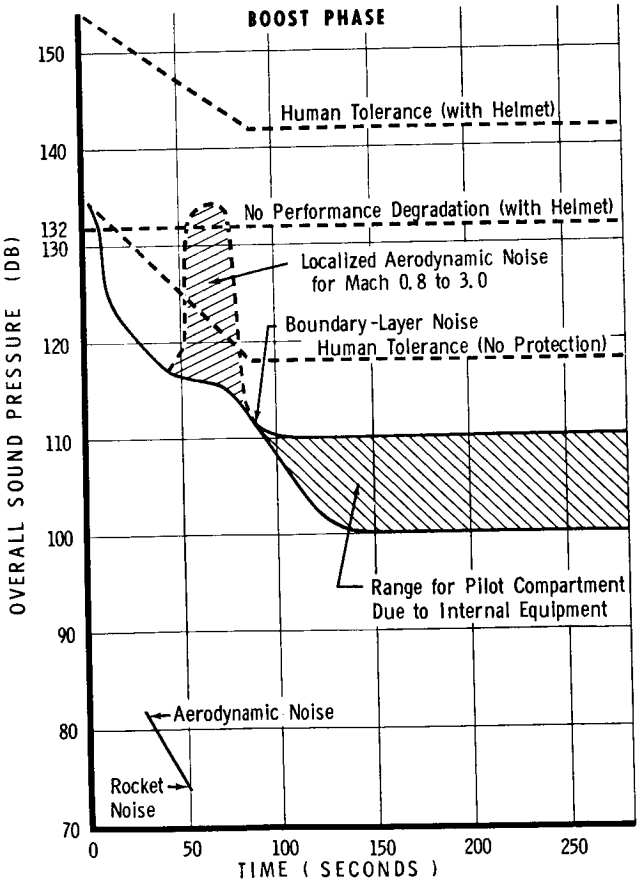

Figure 7 HUMAN THERMAL TOLERANCE AND DYNA-SOAR THERMAL ENVIRONMENT

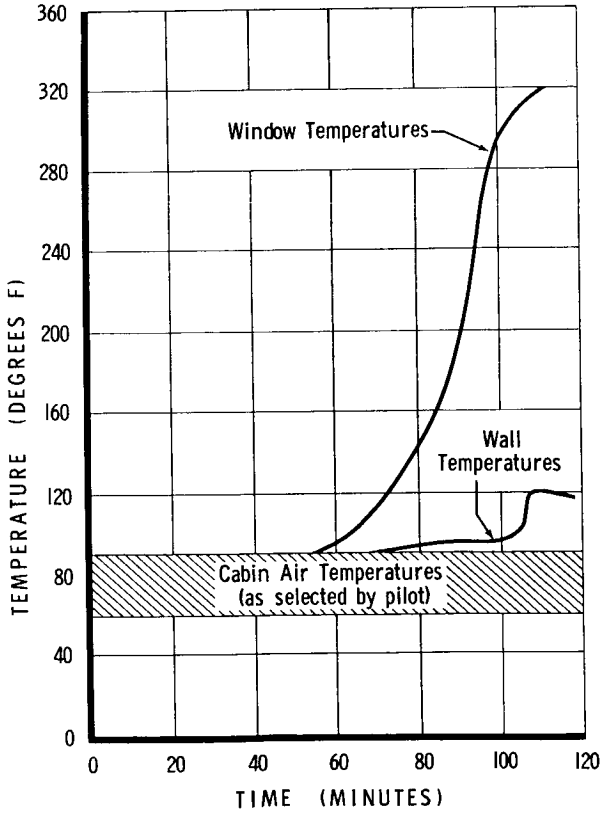

Figure 9 DYNA-SOAR RANDOM VIBRATION ENVELOPE

REGENERATIVE ENVIRONMENTAL CONTROL SYSTEMS FOR MANNED EARTH-LUNAR SPACECRAFT

N62-14473

Michael G. Del Duca, Ph.D.
Richard G. Huebscher, M. Sc.
Anthony E. Robertson, Ph.D.

Thompson Ramo Wooldridge, Inc.
New Devices Laboratories, Tapco Division

INTRODUCTION

The historic earth orbital flight of the Mercury space capsule on February 20, 1962 has illustrated that man has the capability of creating instrumentation and equipment which permit him to survive outside the protective earth atmosphere which, in time, has served both as a shield and a barrier. Because of this great achievement man need no longer restrict himself to earth-space but may direct his resources to expand his zone of operation to earth-moon space. However, in order to exploit this new frontier many problems must be solved which are not mere extensions or extrapolations of those already treated. The problem associated with providing man with an adequate environment for extended periods in the earth's atmosphere, earth-moon space and on the lunar surface is indeed extensive. Trapped radiation, solar flare activity, meteoroid bombardment, solar radiation and the hard vacuum of space are no longer merely phenomena of scientific interest; they describe the operating environment of manned earth-lunar spacecraft.

In order that man may effectively operate in the earth-moon space, myriads of systems and subsystems of varying types and functions must be devised and integrated into an efficient, reliable man-machine complex.

This paper will consider only one small aspect of this problem--that is, the problem of providing man with an adequate gaseous and thermal environment in earth-lunar spacecraft. Control of atmospheric gases in manned sealed environments will be treated in Part I. Part II treats thermal regulation and atmosphere control requirements of mobile life support systems for lunar exploration.

PART I
ATMOSPHERE CONTROL SYSTEMS FOR ADVANCED SPACECRAFT

A. General Remarks

Providing man with a gaseous environment in the earth-moon space must be considered within the framework of the sealed environment. The problem is not restricted to providing breathing oxygen and diluent nitrogen, removing metabolic CO_2, H_2S, CH_4, etc., at optimum temperatures and pressures. For purposes of this paper, however, attention will be focused on methods for providing breathing gases and removal of metabolic products.

Many methods may be used to provide oxygen and remove metabolic carbon dioxide in manned sealed environments. The problem is the selection of the method which integrates into the vehicle complex in the optimum manner. For the past several years much attention has been focused on analyses attempting to select optimum atmosphere control systems for specific mission times. Data and information have been accrued which permit us now to make tentative selections of systems for particular mission requirements. In Figure 1, the areas of application of regenerative systems are compared to those for storage systems. Some of the major criteria which must be considered in the comparison are weight, volume, and power requirements associated with a particular atmosphere system operating for a specific time and in a specific mission phase. These criteria must be considered as they relate to state of the art and projected future developments.

The basis for the future development of environmental control systems was taken to be the weight of breathing oxygen needed for a given mission. Missions considered have been divided into broad categories, descriptive of those anticipated for the next fifteen years.

As illustrated in Figure 1, completely regenerative systems cannot compete -- from the standpoint of weight, volume, and power -- with chemical storage systems or chemical partial regenerative systems for missions requiring less than the order of 100 pounds of oxygen. Above the 100-pound mission requirement, however, regenerative systems become increasingly attractive. Based on projected mission requirements, storage systems show optimum applicability for the next few years. As mission requirements change, however, stored superoxide and partially regenerative systems will probably displace the simple storage systems. Chemical regenerative methods, such as H_2 reduction of CO_2 followed by electrolysis, will become operative by about 1965. These systems will be most useful for missions requiring between 100 and 2000 pounds of breathing oxygen.

Chemical regenerative systems may accumulate some by-product wastes. Handling of these wastes makes the use of such systems somewhat unwieldy for high O_2 consumption. The area delegated to these chemical systems is therefore shown as limited to missions requiring a total O_2 consumption less than several thousand pounds.

Completely regenerative biological systems will be useful for almost any level of oxygen regeneration. Their application to future missions will be limited by (a) physical size, which is dependent on the number of men in a mission rather than on length of mission, and (b) type and magnitude of available power. The results shown suggest that it is rather important that efforts in the development of regenerative systems be maintained, especially when we consider environmental requirements for extended missions such as moon colonization or deep space manned explorations.

Several storage, partially regenerative, and completely regenerative systems for providing atmospheric gases in manned sealed environments are discussed below. Those methods to be considered include:

1. Storage of gases as liquids.
2. Generation of oxygen and absorption of CO_2 by means of stored chemicals.
3. Regeneration of oxygen from waste products.
   a. Electrolysis of water.
   b. Regeneration of oxygen from carbon dioxide by chemical means.
   c. Regeneration of oxygen from carbon dioxide by biological methods.

B. Methods for Atmosphere Control

1. Storage Systems

a. Storage of Oxygen and Nitrogen as Liquids and Gases

While pure oxygen at 5 psi is considered satisfactory for the Mercury spacecraft, for flights of longer duration a mixture of oxygen and nitrogen at a pressure of 380 mm Hg, with a partial pressure of oxygen of about 160 mm Hg (corresponding to that in sea level air), is recommended. [1] The preferred diluent gas is nitrogen.

In Figure 2, systems weights for cryogenic and pressure vessel storage of oxygen are presented as a function of mission time. Supplying the required oxygen from a pressure vessel at ambient temperature is not advantageous because of the large weight penalty. For example, for a 14-day, 3-man mission, with a consumption rate of 6.2 lb/day, a tankage weight of 1,8 lb. is required to carry one pound of oxygen.[2] With cryogenic storage, however, the weights are more moderate. (By cryogenic storage is meant storage at temperatures and pressures that are above, but near, the critical values. This insures that all material will be in the gas phase, and avoids the spearation problems that would arise with liquid oxygen storage under zero gravity conditions.) Results of cryogenic storage studies on oxygen are presented in Figure 2.

b. Generation of Oxygen and Absorption of CO_2 with Stored Chemical Systems

The provision of breathing oxygen and the removal of CO_2 in space cabins from stored chemicals appears quite attractive for missions requiring O_2 consumption of less than 100 pounds. As indicated in Table 1, the oxygen-CO_2 balance may be maintained by several methods utilizing stored chemicals. These include:

1. Generation of oxygen by the thermal decomposition of oxygen compounds, and the removal of CO_2 by the absorption or reaction with stored chemicals.
2. Simultaneous generation of oxygen and removal of CO_2 by the chemical reaction of stored oxygen compounds with metabolic water vapor and the absorption of CO_2 on the products of the water vapor - O_2 compound reaction.

Representative systems for these methods will be described below.

(1) Oxygen Generation by the Thermal Decomposition of Oxygen Compounds and the Absorption on Stored Chemicals

The chlorates and perchlorates of the alkali and alkaline earth metals show great potential for oxygen generation in space systems. Particular applications include oxygen generation in emergency conditions, oxygen supply in re-entry modules, and oxygen provisions in short-time (1-12 hr.) lunar exploration missions by manned overland capsules.

The chlorates and perchlorates evolve oxygen when heated to a sufficiently high temperature. This reaction is usually slightly exothermic in the case of the chlorates. In the case of the perchlorates, the heat of reaction is less exothermic and in some cases may be slightly endothermic. Reactions of typical chlorates and perchlorates, together with heat evolution data, are presented below.

$$NaClO_3 \rightarrow NaCl + 1.5\ O_2 \qquad \Delta H_{25} = -12.5 \text{ kcal/mole}$$

$$LiClO_4 \rightarrow LiCl + 2O_2 \qquad \Delta H_{25} = +0.25 \text{ kcal/mole}$$

(Note: A minus ΔH value indicates that heat is evolved)

In general, the heat of reaction is insufficient to raise the temperature of the chlorate or perchlorate to the high temperature required for the reaction. The temperature required for sodium chlorate candles is 700 to 800°C.[3] To supply the needed heat, a fuel is incorporated in the candle. This fuel consumes part of the oxygen produced. Metallic iron, the fuel most commonly used, is normally oxidized to the ferrous oxide (FeO) when the candle burns.

Owing to the fact that the decomposition temperature of chlorates and perchlorates is above that of their melting points, it is essential to provide a fibrous binder to minimize the flow of the molten salts. Asbestos and fiberglass are commonly used for this purpose[3], although steel wool has been used with good results.[4]

One of the serious problems encountered in the development of chlorate candles has been the contamination of the oxygen produced with varying amounts of chlorine and carbon monoxide. Since these are both poisonous gases, their concentrations must be kept very low if the oxygen is to be used for respiration. It has been found possible to keep the concentration of carbon monoxide acceptably low by scrupulously excluding carbon from the candle constituents. It has been common practice to add barium peroxide to the composition to suppress the chlorine concentration in the evolved oxygen.

TABLE 1

CHEMICALS THAT CAN SERVE AS OXYGEN SOURCES AND CARBON DIOXIDE REMOVERS IN SEALED CABINS

CHEMICAL COMPOUND	FORMULA	USE		AS OXYGEN SOURCE		FOR CARBON DIOXIDE REMOVAL	REMARKS
		Oxygen Source	CO_2 Removal	Mechanism of Oxygen Release	Wt. Compound Per Wt. Oxygen	Wt. Compound Per Wt. CO_2 Removal	
Hydrogen Peroxide	H_2O_2	X		Catalytic Decomposition	2.1		
Lithium Hydroxide	LiOH		X			1.09	
Lithium Oxide	Li_2O		X			0.68	
Lithium Perchlorate	$LiClO_4$	X		Thermal Decomposition	1.66		
Lithium Peroxide	Li_2O_2	X	X	Reaction with H_2O or CO_2	2.88	1.05	Not Commercially Available
Lithium Superoxide	LiO_2	X	X	Reaction with H_2O or CO_2	1.62	1.77	Not Prepared in Pure Form
Magnesium Perchlorate	$Mg(ClO_4)_2$	X		Thermal Decomposition	1.74		
Magnesium Superoxide	MgO_4	X	X	Reaction with H_2O or CO_2	1.84	2.01	Not Commercially Available
Potassium Superoxide	K_2O_4	X	X	Reaction with H_2O or CO_2	2.96	3.23	
Sodium Hydroxide	NaOH		X			1.82	
Sodium Perchlorate	$NaClO_4$	X		Thermal Decomposition	1.91		
Sodium Superoxide	NaO_2	X	X	Reaction with H_2O or CO_2	2.29	2.50	

An optimized lithium perchlorate candle consists of the following ingredients in addition to lithium perchlorate:

a. A fuel to supply the heat of decomposition of the lithium perchlorate and to bring it to its decomposition temperature.

b. A material to mechanically support the composition when it is in a molten state.

c. A catalyst to facilitate the decomposition of the lithium perchlorate.

d. A material to prevent the occurrence of toxic ingredients in the evolved oxygen.

The amount of lithium perchlorate required to produce 2.0 pounds of oxygen is 3.3 pounds. The schematic of a one man-day candle is shown in Figure 3. If the atmosphere is continuously maintained by adding oxygen from a stored source, provisions must be made for removing carbon dioxide. The amount of the latter that must be removed is about 2.25 lb/man-day[1].

Various possibilities of CO_2 removal have been considered. These may be classified broadly as regenerative and non-regenerative. The regenerative class includes those systems where the carbon dioxide is adsorbed on molecular sieves that are regenerated by heat and vacuum. It also includes regenerable liquid absorbers such as monoethanolamine.

In the non-regenerative category, chemisorption, freezing out, and diffusion separation with exhaust to space may be mentioned. A list of selected chemicals that may be used to absorb CO_2 is presented in Table 1.

Lithium hydroxide is perhaps the most widely used of the chemisorbers for submarine and space applications. Its characteristics and performance have been well treated in published reports and papers 1,2,4 and will not be considered further.

Magnesium oxide has been studied by the Naval Research Laboratory [4], but results showed that the material absorbed too slowly for practical use. Nevertheless this material may be worthy of further investigation in view of the wide divergence in reactivity of magnesium oxide depending on method of preparation and subsequent treatment.

(2) Combined O_2 Generation and CO_2 Removal with Stored Chemicals

The alkali metal peroxides and superoxides are of particular interest because of their dual role of removing CO_2 and supplying oxygen. The lithium superoxide, theoretically of great interest, has not been prepared in the pure state in any quantity. It is expected that work in this area will be intensified. Sodium superoxide is also a most desirable chemical for atmosphere control in sealed cabins. This material, readily prepared from sodium peroxide[5], reacts with CO_2 to produce oxygen and sodium carbonate:

$$2\ NaO_2 + CO_2 \longrightarrow Na_2CO_3 + 1.5\ O_2 \qquad (1)$$

In practice the RQ of the human component may vary from 0.7 to 1.0, with 0.9 being considered about normal [2]. The RQ of the sodium superoxide system according to equation (1) is 0.67. Thus the reaction may produce excess oxygen and in any event, cannot be controlled to conform to the actual requirements.

Lithium peroxide reacts in the following way:

$$Li_2O_2 + CO_2 \longrightarrow Li_2CO_3 + 0.5\ O_2 \qquad (2)$$

This reaction corresponds to an RQ of 2.0. Thus by the use of mixed oxides and superoxides in air regeneration equipment it is possible to devise a system which compensates for any RQ variation between 0.67 and 2.0.

One approach which suggests itself is to provide two cannisters for atmosphere regeneration. One would contain an alkali superoxide such as sodium superoxide, while the other would contain lithium oxide or peroxide. The atmosphere flow is divided depending on the air composition. A schematic is shown in Figure 4.

c. Comparative Weights of Chemical Storage Atmosphere Control Systems

Table 2 presents a systems comparison between several representative stored systems for a 3-man, 14-day mission in which each man consumes 2.0 lb. of oxygen and produced 2.25 lb. of CO_2 per day. This corresponds to an RQ of 0.82. The tabulation indicates the weights of chemicals required to produce the required 84 lb. of oxygen and remove the necessary 94.5 lb. of CO_2.

The mixed oxide-superoxide system shows a moderate superiority on a weight basis. The actual advantage of the superoxide system is believed to be greater because of its inherent simplicity and potentially high reliability. It is further pointed out that if lithium superoxide could be used to replace sodium superoxide, the weight of the superoxide would be 121 lb., or a total weight of 168 lb. for the conditions specified.

2. Regenerative Atmosphere Control Systems

Many methods have been considered for the provision of breathing oxygen by the regeneration of metabolic products such as water vapor and CO_2. These methods include the thermal decomposition of water and CO_2, photolysis and radiolysis of water, electrolysis of carbonates and aqueous solutions, the chemical reduction of CO_2 with H_2 followed by electrolysis, and the biological regeneration of oxygen from CO_2 by photosynthesis.

Because of the possibility of relatively low weights, volumes, and power requirements of chemical reduction and electrolytic systems, and because of the potential and advantages afforded by the integration of the photosynthetic method into a completely closed ecological system, these latter systems have received considerable attention.

TABLE 2

STORED ATMOSPHERE CONTROL SYSTEMS

WEIGHT REQUIREMENTS FOR 14-DAY, 3-MAN MISSION

$LiClO_4$-LiOH		NaO_2 - Li_2O_2		Cryogenic O_2 - LiOH		Pressurized O_2 (7000 psia) - LiOH	
$LiClO_4$	140 lb.	NaO_2	171 lb.	LiOH	103 lb.	LiOH	103 lb.
LiOH	103 lb.	Li_2O_2	27 lb.	O_2	84 lb.	O_2	84 lb.
Structure	25 lb.	Structure	20 lb.	Structure	90 lb.	Structure	150 lb.
Total Weight	268 lb.	Total Weight	218 lb.	Total Weight	277 lb.	Total Weight	337 lb.

Table 3 presents representative equations for these systems; Table 4 presents volumes, power and weight requirements exclusive of powerplant weights.

The material presented in Table 4 should not be considered as absolute for all suggested missions since different values can be obtained depending upon vehicle requirements. These values, however, do indicate relative weights, powers, and volumes required to provide the gaseous environment for manned space cabins. It is evident from Table 4 that certain systems offer certain weight, volume, and power advantages; for example, the hydrogen reduction system and the LiOH system. However, if one considers operating temperatures and hazards, other systems (such as the photosynthetic system) may offer advantages which offset the weight, volume, and power advantages of the hydrogen reduction or LiOH system. Both the CO_2-H_2 electrolytic and the photosynthetic systems have been more than adequately described in previous publications. Brief descriptions are included in the following for convenience in (1) presenting the present state of development, and (2) describing experimentation necessary to insure availability of such systems for future mission requirements.

TABLE 3

PROMISING O_2 REGENERATIVE SYSTEMS

1. Biological

   A. Algae photosynthetic method

   $CO_2 + H_2O$ + algae + light energy $\longrightarrow O_2$

   + cellular material (C H_2O) + H_2O

   B. Microbial-Electrolysis

   $CO_2 + 2H_2$ (H_2X) + hydrogen bacteria $\longrightarrow$

   cellular material (CH_2O) + H_2O

   $2\ H_2O \xrightarrow{\text{Electrolysis}} 2\ H_2 + O_2$

2. Electrolytic

   A. Anodic generation of O_2 by electrolysis of LiOH

   $2\ LiH + CO_2 \longrightarrow 2\ LiOH + C$

   $2\ LiOH \xrightarrow{\text{Electrolysis}} 2\ LiH + O_2$

   B. Generation of O_2 by electrolysis of NaOH

   $4\ NaOH \xrightarrow{\text{Electrolysis}} 4\ Na + 2O_2 + 2\ H_2$

   $4\ Na + CO_2 \longrightarrow 2\ Na_2O + C$

   $2\ Na_2O + 2\ H_2O \longrightarrow 4\ NaOH$

   $2\ H_2 + 2\ O_2 \longrightarrow 2\ H_2O + O_2$

   C. Hydrogen reduction of CO_2 and O_2 generation by electrolysis of water

   $CO_2 + 2\ H_2 \longrightarrow C + 2\ H_2O$

   $2\ H_2O \xrightarrow{\text{Electrolysis}} 2\ H_2 + O_2$

TABLE 4

TOTAL WEIGHT, VOLUME, AND POWER REQUIREMENTS PER MAN FOR VARIOUS GASEOUS REGENERATIVE SYSTEMS

	Weight lb	Volume ft^3	Power,[b] kw
Photosynthetic			
Elec. Illum.	255	6.15	5.5
Solar Collector	227	9.45[a]	1.7
Microbial-Electrolysis	110-130	~2.2-2.4	.35
LiOH	275	0.7	1.4
NaOH	340	0.9	7.68
CO_2 - H_2	75	1.3	0.36

[a] Folded collector volume

[b] Electrical power required for cooling not included

a. Regeneration of O_2 from CO_2 by Hydrogen Reduction and Electrolysis

This chemical system generates oxygen in a closed environment by the reduction of CO_2 with H_2 to produce solid carbon and water. The water is decomposed by electrolysis to produce hydrogen and breathing oxygen. A system design presently under investigation is shown in Figure 5.

As shown in the illustration, the oxygen regenerator consists of essentially three individual, yet functionally interdependent, components:

1. Chemical reactor for CO_2 reduction with H_2; produces H_2O and carbon.

2. Components for H_2O transfer from reactor into the electrolytic cell.

3. H_2O electrolytic cell for generation of H_2 and O_2.

Each of these three basic components must function so as to provide an operation that satisfies equilibrium conditions between the CO_2 supplied to the generators and the O_2 generated in the electrolytic cell.

The system shown in Figure 5 incorporates the following major provisions:

a. Continuous carbon removal by a rotating catalytic wire mesh belt.

b. Continuous water transfer from the reactor section into the electrolytic cell via porous membranes(water cooled).

c. Hollow electrodes of porous material for removal of gases from the electrolytic cell into the gas phase.

The actual performance of the oxygen regenerator shown in Figure 5 is governed primarily by the chemical constants such as the thermodynamic equilibrium, the chemical kinetics and the catalytic activity of the materials participating in the process of CO_2 reduction, the materials regulating the water transfer into the electrolyte,and electrolysis rates.

One of the critical components in the H_2-CO_2 reduction system is the electrolytic cell. Since this component utilizes the majority of the electrical power required by the system,continued efforts are being made to insure high efficiency electrolysis. In conventional electrochemical systems, gases are generated in the gas-liquid interface; however, in zero-gravity operation, provisions must be made for the circulation of both gases and electrolyte, the separation of the gases from the electrolyte, and the return of the electrolyte to the cell.

In a system being studied at the Tapco Division of Thompson Ramo Wooldridge, double porosity metal electrodes and ion exchange membranes are utilized for the generation of gases in the gas phase, thus avoiding the gas-liquid separation operation. This is accomplished by the use of a double porosity electrode system with fine pores on the liquid side and coarse pores on the gas side.

In summary, it may be stated that an electrolytic cell for space operation should have the following features:

1. No rotating components

2. Low liquid flow rates

3. High current densities

4. High electrical and thermodynamic efficiencies

5. No gas-liquid separation problems.

Continued research is being conducted on the critical components of this system, namely, (1) the choice of appropriate catalysts for the chemical reactor utilized in the chemical reduction of CO_2 with hydrogen, (2) heat and water transfer from the reactor into the electrolytic cell, and (3) gas phase electrolytic systems. However, in order to critically evaluate the feasibility of this system as an atmosphere control device in sustained reduced gravity environments, zero-gravity experimentation must be conducted. Figure 6 shows the required parameters which must be evaluated under zero-gravity conditions. Figure 7 shows a 0.1 man system integrated into a scientific passenger pod for zero-gravity testing. Since there are many missions in which the H_2-CO_2 system shows maximum application, continued work must be carried on to insure the availability of this atmospheric control device for those missions.

b. Regeneration of O_2 from CO_2 by Photosynthetic Methods

Certain plants and micro-organisms, utilizing CO_2 and other chemical nutrients, produce O_2 by photosynthesis.

For each mole of O_2 utilized by man, about 0.85 moles of CO_2 are expelled. The ratio of CO_2 intake by algae to O_2 output can be regulated to lie between about 0.7 to 0.9 by appropriate choice of nutrients. If this ratio is set to 0.85 then a balance can be set between the algae and all the O_2 output of the algae available to man. A schematic representation of such a gas exchange system which would provide O_2 and remove CO_2 photosynthetically in a manned vehicle is presented in Figure 8.

In the system presented in Figure 8, algae in an aqueous medium is pumped from a central reservoir through a light system in which CO_2 is assimilated by the algae and O_2 produced. The temperature of the algae culture is controlled by circulating coolant through coils in the lighting system. The algae is subsequently mixed with CO_2-enriched air from the cabin. The gas-algae mixture is then transported to a gas-liquid separator where O_2-enriched gas is separated from the algae culture. The algae culture is returned to the central reservoir and the enriched gas saturated with water vapor is circulated through an air-conditioning system to the cabin.

Water vapor condensed in the air conditioner may be used for drinking. In addition to providing drinking water, the air conditioner also purifies and regulates the temperature of the gas. The reject heat from the conditioner and the reject heat from the light system cooler is upgraded in temperature and emitted by radiation.

To maintain the desired algae concentration, a portion of the algae mixture is pumped from the central reservoir through a separator. The medium is returned to the reservoir and the harvested algae are either removed to waste storage or reprocessed into nutrients. Nutrients are also provided from a stored nutrient tank which contains necessary chemicals to maintain the nutritional balance of the algae.

The majority of the energy required by the photosynthetic gas exchange system is light energy. To increase the efficiency of such a device, particular attention must be given to the geometry of the illumination system, and the method of providing light of required wave lengths. Of special importance is the selection of an illumination system which integrates with mission and vehicle requirements.

Two possible lighting systems suggest themselves; one utilizes fluorescent lamps, the other uses a solar collector. In the solar collector illuminator, the algae media is illuminated as it passes through a flat duct placed at the focal plane of a semi-circular cylindrical solar collector. Figure 9 presents a system, currently under investigation, which uses fluorescent lamps. As indicated in Table 4, both fluorescent lights and solar collectors are comparable methods of supplying light energy from a weight standpoint, but fluorescent illumination is somewhat more favorable from a volume viewpoint.

In any studies aimed at determining the optimum manner of providing illumination for a specific mission and vehicle system, one must take into careful consideration the feasibility of integrating the illumination devices into the vehicle complex. In order to provide the gaseous requirements for one man, the lower volume fluorescent illumination device requires on the order of 4 kw if one considers a 20% efficient photosynthetic system illuminated by means of 20% efficient fluorescent tubes. However, approximately 3.2 kw heat must be rejected from the photosynthetic system at relatively low temperatures. Solar illuminated devices,on the other hand, require electrical power only for associated components (such as pumps), and heat may be rejected by radiation to space from the backside of required solar collecting surfaces. Choice of this latter type illumination is determined in part by the availability of larger volumes and surfaces.

The photosynthetic systems offer great promise as complete environmental control systems for missions requiring an excess of 150 pounds of oxygen. Their major drawback however, consists in the large power requirements and the associated weight penalties of long-time power systems. The biological systems which should be further investigated are those employing the reduction of metabolic carbon dioxide with hydrogen, utilizing hydrogen-fixing bacteria. Water formed as a result of microbial action is subsequently electrolyzed to breathing oxygen and hydrogen.

This system requires further investigation into methods for matching systems RQ to the human RQ. The advantage of the hydrogen-fixing biological system is its lack of a requirement for light. Because illumination of microbial systems requires large surfaces and associated volumes, the photosynthetic system may be restricted to large fixed installations with large power stations or large solar collector volumes.

PART II

THE CONTROL OF THE THERMAL AND GASEOUS ENVIRONMENT IN LUNAR LIFE SUPPORT SYSTEMS

A. Introduction

The life support system for lunar exploration must provide an environment for the astronaut conducive to the highest level of human performance. Since most of his physical functions as an explorer could be fulfilled by an unmanned probe, the astronaut will be of value primarily in the roles of observation and decision-making. These higher-order functions of the astronaut's capabilities require optimum comfort. In order to achieve an optimum comfort system, the design of the lunar life support system must be based upon a knowledge of the lunar environment, the objectives of the exploratory mission, and the physiological requirements of the astronaut.

B. Factors in the Design of Life Support Systems for Lunar Exploration

As shown in Table 5, the lunar environment is extremely hostile to human life, and exhibits many factors peculiar to itself which must be considered in the determination of design requirements for lunar landing life support systems. Figure 10 shows the temperature variation on the lunar surface from the subsolar point to the limb. Shown in Figure 11 are the changes of surface temperature near the limb, during a lunar eclipse. In 3-3/4 hours, the temperature may drop from 156°F to -186°F; since lunar night is 13 earth days long, it is believed that the temperature on the dark side must approach absolute zero prior to lunar sunrise.[10]

In order to provide an optimum thermal environment for the astronaut in the environment of the moon, in any design analysis, attention must be directed toward elucidation of those factors affecting man's thermal requirements on the lunar surface. These factors may include: (1) reduced gravity; (2) rates of change of temperature; (3) pressure level, atmospheric composition, level of contaminants, atmospheric temperature, humidity, and air motion, and mean radiant temperature of protective garment; and (4) intensity of transmitted solar radiation through transparent portions of the life support system and subsequent heating effects on the astronaut's body.

In order to utilize optimum design criteria, it is necessary to consider the mechanism of thermal regulation in the human body. For example, up until recently, it was hypothesized that heat loss or production was initiated in response to skin temperature. In 1961, Benzinger shed new light on the mechanism of thermal regulation in the human.[11,12] Neurosurgical evidence led him to believe that the temperature-regulating centers are located in the brain. By use of the gradient calorimeter (for measurement of heat loss), respiratory gas analysis equipment (for measurement of heat production), and skin and cranial thermometry (for measurement of the stimulus), a unique experimental approach was developed which verified his hypothesis. He

TABLE 5

SELECTED CHARACTERISTICS OF THE LUNAR ENVIRONMENT

	Factor	Value	Comments
1.	Mean distance from earth	238,857 miles	
2.	Mean diameter	2,160 miles	
3.	Rotational period	27.322 mean solar days	
4.	Intensity of solar radiation	442.2 Btu/hr-ft^2	
5.	Albedo	0.07 [6]	Indicates dark colored, dust covered surface.
6.	Radiation	?	Very little information on magnitude and type of radiation at lunar surface.
7.	Gravity at surface	5.32 ft/sec^2	
8.	Atmospheric pressure	10^{-13} terrestrial atmosphere	Very nearly that in deep space. Moon may serve as excellent location for high-vacuum experimentation. [6,7]
9.	Height range of topographical features	+30,000 ft to -17,000 ft [7]	
10.	Surface texture	Non-uniform; dust-covered	Polarization curves of moonlight are typical of powdery opague surface. [8] Radar signals of 10 cm wavelength indicate particle size in micron to millimeter range. Variation of temperature during lunar eclipse indicates thermal properties of a powdery material in a vacuum. [8] Non-uniform distribution due to hyper-velocity meteorites impacting on surface and accelerating much of dust layer to escape velocity. [8]
11.	Bearing properties of surface	?	Unknown, but will be under intensive investigation in order to define engineering requirements of Apollo landing gear. [8]
12.	Surface temperature	273°F to -460°F [10]	
13.	Sub-surface temperature	< 32°F 5-10 cm below surface	From long-wave, infra-red analysis. [8]
		-22°F c. one meter below surface	May be too low. [7]
14.	Meteor flux	$\phi = 10^{-12}\ m^{-10/9}$ [9]	ϕ = meteor flux (number of particles/met^2-sec) m = particle mass (gms) Same flux as incident to earth atmosphere. This relationship verified by earth satellite instrumentation.
15.	Penetrating flux for aluminum	$\psi = 5.20 \cdot 10^{-12}\ t^{-10/3}\ v^{10/9}$ [9]	ψ = penetrating flux (penetrations/met^2-sec) t = thickness of thin sheet (cm) v = impact velocity (km/sec)

found that evaporative heat loss is nearly proportional to the increase in cranial temperature above a 37.11°C set point, and increases to four times the resting heat loss for an increase in cranial temperature of only 0.5°C. These findings are shown in Figure 12. In addition, it has been demonstrated that the relation between cranial temperature and sweat rate is independent of work rate and skin temperature; thus it may be concluded that a unique relationship exists between cranial temperature and the powerful heat loss mechanism of sweating. This finding should be explored further in order to ascertain the feasibility of incorporating sensors in the thermal helmet portion for control of the sealed capsule's regulation system. In addition, further work in this area is required in order to define the required state, flow rate, and distribution of gaseous atmosphere over each segment of the body in protective garments under reduced pressures and gravity.

In the design of lunar life support systems, attention should be given to matching work loads to system requirements. For sedentary individuals, the optimum environmental conditions have been thoroughly investigated. However, the required thermal conditions for working individuals in reduced pressure atmospheres and reduced gravity conditions are not so well defined. It has been found that in the terrestrial environment, the required temperature for a work rate corresponding to a metabolic rate of 850 btu/hr (approximately equivalent to walking at 2-½ miles per hour) is 69°F at an RH of 50 percent.[13] The radiation and convection loss will total 425 btu/hr, and evaporative heat loss will also be 425 btu/hr. Continued theoretical and experimental work must be conducted however, to determine relative effects under conditions simulating the life support system in the lunar environment.

Another factor of prime importance in the design of a thermal environment for lunar spacecraft is the mean radiant temperature. As shown in Table 6, radiation exchange is the larger fraction of human heat loss. Since in reduced gravity and pressures, convective heat loss is reduced*, thermal regulation by control of radiant interchange becomes extremely important.

TABLE 6

HEAT EXCHANGE PARTITION,

77°F db = 77°F mrt

Partition	Heat Loss, Btu/hr	% of Total
Radiation	163	40.8
Convection	87	21.7
Evaporation	150	37.5
	400	100.0

In a terrestrial environment (with natural convection) at an ambient temperature of 77°F, the average body surface temperature is 87°F.[17] In a reduced gravity sealed environment, with air at 14.7 psia and forced convection with a velocity of 10 ft/min., the ambient air temperature should be 75°F in order to provide a body surface temperature of 87°F.

With an oxygen environment at 5 psia and forced convection with a velocity of 10 ft/min., the ambient temperature should be 73°F. Although the required ambient gas temperature is not appreciably changed, the proportion of radiation to convection is appreciably altered. In the case of the terrestrial environment, a decrease in mean radiant temperature of 1°F can be compensated for by an increase in air temperature of 0.5°F. In the case of air at 14.7 psia and a reduced gravity environment, a decrease in mean radiant temperature of 1°F is compensated for by an increase in air temperature of 3.4°F. For oxygen at 5 psia, the ratio is 1°F mean radiant temperature change to 5.8°F air temperature change.

Much work remains to be done in the design of optimum thermal control instrumentation for lunar life support systems. Obviously, the extrapolation of subjective comfort evaluations (as well as objective physiological data) from terrestrial

---

* The free convection heat transfer coefficient for the human body takes the form: $h = C \cdot \frac{k}{L} (N_{Gr} \cdot N_{Pr})^{\frac{1}{4}}$ where: h = free convection heat transfer coefficient; C = a constant; k = thermal conductivity of gaseous atmosphere; L = a characteristic length = 1 ft. for a man in an air atmosphere; N_{Gr} = Grashof number; and N_{Pr} = Prandtl number.

Assuming an air pressure of 5 psia in the lunar life support system, the ratio of heat transfer coefficient on the moon as compared to the terrestrial environment is obtained from the definition of Grashof number and the variables of interest:

$$\frac{h_m}{h_e} = \left(\frac{g_m}{g_e} \cdot \frac{p_m^2}{p_e^2} \right)^{1/4}$$

where: g = gravitational acceleration, ft/sec^2; e = earth; m = moon; and p = pressure of atmosphere, psia.

Thus, $h_m/h_e \approx \left(\frac{1/6\ g}{g} \cdot \frac{5^2}{15^2} \right)^{\frac{1}{4}} \approx 0.49$

It is therefore apparent that an appreciable amount of natural convection may occur in the lunar life support system; however, it should be recognized that inertial forces on the gas mass induced by the motion of the system as well as by the gas flow and distribution system will cause forced convection heat transfer to predominate.

environments to the environment of the life support system on the lunar surface, through heat transfer analysis alone, is open to criticism. Additional partitional calorimetry studies are needed to define the effects of gas composition, pressure,and motion on objective as well as subjective physiological reactions. Although a great deal of fundamental information is lacking, preliminary analyses of requirements for lunar environmental control systems should be conducted in order to ascertain critical problem areas. Such an analysis is presented in the following section.

C. Analysis of Requirements for Lunar Environmental Control Systems

A preliminary analysis of the lunar environment, the physiological requirements for sustaining man in this environment, and the mission objective for lunar exploration indicate that the lunar life support system must be a mobile capsule - suit combination. The requirements for this life support system are shown schematically in Figure 13. In order to determine the types of instrumentation and equipment which would meet the requirements of the lunar life support system in an optimum manner, preliminary engineering analyses of expected loads, and of methods for protecting the human component from these loads, must be conducted.

1. Sealed Cabin Atmosphere Selection

Several atmospheric compositions have been considered for space vehicle environment, such as an oxygen-nitrogen mixture at a total pressure of 11.0 psia, oxygen-helium at 6.5 psia, oxygen at 11.0 psia, oxygen at 5.0 psia, and oxygen-neon at 11.0 psia.[14] The physiologically acceptable partial pressure range of oxygen in the atmosphere is limited by a decrease in human performance below a pressure of 1.64 psia, and by the toxic effects of breathing pure oxygen at a pressure above 8.2 psia. To reduce the hazard of decompression sickness under conditions of slow cabin leakage, a pressure of 3.5 psia is desirable.[15] The inert component of the atmosphere is selected to minimize fire hazard,blower power requirements, and vocal pitch change, and to maximize heat transport properties.

It may be assumed that the volume of the lunar life support system is small, and as a consequence the decompression time in the event of meteor puncture would be small, regardless of the initial pressure. Thus, rapid decompression could best be prevented by a self-sealing layer and an atmospheric gas supply sufficient to maintain pressure until a return to the operational base. In order to minimize leakage and insure flexibility of any movable portions of the system, a total pressure in the range 5 to 10 psia is desirable.

An optimum system may incorporate a neck seal which permits ventilation of the helmet portion with 5.0 psia oxygen, and the ventilation of the balance of the system with low-pressure nitrogen.

2. Thermal Shielding from Lunar Environment

The temperature of the lunar surface varies from a high of 273°F at the subsolar point to perhaps as low as -460°F before lunar sunrise. Consequently, it is necessary to minimize thermal interchange with the lunar surface insofar as possible. In addition, solar radiation reaches the lunar surface unattenuated; thus both direct solar and reflected solar radiation are incident upon the life support system. In the following paragraphs, a brief analysis is presented on the thermal loads transmitted to a lunar life support system assumed to have an area 1.3 times the area of the human component and insulated by means of super-insulation.

Super-insulation is considered due to its many advantages in the lunar environment. These advantages include:

1. Extremely low transmittance
2. Light weight
3. No need to evacuate the insulation in the lunar environment
4. Ease of application of selective metal coatings
5. May serve as shield to protect against meteorite puncture.

The primary disadvantage of super-insulation, however, is its fragility and lack of flexibility. Approximately 1/4 inch thickness will be required, and this thickness may comprise 10 to 20 layers of foil.[16] It is desirable to select a surface for the system that will provide minimum absorption of solar and infra-red radiation. A silver coating, for example, will provide this function, due to its low solar and infra-red absorptivities, 0.07 and 0.02 respectively.

The thermal load transmitted to the interior of the lunar life support system is the net sum of the load components:

$$q_{system} = q_{solar} + q_{albedo} \pm q_{thermal\text{-}lunar} - q_{space}$$

The heat transferred through the insulation surrounding the system is:

$$q_{system} = U A_s (T_s - T_e)$$
$$= 0.02 \cdot 25.4 (T_s - 537)$$
$$= 0.508 (T_s - 537)$$

where:

U = transmittance of insulation, 0.02 Btu/hr-ft^2

A_s = system area = 19.5 x 1.3 = 25.4 ft^2

T_s = temperature of system exposed to lunar environment, °R

T_e = environmental temperature within system = 77°F = 537°R

The solar radiation absorbed by the system is:

$$q_{solar} = I_s A_{ps} \alpha_s$$
$$= 442.2 \cdot 3 \cdot 0.07 = 92.9$$

where:

I_s = solar intensity on lunar surface, 442.2 btu/hr-ft^2

A_{ps} = irradiated area of system, assume 3 ft^2

α_s = solar absorptivity, 0.07

The albedo absorbed by the system is:

$$q_{albedo} = a\, I_s\, \alpha_s\, A_{rs}\, F_{rs-m}$$
$$= 0.07 \cdot 442.2 \cdot 0.07 \cdot 20.3 \cdot 0.5$$
$$= 22 \text{ btu/hr}$$

where:

a = moon albedo = 0.07

A_{rs} = surface area of astronaut x (system area/surface area) x (radiating area/system area)

$= 19.5 \cdot 1.3 \cdot 0.8 = 120.3$ sq. ft.

F_{rs-m} = view factor (system surface to lunar surface) = 0.5

The thermal interchange between the system and the lunar surface is:

$$q_{thermal-lunar} = \sigma A_{rs} F_{rs-m} \alpha_t \cdot (T_m^4 - T_s^4)$$
$$= 0.173 \cdot 20.3 \cdot 0.5 \cdot 0.02 \cdot \left[\left(\frac{T_m}{100}\right)^4 - \left(\frac{T_s}{100}\right)^4\right]$$
$$= 0.0351 \left[\left(\frac{T_m}{100}\right)^4 - \left(\frac{T_s}{100}\right)^4\right]$$

where:

σ = Stefan-Boltzmann constant

α_t = thermal absorptivity = 0.02

T_m = temperature of lunar surface, $^\circ$R

The thermal radiation to space is:

$$q_s = \sigma A_{rs}\, \alpha_t\, T_s^4$$
$$= 0.173 \cdot 20.3 \cdot 0.02 \left(\frac{T_s}{100}\right)^4$$
$$= 0.0703 \left(\frac{T_s}{100}\right)^4$$

Summing the above equations provides

$$0.508\,(T_s - 537) = -0.105 \left(\frac{T_s}{100}\right)^4$$

on the shade side of the moon.

And,

$$0.508\,(T_s - 537) = 115 + 0.035 \left(\frac{733}{100}\right)^4 - 0.105 \left(\frac{T_s}{100}\right)^4$$

on the sun side at the sub-solar point.

These relationships are plotted in Figure 14, from which it is seen that the maximum heat gained by the life support system at the sub-solar point is 50 btu/hr with the outside surface temperature of the system reaching 175°F. On the shade side of the moon, the heat loss is 45 btu/hr with the surface temperature dropping to -10°F.

Since shading devices can be provided to minimize heat gains from the transmission, and ultimate absorption, of solar radiation passing through transparent sections of the system at as low a value as desired, this load source is purposely neglected.

3. Meteor Shielding

Bjork[9] gives the following relationship between penetrating flux, sensitive area, and time of exposure for a 0.99 probability of no puncture in the sensitive area,

$$\exp(-\psi A \tau) = 0.99$$

where:

A = sensitive area, meters^2

τ = time of exposure, seconds

ψ = penetrating flux

Combining the relationship for penetrating flux with the above yields the required aluminum thickness to protect with a 0.99 probability of no puncture.

$$t = 1.9 \cdot 10^{-3} \cdot v^{1/3} \cdot (A\tau)^{3/10}$$

The above expression for t is plotted against A in Figure 15 for the appropriate meteor velocities.

For a life support system with a sensitive area of 1.90 sq. meters, in a six-hour mission

$$A\tau = 1.90 \cdot 6 \cdot 3600 = 40{,}800$$

and $\log_{10} A\tau = 4.61$

and consequently, from Figure 15, the required armor must be 0.1 cm or 0.039 in. thick.

Multiple foils of thermal insulation will serve the dual purpose of insulation and meteorite shielding. Due to particle break-up with multiple shields, it has been demonstrated that materially less total shield thickness may be required than the single 0.039 in. shield calculated above.

4. Atmospheric Temperature and Humidity Control

The individual in the lunar life support system might induce a sensible load of 425 btu/hr and a latent load of the same magnitude during maximum work. For optimum comfort, the cabin atmosphere and mean radiant temperature should be 65°F. An atmospheric relative humidity of 50 percent is desirable.

The total maximum sensible load on the cooling system will be the sum of the conduction load through transparent sections of the system, person load, and equipment load. The aggregate of these loads is 500 btu per hour. Assuming no moisture sources in the system other than the man, the maximum latent load is 425 btu per hour. The total cooling load is thus 925 btu per hour.

The high temperature on the sun side of the lunar surface precludes the direct rejection of the sensible load to the lunar environment; therefore some form of refrigeration must be provided.

Methods which suggest themselves include:

1. Vapor cycle refrigeration
2. Evaporative cooling
3. Regenerative ice refrigeration

Schematics of these three systems are shown in Figure 16. System specifications are found in Table 7.

A psychrometric analysis of the atmosphere-conditioning process discloses that the heat exchanger surface temperature should be approximately 40°F in order to remove the required amount of sensible and latent heat.

The vapor cycle system requires a space radiator for heat rejection. A high radiator inlet temperature provides a small radiator area, a low cycle efficiency and a large power supply for the compressor. Thus, the system weight must be optimized.

The optimum mounting position of a radiator with selective surface coating would be on the top of the lunar life support system. The equivalent space temperature, assuming the worst condition (normally incident solar radiation), for this radiator would be approximately 86°F. Equivalent space temperature for a side-mounted radiator would be higher, due to the fact that the unit would "see" the high-temperature lunar surface.

If dehumidification by adsorbent bed or absorbent spray is used, the surface temperature of the heat exchanger can be materially higher and the coefficient of performance of the refrigeration system can correspondingly be raised. Such systems require high temperature reactivation, however, and water reclamation is awkward.

As noted earlier, it has been postulated that the temperature a few centimeters under the lunar surface is below the freezing point of water. Assuming that the dust layer can be removed from underneath the lunar life support system by jet blast or other means, a low temperature heat sink would be available. A flexible bag enclosing a substance of large heat-of-fusion such as water might be placed in good thermal contact with the lunar surface in the cleared area when the life support system is stationary. During this period the water would freeze. During mobile operations, the bag would be retracted, and the heat generated in the life support system would be rejected to it by suitable means.

TABLE 7

SYSTEM SPECIFICATIONS

	Vapor Cycle Refrigeration	Evaporative Cooling	Heat Transfer to Lunar Sub-Layers
Minimum heat exchanger surface temperature, °F	40	40	40
Refrigerant temperature, °F	30	30	30
Radiator temperature, °F	200	-	-
COP	1.56	-	-
Compressor power, HP	0.2	-	-
Blower power, HP	0.02	0.02	0.02
Battery requirement for 6-hour mission, w-hr	1014	90	90
Radiator area, ft^2	17	-	-
Fixed weight, lb.	12	2	18*
Weight determined by 6-hour mission, lb	32	10	2
Total wt., 6-hour mission	44	12	20

* Assuming regeneration every 2 hours.

System weights as a function of mission length are shown in Figure 17. For the vapor refrigeration cycle, the fixed weight items are the compressor, radiator, heat exchanger, fan, and expansion valve. The battery weight depends upon mission time. In the water boil-off system, fixed weight items are the heat exchanger and fan. Battery weight and initial water inventory depend upon mission time. The fixed weight items in the regenerative ice refrigeration system are the heat exchanger, fan, pump, and ice inventory. It is assumed that regeneration is provided every two hours. Battery weight depends upon mission time.

The secondary batteries of all three systems are rechargeable at the operational base (or vehicle). No working media are expended in the vapor-cycle

TABLE 8

CHARACTERISTICS OF A LUNAR LIFE SUPPORT SYSTEM

Form	Suit-Capsule Combination	
Thermal shielding	Aluminum foil super-insulation, $\frac{1}{4}$ inch thickness with silver coating on outside.	
Meteor shielding	For 0.99 probability of no puncture in six-hour mission, 0.039 inch aluminum sheet required. May be integrated with thermal shield.	
Atmosphere	In Helmet	In Capsule
Composition	O_2	N_2
Pressure	3.5 psia minimum 5.0 psia recommended	5.0 psia
Regeneration	Passive mixed super-oxide chemical	Dehumidification and cooling by heat-exchanger

Optimum state of atmosphere	At Rest	Working
	73°F	65°F @ 50% RH

Cooling load: Btu/hr	Sensible	Latent
Conduction from lunar environment	50 gain on sun side [a] 45 loss on shade side [b]	
Person load	425	425
Misc. load	25	
Total max. sensible	500	500
Total max. cooling load		925

Probable heat sink	Water boil-off
Mobility provided by	Jet propulsion or land contact

a. Outer surface temperature = 175°F

b. Outer surface temperature = -10°F

or regenerative ice refrigeration systems. In the water boil-off system, water is lost; however, excess water produced by the power and atmosphere control systems in the mother vehicle can be used for this supply. In conclusion, water boil-off shows desirable weight and systems features for thermal control of lunar life support systems for mission times of at least 6 hours.

D. Characteristics of a Mobile Lunar Life Support System

In summary, it may be stated that the results of a preliminary analysis of a lunar life support system indicate that the system must be of a capsule-suit combination. Due to the texture and topographic features of the lunar surface, it may be desirable to propel the life support system by both jet and land contact, as required by the mission objectives. Mobility can be provided by jet propulsion in order to explore topographical features of considerable height range or areas remote to the operational base. Provision for over-land propulsion would be desirable in order to allow vernier control of position for close inspection and minimum disruption of surface detail. From reliability considerations, it would be desirable to provide means of propelling the system by muscle power in the event of component or subsystem failure. The outer surface of the system may be lined with a metallic foil, serving both as a vacuum super-insulation and meteoroid shield.

In order to minimize leakage and rigidity of flexible parts, a low-pressure atmosphere should be selected. The optimum system may incorporate a neck seal to permit ventilation of the helmet portion with 5.0 psia oxygen, and ventilation of the balance of the system with low-pressure nitrogen. The environmental temperature should be adjusted automatically over the range of 73°F to 65°F. The adjustment of the optimum temperature would preferably be controlled by work rate. Manual overrides should be provided. Controlled water removal should result in an ambient humidity at a value near 50 percent. Cooling by water boil-off and the control of breathing by a passive mixed superoxide chemical reactor appear promising as thermal and atmosphere control techniques for missions up to 6 hours in duration.

Suggested characteristics of a life support system for lunar exploration are summarized in Table 8.

REFERENCES

1. Waggoner, J.N., and W.L. Burriss, "Problems and Progress in Providing an Earth Environment for Manned Space Flight", ARS Paper 2102-61.

2. "Propellant-Atmosphere System Study", Thompson Ramo Wooldridge Inc., Contract No. AF 33(616)-6514, WADD Technical Report 60-622, March 1961.

3. Schecter, W.H., R.R. Miller, R.M. Jackson, and J.R. Pappenheimer, "Chlorate Candles as as a Source of Oxygen", Ind. and Eng. Chem., 42, 2348, 1950.

4. Miller, R.R., and V.R. Piatt (editors), "The Present Status of Chemical Research in Atmosphere Purification and Control on Nuclear-Powered Submarines", Naval Research Laboratory Report 5465, p. 119.

5. Stephanou, S.E., W.H. Schecter, W.J. Argersinger, and Jacob Kleinberg, "The Absorption of Oxygen by Na_2O_2: Preparation and Magnetic Properties of Sodium Superoxide", Journal Am. Chem. Soc., II, 1819, May 1949.

6. Ballinger, J.C., J.C. Elizalde, and E.H. Christensen, "Thermal Environment of Interplanetary Space", SAE Paper 344B, 1961.

7. Campbell, Paul A., "Research Programs - II; The Lunar Colony", Lectures in Aerospace Medicine, School of Aviation Medicine, USAF Aerospace Medical Center (ATC), Brooks AFB, Texas, January 1960.

8. Shoemaker, Eugene M., "Exploration of the Moon's Surface", American Scientist, 50, 1, March 1962.

9. Bjork, R.L., "Meteoroids versus Space Vehicles", ARS Paper 1200-60, 1960.

10. Tombaugh, Clyde W., "Moon, Mars, and Venus", Lectures in Aerospace Medicine, USAF Aerospace Medical Center (ATC), Brooks Air Force Base, Texas, January 1960.

11. Benzinger, T.H., A.W. Pratt, and Charlotte Kitzinger, "Thermostatic Control of Human Metabolic Heat Production", Proceedings of the National Academy of Sciences, 47, 5, 730-739, 1961.

12. Benzinger, T.H., "Sensory Reception and Control of Temperature in Man", ASME Paper No. 59-A-214, 1959.

13. ASHRAE Guide - 1959, American Society of Heating, Refrigerating, and Air Conditioning Engineers, pp. 66-67, 1959.

14. Breeze, R.K., "Space Vehicle Environmental Control Requirements Based on Equipment and Physiological Criteria", ASD Technical Report 61-161, Part I, pp. 96-100, 1961.

15. Ibid., pp. 37, 95.

16. Barron, Randall R., "Superinsulations", Machine Design, 33, 5, 116, 1961.

17. Janssen, J.E., "Thermal Comfort in Space Vehicles, ASME Paper 59-A-209, December 1959.

ACKNOWLEDGEMENTS

The authors respectfully acknowledge the contributions of Drs. N. Fatica and F. Miraldi and of Mssrs. A.D. Babinsky and R.S. Pauliukonis, without whose helpful contributions this report would not have been possible. We also wish to express appreciation to Miss Joyce Scheatzle for her help in preparation of the manuscript.

ATMOSPHERE CONTROL SYSTEMS FOR MANNED SEALED ENVIRONMENTS

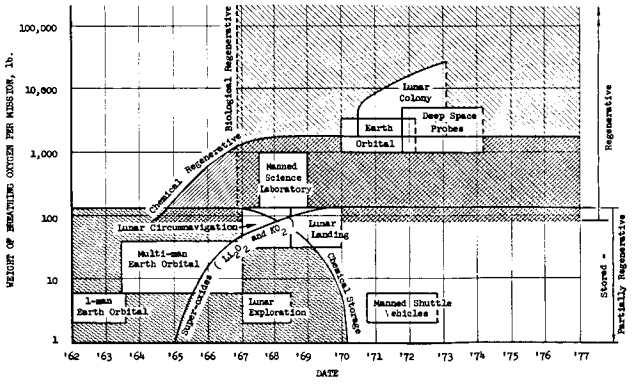

FIGURE 1

SYSTEM WEIGHT VS. MISSION DURATION FOR MOLECULAR O_2

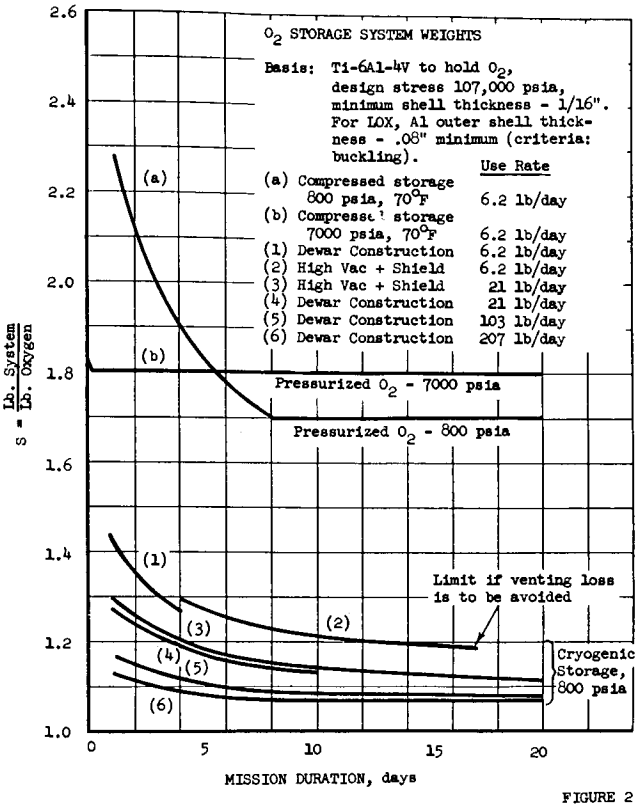

FIGURE 2

SCHEMATIC OF A ONE MAN-DAY PERCHLORATE CANDLE

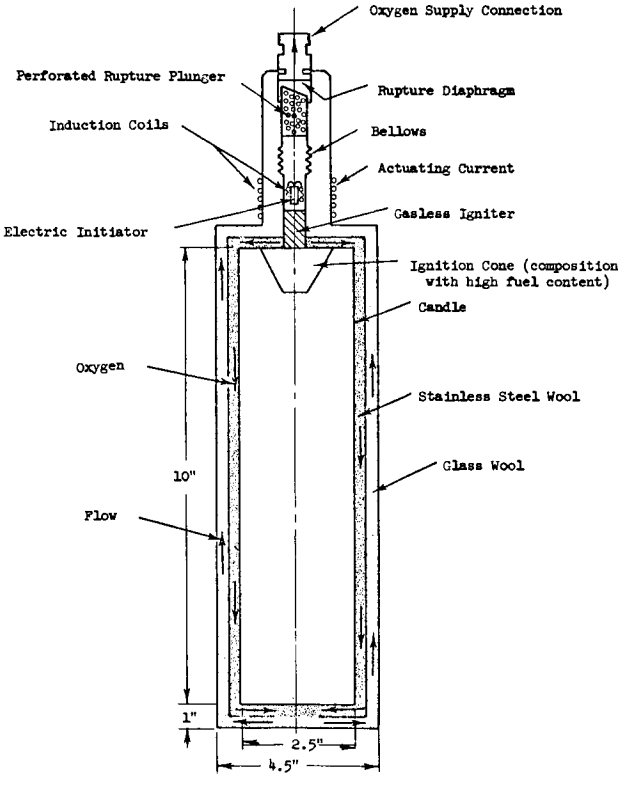

FIGURE 3

SCHEMATIC OF ATMOSPHERE REGENERATION SYSTEM USING SODIUM SUPEROXIDE AND LITHIUM PEROXIDE

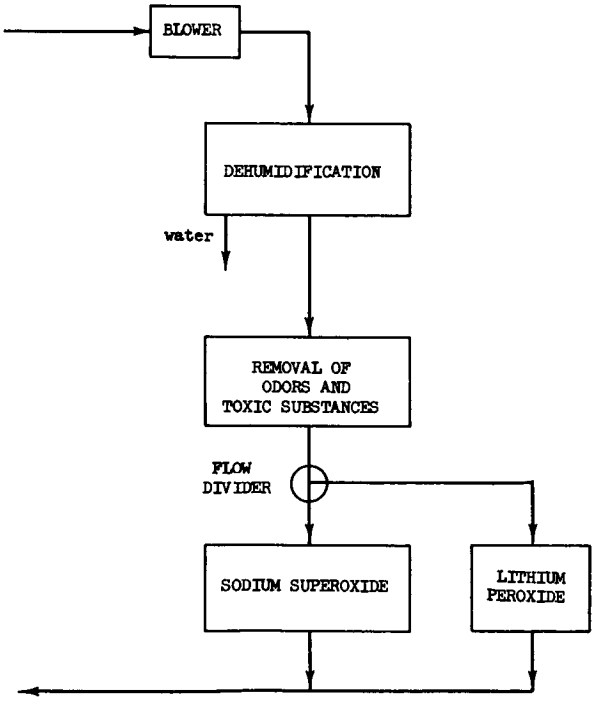

FIGURE 4

OXYGEN REGENERATION (FLIGHT TEST SYSTEM)

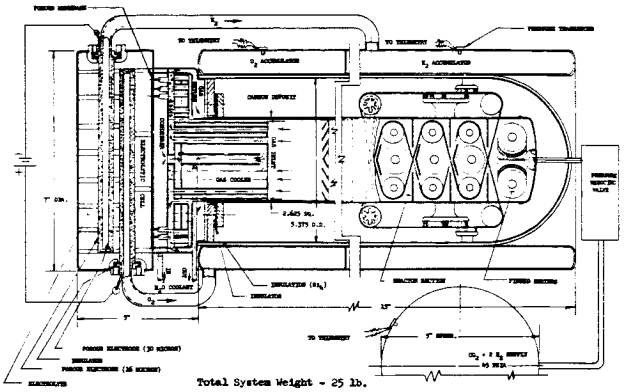

Total System Weight - 25 lb.

FIGURE 5

Photosynthetic Oxygen Regeneration System

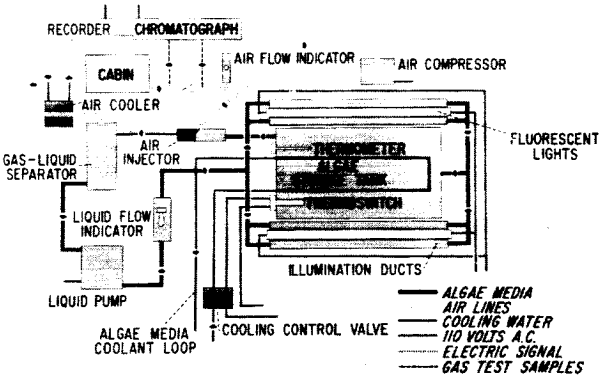

FIGURE 8

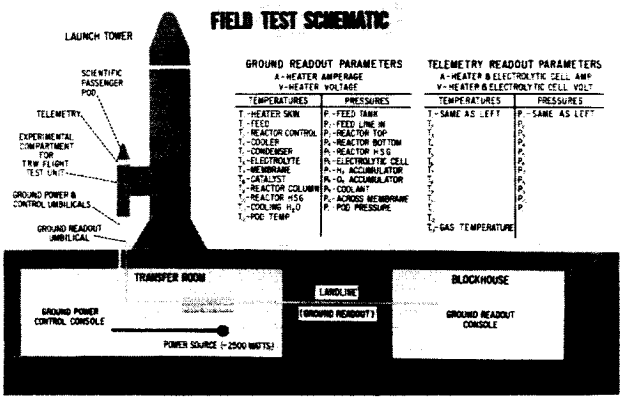

FIGURE 6

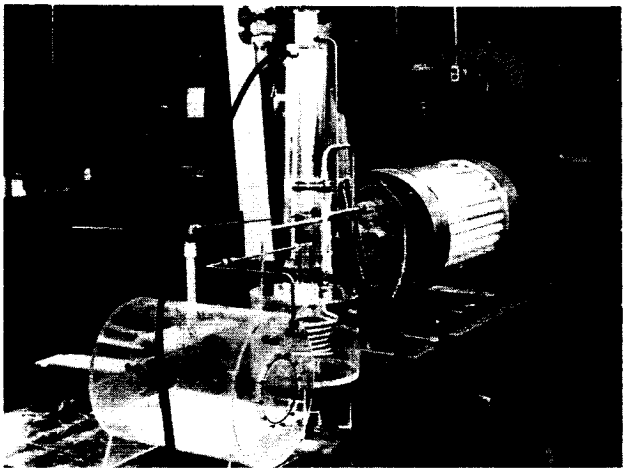

FIGURE 9 ALGAE ILLUMINATION CHAMBER

TEMPERATURES OF VARIOUS AREAS ON THE EARTH'S FACE OF THE MOON
(from Pettit and Nicholson)

FIGURE 10

SIMPLIFIED SYSTEM DIAGRAM INTEGRATED SCIENTIFIC PASSENGER POD

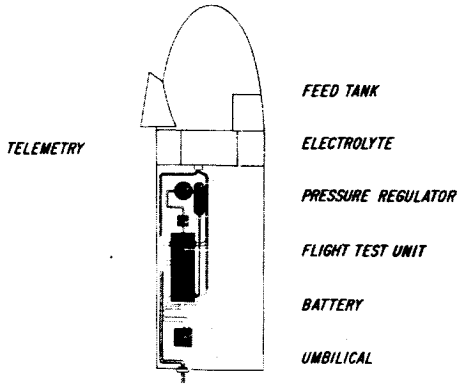

FIGURE 7

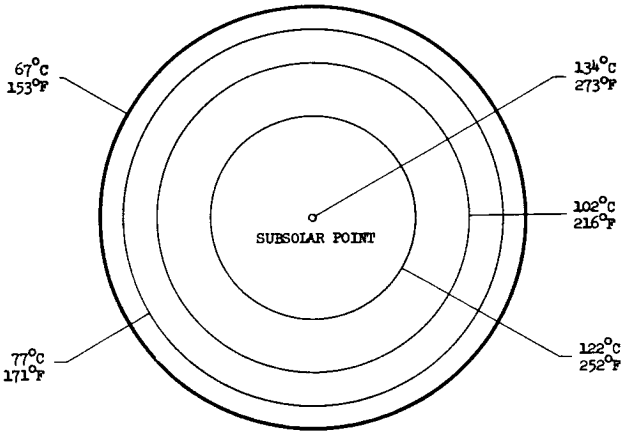

This page is reproduced again at the back of this report by a different reproduction method so as to furnish the best possible detail to the user.

TEMPERATURES ON THE EARTH'S FACE OF THE MOON DURING LUNAR ECLIPSE
TAKEN 2 MIN. FROM SOUTH LIMB
(from Pettit and Nicholson)

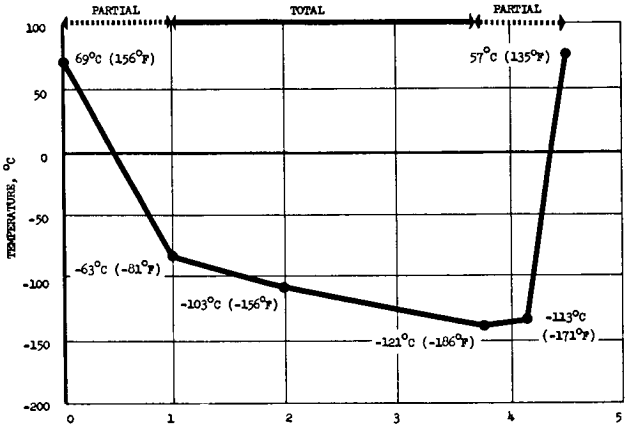

FIGURE 11

LUNAR LIFE SUPPORT SYSTEM REQUIREMENTS

FIGURE 13

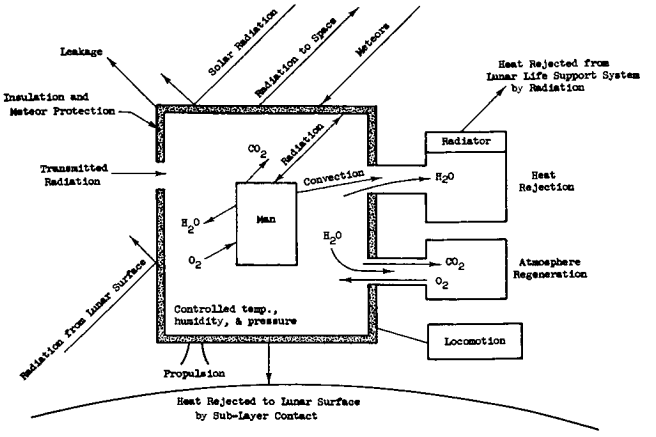

METABOLIC HEAT PRODUCTION AND EVAPORATIVE HEAT LOSS AS A FUNCTION
OF CRANIAL AND SKIN TEMPERATURE

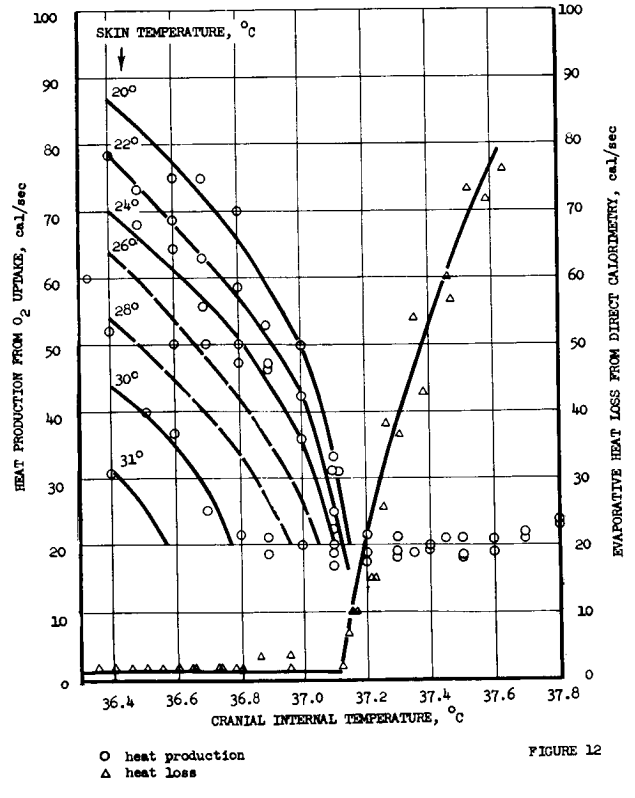

FIGURE 12

THERMAL LOADS FROM LUNAR ENVIRONMENT

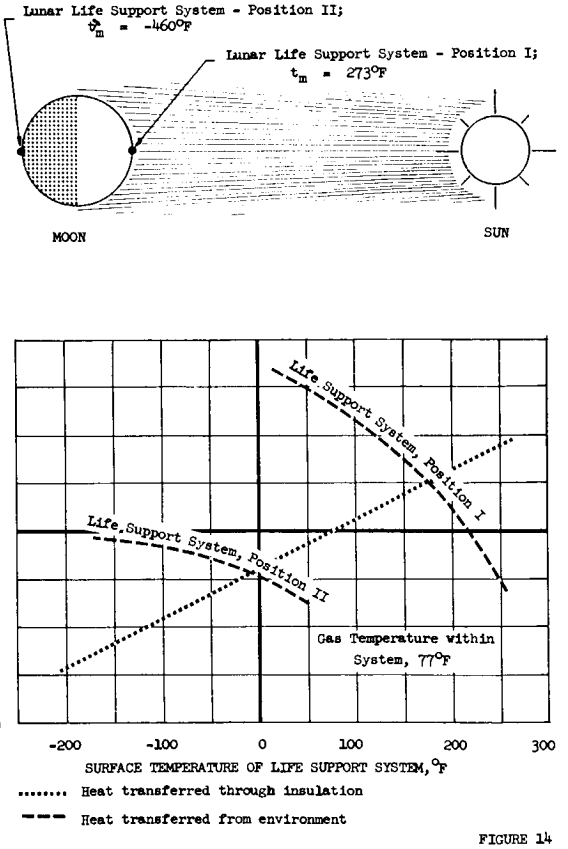

FIGURE 14

ALUMINUM SKIN THICKNESS REQUIRED FOR METEOROID PROTECTION

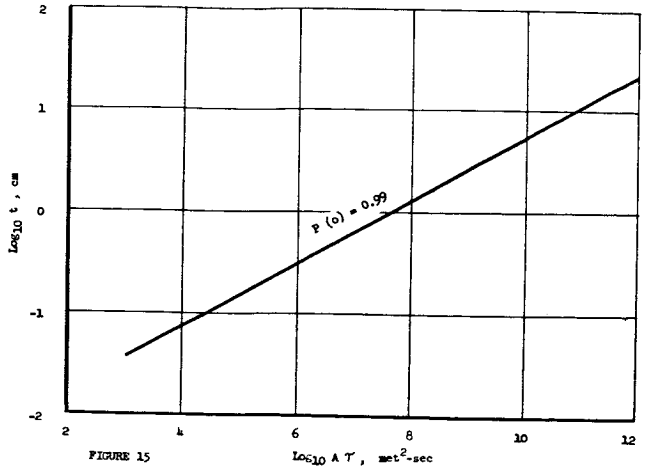

FIGURE 15

SYSTEM WEIGHT AS A FUNCTION OF MISSION TIME

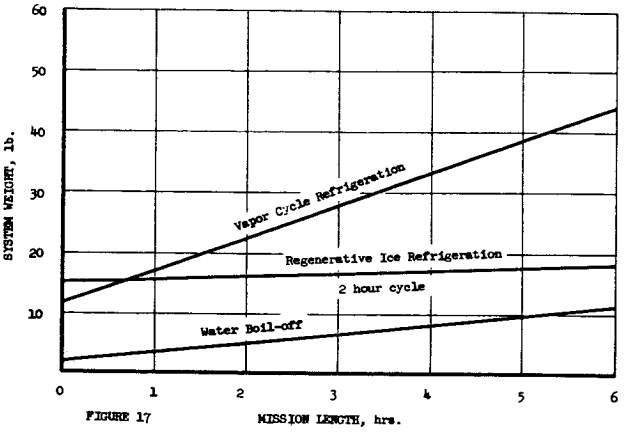

FIGURE 17

SCHEMATICS OF ATMOSPHERE COOLING SYSTEMS

FIGURE 16

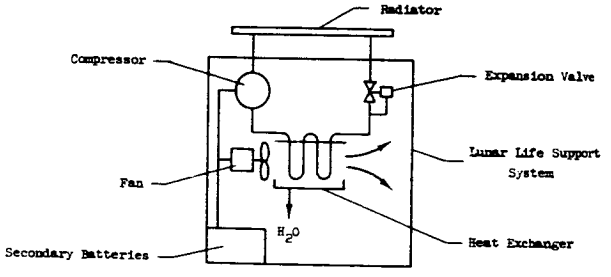

Vapor Cycle Refrigeration

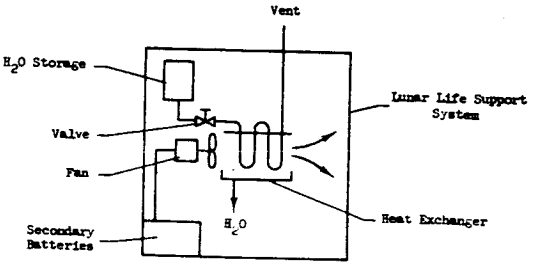

Water Boil-off

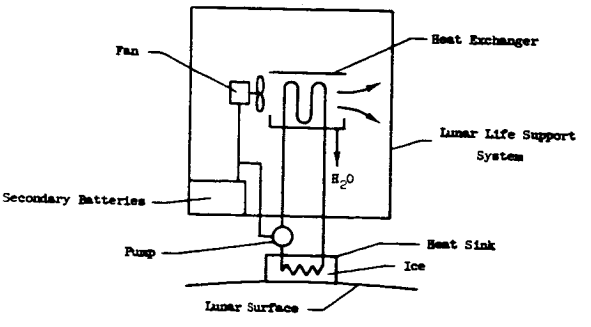

Regenerative Ice Refrigeration

ADVANCED ENVIRONMENTAL SYSTEMS

N62-14474

John L. Mason
Chief Engineer
AiResearch Mfg. Co.

William L. Burriss
Staff Engineer
AiResearch Mfg. Co.

Abstract

Atmosphere controls for advanced manned space vehicles will in some cases require techniques different from those selected as optimum for the Mercury environmental control system (ECS). Water conservation will be rigorous for vehicles which use a solar or nuclear auxiliary power unit (APU). For missions longer than a few hundred hours, CO_2 will be removed in a regenerable process. Several promising regenerable CO_2 removal systems are presented, including freeze-out.

Regeneration of oxygen from CO_2 is discussed as the next step in atmosphere control advancement. Test work on CO_2 hydrogenation by the Sabatier process is cited. The recommended makeup of ECS elements is presented as a function of mission duration.

Introduction

Environmental control systems (ECS) include at least the following functional elements:

1. Thermal management
2. Water management
3. Atmosphere composition management
4. Food management
5. Waste management
6. Power management

In terms of the equipment selected to perform these functions, considerable overlap exists because of multi-function elements. For example, a cooler-condenser-water separator performs in one component essential functions of thermal management, water management, and atmosphere composition management. Functional tie-ins exist between the ECS and other subsystems. For example, thermal management should extend to the thermal design of power-consuming equipment, to provide a suitable path for heat flow from source to sink, compatible with low-penalty liquid cooling media[1,2].

This paper considers in detail the subjects of water management and the part of atmosphere composition management related to CO_2 removal. Other ECS elements are considered only in a summary chart which makes recommendations as a function of mission duration.

Water Management

Water management is a key problem in space vehicle environmental control, for three reasons:

1. Water is essential to human life over time spans short compared to durations of presently planned space missions.

2. The quantities of water required for life support are larger than required quantities of any other constituent.

3. Water management is functionally interrelated to several other elements of environmental control, such as energy-balance comfort in terms of atmosphere humidity control, and CO_2 removal.

Table I shows a typical human material balance, as estimated for a space mission of several days or longer. As shown by the footnotes to the table, the numbers contain varying degrees of arbitrariness; however, they should be quite adequate for purposes of system parametric analysis and evaluation.

Table II is made up of the water entries from Table I. The listing shows a total of water produced of 12.25 lb/man day, compared with a total consumption of 11.0 lb/man day. The excess of 1.25 lb represents approximately 1.0 lb metabolic water (formed by oxidation of hydrogen in food) and 0.25 lb of water present as H_2O in the food supply. (The 0.25 lb of water in the food supply represents a free source of water as long as stored food is carried. Missions for which food is reprocessed are beyond the scope of this paper.)

Given the objective of closing the water loop to the extent of providing all the drinking, cooking and wash water needed, the favorable margin of 1.25 lb/man day is narrow enough to pose a challenging problem to the vehicle and ECS designers. They must not only design efficient water recovery equipment, but also minimize casual losses of water from the system, as by leakage overboard or migration into unrecoverable areas on the vehicle.

A more ambitious water loop closure would include oxygen recovery from the metabolic water as well as purification of the waste water. This is not recommended, even for a 3000 hour mission, although on a mission of this length oxygen would be recovered from CO_2. Some material losses are inevitable in a nominally closed system. Water storage can be provided to make up these losses. Oxygen recovery will be discussed further under CO_2 management.

The allocation of 5.7 lb/man day for production of exhaled and perspired water vapor merits some discussion. This water production is consistent with a metabolic rate approximately 150% of the basal metabolic rate (BMR) for a 90 percentile man, and with a 50-50 split of the metabolic heat output between latent and sensible cooling. The assumed metabolic level appears reasonable for space missions of a few days or longer, where physical activity will be inherently somewhat limited. The 50-50 latent-sensible split of the metabolic heat load is based on the assumption that the astronaut spends about half his time in a pressure suit (where the cooling load is

about 65% latent), and the other half of his time in a shirt-sleeve environment (where the cooling load is about 65% sensible). The cooling load for suit occupation is largely latent because of the restricted suit ventilation rates compatible with reasonable power consumption.

The 5.7 lb/man day figure is representative of the average quantity of exhaled and perspired water vapor available for recovery; the actual design of recovery equipment could well be predicated on even higher peak rates.

As far as the human water balance is concerned, any recovery system which comes within (approximately) 1.25 lb/man day of recovering all the produced water will be satisfactory. A high latent load will increase water vapor produced and drinking water consumed by equal amounts.

The water sources listed in Table II are designated primary sources. They are: water vapor (exhaled and perspired), waste water (urine and wash water), and fecal water. It has been pointed out that operating at a break-even or favorable water balance is a feasible but challenging problem, requiring highly efficient recovery equipment. Fortunately, this problem will be relaxed in space missions where by-product water sources are available. Table III repeats the primary water balance of Table II, with supplemental entries for two by-product water sources expected to be available in space missions in the two-week class. The two enumerated by-product sources are LiOH (used for CO_2 removal) and a hydrogen-oxygen APU, which could be either a fuel cell or a combustion heat engine.

When absorbing CO_2, LiOH produces water vapor according to the reaction

$$2LiOH + CO_2 = Li_2CO_3 + H_2O$$

Practically all the water produced by this reaction shows up as vapor in the gas flow out of the bed, and is therefore recoverable to the same extent as is the exhaled and perspired water vapor. The quantity of water produced by LiOH (0.9 lb/man day) could be a significant entry on the plus side of the water balance, were it not overshadowed by the much larger quantity of water available from the APU.

The water available from the APU has been estimated to be 8.0 lb/man day, consistent with an average electrical load of 1/3 KW/man, and a specific fuel consumption of 1 lb/KW hr. Lower rates of APU water availability per man are believed unlikely.

Table IV shows the effect on water balance of various combinations of water recovery sources, primary and by-product. Combinations of the primary sources are listed as column headings. The first column depicts an all-out recovery effort utilizing all three primary sources (fecal, waste, vapor). The other columns depict successively less rigorous recovery schemes. The rows show the effect on water balance of the two by-product recovery sources, alone or in combination. Unfortunately, neither the hydrogen-oxygen APU nor LiOH for CO_2 removal is compatible with long space missions (of the order of months in duration); so that in the absence of by-product water, these missions will require the most rigorous water management.

A brief discussion of water recovery techniques is now in order. Exhaled and perspired vapor, together with any LiOH-generated water vapor, is recovered by condensation and separation from the space vehicle atmosphere. Figure 1 shows typical atmosphere, water and water-glycol coolant flow rates for handling cooling and dehumidifying requirements of one man. The water-glycol would of course be cooled in a space radiator.

For comparison, a comparable process without water recovery is shown in Figure 2. Here, the load on the water-glycol coolant is reduced by reevaporation (to space vacuum) of the condensed water, providing full thermodynamic recovery of the heat of water condensation.

Equipment capable of functioning as indicated by Figure 1, Figure 2, or an intermediate case where the water condensate is partially recovered and partially reevaporated has been built and tested. Figure 3 is a photograph of a development cooler-condenser-water separator. The unit is a conventional plate-fin liquid-cooled heat exchanger, with the addition of bats of wicking material between adjacent fin rows on the atmosphere side. The cooling liquid keeps the metal surfaces of the heat exchanger below the dew point. Water from the moist atmosphere throughflow is condensed on these surfaces, forming a thin condensate film from which it is drawn into the wicking material by capillarity. The wicking bats pass through a side wall of the heat exchanger into a water-collecting manifold. This manifold is packed with material which, when wet, effectively blocks the flow of air, thereby preventing air entrainment in the recovered water.

Tests of this device have been encouraging, having demonstrated negligible air loss and 100% water separation efficiency with the atmosphere flow downward. Performance with flow downward, the least favorable direction for full water recovery, indicates a probable performance margin under zero-g conditions.

Development of this water recovery unit is believed to represent a significant advancement in the technology of zero-g water separation, for the following reasons:

1. The device is passive.

2. Negligible power is required.

3. Weight penalty chargeable to separation is small.

4. Water is removed at ths point of condensation, eliminating the need for back-pressure producing blowoff of the water from the cooler-condenser.

5. Ultimate performance in terms of separation efficiency and air loss is achieved.

Order-of-magnitude estimates of the penalty involved in condensing and recovering water have resulted in a penalty of 10 lb of fixed weight per lb/hr of water recovered. This figure includes the portion of radiator, liquid coolant system and coolant pumping power chargeable to water condensation. It does not include tankage for stored water. This figure indicates the desirability of recovering exhaled and perspired water vapor from the space vehicle atmosphere in missions of duration

beyond a few hours.

Urine-waste water recovery poses a number of problems, the most important of which is purity of the product. Pretreatment of the feed with acid to a pH of 4 or 5, processing at a low temperature, and charcoal filtration (and possibly ultraviolet radiation) of the product are recommended.

Although many schemes of waste water treatment are possible, batch distillation under vacuum conditions appears to be the best. In the absence of forced flow, both the evaporation and condensation portions of the process have to be designed carefully to work in a zero-g environment. The distillation process is thermodynamically straightforward. For a nominally constant-pressure process, a temperature difference of about $5^{0}F$ (at $150^{0}F$) is required; for a nominally isothermal process, a pressure lift of about .5 psi is necessary. These lifts are those required to overcome the vapor pressure depression associated with the solids dissolved in urine at the end of a batch recovery process. An additional temperature difference is required for heat transfer. Figure 4-a, b, and c shows three ways of providing the required temperature or pressure lift: use of an available heat source and sink, vapor compression, and a thermoelectric heat pump. Because of the low flow rates (in the range of 1 lb/man hr), power requirements are low enough that comparison of these three approaches on a formal penalty basis will not show significant differences.

Figure 5 shows schematically a waste water recovery device, now under development, which utilizes a spray condenser for the dual purpose of generating the pressure lift required for condensation and for providing a g-insensitive condensation mechanism. Water is recirculated by a small pump through the spray condenser where it provides a heat sink and sufficient ejector action to condense the waste water vapor. The condenser outlet water is circulated through a heat exchanger which furnishes heat to the waste water evaporator, from which the flow is divided, part returning to the spray condenser, part being drawn off as product. The evaporator is batch-type, packed with a sponge-like material for g-insensitivity. The key to successful operation of the cycle is getting enough pressure lift out of the spray condenser to condense the vapor.

Preliminary distallation tests, conducted in glassware, have been successfully run at a temperature of $157^{0}F$, with 90 per cent recovery of a product which when filtered with activated charcoal met the U.S. Public Health standards for drinking water[3].

The following conclusions may be drawn regarding water management:

1. Manned space missions of duration from a few days to a few weeks, using a hydrogen-oxygen APU (fuel cell or heat engine) can operate at water parity (that is, consumption equal to production) by recovery of APU water and approximately 50 per cent of the exhaled and perspired water. Recovery of fecal water, water from urine, or wash water waste (the latter budgeted at 3.0 lb/man day) is not necessary in this case. The use or non-use of LiOH for CO_2 removal does not materially change this picture.

2. Manned space missions too long for use of a hydrogen-oxygen APU (and therefore requiring solar or nuclear power) will operate under rigorous water management discipline. Water must be kept not only on board the vehicle, but within the consumption-recovery cycle. Water parity can be obtained in this case without recovery of fecal water, if slightly more than 90 per cent of the exhaled and perspired water vapor is recovered, together with 90 per cent of the waste water, including water from urine.

3. Water balance must be considered as a constraint on the design of related equipment, such as CO_2 removal equipment which concurrently separates water and CO_2 and is subsequently regenerated by venting both water and CO_2 overboard. Such a CO_2 removal system may or may not be applicable to missions with by-product (APU) water, depending on the amount of overboard water loss; it will almost certainly not be applicable to long missions which have no by-product water.

CO_2 Management

The human CO_2 production (nominally 2.25 lb/man day) must be removed in a way that avoids excessive CO_2 concentrations in the breathing atmosphere. Figure 6 shows representative human tolerance curves for CO_2 in terms of allowable concentration versus time duration. Curve A is the desirable standard for normal operation. Curve B sets emergency limits, consistent with maintaining astronaut performance at a functional level[4].

The many different ways of removing CO_2 from a space vehicle atmosphere can be combined into four basic processes, listed here in order of increasing complexity:

1. Open-cycle
2. Non-regenerable
3. Regenerable
4. O_2-recoverable

The open-cycle system, in which CO_2 is simply purged overboard by a relatively high ventilation rate, has a definite place in backpack or emergency breathing systems. Such systems will be important for many manned space missions. In spite of its high ventilating flow rates, the open-cycle system has been found to be optimum for a backpack emergency life support system of as long as 4 to 5 hours duration, in comparison with a non-regenerable CO_2 absorbent such as LiOH. The open system has the definite advantage of greater tolerance of leakage than the system using LiOH, an important consideration in suit-backpack applications.

The non-regenerable systems are mainly chemicals of two types: metal oxides or hydroxides, and superoxides. LiOH has been successfully used for CO_2 removal in the Mercury project. Its stoichiometry is predictable. Utilization efficiency is 90 per cent or better, requiring about 1.2 lb LiOH per lb of CO_2 absorbed.

As previously mentioned, LiOH evolves water when absorbing CO_2. If the evolved water cannot be credited to the system (and typically it

cannot, because LiOH will be used on missions where the water balance is not critical) there is incentive to consider Li_2O. Tests on CO_2 absorption with Li_2O are now in progress. If Li_2O proves successful it will result in a 37.5 per cent weight saving, since (at 90 per cent efficiency) only 0.76 lb Li_2O per lb of CO_2 will be required. Unfortunately, there will not be a corresponding volume saving. Li_2O is about 30 per cent less dense than LiOH.

By comparison, superoxides, such as NaO_2 or KO_2, absorb CO_2 and water vapor and produce oxygen, according to reactions such as:

$$2NaO_2 + CO_2 = Na_2CO_3 + 1.5\ O_2$$

$$2NaO_2 + 2CO_2 + H_2O = 2NaHCO_3 + 1.5\ O_2$$

Ideally, the relative rates of these reactions should be controlled to maintain an $O_2 - CO_2$ balance with man's metabolism. For example, for a respiratory quotient of 0.82, the proper over-all reaction would be:

$$2NaO_2 + 1.23\ CO_2 + 0.23\ H_2O = 0.77\ Na_2CO_3 + 0.46\ NaHCO_3 + 1.5\ O_2$$

A simple material balance based on the above reaction shows that NaO_2 appears to be reasonably competitive with LiOH on a weight basis:

$$\frac{2NaO_2 - 1.5\ O_2}{CO_2} = 1.18$$

$$\frac{2LiOH}{CO_2} = 1.09$$

Detailed comparisons, reported elsewhere, show that NaO_2 is actually non-competitive with LiOH for CO_2 removal, even when NaO_2 is credited with the O_2 produced, and LiOH is not credited with the water produced[5]. Also, it appears infeasible to rely solely on chemical reaction with CO_2 to produce breathing oxygen; the process is too vulnerable to leakage, repressurization requirements, and unbalance in $O_2 - CO_2$ ratio. For this reason, the superoxide would have to be used as a supplemental oxygen source. On this basis, the superoxide loses its primary potential advantage, namely that of eliminating a separate oxygen supply. In short, superoxides are non-competitive with LiOH for CO_2 removal, when evaluated on an overall basis.

Typically, regenerable CO_2 systems utilize a process which is reversible by exposure to vacuum. The process must be periodic, to avoid the sealing problems inherent in a rotary regenerator. In simplest form, as shown in Figure 7, the device contains two sorbent beds with interconnecting valving to permit regeneration of one bed by exposure to vacuum, while the other is sorbing CO_2. Practical devices are somewhat more complex.

LiOH is unsuitable as a regenerable absorbent, since it requires excessive temperature for its regeneration. A survey of all common metal oxides and hydroxides has not yet led to any that are proven satisfactory as regenerable absorbents. In this connection, Ag_2O is of particular interest. The O_2 dissociation pressure vs temperature curve for Ag_2CO_3, shown in Figure 8, suggests the possibility of absorption of CO_2 by Ag_2O at a temperature near 50°F and vacuum desorption at a temperature near 175°F, both temperatures being within the range of temperatures available from the ECS. The decomposition of Ag_2O to Ag and O_2 during vacuum desorption of the Ag_2CO_3 is suggested by the dissociation pressure of O_2 over Ag_2O, but there is some evidence that the rate of decomposition of Ag_2O is slow enough not to cause trouble. Tests of Ag_2O were not successful in achieving practical CO_2 absorption rates, even at gas concentration of CO_2 in excess of 50 per cent[6]. Apparently the reaction of Ag_2O with CO_2 proceeds until the oxide surface is covered with Ag_2CO_3, after which it becomes very slow. Clearly, a way of improving the reaction rate is needed. If Ag_2O can be brought close to its potential performance in absorbing CO_2, and if it proves stable under vacuum desorption, it deserves serious consideration as a regenerable absorbent, since it has no affinity for water vapor.

The synthetic zeolites (molecular sieves or microtraps) are good regenerable adsorbents. They show good dynamic efficiency, are stable, and can be regenerated by adiabatic exposure to vacuum. Unfortunately, they adsorb water preferentially to CO_2, so that water must be removed rather completely in advance of CO_2 adsorption. The subsequent processing of the removed water has an important effect on the water balance, as already noted.

Regenerable adsorbent systems tend to use more power than the best proved non-regenerable system, (LiOH), because of the pressure drop associated with flow through the extra equipment which processes water vapor and CO_2, and (in some schemes) because of the need for heat to carry out the regenerative process. (Development of a regenerable substance like Ag_2O, specific to CO_2 and unaffected by water vapor would materially reduce the power consumption of the regenerable CO_2 system.)

Figure 9 shows schematically a regenerable CO_2 system using a molecular sieve as a CO_2 adsorbent, with vacuum regeneration. The process gas is predried by a silica gel adsorbent bed, which is periodically regenerated by the dry, essentially CO_2-free, effluent gas. Heat is required to aid in regeneration of the silica gel. This system retains the water vapor (temporarily adsorbed in the silica gel) in the system; this feature is essential for long missions with a tight water balance.

Missions in the 300 to 500-hour class will be characterized by chemical APU's with relatively high power penalties (of the order of 600 lb/kw), at least until a solar or nuclear APU is available. For such missions, the high power consumption of the system of Figure 9 places it at a distinct disadvantage compared to the non-regenerable LiOH absorbent.

Figure 10 is a photograph of a regenerable CO_2 system now under development. The same system is shown schematically in Figure 11. The design objective of this device is to be competitive with the non-regenerable LiOH for missions in the 300 to 500 hour class, which, with a chemical APU, are characterized by high power penalties and available by-product water. The system of Figure 10

has therefore been designed to minimize power consumption, at the expense of water recovery. This system differs from the system in Figure 9 in two ways:

1. Silica gel is regenerated by vacuum desorption rather than by purging.

2. Heat is provided for regeneration of the vacuum-exposed silica gel bed by conduction from the other silica gel bed, which is absorbing water.

Heat is transferred between the two silica gel beds by virtue of their being located on each side* of a conventional plate-fin heat exchanger. In essence, the water adsorbed in the silica gel on one side of the heat exchanger releases heat which is partly transferred to the gas flowing through the silica gel on the same side of the exchanger, and partly transferred to the vacuum-exposed silica gel bed on the other side. Calculations have shown that about 80 per cent of the heat released from the active bed is conducted to the vacuum-exposed bed, with only 20 per cent being transferred to the gas.

The two molecular sieve beds are also packed into two sides of a heat exchanger, primarily for convenience in packaging.

Existing valves, linked by Teleflex cable, were used for flow switching in this development unit. It may be desirable to vacuum-desorb the water vapor from both ends of the silica gel bed; the present valve arrangement provides for desorption of both water vapor and CO_2 through the same valve. One such valve is located between the silica gel and molecular sieve beds on each side of the unit.

Design conditions for the unit are shown in Table 5. Preliminary tests are now being run to measure the completeness of vacuum desorption of silica gel. If silica gel does not vacuum desorb adequately, one of the molecular sieves will be tried as a water adsorbent.

Table 5 shows a water loss of 1.52 lb/man day by vacuum desorption of the silica gel. This water loss is quite tolerable if a chemical APU is on board, thereby providing a by-product water source. The system has a lower power consumption than the purge-regenerated system of Figure 9 for two reasons:

1. Process gas flows through only two beds (one silica gel, one sieve). Hence pressure drop is reduced.

2. No external heat is required to regenerate the silica gel bed.

Another process of regenerative CO_2 removal is by freeze-out. Temperatures in the range of 225^0R are required to give adequately low CO_2 partial pressure. Given the availability of cryogenic fluids stored on the vehicle, either for atmosphere storage or for APU fuel, the potential exists for a heat sink which is both cold enough and adequate in capacity. The problem of water management is similar to that with the adsorbents, since water ice must be precipitated either upstream or together with the CO_2.

Figure 12 shows schematically a typical CO_2 freeze-out system, consisting of four thermally linked flow passes, numbered for identification. During the operating mode shown, process gas from the vehicle atmosphere, containing both CO_2 and water vapor, flows into pass 2 where it is cooled by heat transfer to both pass 1 and pass 3. Both the water vapor and CO_2 from the process gas freeze out on the surface of pass 2. The gas leaving pass 2 is essentially dry and has a CO_2 partial pressure well under 1 mm Hg. This gas is mixed with makeup LOX from storage, and the mixture flows to pass 1. The LOX, admixed with the cold, dry, nearly CO_2-free process gas provides part of the heat sink for pass 2. Discharge gas from pass 1 is returned to the space vehicle atmosphere. The remainder of the heat sink for pass 2 is provided by sublimation to vacuum of the CO_2 and H_2O vapor in pass 3. Pass 4 is inactive.

The complementary operating mode reverses all valve positions from those shown in Figure 12, making pass 1 inactive, pass 2 open to vacuum for desorption of water vapor and CO_2, pass 3 the receiver of inlet gas, and pass 4 the regenerative pass.

Figure 13 shows the performance potential of a regenerative freeze-out system using subcritically stored metabolic oxygen as a heat sink. The ordinate is the ratio of oxygen required to effect freeze-out to the metabolic oxygen. The abscissa is total pressure, which controls the total quantity of gas circulated. Operation below an ordinate of 1.0 is essential if the system is to work on metabolic oxygen alone. This is possible for pressures up to 7 psia, 70 per cent CO_2 recovery, and 3.8 mm Hg partial pressure of CO_2. In practice, supplemental oxygen (and possibly nitrogen) will be used by the ECS for leakage makeup, providing a performance margin.

Cryogenic hydrogen is an excellent heat sink for CO_2 freeze-out, if available. A space radiator heat sink is also feasible. A small, oriented radiator panel is required. The radiator sink would be used for long missions where cryogenic APU fuel is not available, being precluded by the use of solar or nuclear power, and where the supply of stored oxygen is limited by the existence of an oxygen-recoverable CO_2 cycle. In such a case, the CO_2 freeze-out system would give up its CO_2 to the O_2-recovery system. The tolerability of water-ice admixed with the CO_2-ice depends on the mechanics of the O_2-recovery system; if a mixture is not tolerable, the H_2O and CO_2 can be frozen out separately at different temperature levels, and therefore recovered separately.

Long space missions, greater than about 2000 hours, will require such large quantities of metabolic oxygen that it will become economical to recover O_2 from CO_2. Such missions will have solar or nuclear power at reasonable penalties, probably in the range of 200 to 500 lb/KW. The theoretical minimum power available for regeneration of O_2 from CO_2 is given by the free energy of formation of CO_2, which is 1.13 KWh/lb CO_2 or 1.55 KWh/lb O_2. Practical processes can be

*In heat exchanger terminology, "side" refers to a set of parallel flow passages taken together, as hot-side face area.

expected to consume several times the theoretical minimum energy.

Clearly, power from a chemical APU (fuel cell or heat engine) which produces no more than about 1.0 KWh/lb of fuel consumed, is not attractive for regeneration of O_2, with a power requirement no less than 1.55 KWh/lb. O_2 recovery is therefore definitely tied to missions with solar or nuclear power available.

Direct thermal or electrolytic decomposition of CO_2 has been extensively studied, with only limited progress toward a system useful in a space vehicle. As an alternate, processes producing intermediate products have been considered. A promising example is the hydrogenation of CO_2 by the Sabatier process, followed by pyrolytic decomposition of methane and electrolysis of water. The reactions are:

$$CO_2 + 4H_2 = CH_4 + 2H_2O \quad \text{(Sabatier)}$$

$$CH_4 = C + 2H_2 \quad \text{(pyrolysis)}$$

$$2H_2O = 2H_2 + O_2 \quad \text{(electrolysis)}$$

The sum of these reactions gives the desired end result:

$$CO_2 = C + O_2$$

Except for a small initial and makeup supply, the required hydrogen would be regenerated by the process. Similarly, the intermediate products, methane and water, would be decomposed as shown.

Use of the water in the Sabatier reaction to augment the space vehicle water supply is not recommended, nor does it appear advantageous to use methane as fuel for a chemical APU.

The Sabatier reaction has a favorable equilibrium (99 per cent conversion of CO_2 at 400°F; 95 per cent at 640°F). Catalysis of the reaction is necessary for any practical reaction temperature; catalyst development is naturally aimed at a reasonable reaction at a low temperature, where the equilibrium is favorable relative to competing side reactions, such as:

$$CO_2 + 2H_2 = C + 2H_2O$$

(This is the reverse of the commercial water gas reaction used to produce hydrogen from coal and steam. This reaction, catalyzed, proceeds from left to right at about 1000°F.)

Methane spontaneously pyrolyzes at 1600°F or higher. The reaction is substantially complete at 2000°F. Reaction at lower temperatures is is desirable for space applications. In particular, it would be desirable to pyrolyze methane at a temperature low enough to absorb the heat produced by the Sabatier reaction:

$$CO_2 + 4H_2 = CH_4 + 2H_2O + 1640 \text{ Btu/lb } CO_2$$

$$CH_4 = C + 2H_2 - 830 \text{ Btu/lb } CO_2$$

The Sabatier reaction has plenty of heat available, but for this heat to have a chance of being used to pyrolyze methane, the temperature would have to be at least 600°F, with some sacrifice of completeness of CO_2 conversion. Even at this temperature, the equilibrium conversion of CH_4 to C and H_2 is less than 10 per cent. To make the CH_4 pyrolysis complete at 600°F, carbon would have to be continuously removed. Process-development tests of low-temperature pyrolysis of methane are planned as a supplement to test work recently completed on the Sabatier reaction[7]. The latter will be briefly summarized in the next few paragraphs. It is of course not essential that the heat to pyrolyze methane be obtained from the Sabatier reaction, but it is desirable to do so.

The Sabatier reaction will not work in the presence of appreciable oxygen because of the preferential reaction with hydrogen to form water. Thus, space vehicle atmospheres, with only about 1 per cent CO_2 content, cannot be hydrogenated. It is necessary to work with relatively pure CO_2. In the test work reported in Reference 7, CO_2 was obtained by desorption of a molecular sieve bed (Linde type 5A). Rather than desorb the sieve by the usual process of exhausting to low pressure (which in this case would require a pump) the CO_2 was removed by purging with hydrogen at 300°F. Approximately 75 per cent desorption was obtained in a once-through process. Complete desorption of CO_2 from the sieve is unnecessary.

The advantage of H_2-purge desorption is the power saved. Figure 14 shows typical power requirements for pumping CO_2 (temperature = 100°F) from a desorption pressure of 0.05 mm Hg to the pressures shown. The disadvantage of H_2-purge desorption is the variable composition of the purge gas, which was found to have an unfavorable effect on the completeness of the Sabatier reaction.

In a typical run on purge gas, 85 per cent conversion of the CO_2 to CH_4 was obtained at 600°F in one pass through the reactor, with a nickel catalyst. The effect of the unconverted CO_2 on the subsequent processing (especially pyrolysis) has not been investigated. Hopefully, small percentages of CO_2 would be tolerable, passing through the process and being recycled to the sieve inlet with the produced hydrogen.

CO formation should be avoided on principle. This is one of the best reasons for keeping the temperatures reasonably low, since CO formation is thermodynamically favored at high temperatures.

Figure 15 shows the elements of a complete, steady-flow, O_2 recovery system using H_2-purge desorption of the sieve bed, a catalytic reactor for the Sabatier process, a cooler-condenser to separate the water produced, an electrolyzer for the water, and a pyrolyzer for the methane.

The major power requirement would be for the gas blowers and for the electrolysis of water. Figure 16 compares the theoretical energy requirement for electrolysis of water with that achieved by actual electrolytic cells. Efficiencies of 50 to 80 per cent are typical. O_2 is drawn from the electrolytic cell and returned to the breathing system. The hydrogen from the electrolytic cell is dehumidified, combined with the hydrogen from CH_4 pyrolysis, and returned to the desorbing sieve bed.

Work to date on the Sabatier reaction has gone a long way toward establishing its feasibility for O_2 recovery in space ECS, but substantial development of the process remains.

Certain ion exchange resins absorb CO_2 from gas streams. Since these resins can be regenerated electrically, the materials can be used in regenerable CO_2 removal systems using the fundamental process of electrodialysis. Cationic and anionic exchange membranes which are permeable to ions of opposite charges are placed in contact with the ion exchange resin bed. These membranes, which are essentially the ion exchange resins in film form, provide the means for CO_2 removal from the resin bed.

Operation of an electrodialysis removal system involves absorption of the CO_2 in a basic ion exchange resin bed to form carbonate ions:

$$2(R^+ + OH^-) + CO_2 = (2\,R^+ + CO_3^=) + H_2O$$

As shown in Figure 17, the carbonate ions migrate from the absorption bed through an anionic membrane into an adjacent reaction bed. Hydrogen ions migrate into this reaction bed through a cationic membrane on the opposite side of the reaction bed. The hydrogen ions and carbonate ions react to liberate CO_2 and H_2O:

$$CO_3^= + 2H^+ = H_2O + CO_2$$

Hydrogen and oxygen are generated at the cathode and anode, respectively. The ratio of the gas generation rate to the CO_2 removal rate depends upon the internal arrangement of the cell. If the cell is designed primarily for CO_2 removal, it will have a relatively large number of removal passages per pair of electrodes. If the cell is to be used in an oxygen recovery system, the electrode area will be sized to provide the required O_2 flow while removing the CO_2. Of course, increased O_2 production will involve increased power consumption over that needed for CO_2 removal alone. The theoretical power required for CO_2 removal alone is 65 watts/man. Present prototype electrodialysis cells require approximately 350 watts/man. There is reason to believe that the power consumption can be reduced to less than 100 watts/man. Because of the continuous flow and static nature of the process, electrodialysis may be used to advantage for long-duration space missions.

Table VI contains recommended ECS elements for missions of length 3, 30, 300, 1000, and 3000 hours. The 3 and 30 hour missions are assumed to carry 1 man; the other missions are assumed to carry 3 men. Recommended power source is included in the table together with a power penalty figure. Power selection is included because of its effect on ECS element selection. The quoted penalty range for solar-nuclear power (200-500 lb/kw; 100-300 lb/kw) reflects a range of system advancement status and also a range of power levels, as shown.

Weights of expendables produced and consumed per man are shown for the mission lengths indicated. These quantities are the theoretical calculated minima; for example, the O_2 shown is metabolic O_2 only. Where closed cycles are used for O_2 or H_2O recovery, the numbers in parentheses reflect an arbitrarily selected inventory for makeup and emergencies. Where total water utilization differs from the makeup quantity required, because of partial water recovery, both numbers are shown. For example, on a 1000-hour mission, the total water utilized is 460 lb/man, of which all but 75 lb/man is provided by water recovery.

There are few surprises in the table. The longest mission shown (3000 hours) is clearly in the stored food and stored solid waste regime. (The latter would probably be dehydrated to save volume.) Only the 3000 hour mission, of those shown, utilizes oxygen recovery.

Acknowledgment

Certain of the work cited herein was performed by AiResearch for North American S & ID under the Air Force Space Vehicle Thermal and Atmospheric (T&A) Study, Contract AF33(616)-7536, directed by W. S. Savage and A. L. Inglefinger, ASD. The suggestions of A. Shaffer, Apollo ECS chief engineer, and R. Nelson, Gemini ECS chief engineer, are also gratefully acknowledged.

References

1. "Development of Analytical Cooling Design Techniques and Procedures for Airborne Electronic Equipment," C. H. LaFranchi, AiResearch Report L-9033-R; Progress Report, NADC Contract N62269-1353.

2. "How to Select an Adequate Cooling System," A. L. Johnson, Electronics, Oct. 20, 1961.

3. "Waste Water Recovery System," F. Fujimoto; AiResearch Report L-9099-MR; Progress Report, Contract AF33(657)-7252 for Aerospace Medical Laboratory, ASD

4. Data received from Department of Aerospace Medicine and Bioastronautics, the Lovelace Foundation.

5. "Atmospheric Control Systems for Space Vehicle," J. Rousseau; AiResearch Report SS-716-R. To be published by ASD in T&A series.

6. "Analytical Methods for Space Vehicle Atmosphere Control Processes--Part 2," C. S. Coe, J. Rousseau, A. Shaffer; AiResearch Report SS-595-R, to be published by ASD in T&A series.

7. "Space Vehicle Atmospheric Control Study: Investigation of Integrated CO_2 Hydrogenation Systems," R. F. Rydelek; AiResearch Report SS-712-R, to be published by ASD in the T&A series.

8. "Low Temperature Absorption of CO_2 by Molecular Sieves," G. Christensen and J. R. Wenker; AiResearch Report SS-715-R. To be published by ASD in T&A series.

9. "Contaminant Freeze-out Study for Closed Respiratory Systems," AiResearch Report SS-596-R. Technical Documentary Report No. MRL-TDR-62-7. C. C. Wright; Prepared for Aerospace Medical Laboratories, ASD, under Contract AF33(616)-7768.

10. "Problems and Progress in Providing an Earth Environment for Manned Space Flight," J. N. Waggoner, W. L. Burriss; ARS Space Flight Report to the Nation, October 1961.

11. "Problems Associated with Environmental Control in Manned Spacecraft with Mission Durations up to Two Weeks," J. N. Waggoner, W. L. Burriss; J. ARS (In press).

TABLE I HUMAN MATERIAL BALANCE

CONSUMED	LB/MAN DAY	PRODUCED	LB/MAN DAY
FOOD	1.80	CO_2	2.25
		WATER VAPOR (EXHALED & PERSPIRED)	5.70
OXYGEN	2.00	WATER (URINE)	3.25
		WATER (FECAL)	0.30
DRINKING WATER	8.00	SOLID WASTE (URINE + FECAL)	0.30
WASH WATER	3.00	WASH WATER	3.00
TOTAL	14.80	TOTAL	14.80

BASED ON:
1. AVERAGE METABOLIC LEVEL ANTICIPATED IN SPACE FLIGHT.
2. RESPIRATORY QUOTIENT (CO_2 PRODUCED/O_2 CONSUMED) =.82.
3. 50-50 SPLIT OF SENSIBLE AND LATENT COOLING LOAD.
4. ARBITRARY WASH WATER ESTIMATE.

TABLE II HUMAN WATER BALANCE

CONSUMED	LB/MAN DAY	PRODUCED	LB/MAN DAY
DRINKING WATER	8.00	WATER VAPOR (EXHALED & PERSPIRED)	5.70
WASH WATER	3.00	WASTE WATER (URINE & WASH)	6.25
TOTAL	11.00	FECAL WATER	0.30
		TOTAL	12.25

BASED ON WATER QUANTITIES OF TABLE I. EXCESS OF 1.25 LB REPRESENTS WATER TAKEN IN WITH FOOD (0.25 LB) AND METABOLIC WATER (1.00 LB).

TABLE III SPACE VEHICLE WATER BALANCE

CONSUMED	LB/MAN DAY	PRODUCED	LB/MAN DAY
HUMAN	11.0	HUMAN	12.25
		BY-PRODUCT SOURCES	
		LiOH	0.90
		$H_2 \mid O_2$	8.00
		TOTAL	21.15

BASED ON:
1. $CO_2 = 2.25$; $2\,LiOH + CO = Li_2\,CO_3 + H_2O$
2. APU POWER = .33 KW/MAN DAY (AVERAGE)
   SFC = 1.00 LB/KW HR

TABLE IV SPACE VEHICLE WATER BALANCE FOR VARIOUS RECOVERY SOURCES

		PRIMARY WATER RECOVERY SOURCES			
		VAPOR (EXHALED AND PERSPIRED) WASTE (URINE AND WASH) FECES	VAPOR (90%) WASTE (90%)	VAPOR (90%)	NONE
BY-PRODUCT WATER RECOVERY SOURCES	APU AND LiOH	10.1	8.6	3.0	-2.1
	APU	9.2	7.7	2.1	-3.0
	LiOH	2.1	0.6	-5.0	-10.1
	NONE	1.2	-0.2	-5.9	-11.0

POSITIVE NUMBERS DENOTE WATER SURPLUS, LB/MAN DAY
NEGATIVE NUMBERS DENOTE WATER DEFICIT, LB/MAN DAY

TABLE V

OPERATING CONDITIONS, REGENERABLE CO_2 SYSTEM

ATMOSPHERE MOLECULAR WEIGHT	MW =	30	
INLET PRESSURE	P_I =	7.0	psia
INLET TEMPERATURE	T_I =	45	^oF
INLET HUMIDITY	γ_I =	0.013	lb/H_2O lb atmosphere (saturated)
OUTLET HUMIDITY	γ_2 =	0	
AVERAGE INLET CO_2 CONCENTRATION	Y_I =	0.0207	lb/lb atmosphere
INLET CO_2 PARTIAL PRESSURE	p_I =	5.0	mm Hg
AVERAGE OUTLET CO_2 CONCENTRATION	Y_2 =	0.0021	lb/lb atmosphere
OUTLET CO_2 PARTIAL PRESSURE	p_2 =	0.5	mm Hg
CO_2 REMOVAL RATE	Y =	7.5	lb/day (3 men)
CO_2 REMOVAL RATE	Y =	0.313	lb/hr
ATMOSPHERE FLOW RATE	W =	16.8	lb/hr
WATER LOSS	L =	0.19	lb/hr
WATER LOSS	L =	4.56	lb/day (3 men)
WATER LOSS	L =	1.52	lb/man day
SILICA GEL BED WEIGHT	X =	3.0	lb silica gel (per pass)
MOLECULAR SIEVE BED WEIGHT	Z =	3.3	lb zeolite (per pass)
SILICA GEL BED	ΔP =	3.73	psf
MOLECULAR SIEVE BED	ΔP =	7.90	psf
DESIGN CYCLE TIME (BOTH BEDS)	θ =	20	min

TABLE VI

RECOMMENDED ECS ELEMENTS

MISSION DURATION, HOURS	POWER SOURCE AND PENALTY, LB/KW ESTIMATED POWER LEVEL	HEAT SINK	ATMOSPHERE SOURCE		CO_2 REMOVAL	CO_2 RECOVERY AND O_2 REGENERATION	H_2O REMOVAL	H_2O RECOVERY FROM ATMOSPHERE	FOOD MANAGEMENT	WASTE MANAGEMENT INCLUDING H_2O RECOVERY FROM WASTE	TOTAL WATER CONSUMED, (DRINKING, FOOD PREPARATION, WASH)	TOTAL EXPENDABLES CONSUMED (NOT INCLUDING POWER PENALTY)	TOTAL EXPENDABLES PRODUCED AND STORED
			OXYGEN	NITROGEN									
3	BATTERIES 60 LB/KW 50 W	CRYOGENIC O_2	CRYOGENICALLY STORED (8 LB), SET BY COOLING LOAD	NONE	OPEN CYCLE VENTILATION BY O_2	NONE	COOLER-CONDENSER-SEPARATOR	NONE (ALL CONDENSED WATER IS RE-EVAPORATED)	NONE	NONE	NONE	(8 LB)	NONE
30	H_2-O_2 APU; 300 LB/KW 1 KW	WATER (7.5 LB) + CRYOGENIC O_2 AND H_2 AS AVAILABLE	CRYOGENICALLY STORED (2.5 LB)	NONE	LiOH (3.4 LB)	NONE			STORED (22 LB)	STORED (3.8 LB)	(10 LB)	(25.6 LB)	(3.8 LB)
300	H_2-O_2 APU; 600 LB/KW (SOLAR-NUCLEAR APU WHEN AVAILABLE: 200-500 LB/KW 2 KW	RADIATOR + CRYOGENIC O_2 AND H_2 AS AVAILABLE	CRYOGENICALLY STORED (25 LB)	CRYOGENICALLY STORED; QUANTITY DEPENDS ON LEAKAGE AND REPRESSURIZATION REQUIREMENTS	LiOH (34 LB)	NONE		PARTIAL RECOVERY	STORED (22 LB)	STORED (85 LB)	140 LB; PARTIALLY MET BY WATER RECOVERY; WATER INVENTORY: (35 LB)	(117 LB)	(85 LB)
1000	H_2-O_2 APU; 1200 LB/KW (SOLAR-NUCLEAR APU WHEN AVAILABLE; 200-500 LB/KW) 5 KW		CRYOGENICALLY STORED (83 LB)		REGENERABLE: MOLECULAR SIEVE OR FREEZE-OUT	NONE	COOLER-CONDENSER SEPARATOR, WITH FURTHER WATER REMOVAL PRIOR TO CO_2 PROCESSING	POTENTIAL RECOVERY WITH CHEMICAL APU, NEARLY COMPLETE WITH SOLAR-NUCLEAR APU	STORED (75 LB)	WATER RECOVERY AS NEEDED FOR WASTE WATER. STORAGE OF FECAL WASTE AND URINE RESIDUE (42 LB)	460 LB; PARTIALLY MET BY WATER RECOVERY; WATER INVENTORY: (75 LB)	(158 LB)	(42 LB)
3000	SOLAR-NUCLEAR APU; 100-300 LB/KW 10 KW	RADIATOR	STORED AS GAS FOR MAKEUP AND EMERGENCIES (75 LB)	STORED AS GAS; LEAKAGE MUST BE LOW (75 LB)		SABATIER + CH_4 PYROLYSIS + H_2O ELECTROLYSIS		AS COMPLETE AS POSSIBLE	STORED (225 LB)	WATER RECOVERY FROM WASTE WATER. DEHYDRATION OF FECES TO SIMPLIFY STORAGE (105 LB)	1400 LB; PARTIALLY MET BY WATER RECOVERY; WATER INVENTORY: (150 LB)	(525 LB)	(105 LB)

NOTE: Weights in parentheses indicate theoretical minimum quantity of indicated expendables consumed or produced per man for the mission length indicated. System selection is based on 1 man for the 3 and 30 hour missions, 3 men for longer missions.

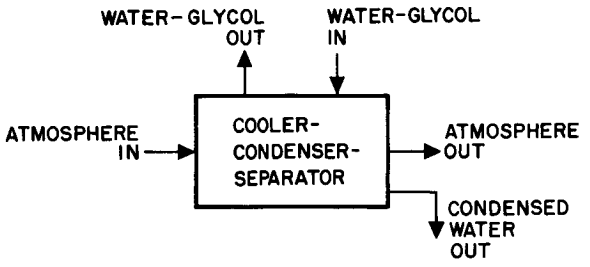

FIGURE 1. COOLING, DEHUMIDIFYING, AND WATER RECOVERY PROCESS

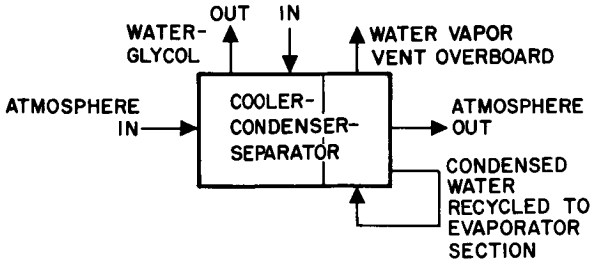

FIGURE 2. COOLING AND DEHUMIDIFYING PROCESS

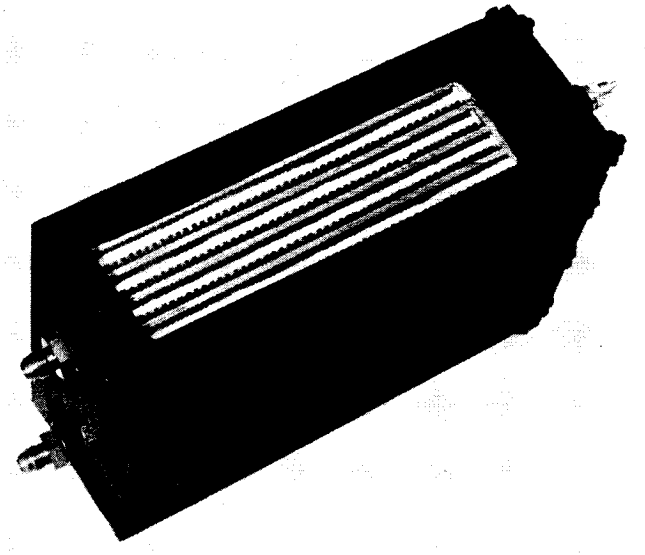

FIGURE 3. Integral Cooler--Condenser--Water Separator

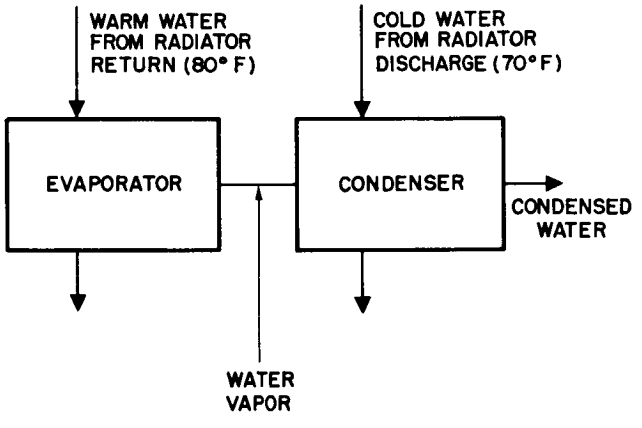

FIGURE 4. WASTE WATER RECOVERY SCHEMES
a. Available Heat Source and Sink

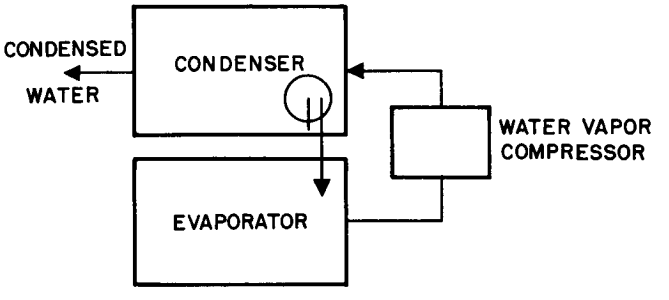

FIGURE 4. WASTE WATER RECOVERY SCHEMES
b. Vapor Compression

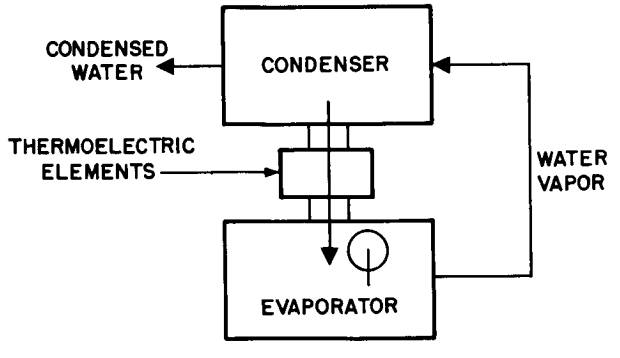

FIGURE 4. WASTE WATER RECOVERY SCHEMES
c. Thermoelectric

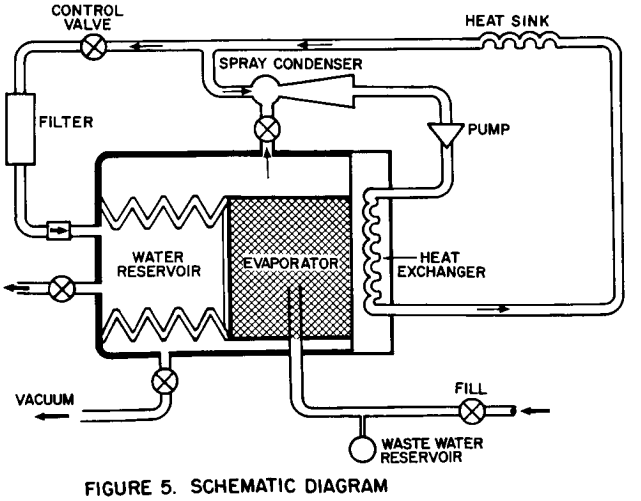

FIGURE 5. SCHEMATIC DIAGRAM
WASTE WATER RECOVERY SYSTEM

This page is reproduced again at the back of this report by a different reproduction method so as to furnish the best possible detail to the user.

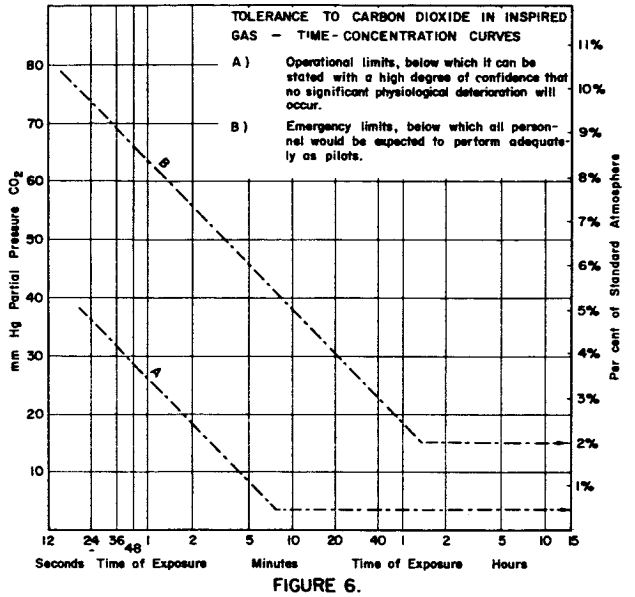

FIGURE 6.

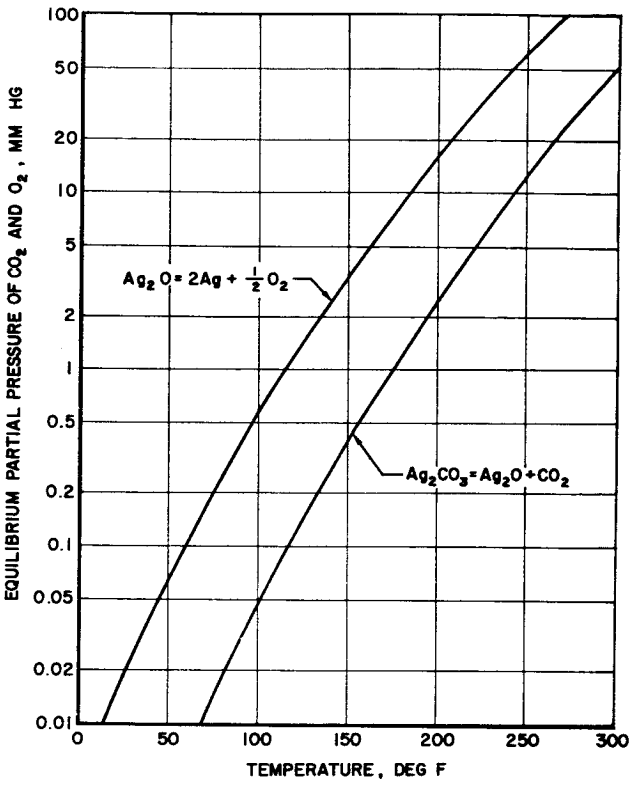

FIGURE 8. EQUILIBRIUM PARTIAL PRESSURES

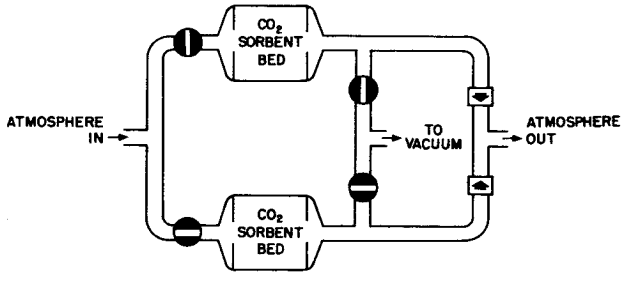

FIGURE 7. SIMPLIFIED REGENERABLE CO_2 SORBENT SYSTEM

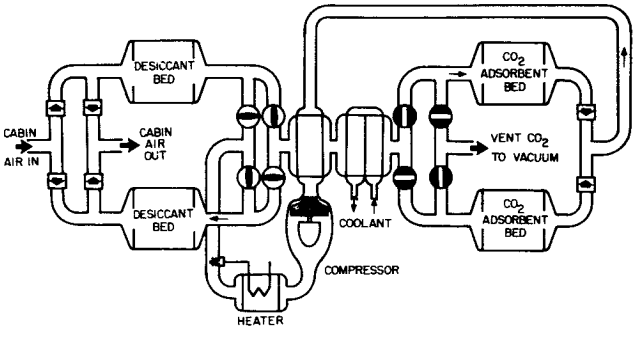

FIGURE 9. RECUPERATIVE CYCLE REGENERABLE CO_2 REMOVAL SYSTEM

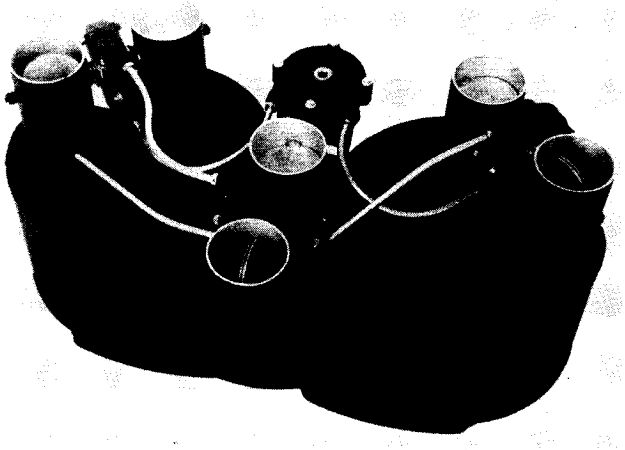

Figure 10. Regenerable CO_2 Removal System

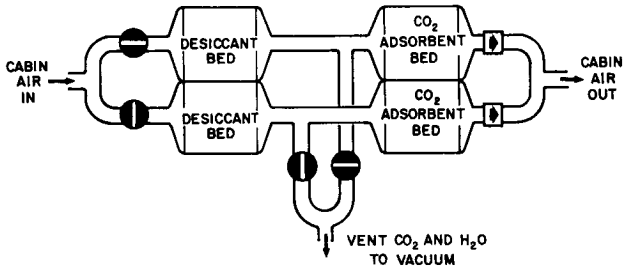

FIGURE 11. REGENERABLE CO_2 REMOVAL SYSTEM WITH VACUUM DESORPTION OF CO_2 AND H_2O

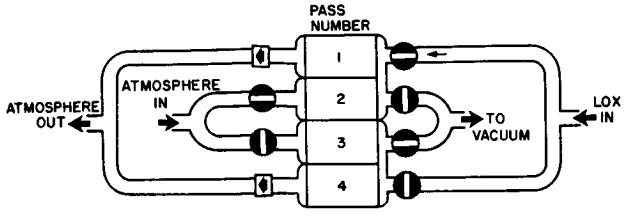

FIGURE 12. REGENERABLE CO_2 FREEZE-OUT SYSTEM

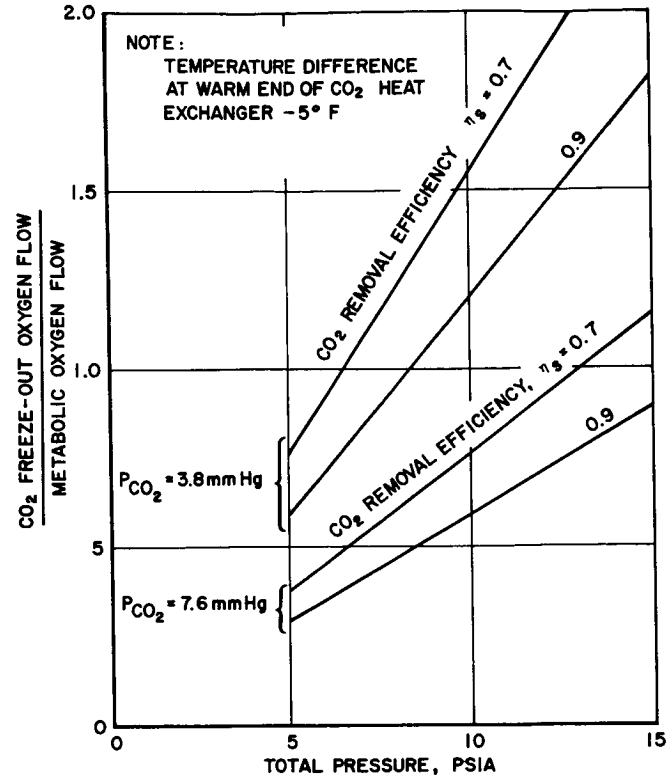

FIGURE 13. PERFORMANCE OF CO_2 FREEZE-OUT SYSTEM

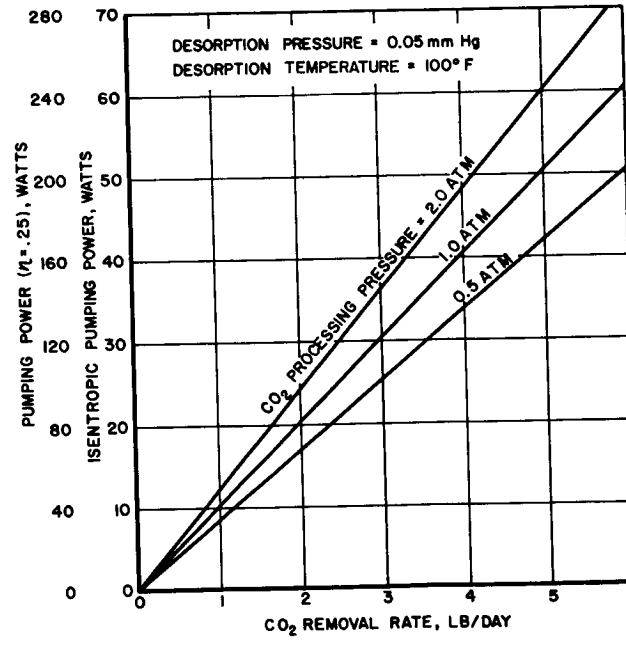

FIGURE 14. PUMPING POWER FOR DESORPTION OF REGENERABLE ADSORBENT

This page is reproduced again at the back of this report by a different reproduction method so as to furnish the best possible detail to the user.

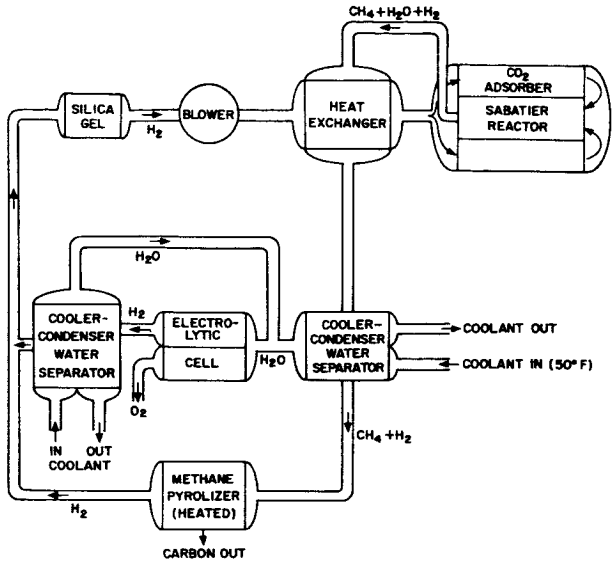

FIGURE 15. O_2-RECOVERABLE CO_2 PROCESSING SYSTEM

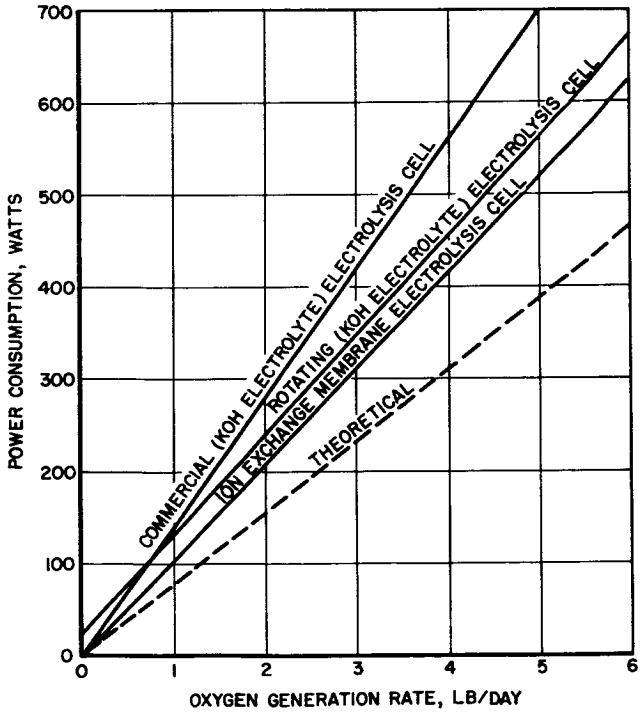

FIGURE 16. POWER REQUIRED FOR ELECTROLYSIS OF WATER

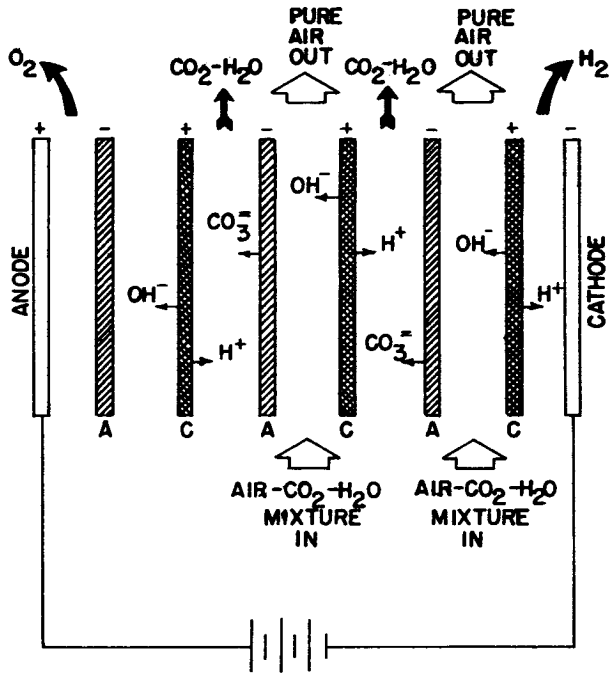

A ANIONIC MEMBRANE

C CATIONIC MEMBRANE

FIGURE 17. ION EXCHANGE ELECTRODIALYSIS UNIT FOR CONTINUOUS CO_2 REMOVAL

THERMAL BALANCE OF A MANNED SPACE STATION

by

George B. Patterson - Advanced Development Engineer

Arthur J. Katz - Group Head, Thermophysics Group

GRUMMAN AIRCRAFT ENGINEERING CORPORATION

INTRODUCTION

The early artificial satellites, all unmanned, had relatively simple temperature control requirements. In designing such systems it was only necessary to prevent temperatures from exceeding the maximum and minimum allowable limits of the electronic equipment aboard. Manned spacecraft, on the other hand, imposed new and more severe restrictions on the allowable internal temperature variations. While man can survive in an environment ranging from less than 400°R to over 600°R, his ability to perform useful work for extended periods of time is severely compromised unless temperature, pressure, and humidity variations are kept to a minimum.

This problem is further magnified, in the case of an orbiting vehicle, by the extreme variation in the external radiation which it receives as it moves into and out of the earth's shadow. Added to this are the variations resulting from changes in the orientation of the vehicle with respect to the earth and the sun. It would seem, then, that the temperature control of such spacecraft might present some difficulty. It is the purpose of this paper to describe a scheme for analyzing the thermal balance of a manned space station and to propose a passive temperature control system for such a vehicle.

A survey of the available literature on the subject discloses considerable coverage of the thermal radiation environment of space. However, the suggested analytical techniques are usually applied to simple geometric shapes and are restricted to determining equilibrium radiation temperatures.

In order for any analysis to yield reasonable results when applied to a realistic configuration, it must account for convective, conductive, and radiative heat transfer through and within the vehicle, and, unless the vehicle surface is wholly convex, for the complex interchange of radiation between external surfaces. The following is a comprehensive view of the entire heat balance problem, including internal and external radiation, conduction, and internal convection heat transfer. In addition, a specific method of temperature control, particularly suited to manned space stations is suggested. The method makes use of the "atmosphere" within the space station as a major factor in the process of heat distribution. The vehicle air is circulated between the living quarters and an area containing the bulk of the heat generating equipment. By regulating the flow rate, temperature changes in the living quarters are minimized at the expense of increased fluctuation of the equipment area temperature. This technique has been applied to a manned orbital space station (MOSS) configuration, suggested by NASA's Langley Research Center. The feasibility of this approach has been demonstrated in terms of required and available flow rates, and the range of allowable equipment temperatures[1].

GENERAL PROCEDURES OF THE ANALYSIS

The methods applied to the space station heat balance can be considered extensions of the basic methods of transient temperature analysis applied to any large or complex configuration. For the purposes of analogy, consider the case of non-steady state conduction heat flow in a rod. The rod is divided into differential segments of length dx, where x represents the longitudinal axis of the rod. The equation for the time derivative of temperature,

$$\frac{\partial T}{\partial t} = \frac{k}{c_p} \frac{\partial^2 T}{\partial x^2} \qquad (1)$$

may then be written. Since the rate of heat flow by conduction is proportional to the temperature gradient, dT/dx, the second derivative represents the rate of change of heat flow in the x-direction. The equation properly reflects that the time derivative of the temperature of a segment is proportional to the net heat flow into that segment. This equation may be solved analytically for most types of boundary conditions. However, the more difficult problems represented by the two- or three-dimensional form of the equation must be treated by numerical methods. In such a case, the body is divided into a finite number of "differential" segments, each of which is assumed to be isothermal (each of uniform temperature, varying with time). A difference equation may then be written for the time rate of change of the temperature within any segment as a function of its temperature and the temperatures of the adjacent segments. Once the initial temperatures are assigned and the boundary conditions specified, a numerical integration will yield the transient temperature time history. Such a procedure can, theoretically, produce any desired degree of accuracy, however the accuracy is governed by the size of the segments and the computing interval. In practice there is always some compromise between accuracy and the amount of time and effort expended.

For this analysis, the entire vehicle is subdivided into sections, where each section is assumed to be isothermal as defined above, and in "thermal contact" by means of radiation, conduction, and/or convection with other sections. The boundary conditions for the system are described in terms of the thermal radiation environment. This environment is dependent on the position and angular orientation of the space station with respect to the earth and the sun, the two sources

of external radiation. The success of the analysis depends on the ability to adequately describe both the effect of this complex thermal environment on the space station exterior and the physical relationship between the section which determine the internal heat transfer rates. Once this information is compiled, the numerical integration can be programmed for a high speed digital computer.

The general equation governing the entire analysis represents a complete heat balance on any section. This equation, which must be evaluated and integrated numerically for each section of the station is given by

$$C_p \frac{dT}{dt} = Q_{SUN} + Q_{EARTH} + Q_{ALBEDO} + Q_{RAD} + Q_{COND} + Q_{CONV} + Q_{FLOW} + Q_{EQUIP} \quad (2)$$

where Cp is the thermal capacity of the section. The different Q terms represent all available means of heat input or exchange for any section.

Not all the sections will receive heat from all the available sources. For example, Q_{sun}, Q_{earth}, and Q_{albedo} can only affect sections which constitute external surfaces of the station. The rate of heat input will be dependent on the space station configuration, the surface characteristics, and the orientation of the station with respect to the sun and the earth. For missions other than earth orbits, Q_{earth} and Q_{albedo} may be neglected or used to represent radiation from any other body which reflects solar radiation or is itself a source of thermal radiation. Q_{rad} includes both the heat lost by a surface through radiation to space, and the heat exchanged between sections by thermal radiation. The remaining terms describe the internal flow of heat within the station. Q_{cond}, Q_{conv}, and Q_{flow} are the rates at which heat is exchanged by conduction, convection, and the mass transfer of air within the station. Q_{equip} is the rate at which heat is generated internally, both by the occupants of the station and any heat generating equipment which is on board

Subdivision Into Sections

The entire analysis requires the judicious division of the station into a number of separate sections, each of which exhibits a reasonable degree of isothermal behavior. The subdivision must be the initial step in the procedure since all the detailed information governing heat flow rates derives from the characteristics and interrelations of the different sections. Any alteration of the subdivision scheme later in the analysis will require recalculation of most of these data.

While all sections will be subject to the same general equation governing heat flow, they may be divided into four distinct types, for which different terms will have greater importance and which may betreated with differing degrees of accuracy. The types of sections are:

1. External surface, or skin sections
2. Internal structure and non-heat-generating equipment
3. Heat generating equipment
4. Air masses contained within the station

Skin Sections These sections, which compromise the entire surface of the vehicle are the most critical since it is through them that the vehicle receives heat from the earth and the sun and dissipates heat by radiating to space. The two major criteria governing the division of the skin into the different sections are the requirement of a relatively uniform temperature over any given section, and a desire to maintain reasonably simple geometrical outlines for each section. In order to evaluate what constitutes a relatively uniform temperature it is necessary to consider the effects of a temperature variation within a section. The assumption of uniform temperature over a section affects the evaluation of the total heat radiated by the section and the determination of the rate of conduction to the adjacent sections. A plate at a uniform temperature will radiate at a rate 2% less than a plate at the same mean absolute temperature but with a linear variation of 10% between its end temperatures. The error varies with the square of the temperature variation with respect to the mean. This would indicate that a temperature range of 10°-20° is acceptable for a mean temperature of the order of 500°R. In speaking of temperature variation over a section we do not mean fluctuations in small areas as might result from fittings or small structural details. Rather, it is the variation in temperature such as might occur from one end of a section to the other. A good indication of the variation within a section is given by the temperature difference between two adjacent sections. On this basis, sections should be established to restrict adjacent section temperature differences to less than 50°.

In addition to the error in radiation. we must consider the method used to estimate the rate of conduction between adjacent sections. Since the only information about temperature that is available during the analysis is the mean temperature of a section it is necessary to assume the gradient at the interface between two sections is proportional to the temperature difference between the sections. Such an assumption becomes progressively less accurate as the variation of temperature within the sections increases.

The second requirement for skin division, that of maintaining simple geometric shapes wherever possible, arises from the inherent difficulty of determining the rates of radiative heat transfer between the sections. This problem, which is discussed later in the paper, is simplified to some extent if the sections have regular outlines and only slight curvature. One important exception to this situation is an axially symmetric vehicle which rotates about its axis of symmetry. If the vehicle rotates rapidly enough, the radiation inputs from the earth and the sun may be averaged around the periphery. In this case, the sections may be taken as circumferential rings.

The temperature gradients which exist along the skin sections have been discussed above. If, in addition, a gradient exists through the skin it may be accounted for without additional subdivision, as follows. The heat flow rate through the skin is known from the rates of heat flow into and out of each face. The value of the temperature difference through the skin may be determined from this information. Since the mean temp-

erature is assumed to be the average of the two face temperatures, the correct face temperatures can be calculated. These will be used for determining convection and radiation from the faces while the mean temperature is used for conduction through the edges.

For some configurations, there may be a large portion of the vehicle, such as a solar collector or shield, which is not an integral part of the vehicle and transfers heat to the vehicle proper only by radiation. It is often possible to separate such an item from the general analysis and treat it as an external source of radiation whose temperature can be predicted independent of the vehicle analysis. This situation will be discussed in a later section.

Internal Structure This classification comprises all portions of the station which are neither skin nor heat generating equipment. While the bulk of this may well be actual structural framing and internal paneling, the category also includes any equipment which does not generate heat, any storage tanks, furnishings, or, in general, any mass with a thermal capacity which cannot be neglected. The decision as to whether or not certain of these items are to be included in the balance depends on the heat transfer function they perform. The major contribution of internal structure items is their heat capacity. The amount of heat that is conducted through them is generally not of great importance except in the case where structural framing constitutes a conduction path from high temperature equipment to some heat sink, such as the skin. Usually, the heat transfer rates to these items are taken into account only so as to allow the effects of the heat capacity to appear in the balance. When the heat transfer paths to any of these items are not sufficient to cause a variation in their temperature of more than several degrees when the temperatures of the section with which they exchange heat vary greatly, the items need not be included in the balance. It is difficult to state any general rules for structure subdivision since configurations can vary so greatly, however, the number of sections should be restricted to as few as possible for the sake of expediency.

Heat Generating Equipment Any reasonably compact group of components which can be represented by one mean temperature should be treated as a single section. The rate of heat generation is assumed equal to the rate at which this equipment dissipates power. This is treated as a direct heat input to the section and will result in the temperature of the equipment section rising to the point where this heat can be dissipated by the normal means of conduction, convection and radiation.

Air Masses While the atmosphere within a space station does not have a large heat capacity, the fact that it can be circulated between areas of widely different temperatures makes it an important factor in the heat balance. Rather than attempt to identify a certain quantity of air and follow its movement between different compartments, it is best to subdivide it according to location. The air in each compartment is treated as a separate section, and, while its identity is constantly changing as the air is circulated between different compartments, the quantity of air in each compartment remains constant. The rate of heat exchange between these air mass sections is then dependent on the rates of circulation and their temperature differences.

Radiative Heat Transfer

In calculating the heat balance of a vehicle in a fluid medium, the heat flux by radiation usually represents a minor, if not insignificant, percentage of the overall amount. With space vehicles, however, as a result of the vacuum in which they operate. radiation must act as a major contributor to the heat transfer process. Indeed, the heat exchange between the vehicle and its environment takes place solely by radiative transfer.

This environment contains radiation of three types, direct solar radiation, direct earth radiation, and solar radiation reflected from the earth (albedo radiation). During each orbit, there may be an extreme variation in the rate of heating by direct solar and albedo radiation. This results from the vehicle "seeing" varying amounts of the day side of the earth, and passing into and out of the earth's shadow. The variation is so great that radiation equilibrium temperatures for the two extremes range from 250°F. to -200°F. Such a variation is, of course, intolerable for a manned vehicle. It may be controlled to a large degree, however, by insulating the skin from the station interior, using a shield against solar radiation, or applying special coatings to alter the rates at which external radiation is absorbed.

A second area where the vehicle heat balance is affected by radiation is that of radiant interchange between the different sections of the station. This exchange occurs not only between skin sections but also between the structure and equipment sections. The rates of exchange by this method are usually of the same order of magnitude as those of conduction or convection between sections.

Mechanism of Radiation The potential rate of emission of thermal radiation from an opaque body is given by the Stefan-Boltzmann law as:

$$Q = \sigma A T^4 \qquad (3)$$

where A is the surface area and T is the absolute temperature of the surface. Such radiation is called "black body" radiation, and is emitted over the entire electromagnetic spectrum with a particular spectral distribution which is also a function of temperature. No real body ever completely attains this ideal maximum rate of radiation. The surface of the radiating body and/or its molecular structure have an attenuating effect on the rate at which this radiation is emitted. The degree of attenuation varies with wavelength and is primarily a result of the surface characteristics. The fraction of "black body" radiation actually emitted at any wavelength is known as the spectral emittance, ϵ_λ, while the fraction emitted over the entire spectrum is the total emittance, ϵ. The surface characteristics have a similar effect on incoming radiation, so that the fraction, α_λ, of the impinging radiation at wavelength λ is absorbed and the remainder reflected. The fraction representing the amount reflected is called the reflectivity, ρ, which may also vary with wavelength. The spectral absorptance, α_λ, of a surface is equal to the spectral emittance, ϵ_λ, at

any wavelength provided no artificially stimulated emission takes place. However, since the incoming radiation may not have the same spectral distribution as a "black body" at the temperature of the surface, total emittance and total absorptance are not necessarily equal. While a complete description of the radiative properties of a surface requires a determination of the spectral emittance over the entire spectrum, it is usually sufficient to work with the total emittance and the total absorptances with respect to each of the various radiation spectra which will exist at the vehicle surface.

The earth radiates with the same intensity and nearly the same spectral distribution as a "black body" at 450°R. Since the spectral distribution of "black body" radiation does not change greatly between 450°R and the expected temperatures on the space station skin, the total absorptance of these surfaces to earth radiation may be considered equal to the total emittance.

The sun, on the other hand, radiates as a "black body" at a temperature of 6000°R. This represents a spectral distribution radically different from that of the space station surface radiation, and therefore, the total absorptance with respect to solar radiation, α_s, is, in general, different from the total emittance. It is possible, by choosing coatings with a spectral emittance which is low for wavelengths shorter than three microns, the region where most of the solar energy is radiated, to obtain surfaces with α_s/ϵ ratios as low as 0.1. Generally the ratio may be used as a rough measure of equilibrimum temperature. By reducing the amount of solar radiation absorbed while maintaining a high rate of surface heat loss by radiation, the surface temperature can be regulated.

Emitted and reflected radiation exhibit directional properties. The directional distribution of emitted radiation is usually such that the intensity of radiation in any direction is proportional to the cosine of the angle between the direction of radiation and a normal to the radiating surface. (Lambert's Cosine Law) Such radiation is termed "diffuse". While deviations from diffuse emission will sometimes occur with polished surfaces, in general, these deviations are small enough to be ignored. Reflected radiation may also be diffuse, in which case the cosine law for distribution is followed, regardless of the direction of the incident radiation. The opposite extreme is "specular" reflection in which the angle of reflection is equal to the angle of incidence. While no surface is a purely specular reflector at all wavelengths, most polished surfaces will exhibit a significant degree of specularity, particularly at low angles of incidence.

View Factors While the rate at which a surface radiates is easily determined from its temperature and surface characteristics, the determination of the eventual destination of the emitted radiation, which may either "escape" to space or be reabsorbed by another surface, is a complex problem.

Assuming diffuse emission, the rate at which radiation leaves an elemental area dA_1 and impinges on a second elemental area dA_2 is given by

$$dQ_{1-2} = \frac{\sigma \epsilon T^4 \cos \eta_1 \cos \eta_2 \, dA_1 dA_2}{\pi r^2} \quad (4)$$

where η_1 and η_2 are the angles between the normals to the areas and the line between their centers, and r is the distance between them. In order to find the rate of radiation for two finite surfaces, A_1 and A_2, this expression must be integrated over both areas. The ratio of the radiation which leaves the emitting surface, A_1, and initially impinges on A_2, to the total radiation emitted by A_1 is called the direct view factor, or angle factor, from A_1 to A_2, and is denoted by F_{1-2}. The first step in the process of determining the rates of radiative heat exchange between the different sections of the space station is the calculation of these direct view factors between all sections which can "see" each other. Any method of evaluation of the direct view factors will involve the integration of Eq. 4, either exactly or by an approximate method. To perform the integration exactly, both surfaces must be represented analytically and Eq. 4 integrated in closed form between the required limits. This procedure can be carried out for simple shapes, most of which have already been investigated, and the results made available in generalized form.[2,3] At the opposite extreme from exact integration is the simplest approximation, both surfaces being treated as "incremental" plane areas and Eq. 4 applied directly without integration. This is a good approximation when the distance between the surfaces is large relative to the surface dimensions. Intermediate degrees of approximation can be used by subdividing each surface into some number of small "incremental" areas and summing the radiation between them.

The direct view factors must be found in both directions (i.e. both F_{1-2} and F_{2-1}), and therefore it is usually convenient to apply the reciprocity relation

$$A_1 F_{1-2} = A_2 F_{2-1} \quad (5)$$

to find the one from the other. Another relation between the view factors which must be observed expresses the conservation of energy. When the direct view factor of space (fraction of radiation from a surface which does not impinge on another surface) is taken into account, the sum of the direct view factors for radiation leaving any surface must be unity.

When integrating Eq. 4, it must be assumed that radiation is emitted uniformly over all of A_1. This may not always be the case. For example, skin sections may either have strong gradients through them so that the inner and outer faces radiate at different temperatures, or else have different values of emittance for the two faces. In such cases, separate view factors must be determined for each of the portions of the surface of a section which emit at a different rate

Once the direct view factors between the sections have been determined, one additional step is necessary before the rate of radiative heat transfer between the sections can be calculated.

$$\sigma \epsilon_1 A_1 T_1^4 F_{1-2} \alpha_2 \quad (6)$$

denotes the rate at which heat is radiated from A_1, impinges on A_2, and is absorbed. However, the radiation which is reflected from A_2 must still be accounted for. This radiation may be reflected back and forth any number of times between A_1 and A_2 and any other nearby surfaces, some of it being absorbed at each reflection.

The total view factor, $\mathcal{F}_{1-2}$, is the ratio of the radiation emitted by A_1 which is eventually, after any number of reflections, absorbed by surface A_2, to the total radiation emitted by A_1. Unless the surfaces are completely absorptive (in which case the direct and total view factors are equal), the total view factors cannot be estimated or calculated directly. However, once the direct view factors and the surface absorptances are known, it is theoretically possible to trace the paths of all emitted radiation, as it is reflected, by the repeated application of the direct view factors. This process has been formalized in slightly differing ways by Hottel,[3] Eckert,[4] and Gebhart,[5] all of whose methods are based on the following assumptions.

First, each of the surfaces must be isothermal, a requirement which is basic to the entire analysis. Second, the surfaces must be "gray". A gray surface is one which has a constant spectral emittance over all wavelengths. While this is rarely the actual case, most surfaces may be treated as effectively gray if the emittance is constant over the wavelength band in which the major portion of the radiant energy is concentrated. When this is not the case, the wavelength range of interest must be divided into bands over which the surfaces are effectively gray. The calculation will be carried out for each band and the results added together to give a final value for the total view factor. The third assumption is that the surfaces are perfect diffuse reflectors. In actuality, most materials deviate from this condition. The external surfaces of a space station would probably be given a highly reflecting coating in order to minimize the rate at which heat is absorbed. Such coatings are rarely purely diffuse reflectors. If the degree of specularity is too great to be ignored, a modification to this method must be used.[6]

Whether or not the errors in the total view factors due to specular reflectance are too great to ignore depends on the ultimate use of the view factors. If they are only to be used to determine the rates of exchange between the sections, a high degree of accuracy is not required. However, if they are to be used to determine the rates at which the sections absorb radiation from the earth and sun, greater accuracy is desired. If the space station does not lend itself to the analytical procedures referred to above, either as a result of extreme geometric complexity or difficulties with surface specularity, an alternate method may be used to determine the rates of absorption of external radiation. This method, involving reflectance tests on a scale model, is described in the following section.

It was pointed our previously that many coatings respond differently to solar radiation and radiation from lower temperature sources. Because of the difference between the values of α_s and ϵ for most coatings, the two types of radiation sources must be treated separately. Therefore, two sets of total view factors must be generated. One set will be used to determine the radiation between the skin sections, and the rate at which earth radiation is absorbed, while the second set will be used to determine the rate at which solar and albedo radiation are absorbed.

Radiation Heat Input While the heat exchange rates between the sections are dependent on the temperatures of the sections, the rates of heat input by external radiation are only dependent on the vehicle configuration, the radiative characteristics of the skin sections, and the relative positions of the earth, the sun, and the space station. Therefore, these rates may be computed independently of the overall transient heat balance analysis. The heating rates should be computed for a sufficient number of positions in the orbit so that the results may be tabulated and interpolated accurately when used in the actual transient calculations.

The calculation of the rates of heat absorption by each section is performed in two steps. First, the rates at which the radiation impinges directly (before reflections) on each section are determined, after which, the rates at which this radiation is absorbed can be calculated, taking into account the possible multiple reflections between the different sections.

In order to determine the rates at which the earth and albedo radiate to each section, Eq. 4, the basic relation for radiation interchange between two surfaces must be used. In general, it is necessary to integrate Eq. 4 over that portion of the earth which radiates to the station. This "visible cap" of the earth is treated as the emitting area, A_1, and is divided geometrically into a finite number of incremental areas. Each section of the skin is treated as a receiving area, dA_2, and Eq. 4 is integrated numerically by summing the radiation from each increment of A_1. For earth radiation, $\sigma\epsilon T^4$ is taken as 68.8 BTU/hr-ft^2 of radiating surface. η_1 is the angle between the normal to the incremental area and the line from the area to the station. η_2 is the corresponding angle for the normal to the skin section. When the skin section is treated as a single incremental receiving area, so that no integration over A_2 is performed, it is assumed that the section is a flat plate. In this case, $\cos\eta_2 dA_2$ of Eq. 4 represents the area of the section projected into a plane normal to the line of sight to the emitting earth surface. When the skin section is not a plane area it may be handled either by subdividing it further until it can be approximated by plane sections, or by treating it as a single unit, in which case the projected area in the appropriate direction is substituted for $\cos\eta_2 dA_2$. Two additional factor must be introduced into Eq. 4 when determining radiation input. When $\eta_2 > 90°$, the skin section is turned away from the incremental area on the earth and can receive no radiation from it. It is also possible that a section which is oriented so that it should be able to see the radiating area has its view blocked by another part of the station. As a result of this possibility, each section has associated with it a "shadow" factor which describes whether or not another section of the station casts a shadow upon it when radiation comes from a particular direction, and if so, what amount of the section is shadowed. For a complex configuration, these factors may be very difficult

to determine analytically. In such a case, sufficiently accurate approximations may be obtained by using a scale model and a collimated visible light source to show the radiation shadow pattern.

The process for albedo radiation is similar to earth radiation, however, only that portion of the visible cap which is lighted by the sun is treated as emitting area. To determine the intensity of radiation from each incremental area, of Eq. 4 is replaced by $442 \rho_E \cos \eta_3$ BTU/hr-ft^2, where η_3 is the angle between the normal to the incremental area and the earth-sun line, and ρ_E is the albedo reflectivity of the earth, usually taken as 0.38.

No integration is required for solar radiation since the sun may be treated as a point source. Eq. 4 may be replaced by

$$dQ_{SUN} = C_s \cos \eta_2 \, dA_2 \qquad (7)$$

where C_s is the solar constant, 442 BTU/hr-ft^2 of vehicle surface, for any location within several thousand miles of the earth. The shadow factor must still be used, and in addition, there is the possibility that the station lies in the earth's shadow, where it will receive no solar radiation. The geometry involved in determining the orientation of the earth, the sun and the station, and the procedure to be followed in performing the integration over the visible cap of the earth is covered in Ref. (7)

The information resulting from this work is a tabulation of the earth, albedo, and solar radiation incident upon each section of the space station for a number of positions throughout the orbit. It remains to determine how much of this radiation is actually absorbed. The initial absorption rates are given by α_s and ϵ, while the radiation reflected from each section will be additionally absorbed as it impinges on other sections. If the radiation incident on a section is reflected diffusely, its directional distribution will be the same as if it were being emitted by the section. Therefore, the total view factors may be applied to determine the amount absorbed by each section as a result of multiple reflections. The amount of solar radiation absorbed by the i^{th} section is given by

$$Q_{SUN}(i) = Q'_{SUN}(i)\alpha_s(i) + \sum_j Q'_{SUN}(j)\left[1-\alpha_s(j)\right]\mathcal{F}_{ji} \qquad (8)$$

where Q'sun is the solar radiation directly incident on a section, and the summation is taken over all the skin sections. Albedo and earth radiation are treated in an identical manner, with ϵ substituted for α_s in the case of earth radiation. In addition, since the total view factors are dependent on the surface absorptances, the total view factors used to determine the rate of absorption of earth radiation will, in general, differ from those used for solar and albedo radiation.

This relatively straightforward procedure may not be applicable, either because the surfaces are highly specular, or because the total view factors cannot be determined with sufficient accuracy. Under such circumstances it is necessary to resort to scale model testing to determine the thermal radiation inputs. The basic theory of radiation model testing, which follows a procedure published by Tea and Baker[8], requires a scale model which duplicates the external configuration and surface radiation characteristics of the space station. Radiation is simulated by a collimated light source, measurements of which are made with light sensitive cells such as solar cells. These cells are placed on the model in positions which are representative of the subdivision of the space station surface. As the model orientation is changed with respect to the light, readings are taken on the cells and compared with a monitoring cell to show the radiation incident on each section as a percentage of the full intensity of the beam. These readings give the total of directly incident radiation and reflected radiation ultimately incident on each section. This procedure was utilized for the MOSS study and was shown to be accurate and practicable.

Some individual considerations which must be observed are as follows:

1. The model must be in a sufficiently "black" enclosure to eliminate stray radiation and prevent radiation reflected off the model from returning.

2. The light source must illuminate the model with a field of uniform intensity and should be sufficiently collimated or far enough from the model so that the beam is essentially unidirectional.

3. The cells must be small enough so as not to interfere with the reflectance pattern of the model.

4. The response of the cells should be linear over the range to which they are sensitive. (Filtering of either cells or source may be necessary.)

5. The surface coating of the model must be "grey" in the spectral range which the cells respond to.

Since both the direct and reflected radiation are measured together in this procedure, the reflectance of the model must match that of the space station. Specifically, the model must have the same total reflectance over the spectrum to which the metering cells respond, as the station has to the solar or earth radiation spectrum. If α_s and ϵ of the station differ, two test runs must be made so that both may be duplicated. Ideally, the tests should be run over a range or reflectances, and the results fitted with a power series in terms of ρ. This will allow investigating the effects of changes in the space station coatings during the analysis. In addition, if the desired coating for the station is not "grey", it is possible, with this information, to go through the proper procedure of breaking the spectrum down into bands over which reflectance is constant.

The data resulting from the experimental reflectance tests will be tabulations of the percentage of full intensity radiation on each section of the station as a function of the angular orientation of the radiation source with respect to a coordinate system fixed on the station.

In calculating the radiation from the incremental areas of the visible cap of the earth, the term $\cos \eta_2$ was used to describe the percentage of full intensity radiation directly incident on a section as a result of its angular orientation with respect to the direction of the incoming radiation. Since the function evaluated in the reflectance tests gives the same information for the sum of both direct and reflected radiation, it may be substituted for $\cos \eta_2$ in Eq. 4 to obtain the total radiation incident on each section. The fraction of this radiation which is absorbed, according to the values of α_s and ϵ of each section is the total external radiation heat input to the section.

Radiation Between Sections In addition to absorbing radiation from the earth, the sun, and the albedo, the external surfaces of the space station reject heat by radiation to space. At the same time, all sections of the station are involved in a mutual interchange of thermal radiation. To properly evaluate radiation between sections both the amount of radiation emitted by each section and the total view factors which describe how the radiation is reabsorbed must be known. It is best to consider the radiation between external skin sections separately from radiation between sections within the vehicle.

The entire external surface of the station emits thermal radiation according to the Stefan-Boltzmann Law, modified by the total emittance. The emitted radiation may either "escape" directly to space, or impinge on other sections of the space station skin. The radiation which impinges on other surfaces is partly absorbed and the remainder is reflected. This process is identical to the reflection and absorption situation described for radiation inputs from external sources and, correspondingly, the fractions of radiation leaving a given section which are eventually reabsorbed are given by the total view factors for the external skin. Applying these view factors directly to the emitted radiation we obtain the rates of radiation exchange for the external skin.

$$Q_i = -\sigma \epsilon_i A_i T_i^4 + \sum_j \sigma \epsilon_j A_j T_j^4 \mathcal{F}_{j,i} \qquad (9)$$

The view factors of space, $\mathcal{F}_{i,\,space}$, the fraction of radiation emitted by a section which is not reabsorbed by any section, does not appear explicitly in this equation, however, it is related to the other total view factors by

$$\mathcal{F}_{i,SPACE} = 1 - \sum_j \mathcal{F}_{i,j} \qquad (10)$$

thus assuring that all radiation leaving a section is accounted for. When the total view factors between external skins sections have been evaluated to a sufficient degree of accuracy to assure that they properly indicate the amount of radiation absorbed and consequently, the amount "escaping", they may be used directly. However, when these factors have not been evaluated with great accuracy, either as a result of too complex a configuration or difficulties with surface specularity, it is necessary to perform an independent calculation to determine the view factors of space. The experimental procedure used to determine the external radiation input may be utilized to evaluate $\mathcal{F}_{i,\,space}$. The results of these experiments, which were used to compute the amount of radiation absorbed by each section from any external source, should be used to compute the amount of radiation to each section from a hypothetical sphere surrounding the station. The ratio of radiation absorbed by each section to the total amount emitted by the sphere will be equal to the view factor from space to the section, $\mathcal{F}_{space,i}$. By the reciprocity relation, (Eq. 5), $\mathcal{F}_{i,\,space}$ may be determined. The expression for $\mathcal{F}_{i,\,space}$ derived from this procedure is

$$\mathcal{F}_{i,SPACE} = \frac{1}{\pi} \int_{\theta_1=0}^{\pi} \sin\theta_1 \int_{\theta_2=0}^{2\pi} F_i(\theta_1, \theta_2)\, d\theta_1\, d\theta_2 \qquad (11)$$

With this independent evaluation of $\mathcal{F}_{i,\,space}$ the rough estimates of the total view factors may be adjusted to satisfy Eq. 10 and then used in Eq. 9 to evaluate the radiation exchange. While the errors in the total view factors will result in some discrepancies in the radiation between the sections, the heat loss to space will now be correctly represented.

Radiation between sections which occurs within the space station is also determined from Eq. 9 and hence is completely defined when the rates of emission from each section and the total internal view factors are known. The rates of emission can be determined from the mean temperature, emittance, and surface area of each section. While this information is not difficult to obtain for the internal surfaces of the skin or large panels of the internal structure, the structural framing and the heat generating equipment usually have rather complex radiating surfaces. In addition, the analysis must often be performed before the space station is thoroughly designed, so that structural details may not be available. Therefore, rough estimates of the amount of emitting surface must usually be made. Since most of the internal radiation exchange occurs between the skin and compartment walls, these inaccuracies for the detailed structure can generally be tolerated. The problem is more critical for heat generating equipment since a large portion of its heat dissipation may occur by radiation. When the details of the equipment are not available, an upper limit on its capacity to reject heat may be determined, since its "effective" radiating surface area may not exceed the area of the surfaces to which it radiates.

As was the case with the external skin, the total internal view factors must be derived from the direct view factors and the surface reflectances. The direct view factors of greatest importance, those between the inner skin, structural paneling, and compartment walls, can usually be determined by analytical procedures. Those involving the less well defined structural components and equipment must be estimated as well as possible. However perfunctory these estimates may be, both the direct and total view factors must satisfy the restriction that

$$\sum_j F_{i,j} = \sum_j F_{i,j} = 1 \qquad (12)$$

in order to insure that no radiation is inadvertantly "lost".

Unlike the space station exterior, the interior surfaces may have highly absorptive coatings in order to reduce temperature variations and eliminate "hot spots". If the surfaces are highly absorptive, the procedure for deriving the total view factors may be applied without

great concern for the restricting assumptions. When this is not the case, the restrictions must be adhered to, particularly the assumption that an entire surface is exposed to a uniform radiation environment. This may require further subdivision of the sections in order to determine the view factors.

Conductive Heat Transfer

Conduction of heat will take place between any of the skin, structure, or equipment sections which are in thermal contact with each other. When two sections are in contact through an interface of area A, the rate of conduction between them is given by

$$Q = \frac{\partial T}{\partial x}\bigg|_i k_i A = \frac{\partial T}{\partial x}\bigg|_j k_j A \qquad (13)$$

where $\frac{\partial T}{\partial x}$ is the temperature gradient normal to the interface and k is the conductivity. When the conductivity is different on the opposite sides of the interface, the gradient is discontinuous. While this equation is an exact representation of the conduction rate, there is not sufficient information available from the analysis to correctly evaluate the gradient. The major limitation on our ability to estimate the gradient is that our knowledge of the temperature distribution within a section does not go beyond a knowledge of the mean temperature. To obtain any further information it would be necessary to additionally subdivide the sections.

A general procedure for handling this problem requires the determination of the nominal resistivity of the conducting path between the geometric centers of the two sections. It is assumed that steady state conditions exist, the mean temperatures occur at the centers of the sections, and the only heat flow present is conduction through the sections and across the interface. Then, if L is the distance from the interface to the center of a section, and A is the average cross section perpendicular to L, the conduction rate is given by

$$Q = \frac{T_i - T_j}{\frac{L_i}{A_i k_i} + \frac{L_j}{A_j k_j}} \qquad (14)$$

The denominator of this expression, the thermal resistivity of the conducting path, is essentially a constant of proportionality between the heat flow rate and the temperature difference between the sections. While the approach may seem to leave something to be desired from the point of view of rigor, it represents the same order of accuracy as the assumption of isothermal sections. In addition, this approach is usually a good representation of one of the more important conduction activities which occurs, the removal of heat from heat generating equipment. Here, the flow is generally unidirectional, from the high temperature source, the equipment, through structural members, to a lower temperature sink, the skin. In the preliminary design stages, it is often an important part of the problem to determine how good a conducting path is required to keep the equipment temperatures at a reasonable level. For this purpose, the thermal resistivity is the simplest parametric representation of a generalized conducting path.

Convective Heat Transfer

Convective heat transfer occurs between the air masses and the surfaces which they contact. The basic equation for convection is

$$Q = A h_f (T_s - T_a) \qquad (15)$$

where A is the surface area, T_s and T_a are the surface and air temperatures respectively, and h_f is the convective film coefficient.

While it is not absolutely necessary that a manned space station contain an atmosphere, it is assumed that this will be the usual case. In this event, the effective operating temperatures of the station will be determined by the temperature of the air within the different compartments. Therefore, careful treatment of the convective heat transfer process is necessary since it is the only means by which the air can absorb or reject heat.

The item which introduces the greatest complication in the determination of the convection rates is the film coefficient. The film coefficient is dependent on the composition of the space station atmosphere, its pressure, the condition of the surface, and the velocity with which the air passes over the surface. The most difficult factor to determine is the velocity of the air over the surface. This will be affected by the rate of air circulation between compartments, the expected pattern of flow, the degree of free access of the air to the surface, natural convection due to rotationally induced gravity, and a host of other items. In general, the situation is very similar to the problems encountered in aircraft air conditioning and ventilation, and liberal reference should be made to the available literature on this subject.

While the convective heat transfer to the equipment is correctly described by Eq. 15, there is rarely sufficient information available to allow a description of the equipment in terms of convective surfaces and film coefficients. When a rough estimate of the effects of equipment heating is needed, it may be assumed that the equipment operates at a constant temperature and manages to reject its entire heat load to its surroundings. The rates of heat rejection by conduction and radiation are then determined from estimates of the effective radiating surface and the conduction paths. The remainder of the heat load is then assumed to be taken up by the air within the compartment. From the analysis, it may be determined whether the air remains at a low enough temperature for such a heat rejection rate to be possible.

Air Mass Flow

When the space station contains an atmosphere, the air mass sections exchange heat with their surroundings by convection and with each other by an interchange of mass flows. The air mass sections are initially determined by subdividing the volume which is occupied by the air, usually according to vehicle compartmentation. When there is mass exchange by flow between the sections, the identity of the air comprising any section will be constantly changing. However, since the total mass of each section is constant,

a heat balance may easily be written. The rate at which air leaves any section is equal to the rate at which it is returned from the other sections. The heat gained by a section is equal to the heat content of the incoming air, less the heat content of the outgoing air.

Some care should be taken to avoid a possible numerical integration difficulty which can arise when high flow rates between the sections are used. If a large portion of the air in any section is exchanged in one integration interval, a divergent oscillation in the sections temperatures may result. This may be avoided by reducing the integration interval or by eliminating rapid changes in the air flow rates.

MOSS Study

The methods described in this paper have been applied to a manned orbital space station, (MOSS), in a study for NASA's Langley Research Center. The configuration studied consisted of an inflatable torus, 32 ft. in diameter, connected by inflatable spokes to a rigid cylinder in the center. The torus was to be used as the living quarters and work area for the crew, while the cylinder housed the bulk of the equipment. An erectable solar collector, which was used as a source of power, protected the vehicle from directly incident solar radiation. The steady power requirements resulted in an internally generated heat load of 10,000 BTU/hr.

The object of the study was to determine a method for regulating the temperature within the torus without resorting to an active thermal control system which would require changes in the heat load, the use of variable surface coatings or any method of altering the thermal radiation input rates. The procedure developed was based on the regulation of air flow between the torus and the equipment cylinder.

The torus was given an aluminized surface with an $\alpha_s = .25$ and an $\epsilon = .08$. The cylinder had a porcelain enamel finish with an $\alpha_s = .25$ and an $\epsilon = .75$. With no circulation of air between the torus and the cylinder, the torus temperature varied from 50°F to 70°F during an orbit, while the cylinder temperature varied from 120°F to 170°F. In order to reduce the fluctuation of temperature in the torus, air was circulated between the torus and the cylinder during the cold portion of the orbit. When the rates of flow were properly controlled, the torus could be maintained at a constant temperature of 70°F while the cylinder varied from 80°F to 170°F.

REFERENCES

1. A.J. Katz, G.B. Paterson, Theoretical Heat Balance Study of a Manned Orbital Space Station, ADR 03-04-61.1, Bethpage, N.Y., Grumman Aircraft Engineering Corp., June, 1961

2. D.C. Hamilton, W.R. Morgan, Radiant-Interchange Configuration Factors, NACA TN 2836, Washington, D.C. 1952

3. W.H. McAdams, Heat Transmission, 3rd ed., New York, McGraw-Hill, 1954

4. E.R.G. Eckert, R.M. Drake, Heat and Mass Transfer, New York, McGraw-Hill, 1959

5. B. Gebhart, Heat Transfer, New York, McGraw-Hill, 1961

6. E.R.G. Eckert, E.M. Sparrow, Radiative Heat Exchange Between Surfaces With Specular Reflection, International Journal of Heat and Mass Transfer, vol. 3, 1961

7. A.J. Katz, Determination of Thermal Radiation Incident Upon the Surfaces of an Earth Satellite in an Elliptical Orbit, Memorandum Report XP12.20, Bethpage, N.Y., Grumman Aircraft Engineering Corp., May 1960

LIFT CONTROL DURING ATMOSPHERE ENTRY FROM SUPERCIRCULAR VELOCITY

By Rodney C. Wingrove and Robert E. Coate
Research Scientists
NASA, Ames Research Center, Moffett Field, Calif.

Summary

This paper presents an analysis of a guidance method which uses a reference trajectory. The four state variables needed to prescribe the trajectory are used as follows: Velocity is made the independent variable, and the errors in the rate-of-climb, acceleration, and range variables away from the reference are used to govern the lift. A linearized form of the motion equations is used to show that this represents a third-order control system. First- and second-order control terms (rate of climb and acceleration inputs) are shown to determine the entry corridor depth by stabilizing the trajectory so that the vehicle does not skip back out of the atmosphere or does not exceed a specified acceleration limit. The destabilizing effect that range input (the third-order control term) can have is illustrated and the results indicate that a low value of range input gain must be used at the high supercircular velocities while larger values of range input gain can be used at lower velocities.

The usable corridor depth and range capability with this guidance system are demonstrated for a lifting capsule ($L/D = 0.5$). The practical applications of this system are illustrated with a fixed trim configuration wherein roll angle is used to command the desired lift. The results show that the guidance system requires only one reference trajectory for abort entry conditions as well as for entry conditions near the design values.

Introduction

Current and future manned space flight projects require the development of entry guidance methods applicable to blunt-shaped vehicles entering the earth's atmosphere at supercircular velocities. These guidance systems must regulate small lift changes in such a manner that constraints, such as acceleration and heating, are not exceeded and that the vehicle arrives at a predetermined destination. Various entry guidance and control methods which meet some or all of these needs have been considered[1-13] and although these studies do present solutions to the problem, they do not analyze in detail the control parameters which strongly influence the entry guidance system. It is the purpose of this paper to demonstrate, by means of control system analysis techniques, the influence of various control parameters upon the trajectory motion. A simple guidance method, using a reference trajectory, will be developed from these principles, and a linearized form of the entry motion equations will be used to describe mathematically the trajectory dynamics resulting from this guidance method.

This guidance technique will be demonstrated for entries of a low-lift ($L/D = 0.5$, $W/C_DS = 48$ psf) vehicle with entrance conditions (a velocity of 36,000 ft/sec at an altitude of 400,000 ft) that are to be expected in the return from a lunar mission. As previously shown[14,15] the entrance velocity requires that lift be varied in such a manner that it does not let the vehicle skip out of the atmosphere or exceed a given acceleration limit. The use of lift variations to keep the vehicle within these constraints will be studied and the manner in which range must be controlled to reach a desired endpoint will be considered. Finally, as a practical application, the control system is illustrated with a fixed-trim configuration in which roll angle is used to control lift during entry. The guidance characteristic of this system is shown for entries from a lunar mission as well as for entries at possible abort conditions.

Control System Analysis

Dynamics of Entry Motion

In order to study the dynamics of entry motion a set of equations is needed which not only describes the important aspects of the motion but which also has simple analytical solutions for use with control system analysis techniques. The equations of motion in the plane of the trajectory in their standard form - two second-order nonlinear differential equations with time as the independent variable - can only be solved by a computer and they do not, as such, lend themselves to a general analytical solution. Chapman[16] has shown that these equations may be approximated by one second-order nonlinear differential equation with normalized velocity, $\bar{u}$, as the independent variable. Although his equation does indicate the important control aspects in entry motion, its nonlinear nature does not allow the use of standard control system analysis techniques. Before the Chapman equation can be used to analyze the trajectory motion, it must be linearized. The linearization given in the appendix will be used throughout this paper to illustrate the effects of various trajectory parameters that might be used to govern lift variation.

Fig. 1(a) shows a block diagram of the linearized equation of motion derived in the appendix. The equation of motion is a second-order differential equation in either altitude, acceleration, or temperature along the trajectory. However, when range is considered, the equation becomes a third-order differential equation. To illustrate the dynamics graphically in terms of the variation of trajectory parameters with velocity, $\bar{u}$, a simplified representation of the motions at the bottom of skip is shown in Fig. 1(b). When the altitude, acceleration, and temperature are near a maximum (or minimum) their corresponding rates of change must, of course, change sign. Also near this point, the range curve has an inflection point. The curves on Fig. 1(b) indicate graphically the integrations ($1/s$) shown in the block diagram.

It is interesting to note the loops inherent in the motion equation shown in Fig. 1. The upper loop, $(1 - \bar{u}^2)/A^2$, corresponds to the spring constant of the second-order differential equation, and, therefore, it determines the natural frequency of the trajectory oscillation. This loop is stabilizing when velocity, $\bar{u}$, is less than 1 (local circular velocity), but it is destabilizing when velocity is greater than 1. The lower loop, $1/\bar{u}$, is a first-order damping term that adds damping to the trajectory oscillations.

This simplified representation of the dynamics gives some insight into the terms a lift control system should incorporate. For instance, lift variation controlled by range measurements represents a third-order system. It can be reasoned that this third-order system, like any other classical third-order control system, needs first- and second-order feedback terms for satisfactory dynamic response. The first-order term in this case is represented by the rate of change of altitude, acceleration, or temperature and the second-order term can be represented by the value of altitude, acceleration, or temperature. It appears that simple entry control techniques can be conceived by consideration of these system dynamics. One method which will be demonstrated here is the guidance about a stored reference trajectory. The system chosen uses the difference in range from that of the reference trajectory as the third-order feedback term, with errors in acceleration and in rate of climb used as second- and first-order feedback terms. The command equation for lift-drag ratio is

$$L/D = (L/D)_{ref} + K_1\Delta\dot{h} + K_2\Delta A + K_3\Delta A$$

where $(L/D)_{ref}$ is the L/D function used to describe the reference trajectory, and the error quantities, $\Delta\dot{h}$, ΔA, and ΔR, are the difference between measured variables and the stored reference variables as a function of the velocity, $\bar{u}$, along the trajectory. A block diagram of this control system is shown in Fig. 2.

The trajectory dynamics associated with each of the feedback terms in this control system will be shown. Comparison of the trajectory motions resulting from simulated controlled trajectories will be made with the linearized analytical expression of the motion taken from the appendix. The use of first- and second-order terms ($\dot{h}$, A) to control the trajectory and thus assure a satisfactory corridor depth will first be discussed. Then the manner in which the third-order range term must be used will be demonstrated and the maximum value of downrange and crossrange available will be determined.

Design Reference Trajectory

The reference trajectory to be used must be precomputed for the desired path through the atmosphere to the desired touchdown. The entrance conditions for the reference trajectory are limited to those within the safe entry corridor. This corridor, which can be defined in terms of possible initial entrance angles, is presented in Fig. 3 in relation to the overshoot boundary, where the vehicle will just stay within the atmosphere, and the undershoot boundary, where the vehicle will reach a specified deceleration limit. The reference trajectory is computed for a prescribed L/D variation which gives the desired path through the atmosphere. In this report the computed reference trajectory is expressed as an L/D function proportional to rate of climb.

$$(L/D)_{ref} = K_1\dot{h}_{ref}$$

Fig. 4 shows typical trajectories obtained when L/D is controlled by a constant-gain ($K_1 = -0.001$/fps) feedback for various initial entry angles. With this program for L/D the maximum value of L/D is commanded for the initial portion of the entry; L/D is then varied, as the function of rate of climb, to stabilize the trajectory; and, finally, at subcircular velocities, about half of the maximum L/D available is commanded, thus giving a trajectory within the center of the subcircular maneuvering capability of the vehicle. The reference trajectories in Fig. 4 have a particular variation of rate of climb, acceleration, and range with respect to velocity which can be used for the reference values in the complete control equation

$$L/D = (L/D)_{ref} + K_1\Delta\dot{h} + K_2\Delta A + K_3\Delta R$$

The $(L/D)_{ref}$ is that L/D used to describe the reference trajectory, $(L/D)_{ref} = K_1\dot{h}_{ref}$. A simplification can be made in this equation by noting that with this particular reference trajectory

$$(L/D)_{ref} + K_1\Delta\dot{h} = K_1\dot{h}_{ref} + K_1(\dot{h} - \dot{h}_{ref}) = K_1\dot{h}$$

so that the equation reduces to

$$L/D = K_1\dot{h} + K_2\Delta A + K_3\Delta R$$

Trajectories, also shown in Fig. 4, represent limiting values for the constraints used in this study. The overshoot trajectory ($\gamma_1 = -4.6^\circ$) defines the skipout limit since the maximum negative lift, in this case $L/D = -0.5$, fails to keep the vehicle within the atmosphere. The steepest entrance angle $\gamma_1 = -7.5^\circ$ shown in Fig. 4 is determined by the acceleration limit (-10g) which is a function of the maximum acceleration force that can be tolerated by the vehicle or crew. The -10g acceleration limit is shown[17] to be a realistic value for humans. The effect of the permissible acceleration level on the corridor boundary will be demonstrated.

Control System With Acceleration and Rate-of-Climb Inputs

The effects of the various feedback quantities upon the entry trajectory can be shown by using the input quantities independently and in combination. The first quantity to be considered is acceleration feedback which is used to control L/D in the following manner,

$$L/D = (L/D)_{ref} + K_2\Delta A$$

Fig. 5 shows trajectories for various entry conditions where L/D was controlled only by the acceleration error. It can be seen in Fig. 5 that the resulting trajectories are very oscillatory about the reference trajectory. The oscillatory character of this control is to be expected because, as was pointed out earlier, the acceleration feedback is of second order and would thus modify the frequency, but not the damping, in the equation of motion.

Since the trajectories are highly oscillatory when only acceleration feedback is used, it would seem reasonable that the addition of rate of climb, which is essentially a first-order feedback quantity, will damp the motions. The combined acceleration and rate-of-climb trajectory control is specified by the following equation

$$L/D = (L/D)_{ref} + K_1\Delta\dot{h} + K_2\Delta A$$

This method of control is illustrated in Fig. 6 wherein the acceleration error ΔA is shown versus

velocity for various constant K_1 gains in the trajectory control equation. The effect of the rate-of-climb control is particularly evident in this figure because, as can be seen from the curves, when the K_1 gain is increased, the resulting vehicle acceleration damps quite rapidly to the acceleration profile of the reference trajectory. When rate-of-climb feedback gain is approximately -0.001/fps, the damping, as can be seen in Fig. 6, is almost critical and the vehicle acceleration reaches the design trajectory acceleration with a small amount of overshoot by the time the vehicle velocity has decreased to local circular velocity ($\bar{u} = 1$).

An approximate analytical description of the trajectory dynamics for this combined rate of climb and acceleration feedback can be obtained from the linearized equations in the appendix. From the appendix the linearized characteristic equation with combined rate of climb and acceleration feedback is

$$s^2 + \left(\frac{1}{\bar{u}} - 25{,}800K_1\right)s + 900\left(\frac{1 - \bar{u}^2}{A_{ref}^2} - K_2\right) = 0$$

from this equation

$$2\zeta\omega_n = \frac{1}{\bar{u}} - 25{,}800K_1, \text{ (radians/unit of } \bar{u})$$

and

$$\omega_n^2 = 900\left(\frac{1 - \bar{u}^2}{A_{ref}^2} - K_2\right), \text{ (radians/unit of } \bar{u})^2$$

If K_1 and K_2 are set equal to zero, these expressions for damping and frequency reduce to the values inherent in equations of motion with no L/D variations. It can be seen that if K_1 and K_2 are negative numbers, they will increase the damping and the frequency of the trajectory oscillations. If, for example, we set $K_1 = -0.001$/fps, $K_2 = -0.33/g$ at $\bar{u} = 1$, the computed damping factor is $\zeta = 0.78$. The corresponding curve of Fig. 6 compares favorably with this result. The approximate formulas for damping and natural frequency can be seen to give a quantitative as well as a qualitative insight into the effect of the rate-of-climb and acceleration gains upon the vehicle trajectory.

Typical rate-of-climb and acceleration-controlled trajectories are shown in Fig. 7 for various initial entry angles. It can be seen that for the usable range of entry angles, the vehicle trajectory damps to the reference trajectory by the time the vehicle velocity has decreased to approximately local circular velocity.

Usable Corridor Depth

The limits of entrance angle within which a specific vehicle will enter the atmosphere without violating any of the constraints placed upon its trajectory determine the usable corridor depth. A comparison is made in Fig. 8 of the usable corridor depth for the three control combinations considered thus far. From Fig. 8 it is seen that with L/D variation controlled by combined acceleration and rate of climb, the usable corridor depth is almost equal to the available corridor depth. When L/D variation is controlled by acceleration errors, the usable corridor depth is approximately 10 miles less than the available corridor depth regardless of the acceleration constraint placed upon the trajectory. When L/D is controlled only by rate of climb, the usable corridor depth is about 13 miles less than that available. The data in Fig. 8 represent the maximum usable corridor depths to be expected with the given K_1 and K_2 gains. The usable corridor is primarily a function of the first- and second-order feedback terms. Additional effects of range, the third-order feedback term, upon the trajectory characteristics will next be considered.

Control System With Range Input

A control system using range measurements in a fashion that will assure the vehicle's arrival at a desired destination at the end of the reentry is prescribed in the following manner:

$$L/D = (L/D)_{ref} + K_1\Delta\dot{h} + K_2\Delta A + K_3\Delta R$$

or, for the particular case considered herein,

$$L/D = K_1\dot{h} + K_2\Delta A + K_3\Delta R$$

The range error term, ΔR, is the difference between range to the destination and range the reference trajectory will traverse. If this error is zero by the end of the trajectory, then the vehicle will reach its destination. The terms $K_1\Delta\dot{h}$ and $K_2\Delta A$ are those described in the previous sections and are used to give acceptable control of L/D.

The effect of range input gain, K_3, is shown in Fig. 9 for a given initial range error about a given reference trajectory. Using a low value of gain does not correct entirely the range error by the end of the trajectory. On the other hand, large values of range input gain will overcontrol the vehicle and can cause it to skip out as shown in the figure. In order to gain a better understanding of the problem, an approximate analytical expression for the trajectory dynamics derived in the appendix can be used to assess the effect of range-error gain. From the appendix the linearized motion equation at local points along the trajectory can be stated:

$$s^3 + \left(\frac{1}{\bar{u}} - 25{,}800K_1\right)s^2 + 900\left(\frac{1 - \bar{u}^2}{A_{ref}^2} - K_2\right)s + \frac{3.6\times10^6\bar{u}}{A_{ref}^2}K_3 = 0$$

This is a linear third-order equation and the standard methods of control analysis can be used to gain insight into the trajectory dynamics. One simple method of analysis is to determine the values of K_3 which make this equation stable. From Routh's criterion for stability, K_3 must be positive and also

$$K_3 < \frac{\left(\frac{1 - \bar{u}^2}{A_{ref}^2} - K_2\right)\left(\frac{1}{\bar{u}} - 25{,}800K_1\right)A_{ref}^2}{4{,}000\,\bar{u}}$$

The above expression can be used to determine the upper limit on K_3 (i.e., the upper limit based on stability consideration) and can be used to observe the qualitative interaction of K_1, K_2, K_3, and $\bar{u}$ on trajectory stability. From the above equation, increasing the magnitude of K_1 and K_2 will allow the upper limit on K_3 to increase and it is

important to note that the upper limit of K_3 will increase as $\bar{u}$ decreases. To maximize range capability and drive the range error to zero by the end of the trajectory it is desirable to have a large value of range input gain, K_3, but still maintain a margin of system stability. This value of gain must be small, then, when $\bar{u}$ is large (i.e., $\bar{u} \gtrsim 1$) and larger values of gain can only be used when $\bar{u}$ is small (i.e., $\bar{u} < 1$).

The maneuvering longitudinal range capability boundaries as a function of initial entry angle that result from various range input techniques are presented in Fig. 10. In this figure the range of the reference trajectory is 3400 miles and rate-of-climb feedback gain and acceleration feedback gain are held constant. The curves labeled range input from $\bar{u} \approx 1$ were obtained with $K_3 = 0$ when $\bar{u} > 1$ and $K_3 = 0.006$/mile when $\bar{u} \lesssim 1$, and the curves labeled "range input" from $\bar{u} = 1.4$ mean that $K_3 = 0.0008$/mile when $\bar{u} > 1$ and $K_3 = 0.006$/mile when $\bar{u} \lesssim 1$. It can be seen that if range control is exerted only when velocity is less than local circular velocity, the vehicle has a range capability of approximately 2000 miles for any entry angle within the usable entry corridor. In contrast, when two-step range input is used from $\bar{u} = 1.4$ the range capability is increased 500 to 2000 miles, depending upon the initial entry angle. However, for shallow entry angles and for flight ranges greater than the reference trajectory, there is an approximate 6-mile reduction in the usable entry corridor. This is because, if for shallow-entry angles an attempt is made to extend range when $\bar{u} > 1$, the range input will overpower the first- and second-order input terms and cause the vehicle to skip out. Even though there is this slight loss in usable corridor depth, this use of a small range input gain at the higher velocity adds considerably more usable range.

The attainable ground area for two different corridors is shown in Figs. 11(a) and 11(b). The conics in these figures represent the vacuum trajectories for the extreme entry angles at the boundaries of the corridor in each case and the shaded areas represent the ground area that can be reached from any entry angle within the corridor. In Fig. 11(a) for the 34-mile usable entry corridor depth between $\gamma_1 = -5.3^\circ$ and $\gamma_1 = -7.5^\circ$ the attainable ground area is about 2200 miles of downrange capability and from ±250 to ±350 miles of crossrange capability. In Fig. 11(b) for the 11-mile usable entry corridor depth between $\gamma_1 = -5.8^\circ$ and $\gamma_1 = -6.5^\circ$ the attainable ground area for the vehicle is 3900 miles downrange and ±250 to ±550 miles crossrange. These data illustrate the trade off that must be considered between the specified corridor depth and attainable ground area. This demonstrates that the largest ground area can be attained if the entry can be made within the smallest specified corridor. These data also show the capabilities that can be expected for the supercircular entries. The following section illustrates the application of these control-system principles to a particular vehicle.

Control-System Application

The control-system principles described in this study will now be demonstrated by application to a particular entry vehicle. The vehicle chosen is a lifting capsule configuration trimmed by center-of-gravity position to give a constant angle of attack that produces a ratio of 0.5 between the force normal to flight path and the drag force along the flight path. The vehicle roll angle is then used to control the lift force in the vertical plane during entry. This roll-angle command method will be illustrated for entries from a lunar mission, as well as for entries from abort conditions.

Roll-Angle Command

The control method described in this study is used merely to null errors in the trajectory variables. It is therefore reasonable to expect that the full transformation that relates roll angle to $L/D\,[L/D = (L/D)_{max} \cos\varphi]$ need not be used in the command equation. Instead, the following simplified command equation, which was found to be adequate, will be used.

$$|\varphi| - 90^\circ = K_1'\dot{h} + K_2'\Delta A + K_3'\Delta R$$

The predetermined reference trajectory that is needed for this control system is computed by controlling a trajectory with $|\varphi| - 90^\circ = K_1'\dot{h}$ exactly as was done in the previous section. During an entry, the $K_1'\dot{h}$ and $K_2'\Delta A$ terms in the command equation cause the vehicle trajectory to converge to the design trajectory; the range input term, $K_3'\Delta R$, can be used to null the range error so that the vehicle reaches a prescribed destination. In the command equation a low value of range gain, K_3', is used when vehicle velocity is greater than local circular velocity. Larger values of range gain, compatible with the previous stability considerations, are used when vehicle velocity is less than local circular velocity.

The command equation determines the magnitude of the roll angle, and the sign of the roll angle is determined by crossrange. The method of determining the sign of the command roll angle by crossrange to the destination is shown in Fig. 12. The method is to let the vehicle fly to one side until the crossrange to the destination exceeds a value specified by a design envelope at which time the sign of the roll-angle command is reversed. The allowable crossrange design envelope is made a function of $\bar{u}^2$ which is shown[18] to be a good approximation for crossrange capability of a vehicle, particularly when its speed is less than local circular velocity. For the control system used here the crossrange to the destination is allowed to become equal to approximately one-half ($100\ \bar{u}^2$, miles) the maximum crossrange capability of the vehicle, at which time the sign of the roll-angle command is reversed. This procedure usually entails a maximum of four to six roll reversals during typical entry trajectories.

Entry From Lunar Trajectory

Both automatic and piloted control have been studied for this type of roll-angle command system. Fig. 13 shows a typical trajectory in which roll angle is controlled by the automatic system. It can be seen that the crossrange error becomes zero by the end of the trajectory, and the downrange error, which is initially -1500 miles, converges to zero at the end of the trajectory. The attainable ground area and usable corridor depth obtained with this roll command system is essentially the same as given by Fig. 10, where a similar 3400-mile design trajectory was used. It is important to note that this range capability is achieved with one design

trajectory. If greater ranges are required than those shown in Fig. 10, another design trajectory will have to be used. The range capability is essentially the same for either automatic or piloted control because under normal conditions the task of following the command roll angle can be accomplished by either with nearly equal facility. However, the pilot will strongly influence the successful completion of an entry mission when an emergency situation occurs. For instance, simulation studies with NASA test pilots indicate that this particular roll-angle control task can be accomplished even when the short-period stability augmentation system fails.

Entry From Abort Trajectories

The possibility of an abort during a lunar mission poses the most stringent requirement that can be placed upon a guidance system - that it be able to cope with those conditions which are extremely far from the design trajectory. Typical abort trajectories were flown using this roll command guidance system and are shown in Fig. 14. These trajectories represent reentries at 26,000 ft/sec and 32,000 ft/sec where the destination is 1,500 miles from entry into the atmosphere. Many extreme abort conditions were investigated. The sensitive situation for this guidance system, and one which would be difficult for most guidance methods, was found to be emergency entry in which the vehicle at the bottom of the first skip is near circular velocity and range extension is needed from this point to reach the destination. The entry at 26,000 fps in Fig. 14 illustrates such a sensitive situation. Although these entry conditions are quite different from the reference trajectory, the guidance system is able to govern the trajectory so that the vehicle reaches its destination and none of the acceleration constraints are violated.

The ability of this control system, which uses only one reference trajectory, to handle these off-design entrance conditions is due primarily to the fact that the four state variables needed to describe the trajectory are contained in the guidance law. This is equivalent to the fact that all three of the feedback loops are used in the third-order control system described as a function of velocity. This control system therefore is able to damp out the oscillations along the trajectory and guide the vehicle to a desired end point.

Conclusions

It has been shown in this paper that reentry-trajectory control systems can be represented as a third-order control system described with respect to velocity. The first- and second-order feedback terms determine the vehicle's usable corridor depth because they damp the vehicle trajectory to the reference trajectory in such a way that the vehicle does not skip out of the atmosphere or exceed specified acceleration limits. Range error feedback, the third-order term of the control system, must have a high gain at velocities less than local circular velocity to insure that range errors are zero by the end of the trajectory, and the feedback gain must be low at higher velocities to insure trajectory stability.

A system using one reference trajectory was investigated for a low L/D vehicle and supercircular entry velocities. The results indicate that for a 34-mile usable corridor depth, attainable downrange increment is on the order of 2200 miles, and for an 11-mile usable corridor depth, attainable downrange increment is on the order of 3900 miles.

This reference trajectory system was demonstrated for a lifting capsule configuration where roll angle is varied to modulate lift. The control system using only one reference trajectory gives satisfactory guidance for entries from design supercircular velocities as well as entries from abort or emergency conditions.

Appendix

An approximate equation that represents the dynamics of the equations of motion about a reference trajectory can be derived by a linearization of the following Chapman equation[18]

$$Z'' - \frac{Z'}{\bar{u}} + \frac{Z}{\bar{u}^2} - \frac{1 - \bar{u}^2}{\bar{u}^2 Z} = - \frac{\sqrt{\beta r}\,(L/D)}{\bar{u}} \qquad (1)$$

where

$$Z = \frac{\rho \bar{u}}{2(m/C_D S)} \sqrt{\frac{r}{\beta}}$$

Z' and Z'' are the first and second derivatives with respect to $\bar{u}$.

Let $\Delta Z''$, $\Delta Z'$, and ΔZ denote the variations of the vehicle trajectory from a reference trajectory; then equation (1) can be written in the following form:

$$(Z''_{ref} + \Delta Z'') - \frac{1}{\bar{u}}(Z'_{ref} + \Delta Z') + \frac{Z_{ref} + \Delta Z}{\bar{u}^2}$$

$$- \frac{1 - \bar{u}^2}{\bar{u}^2 (Z_{ref} + \Delta Z)} \left(\frac{Z_{ref} - \Delta Z}{Z_{ref} - \Delta Z} \right) = - \frac{\sqrt{\beta r}\,(L/D)}{\bar{u}} \qquad (2)$$

Now if this equation is linearized by neglecting $(\Delta Z)^2$ compared to Z^2_{ref}, it becomes:

$$\Delta Z'' - \frac{\Delta Z'}{\bar{u}} + \left(\frac{1}{\bar{u}^2} + \frac{1 - \bar{u}^2}{\bar{u}^2 Z^2_{ref}} \right) \Delta Z$$

$$= -Z''_{ref} + \frac{Z'_{ref}}{\bar{u}} - \left(\frac{1}{\bar{u}^2} - \frac{1 - \bar{u}^2}{\bar{u}^2 Z^2_{ref}} \right) Z_{ref} - \frac{\sqrt{\beta r}\,(L/D)}{\bar{u}} \qquad (3)$$

This is a linear differential equation in ΔZ with variable coefficients. The left side is the "characteristic equation" that describes oscillations of the trajectory about the reference trajectory defined by the right side of equation (3) when $L/D = (L/D)_{ref}$. Then when $L/D = (L/D)_{ref}$ the right side of the equation is the Chapman equation, (1), for the reference trajectory and may be set equal to zero.

By noting that $-\sqrt{\beta r}\,\bar{u} Z_{ref} = A_{ref}$ and that $1/\bar{u}^2$ is small compared to $(1 - \bar{u}^2)/(\bar{u}^2 Z^2_{ref})$, equation (3) may be written:

$$\Delta Z'' - \frac{\Delta Z'}{\bar{u}} + \frac{\beta r (1 - \bar{u}^2)}{A^2_{ref}} \Delta Z = - \frac{\sqrt{\beta r}\,\Delta(L/D)}{\bar{u}} \qquad (4)$$

The operator transform of equation (4) may be written: (Note that $d\bar{u}$ in eq. (1) is negative during solution of an entry trajectory.)

$$\left[s^2 + \frac{1}{\bar{u}}\,s + \frac{\beta r(1 - \bar{u}^2)}{A_{ref}^2}\right]\Delta Z = -\frac{\sqrt{\beta r}\,\Delta(L/D)}{\bar{u}} \quad (5)$$

The dynamics of this characteristic equation will be described for various functions controlling $\Delta(L/D)$.

Rate-of-Climb Input

The expression for rate of climb in the Z function notation[16] is $\dot{h} = \sqrt{g/\beta}\,(\bar{u}Z' - Z)$, fps; L/D is controlled by $\dot{h}$ errors about the reference trajectory in the following manner:

$$\Delta(L/D) = K_1\Delta\dot{h} = K_1\sqrt{g/\beta}\,(\bar{u}\Delta Z' - \Delta Z)$$

This $\Delta(L/D)$ can be substituted into equation (4) to obtain the following result:

$$s^2 + \left(\frac{1}{\bar{u}} - K_1\sqrt{gr}\right)s + \frac{\beta r(1 - \bar{u}^2)}{A_{ref}^2} - \frac{K_1\sqrt{gr}}{\bar{u}} = 0$$

Then at each local point along the trajectory, the damping and natural frequency can be approximated by:

$$2\zeta\omega_n \approx \frac{1}{\bar{u}} - K_1\sqrt{gr}, \text{ radians/unit of } \bar{u}$$

$$\omega_n^2 \approx \frac{\beta r(1 - \bar{u}^2)}{A_{ref}^2} - \frac{K_1\sqrt{gr}}{\bar{u}}, \text{ (radians/unit of } \bar{u})^2$$

From these approximate solutions, important features of the dynamics can be noted. The gain K_1 must be negative to increase the damping of the trajectory and this in turn increases the natural frequency. The increase in ω_n^2 is very slight, however, for the K_1 large enough to give near critical damping ($\zeta = 1$); so then rate of climb is essentially a simple first-order feedback term, that is, affecting the damping only. In future derivations the K_1 contribution to natural frequency will be omitted.

Acceleration Input

The expression for acceleration in the Z function notation[16] is $A = -\sqrt{\beta r}\,\bar{u}Z$, g. Acceleration errors control L/D about the reference trajectory in the following manner:

$$\Delta(L/D) = K_2\Delta A = -K_2\sqrt{\beta r}\,\bar{u}\Delta Z$$

This value $\Delta(L\ D)$ can be substituted into equation (4) to obtain:

$$s^2 + \frac{1}{\bar{u}}\,s + \beta r\left(\frac{1 - \bar{u}^2}{A_{ref}^2} - K_2\right) = 0$$

At each local point along the trajectory, the dynamics may be approximated by:

$$2\zeta\omega_n \approx \frac{1}{\bar{u}}, \text{ radians/unit of } \bar{u}$$

$$\omega_n^2 \approx \beta r\left(\frac{1 - \bar{u}^2}{A_{ref}^2} - K_2\right), \text{ (radians/unit of } \bar{u})^2$$

It is apparent then that if K_2 is negative, the natural frequency is increased and K_2 will not affect the damping.

Range Input

The expression for range in the Z function notation[16] is

$$R = \frac{r}{5280\sqrt{\beta r}}\int_{\bar{u}_2}^{\bar{u}_1}\frac{d\bar{u}}{Z}, \text{ miles}$$

The L/D is controlled by range errors about the reference trajectory in the following manner:

$$\Delta\frac{L}{D} = K_3\Delta R = K_3\frac{r}{5280\sqrt{\beta r}}\left[\int_{\bar{u}_2}^{\bar{u}_1}\frac{(Z_{ref} - \Delta Z)\,d\bar{u}}{(Z_{ref} - \Delta Z)(Z_{ref} + \Delta Z)} - \int_{\bar{u}_2}^{\bar{u}_1}\frac{d\bar{u}}{Z_{ref}}\right]$$

If ΔZ^2 is neglected compared to Z_{ref}^2 this becomes

$$\Delta\frac{L}{D} = -K_3\frac{r}{5280\sqrt{\beta r}}\int_{\bar{u}_2}^{\bar{u}_1}\frac{\Delta Z}{Z_{ref}^2}\,d\bar{u}$$

This value of $\Delta(L/D)$ may be substituted into equation (4) and the equation becomes

$$s^3 + \frac{1}{\bar{u}}\,s^2 + \frac{\beta r(1 - \bar{u}^2)}{A_{ref}^2}\,s + \frac{\beta r^2\bar{u}K_3}{5280A_{ref}^2} = 0$$

For this third-order equation not to have a positive root, K_3 must be greater than zero and $\bar{u}$ must be less than unity. An upper limit for K_3 may be determined by using Routh's criterion for stability; that is, the trajectory will be stable if

$$K_3 < \frac{1 - \bar{u}^2}{\bar{u}^2}\left(\frac{5280}{r}\right)$$

As is shown in the text, other inputs (i.e., accelerations and rate-of-climb control) will add damping to the control system and permit a larger value of K_3 than the one shown here for range error input alone.

Notation

A	horizontal acceleration, g units
C_D	drag coefficient, $\frac{D}{(1/2)\rho V^2 S}$
D	drag force, lb
g	local gravitational acceleration, ft/sec^2
h	rate of climb, fps
K_1, K_2, K_3	gain constants
L	lift force, lb
m	mass of vehicle, slugs.
r	distance from planet center, ft
R	downrange value along a local great circle route in space, miles
S	surface area, ft^2
u	circumferential velocity component normal to radius vector, fps
$\bar{u}$	dimensionless ratio, $\frac{u}{\text{circular orbital velocity}}, \frac{u}{\sqrt{gr}}$
V	resultant velocity, fps
W	weight of vehicle, lb
β	atmospheric density decay parameter, ft^{-1}
γ	flight path angle relative to local horizontal; positive for climb
ρ	atmosphere density, slugs/cu ft
φ	roll angle, deg
ζ	damping factor
ω_n	natural frequency, $\frac{\text{radian}}{\text{unit of } \bar{u}}$

Subscripts

ref	respect to reference trajectory
1	initial value

References

1. Eggleston, John M., and Young, John W.: Trajectory Control for Vehicles Entering the Earth's Atmosphere at Small Flight-Path Angles. NASA TR R-89, 1961.

2. Creer, Brent Y., Heinle, Donovan R., and Wingrove, Rodney C.: Study of Stability and Control Characteristics of Atmospheric-Entry Type Aircraft Through Use of Piloted Flight Simulators. Paper no. 59-129, Inst. Aero. Sci., 1959.

3. Cheatham, Donald C., Young, John W., and Eggleston, John M.: The Variation and Control of Range Traveled in the Atmosphere by a High-Drag Variable-Lift Entry Vehicle. NASA TN D-230, 1960.

4. Assadourian, Arthur, and Cheatham, Donald C.: Longitudinal Range Control During the Atmospheric Phase of a Manned Satellite Reentry. NASA TN D-253, 1960.

5. Foudriat, Edwin C.: Study of the Use of a Terminal Controller Technique for Reentry Guidance of a Capsule-Type Vehicle. NASA TN D-828, 1961.

6. Young, John W.: A Method for Longitudinal and Lateral Range Control for a High-Drag Low-Lift Vehicle Entering the Atmosphere of a Rotating Earth. NASA TN D-954, 1961.

7. Lowry, James H., Jr., and Buehrle, Clayton D.: Guidance and Control of Point Return Vehicles. Proc. Nat. Specialists Meeting on Guidance of Aerospace Vehicles (Boston, Mass.), Inst. Aero. Sci., May 1960, pp. 28-33.

8. White, J. A., Foudriat, E. C., and Young, J. W.: Guidance of a Space Vehicle to a Desired Point on the Earth's Surface. Preprint no. (61-41) American Astronautical Soc., Jan. 1961.

9. Wingrove, Rodney C., and Coate, Robert E.: Piloted Simulator Tests of a Guidance System Which Can Continuously Predict Landing Point of a Low L/D Vehicle During Atmosphere Re-entry. NASA TN D-787, 1961.

10. Wingrove, Rodney C., and Coate, Robert E.: Piloted Simulation Studies of Re-entry Guidance and Control at Parabolic Velocities. Paper no. 61-195-1889, Inst. Aero. Sci., 1961.

11. Dow, Paul C., Jr., Fields, Donald P., and Scammell, Frank H.: Automatic Re-entry Guidance at Escape Velocity. Preprint no. 1946-61, American Rocket Society, 1961.

12. Bryson, Arthur E., and Denham, Walter F.: A Guidance Scheme for Supercircular Re-entry of a Lifting Vehicle. ARS Space Flight Report to the Nation, Oct. 1961.

13. Morth, Raymond, and Speyer, Jason: Control System for Supercircular Entry Maneuvers. IAS Paper No. 62-3, Jan. 1962.

14. Chapman, Dean R.: An Analysis of the Corridor and Guidance Requirements for Supercircular Entry Into Planetary Atmospheres. NASA TR R-55, 1960.

15. Wong, Thomas J., and Slye, Robert E.: The Effect of Lift on Entry Corridor Depth and Guidance Requirements for the Return Lunar Flight. NASA TR R-80, 1961.

16. Chapman, Dean R.: An Approximate Analytical Method for Studying Entry Into Planetary Atmospheres. NASA TR R-11, 1959.

17. Creer, Brent Y., Smedal, Harald A., Capt. USN (MC), and Wingrove, Rodney C.: Centrifuge Study of Pilot Tolerance to Acceleration and the Effects of Acceleration on Pilot Performance. NASA TN D-337, 1960.

18. Slye, Robert E.: An Analytical Method for Studying the Lateral Motion of Atmosphere Entry Vehicles. NASA TN D-325, 1960.

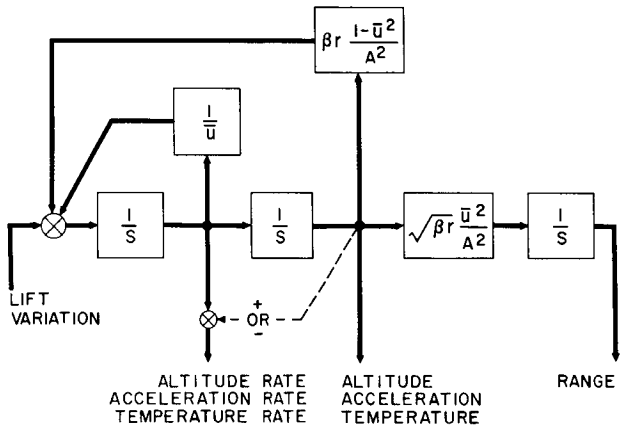

Fig. 1. - Dynamics of entry motion.
(a) Linearized form of entry motion.

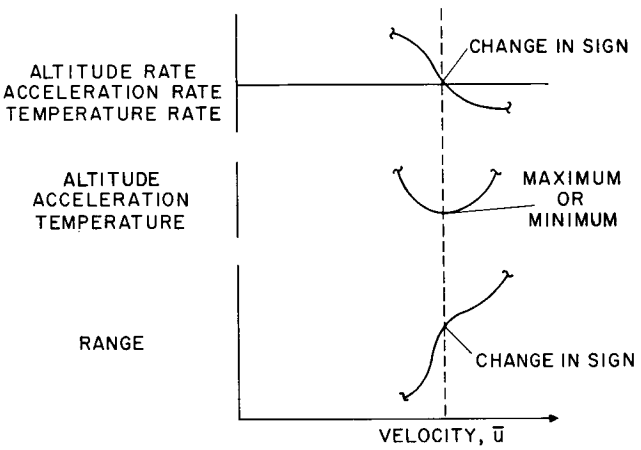

Fig. 1. - Dynamics of entry motion.
(b) Typical dynamics in entry motion.

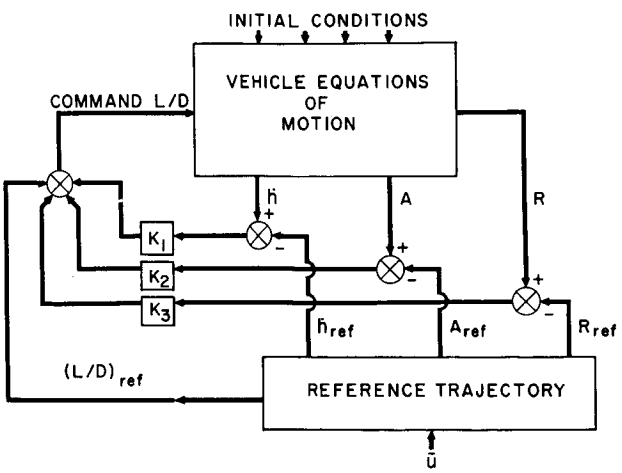

Fig. 2. - Block diagram of reference-trajectory control system.

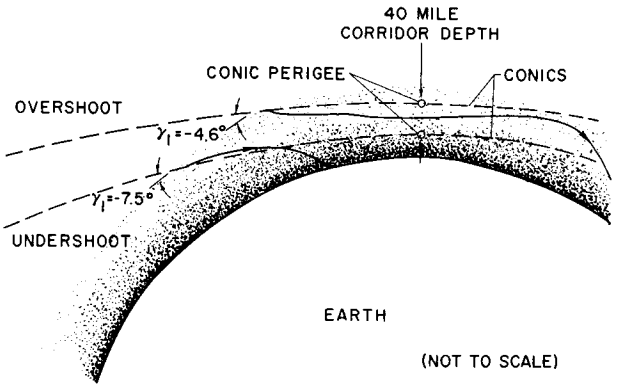

Fig. 3. - Definition of corridor depth.

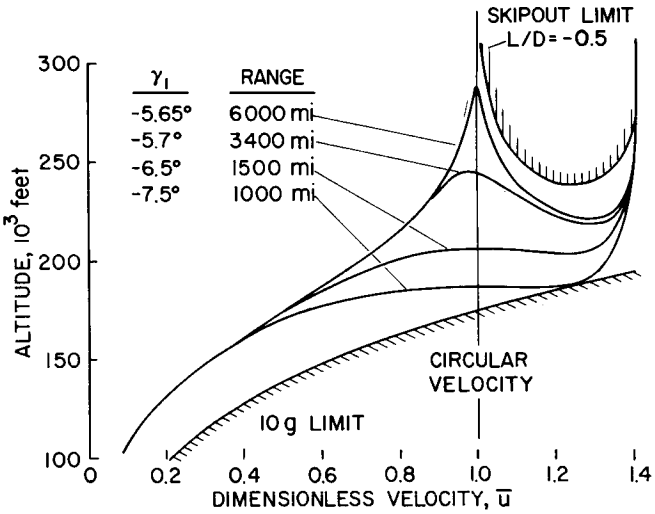

Fig. 4. - Entry trajectories controlled with rate-of-climb input; $\dot{K}_1 = 0.001$/fps.

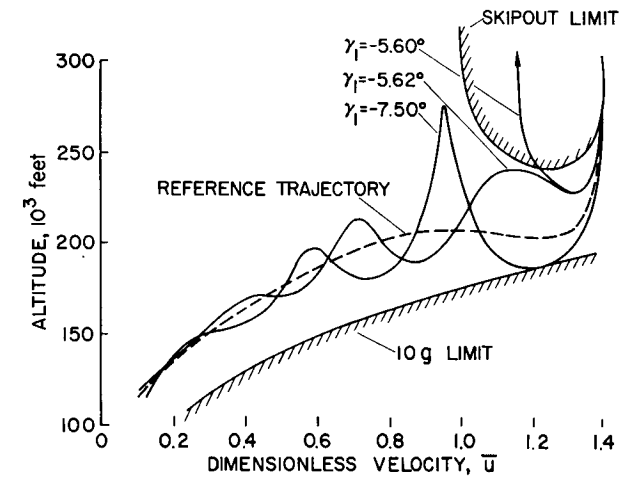

Fig. 5. - Acceleration input used for control about the reference trajectory with design of $\gamma_1 = -6.5°$; $K_2 = -0.33$/g.

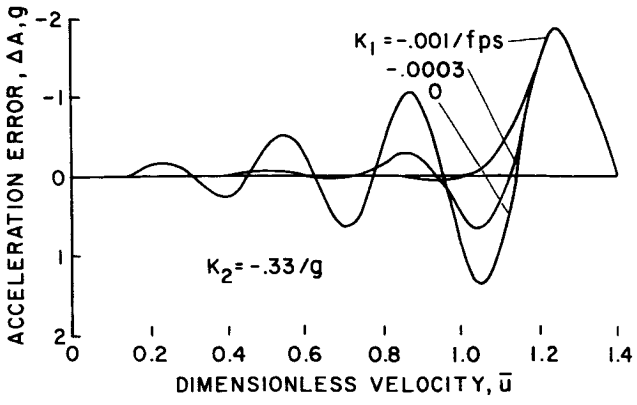

Fig. 6. - Effect of control gain on acceleration errors about the reference trajectory with design $\gamma_1 = -6.5^\circ$; $\gamma_1 = -7^\circ$.

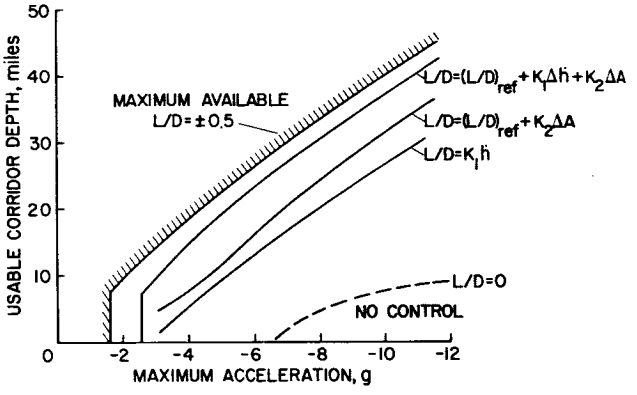

Fig. 8. -Usable corridor depth for various methods of controlling L/D; K_1 = -0.001/fps; K_2 = -0.33/g.

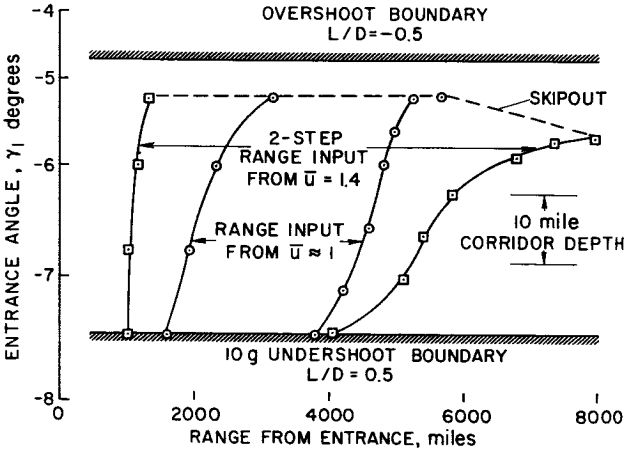

Fig. 10. - Downrange capability as a function of entrance angle for the 3400-mile trajectory; K_1 = -0.001/fps; K_2 = -0.33/g; K_3 = 0.0008 and 0.006/mile.

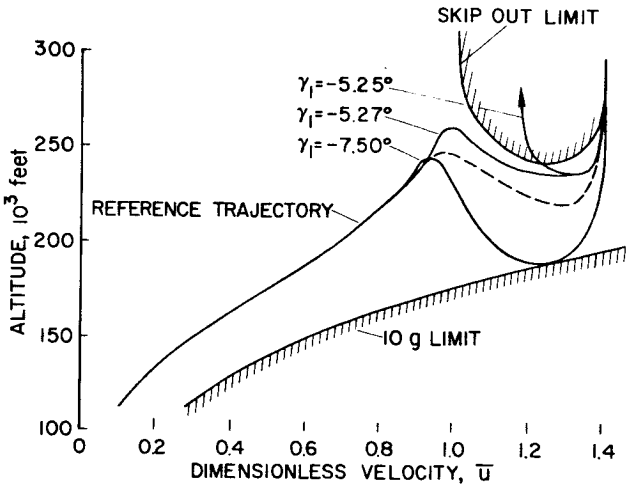

Fig. 7. - Combined acceleration and rate-of-climb inputs used for control about the reference trajectory with design $\gamma_1 = -5.7^\circ$; K_1 = -0.001/fps; K_2 = -0.33/g.

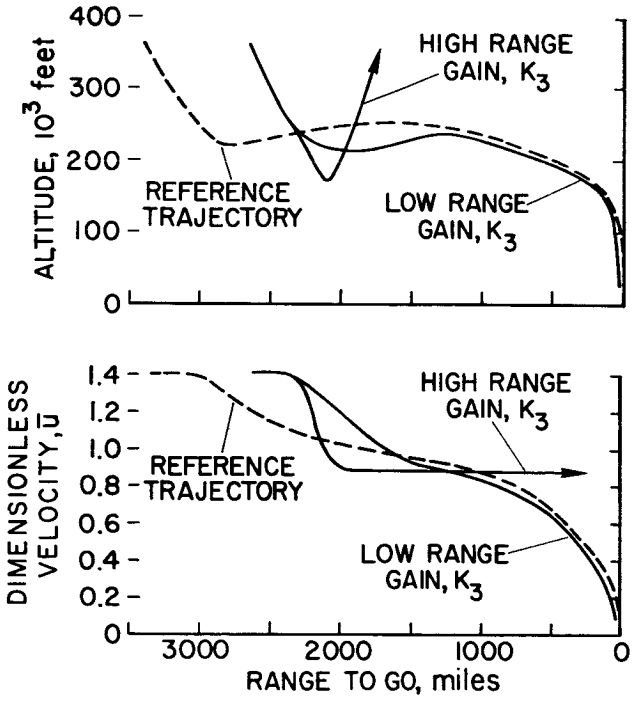

Fig. 9. - Effect of range input gain on the controlled trajectory with design range to go = 3400 miles; range to go = 2500 miles; $\gamma_1 = -5.7^\circ$; K_1 = -0.001/fps; K_2 = -0.33/g; K_3 = 0.0008 and 0.006/mile.

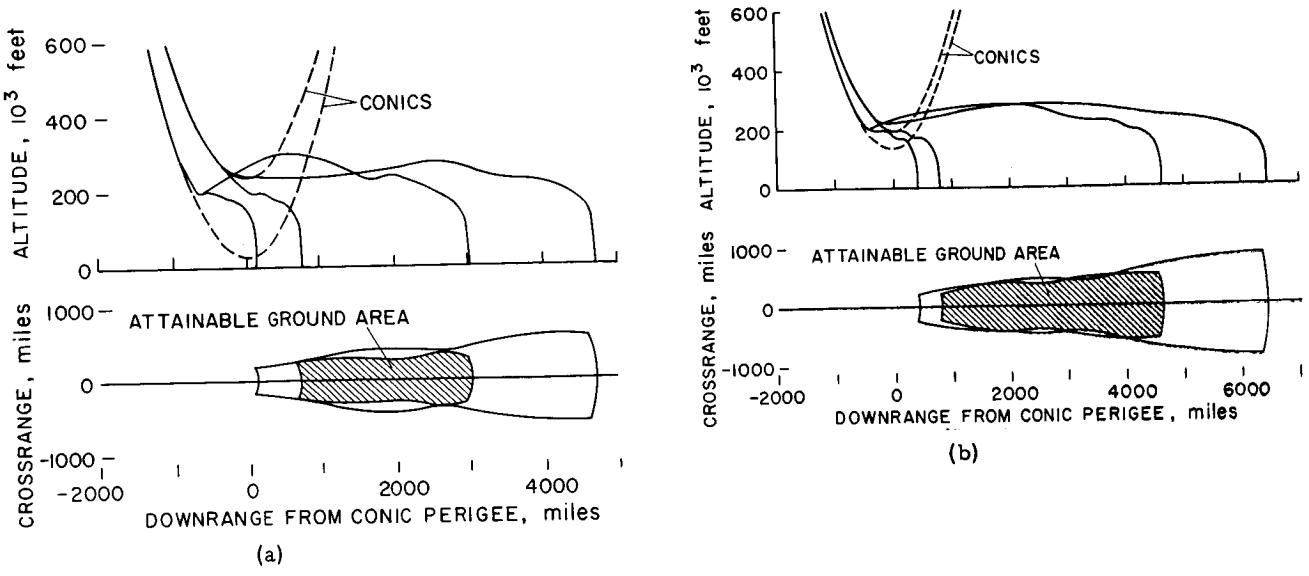

Fig. 11. - Attainable ground area for various combinations of entrance angle using the 3400-mile design reference trajectory. (a) γ_1 = -5.3° and -7.5°; 34-mile usable corridor depth. (b) γ_1 = -5.8° and -6.5°; 11-mile usable corridor depth.

Fig. 12. - Method of crossrange control for lifting capsule.

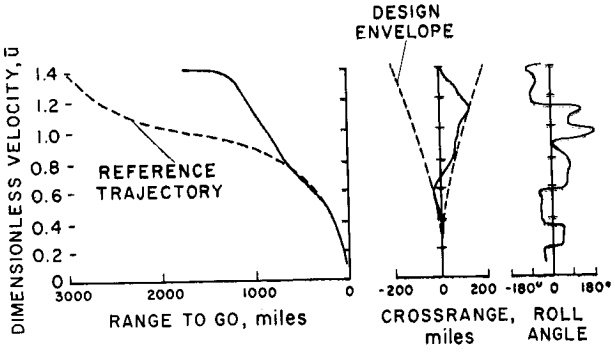

Fig. 13. -Trajectory controlled by roll-angle command; V_1 = 36,000 fps; h_1 = 400,000 feet; γ_1 = -5.8°; range to go = 1,700 miles; design range to go = 3,400 miles.

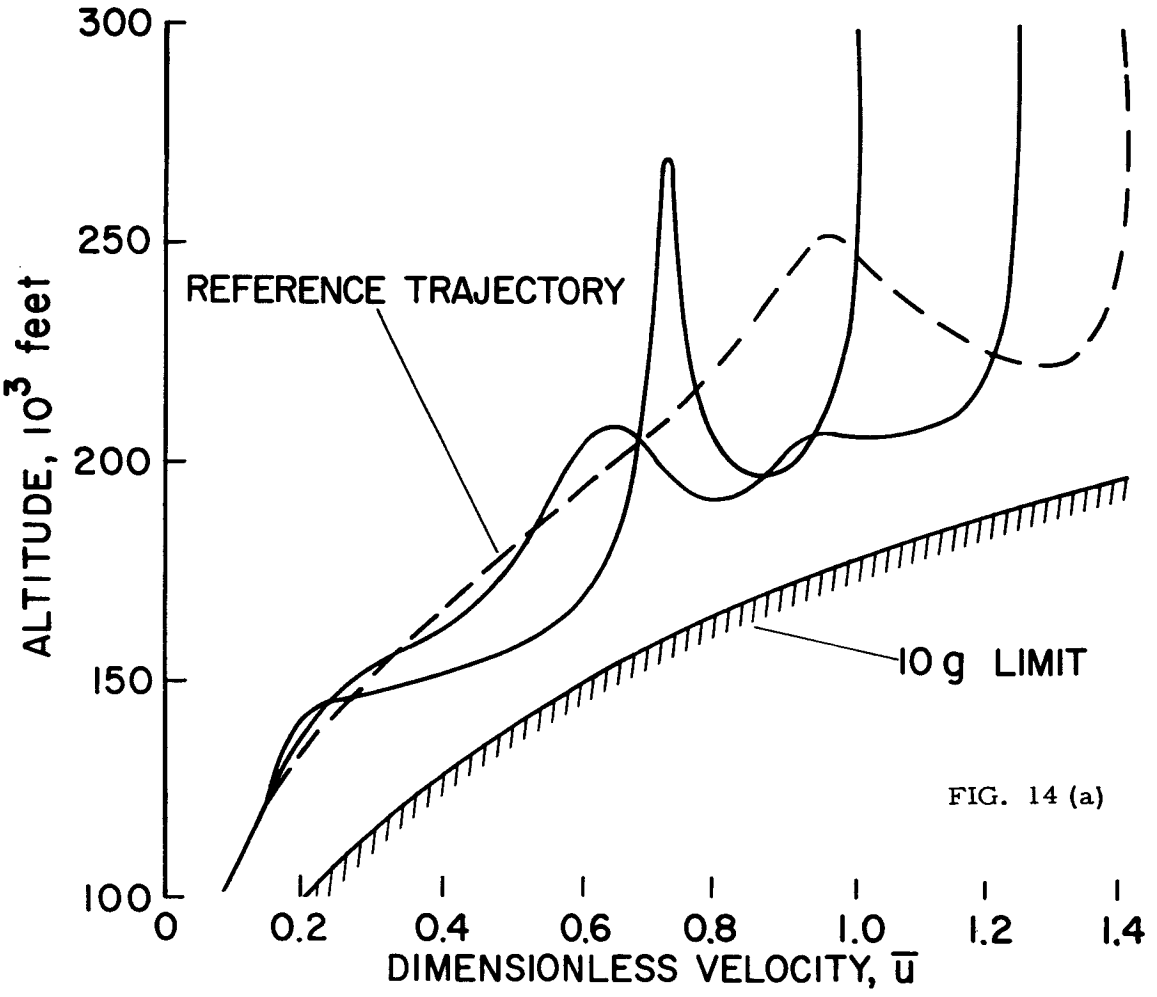

FIG. 14 (a)

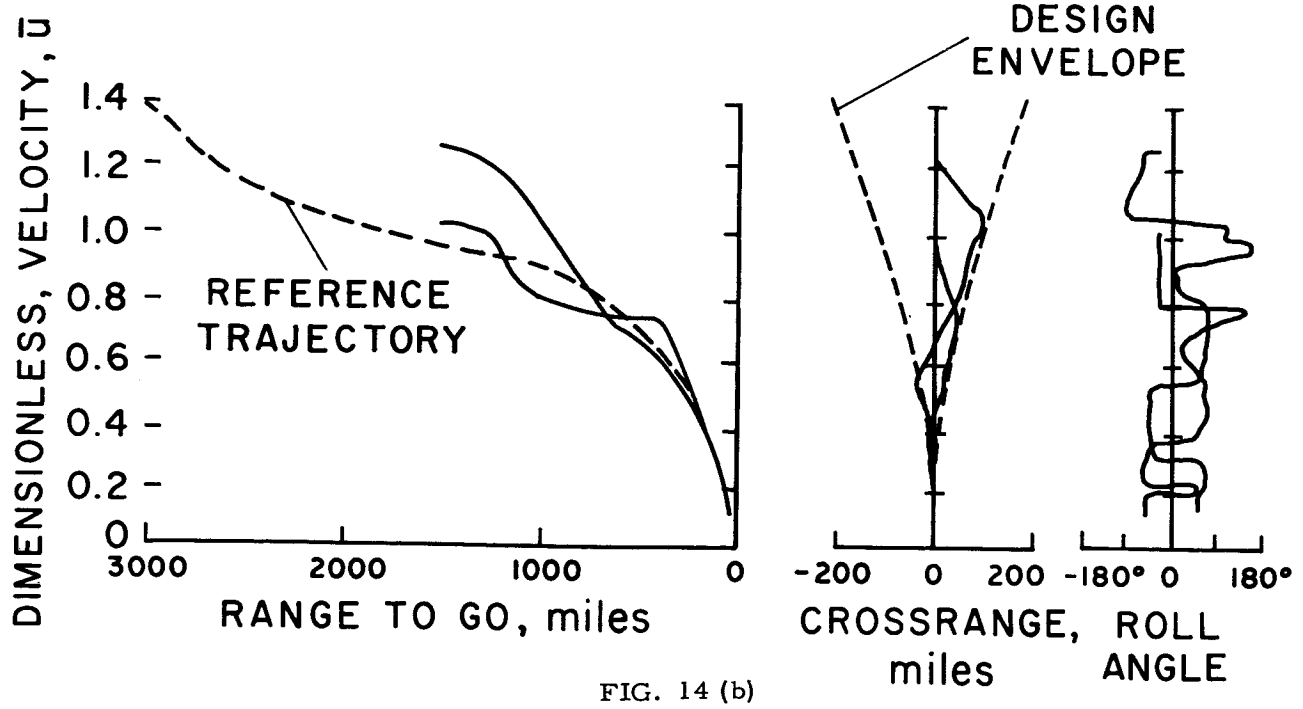

FIG. 14 (b)

Fig. 14. - Abort trajectories controlled by roll-angle command; V_1 = 26,000 and 32.000 fps; h_1 = 300,000 feet; γ_1 = -4°; range to go = 1,500 miles; design range to go = 3,400 miles at 36,000 fps. (a) Altitude variation with velocity. (b) Downrange, crossrange, and roll-angle variations.

RENDEZVOUS GUIDANCE TECHNOLOGY N62-14476

Robert S. Swanson, Consultant
Peter W. Soule, Senior Scientist
Northrop Space Laboratories

SUMMARY

The literature on rendezvous guidance technology is reviewed and a bibliography of about 160 documents is presented. The importance of the proper selection of the ascent trajectory and of the orbit for a manned space station or an orbiting launch complex is emphasized. The way the launch delay problem affects the selection of the ascent trajectory and the target orbit is discussed. A specific ascent trajectory and an orbit for a manned space station or an orbiting launch complex is recommended on the premise that launch delay problems will continue to outweigh most of the other orbit selection criteria.

A new method for determining the velocity corrections required for mid-course guidance is proposed. The proposed methods consist of an "exact-numerical" solution of the relative equations of motion in the "Shell-coordinate system." The proposed "exact-numerical" method extends the applicability of the mid-course equations to a much greater range than that of the currently available linear methods.

TABLE OF CONTENTS

SUMMARY
INTRODUCTION
ASCENT PHASE
  System Variables and Criteria
  Summary of Past Studies
  Recommended Ascent Trajectory and Target Satellite Orbit
MID-COURSE GUIDANCE PHASE
  Requirements for Mid-Course Guidance
  Summary of Past Studies
    Equations of Motion and Coordinate Systems
    Impulsive Techniques
    Guidance Simulation Studies
  Criteria for "Best" Mid-Course Guidance
  Proposed "Exact-Numerical" Methods for Mid-Course Guidance Using the "Shell-Coordinate System"
TERMINAL-HOMING PHASE
DOCKING PHASE
COUPLING PHASE
EQUIPMENT MECHANIZATION STUDIES
ERROR ANALYSES
CONCLUDING REMARKS
REFERENCES AND BIBLIOGRAPHY
FIGURES

APPENDICES
  A. The "Exact-Numerical" Solution of the Rendezvous Equations of Motion in the "Shell-Coordinate" System
  B. The "Exact-Numerical" Prediction of the Velocity Component Requirements for Two-Impulse Rendezvous Guidance Using the "Shell-Coordinate" System
  C. Summary of Rendezvous Equations

INTRODUCTION

One of the essential requirements for a strong National manned space effort is a satisfactory rendezvous capability. By means of this capability we can assemble, supply, and maintain manned space stations and orbital launch facilities; and can expedite our most important current National space project, the Apollo, by at least a year. Over the last four years the development of the analytic portion of rendezvous guidance technology has been proceeding, and now two experimental rendezvous projects, the Air Force's unmanned "Satellite Interceptor" and the National and Space Administration's manned "Gemini" are in progress.

While this review of the rendezvous guidance literature naturally has some application to these current projects, the specific proposals which are presented herein for ascent trajectories and for mid-course guidance apply primarily to more advanced systems, such as those associated with a permanent manned space station and/or an orbiting launch complex. A fairly complete bibliography of about 160 rendezvous guidance technology reports was prepared for this report. During the last four years at Northrop Corporation alone, over 50 technical reports on various aspects of rendezvous technology have been written (in addition to numerous progress reports and proposals). Two years ago Robert E. Roberson presented a comprehensive review[1] of rendezvous guidance in which he listed 22 selected technical reports (about half of the reports available at that time). A similar "selection" from the reports available today would total about 65 reports. This gives a rough indication of the current nature of rendezvous studies (and of the percentage decrease in quality of the published reports).

The problems associated with guiding a maneuverable astrovehicle (to be called a "space ferry" in the following discussion) either from the earth or from another orbit, to an orbiting space statin or orbiting launch complex (to be called the "target satellite" in the following), cover a number of astronautical technologies. For example, some of the more important considerations in rendezvous operations are: the characteristics of the launch vehicles, the trajectories to be followed, the sensing equipment, the mathematical models used, the computing equipment used, the propulsion system and attitude control system used, the docking and coupling system used and, most important, the over-all mission of the system.

The development of a strong rendezvous guidance technology is important for both civilian and military applications. The special features of military applications of rendezvous techniques will not be discussed here, although it should be noted that many of the logistics problems associated with military operations in space are substantially identical to the civilian space logistics problems.

The word, "rendezvous," has many meanings — even when used in a strict astronautic sense. "In-transit-rendezvous" is the rendezvous between vehicles while in route to the lunar surface or the planets. The term, "planetary rendezvous," denotes the rendezvous of a man-made astrovehicle and one of the planets in the solar system (usually a planet other than "earth" unless the astrovehicle was launched from another planet). "Rendezvous" will be used in this paper to denote the process of bringing a maneuverable astrovehicle, or space ferry, into gentle contact with a non-maneuvering orbital vehicle in a near-earth orbit.

Note also that the mid-course guidance problems associated with the rendezvous between a space ferry and a target satellite, and the mid-course guidance problems associated with "planetary rendezvous" are very similar. In the terminal phases of planetary rendezvous the influence of gravitational field of the planet and the influence of its atmosphere are of predominant importance, while the gravitational attraction between a space ferry and a target satellite is completely negligible, and they have no atmosphere. Because the mid-course guidance problems are similar, the bibliography presented in this report contains some papers dealing with the mid-course guidance problems associated with planetary rendezvous.

The cost of rendezvous operations, even the success or failure of such operations, depends to a major extent upon the proper selection of the target satellite orbit and the ascent trajectories used by the space ferry. As a result of studies of the way the rendezvous problems affect the over-all system optimization, some specific recommendations for the over-all staging design of large launch vehicles will be made. The staging and, in general, the ascent trajectories will be discussed in some detail in the section entitled, "ASCENT PHASE."

In the section entitled, "MID-COURSE GUIDANCE PHASE," are presented some of the requirements for mid-course guidance and a summary of past studies. The mid-course guidance phase is considered herein to include all operations from the moment of leaving the waiting orbit (or another orbit) until the terminal homing phase starts. The initial range may be of the order of 450 nautical miles and this, of course, requires the use of powerful beacons in the target satellite. This definition includes what has sometimes in the past been called terminal-impulsive guidance. Since substantially the same techniques are required for both terminal-impulsive and mid-course-impulsive guidance, it is believed more desirable to broaden the definition of mid-course guidance to include substantially all near-impulsive corrections given to the maneuvering vehicle. The authors also present a proposed new method for mid-course guidance, using the "Shell-coordinate system," which they have previously proposed[2,3], and an "exact-numerical" solution of the relative equations of motion (see Appendices A and B). The solution is so arranged that the velocity components required for rendezvous at a specified time can be calculated more accurately than will be required when consideration is given to the errors due to the sensing equipment (the radar equipment, for example). The proposed method allows a great extension in the range of applicability of mid-course guidance — above that of currently available linear systems. The scheme does, however, require greater spaceborne digital computer capability than would be required by the linear system. Greater radar range (using beacons, of course, for the friendly rendezvous case) is also desirable to fully utilize all the potential of the proposed scheme. It is believed the desired sensors and computer equipment will be available for the suggested applications.

As was previously mentioned, the mid-course guidance phase of planetary rendezvous is similar to the mid-course guidance phase of orbital rendezvous. For this reason the proposed new procedure for calculating the velocity corrections required for orbital rendezvous mid-course guidance may have direct application to planetary rendezvous operations. Further investigation will be required to establish the relative usefulness of the methods proposed in Appendices A and B with those currently suggested for planetary rendezvous mid-course guidance.

Although the main emphasis in this report is on the ascent and mid-course guidance phases, some consideration is also given to the terminal homing phase, the docking phase, and the coupling phase. While it is certainly necessary to perform these maneuvers accurately and with high reliability, it is expected that the selection of a specific method of performing these maneuvers will, in general, have little effect on the over-all performance characteristics, i.e., the total payload which can be placed in orbit. The discussion of the studies available on equipment mechanization and error analyses is also rather limited, since few such studies are currently available for the type of rendezvous applications mainly under consideration herein.

This paper has three appendices. The first two appendices (A and B) discuss in some mathematical detail the "exact-numerical" solution of the rendezvous equations of relative motion in the "Shell-coordinate system," and the methods of using the numerical solutions of these equations for two-impulse mid-course rendezvous guidance. Because the formulation of the equations and the method of solution are new, it was felt desirable to present it in some detail. The essence of these two appendices is, however, summarized in the body of the paper for those not directly working in the field. In Appendix (C) is given a summary of the various forms of the rendezvous equations of motion which are used. The material in this appendix is included primarily for convenient reference.

Three "Flight Performance Manuals for Orbital Operations" have recently been prepared for the Marshall Space Flight Center/NASA, and contain many useful design charts[4,5,6]. The material contained in each of the three handbooks is somewhat different, but it is all valuable. It was not felt desirable to reproduce herein the material on rendezvous given in these manuals but, rather, the recommendation is made that any serious student of rendezvous technology acquire access to these three unclassified handbooks.

ASCENT PHASE

System Variables and Criteria

The rendezvous of a vehicle launched from the surface of the earth with an orbiting target satellite in an orbit with arbitrary inclination, altitude, and epoch angle involves large performance penalties and severe guidance problems. While this is the normal military interception problem, and the inefficiencies must be accepted in the military situation, it is certainly intolerable for the routine, but expensive, logistics operations associated with a manned space station or an orbiting launch complex. Although it is possible that we will have a major launch base near the equator at some future time or that we may develop oceanic portable launch sites, it is most likely that the free-world establishment of a manned space station or an orbiting launch complex will take place from the Atlantic Missile Range. The orbit of these systems should thus be selected in such a way as to optimize the required rendezvous operations for launches from the Atlantic Missile Range.

It is quantitatively very difficult to measure the "cost" of a rendezvous operation which is not performed because adequate allowance was not made for possible aborts, launch delays, etc. The over-all cost is probably much more than that of the cost of the single launched vehicle. It may involve some danger to the well-being of the whole space station or, if additional back-up launch capability is maintained at all times, the rather tremendous cost of such an additional capability must be charged against the unreliable, poorly designed rendezvous system. The numerical evaluation problem is difficult but, fortunately, it is not the purpose in this paper to make a quantitative operational research study of rendezvous operations but, rather, to point out some of the fundamental system variables that must be considered.

The expected "cost" of rendezvous operations thus depends on the following:

1. Probability of a successful rendezvous.
2. The over-all payload capability of the launch vehicle.
3. The relative size of the launch vehicle stages.
4. The way the ascent phase errors affect the mid-course and terminal guidance phases.
5. Payload penalty required for corrective guidance.
6. The operational problems associated with launch (these problems can be measured both by the statistical distribution of launch delays and the monetary cost of launch operations).
7. The weight and size of the required life-support system in the space ferry (as it affects the time in a waiting orbit).
8. Launch base location and facilities available.
9. Safety provisions during launch.
10. Mission of manned space station or orbiting complex.
11. Characteristic velocity requirements to maintain vehicles in the target orbit.
12. Radiation hazard associated with target orbit altitude.
13. Payload penalties for ferry vehicle associated with target orbit altitude.
14. Payload penalties for ferry vehicle associated with earth rotation effects.
15. Personnel morale problems associated with rescue capability.

In the selection of the optimum ascent phase consideration must be given to all of the system variables specified above. Certain qualitative criteria can be postulated which are, for the most part, rather obvious. It is desirable to have a high probability of a successful rendezvous, and usually it will be worthwhile to have a rather conservative design, for the factors relating to the high probability of a successful rendezvous most likely outweigh the performance criteria. On the other hand, it is very possible to "have one's cake and eat it too" by careful selection of the target satellite orbit and ascent trajectory along with the selection of the staging of the launch vehicle. For example, if all of the characteristic velocity margin (required to overcome some of the factors that would decrease the probability of a successful rendezvous) is placed in the space ferry, then this margin, when not actually used, can be considered useful payload, since it will always be desirable to accumulate fuel in orbit. The launch delay problem mentioned in item number 6 is quite important. To avoid unnecessary repetition the launch delay problem and the other criteria will be discussed in more detail in the next two sections.

Summary of Past Studies

"Rendezvous-Compatible-Orbits" are a class of orbits which are designed[7-13] to allow efficient rendezvous operations. An example of a desirable rendezvous-compatible-orbit is shown in Fig. 1. A rendezvous-compatible-orbit is one in which the satellite traces over the earth are synchronized with the rotational period of the earth. This synchronization is obtained by the proper selection of the period of a satellite in a near-circular orbit and of the orbital inclination. It is necessary, however, to maintain the period of the satellite by a station-keeping procedure since, otherwise, there will be a continuous but varying drift due to the various perturbations acting on the satellite.

If the satellite is placed in any synchronous orbit in the proper epoch angle relative to the launch base, one efficient rendezvous per earth's rotation is possible. If the orbital inclination is simultaneously selected with the orbital altitude, it is possible to select points on the earth where one of the ascending (relative to the equator crossing) intersect. If these intersections are placed over a launch site, two efficient rendezvous are possible each day.

In actual practice the vehicles cannot rendezvous directly over a launch base; therefore, when it is desired to determine the orbit which allows two possible rendezvous per earth's rotation, it is necessary to make some assumptions concerning the trajectory of the launch vehicle. A simple, surprisingly realistic, assumption which can be made is that the injection point is a given distance downstream from the launch base — regardless of the direction of launch. That is, the

injection point is assumed to lie on a small circle of constant radius from the launch base.

It was pointed out in the reports[7-13] on rendezvous-compatible-orbits that the more important of the over-all system requirements for the selection of target orbits can be met by having the target satellite in an orbit with an altitude so selected as to give a synchronous ratio between the rotational period of the satellite and of the earth of exactly 15 to 1. In Ref. 7, the problems associated with the selection of the inclination of the "rendezvous-compatible-orbit" were discussed and a low inclination orbit was recommended, primarily based on the belief that a pessimistic view should be taken of the precision with which the timing of launch operations will occur. It was pointed out that a low-inclination orbit is more tolerant of launch delays than is a high-inclination orbit.

It should be noted that larger orbital plane inclinations allow rescues from ground-launched vehicles a much greater percentage of the day with moderate plane angle change capability. For example, a plane inclination of about 35° and a 10° plane angle change capability allows six hours per day rescue capability. However, it seems preferable to provide "lifeboat" type return capability in the space station, rather than hope to "rescue" the personnel — mainly because of the tremendous cost of maintaining a fully equipped launch facility for rescue. Thus, a lower inclination orbit plane of about 29.2° is recommended.

Since these rendezvous-compatible-orbits are described in detail in these six references, a detailed description will not be repeated here. It should be noted, however, that the prime advantage of rendezvous-compatible-orbits is that two efficient rendezvous can be performed each day (more exactly each "effective" earth's rotation, i.e., the time required for the earth to rotate one revolution with respect to the target satellite orbit plane). If launches are made at precisely the right time these two rendezvous are made without any plane angle change. If there is a slight launch delay, a small orbit plane angle change is required — the magnitude of the plane angle change depending on the amount of the delay and of the particular inclination rendezvous-compatible-orbit chosen.

A rendezvous-compatible-orbit clearly requires that the initial errors in orbit establishment of space station be corrected and that the proper epoch angle be maintained by a station-keeping control system. These problems were discussed by the authors[14] and a recommended "zero cost" station-keeping technique was suggested.

It has been suggested by John Bird, David Thomas, and John Houbolt[15,16] that only a very small plane angle change would be required to perform a rendezvous once-a-day, provided the inclination of the target orbit plane was only slightly greater than the launch base latitude. The scheme, as suggested in these references, requires an accurate launch time (when the target is in the proper epoch angle), although it clearly could be modified by the use of waiting orbits. Utilizing this technique, there is no requirement for station-keeping of the target satellite and no requirement for the accurate selection of the orbital altitude. In general, the plane angle changes required for this technique are about half of the difference between the inclination of the target orbit plane and the launch base latitude. The plane angle change can thus be maintained quite small with a small orbit inclination.

W. H. Straly[17] has discussed the general problems associated with launch timing and has recommended a technique which utilizes a small plane angle change and the "phasing technique," which is essentially a waiting orbit. The technique he recommended was thus, in effect, an extension of that recommended by Bird[15] and Houbolt[16] to include the use of waiting orbits to avoid the accurate launch time restriction. Straly[17] did not place any restrictions on the target orbit altitude, nor did he suggest any station-keeping technique to control the epoch angle. The orbital inclination was merely suggested to be only slightly greater than the launch base altitude. Because there was no restriction on the altitude and thus the epoch angle, relatively long waiting times in orbit could be required.

The technique of using waiting orbits is by no means new. Various aspects of waiting orbits are discussed by Swanson,[18] Steinhoff,[19] Ehricke,[20,21] Keller,[22] Brunk and Flaherty,[23] Paiewonsky,[24] and Pierce.[25] A number of other papers which deal with the problems associated with the ascent phase, including discussion of the actual Saturn guidance system, are listed as Refs. 26 through 33, and, of course, much useful information is included in the three Flight Performance Manuals.[4,5,6]

Recommended Ascent Trajectory and Target Satellite Orbit

The logistics requirements associated with a large manned space station or an orbiting launch complex are sufficiently great so as to demand a great deal of care in the selection of the optimum orbit and the selection of the best nominal ascent trajectory. This selection should take due account, not only of the optimum conditions, but also of the various possible errors or tolerances associated with the logistics operations. While there are many who believe that launch timing problems can be made non-existent in the 1970 time period, it appears desirable to select the target satellite orbit so that not only can efficient launches be obtained for on-time launch operations, but also the penalties associated with launch delays are minimized.

The recommended orbit is the lowest possible inclination "rendezvous-compatible-orbit." The basic concept of rendezvous-compatible-orbits is believed to be very sound for multi-rendezvous operations. In a negative sense it simply appears to be very foolish from a logistics viewpoint not to establish and maintain the target satellite in an orbit which optimizes the logistics system, since even, at best, maintaining space stations and orbiting launch complexes are very expensive. The selection of the specific rendezvous-compatible-orbit out of the multitude that are available depends on many criteria. A synchronous ratio 15:1 orbit with an altitude of about 260 nautical miles is selected as a best compromise. The

alternates for two-per-day rendezvous are a synchronous ratio of 14:1 rendezvous-compatible-orbit with an altitude of over 440 nautical miles which is in the lower part of the Van Allen radiation belt, and an altitude of 98 nautical-miles-orbit associated with a synchronous ratio of 16:1. The lower altitude, while ideal for a short duration parking orbit, is too low for a permanent manned space station. The cost in characteristic velocity to maintain a space station at this low altitude on a continuous basis is prohibitive. Intermediate altitudes can be obtained by using synchronous ratios allowing two rendezvous every two or three days. These lower intermediate altitudes (150, 175, and 205 nautical miles) have only slight payload advantages for launch vehicles which are properly staged to utilize the 98 nautical-mile parking orbit and general ascent trajectory recommended herein, and would require much longer times in the waiting orbit for both optimum and non-optimum days. The intermediate orbits would have the same general payload penalties associated with launch delays for launches scheduled for the optimum days, but the possible penalties on the other days would be much larger. The payload advantage of the intermediate altitudes is, however, quite pronounced for current two-stage launch vehicles. The intermediate altitude trajectories may thus have real advantages for the current experimental program, Project Gemini.

Note that if a Hohmann transfer is used from the parking orbit and the mission is an orbital-launch refueling operation, then part of the additional characteristics velocity required by the 260 nautical miles orbit over that of, say, the 175 nautical miles orbit is regained due to the small escape velocity required from the higher altitude.

The net penalty for this example is about 100 feet/second of characteristic velocity (for the orbital launch vehicle). For permanent orbital launch facilities this is more than compensated for by the fact that about eight times more characteristic velocity (about 250 feet/sec/year for the whole facility if it weighs 100 pounds/square foot frontal area) is required to maintain the lower orbit against air drag than to maintain the 260 nautical mile orbit.

The selection of the orbital inclination depends on the specific mission of the space station but, in general, one may expect that any orbital inclination from 28.5 degrees to 35 degrees will meet most of the purposes of the space station. The selection of an inclination of 29.2 degrees for vehicles launched from the Atlantic Missile Range (with an assumed latitude of 28.5°) gives an offset angle (i.e., a difference between the orbital inclination and launch base latitude) of about two-thirds of a degree. This inclination of 29.2 degrees allows zero plane angle change rendezvous for two successive satellite passes. The use of parking orbits and a two-thirds degree plane angle change capability (which can be partially accomplished by the more efficient boost-turn trajectory during the first and second launch stages) allows a rendezvous to be accomplished at any time within a period of two hours and twenty minutes. It is believed that this time period is more than adequate for launch delays to be encountered in the next few years, and certainly more than adequate in the 1970 time period. The relatively small payload penalties associated with the two-thirds-of-a-degree plane angle change are expected to be more than compensated for by the increase in payload capability obtained by utilizing a low-altitude (98 nautical miles) parking orbit.

Although this scheme allows a launch window of about two hours and twenty minutes, there are clearly some times for which it is more optimum to launch than others. The specific rendezvous-compatible points are obviously the desired times for launching. It is believed desirable to partially close this 2.3-hour window. The exact readjustment would require a detailed study of the possible sources of launch delay and of the propellant boil-off cost associated with the specific launch vehicle. (A possible compromise closing of the launch window is suggested below.)

It is desirable to examine in somewhat more detail the specific recommended orbit and the trajectory to be followed as a function of the launch delay time. The target orbit inclination is 29.2 degrees, and the nodes of the target orbit are so oriented that the injection point for a launch from Cape Canaveral lies exactly in the plane of the orbit in two successive passes over the launch base. Since the launch vehicle and space ferry are designed with enough margin to allow a minor boost-turn and orbit plane angle change capability (about 0.67 degrees), the launch can actually be scheduled 23 minutes (about one-fourth orbital period) prior to the ideal rendezvous-compatible launch time. If the epoch angle is made compatible with this early launch period, when the launch actually occurs at 23 minutes prior to the condition of zero plane angle change, the time the vehicle is required to remain in the 98-nautical-mile waiting orbit will be only that time required to separate from the second stage and acquire the target satellite on the radar and compute the desired mid-course trajectory, and start a near-Hohmann transfer to the target satellite. If the launch delay is 23 minutes later then no plane angle change will be required, but the space ferry must remain in the waiting orbit for four-parking-orbit revolutions prior to injecting into the Hohmann transfer. Additional launch time delays will require plane angle corrections and additional time in the waiting orbit until a maximum of 94 minutes of launch delay results in 16 waiting orbit periods (or one effective earth's rotation). For launch delays of 94 minutes, it is no longer necessary to wait in the parking orbit but, rather, conditions are once again compatible for a zero time in the parking orbit. The time in the waiting orbit again increases continuously as additional launch delay occurs, but for the next 23 minutes the orbit plane angle change requirement decreases to zero. For launch delays greater than 117 minutes, the plane angle change required increases nearly linearly to the maximum of two-thirds of a degree at 23 minutes after the zero-plane-angle requirement and a total time in the waiting orbit of 140 minutes (or 2 hours and 20 minutes). Between the times of about 47 minutes after the first opportunity for a launch until 94 minutes from the first opportunity is the most unfavorable launch time. Nearly the full two-thirds-degree plane angle change is required along with a time in the waiting orbit in excess of one-half day. It would generally appear desirable to

postpone launch during this time, if possible, and reschedule launch for 94 minutes after the original schedule. If this is done, a total launch time of 94 minutes, nearly equally spaced around the two efficient (zero plane angle change) rendezvous is obtained. (It appears completely unreasonable to expect to perform launch operations of manned rendezvousing systems with launch vehicles which are sufficiently unreliable that a total tolerance launch time of about an hour-and-a-half-per-day is unsatisfactory.) In this case, the maximum time in a waiting orbit is one-half day or eight waiting orbital periods. This is considered quite satisfactory, since in the advanced time period considered and the complex operations involved in space, if there is any appreciable decrease in the reliability of this system associated with one-half day spent in a waiting orbit, then the whole logistic system is too marginal to be considered.

One can characterize the recommended target satellite orbit as a station-kept,[14] "rendezvous-compatible-orbit" which utilizes an ascent trajectory containing most of the best features of the one-rendezvous-a-day scheme of John Bird[15] and John Houbolt,[16] and of the phasing technique described most recently by W. H. Straly[17] for those launch operations which involve possible launch delays. The target satellite orbit and recommended ascent trajectory allow efficient on-time launches but are also extremely tolerant of launch delays, and these delays can be as great as two hours and twenty minutes without exceeding a penalty of more than about 250 per second of characteristic velocity. The propellants associated with this characteristic velocity will be accumulated in orbit, for other uses, if the launch is on time.

The trajectory has been selected to include a parking orbit in order to account for launch delays. It is desirable to stage the launch vehicles so as to fully utilize the characteristics of the parking orbit so that the maximum payload may be carried to the manned space station or orbiting launch complex. The use of three-stage vehicles (where the space ferry is considered to be the third stage) seems to be most desirable for such space logistics operations. The first two stages are required to boost the space ferry to an apogee of 98 nautical miles, the parking orbit altitude. The flight path should be so arranged that the first two stages burn all their propellants, the flight-path angle being so controlled that the apogee is equal to 98 nautical miles. The velocity decrement at that altitude required to inject in a circular orbit will be provided by the space ferry. The amount of this decrement will, of course, depend on the specific characteristics of the first two stages. Such a procedure is allowable, since the vehicle is going into a parking orbit and exact timing during the operation of the first two stages is not required. The relative position of the space station and of the space ferry in the parking orbit must be so arranged that under the worst tolerance conditions associated with the first two stages that adequate time is still available for a near-Hohmann transfer between the parking orbit and the space station rendezvous-compatible altitude orbit when the launch was on-time.

By means of such staging it is possible to have all of the propulsion margin placed in the space ferry and, thus, propellants will be accumulated in orbit for other uses such as station-keeping, attitude control, refueling of astrotugs and refueling of lunar launched vehicles, etc. The other distinct advantage of this type of staging is that we do not require a two-stage launch vehicle to inject directly into a high 260-nautical-mile orbit, since the degradation of the performance of a two-stage vehicle with orbital altitude is notorious. Because the space ferry must have propulsion capability in order to perform the rendezvous, it is highly desirable to utilize it in other ways to make sure the maximum payload is carried to the space station or orbiting complex.

It generally appears to be undesirable to utilize parking orbits which are above the rendezvous-compatible-orbit. First, because they require more characteristic velocity and, second, because under the conditions which we would normally like to utilize a high-altitude parking orbit, a plane angle change is also required to further increase the characteristic velocity penalty. The additional time which must be spent in a low-altitude waiting orbit seems preferable to the large increase in characteristic velocity associated with the high-altitude parking orbit — at least for routine logistics applications.

It should be noted that there is a difference in the precessional rate of the orbit plane of the space ferry in the 98-nautical-mile waiting orbit and the target satellite orbital plane in the 260-nautical-mile rendezvous-compatible-orbit of about one degree per day. This difference in the precession of the orbit planes must be accounted for in such a way that the launch azimuth into the waiting orbit will allow a near-Hohmann transfer without any required orbit plane angle change when the transfer from the waiting orbit to the final target orbit is accomplished. With a low-inclination orbit, such as the recommended 29.2 degrees, rather minor changes in the launch vehicle flight path result in an azimuth angle at injection which produces a very large change in the nodal angle and, thus, there are substantially no penalties associated with allowing for differential precession angles as much as one degree.

MID-COURSE GUIDANCE PHASE

Requirements for Mid-Course Guidance

In the discussion of the friendly rendezvous for the purpose of supplying a manned space station or orbital launch facility, it was shown that parking orbits are required to cope with moderate to large uncertainties in the timing of launch operations. Even if parking orbits are not used, it is generally most efficient to stage the launch vehicles such that the space ferry is injected into a near-Hohmann transfer from a low altitude of from 60 to 100 nautical miles. In either case, with a coasting trajectory of nearly 180 degrees and with an altitude difference of over 160 nautical miles, it is very desirable to utilize long-range mid-course corrections in order to minimize the requirements on the final terminal-homing phase and, in general, to accomplish a rendezvous with the maximum efficiency and safety. In fact,

it would be desirable to leave the parking orbit for the 260-nautical-mile rendezvous-compatible-orbit only after the radar guidance has acquired and locked on the target satellite if the radar is in the space ferry. (For routine operations it is expected that radars will actually be available in both vehicles for improved reliability.) This requires a total radar range of about 450 nautical miles, a range which is not available with current radars but which does not require large increases in the state-of-the-art for the cooperative rendezvous situation in which the target carries a beacon. If the target satellite orbit is well-known and the ascent guidance fairly accurate, the initiation of the near-Hohmann transfer could almost be based only on range information without regard to range rate or angle rate information, provided the mid-course corrections were within about 10 minutes. This would give more than adequate time for radar data smoothing.

Once on the transfer orbit, it is desirable to have a form of mid-course guidance logic, which would require no corrections at all if the data were perfect and the satellite was on a collision course with the target. Unfortunately, as some detailed computer studies by the authors and by Eggleston[34,35] have shown, the popular linearized guidance formula[2,3,34-38] do not work too well for orbits which are as far below the target orbit as these will be. Here it would seem that some improvement in guidance technique is required, and a proposed procedure for solving this problem will be discussed below, as well as in Appendix B. When the range between the interceptor and the target decreases the closed loop logic using linearized equations (similar to that described by Eggleston[34]) proves quite adequate.

Summary of Past Studies

Equations of Motion and Coordinate Systems. It is very desirable to have available and to use approximate equations of motion when studying the rendezvous problem; first, because a clearer understanding of the physical situation is then possible; and, second, because the actual computations required for the rendezvous must be performed with a space-borne computer. If approximate equations can be used the computer can be made simpler and of lighter weight. It is, of course, necessary to know the range of validity of the approximate equations. If the approximate equations are not valid over the range for which they must be applied, then methods of solving the more exact equations must be developed. "Exact-numerical" solutions of the exact equations are presented in Appendices A and B.

The first approximation to the equations of motion (and their solution) to be discussed is the "free-space" approximation. The assumption is made that the two vehicles are sufficiently close together so that the effects of the earth's gravitational attraction are almost the same on both vehicles and, therefore, we can assume that the net effect of the gravitational attraction terms is negligible and the equations of motion in inertial free space apply. Such an assumption, it is clear, will only apply when the two vehicles are rather close together and, furthermore, when the time interval for the completion of the maneuver is relatively short. If the time is long, even when they are close together, the effects of gravitational forces will result in significant modifications of the motion; and if the bodies are far apart then the gravitational differences may produce significant forces. These two criteria have different implications. The fact that the bodies are close together merely defines that it is the very terminal phase of the motion for which this approximation can apply, but the fact that the time must be short implies that rather large thrust forces are utilized to make the rendezvous, so that these forces will be large relative to the differential effects of gravity. This very well may have the connotation of inefficiency, since the gravitational forces are negligible in a percentage sense only, and if the thrust forces are very large it may require a tremendous quantity of propellant to perform the maneuver.

One exception to this rule is when the closing velocity is large because it is obtained from previously required impulses and/or because the motion of the intercepting satellite is at a much lower velocity than that of the target satellite, so that the target satellite is catching up with the intercepting satellite. Under these conditions a large force is not required to initiate the motion, but only to stop it, and there are no great inefficiencies associated with this type of use of the free-space equation concept. Thus, the free-space approximation to the equations is most useful for the homing guidance equations.

The free space concept was discussed by Mr. R. A. Hord,[39] and H. Oberth.[40] The errors involved in using the free space concept are best discussed by evaluating the differential gravitational effects (which are also termed "tidal accelerations").

If the first-order effects of the earth's gravitational potential are included in the equations of motion the range of validity of the equations is greatly extended. This was first shown independently by three different groups: Albert Wheelon,[36] Clohessy and Wiltshire,[37] and Louis Spradlin.[38] All of these three studies used the rectangular rotating coordinate system. The rectangular rotating coordinate system is less accurate in general than the shell-coordinate system developed by Swanson, Petersen, and Hoover,[2] and by Soule.[3] Independent studies showing the advantages of the shell-coordinate system were conducted by Eggleston and Beck[41] and Stapleford.[42] The fact that the shell-coordinate system is appreciably better for rendezvous studies than is the rectangular coordinate system can be seen most easily for those cases where the x coordinate is large, where the x direction is along the flight path. If two bodies are in precisely the same orbit, they will have the same altitude in the shell-coordinate system (see Fig. 2), but will have a different altitude in the rectangular system depending on the value of x. The time interval of the motion is no longer of quite such importance as in the free-space case, but the relative displacements between the two bodies are important, since the first-order gravitational effect type of an approximation is directly associated with the geometrical relations between the two satellites and the earth. Furthermore, greater efficiency is obtained since the "natural" gravitational forces can be used to advantage.

Impulsive Techniques. The two-impulse rendezvous guidance technique has been developed by Clohessy and Wiltshire,[37] Soule,[3] and Eggleston.[34] While the two-impulse technique is by no means optimum, its simplicity makes it very attractive. The first impulse is given shortly after booster burn-out, and the second is usually replaced by a terminal-homing phase. When the characteristic velocity required for rendezvous is small, then the use of a simple non-optimum scheme such as the two-impulse technique is much to be recommended. The technique is also very useful as a secondary correction procedure.[2] Useful design curves are given in the Flight Performance Handbook.[6]

A three-impulse technique suggested by Irving, and discussed by Wheelon,[36] consists of a tangential velocity increment just sufficient to neutralize any steady drift, later followed by two radial velocity increments; the first, when the vehicle crosses the same radial altitude as the target vehicle; and the second, just before impact with the target vehicle. This scheme is more expensive in final requirements than the two-impulse scheme.

A four- or five-impulse technique, called "Quasi-Optimal Rendezvous Guidance System", or "QORGS," was developed[2] — which gives a near-optimum rendezvous in that the impulses are given tangentially so that the minimum characteristic velocity is required to achieve rendezvous within exactly one orbital period. The four-impulse method requires less characteristic velocity than the five-impulse method; however, the five-impulse method is considered more optimum when the guidance sensor accuracy requirements are considered, as well as the characteristic velocity requirements.

Guidance Simulation Studies. The only orbital rendezvous mid-course guidance problem which has been simulated on digital computer is that of Eggleston.[34] This study clearly shows some of the shortcomings of the rectangular coordinate system and linearized equations of motion for long-range mid-course guidance. Eggleston also studied the effects of dead-band and of radar inaccuracies (a study similar to that of Eggleston[34] but using the guidance law suggested in Appendix B is very desirable).

Other reports which discuss the mid-course guidance problem are given in the bibliography.[43-55]

Criteria for "Best" Mid-Course Guidance.

The "best" mid-course guidance to use is hardly a subject that lends itself to dogmatic statements. The multiplicity of factors entering into the decision makes it difficult to say anything important unless specific information on the space system in question is available.

Anticipating the major characteristics of future space systems will, however, bring out some facts. In the friendly, logistic rendezvous emphasized in this paper, future rendezvous vehicles will become considerably more massive, while computer capability per unit of computer mass will increase so that the cost of improving the quality of guidance information by means of additional computing (smoothing plus exact equations of motions) will be a much smaller fraction of total vehicle mass than is now required while the potential savings will be greater. Furthermore, large digital computers can be boosted into orbit during the initial assembly of the space station and can be used for subsequent rendezvous operations (with a radio communications link). Again, the increased efficiency of rendezvous operations more than offsets the larger computer installation. It is apparent, then, that as sensors are improved more accurate guidance equations than have been suggested previously will be required to bring desirable over-all improvements in the system.

In homing systems similar to those proposed for the Air Force Satellite Interceptor System, the guidance formulas are derived on the assumption of free space (no force-field gradient). The rendezvous guidance systems typified by the Clohessy and Wiltshire paper[37] and by Swanson, Petersen and Hoover[2] derive guidance formula on the basis of linearized force-field gradients. In each of these types of guidance formulas the accuracy deteriorates with increasing range, but with closed-loop, guided trajectories these guidance laws will, of course, actually produce a rendezvous even when applied far beyond the limits that make the guidance formulas "good assumptions." The question to be answered in the choice of a mid-course guidance scheme is whether the waste of thrust is compensated by the simplicity of the guidance system. And the answer clearly depends on the operational time period in question.

Appendix B gives a basis for a guidance scheme which is one step more advanced than the two basic types referred to previously. This system gives an "exact" solution under the assumption of a central force field and, therefore, brings about another improvement in accuracy. Still more accuracy would require the consideration of very minute forces acting on the satellite — such as aerodynamic forces, those due to oblateness, and so on. Since these forces are very small and not too greatly different from each other in order of magnitude, a great number of them would have to be considered in order to bring about a unified treatment. The accuracy to be gained by these additional considerations is very small. Some of the effects of oblateness and the slight eccentricity of the orbit may be taken into account by the use of a reference orbit. The requirement in the selection of such a reference orbit is that the position of the reference point in the reference orbit will coincide with that of the target at the time of rendezvous.

The method proposed requires a successive approximation to be computed until a satisfactory numerical convergence is obtained. Once started, this method requires no evaluation of trigonometric functions so that the increase in required computational labor just for the operations of Appendix B is less than an order of magnitude when compared with previous methods. When looked at in the light of all the computation required (i.e., data smoothing, data conversion, etc.), the actual over-all increase in computer complexity is expected to be relatively minor.

In general, the factors that affect the choice of the mathematical model to use for the guidance system are:

1. The quality of the sensed information.
2. The range over which the system must operate.

An increase in either of these two tends to promote the selection of a more accurate guidance formula, and vice versa; there is little point in trying to make improvements beyond a certain limit in sensor accuracy for a short-range system. In this case the crudest of models, force-free space, is adequate.

Proposed "Exact-Numerical" Methods for Mid-Course Guidance Using the "Shell-Coordinate System"

Efforts to obtain a more accurate model of the relative motion in a rendezvous maneuver than that of the linear gravity gradient, culminated in the analysis given in Appendix A. The fact that the use of shell coordinates allows one to obtain two exact first integrals of the equations of motion is a strong point in its favor, but the more important consequence is that the "exact" equations of motion can be written in such a manner as to only have functional dependence on one (the altitude coordinate) of the dependent variables (the word, "exact," in this case implies the solution of the equations of motion for a central-force field and neglects the small perturbations due to earth's oblateness, atmospheric density, solar, lunar and planetary perturbations, etc. While some of these effects are of importance — when one is in a waiting orbit, for example — they are quite negligible during the mid-course guidance phase. In fact, the magnitude of these quantities can be used to estimate a limit on the required accuracy of the numerical calculations as performed in Appendices A and B. It is the fact that the equations have a functional dependence only on the altitude coordinate which allows the rapid numerical solution of the exact relative velocity required to produce a collision with the target in a specified time as is done in Appendix B. In addition, an improved version of the linearized equation has been derived by the rather obvious device of discarding (i.e., including in the non-linear part of the equations for numerical integration) only second-order small variable quantities. The resulting new linear equations are more accurate, in general, although a few specific instances have been found when they have made no improvement. These new linear equations, however, are not as easy to use as the previous ones for guidance purposes. The reason for this is that they contain the initial conditions in the coefficients in a complicated manner. The use of these equations for guidance would require a numerical iterative solution. The details of this are not given, however, since it is felt that if numerical integrations are to be used the non-linear terms should also be included (as in Appendix B) to give an exact solution to the rendezvous problem.

The work in Appendix A led to the application of the numerical method of successive approximation to the solution of the equations with rendezvous in a fixed time as a boundary condition. The formulation in Appendix A which makes the derivatives functions of only one dependent variable, makes the application of this method straightforward. This method takes an approximate curve which exactly fits the boundary conditions and refines it in a series of steps (see Appendix B).

The proposed procedure, then, is to start the near-Hohmann transfer maneuver from the parking orbit at the optimum time which is indicated by the orbit altitude difference and the epoch angle between the target and the interceptor. Once this optimum position is arrived at, the time to rendezvous of almost 180 degrees of target travel is selected and the exact impulse required to establish a collision course is computed by the method given in Appendix B. This impulse is given to the interceptor and then at periodic intervals along its ascent to the target, its relative velocity is measured and compared with the correct relative velocity as computed from the time to go and the exact methods given in Appendix B. As the rendezvous vehicle gets closer to the target the method of Appendix B degenerates to the more common linearized equations. From this point on into the final homing phase the mid-course guidance is achieved by conventional methods (discussed in detail by Soule[3] and Eggleston[34]).

TERMINAL-HOMING PHASE

There have been more analytic studies and more simulator work done on the manned and unmanned terminal-homing phase of rendezvous guidance than on any other aspect of rendezvous.[56-80] Although the various papers differ in specific details of the method of mechanization of the closed-loop terminal-homing guidance problem, they universally agree that fairly efficient homing guidance schemes can be developed. It is desirable that the mid-course guidance be so designed to bias the initial conditions for the terminal phase, that closing velocities are already established and the primary purpose of the terminal-homing system is then to decrease to zero these already established closing velocities.

The differences between the various proposed terminal guidance schemes depend upon the basic assumptions made as to the availability, accuracy and reliability of various types of equipment and the proposed schemes to minimize the errors. Schemes which require a throttleable propulsion system have been suggested in a number of papers by Sears and Felleman,[56-58] while schemes that involve constant thrust but require restartable engines have been proposed by several authors.[66, 67, 73] Another variation of the basic propulsion system which has been suggested by Kidd[72] and Soule[70] is to use a constant thrust engine on throughout the homing phase and achieve guidance by controlling the direction of the engine thrust.

The various proposed homing guidance schemes may also be specified by consideration of the methods they suggest for computation, i.e., whether analog or digital, and the particular coordinate axis system they suggest using during the terminal-homing phase. Stapleford[73] has suggested an equipment mechanization scheme designed for minimum complexity. Such a scheme is believed to be very useful for unmanned rendezvous, but for the type of operations which is envisioned herein, for an advanced time period, and where both ascent guidance and mid-course guidance as well as other operations are to be performed with rather high capacity digital computers, it is doubtful that

such a scheme need be used.

The capability of man to conduct the terminal phases of rendezvous has been studied.[78-84] However, it is not clear that there is any advantage to his participation in the terminal phase of rendezvous as a part of the closed loop. There is obviously a great need to have him aboard the vehicle to increase the over-all reliability by performing monitoring and maintenance functions. Obviously, he can only satisfactorily perform maintenance functions if adequate propulsion capability is available for him to interrupt the rendezvous sequence for several orbits while repairing the equipment and again make a satisfactory approach and rendezvous. The problem of how to best utilize man in space has been extensively discussed to date and clearly requires still further thought and experimentation before satisfactory answers can be obtained.

DOCKING PHASE

The docking phase begins either when the interceptor satellite is moved as close to the target satellite as is practical with the terminal-homing guidance and the moderate to large maneuvering rockets, or when the docking guidance and control system can adequately take over (even though the terminal phase homing system may still be performing well). The distance between the two vehicles will have been reduced to only hundreds of meters at the start of this phase. The docking phase has been discussed for both manned[85] and unmanned[86] systems.

The docking phase may require the space ferry to approach the target satellite from a particular azimuth and elevation for some operations. Additional sensory information would then be necessary, and would probably be obtained from measurements made from the target satellite and transmitted to the space ferry. Vernier thrusting would be required to utilize this added information.

The docking maneuver is less complicated than the terminal maneuver from the standpoint of the equations of motion used to guide the docking procedure. The equations can be, if desired, reduced to their free-space forms with negligible loss of accuracy due to the relatively small distances involved.

In some other respects the docking phase is rather difficult. The interceptor satellite must usually be able to approach the target satellite at a given azimuth and elevation. The selection of the best sensory and guidance equipment to handle this requirement is a problem that depends on the specific space station configuration, etc. In addition, the design of an effective docking system must be done concurrently with that of the sensory and coupling mechanism system because of their interdependence.

COUPLING PHASE

The termination of the docking phase and the start of the coupling phase begins with the initial contact between the two rendezvousing vehicles. At this instant the interceptor satellite no longer actuates its maneuvering and attitude control rockets so that the two control systems will not oppose each other. Note that any maneuvering rockets whose jets are pointed at the target satellite must have been shut off a short distance before contact was made. As the two vehicles meet the coupling mechanisms of each will meet and engage.[86] The proper parts are aligned and then locked. All unnecessary angular and linear motion perturbations present after coupling is completed are removed, and the phase is complete.

A different guidance scheme for the coupling phase must be worked out for each coupling scheme that is suggested. A proper error analysis should show the probability of success of each. Those schemes which seem to have the highest probability of success should then be laboratory-tested. The best scheme is determined on the basis of test success. Upon contact the latching must be positive and solid to prevent the space ferry from shaking loose and becoming separated.

EQUIPMENT MECHANIZATION STUDIES

Stapleford and Jex[53] made a comprehensive study of the requirements which are placed on the flight control system during the terminal phase of orbital rendezvous. The report not only specifies some of the requirements but presents a preliminary analysis of several possible methods of achieving satisfactory flight control systems, using both manual and automatic systems.

As a part of an over-all study of orbital launch operations being conducted by Chance Vought under contract to the Marshall Space Flight Center of NASA, a rather complete study not only of the theoretical aspects of rendezvous but also many of the mechanization problems associated with the attitude control system and the instrumentation sensors, was conducted by the Raytheon Company.[30]

Considerable information on the guidance sensors is presented in the STL Flight Performance Handbook[5] along with methods of processing the signals to smooth out the noise.

Propulsion system restart problems are discussed by Radcliff and Transue.[87]

ERROR ANALYSES

Analyses of the errors made in each of the major guidance phases are among the most important parts of any rendezvous program. In fact, before any proposed over-all rendezvous guidance scheme (ascent, mid-course, terminal, coupling and docking) and the corresponding specific equipment proposed can be seriously considered for adoption, a careful error analysis of all aspects of the system must be made.[5,67,88,89]

Error associated with inaccurate thrust magnitude, duration of thrust, measurement, computation, etc., is the first type to be analyzed. These errors fall broadly under the classification of "mechanical errors." Errors of this type must, first, be examined upon an accurate physical model under simulated conditions. Even though most of the errors of this type produce only small results on an individual basis, they often combine to create large over-all errors. If accurate analysis is desired, it will be found necessary to make use of digital computation.

The second type error encountered is that associated with the guidance law. Even with the most perfect equipment, the thrust computed under the guidance law and the thrust actually required for the space ferry rockets will not be identical. This is especially true when simplified equations of motion are used to derive the guidance law. This type of error has greater effect during the mid-course maneuver phase than it does in the terminal and docking phases, where the simplified equations more nearly approximate actual operating conditions.

The performance for such error analysis often leads directly to improved systems. For example, the scheme proposed herein for an "exact-numerical" guidance law resulted directly from an error analysis of linearized guidance laws which pointed up the need for an improvement and further showed that numerical processing of computed errors could lead directly to a near-exact mid-course-guidance law.

CONCLUDING REMARKS

The first 90 publications listed in the references and bibliography deal primarily with the ascent and the mid-course guidance phase, the terminal-homing phase, the docking phase, the coupling phase, equipment mechanization problems and error analyses. About 70 additional items are in the references and bibliography on related subjects, such as orbital transfers in space, the effects of the oblateness of the earth on the orbital motion, and system studies of space complexes.

In addition to a summary of the general status of rendezvous guidance technology, the specific contributions of this report are:

1. A recommended ascent trajectory and orbit for a manned space station or orbiting launch complex, which not only allows efficient on-time launches but is tolerant of launch delays up to two hours and twenty minutes. The implications of the use of this ascent trajectory for the efficient staging of launch vehicles are pointed out.
2. A proposed "exact-numerical" method for long-range mid-course guidance using the "shell-coordinate system."

REFERENCES AND BIBLIOGRAPHY

1. Roberson, Robert E., "Path Control for Satellite Rendezvous," Advances in the Astronautical Sciences, Vol. 6 (Proceedings of the Sixth Annual Meeting of the American Astronautical Society, New York City, 18-21 January 1960), Macmillan Company, New York, 1961, pp. 192-228.

2. Swanson, Robert S., Petersen, Norman V., and Hoover, LeRoy R., "An Astrovehicle Rendezvous-Guidance Concept," Astrosystems and Research Lab., Norair Division, Northrop Corporation, Hawthorne, California (presented to the American Astronautical Society, January, 1960). Also published in Advances in the Astronautical Sciences, Vol. 6 (Proceedings of the Sixth Annual Meeting of the American Astronautical Society, New York City, 18-21 January 1960), Macmillan Company, New York, 1961, pp. 147-160. Also published in Western Aviation, Vol. 40, No. 2, February, 1960, pp. 12-15,31.

3. Soule, Peter W., "Rendezvous with Satellites in Elliptical Orbits of Low Eccentricity," AAS Preprint No. 60-71, presented at American Astronautical Society Third Annual West Coast Meeting, Seattle, Washington, 8-11 August 1960.

4. Townsend, George E., "Satellite Rendezvous," Chapter VIII of Orbital Flight Manual, ER 11648, Martin Company, July, 1961.

5. Wolverton, Raymond W. (ed.), "Flight Performance Handbook for Orbital Operations," Space Technology Laboratories (prepared under contract NAS 8-863 to NASA), September, 1961.

6. Gedeon, Geza S. (Project Manager), "Flight Performance Manual for Orbital Operations," ASG-TM-61-68, Norair Division, Northrop Corporation, Hawthorne, California, revised January, 1962.

7. Swanson, Robert S. and Petersen, Norman V., "The Influence of Launch Conditions on the Friendly Rendezvous of Astrovehicles," Advances in the Astronautical Sciences, Vol. 5 (Proceedings of the Second Western Meeting of the American Astronautical Society, Los Angeles, California, 4-5 August 1959), Plenum Press, Inc., New York, 1960, pp. 218-236. Also published by Astrosystems and Research Laboratories, ASRL-TM-59-8, NB-59-196, Norair Division, Northrop Corporation, Hawthorne, California, 1959.

8. Swanson, Robert S. and Petersen, Norman V., "Rendezvous-Compatible-Orbits," ASRL-TM-59-6, Norair Division, Northrop Corporation, Hawthorne, California, 1959.

9. Petersen, Norman V. and Swanson, Robert S., "Rendezvous-Compatible-Orbits," Astronautical Sciences Review, October-December, 1959.

10. Petersen, Norman V. and Swanson, Robert S., "Rendezvous in Space - Effects of Launch Condition," Proceedings of the Manned Space Station Symposium, Los Angeles, 20-22 April 1960 (sponsored by IAS, NASA and Rand Corporation), Institute of the Aeronautical Sciences, Inc., New York, 1960, pp. 165-170. Also published in Aero/Space Engineering, Vol. 19, No. 5, May, 1960, pp. 72-73, 106.

11. "Rendezvous-Compatible-Orbits," NB-60-166-R, Astro-Systems and Research Laboratories, Norair Division, Northrop Corporation, Hawthorne, California, April, 1961.

12. Swanson, Robert S. and Petersen, Norman V., "Summary Report of Rendezvous-Compatible-Orbits," ASG-TM-61-10, Norair Division, Northrop Corporation, Hawthorne, California, January, 1961.

13. Soule, Peter W., "Application of Rendezvous Compatible Orbits to ORBS," ASG-TM-61-81, Norair Division, Northrop Corporation, Hawthorne, California, November, 1961.

14. Swanson, Robert S., Petersen, Norman V., and Soule, Peter W., "Station-Keeping of Satellites in Rendezvous Compatible Orbits," ASG-TM-61-11, Norair Division, Northrop Corporation, Hawthorne, California, May, 1961.

15. Bird, John D. and Thomas, David F., Jr., "A Two-Impulse Plan for Performing Rendezvous on a

"Once-A-Day Basis," NASA TN D-437, November, 1960.

16. Houbolt, John C., "Considerations of the Rendezvous Problems for Space Vehicles," Preprint No. 175A, Society Automotive Engineers, April, 1960 (presented at the SAE National Aeronautics Meeting, New York, N.Y., 5-8 April 1960).

17. Straly, W. H., "Utilizing the Phasing Technique in Rendezvous," ARS Preprint No. 2295-61, American Rocket Society Space Flight Report to the Nation/New York Coliseum, 9-15 October 1961.

18. Swanson, Robert S., "Maneuverable Astrovehicle Guidance Systems," ASRL-TM-59-5, Norair Division, Northrop Corporation, Hawthorne, California, October, 1959.

19. Steinhoff, Ernst A., "Orbital Rendezvous and Guidance," Proceedings of the Manned Space Station Symposium, Los Angeles, California, 20-22 April 1960 (sponsored by IAS, NASA and the Rand Corporation), Institute of the Aeronautical Sciences, Inc., New York, 1960, pp. 151-164.

20. Ehricke, K. A., "Establishment of Large Satellites by Means of Small Orbital Carriers," Proceedings of the Third International Astronautical Federation Congress, Stuttgart, 1952, pp. 111-145.

21. Ehricke, K. A., "Ascent of Orbital Vehicles," Astronautica Acta, Vol. 2, 1956, pp. 175-190.

22. Keller, C. L., "Satellite Ascent Paths," Sperry Engineering Review, 1958, pp. 2-14.

23. Brunk, W. E. and Flaherty, R. J., "Methods and Velocity Requirements for the Rendezvous of Satellites in Circumplanetary Orbits," NASA TN D-81, October, 1959.

24. Paiewonsky, Bernard H., "Transfer Between Vehicles in Circular Orbits," Jet Propulsion, Vol. 28, February, 1958, pp. 121-123.

25. Pierce, David A., "Velocity and Time Requirements for Satellite Rendezvous Trajectories," ASG-TM-61-12, Norair Division, Northrop Corporation, Hawthorne, California, May, 1961.

26. Swanson, Robert S., "Non-Coplanar Astro-Vehicle Rendezvous Maneuvers," ASG-TM-59-3, Norair Division, Northrop Corporation, Hawthorne, California, October, 1959.

27. Garber, T. D., "Ascent Guidance for a Satellite Rendezvous;" Proceedings of the Manned Space Station Symposium, Los Angeles, California, April 20-22, 1960 (sponsored by IAS, NASA, and the Rand Corporation), Institute of the Aeronautical Sciences, Inc., New York, 1960, pp. 171-178.

28. Edelbaum, T. N., "Preliminary Comparison of Air and Ground Launching of Satellite Rendezvous Vehicles," IAS Paper No. 61-10, presented at the IAS 29th Annual Meeting, New York, 23-25 January 1961.

29. Carstens, J. P., and Edelbaum, T. N., "Optimum Maneuvers for Launching Satellites into Circular Orbits of Arbitrary Radius and Inclination," ARS Preprint No. 1450-60, December, 1960.

30. "Study of Orbital Launch Operations," Vol. II (Rendezvous and Escape Window), Phase 2, Progress Report (14 June 1961 - 16 January 1962), Report submitted by Vought Astronautics Division, Chance Vought Corporation; Norair Division, Northrop Corporation; and Missile and Space Division, Raytheon Company, Report No. 00.26, Contract No. NAS 8-853, 16 January 1962.

31. Miner, W. E. and Schmieder, D. H., "The Path-Adaptive Mode for Guiding Space Flight Vehicles," 1944-61, ARS Guidance, Control and Navigation Conference, Stanford University, Stanford, California, 7-9 August 1961.

32. Schmieder, D. H., and Braud, N. J., "Implementation of the Path-Adaptive Guidance Mode in the Steering Techniques for Saturn-Multistage Vehicles," 1945-61, ARS Guidance, Control and Navigation Conference, Stanford University, Stanford, California, 7-9 August 1961.

33. Gedeon, Geza S., "A Rapid Method for Selecting Trajectories," ASRL-TM-60-11, Norair Division, Northrop Corporation, Hawthorne, California, July, 1960.

34. Eggleston, John M., and Dunning, Robert S., "Analytical Evaluation of a Method of Midcourse Guidance for Rendezvous with Earth Satellites," NASA TN D-883, June, 1961.

35. Eggleston, John M., "The Trajectories and Some Practical Guidance Considerations for Rendezvous and Return," IAS Paper No. 61-36, presented at the IAS 29th Annual Meeting, New York, N. Y., January 23-25, 1961.

36. Space Technology, edited by Howard Seifert, New York, John Wiley and Sons, Inc., 1959. (See Chapter 26 by Albert D. Wheelon, "Midcourse and Terminal Guidance.")

37. Clohessy, W. H., and Wiltshire, R. S., "Terminal Guidance for Satellite Rendezvous," IAS Paper No. 59-93, presented at the IAS National Summer Meeting, Los Angeles, California, June 16-19, 1959. Also published in Journal of the Aero-Space Sciences, September, 1960, pp. 653-658,674.

38. Spradlin, Louis W., "The Long Time Satellite Rendezvous Trajectory," Aero/Space Engineering, June, 1960, pp. 32-37.

39. Hord, R. A., "Relative Motion in the Terminal Phase of Interception of a Satellite or a Ballistic Missile," NACA TN 4399, September, 1958.

40. Oberth, Hermann, "A Precise Attitude Control for Artificial Satellites," Vistas for Astronautics, Vol. I, pp. 217-255, Pergamon Press, New York, 1958.

41. Eggleston, John M., and Beck, Harold D., "A Study of the Positions and Velocities of a Space Station and a Ferry Vehicle during Rendezvous and Return," NASA TR R-87, 1961.

42. Stapleford, Robert L., "A Study of the Two Basic Approximations in the Impulsive Guidance Techniques for Orbital Rendezvous," ASD TDR 62-83, System Technology, Inc., 1962.

43. Swanson, Robert S., "First Interim Report on the Northrop Study of Astrovehicle Rendezvous Operations," ASRL-TM-59-1, Norair Division, Northrop Corporation, Hawthorne, California, 2 June 1959.

44. Petersen, Norman V., "Satellite Rendezvous Operations," Advances in Astronautical Sciences, Vol. 4 (Proceedings of the Fifth Annual Meeting of the AAS, November, 1958), Plenum Press, New York, 1959, pp. 355-382.

45. Lieberman, Stanley I., "Rendezvous Acceptability Regions Based on Energy Considerations," ARS Journal, February, 1962, pp. 287-290.

46. Kenner, L. M., "Iso-Orbital Rendezvous by Means of an Intersecting Ellipse," NORAIR WSDS-30, Northrop Corporation, Hawthorne, California, June 24, 1959.

47. Kenner, L. M., "Charts for the Rapid Estimation of Velocity Impulse for Three Basic Orbital Transfers," NORAIR, Northrop Corporation, Hawthorne, California, August 25, 1959.

48. Petersen, Norman V., "Rescue and Retrieve Space Missions," NB-59-237, Norair Division, Northrop Corporation, Hawthorne, California, November 5, 1959.

49. Eggleston, John M., "Optimum Time to Rendezvous," ARS Journal, Vol. 30, no. 11, November, 1960, pp. 1089-1091.

50. Soule, Peter W., "An Error-Compensating Version of GORGS and the Theory of Some Terminal Rendezvous Maneuvers," ASG-TM-61-4, Norair Division, Northrop Corporation, Hawthorne, California, January, 1961.

51. Conrad, K. P., "Satellite Epoch Angle Control in Orbit," Technical Memorandum No. 851 (R-213-461-1), Aerojet-General Corporation, Azusa, California, April, 1961.

52. Jantscher, H. N., Olson, D. N., and Saari, A. E., "Minimum Energy Analysis for the General Problem of Rendezvous in Earth Orbital Space," ARS Journal, February, 1962, pp. 292-294.

53. Stapleford, Robert L., and Jex, Henry R., "A Study of Manual and Automatic Control Systems for the Terminal Phase of Orbital Rendezvous," ASD TDR 62-82, System Technology Inc., 1962.

54. Thompson, Hugh V., and Stapleford, Robert L., "Basic Guidance and Control Information for the Terminal Phase of Orbital Rendezvous," ASD TDR 61-344, System Technology, Inc., August, 1961.

55. Gilbert, E. O., "Orbit Control and Analysis Techniques for Equatorial 24-Hour Satellites," STL/TN-60-0000-27149, Space Technology Laboratories, August, 1960.

56. Sears, N. E., Jr., and Felleman, P. G., "Continuously Powered Terminal Maneuver for Satellite Rendezvous," ARS Journal, Vol. 30, no. 8, August, 1960 (presented at the ARS Controllable Satellite Conference, MIT, April 30-May 1, 1959).

57. Felleman, P. G., and Sears, N. E., Jr., "A Guidance Technique for Achieving Rendezvous," Proceedings of the Manned Space Station Symposium, Los Angeles, California, April 20-22, 1960 (sponsored by IAS, NASA, and the Rand Corporation) Institute of the Aeronautical Sciences, Inc., New York, 1960, pp. 179-183.

58. Felleman, P. G., "Analysis of Guidance Techniques for Achieving Orbital Rendezvous," AAS Preprint 62-9, Instrumentation Laboratory, MIT, January, 1962.

59. Nason, Martin L., "Terminal Guidance and Rocket Fuel Requirements for Satellite Interception," ARS Preprint 778-59, presented at the ARS Controllable Satellite Conference, MIT, April-May, 1959.

60. Nason, Martin L., "A Terminal Guidance Law Which Achieves Collision Based on Coriolis Balance Techniques," AAS Preprint No. 61-40, presented at the 7th Annual Meeting, American Astronautical Society, Dallas, Texas, January 16-18, 1961.

61. Hollister, Walter M., "The Design of a Control System for the Terminal Phase of a Satellite Rendezvous," MS Thesis, MIT, June, 1959.

62. Nason, Martin L., "A Terminal Guidance Technique for Satellite Interception Utilizing a Constant Thrust Rocket Motor," ARS Journal, November, 1960.

63. Stalony-Dobrzanski, J., and Imai, O., "Attitude and Flight Path Control System for a Space Station Supply Vehicle," Proceedings of the Manned Space Station Symposium, Los Angeles, California, April 20-22, 1960 (sponsored by IAS, NASA, and the Rand Corporation), Institute of the Aeronautical Sciences, Inc., New York, 1960, pp. 281-315.

64. Simon, Edward, Jr., "A Proposed Control System to Facilitate the Terminal Stages of Manned Rendezvous," ARS Paper 1480-60, presented at the ARS 15th Annual Meeting, Washington, D.C., December 5-8, 1960.

65. Kerfoot, H. T., Bender, D. F., and Des Jardins, P. R., "Analytic Study of Satellite Rendezvous Final Report," Report No. MD 59-272, North American Aviation Company Aero/Space Laboratories, October 20, 1960.

66. Steffan, Kenneth F., "A Satellite Rendezvous Terminal Guidance System," ARS Preprint 1494-60, presented at the ARS 15th Annual Meeting, Washington, D.C., December 5-8, 1960.

67. Luke, W. M., Goldberg, E. A., and Pfeffer, I., "Error Analysis Considerations for a Satellite Rendezvous," ARS Paper 1198-60, presented at ARS Semi-Annual Meeting, Los Angeles, California, May 9-12, 1960.

68. Passera, A. L., "Conditional Switching Terminal Guidance (A Terminal Guidance Technique for Satellite Rendezvous)", PGANE-IRE, December, 1960.

69. Shapiro, M., "An Attenuated Intercept Satellite Rendezvous System," 61-155-1849, National IAS-ARS Joint Meeting, Los Angeles, California, June 13-16, 1961.

70. Cicolani, Luigi S., "Trajectory Control in Rendezvous Problems Using Proportional Navigation," NASA TN D-772, April, 1961.

71. Soule, Peter W., and Kidd, Alan T., "Terminal Maneuvers for Satellite Ascent Rendezvous," 61-206-1900, National IAS-ARS Joint Meeting, Los Angeles, California, June 13-16, 1961.

72. Kidd, Alan T., "Terminal Maneuvers for Satellite Ascent Rendezvous," AS-TM-60-13, Norair Division, Northrop Corporation, Hawthorne, California.

73. Stapleford, R. L., "An Automatic Flight Path Control System for the Terminal Phase of Orbital Rendezvous," AAS Preprint 62-10, presented at AAS 8th Annual National Meeting, Washington, D.C., January 16-18, 1962.

74. Niemi, N. J., "An Investigation of a Terminal Guidance System for a Satellite Rendezvous," ARS Preprint 1176-60, presented at the ARS Semi-Annual Meeting, Los Angeles, California, May 9-12, 1960.

75. Harrison, E., "Some Considerations of Guidance and Control Techniques for Coplanar Orbital Rendezvous," Proceedings of the National Specialists Meeting on Guidance of Aerospace Vehicles, Boston, Massachusetts, May 25-27, 1960, Institute of the Aeronautical Sciences, New York, 1960.

76. Tassera, A. L., "Conditional-Switching Terminal Guidance (A Terminal Guidance Technique for Satellite Rendezvous)," IRE Transactions on Aeronautical and Navigational Electronics, Vol. ANE 7, No. 4, December, 1960.

77. Kamm, Laurence J., "Satrac Satellite Automatic Terminal Rendezvousing and Coupling," ARS Preprint No. 1497-60, presented at the ARS 15th Annual Meeting, Washington, D.C., December 5-8, 1960.

78. Kurbjun, M. C., Brissenden, R. S., Foudriat, E. C., and Burton, B. B., "Pilot Control of Rendezvous," Aero/Space Engineering, March, 1961.

79. Wolowicz, Chester H., Drake, Hubert M., and Videan, Edward M., "Simulator Investigation of Controls and Display Required for Terminal Phase of CoPlanar Orbital Rendezvous," NASA TN D-511, October, 1960.

80. Brissenden, Roy F., Burton, Bert B., Foudriat, Edwin C., and Whitten, James B., "Analog Simulation of a Pilot-Controlled Rendezvous," NASA TN D-747, April, 1961.

81. Hopkins, C. O., "Determination of Human Operator Functions in a Manned Space Vehicle," IRE Transactions on Human Factors in Electronics, Vol. HFE-1, No. 2, September, 1960.

82. Ritchie, Malcolm L., Hanes, Lewis F., and Hainsworth, Thomas E., "Some Control-Display Aspects of Manual Attitude Control in Space," Advances in the Astronautical Sciences, Vol. 6 (Proceedings of the Sixth Annual Meeting of the American Astronautical Society, New York City, January 18-21, 1960), Macmillan Company, New York, 1961, pp. 170-191.

83. Hopkins, Charles O., Bauerschmidt, Donald K., and Anderson, M. J., "Display and Control Requirements for Manned Space Flight," WADD TR 60-197, April, 1960.

84. Baker, C. A., "Man's Visual Capabilities in Space," Proceedings of the Seventh Annual East Coast Conference on Aeronautical and Navigational Electronics, Baltimore, Maryland, October 24-26, 1960, The Institute of Radio Engineers, Inc., New York, 1960.

85. Levin, E., and Ward, J., "Man Control of Orbital Rendezvous," Proceedings of the Manned Space Station Symposium, Los Angeles, California, April 20-22, 1960 (sponsored by IAS, NASA, and the Rand Corporation), Institute of the Aeronautical Sciences, Inc., New York, 1960.

86. Schroeder, W., "A Terminal Guidance Scheme for Docking Satellites," 1952-61, ARS Guidance, Control and Navigation Conference, Stanford University, Stanford, California, August 7-9, 1961.

87. Radcliff, William F., and Transue, John R., "Problems Associated with Multiple Engine Starts in Space Craft," Preprint No. 1122-60, presented at the ARS Semi-Annual Meeting, Los Angeles, California, May 9-12, 1960.

88. DeBra, D. B., "Ascent Error Analysis and Correction Maneuvers for Circular Orbits," Lockheed Missiles and Space Division, Report No. 446130, February 22, 1960.

89. Braham, Harold S., and Skidmore, Lionel J., "Guidance Error Analysis of Satellite Trajectories," presented at the IAS 29th Annual Meeting, New York, January 23-25, 1961.

90. Van Gelder, A., Beltrama, E., and Munick, H., "On Minimum-Time Minimum-Fuel Rendezvous," Journal, The Society of Industrial Applied Mathematics, Vol. 9, September, 1961, pp. 474-480.

91. Petersen, N. V., "Rendezvous in Space Brochure," ASRL-TM-59-18 NB-59-85, Norair Division, Northrop Corporation, Hawthorne, California, April, 1959.

92. Petersen, N. V., Pode, L., and Hoover, L. R., "Satellite Rendezvous Navigational Requirements," ASRL-TM-59-50, Norair Division, Northrop Corporation, Hawthorne, California, June, 1959.

93. Swanson, Robert S., "Co-Planar Iso-Orbit (Same Orbit) Rendezvous Maneuvers," ASRL-TM-59-4, Norair Division, Northrop Corporation, Hawthorne, California (to be published).

94. Swanson, Robert S., "First Interim Report on Study of Maneuverable-Astrovehicle Problems with Special Reference to Rendezvous Problems," ASRL-TM-59-1, Norair Division, Northrop Corporation, Hawthorne, California, June, 1959.

95. Swanson, Robert S., "Propulsion Systems Useful for Astrovehicle Maneuverability and Rendezvous Operations," ASRL-TM-59-2, Norair Division, Northrop Corporation, Hawthorne, California, July, 1959.

96. Clohessy, W. H., and Wiltshire, R. S., "Problems Associated with the Assembly of a Multiunit Satellite in Orbit," presented at the ASME, Aviation Conference, Los Angeles, March, 1959, ASME reprint 59-AV-25.

97. Pierce, D. A., "Satellite Rendezvous Trajectories," ASRL-TM-60-24, Norair Division, Northrop Corporation, Hawthorne, California, October, 1960.

98. Gedeon, G. S., "Optimized Satellite Interception Trajectories," ASRL-TM-60-28, Norair Division, Northrop Corporation, Hawthorne, California, 1960 (presented at the 7th Annual Meeting of the AAS, Dallas, Texas, January, 1961).

99. Reich, H., and Wolpert, R., "Orbital Rendezvous Base System Flight Mechanics," ASG-TM-61-40, Norair Division, Northrop Corporation, Hawthorne, California, 1961.

100. Reich, H., "Summary Report for an Orbital Rendezvous Base System," ASG-TM-61-50, Norair Division, Northrop Corporation, Hawthorne, California, December, 1961.

101. "Preliminary Parametric Analysis for Orbiting Rendezvous Base System," ASG-TM-61-59 NB-61-204, Norair Division, Northrop Corporation, Hawthorne, California, August, 1961.

102. Tempelman, Wayne, "Comparison of Minimum Energy Paths and Apogee Designation Paths," ARS Journal, November, 1959, pp. 865-868.

103. Petersen, N. V., "A New Route to the Moon - Orbital Assembly and Launch," ASG-TM-61-76, Norair Division, Northrop Corporation, Hawthorne, California, October, 1961.

104. Petersen, N. V., "Engineering for a Shot to the Moon," ASG-TM-61-78, Norair Division, Northrop Corporation, Hawthorne, California, October, 1961.

105. Petersen, N. V., Reich, H., and Swanson, R. S., "Earth-Lunar Logistics Employing Orbital Assembly and Launch," ASG-TM-61-86, Norair Division, Northrop Corporation, Hawthorne, California, November, 1961. (To be published in Space Logistics, John Wiley and Sons, 1962).

106. Conrad, K. P., "Satellite Epoch Angle Control in Orbit," Technical Memorandum No. 851 (R-213-416-1), Aerojet-General Corporation, Azusa, California.

107. Hill, Fosdick Emerson, "Orbital Rendezvous Feasibility Study," NORAIR WSDS-56, Northrop Corporation, Hawthorne, California.

108. Silber, Robert, and Horner, James, "Geo-Stationary Orbits: Flight-Mechanical Outlay and Analysis of Vernier-Scheme for Fine-Positioning," DA-TM-104-59, Army Ballistic Missile Agency, Redstone Arsenal, Alabama, 20 August 1959.

109. Friedlander, Alan L., and Harry, David P., III, "An Exploratory Statistical Analysis of a Planet Approach-phase Guidance Scheme Using Angular Measurements with Significant Error," NASA TN D-471, September, 1960.

110. Harry, David P., III, and Friedlander, Alan L., "Exploratory Statistical Analysis of Planet Approach-phase Guidance Schemes Using Range, Range-rate, and Angular-rate Measurements," NASA TN D-268, March, 1960.

111. Friedlander, Alan L., and Harry, David P., III, "Requirements of Trajectory Corrective Impulses during the Approach Phase of an Interplanetary Mission," NASA TN D-255, January, 1960.

112. Schmaedeke, Wayne, and Swanlund, George, "Optimalizing Techniques for Injection Guidance," 1943-61, ARS Guidance, Control and Navigation Conference, Stanford University, Stanford, California, August 7-9, 1961.

113. Swanson, Robert S., "Two Approximate Concepts for Satellite Interception and Rendezvous," ASRL-TM-60-15, Norair Division, Northrop Corporation, Hawthorne, California, November, 1960.

114. "Quasi-Optimum Rendezvous Guidance System (QUORGS) Brochure," ASG-TM-60-34 NB-60-167, Norair Division, Northrop Corporation, Hawthorne, California, May, 1960.

115. Kenner, L. M., "Charts for the Rapid Estimation of Velocity Impulse for Three Basic Orbital Transfers," ASRL-TM-59-10, Norair Division, Northrop Corporation, Hawthorne, California, August, 1959.

116. Wheelon, A. D., "An Introduction to Midcourse and Terminal Guidance," STL Report GM-TM-0165-00252, 10 June, 1958.

117. Mundo, C. J., Jr., "Trade-off Considerations in the Design of Guidance Equipment for Space Flight," Aero/Space Engineering, June, 1959, pp. 31-34.

118. Morgenthaler, G. W., "On Mid-Course Guidance in Satellite Interception," Astronautica Acta, Vol. 5, 1959, pp. 328-346.

119. Skalafuris, A. J., and Schiller, D. H., "Midcourse Guidance Problem in Satellite Interception--1," JARS, Vol. 30, 1960, pp. 41-46.

120. Kidd, A. T., "Manned Early Rendezvous System for Apollo/ORBS," ASG-TM-61-39, Norair Division, Northrop Corporation, Hawthorne, California, November, 1961.

121. Hoover, L. R., "Analogue Simulation of a Pilot Operated Maneuverable Satellite Control System," ASRL-TM-59-9, Norair Division, Northrop Corporation, Hawthorne, California, August, 1959.

122. Benedikt, E. G., "Electromagnetic Docking and Coupling Operations in Space," ASG-TM-61-51, Norair Division, Northrop Corporation, Hawthorne, California, August, 1961 (presented at the Fourth National Meeting of the American Astronautical Society, San Francisco, August, 1961).

123. Post, J., "Automatic Positioning, Indexing, and Coupling to a Quiescent or Tumbling Satellite," ASG-TM-61-61, Norair Division, Northrop Corporation, Hawthorne, California, August, 1961.

124. Post, J., "Orbital Rendezvous Positioning, Indexing, and Coupling System," ASG-TM-61-77, Norair Division, Northrop Corporation, Hawthorne, California, October, 1961.

125. Moore, R., "Vehicle Design Concepts for Orbital Rendezvous Missions," ASG-TM-61-28, Norair Division, Northrop Corporation, Hawthorne, California, December, 1961.

126. Gabloffsky, H., "Optical Acquisition of a Satellite Aboard a Space Vehicle to Assist in Rendezvous Maneuvers," ASRL-TM-60-29, Norair Division, Northrop Corporation, Hawthorne, California, 1960.

127. Smith, R. A., "Establishing Contact Between Orbiting Vehicles," Journal of the British Interplanetary Society, Vol. 10, 1951, pp. 295-299.

128. Gatland, K. W., "Orbital Rockets I. Some Preliminary Considerations," Journal of the British Interplanetary Society, Vol. 10, 1951, pp. 97-101.

129. Potter, Norman S., "The Controlled Rendezvous of Orbiting Space Stations," ARS Preprint No. 1483-60, presented at the ARS 15th Annual Meeting, Washington, D. C., December 5-8, 1960.

130. Peterson, Norman V., Pode, Leonard, and Hoover, Leroy R., "Satellite Rendezvous Navigational Requirements," NB 59-225, Norair Division, Northrop Corporation, Hawthorne, California, 18 June 1959 (presented at the 5th Annual Meeting of the Institute of Navigation, Kings Point, New York, June 18-20, 1959).

131. King-Hele, D. G., Gilmore, D. M. C., "The Effect of the Earth's Oblateness on the Orbit of a Near Satellite," R.A.E. TN G.W. 475, October, 1957.

132. Blitzer, Leon, "On the Motion of a Satellite in the Gravitational Field of the Oblate Earth," GM-TM-0165-00279, Space Technology Laboratories, September 5, 1958.

133. Hill, F. E., "Orbital Rendezvous Feasibility Study," Vol. I, ASRL-TM-59-11, Norair Division, Northrop Corporation, Hawthorne, California, September, 1959.

134. Hill, F. E., "Preliminary Operational Determinations for an Orbital Fighter-Bomber," ASRL-TM-59-12, Norair Division, Northrop Corporation, Hawthorne, California, October, 1959.

135. Hill, F. E., "Preliminary Operational Determinations for an Orbital Logistic Fleet," ASRL-TM-59-13, Norair Division, Northrop Corporation, Hawthorne, California, October, 1959.

136. Hohmann, W., "Die Erreichbarkeit der Himmelskorper," R. Oldenbourg, Munich, 1925.

137. Lawden, D. F., "Transfer Between Circular Orbits," Jet Propulsion, Vol. 26, Part I, July, 1956, pp. 551-558.

138. Lawden, D. F., "Correction of Interplanetary Orbits," Journal of the British Interplanetary Society, Vol. 13, no. 4, July, 1954, pp. 215-223.

139. Lawden, D. F., "Minimal Rocket Trajectories," Journal of the American Rocket Society, Vol. 23, no. 6, November-December, 1953, pp. 360-367.

140. Kelber, C. C., "Next-Maneuverable Satellites," Proceedings of the American Astronautical Society, Western Regional Meeting, August, 1958.

141. Vargo, L. G., "Optimal Transfer Between Two Coplanar Terminals in a Gravitational Field," Proceedings of the American Astronautical Society, Western Regional Meeting, August, 1958.

142. Gedeon, G. S., "Orbital Mechanics of Satellites," Proceedings of the American Astronautical Society, Western Regional Meeting, August, 1958.

143. Dobrowalski, A., "Satellite Orbits and Interorbital Transfer," Proceedings of the American Astronautical Society, Western Regional Meeting, August, 1958.

144. Petersen, N. V., "Rescue and Retrieve Space Missions," Proceedings of the Second International Symposium on the Physics and Medicine of the Atmosphere and Space, John Wiley and Sons, 1959.

145. Hill, Fosdick Emerson, "Preliminary Operational Determinations for an Orbital Rendezvous," AAS 8th Annual National Meeting, Washington, D.C., January 16-18, 1962.

146. Munick, H., "Optimum Orbital Transfer Using N-Impulses," American Rocket Society 2078-61, Space Flight Report to the Nation, New York Coliseum, October 9-15, 1961.

147. Ting, Lu, "Optimum Orbital Transfer by Impulse," ARS Journal, Vol. 30, November, 1960, pp. 1013-1018.

148. Gedeon, G. S., and Pierce, D. A., "Terminal Velocity and Orbiting Times," ASG-TM-61-41 NB 61-78, Norair Division, Northrop Corporation, Hawthorne, California, June, 1961.

149. Gedeon, G. S., "Orbital Segment Mechanics," ASG-TM-61-43, Norair Division, Northrop Corporation, Hawthorne, California, June, 1961 (presented to the International Astronautical Congress, Washington, D.C., October, 1961).

150. Gedeon, G. S., "A Minimal Set of Orbital Equations," ASG-TM-61-63, Norair Division, Northrop Corporation, Hawthorne, California, October, 1961.

151. Gedeon, G. S., "Satellite Interception," ASRL-TM-60-1, Norair Division, Northrop Corporation, Hawthorne, California, April, 1960.

152. Gedeon, G. S., "Kinematics of Orbital Motion," ASRL-TM-60-2, Norair Division, Northrop Corporation, Hawthorne, California, April, 1960 (presented at the AAS Third Annual West Coast Meeting, August 8-11, 1960, Seattle Washington).

153. Travers, E., "Preliminary Coast Trajectory Analysis for Satellite Interception," ASG-TM-60-42, Norair Division, Northrop Corporation, Hawthorne, California, 1960.

154. Kaemten, Charles E., "Space Refueling," Space World, Vol. 1, no. 1, April, 1961, pp. 37-39, 54-56.

155. Darby, W. O., "Primary Aiming Relationships for Ship to Ship Missiles in Space," ARS Journal, February, 1962.

156. Magness, T. A., McGuire, J. B., and Smith, O. K., "Accuracy Requirements for Interplanetary Ballistic Trajectories," Proceedings of the IX International Astronautical Congress, Amsterdam, 1958, Springer-Verlag, Vienna, 1959, Vol. I, pp. 286-306.

157. Carstens, J. P., and Edelbaum, T. N., "Optimum Maneuvers for Launching Satellites into Circular Orbits of Arbitrary Radius and Inclination," ARS Journal, July, 1961, pp. 943-950.

158. Roth, Harvey L., "Transfer from an Arbitrary Initial Flight Condition to a Point Target," Journal of the Aerospace Sciences, September, 1961, pp. 693-701.

159. Tempelman, Wayne H., "Velocity and Range Considerations for the Attainment of Given Intercept Angles," Journal of the Aerospace Sciences, September, 1961, pp. 681-684,701-702.

160. "Bibliography of Technical Reports - 1961," ASG-TM-61-1, Astro Sciences Group, Norair Division, Northrop Corporation, Hawthorne, California, 1961.

161. Moulton, Forest Ray, An Introduction to Celestial Mechanics, The Macmillan Co., New York, 1959.

162. Milne, W. E., Numerical Solution of Differential Equations, John Wiley and Sons, New York, 1953.

APPENDIX A: THE "EXACT-NUMERICAL" SOLUTION OF THE RENDEZVOUS EQUATIONS OF MOTION IN THE "SHELL-COORDINATE" SYSTEM

Summary

The "exact" equations of motion of a point mass in a central force field relative to a reference circular orbit are examined. The effects of earth's oblateness, air drag, lunar and solar gravitational perturbations, etc. are neglected. Since the out-of-plane motion is very weakly coupled with the in-plane motion, the case of coplanar motion is singled out for study and the resulting differential equations of motion are reduced to linear and nonlinear parts. The linear part is solved analytically, while the solution to the nonlinear part is of second-order small magnitude and is obtained numerically as a perturbation to the linear equations.

The linear equations are somewhat more accurate than those used previously,[2,3,34-38] their constant coefficients and independent variables differing by quantities of second order when compared with the earlier ones. This method, therefore, provides a very accurate solution to the equations of motion in that the only errors made are those that are committed in the numerical integration of quantities of second order. The integration method used permits this error in second order and all smaller quantities to be held to one part in one hundred thousand for typical cases.

The relative size of the nonlinear correction is a function of the time of flight and the magnitude of the relative motions. This appendix attempts to establish some qualitative idea of the error introduced by using the linearized equations. Numerical comparisons of the exact solution with the "old" and the "new" linearized expressions are made for several specific cases.

Introduction

The equations of motion of point mass in a central force field relative to a circular or elliptic reference orbit have been derived previously[2] in the shell-coordinate system. With this derivation, when coplanar motion is considered, each equation of motion has an exact first integral (corresponding to the conservation of angular momentum and the vis-viva integral).

The "question" of whether to use rectangular coordinates or spherical shell coordinates is not of direct importance here, as it is only possible to use the latter with this method. It may be of interest to observe that computer studies made by the authors have satisfied us that there is no question but what the shell coordinates are, on a whole, superior to rectangular coordinates for rendezvous guidance. These studies showed that the rectangular coordinates were best only when the initial conditions were such that the target was almost directly below or above the space ferry. It was this reason that prompted us to use as a check case for the linear formula advanced here the "worst" case of motion, a large altitude discrepancy. In the case of large epoch angle errors and relatively long-time rendezvous maneuvers, the use of the shell coordinate system produced usable answers while the rectangular coordinate system indicates initial impulses which are quite ridiculous.

It has become common practice[2,3,34-38] to linearize the exact equations and solve the resulting linear, constant-coefficient, differential equations, analytically. The linearization is performed under the assumption that the distance and velocities, when nondimensionalized by the reference orbit radius and velocity respectively, are first-order small when compared with unity. The products, squares, and higher powers of terms like this are neglected. The approximations made result in an accuracy that is unknown and which deteriorate with increasing scale of the motion. The following analysis will attempt to improve on the basic equations and provide a method of computing the exact motion which in turn will

provide an error analysis of the approximate solution.

In this work the most general form of the linear equations will be sought; that is, the most general linear, constant-coefficient equation without regard to the order of magnitude of the terms included. The difference between the solution of this equation, which is analytical in nature, and the exact solution, which is implied by the differential equation, is termed the perturbation solution. This perturbation is second-order small and has its own differential equation which may be solved by a numerical integration procedure. In actual fact the problem of determining the solution is practically one of quadratures which makes the numerical analysis inherently more accurate.

Analysis

Differential Equations for Relative Motion. The situation to be studied is shown in Fig. 2 . A reference point is moving uniformly at a rate $\dot{\theta}$ in a circular orbit of radius r . As this is the target satellite the relationship between $\dot{\theta}$ and r is fixed by the two-body result for a circular orbit $\dot{\theta}^2 r^3 = G$. The coordinates of the position of the space ferry with respect to the reference point (may be the target satellite if the target satellite is in a perfect circular orbit) are x , arc length along the reference orbit, and z radially out from the reference orbit.

To derive the differential equations of motion by Lagrange's equations the expression for the kinetic and potential energy (T and V) are set down.

$$T = \frac{m}{2}\left\{\left[\frac{d}{dt}(r+z)\right]^2 + \left[(r+z)\,\frac{d}{dt}(\theta + x/r)\right]^2\right\}$$
$$= (m/2)\left[\dot{z}^2 + (r+z)^2(\dot{\theta}+\dot{x}/r)^2\right]$$
$$V = -Gm/(r+z)$$
$$= -m\dot{\theta}^2 r^3 (r+z)^{-1}$$

Letting L=T-V, the following two differential equations result:

$$(\partial L/\partial x) - d/dt\,(\partial L/\partial \dot{x}) = 0$$
$$(2m/r^2)\,d/dt\left[(r+z)^2(\dot{\theta}+\dot{x}/r)\right] = 0 \qquad (1\text{-A})$$
$$(\partial L/\partial z) - d/dt\,(\partial L/\partial \dot{z}) = 0$$
$$m\ddot{z} - m(r+z)(\dot{\theta}+\dot{x}/r)^2 - m\dot{\theta}^2 r^3 (r+z)^{-2} = 0 \qquad (2\text{-A})$$

The equations may be nondimensionalized by the new variables,

$$\zeta = z/r \qquad \xi = x/r \qquad \theta = \dot{\theta}t \qquad (3\text{-A})$$

and become, after simplification:

$$d/d\theta\left[(1+\zeta)^2(1+\xi')\right] = 0 \qquad (4\text{-A})$$

$$\zeta'' - (1+\zeta)(1+\xi')^2 + (1+\zeta)^{-2} = 0 \qquad (5\text{-A})$$

where a prime indicates differentiation with respect to theta, θ .

Solution of the Differential Equations. The differential equations above are really no more than the conventional equations of two-body motion with a transformation of variables. These equations can be solved in the same manner as orbit equations, however, this is not satisfactory for rendezvous studies. What is desired, of course, is an equation for ξ and ζ as functions of θ . (Something like this has been done and appears in Moulton[16] on p. 171. Moulton's equations, unfortunately, cannot be evaluated readily when only the motion relative to the target is known.) When the target and interceptor are close it is known that the motion approximates that in free space and it is desired to have the equations of rendezvous have this behavior.

The solution to the two differential equations above may be partly accomplished by the two exact first-integrals available. These correspond to the conservation of angular momentum and vis-viva integrals respectively. The constants of integration will be denoted by small k 's.

$$(1+\zeta)^2(1+\xi') = k_1 \qquad (6\text{-A})$$

comes directly from the first differential equation (4-A). To get the second first-integral, insert this relation into the second equation (5-A):

$$\zeta'' + (1+\zeta)^{-2} - k_1^2(1+\zeta)^{-3} = 0 \qquad (7\text{-A})$$

This equation may be integrated by multiplying through by $2\zeta'$ which produces an exact differential.

$$(\zeta')^2 - 2(1+\zeta)^{-1} + k_1^2(1+\zeta)^{-2} = k_2 \qquad (8\text{-A})$$

This last equation, however, is not used by the procedure outlined in this note, but the equation from which it is derived is used instead. The differential equations then become:

$$\zeta'' + (1+\zeta)^{-2} - k_1^2(1+\zeta)^{-3} = 0 \qquad (9\text{-A})$$

$$\xi' + 1 - k_1(1+\zeta)^{-2} = 0 \qquad (10\text{-A})$$

where k_1 is to be evaluated by the initial conditions.

Introducing additional notation to distinguish between orders of magnitude of constants, let

$$K_1 = k_1 - 1 \qquad (11\text{-A})$$

$$K_2 = 2K_1 - K_1^2 \qquad (12\text{-A})$$

If this notation is used the differential equations become:

$$\zeta'' + (1+\zeta)^{-2} - (1+K_2)(1+\zeta)^{-3} = 0 \quad (13\text{-A})$$

$$\xi' + 1 - (1+K_1)(1+\zeta)^{-2} = 0 \quad (14\text{-A})$$

where all symbols appearing are first-order. It is now possible to separate the differential equations into their linear and nonlinear parts by the following substitutions:

$$(1+\zeta)^{-2} = 1 - 2\zeta + \beta(\zeta) \quad (15\text{-A})$$

where:

$$\beta = \zeta^2 \left[\frac{3+2\zeta}{(1+\zeta)^2}\right] \quad (16\text{-A})$$

and

$$(1+\zeta)^{-3} = 1 - 3\zeta + \gamma(\zeta) \quad (17\text{-A})$$

where:

$$\gamma = \zeta^2 \left[\frac{6+8\zeta+3\zeta^2}{(1+\zeta)^3}\right] \quad (18\text{-A})$$

The differential equations are now written in two parts below:

$$\left[\zeta'' + \zeta(1+3K_2) - K_2\right] + \left[\beta - \gamma(1+K_2)\right] = 0 \quad (19\text{-A})$$

$$\left[\xi' + 2\zeta(1+K_1) - K_1\right] + \left[-\beta(1+K_1)\right] = 0 \quad (20\text{-A})$$

Each equation is the sum of a linear and a nonlinear part, and each equation is also exact in that no simplifying assumptions have been in addition to the basic assumptions.

The linear part of the differential equation differs from the usual equations only in that, the constants contain, in addition to the usual first order terms, some quantities which are usually neglected because they are an order of magnitude smaller than the basic part of the term. These extra terms in the constants, however, do effect an improvement in the accuracy of the linear approximation to the motion which is most noticeable in the analysis of very long time motions.

Let ξ_L and ζ_L be the complete solutions to the linear parts of the equations above. The complete solution to the equations will then appear as the sum of a linear and a "perturbational" part, as shown below:

$$\xi = \xi_L + \xi_p \quad (21\text{-A})$$

$$\zeta = \zeta_L + \zeta_p \quad (22\text{-A})$$

In order to write the linear solution explicitly the following notation is employed:

$$\omega = (1+3K_2)^{1/2} \quad (23\text{-A})$$

so that the linear solution becomes:

$$\zeta_L = C_1 \sin\omega\theta + C_2 \cos\omega\theta + K_2/\omega^2$$

$$\xi_L = \left[\frac{2(1+K_1)}{\omega} C_1\right] \cos\omega\theta - \left[\frac{2(1+K_1)}{\omega} C_2\right] \sin\omega\theta \quad (24\text{-A})$$

$$- \left[\frac{2(1+K_1)K_2}{\omega^2} - K_1\right]\theta + \left[\xi_0 - \frac{2(1+K_1)C_1}{\omega}\right]$$

where:

$$C_1 = \zeta_0' \qquad C_2 = \zeta_0 - K_2/\omega^2 \quad (25\text{-A})$$

Substituting these into the complete differential equation along with the unknown nonlinear part of the solution, one gets the differential equation of the nonlinear parts:

$$\zeta_p'' = -(1+3K_2)\zeta_p + (1+K_2)\gamma - \beta \quad (26\text{-A})$$

$$\xi_p' = -2(1+K_1)\zeta_p + (1+K_1)\beta \quad (27\text{-A})$$

where the functions γ and β are as defined before and are functions of the complete solution ζ. If, in the equations above, the linear instead of the complete solution were used to substitute in γ and β these functions would be in error only by terms that are first-order small when compared with the true value of γ and β. This means that the perturbation solution would be off by an amount one order smaller than the size of the true perturbation solution itself. The perturbation solution would be added to the linear to result in second-order small errors in the total solution; therefore, the problem is practically one of quadratures. The actual solution of the nonlinear perturbation equations above, however, was carried out on a IBM 7090 by a numerical method that permits error control to within one part in one hundred thousand for normal applications. The equations above were solved (using the complete solution to evaluate the ζ_p and ξ_p functions) by a method which is limited in its accuracy only by the number of significant digits carried in the calculation. The numerical integration was carried out by an Adams-Moulton fourth-order, fixed-interval method.

The linear equations can be reduced to the more common form by elimination of all quantities of second order in the constants.

The computer program calculated the value of the "old linear" equations as a check on the calculations. In addition, it calculated the "new linear" solution, the perturbation solution and their sum, the exact solution. The program can take any set of initial conditions in either the non-dimensional form written here or in dimen-

sional form, and give the answers either in dimensional or non-dimensional form.

An inspection of the perturbation equations will show that the "forcing function" has an amplitude proportional to the square of the coordinate ζ. Intuition would say, then, that the error in the linear solution to the equations would be proportional to the square of the average excursion from the origin and would increase directly with the time of flight in the worst instance. The preliminary investigations with the program have been carried out with the model above in mind, and some of the results are shown in the next section.

As a sidelight, the equivalent operation of splitting into a linear and a smaller nonlinear differential equation can also be accomplished, using the second integral available. The constants are adjusted:

$$K_3 = k_2 + 1$$

The following substitutions made:

$$(1+\zeta)^{-1} = 1-\zeta+\zeta^2-\epsilon \qquad \epsilon = \zeta^3/(1+\zeta)$$

$$(1+\zeta)^{-2} = 1-2\zeta+3\zeta^2-\delta \qquad \delta = \zeta^3(4+3\zeta)(1+\zeta)^{-2}$$

$$[(\zeta')^2+\zeta^2-2\zeta K_2+(K_2+K_3)] +$$

$$[2\epsilon-\delta+3\zeta^2K_2-\delta K_2] = 0$$

The expression in brackets on the left has as its solution the linear relation outlined above, however, it can be seen that the type of perturbation analysis used earlier is not applicable here.

Results

The equations in the previous section were programmed for solution on an IBM 7090, as was previously mentioned. As a check on the accuracy of the program the "interceptor" was placed in the initial condition equivalent to an orbiting body at perigee with respect to a reference orbit with the same mean motion. The initial conditions for three cases, e = .001, .010, .100, were run and the trajectory for one orbit computed. The "exact" solution reproduced the initial conditions one orbit later to the order of accuracy of the input conditions. In addition, the error in the linear solution checked the predicted error of Ref. (54), the error in the linear solution growing as the square of the initial distance. Agreement between solutions was good for e = .001; see Figs. 3&4 for other cases. The improvement over the "old linear" by the "new linear" is also quite clear in the larger case of motion, the error being reduced by a factor of four.

The initial conditions were computed by a series expansion given on page 171 of Ref. 2, so the check is independent.

APPENDIX B: THE "EXACT-NUMERICAL" PREDICTION OF THE VELOCITY COMPONENT REQUIREMENTS FOR TWO-IMPULSE RENDEZVOUS GUIDANCE USING THE "SHELL-COORDINATE" SYSTEM

In Appendix A is presented a method for determining the "exact-numerical" motion of a space ferry provided the initial conditions, i.e., position and velocity, are given. In order to obtain a set of guidance equations, it is necessary to be able to calculate the velocity components required for rendezvous at a specified time and position in terms of the initial position. In other words, one must have a solution to the equations of motion between fixed boundary conditions (the end points of the motion). The linear equations of relative motion[2,3,32-38] are easy to arrange in guidance laws. The more exact numerical solutions, such as presented in Appendix A, require an iterative procedure such as described in this Appendix in order to invert the solution of the motion into a guidance law.

The need for a more exact guidance law is dependent on the accuracy of the relative position and rate information and on the range and altitude distance between the two rendezvousing vehicles. Even if accurate relative position and rate information are available at the start of a long-range rendezvous maneuver (e.g., at the start of ascent from a parking orbit) use of the linearizedrendezvous guidance equations will result in large errors to be corrected later. Anticipating large systems of the future where computing complexity is a minor consideration and guidance efficiency is a major item, the following scheme computes an accurate numerical approximation to the exact impulse required to put a vehicle on a collision course with the target at a specified time.

The differential equations advanced in Appendix A have proven themselves good for the problem for which they were designed, that is, given certain initial conditions to compute the relative motion that these initial conditions produce. This appendix considers a problem which is somewhat the inverse, namely, what initial conditions will produce a relative motion that ends in rendezvous.

Solutions like those in Appendix A might be used to approximate the nonlinear perturbation and then a linear correction applied to the initial conditions to get a new, corrected, impulse. Such a procedure, however, fails to get at the root of the problem since the case of interest is one in which the nonlinearities play a major role. An attack which produces a good answer, regardless of the distances involved, may be more complicated but may also be a practical necessity.

The differential equations in Appendix A can be used, but in order to solve them with fixed boundary conditions an adaptation of the numerical method of successive approximation is required. A description of this method is given in Milne's Numerical Solution of Differential Equations on pp. 106-109.[162] The adaptation of this method to the mathematical situation of this appendix involves some generalization of this method for a somewhat more simple situation.

The general idea is to establish an approximate trajectory which exactly fulfills the boundary conditions and successively refines it by repeated substitution into the differential equation, adjusting the constants of integration to assure the satisfaction of the boundary condition at each step. In order to illustrate the application of this method the problem will first be formulated in general terms.

The independent variable is θ, and the two dependent variables are ξ and ζ. The boundary conditions are given below:

Boundary conditions

When θ equals	then ξ and ζ equal	
0	ξ_0	ζ_0
θ_*	0	0

Of course, ξ_0, ζ_0, and θ_* are all given. (θ_* is equal to the product of the time to rendezvous and the angular velocity of the rotating coordinate system). The problem is to find the velocity ξ_0' and ζ_0' that will satisfy the boundary conditions.

K is a constant of integration that is a function of the initial conditions. Written symbolically:

$$K = K(\xi_0, \zeta_0, \xi_0') \tag{B-1}$$

Note that with this formulation of the equations of motion (see Appendix A) that K is not a function of ζ_0'; and that ζ'' and ξ' are functions only of ζ and K as shown by the following differential equations:

$$\zeta'' = f_1[\zeta, K] \tag{B-2}$$

$$\xi' = f_2[\zeta] + K f_3[\zeta] \tag{B-3}$$

So that if the initial value of ζ_0' and the correct value of K are found one has an implicit solution to the problem of determining the correct ζ_0' and ξ_0'.

First, form a first trial "solution" $\zeta_1(\theta)$ such that

$$\zeta_1(0) = \zeta_0 \qquad \zeta_1(\theta_*) = 0$$

Of course, the more $\zeta_1(\theta)$ is like the true solution, the faster the solution will converge.

The boundary conditions require that:

$$\xi(\theta_*) = 0 = \xi_0 + \int_{\theta=0}^{\theta_*} \xi' d\theta \tag{B-4}$$

If the first approximation function is substituted into this equation, one has:

$$\xi_0 + \int_{\theta=0}^{\theta_*} f_2[\zeta_1(\theta)]d\theta + K\int_{\theta=0}^{\theta_*} f_3[\zeta_1(\theta)]d\theta = 0 \tag{B-5}$$

The two integrals in this equation are quadratures which may be evaluated in our case by numerical methods. When this is done the first approximation to K may be found, say K_1, where:

$$K_1 = -\left\{\frac{\xi_0 + \int_{\theta=0}^{\theta_*} f_2[\zeta_1(\theta)]\,d\theta}{\int_{\theta=0}^{\theta_*} f_3[\zeta_1(\theta)]\,d\theta}\right\} \tag{B-6}$$

The second boundary condition requires that

$$\zeta(\theta_*) = 0 = \zeta_0 + \zeta_0'\theta_* + \iint_{\theta=0}^{\theta_*} \zeta''\,d^2\theta \tag{B-7}$$

So that the first approximation to ζ_0' may be computed as:

$$\left(\zeta_0'\right)_1 = -\frac{\left[\zeta_0 + \iint_{\theta=0}^{\theta_*} f_1[\zeta_1(\theta)]\,d^2\theta\right]}{\theta_*} \tag{B-8}$$

With the first approximations to the boundary conditions now at hand a new, and presumably better, approximation function can be computed by the formula below:

$$\zeta_2(\theta) = \zeta_0 + \left(\zeta_0'\right)_1\theta + \iint_{\theta=0}^{\theta} f_1[\zeta_1(\theta), K_1]\,d^2\theta \tag{B-9}$$

Repeating this procedure should result in successive refinements of the correct solution. It is not possible to prove with rigor that the solution will converge except for a very limited class of functions, however, the behavior of the sequence $\{\zeta_0'\}$ of initial values should convince one of the validity of the solution since the existence of the solution is known from physical reasoning.

The formula below gives the actual computational algorithim used in their proper order.

Definitions:

$$\begin{aligned}
\beta &= \zeta^2(3+2\zeta)(1+\zeta)^{-2}\\
\gamma &= \zeta^2(6+8\zeta+3\zeta^2)(1+\zeta)^{-3}\\
B_1 &= (1-2\zeta_0+\beta_0)^{-1}\\
B_2 &= B_1(2\zeta_0-\beta_0)\\
K_2 &= 2K+K^2
\end{aligned} \tag{B-10}$$

The subscript i, $i = 1, 2 \ldots$ refers to the values obtained from the i th approximation function.

Given ζ_0, ξ_0 and θ_*, the differential equations,

$$\zeta'' = K_2 - \zeta(1+3K_2) + \gamma(1+K_2) - \beta \tag{B-11}$$

$$\xi' = K\left[1-(2\zeta-\beta)\right] - (2\zeta-\beta) \tag{B-12}$$

and an approximation function $\zeta_1(\theta)$ such that

$$\zeta_1(0) = \zeta_0 \qquad \zeta_1(\theta_*) = 0$$

The logical choice for ζ_i is one predicted by the linearized two-impulse rendezvous formula. Other functional approximations can be used, however. For convenience the formulas for this "first guess" are given at the end of this appendix.

$$F_i = \int_{\theta=0}^{\theta_*} (2\zeta_i - \beta_i)\, d\theta \qquad \text{(B-13)}$$

$$K_i = (F_i - \xi_o)/(\theta_* - F_i) \qquad \text{(B-14)}$$

$$G_i(\theta, K_i) = \iint_0^{\theta} \zeta''(\zeta_i, K_i)\, d^2\theta \qquad \text{(B-15)}$$

$$(\zeta_o')_i = -\left[G_i(\theta_*, K_i) + \zeta_o\right]/\theta_* \qquad \text{(B-16)}$$

$$(\xi_o')_i = (K_i - B_2)/B_1 \qquad \text{(B-17)}$$

$$\zeta_{i+1}(\theta) = \zeta_o + (\zeta_o')_i \theta + G_i(\theta, K_i) \qquad \text{(B-18)}$$

return to Eq. (B-13).

The linear approximation function is the "old linear" solution to the two-impulse rendezvous problem. The sequence of initial velocities is seen to converge numerically by observing the $(\zeta_o')_i$, $(\xi_o')_i$ for $i = 1, 2, 3 \ldots$ until the arbitrary numerical bound for $[(\zeta_o')_{i+1} - (\zeta_o')_i]$ and $[(\xi_o')_{i+1} - (\xi_o')_i]$ is satisfied.

For integration of F, Simpson's rule may be used, while for the integration of G, a version of Störmer's method may be used.

a) For starting:

$$Y_0 = 0$$

$$Y_1 = (h^2/576)\left[140y_0'' + 228y_1'' - 108y_2'' + 28y_3''\right]$$

$$Y_2 = 2Y_1 + (h^2/12)\left[y_2'' + 10y_1'' + y_0''\right] \qquad \text{(B-19)}$$

b) For continuing:

$$Y_{n+1} = 2Y_n - Y_{n-1} + (h^2/12)\left[y_{n+1}'' + 10y_n'' + y_{n-1}''\right] \qquad \text{(B-20)}$$

Formulas for the first approximation function are given below:

$$\zeta_1(\theta) = (4 - 3\cos\theta)\zeta_o + 2(1 - \cos\theta)\xi_o' + (\sin\theta)\zeta_o'$$

$$\xi_o' = \left\{\sin\theta_*\,\xi_o + \left[14(1 - \cos\theta_*) - 6\theta_*\sin\theta_*\right]\zeta_o\right\}/D$$

$$\zeta_o' = \left\{-2(1 - \cos\theta_*)\xi_o + (4\sin\theta_* - 3\theta_*\cos\theta_*)\zeta_o\right\}/D$$

$$D = 3\theta_*\sin\theta_* - 8(1 - \cos\theta_*)$$

The accuracy of the solution, if no errors are present in the initial conditions, is governed by four factors: (1) the accuracy of the differential equations in representing the real situation; (2) the number of points along the curve that are used to define the approximation function numerically; (3) the number of digits carried in the computation; and (4) the accuracy of the numerical integration formula. It seems clear that none of these factors will be nearly as large as measurement errors will be in a practical guidance system. Therefore, the practicality of such a method ultimately rests on the answer to the question, "Does the fuel-saving that may be realized with the measurement and impulse errors that a real system will have warrant the extra computing capability required?" For long range midcourse guidance using computing facilities on board the space station (so that it need be carried into orbit only once) we believe the answer is clearly that the fuel saving is definitely worth while.

Simplification of the computation procedure for actual systems to, say, eliminate the computation of trigonometric functions may certainly be made. For example, one could limit the computation of impulse to specific points, store the sine and cosine for adequate intervals to fit these points and computations then would all be linear arithmetic. The number of iterations could, possibly, be reduced to only one for most cases. It is very easy to make many runs in studies on the ground to arrive at practical minimums for these quantities. As the distance gets smaller no iterations need take place, and the computation stops when the linearized guess for the velocity has been obtained. These formulas, in turn, reduce to the "free space" formula when the time to rendezvous is small. In this manner the guidance scheme successively linearizes itself as it gets closer, making computation time much less when information is needed more rapidly.

APPENDIX C: SUMMARY OF RENDEZVOUS EQUATIONS

The coordinates of an interceptor relative to the target reference circular orbit are shown in figure 2. The reference orbit has an angular velocity $\dot{\theta}$ and is at a distance r from the earth center. G is a constant for the heavenly body in question such that

$$\dot{\theta}^3 r^2 = G$$

If V_c is the reference circular orbit velocity ($V_c = r\dot{\theta}$) then the rendezvous variables are non-dimensionalized by the following formula:

$\xi = x/r$ (along an arc)

$\eta = y/r$ (along an arc through the target normal to reference orbit plane)

$\zeta = z/r$ (outward from force center)

$$\xi' = d\xi/d\theta = \dot{x}/V_c$$

$$\eta' = \dot{y}/V_c$$

$$\zeta' = \dot{z}/V_c$$

If the subscript o refers to conditions at $\theta = 0$ then the linearized motion is:

$$\xi = \xi_0 + 6(\sin\theta - \theta)\zeta_0 + (4\sin\theta - 3\theta)\xi_0' - 2(1-\cos\theta)\zeta_0'$$

$$\zeta = (4 - 3\cos\theta)\zeta_0 + 2(1-\cos\theta)\xi_0' + \sin\theta\,\zeta_0'$$

$$\xi' = -6(1-\cos\theta)\zeta_0 + (4\cos\theta - 3)\xi_0' - (2\sin\theta)\zeta_0'$$

$$\zeta' = (3\sin\theta)\zeta_0 + (2\sin\theta)\xi_0' + (\cos\theta)\zeta_0'$$

$$\eta = (\cos\theta)\eta_0 + (\sin\theta)\eta_0'$$

$$\eta' = -(\sin\theta)\eta_0 + (\cos\theta)\eta_0'$$

The initial value of the velocity which will produce a collision θ_* radians later is given by

$$\xi_0' = \left\{(\sin\theta_*)\xi_0 + [14(1-\cos\theta_*) - 6\theta_*\sin\theta_*]\zeta_0\right\}/D$$

$$\eta_0' = -(\cot\theta_*)\eta_0$$

$$\zeta_0' = \left\{-2(1-\cos\theta_*)\xi_0 + [4\sin\theta_* - 3\theta_*\cos\theta_*]\zeta_0\right\}/D$$

The value of the velocity at the collision can also be computed[2]

$$\zeta_*' = \left\{-2(1-\cos\theta_*)\xi_0 + \sin\theta_*\,\zeta_0\right\}/D$$

$$\eta_*' = (\csc\theta_*)\eta_0$$

$$\xi_*' = \left\{(4\sin\theta_* - 3\theta_*)\xi_0 + 2(1-\cos\theta_*)\zeta_0'\right\}/D$$

where $D = 3\theta_*\sin\theta_* - 8(1-\cos\theta_*)$

In the computation there are five coefficients that appear. Due to the zero in D at $\theta_* = 0$ these become difficult to evaluate for small θ_*. For this purpose, power series or Laurent series should be used for small θ_*. The series below may be used up to $\theta_* = 40°$ with an error never more than $\frac{1}{2}\%$.

$$\sin\theta_*/D = -\frac{1}{\theta_*}\left\{1 - 1/3\theta_*^2 + 7/90\,\theta_*^4 \cdots\right\}$$

$$[14(1-\cos\theta_*) - 6\theta_*\sin\theta_*]/D = -\left\{1 + 1/4\,\theta_*^2 - 7/20\,\theta_*^4 \cdots\right\}$$

$$2(1-\cos\theta_*)/D = -\left\{1 - 1/4\theta_*^2 + 7/180\,\theta_*^4 + \cdots\right\}$$

$$[4\sin\theta_* - 3\theta_*\cos\theta_*]/D = -1/\theta_*\left\{1 + 2/3\theta_*^2 - 17/90\theta_*^4\right\}$$

$$(4\sin\theta_* - 3\theta_*)/D = -1/\theta_*\left\{1 - 5/6\theta_*^2 + 67/360\,\theta_*^4 - \frac{319}{7560}\theta_*^6\right\}$$

$$\cot\theta_* = \frac{1}{\theta_*}\left\{1 - 1/3\,\theta_*^2 - 1/45\,\theta_*^4 \cdots\right\}$$

Inspection of the formulas above show the free space approximation holds when θ_* is very small.

The QORGS guidance scheme[2] has five impulses tangential to the orbit spaced at 90 degree target orbit travel apart. The first impulse is given 360 degrees from collision. These impulses are, as functions of the initial conditions:

time to rendezvous	tangential impulse, $\Delta\xi'$
360°	$-\xi_0' + (1/6\pi)\xi_0 - (15/8)\zeta_0 - (1/3\pi + 1/8)\zeta_0'$
270°	$(1/4)\zeta_0'$
180°	$-(1/4)\zeta_0$
90°	$-(1/4)\zeta_0'$
0°	$-(1/6\pi)\xi_0 + (1/8)\zeta_0 + (1/3\pi + 1/8)\zeta_0'$

Transformation of Coordinates

There are three systems of coordinates to which reference will be made. For simplicity all distances will be divided through by orbital attitude.

1) Shell coordinates defined in Figure 2. ξ is along the orbit, ζ is along local vertical.

2) Rectangular coordinates. X measured tangent to orbit and Z along local vertical through the coordinate system center.

3) Radar coordinates. R distance from coordinate system center. θ angle from Z measured as positive toward X.

The transformation between rectangular and radar coordinates clarifies their relationship.

Notation:

$$S_\varphi \equiv \sin\varphi$$

$$C_\varphi \equiv \cos\varphi$$

$$V_\varphi = 1 - C_\varphi = \text{versin}\varphi$$

starred formula are to be used when R is small.

$$X = RS_\theta$$

$$Z = RC_\theta$$

$$\theta = \tan^{-1}(X/Z)$$

$$R = (X^2 + Z^2)^{1/2}$$

$$X = (1+\zeta)S_\xi$$

$$Z = (1+\zeta)C_\xi - 1$$

$$Z = \zeta - V_\xi(1+\zeta) \quad (*)$$

$$\xi = \tan^{-1}[X/(1+Z)]$$

$$\zeta = [(1+Z)^2 + X^2]^{1/2} - 1$$

(for small R convert X and Z to radar coordinates and use formula below.)

$$R = \left[1 + (1+\zeta)^2 - 2(1+\zeta)C_\xi\right]^{1/2} = \left[\zeta^2 + 2V_\xi(1+\zeta)\right]^{1/2} (*)$$

$$\theta = \tan^{-1}\left\{[(1+\zeta)S_\xi]/[\zeta - V_\xi(1+\zeta)]\right\} \quad (*)$$

$$\theta = \tan^{-1}\left\{[(1+\zeta)S_\xi]/[(1+\zeta)C_\xi - 1]\right\}$$

$$\xi = \tan^{-1}[RS_\theta/(1+RC_\theta)]$$

$$\zeta = (1 + 2RC_\theta + R^2)^{1/2} - 1 = RF_1(\theta) + R^2F_2(\theta) + \cdots\cdots (*)$$

$$F_1 = C_\theta \quad F_2 = 1/2\,S_\theta^2 \quad F_3 = -1/2\,C_\theta S_\theta^2 \quad F_4 = -1/8\,S_\theta^2(1 - 5C_\theta^2)$$

$$F_5 = \frac{1}{8}C_\theta S_\theta^2(3 - 7C_\theta^2) \quad F_6 = \frac{1}{16}S_\theta^2(1 - 14C_\theta^2 + 21C_\theta^4)$$

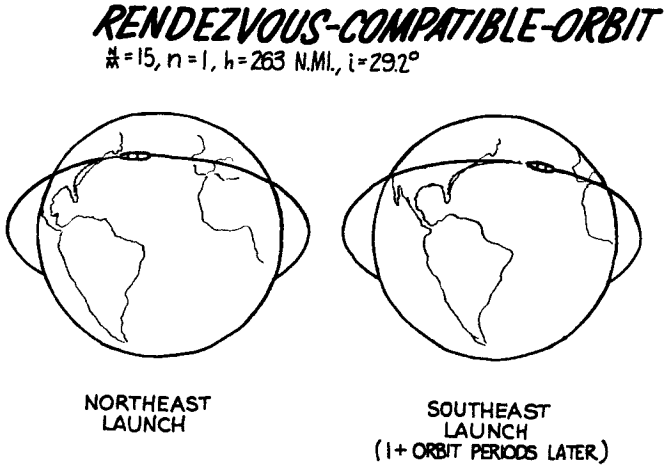

FIGURE 1

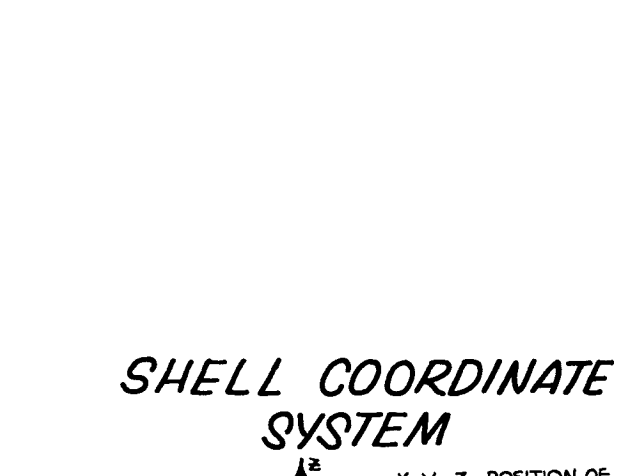

FIGURE 2

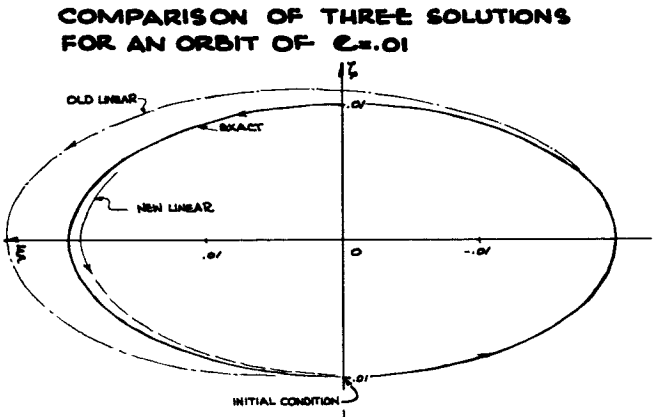

FIGURE 3

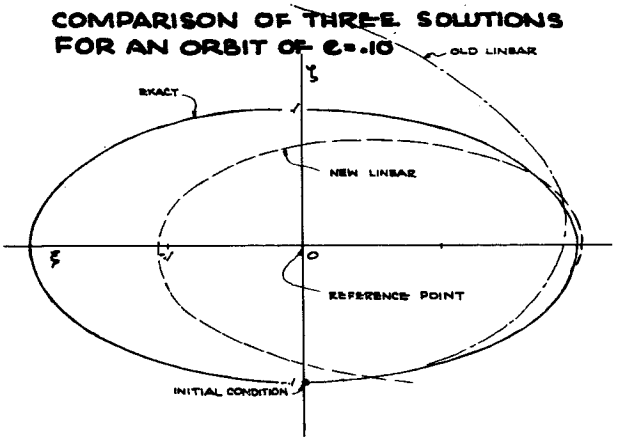

FIGURE 4

THE RESTRICTED THREE-BODY-PROBLEM AS A PERTURBATION OF EULER'S PROBLEM OF TWO FIXED CENTERS AND ITS APPLICATION TO LUNAR TRAJECTORIES

by

Richard Schulz-Arenstorff
Mirt C. Davidson, Jr.
Hans J. Sperling

George C. Marshall Space Flight Center
National Aeronautics and Space Administration

Abstract

The restricted Three-Body-Problem considers the motion of an infinitesimal mass under the gravitational attraction of two finite masses, which revolve about their common center of gravity in coplanar circles. It is well known that Euler's problem of two fixed centers, consisting of the motion of an infinitesimal mass under the gravitational attraction of two finite masses fixed in space, can be solved by elliptic functions.

The idea presented here is to take the solution of Euler's problem as the solution of the restricted Three-Body-Problem by allowing the initial values to be functions of time now. Differential equations for the perturbed initial values are established. These equations can be given in closed form by using the fact that the transformation to the perturbed initial values of Euler's problem is canonical. Thus, an approximation can be obtained for the solution of the restricted Three-Body-Problem. The method can also be used to represent classes of neighboring trajectories for guidance purposes.

Notations

dot: differentiation with respect to time t, e.g. $\dot{x}_1 = dx_1/dt$, $\dot{x} = dx/dt$

small circle: partial differentiation with respect to time t, e.g. $\mathring{x} = \partial x/\partial t$

4-vectors: e.g., $x = \begin{pmatrix} x_1 \\ x_2 \\ x_3 \\ x_4 \end{pmatrix}$, $x_0 = \begin{pmatrix} x_{10} \\ x_{20} \\ x_{30} \\ x_{40} \end{pmatrix}$, $\frac{\partial H}{\partial x} = \begin{pmatrix} \partial H/\partial x_1 \\ \partial H/\partial x_2 \\ \partial H/\partial x_3 \\ \partial H/\partial x_4 \end{pmatrix}$

with the matrix $J = \begin{pmatrix} 0 & 0 & 1 & 0 \\ 0 & 0 & 0 & 1 \\ -1 & 0 & 0 & 0 \\ 0 & -1 & 0 & 0 \end{pmatrix}$ a canonical system $\dot{x}_1 = \partial H/\partial x_3$, $\dot{x}_2 = \partial H/\partial x_4$, $\dot{x}_3 = -\partial H/\partial x_1$, $\dot{x}_4 = -\partial H/\partial x_2$ is written as $\dot{x} = J(\partial H/\partial x)$.

Introduction

For the purpose of guidance of lunar vehicles it would be useful and convenient to possess analytical expressions that give position and velocity at a certain time as functions of position and velocity at an earlier time; in addition, the formulas should be as simple as possible and of sufficient accuracy. This general problem was one of the incentives to a study that shall be outlined in its basic ideas in this paper. Only the simplest case of the problem of motion and guidance in the real earth-moon space has been attacked so far, idealizing as much as possible. Accordingly, in the following the restricted three-body problem in a plane will be considered, treated as a perturbation problem of Euler's problem of two fixed centers, which can be solved in closed form by elliptic functions.

The procedure of attacking the problem is the following: Represent the restricted three-body problem in a rotating coordinate system in which the two finite masses are at rest. Then the Hamiltonian H of the restricted problem can be written as the sum of two terms, $H = H_1 + H_2$, one of which, say H_1, is exactly the Hamiltonian of Euler's problem. Solve Euler's problem - this can be done in principle - and consider the initial values of the solution of Euler's problem as the new variables of the restricted problem. It can be shown that this transformation of the dependent variables is canonical, and that the new variables satisfy canonical differential equations, such that the Hamiltonian of this system is the other term H_2 of the Hamiltonian $H = H_1 + H_2$ of the restricted problem. This process is applied once more to $H_{2_1} = H_3 + H_4$, and the problem is reduced to the solution of a system of canonical differential equations with the Hamiltonian H_4. The solutions of this last system of equations are slowly varying functions for not too large intervals of time.

The object of this study is not so much the approximation of the true trajectory by another simpler trajectory - mathematically usually an initial value problem -, but the development of methods towards the solution of the above-mentioned prediction problem - mathematically closer to a boundary value problem.

Theorem on Canonical Initial Values

The following theorem will be used essentially in the subsequent developments; it will be formulated here without proof. As already mentioned, it states that in certain cases the initial values of the solution of a system of canonical differential equations are canonical variables for another canonical system.

Theorem: Let $\dot{\alpha} = J(\partial H/\partial \alpha)$ be a canonical system with the Hamiltonian $H = H(t, \alpha)$ and initial values t_0, α_0.

Let $H = H_1 + H_2$ and let $\beta = B(t, \beta_0)$ be a solution of the canonical system $\dot{\beta} = J(\partial \tilde{H}_1/\partial \beta)$ with the Hamiltonian $H_1 = \tilde{H}_1(t, \beta) = H_1(t, \beta)$ and initial values t_0, β_0.

Define functions $\gamma = \Gamma(t, \delta) = B(t, \delta)$ and determine the functions $\delta = \Delta(t, \delta_0)$ so that the Γ are a solution of the (original) canonical system $\dot{\gamma} = J(\partial \tilde{H}/\partial \gamma)$ with the Hamiltonian $\tilde{H} = \tilde{H}(t, \gamma) = H(t, \gamma)$ and initial values t_0, $\gamma_0 = \alpha_0$.

Then the functions $\Delta(t, \delta_0)$ are a solution of the canonical system $\dot{\delta} = J(\partial H_2^*/\partial \delta)$ with the Hamiltonian $H_2^* = H_2^*(t, \delta) = H_2(t, \Gamma(t, \delta))$ and initial values $\delta_0 = \alpha_0$.

The Restricted Three-Body Problem in the Plane

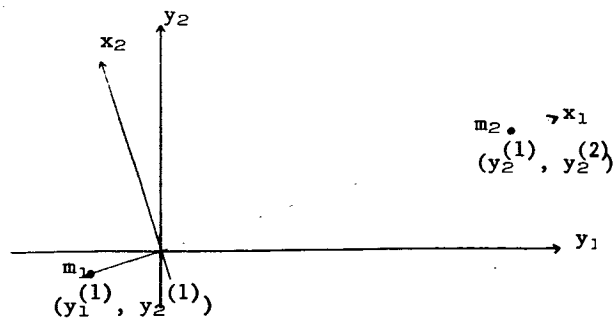

Let y_1, y_2 be cartesian, barycentric, and space fixed coordinates in the plane of motion; let the finite masses m_1 and m_2 revolve in circles about their common center of mass with angular velocity n. The differential equations of motion of a particle with mass zero and position (y_1, y_2) in the gravitational field of m_1 and m_2 read

$$\ddot{y}_1 = -\gamma m_1 \frac{y_1 - y_1^{(1)}}{\rho_1^3} - \gamma m_2 \frac{y_1 - y_1^{(2)}}{\rho_2^3}$$

$$\ddot{y}_2 = -\gamma m_1 \frac{y_2 - y_2^{(1)}}{\rho_1^3} - \gamma m_2 \frac{y_2 - y_2^{(2)}}{\rho_2^3}$$

where

$$\rho_i = \sqrt{(y_1 - y_1^{(i)})^2 + (y_2 - y_2^{(i)})^2} \qquad i = 1,2.$$

The specific kinetic energy is

$$\tilde{T} = \frac{1}{2}(\dot{y}_1^2 + \dot{y}_2^2),$$

the specific potential

$$\tilde{V} = -\gamma m_1 \frac{1}{\rho_1} - \gamma m_2 \frac{1}{\rho_2},$$

and the Lagrangian

$$\tilde{L} = \tilde{T} - \tilde{V}.$$

The equations of motion can also be written as

$$\ddot{y}_1 = -\frac{\partial \tilde{V}}{\partial y_1}; \quad \ddot{y}_2 = -\frac{\partial \tilde{V}}{\partial y_2}.$$

Introduce new coordinates x_1, x_2 by the rotation

$$x_1 = y_1 \cos n(t - t_0) + y_2 \sin n(t - t_0)$$

$$x_2 = -y_1 \sin n(t - t_0) + y_2 \cos n(t - t_0)$$

so that the coordinates of m_1 and m_2 are constant and $x_1^{(1)}$, 0 and $x_2^{(1)}$, 0. In this new coordinate system we get:

specific kinetic energy

$$T = \frac{1}{2}(\dot{x}_1^2 + \dot{x}_2)^2 + \frac{1}{2} n^2(x_1^2 + x_2^2) + n(x_1\dot{x}_2 - \dot{x}_1 x_2)$$

$$= \frac{1}{2}[(\dot{x}_1 - nx_2)^2 + (\dot{x}_2 + nx_1)^2],$$

specific potential

$$V = V(x_1, x_2) = -\gamma m_1 \frac{1}{r_1^3} - \gamma m_2 \frac{1}{r_2^3},$$

where

$$r_i = \sqrt{(x_1 - x_1^{(i)})^2 + x_2^2},$$

the Lagrangian

$$L = T - V,$$

and the differential equations of motion

$$\ddot{x}_1 - 2n\dot{x}_2 - n^2 x_1 = -\frac{\partial V}{\partial x_1}$$

$$\ddot{x}_2 + 2n\dot{x}_1 - n^2 x_2 = -\frac{\partial V}{\partial x_2}.$$

For the following we will write the differential equations of motion in canonical form; introduce in the usual manner the generalized momenta x_3 and x_4 by

$$x_3 = \frac{\partial L}{\partial \dot{x}_1} = \dot{x}_1 - nx_2, \qquad x_4 = \frac{\partial L}{\partial \dot{x}_2} = \dot{x}_2 + nx_1$$

and the Hamiltonian

$$H = H(\dot{x}) = H(x_1, x_2, x_3, x_4) = x_3\dot{x}_1 + \dot{x}_2 x_4 -$$

$$L(x_1, x_2, \dot{x}_1, \dot{x}_2) = \frac{1}{2}(x_3^2 + x_4^2) +$$

$$n(x_2 x_3 - x_1 x_4) + V(x_1, x_2).$$

The canonical equations of motion read

$$\dot{x}_1 = \frac{\partial H}{\partial x_3}, \quad \dot{x}_2 = \frac{\partial H}{\partial x_4}, \quad \dot{x}_3 = -\frac{\partial H}{\partial x_1}, \quad \dot{x}_4 = -\frac{\partial H}{\partial x_2},$$

or in matrix form $\dot{x} = J\frac{\partial H}{\partial x}$.

Let the initial values be t_0, x_0.

Euler's Problem of Two Fixed Centers

Write $H = H_1 + H_2$,

where $H_1 = \frac{1}{2}(x_3^2 + x_4^2) + V(x_1, x_2)$

and $H_2 = n(x_2 x_3 - x_1 x_4)$;

H_1 is the Hamiltonian for Euler's problem of two fixed centers, as can be derived directly or from

the fact that $H_1 = H(n = 0)$. Introduce new coordinates w instead of x for the (formal) solution of Euler's problem, and define a Hamiltonian $\tilde{H}_1$ by

$$\tilde{H}_1 = \tilde{H}_1(w) = H_1(x).$$

The differential equations of motion are

$$\dot{w} = J \frac{\partial \tilde{H}_1}{\partial w},$$

and denote the initial values by t_o, w_o.

Let $w = W(t, w_o)$ be the solution of this system of differential equations, i.e. of Euler's problem; it follows from the theory of differential equations that the $W_j(t, \tilde{w})$ are holomorphic functions of the variables $\tilde{w}_i$ in a sufficiently small neighborhood of the point $\tilde{w}_o = w_o$. Since $W(t_o, \tilde{w}) = \tilde{w}$, one finds, expanding W in a power series of $t - t_o$:

$$W(t, \tilde{w}) = \tilde{w} + \left(\frac{\partial W}{\partial t}\right)_{t_o} (t - t_o) + \ldots$$

and therefore

$$\left(\frac{\partial W_j(t, \tilde{w})}{\partial \tilde{w}_i}\right)_{t_o} = \delta_{ji},$$

and this holds especially for $\tilde{w} = w_o$.

Perturbation

Introduce functions Ω_j, $j = 1, \ldots, 4$, by

$$\omega = \Omega(t, \xi) = W(t, \xi)$$

and determine the functions $\xi_j = \Xi_j(t, x_o)$ in such a way that ω is the solution of the original restricted problem, i.e. that

$$\dot{\omega} = J \frac{\partial \hat{H}}{\partial \omega}$$

with the Hamiltonian $\hat{H} = \hat{H}(\omega) = H(\omega)$ and initial values t_o, $\omega_o = x_o$.

According to the theorem formulated at the beginning one finds that the functions $\xi_j = \Xi_j(t, x_o)$ are determined by the canonical system

$$\dot{\xi} = J \frac{\partial \tilde{H}_2}{\partial \xi},$$

with the Hamiltonian $\tilde{H}_2 = \tilde{H}_2(t, \xi) = H_2(\Omega(t, \xi))$ and initial values t_o, $\xi_o = x_o$.

New Expression for $\tilde{H}_2$

Let us derive another explicit expression for the Hamiltonian $\tilde{H}_2(t, \xi)$ in order to be able to split $\tilde{H}_2$ into the sum of two terms and to apply this perturbation procedure once more. From the definition of H_2 it follows that

$$\tilde{H}_2 = n(\omega_2\omega_3 - \omega_1\omega_4), \quad \omega_j = W(t, \xi).$$

The ω_j are the solution of Euler's problem and consequently satisfy the following set of equations:

$$\dot{\omega}_1 = \omega_3, \quad \dot{\omega}_2 = \omega_4$$

$$\dot{\omega}_3 = -\frac{\partial V(\omega_1, \omega_2)}{\partial \omega_1} = -\gamma m_1 \frac{\omega_1 - \omega_1^{(1)}}{r_1^3} - \gamma m_2 \frac{\omega_1 - \omega_1^{(1)}}{r_2^3}$$

$$\dot{\omega}_4 = -\frac{\partial V(\omega_1, \omega_2)}{\partial \omega_2} = -\gamma m_1 \frac{\omega_2}{r_1^3} - \gamma m_2 \frac{\omega_2}{r_2^3},$$

where $\omega_1^{(i)}$, 0 is the fixed position of m_i, and

$$r_i = \sqrt{(\omega_1 - \omega_1^{(i)})^2 + \omega_2^2}.$$

It follows that

$$\begin{aligned}
\frac{\partial \tilde{H}_2}{\partial t} &= n(\dot{\omega}_2\omega_3 + \omega_2\dot{\omega}_3 - \dot{\omega}_1\omega_4 - \omega_1\dot{\omega}_4) \\
&= n(\omega_4\omega_3 + \omega_2\dot{\omega}_3 - \omega_3\omega_4 - \omega_1\dot{\omega}_4) \\
&= n(\omega_2\dot{\omega}_3 - \omega_1\dot{\omega}_4) \\
&= n\left[\gamma m_1\omega_1^{(1)}\frac{\omega_2}{r_1^3} + \gamma m_2\omega_1^{(2)}\frac{\omega_2}{r_2^3}\right] \\
&= n\gamma m_1\omega_1^{(1)}\omega_2\left(\frac{1}{r_1^3} - \frac{1}{r_2^3}\right),
\end{aligned}$$

since

$$m_1\omega_1^{(1)} + m_2\omega_1^{(2)} = 0$$

in the used barycentric coordinate system.

Integration of $\dot{\tilde{H}}_2$ with respect to time t (the ξ are considered as constants) yields

$$\tilde{H}_2(t, \xi) = \tilde{H}_2(t_o, \xi) + n\gamma m_1\omega_1^{(1)} \int_{t_o}^{t} \omega_2\left(\frac{1}{r_1^3} - \frac{1}{r_2^3}\right) dt;$$

for $\tilde{H}_2(t_o, \xi)$ we find, since $\Omega(t_o, \xi) = \xi$:

$$\tilde{H}_2(t_o, \xi) = n(\xi_2\xi_3 - \xi_1\xi_4).$$

Second Perturbation

Write $\tilde{H}_2(t, \xi) = \tilde{H}_3 + \tilde{H}_4$,

where $\tilde{H}_3 = n(\xi_2\xi_3 - \xi_1\xi_4)$

and $\tilde{H}_4 = n\gamma m_1\omega_1^{(1)} \int_{t_o}^{t} \omega_2\left(\frac{1}{r_1^3} - \frac{1}{r_2^3}\right) dt,$

and $\omega_2 = \Omega_2(t, \xi)$, $r_i = r_i(t, \xi)$.

As in the first perturbation process, we will solve the canonical system with the Hamiltonian $\tilde{H}_3$ and introduce the initial values of the solution as new variables into the full canonical system with the Hamiltonian $\tilde{H}_2$.

Introduce new variables g_1, g_2, g_3, g_4 and solve the canonical system

$$\dot{g} = \frac{\partial H_3^*}{\partial g}$$

with the Hamiltonian

$$H_3^* = H_3^*(g) = \tilde{H}_3(g) = n(g_2g_3 - g_1g_4)$$

and initial values t_0, g_0. The solution $g = G(t,g_0)$ can be given explicitly as the simple rotation

$$g = \begin{pmatrix} \cosn(t-t_0) & \sinn(t-t_0) & 0 & 0 \\ -\sinn(t-t_0) & \cosn(t-t_0) & 0 & 0 \\ 0 & 0 & \cosn(t-t_0) & \sinn(t-t_0) \\ 0 & 0 & -\sinn(t-t_0) & \cosn(t-t_0) \end{pmatrix} g_0$$

or

$$g = R(t)g_0.$$

Now introduce functions $\gamma_j = \Gamma_j(t,\lambda) = G_j(t,\lambda)$ and determine the functions $\lambda_j = \Lambda_j(t,x_0)$ so that the functions Γ_j are solutions of the full canonical system with $\tilde{H}_2$, i.e. of

$$\dot{\gamma} = J\frac{\partial H_2^*}{\partial \gamma}$$

with the Hamiltonian $H_2^* = H_2^*(t,\gamma) = \tilde{H}_2(t,\gamma)$ and initial values t_0, λ_0.

Again it follows by the theorem formulated in the beginning, that the functions $\lambda = \Lambda(t,x_0)$ are determined by the canonical system

$$\dot{\lambda} = J\frac{\partial H_4^*}{\partial \lambda}$$

with the Hamiltonian $H_4^* = H_4^*(t,\lambda) = \tilde{H}_4(t,\Gamma(t,\lambda))$ and initial values t_0, $\lambda_0 = x_0$. The Hamiltonian H_4^* can be written also as

$$H_4^*(t,\lambda) = n\gamma m_1\omega_1^{(1)}\int_{t_0}^{t}\omega_2\left(\frac{1}{r_1^3} - \frac{1}{r_2^3}\right)dt,$$

where ω and r_i have to be expressed as functions of t and λ (λ is a constant for the integration).

Concluding Remarks

By the foregoing developments the restricted three-body problem has been reduced principally to the computation of the functions $\lambda_j = \Lambda_j(t,x_0)$ as the solutions of a system of canonical differential equations.

One can try, for instance, to expand $\Lambda(t,x_0)$ in a power series of $t-t_0$ or in a series of suitably chosen polynomials in t. It is easily seen that

$$\left(\frac{\partial \Lambda}{\partial t}\right)_{t_0} = 0,$$

therefore the power series reads

$$\Lambda(t,x_0) = x_0 + \frac{1}{2}\left(\frac{\partial^2 \Lambda(t,x_0)}{\partial t^2}\right)_{t_0}(t-t_0)^2 + \ldots,$$

i.e., the linear term vanishes. This indicates that $\lambda \approx x_0$ is a good approximation in some neighborhood of t_0.

The coordinates x of the restricted three-body problem can now be written as

$$x = x(t,x_0) = W(t,R(t)\lambda(t,x_0))$$

and, solved for λ,

$$\lambda = \lambda(t,x_0) = R(-t)W(-t,x(t,x_0)).$$

The formulas for the coordinates x in the restricted problem show - as one expects of course from the construction -, that x is represented by the solution W of Euler's problem with varying initial values. Thus, the trajectory of the restricted problem is not approximated in the usual manner by one solution of Euler's problems with the same fixed initial values, but by a one-dimensional point set of a one parameter family of solutions of Euler's problem.

The differential equation for λ is of a very complicated form and it has not been tried yet to approximate its solution analytically. However, the last formula can be used - and it has been used extensively - to compute λ numerically and to fit it then by suitably chosen functions. The results are very promising so far, and the numerical computations show clearly that λ is a slowly varying function of time for the first half (outbound leg) of a circumlunar trajectory; λ is also a slowly varying function for small changes in the initial values, so that families of trajectories can be represented by one expression for λ.

DESIGN COMPARISON OF LUNAR RETURN CONFIGURATIONS*

BY

E. Offenhartz, C. F. Berninger, W. Zeh, and M. C. Adams
Avco Research and Advanced Development Division, Wilmington, Mass.

Abstract

Parabolic manned re-entry design comparisons are made between two classes of slender and blunt configurations capable of conventional horizontal and vertical earth landings. Aerodynamic modulation using flaps and control augmentation requirements are discussed in terms of their effect upon re-entry trajectories and landing footprints. Within the environment defined by the re-entry trajectories, the convective and radiative modes of heat transfer are compared, their differences discussed, and the problems associated with the configurations for planetary return missions indicated. Thermal protection systems are discussed and the factors influencing the selection of a given system for the re-entry environment are indicated. Comparison between reflective and absorptive systems are made and the merits of each for a given flight time indicated. A thermo-structural analysis is presented which shows the trade-off between structural operating temperature and heat protection system thickness requirements. Total heat shield and structural weights are compared for the landing footprints presented and their variation with range shown. Finally, the areas of uncertainty in the aero-thermo structural design analysis are indicated for each class of configuration studied, and the weight differences between conventional horizontal landing and vertical descent configurations are given.

Introduction

Manned circumlunar flight and its associated re-entry phase presents new and novel problem areas. While many of these problems are within the state of the art for solution, the extrapolation of existing types of space vehicle and re-entry vehicle systems to this application requires careful consideration. The problems associated with parabolic re-entry have been treated in detail in the literature (references 1, 2, and 3). These studies indicate significant design parameters but do not enable direct comparison of configuration requirements as needed in determination of final system requirements.

In order to discuss the problems of manned re-entry and compare configurations, certain ground rules were established. A fixed internal volume of 350 ft.^{3} was assumed to be sufficient to house and support three astronauts and their associated equipment for a period of approximately two weeks. Two classes of configurations were then studied. The first were blunt configurations capable of vertical or parachute landings and the other was of the lenticular type capable of horizontal or conventional landing. All configurations considered were to have a hypersonic L/D capability of at least 0.5, considered adequate for maneuverability. Each configuration was designed to use the same basic heat protection system, structural operating temperature, and be operable for the same re-entry corridor and landing area by using a flap arrangement for modulation.

Configurations

The very blunt or high-drag configurations suitable for parachute landings and blunt, moderate-drag bodies suitable for conventional landings were studied. Figure 1 shows the outline and general dimensions of the configurations considered.

The cone had a bluntness ratio of 0.55 and a semi-vertex cone angle of 12 degrees. The calculated hypersonic lift-to-drag (L/D) capability was approximately 0.7. The center of gravity was located along the axis of symmetry and the vehicle trimmed at zero-degree angle of attack without flaps. Pitch and roll control were obtained with flaps located on the aft portion of the blunt cone. The controls operate differentially for roll control and in pairs for pitch control. At an L/D of one-half, the trim angle of attack was calculated to be approximately 19 degrees.

The 30-degree half-blunt cone configuration has a maximum calculated L/D of approximately one-half and trims without flaps at an angle of attack of approximately 4 degrees, the angle being measured from a plane parallel to the top flat surface of the vehicle. Pitch, yaw, and roll control is accomplished by four flaps; two of which extend aft from the top flat surface of the vehicle, the other two extend from the aft conic portion of the body.

The third blunt face configuration studied is shown in figure 1. An L/D of approximately one-half is calculated for this configuration which corresponds to an angle of attack of approximately

*This work was done at the AVCO Research and Advanced Development Division partially funded by subcontract NAS-5-304, GDA 203-429-A, and AVCO Corporate Funds.

35 degrees. At the trim condition the afterbody is not in the flow. Four chin flaps are used to provide pitch and yaw control.

The shapes discussed do not have capability for landing without auxiliary drag and/or lift devices, such as a parachute or a Rogallo Paraglider (reference 4). A configuration which has promise as an acceptable re-entry body with conventional glide landing capability is the lenticular shape (reference 5) where the cross section is elliptical and plan form is circular. The lenticular shape re-enters as a blunt body. After re-entry, the body is pitched to a glide position for landing. Altitude control is provided with flaps as indicated in figure 1.

Trajectory Studies

In order to determine the heating and loads associated with re-entry at parabolic velocities, trajectory studies were undertaken for flight along both the overshoot boundary at an L/D of 0 and by Chapman's 10g undershoot boundary at an L/D of 1/2. The entry corridor so bounded is approximately 30 nautical miles. Figure 2 shows a plot of altitude vs. down-range for re-entry trajectories on the over- and undershoot boundaries. The re-entry flight corridor is established by the range overlap which can be achieved for entries made on both the over- and undershoot boundaries. The maximum range shown is established by flight on the 10g lifting undershoot trajectory. Entry is made with an L/D of $\pm$ 1/2 to pull-up. When the flight path angle reaches $\pm 1.6^{\circ}$, the lift is removed and a ballistic flight is followed to an altitude of about 300,000 feet. At this altitude an L/D of $\pm$ 1/2 is again applied and held constant to impact. This maximum range can also be reached by flight on the ballistic overshoot boundary. On this boundary entry is made with L/D of 0 to impact.

The altitude of near 300,000 feet was chosen as a limiting value for skip-out, since at this altitude aerodynamic forces start to become important for control considerations.

The minimum range is obtained by entry on the ballistic overshoot boundary using a negative lift, trajectory. A modulation is made to limit the load at some point in the trajectory to 10g. This minimum range can also be achieved on the undershoot boundary by a modulation from the pull-up altitude. Ballistic flight from the bottom of the pull-up comes close to providing this range.

Due to the trajectory analysis studies, certain design restraints were established. These restraints are based upon trajectory sensitivity to flight path angle. For example, the initial ballistic overshoot re-entry angle is -5.37°. If the re-entry angle is just .02 degrees shallower or -5.35° then the resultant peak altitude after pull-up is increased by a factor of 6 from 300,000 feet to 1.8×10^{6} feet.

Furthermore, for the 10g lifting undershoot boundary a similar sensitivity exists. However, in this case, the flight path angle associated with the second (ballistic) portion of the flight is the critical parameter. For example, if the lift is removed when the flight path is 3.2° instead of 1.6° then instantaneous, full negative lift will not prevent the vehicle from skipping out.

Hence, these sensitivities to flight path angles and changes in modulation form the basic inputs required to define the guidance and control system (reference 6).

The flight corridor established by the above procedure provides an overlap in down-range of roughly 2,800 n.m. Results of investigations of the requirements of the system, the capabilities of the vehicle, and the guidance and control system indicate that this flight corridor appears to provide a reasonable approach for vehicle design criteria.

Design trajectories of this type were computed for each configuration studied in order to determine the environment which formed the basis of configuration comparison. Altitude-velocity graphs for the ballistic overshoot and 10g lifting undershoot trajectories are indicated in figure 3. The region of high convective heat flux and non-equilibrium radiation phenomena are indicated and are discussed in the re-entry heating section.

The landing capability of a vehicle with $W/C_DA = 50$ lbs./ft.^{2} which enters the atmosphere at the ballistic overshoot and 10g lifting undershoot bounds was examined. The footprint for a given re-entry angle is obtained by suitably banking the vehicle within the trajectory constraints. Once the landing footprints, associated with both entry boundaries, have been established their intersection represents the landing capability.

The maneuver capability was investigated by generating trajectories wherein the L/D and roll angle were represented as step functions. These changes were initiated at the pull-up point and at the top of the ship phase. The landing footprint obtained is indicated in figure 4. The results indicate a down-range maneuvering capability of 2,380 nautical miles and a cross-range capability of $\pm$ 420 nautical miles measured from a minimum down-range impact point which is 870 nautical miles from entry.

If the skip-out altitude requirement is relaxed, the landing footprint can be extended as indicated in figure 4. For an L/D of one-half, increasing the skip-out altitude to 500,000 feet enables the down-range capability of the vehicle to be increased by a factor of approximately 2. Care must be exercised in the choice of re-entry

trajectories and resulting landing footprints. These considerations must include the guidance and control accuracy, total heating to be absorbed as well as many other system requirements.

Re-entry Heating

The convective and diffusive stagnation point heat transfer rates were calculated using the results of Fay and Riddell (reference 7) correlated as,

$$\dot{q}_{STG} = \frac{0.76}{Pr^{0.6}} (\rho\mu)_w^{0.1} (\rho\mu)_{STAG}^{0.4} \left[1 + (Le^{0.52} - 1)\frac{h_d}{H}\right](H - h_w) \sqrt{\left(\frac{du_e}{ds}\right)_{STAG}} \sqrt{\frac{K+1}{2}} \qquad (1)$$

The factor $\sqrt{\frac{K+1}{2}}$ has been used to calculate the correction for the stagnation point velocity gradient for asymmetric configurations. "K" is defined as the ratio of velocity gradients along the principal radii of curvature (reference 8).

For a sphere, the stagnation point velocity gradient is accurately predicted by Newtonian theory. Vinokur (reference 9) evaluated constant density solutions for bodies with elliptic cross-section noses. Comparison of the data obtained for various blunt bodies (reference 10) with Vinokur's results (figure 5) indicates an over-estimation of 20 percent in the predicted velocity gradient, hence, 10 percent in heat transfer rate. In the results to be presented, Vinokur's constant density solutions were used to evaluate the stagnation point velocity gradients.

Equation 1 has been used with great success for correlating data for satellite flight velocities and altitudes less than 250,000 feet. At near escape velocities, however, the electron concentrations and temperatures in the boundary layer are large enough so as to effect transport properties of the air. The results presented in reference 11 indicate that a vehicle entering at parabolic velocity will experience approximately a 15 percent increase in stagnation point heat transfer rate over that predicted by equation 1.

These results have been compared with experimental data (reference 12) at velocities between 32,000 and 39,000 ft./sec. Within the accuracy of the data ($\pm$ 15 percent) the theory is in good agreement with the data and because the integrated electronic effect on heat transfer throughout the entire trajectory results in a smaller increase, this effect was not included in the analysis.

Heat transfer distributions require a knowledge of the pressure distributions. Wherever possible, available data applicable to the configurations studied was used. The prediction of pressure distributions for axisymmetric and/or two dimensional bodies is established in the literature. An approximate blunt body solution and the method of characteristics for equilibrium (reference 13) were employed for applicable configurations. In many cases, simple approximations, which have been found to correlate with data, were used. An approximate method used for the blunt vehicles was the technique of Lees wherein the Newtonian pressure distribution was assumed until the pressure gradient matched the gradient obtained from a Prandtl-Meyer expansion.

The convective and diffuse heat transfer distributions were calculated using the results of Kemp, Rose, and Detra (reference 14) given as:

$$\frac{\dot{q}}{\dot{q}_{STG}} = \frac{\rho_w \mu_w}{\sqrt{2\xi}} \rho_e \mu_e K \left\{2 \rho_w \mu_w \left(\frac{du_e}{ds}\right)\right\}_{ST}^{-\frac{1}{2}} \left(\frac{1 + .096\sqrt{\beta}}{1.068}\right) \qquad (2)$$

Angle-of-attack studies indicate that equation 2 can be applied to nonaxisymmetric flow by considering the flow to be pseudo-axisymmetric and evaluating the distribution along streamlines. Experimental studies (reference 15 and 16) have shown that the heat transfer distribution along meridians located at $\pm$ 90 degrees circumferentially from the windward plane of symmetry are essentially constant for moderate angles of attack. Because of angle of attack, the shift in the position of the stagnation point creates an uncertainty in heating calculations. However, comparison of Newtonian predictions with existing data resulted in empirical estimates of the stagnation point movement.

In addition to the convective and diffuse modes of heat transfer, considerations of equilibrium and non-equilibrium radiation were included in the study. For calculation of equilibrium radiation stagnation point heat transfer, Kivel's method (reference 17) was used in conjunction with shock detachment distances which were estimated using Serbin's (reference 18) and Vinokur's (reference 8) results.

Non-equilibrium Radiation *

The temperature and density gradients in the shock wave enveloping a re-entry configuration act to increase the collision frequency which results in the excitation of the vibrational, dissociative, and electronic states. The reaction rates which govern the excitations are functions of local density and temperature. The temperature, density, and concentration profiles become asymptotic to equilibrium values downstream of the shock wave.

* Reference AERL Report RR 112, "Radiation from the Non-equilibrium Shock Front," by J. D. Teare, S. Georgiev, and R. A. Allen; presented at the October 1961 ARS International Hypersonic Conference in Boston, Mass.

Both shock thickness and relaxation distance vary inversely with density. Up to altitudes where the shock thickness and the average relaxation distance are approximately equal, equilibrium conditions exist immediately behind the shock wave. At higher altitudes, where relaxation distances are much greater than the shock thickness, a temperature overshoot will occur due to the high translational temperature. At the same time, the density increases from its ideal gas value immediately behind the shock wave because dissociation increases the number of particles per unit volume. This reaction zone gives rise to the non-equilibrium radiation effects. As indicated in figure 3, non-equilibrium radiation is expected to occur in an altitude region between 150,000 and 200,000 feet at velocities greater than 30,000 ft./sec. The significance of this effect can be illustrated by the fact that for a velocity of 36,000 feet per second, and an altitude of 200,000 feet, the peak overshoot temperature is approximately four times the equilibrium temperature.

It is interesting to note that the manned lunar return flight becomes one of the first problems wherein non-equilibrium radiation phenomena may play an important design role.

To illustrate the results of the heating calculations, the stagnation point time history for the 12 degree blunted cone configuration is shown in figure 6. The convective, equilibrium, and non-equilibrium values are shown indicating that for this case, the peak radiative contribution is approximately 82 percent of the peak convective rate. The pulses associated with the radiative contribution are short in time and occur slightly earlier than the convective pulse.

The integrated stagnation point heating is shown in figure 7 wherein the integrated non-equilibrium heating is 26 percent of the convective value.

The results shown for the cone are typical of the stagnation point calculations completed for all the configurations studied. In general, the results indicate the relative order of magnitudes of heating associated in decreasing order with convective, non-equilibrium radiative, and equilibrium radiative fluxes.

In addition to the stagnation point calculations equation 2 was used to generate heating distributions and the resultant total integrated flux determined for each re-entry trajectory considered. The results of these studies indicated that the maximum heat to be absorbed by a given configuration was determined by the maximum down-range achievable by flight along the lifting undershoot trajectory. Therefore, the heat protection system was designed for this case and its performance evaluated for the other flight conditions.

Although results are not presented, heating was calculated for each of the flaps associated with a given configuration. In general, the flaps arranged along the forward blunt portion of the body were subject to stagnation point heating whereas trailing edge flaps were subject in part to separated flow as well as the oblique shock ahead of the flaps. Although the flap arrangement presents a difficult local problem, they were designed to meet maneuvering requirements. Certainly maneuvering techniques which eliminate the necessity of flap arrangements result in greater efficiency and less weight.

Thermodynamic Analysis and Materials

The two-pulse heating environment previously described requires a detailed analysis of the thermal protection system capable of dissipating the energy generated during re-entry. In general, two systems capable of achieving this end are concerned with either absorbing or radiating the energy. The absorption systems considered for ballistic missile re-entry have been the heat sink and ablation concepts. The latter system uses heat absorption with phase change and for parabolic re-entry total weight considerations indicate it is preferable to the heat sink. The difference between ablative and radiative heat protection systems is associated with the exposure time and level of aerodynamic heating. Ablative systems are generally restricted to short duration exposure because of the total mass loss. Pure radiation systems are capable of longer exposure but restricted to relatively low aerodynamic heating because of the limitation of materials capable of operating at high surface temperature. The combination of ablation and radiation in a heat protection system has certain possibilities for the two-pulse heating associated with parabolic re-entry. Detailed discussions of the merits and performance of these systems are indicated in references 19, 20, and 21.

The thermal design of a heat protection system requires knowledge of the environment and loading conditions as well as specific materials properties and desired performance. Ablation materials are available over a wide range of ablation temperatures. Epoxy-base plastics are typical of low temperature ablators restricted to an operating range between 1,200-1,700°F. These materials have low densities and thermal conductivities and are suited to satellite re-entry where their performance as pure sublimers with large transpiration contribution to the heat of ablation is desirable. Intermediate ablation temperatures between 2,800 and 3,500°F can be achieved with charring plastics which are reinforced to reduce the rate at which the char spalls during re-entry. High temperature ablators operating between 4,300 and 5,000°F vary in chemical composition and thermal properties and include such materials as nylon and quartz reinforced plastics.

Using the half-blunt cone vehicle for illustrative purposes, examination of the isotherms shown in figure 8 indicate that during the first modulation period a conventional radiation design using a refractory metal or ceramic is not feasible. The lower surface temperature on both boundaries during the second modulation indicates the feasibility of radiation design during that portion of re-entry. This then indicates the possibility of the use of a combined ablation-radiation design.

Because of the many ablation materials available, parametric studies were undertaken to determine the influence of variation in both density and thermal conductivity variations on thermal design. Furthermore, variations in design performance due to ablation temperature were also studied. For purposes of design it was assumed that the basic structural member was a honeycomb structure. As will be shown later, the material used in the honeycomb structure influences the thermal history of the structural members used for longitudinal and circumferential support but does not directly influence the heat shield selection or thickness evaluation. Therefore, evaluation was made using a honeycomb structure backed by a semi-infinite thickness of a typical low strength, low density fibrous glass insulation designed to limit the temperature rise at the vehicle interior to approximately 70°F. The ablation material was an epoxy based reinforced resin capable of operation at 5,000°F. With these ground rules the results of the thermodynamic design are indicated in figure 9. The figure indicates the ablator thickness required to restrict the honeycomb structure temperature to the prescribed values. From a thermal point of view, the advantage of allowing the structure to attain a high operating temperature is obvious. The required thickness of ablation material increases with increasing aerodynamic heat input and decreasing structural operating temperature.

Structural Considerations

Preliminary structural designs and analysis were conducted to determine the relative structural advantages of each configuration. Variation of maximum operating structure temperature and the associated structural material selection was introduced as the only other significant parameter which was independent of vehicle shape.

Structural integrity was provided, in all cases, by a metallic structure behind the ablator which was designed to withstand all loading conditions without consideration of the load-carrying capability of the ablator. Each vehicle structure was designed for both 14.7 and zero psia internal pressure during re-entry. Honeycomb sandwich, reinforced with frames and longerons as required, was selected as the basic type construction. The high rigidity to flexure of this type design provides for structural stability and minimizes deflections between frames and longerons and the associated bending stresses induced in the ablator.

The use of aluminum, titanium, stainless steel, and René 41 were each considered as structure behind the ablator. The required honeycomb sandwich design and weight was computed for the blunt face vehicle for each material using load and temperature data corresponding to the worst design condition in a 10g lifting undershoot trajectory of 2,800 miles down-range distance. The unit weight of structure and heat shield are shown plotted in figure 10. Structural design comparisons of other large areas of the reference vehicles indicated a similar result. It should be mentioned that in certain cases -- particularly using steel and René -- minimum available sheet gages became a governing factor and structural weight was not directly related to operating temperatures. Figure 10 illustrates that appreciable over-all weight saving are possible by operating structure at higher limits, i.e., the savings in ablation material required for insulation more than offset increased structural weights over the temperature range considered. The maximum temperature that may be used in a practical design depends greatly on the maintenance of the heat shield-substructure bond or attachment integrity. This depends upon a number of factors such as detail design and the criteria for maintaining the heat shield on the vehicle and over-all system reliability.

A complete structural analysis is beyond the scope of this paper, however, a few comments on the differences and similarities of the design problems between vehicle shapes and the use of different structural materials is in order.

The half-blunted cone and lenticular shapes required substantial frames to resist the bending moments due to internal pressurization. Difficulty was experienced with thermal gradients and yielding within the frames for the higher temperature structural designs and tension-tie members across the vehicle compartment were used to reduce bending moments and frame depth requirements in order to avoid excessive thermal stresses. This problem was due primarily to the shapes and the internal pressure loads. The full-cone and blunt face type body with the non-symmetric aerodynamic loading did not present a comparable design problem.

Landing impact attenuation with crushable material behind the structure was also considered. Here blunt cone and half-blunt cone have an advantage over the other configurations since in the former the point of impact, on the vehicle, under different vehicle attitudes occurs over a smaller area thus permitting more efficient usage of a limited amount of crushable material and smaller internal volume used for this purpose.

The launch arrangement and tie-down systems studied showed substantial advantages for the axial symmetric bodies (blunt cone and blunt face type vehicles). The half cone and lenticular shapes resulted in more complex and generally heavier booster transition section. The lenticular shape entails considerable complexity for abort requirements and escape pods were considered necessary.

The choice of the structural material had little significance on the nature of the design problems. The membrane stresses in the composite shall (structure and ablator) distribute themselves in the ratio of their modulii; $\sigma_{abl}/E_{abl} = \sigma_{str}/E_{str}$. Since the structural materials considered have approximately the same strength-modulus ratios, each metal may be utilized at approximately the same percentage of its allowable stress for a given maximum ablator stress. The structural materials considered also have approximately the same modulus-weight ratios, and strength-weight ratios, and, since each was designed to the same loading conditions, the rigidities of the sandwich structures were comparable. The lighter materials having lower modulii and strengths had correspondingly thicker sandwich face sheets.

To explain the nature of the re-entry thermal stresses, consider the typical stresses in the ablator shown in figure 11 which corresponds to a "full restraint" such as would occur with a rigid substructure. It can be seen that the internal force ($\int \sigma dy$) occurs primarily due to stresses over a small layer of material (labeled A) which corresponds to temperatures over a range where $E\lambda\Delta T$ is appreciable, where E(T) is Young's Modulus, λ (T) is the thermal coefficient of expansion, and ΔT the temperature rise from the zero stress temperature. Small stresses exist in the outer region B due to the low modulus of the degraded (char) material. Small stresses exist in the inner region C due to the low expansion term $\lambda\Delta T$ in this "cool" region.

The thermal stress behavior for different ablator thicknesses is further illustrated by the stress-time curves shown in figures 12, 13, and 14 which are obtained from a shell solution including the effects of a steel substructure. It will be noted that the stresses on the outer surface (O.D.), mid-point, and inner surface (I.D.) of the ablator all peak at about the same value* (approximately $E\lambda\Delta T$). The peak ablator stresses for different thicknesses (vehicle locations) are all approximately of the same magnitude, although occurring at different times. Qualitatively, the peak of figure 11 "travels through" the ablator and decreases slightly in magnitude as the "restraint of the ablator" decreases with increased penetration of the degraded plastic layer.

*The effects of external pressure cause the peak stresses to be slightly greater than that of figure 11.

It is necessary to consider the relative thermal coefficients of expansions of the structures and ablators. The values given below

	$\lambda (10^{-6}/^{\circ}F)$ @ $200^{\circ}F$
Aluminum	12.9
Titanium	5
Steel	7
Ablator	61

indicate small differences between the structural materials compared to the difference between the structure and ablator. This, together with the comparable structural rigidities already discussed, explains why the nature of the thermal stress problems in re-entry were fundamentally the same for all the structures.

The contact pressure or bond stresses are shown in each case to be small. The contact pressure due to thermal stresses is, however, dependent on the radii of curvatures of the shell and therefore vehicle shape dependent. Estimates of contact pressures can be made by taking ratios of radii of curvatures. Contact stresses 10 to 20 times the values shown were found in the study but even these values do not appear to create design difficulties.

Weight Comparisons

The results of the aerothermodynamic and structural analysis can be summarized in terms of weight. The weight of the heat shield and structure for each of the vehicles studied are shown in Table I, based upon the use of a $1,000^{\circ}F$ René structure and charring ablator.

Within the accuracy of the design analysis, the weights of all blunt bodies capable of conventional parachute landing are the same. It was not possible to determine an obvious advantage between configurations based upon the assumption of a fixed internal volume and identical heat shield and structural operating temperature. Other total system requirements may determine an optimum configuration for the total mission which was not possible from the present analysis.

The weight penalty associated with the lenticular configuration capable of conventional landing is clearly indicated. It was found that a lenticular configuration having a 350 cubic foot volume could not develop sufficient subsonic L/D for landing. Therefore, a 16 foot diameter configuration was studied and the penalty shown.

The relative increase in heat shield weight is a function of down-range distance is shown in figure 15. Also shown as a design parameter are lines of constant deceleration from 4 g's to 10 g's. Confining attention to the 6 g curve, it is apparent that increasing down-range generally produces a heat shield weight penalty up to a range of 13,000 miles. This corresponds to a skip-out altitude

of approximately 750,000 feet. This results from the fact that increasing the range tends to increase the time for heat penetration into the structure and the time for radiation heat loss from the vehicle surface. Beyond this range, the radiation loss exceeds the heat diffusion effect and the weight requirement decreases. It is also apparent that for constant range, increasing the deceleration decreases the relative heat shield weight. Consequently to reduce heat shield weight, the trajectory would be restricted to shorter ranges or greater deceleration levels.

Conclusions

Blunt bodies capable of vertical descent when compared on a fixed volume basis offer little difference in terms of structural and heat protection system weight. The lenticular or conventional landing configurations studied require greater volume than blunt configuration and hence show a weight disadvantage by comparison. For vertical descent vehicles, the choice of configuration may be largely dictated by total system considerations, such as abort requirements, booster interface design, and rendezvous and docking with other vehicles in space.

Acknowledgment

The authors wish to acknowledge the contributions of Messrs. P. T. Andrews, J. A. Collins, and G. J. Cloutier to the details of the analysis presented.

References

1. Chapman, D. R., "An Analysis of the Corridor and Guidance Requirements for Supercircular Entry into Planetary Atmospheres," NASA TR R-55, 1959.

2 Grant, F. C., "Modulated Entry," NASA TN D-452, August 1960.

3. Wong, T. J., Goodwin, G., and Slye, R. E., "Motion and Heating During Atmosphere Reentry of Space Vehicles," NASA TN D-334, September 1960.

4. Rogallo, F. M., Lowry, J. G., Croom, D. R., and Taylor, R. T., "Preliminary Investigation of a Paraglider," NASA TN D-443, August 1960.

5. Jackson, C. M. and Harris, R. V., "Static Longitudinal Stability and Control Characteristics at a Mach Number of 1.99 of a Lenticular-Shaped Reentry Vehicle," NASA TN D-514, October 1960.

6. Dow, P. C., Fields, D. P., and Scammell, F. H., "Automatic Re-entry Guidance at Escape Velocity," ARS No. 1946-61, 1961.

7. Fay, J. A. and Riddell, F. R., "Theory of Stagnation Point Heat Transfer in Dissociated Air," JA/SS, February 1958.

8. Reshotko, E., "Heat Transfer to a General Three-Dimensional Stagnation Point," Jet Propulsion, January 1958.

9. Vinokur, M., "Inviscid Hypersonic Flow Near the Stagnation Point of Oblate Ellipsoidal Noses," JA/SS, July 1958.

10. Boison, J. C. and Curtiss, H. A., "An Experimental Investigation of Blunt Body Stagnation Point Velocity Gradient," ARS Journal, February 1959.

11. Adams, M. C., "A Look at the Heat Transfer Problem at Super Satellite Speeds," ARS No. 1556-60, December 1960.

12. Offenhartz, E., Weisblatt, H., and Flagg, R. F., "Stagnation Point Heat Transfer Measurements at Super Satellite Speeds," Journal of the Royal Aeronautical Society, January 1962.

13. Wood, A. D., "Machine Programming for Method of Characteristics Computation (In Vicinity of Flare Shock)," Avco RAD Technical Release 59-22, February 1959.

14. Kemp, N. H., Rose, P. H., and Detra, R. W., "Laminar Heat Transfer Around Blunt Bodies in Dissociated Air," JAA/SS, July1959.

15. Weisblatt, H., "Experimental Determination of the Laminar Heat Transfer Rate Distribution Along a Slender Blunt-Nose Body from Shock Tube Tests," Avco RAD-7-TM-60-34, June 1960.

16. Weisblatt, H., "Effect of 15° Angle of Attack on Laminar Heat Transfer Rate Distribution of a Slender Blunt-Nosed Cone-Cylinder Model," Avco RAD Technical Release 60-8, January 1960.

17. Kivel, B., "Radiation from Hot Air and Its Effect on Stagnation Point Heating," JA/SS, February 1961.

18. Serbin, H., "The High-Speed Flow of Gas Around Blunt Bodies," Aeronautical Quarterly, pp 313, 1958.

19. Collins, J. A. and Moodie, D., "Thermal Insulation for Lifting Re-entry Vehicles," ARS No. 1684-61, 1961.

20. Collins, J. A., Toscano, C., Moodie, D., and Wolz, W., "Transient Behavior of Composite Thermal Protection Systems," ARS No. 1695-61, 1961.

21. Roberts, L., "Radiation and Ablation Cooling for Manned Re-entry Vehicles," presented at the Second International Congress, International Council of the Aeronautical Sciences, Zurich, Switzerland, September 1960.

Table 1

Configuration	Heat Shield & Structure (lbs.)
Half-Blunt Cone	2,054
Blunt Cone	2,187
Blunt Body	2,136
Lenticular (16'D)	3,570

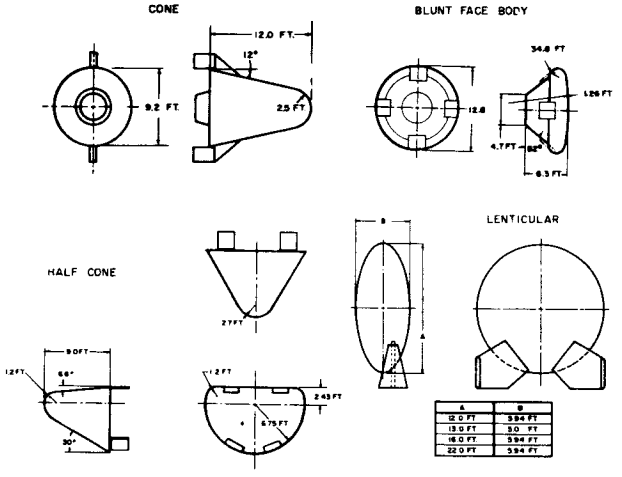

FIG 1 LUNAR RETURN CONFIGURATIONS

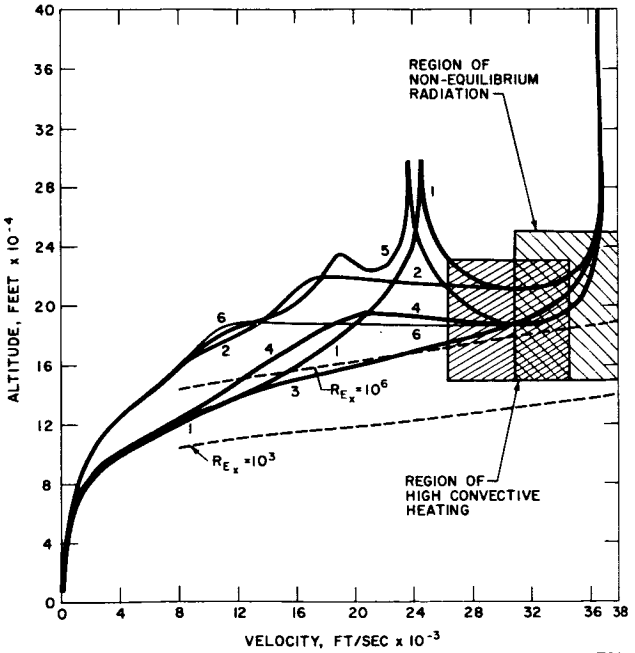

FIG. 3 ALTITUDE-VELOCITY PROFILES FOR PARABOLIC RE-ENTRY TRAJECTORIES

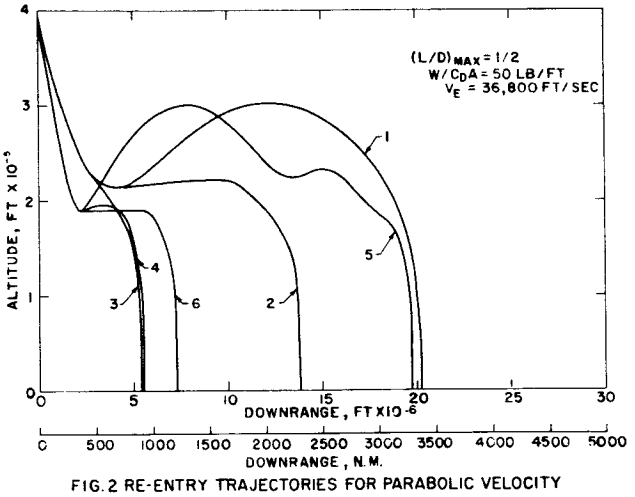

FIG. 2 RE-ENTRY TRAJECTORIES FOR PARABOLIC VELOCITY

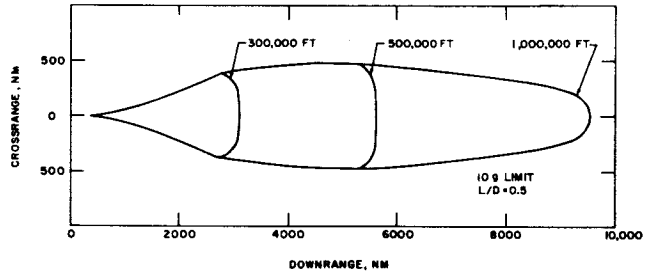

FIG.4 LANDING FOOTPRINT AS A FUNCTION OF SKIP-OUT ALTITUDE

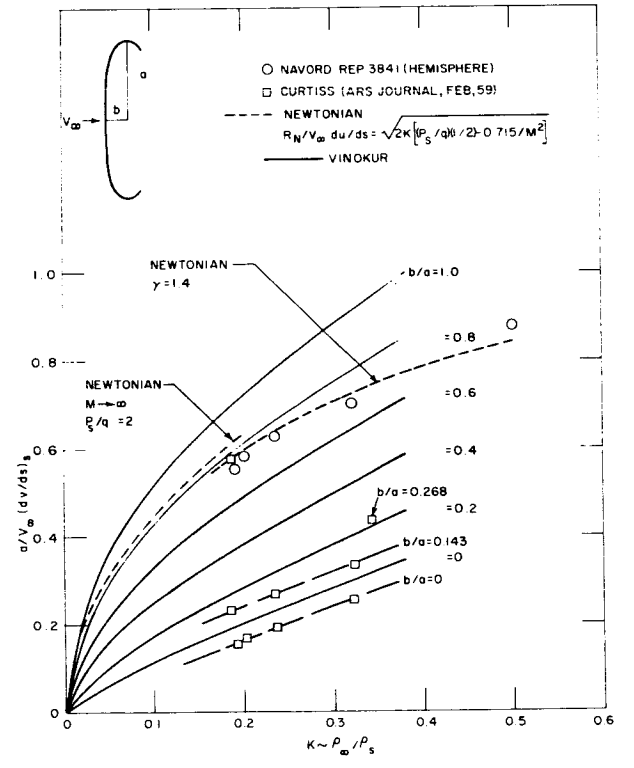

FIG.5 COMPARISON OF VINOKUR RESULTS WITH EXPERIMENTAL DATA AND NEWTONIAN THEORY

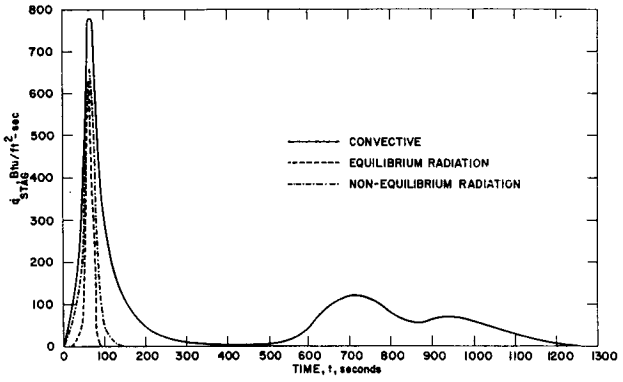

FIG. 6 STAGNATION POINT HEATING–CONE
10 G LIFTING UNDERSHOOT BOUNDARY TO MAXIMUM RANGE

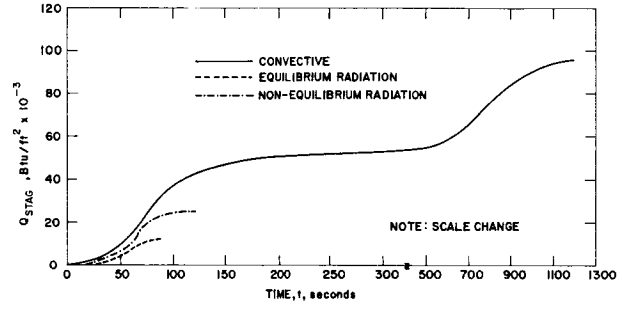

FIG. 7 INTEGRATED STAGNATION POINT HEATING–CONE
10 G LIFTING UNDERSHOOT BOUNDARY TO MAXIMUM RANGE

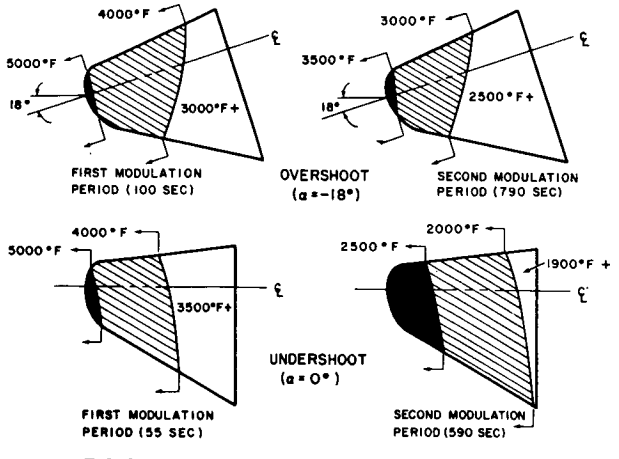

FIG. 8 MAXIMUM SURFACE TEMPERATURE FOR THE BLUNT HALF CONE

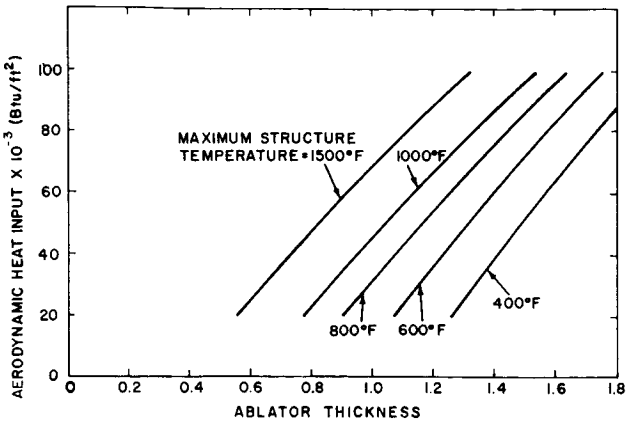

FIG. 9 THICKNESS REQUIREMENTS FOR VARIOUS STRUCTURAL OPERATING TEMPERATURES

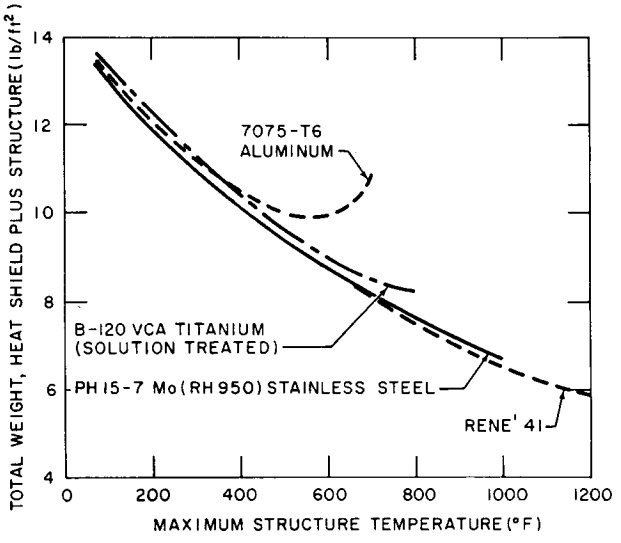

FIG. 10 COMBINED WEIGHT, HEAT SHIELD PLUS STRUCTURE BLUNT FACE VEHICLE

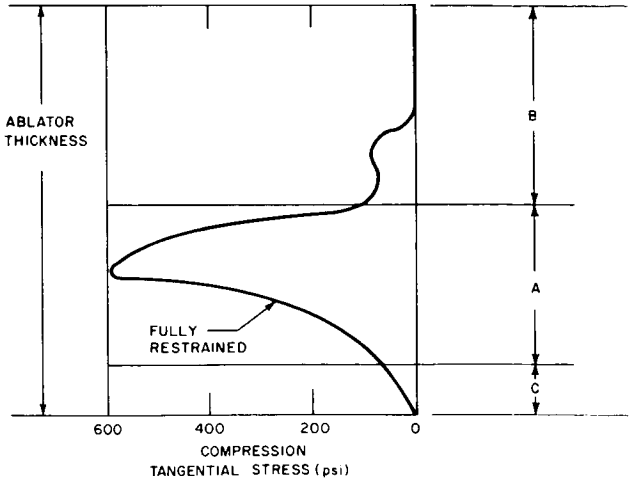

FIG. 11 STRESS DISTRIBUTION THROUGH ABLATOR THICKNESS

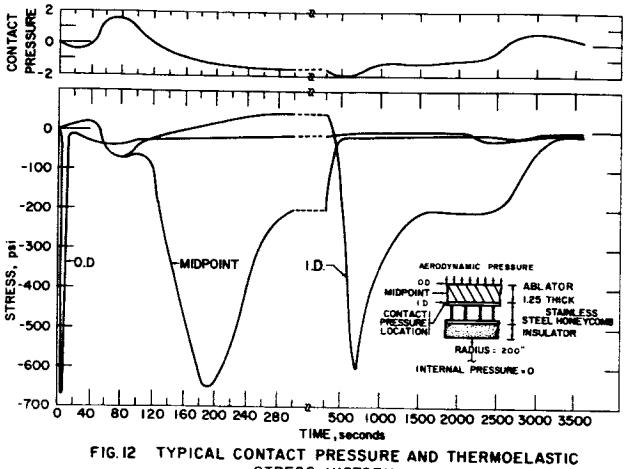

FIG. 12 TYPICAL CONTACT PRESSURE AND THERMOELASTIC STRESS HISTORY

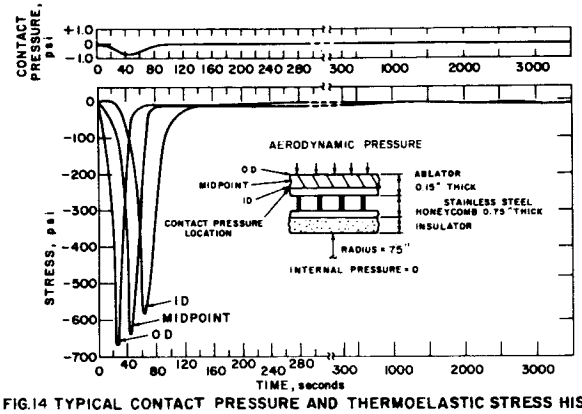

FIG. 14 TYPICAL CONTACT PRESSURE AND THERMOELASTIC STRESS HISTORY

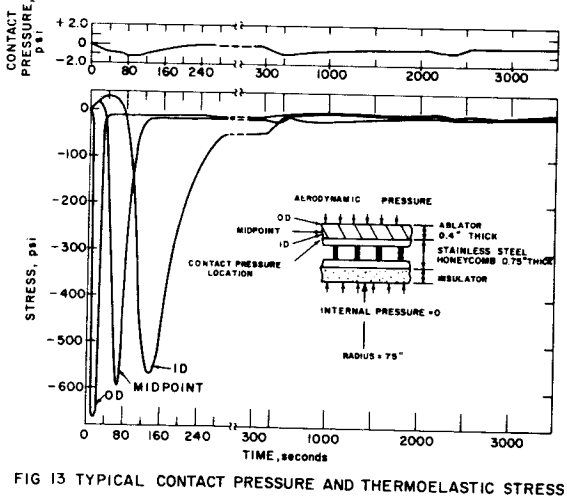

FIG 13 TYPICAL CONTACT PRESSURE AND THERMOELASTIC STRESS HISTORY

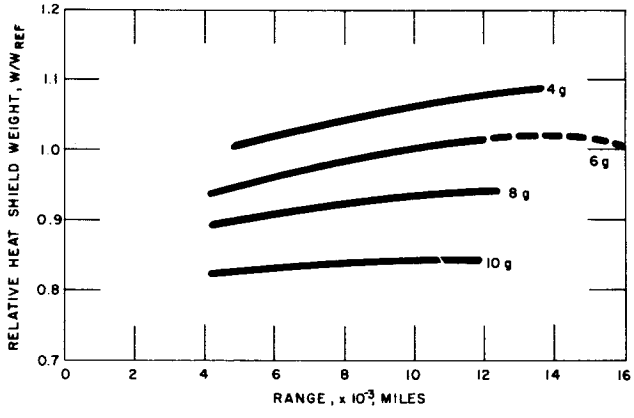

FIG. 15 INFLUENCE OF DOWNRANGE DISTANCE AND DECELERATION ON RELATIVE HEAT SHIELD WEIGHT

SELF ERECTING MANNED SPACE LABORATORY

R. Berglund
Aerospace Technologist
National Aeronautics & Space Administration
and
E. A. Weber
Project Engineer
North American Aviation, Inc.

The Langley Research Center of the National Aeronautics and Space Administration is currently involved in several research programs on manned orbital space stations. This research effort is focused on seeking out and solving the problems which lie in the way of the eventual development of such a vehicle for use as a space laboratory. In conducting this research activity, it has been necessary to consider many vehicle configuration designs and operational concepts in some detail. The Langley Research Center space station study program has been in progress for several years, and it was consisted of both in-house activities and contracted efforts with industry. In the early Langley Research Center studies, only zero-gravity configurations were considered; however, the requirement for artificial gravity simulation for experimental purposes was soon added. Human factors considerations indicated that large diameter vehicles with slow rotational velocities generally permit the most comfortable living conditions for the crew. The configurations which were studied were required to be compatible with the planned launch vehicles such as Saturn, and manned spacecraft such as Mercury.

The most familiar space station configuration is one which is composed of a tubular rim or torus and a central hub which is joined to the rim by a series of tubular spokes. However, it is obvious that a vehicle with sufficiently large diameter to permit a moderate level of artificial gravity to be simulated with a low rotational velocity is not capable of being boosted into orbit in one piece because of geometric factors. It has often been suggested that such a vehicle be disassembled, launched into orbit, and then reassembled by the crew members. With this concept, all equipment can be installed in its proper place in the various sections before launch, and, since the vehicle can be constructed of any material, adequate protection from the space environment can be provided. To obtain an early operational vehicle, it was apparent that emphasis must be placed on a means of obtaining a large volume, large diameter station without the necessity of having the crew assemble a number of smaller units which are launched into orbit either individually or collectively.

Inflatable or expandable spacecraft designs are distinctly advantageous from the standpoint of being able to be packaged as a small-volume booster payload. The Langley Research Center has done a great amount of work on the design and construction of inflatable space stations. Recently, a 24 foot diameter inflatable station was constructed for test purposes. This station plus a Mercury reentry vehicle, could be launched into orbit by a single booster, and after orbit is established, the station could be automatically inflated. There are two primary disadvantages of inflatable space stations. The first is that equipment cannot be installed prior to launch; it must be stored in a hub area and moved into position by the crew. The second is that the inflatable structure is not sufficiently resistant to penetration by meteorite particles for long duration missions.

The Langley Research Center recently developed a concept of self-erecting manned space station which combines the best features of both the rigid and inflatable space station concepts; i.e., the compactness of inflatable/expandable designs and the pre-launch equipment installation features of the rigid configurations.

The concept is a large, multi-manned space station composed of six rigid cylindrical sections joined by inflatable sections and arranged in a toroidal configurations. Three radial elements of inflatable structure join the torus to a central, non-rotating section. It is sized to be folded into a compact payload which can be launched by a single Saturn C-5 booster (S-IB and S-II stages). The Apollo vehicle, launched with the space station, serves only as a personnel transport and resupply vehicle. After the orbit is successfully established, the station can be automatically deployed without the necessity of having men assemble a number of smaller units in orbit. When fully extended, the station can be rotated to simulate gravity in the torus. The crew, launched with the station in an Apollo vehicle, will enter the station after it has been deployed, to set up and check out equipment and begin orbital operations.

Some of the characteristics of the basic NASA design are shown by the photographs of the model in Figure 1. This arrangement was used as a "basepoint" configuration for the North American Aviation, Inc. studies which were performed under NASA contract NAS1-1630. During the study period, a close working relationship was maintained between North American Aviation and the National Aeronautics and Space Administration to insure the evolution of the configuration could incorporate the best ideas of both organizations.

The general arrangement of the space station is shown in Figure 2. Struts, connecting the hub with each of the six rigid cylindrical sections, are used to assure uniform deployment from the launch configuration to the orbital configuration. The orbital configuration, with the non-rigid sections inflated, results in a space station with a 100-foot diameter, although the diameter could be treated as a variable. The hub provides non-

rotating docking facilities for the two Apollo vehicles which serve as the crew escape vehicles as well as the personnel transport and resupply vehicles. One end of the hub has been enlarged to house a small zero-gravity laboratory.

This space station launch configuration is shown in Figure 3. The modules are clustered, as indicated by the cross-section A-A, and the enlarged section of the hub serves as the interstage between the space station and the one Apollo vehicle which is launched with the station. This payload can be launched by a single Saturn C-5 booster (S-IB and S-II stages), while the crew transfer and resupply mission can be accomplished by means of Saturn C-1 or Titan III launch vehicles.

While the diameter of the initial configuration was sized by the limited payload capability of the Saturn C-2 booster, it became apparent early in the investigation that the rotational effects on the crew members might be intolerable. In Figure 4, a number of the parameters affecting the man's tolerance to the conditions aboard a rotating space station have been plotted in a manner such that a "comfort zone" is defined. The bounds of this comfort zone are determined by four parameters - the percent change in gravity between the man's head and feet; the space station angular velocity; the radial velocity; and the radial acceleration. It is believed that the change in gravity or acceleration between the man's head and feet should not exceed 15% in order to prevent impairment of blood circulation and to reduce the discomfort felt when the man changes the relative position of his head and feet by bending over or lying down. The recommended upper limit on the space station angular velocity is approximately 3 rpm to minimize the effects of Coriolis acceleration. Experiments with a rotating room have indicated that 3 rpm, with the human subject at a radius of 40 feet is a tolerable condition. The radial velocity of the space station should be no less than 20 fps in order to minimize the change in gravity the man will experience when he walks along the rim of the station. The upper limit on radial acceleration, or gravity, was set at 0.5 g to reduce fatigue; the lower limit is somewhat arbitrary, it being the minimum acceleration under which normal body processes can continue to function.

It can be seen from Figure 4 that a space station radius of 50 feet does not fall within the comfort zone. Consequently, a radius of 75 feet was selected for subsequent space station designs. With the increased payload capability of the Saturn C-5 booster, this larger diameter station can readily be launched into a low altitude orbit.

An additional factor in the design of the self-erecting space station is the optimum shape of the module. A module can be either a right cylinder or curved, i.e., a section of a torus which has a circular cross-section, as illustrated in Figure 5. A man, walking through a cylindrical module, will experience a change in gravity because his distance from the center of rotation is changing. Also, toward the end of the module, he will feel as if he were on an inclined floor because his body aligns itself with the radius vector. A curved module overcomes these problems, but it is more difficult to manufacture and it creates an undesirable launch configuration. Most of the difficulties in the cylindrical module can be overcome by use of a stepped floor as shown in Figure 5 to approximate the floor in the curved module. This has been exaggerated in the figure to illustrate how this might be accomplished.

A 150-foot diameter space station, using curved modules, was designed. It is shown in Figure 6. It has six modules, connected by inflatable material, and there are three inflatable spokes connecting the hub to the modules. This space station is deployed by means of controlled pneumatic pressure in the spokes, rather than by mechanical actuators which were discussed previously. It was subsequently concluded that this was not a suitable deployment mechanism because the motions of the modules could not be closely controlled. Each module of the configuration has a section of inflatable material at its midsection which is used to reduce the module curvature in the launch configuration as shown on the right-hand side of the figure. If the curvature were not reduced, the payload cross-section would extend as far as the dashed line and it would tend to create aerodynamic buffet during launch.

The space station will be continuously subjected to meteoroid bombardment during its lifetime in orbit. Since the inflatable material which is used in the design has very poor penetration resistance, it has been minimized on all designs. Wherever inflatable material is used, it would be lined with penetration-resistant panels by the crew members after the station has been deployed. The meteoroid environment which was assumed for this study is based on Whipples 1957 estimate as illustrated in Figure 7. The majority of particles are very small, and cause only a gradual erosion of the exterior surface. Of particular concern are those which are sufficiently large to cause a penetration of the structure. Through the use of emperical data on hypervelocity particle impact, a multiwall structure was designed to reduce the number of penetrations of the space station structure as much as possible. This structure is shown in Figure 8. The outer two layers of aluminum skin and glass wood (or polyurethane foam) are used only for the meteoroid bumber. They do not carry any structural loads. All of the structural loads in the modules are carried by the aluminum honeycomb. Sections of the inner wall are welded together to form a pressure tight vessel; consequently, penetrations of the outer three layers of aluminum will not result in a loss in pressure within the space station. If this structure were used throughout the space station, it is estimated that there would be only about 10 to 20 penetrations per year of the inner pressure wall of the entire station.

After an intensive design effort, it was concluded that a self-erecting space station could be designed with a completely rigid rim if the modules were properly hinged. This configuration, Figure 9, is deployed by mechanical actuators located at each hinge position. Since the motion of the modules is critical, the deployment must be carefully phased to prevent binding of the hinges. Several crude models of this configuration have been made in an attempt to demonstrate the feasibility of the concept.

The spokes, leading from the hub to the rim, are of inflatable material and must be lined with panels of rigid structure to prevent meteoroid penetration. The hub of this space station configuration is very large because it is designed to carry all the loads encountered during launch. The lower portion of the hub is utilized as a zero gravity laboratory compartment. Zero gravity is created in the compartment by mounting it on bearings and driving it in a direction opposite to the space station rotation.

Certain requirements, established early in the North American Aviation study had a particular influence on the evolution of the space station configuration. One of these stipulations was that the space station laboratory should be available as early as possible in order to provide information on a variety of subjects which could greatly affect future operations in space. Another was that the station must have a one year operational lifetime. To accomplish this with such a large vehicle meant that a very conservative design approach should be taken. The equipment which is used must be within today's state-of-the-art. Since the space station will be the first long-duration manned vehicle to be placed in space, reliability of operation is exceedingly important. Consequently, one of the major characteristics which was developed was that of a completely self-sufficient life support system in each module. Each module will have its own environmental control system and power supply. With this approach, a failure in one module would not jeoparidize either the mission or the lives of the crew members.

The concept of a "shirtsleeve" environment has been utilized throughout the space station because of the necessity to provide a comfortable working environment for the crew members. Since the tour of duty for the crew members of the space station will be a minimum of six weeks, they cannot tolerate living in a pressure suit as do the crew of Mercury, Gemini, or Apollo. Pressure suits would be worn only in emergency situations. The crew members will have free access to all parts of the space station. There will be pressure tight doors and airlocks between each of the adjoining sections of the station; however, so that if there is a major failure in any one section it can be sealed off from the remainder of the station until it can be repaired.

The dimensions of this station are such that an internal volume of approximately 60,000 cubic feet is available. With such a large volume, it is now reasonable to consider a much larger crew than was originally planned for the 100-foot diameter station. With an increase in crew size, all systems must be resized and docking facilities must be provided for additional Apollo vehicles, since there must be one Apollo vehicle at the station for every three men aboard. Studies have shown that a crew of 27 men can readily be accommodated by the space station; however, a nominal size of 21 was selected on the basis of anticipated duties and work load on the space laboratory mission.

The multiple vehicle docking facility and the zero gravity laboratory compartment have a great influence on the design of the hub of the space station. The Apollo vehicle should have a non-rotating (with respect to the space station) docking attachment. Also, the Apollo vehicles should be stored in a position near the plane of the modules so that the moments of inertia of the space station more nearly resemble those of a disk than those of a sphere. These two requirements lead to the conclusion that the hub should be as short as possible. At the same time, the zero gravity laboratory must be isolated from the normal movements of crew members between the rim and the hub. In Figure 10, the recommended space station configuration is shown. It incorporates all the refinements which have been discussed herein.

A docking facility to accommodate maximum of seven Apollo vehicles is illustrated in Figure 11. When the Apollo approaches the space station, the docking attachment is driven opposite to the space station rotation. The Apollo which was launched with the station is moved to one side. The second Apollo docks, and is moved to a position diametrically opposite the first. The docking attachment then is permitted to approach the station rotational velocity and the crew members exit to the hub by means of tubes which are extended to the Apollo airlock.

Figure 12, a cross-section of the hub, shows how the zero gravity laboratory compartment of the hub can be isolated from the normal flow of traffic between the rim and the hub. It occupies the lower portion of the hub. As in the previous hub design, the compartment is suspended by bearings and mechanically driven opposite to the direction of the space station rotation. The exact method for the suspension and drive has not yet been worked out, but it is apparent that the system must provide some means of isolating the compartment from low magnitude distrubances in the motion of the space station.

Although NAA placed primary emphasis on the configuration analysis in this study, the many systems which would compose the operational space station were also designed. In all these technical areas, particular effort was devoted to developing an approach which would provide the utmost reliability in a very early time period. Only systems which are well within the state-of-the-art were considered.

A typical example of this approach is found in the design of the environmental control system. Each module has a complete system, independent of the other modules, so that a failure in any one module will not result in the loss of the crew members aboard the station. The environmental control system is semi-closed, i.e., it must be resupplied on a periodic basis with oxygen, nitrogen, and a small amount of water. Consideration was given to the use of a completely closed system, which has two primary advantages - lighter weight and no resupply requirement - for long-duration missions. It was found that for a six-week mission on the space station, the weight of the semi-closed system was equal to the weight of a closed system, including the additional weight in the power system required for the electrolysis of water. Despite the obviously desirable characteristics of the closed system, it was concluded that the semi-closed system was more desirable for use in an early time period. Oxygen regeneration equipment,

just now in the early stages of development, will not have had sufficient operational experience by the 1966 time period to completely establish its reliability.

Each module has its own power system to provide the necessary electrical energy for all the equipment within the module. Several power sources - fuel cells, solar cells, nuclear reactors, and solar dynamic units - were studied for possible application to the space station. Only the solar cell system was able to meet the requirements for availability and reliability as well as the many other factors associated with the selection of a system. A solar cell power system is very expensive and requires a very large array area in order to provide the 17 kw peak power load for the space station; consequently, it is not recommended for use in a later time period when the reliability of the other systems would be established. The designs of the other systems were similarly established; however, these were not particularly unique and will not be discussed further here.

It has been found that the space station design which was presented herein has a gross weight of about 121,000 pounds, including all the equipment which would initially be placed in the station. The Apollo vehicle - command module, service module, and launch abort tower - which is launched with the space station plus the required interstage structure bring the total launch weight to approximately 150,000 pounds. Thus, the Saturn C-5 (S-IB + S-II stages) can readily launch the space station into a low altitude orbit, and a Saturn C-1 or a Titan III booster can be used to resupply the station and to transfer crews at scheduled intervals. For short crew mission duration, large numbers of C-1 boosters are required for crew transfer on the 21-man station, as shown in Figure 13. In order to mimimize the number of boosters required, the crew mission duration must be increased or the crew size must be decreased. The other means of overcoming this problem is to develop a multi-man logistics vehicle which could be used to transport all crew members to the station in one launching.

NAA has taken a very conservative design approach in this study. The use of more advanced systems or techniques would result in a decrease in the space station weight, but only at the expense of a decrease in the level of confidence associated with its operation.

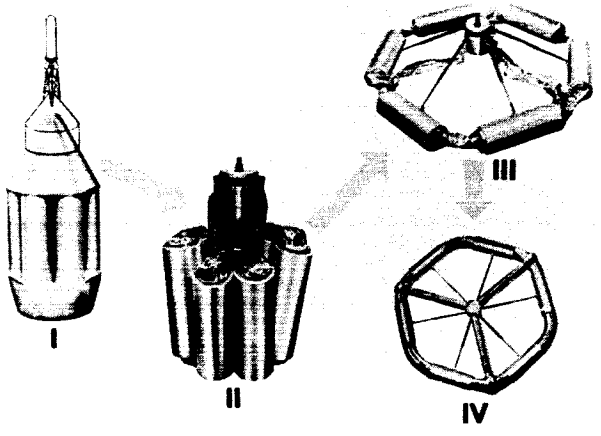

FIGURE 1. ERECTION SEQUENCE

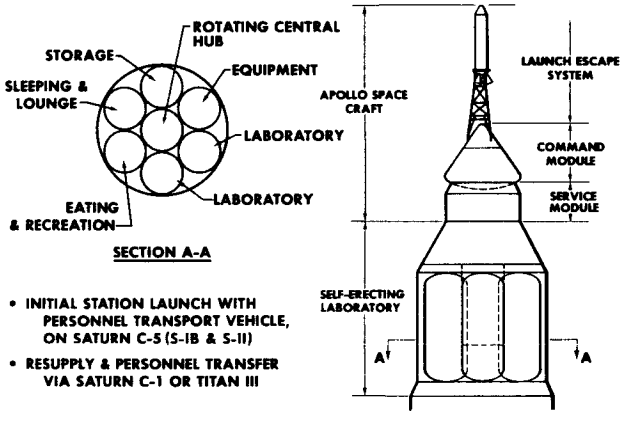

FIGURE 3. LAUNCH CONFIGURATION

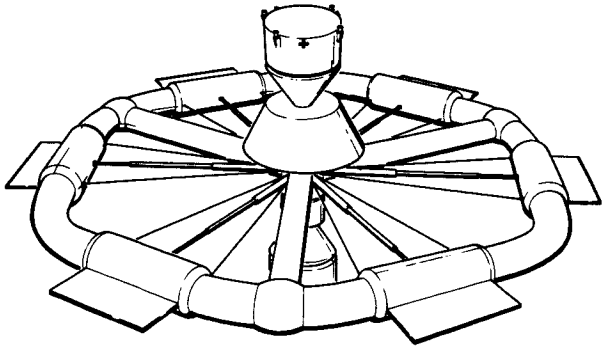

FIGURE 2. INITIAL CONCEPT

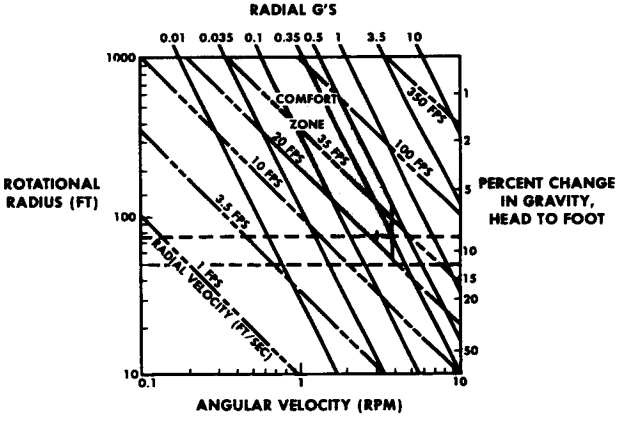

FIGURE 4. ROTATIONAL EFFECTS

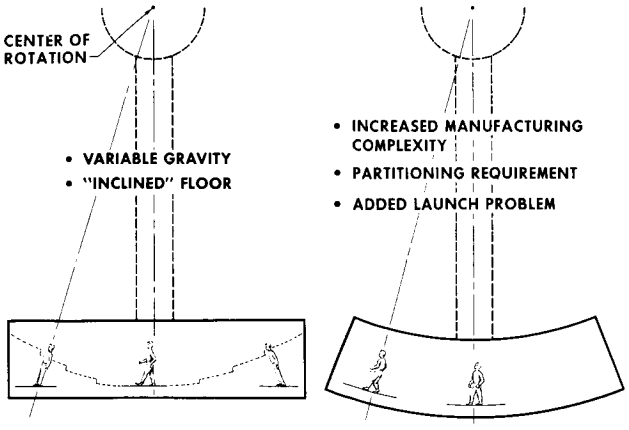

FIGURE 5. MODULE DESIGN CONSIDERATIONS

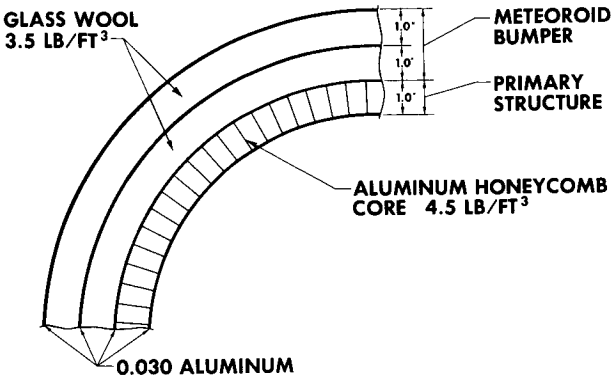

FIGURE 8. TYPICAL WALL STRUCTURE

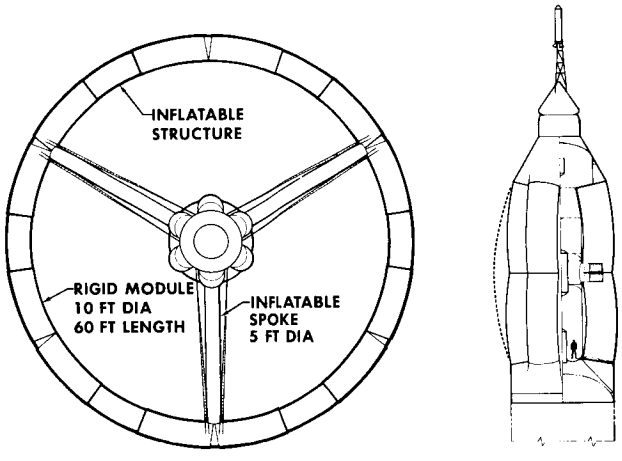

FIGURE 6. SPACE STATION CONFIGURATION (150 FT DIA)

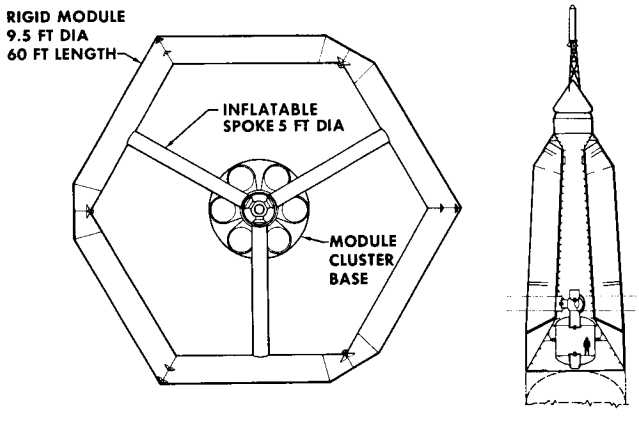

FIGURE 9. SPACE STATION CONFIGURATION (150 FT DIA)

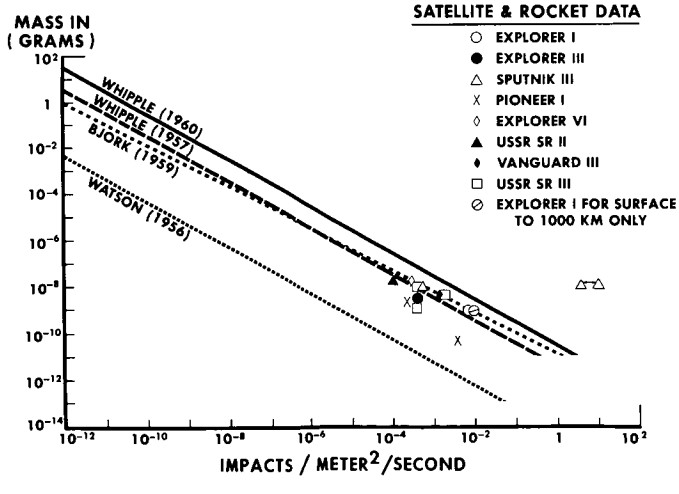

FIGURE 7. METEOROID ENVIRONMENT

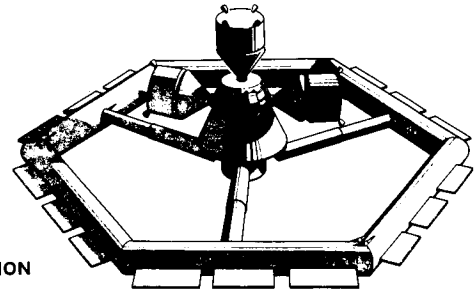

- ALL RIGID CONSTRUCTION
- 21-MAN CREW ACCOMMODATION
- INDIVIDUAL MODULE POWER & ECS

FIGURE 10. SELECTED CONFIGURATION

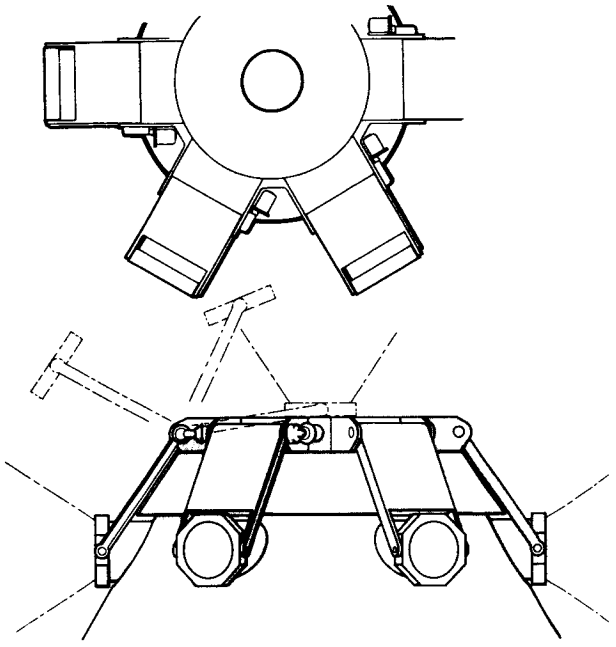

FIGURE 11. MULTIPLE VEHICLE DOCKING

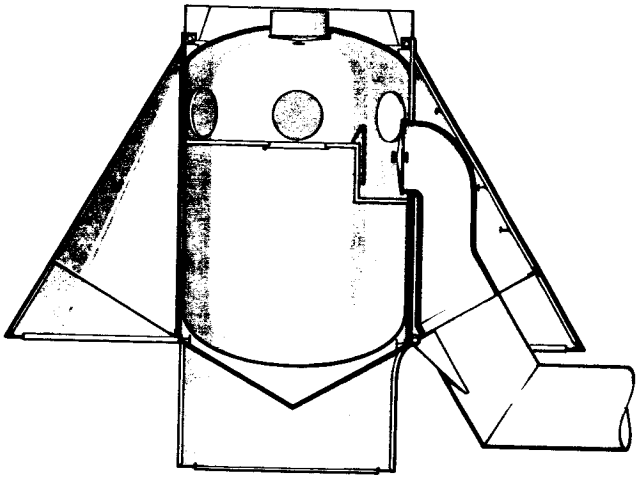

FIGURE 12. HUB SECTION

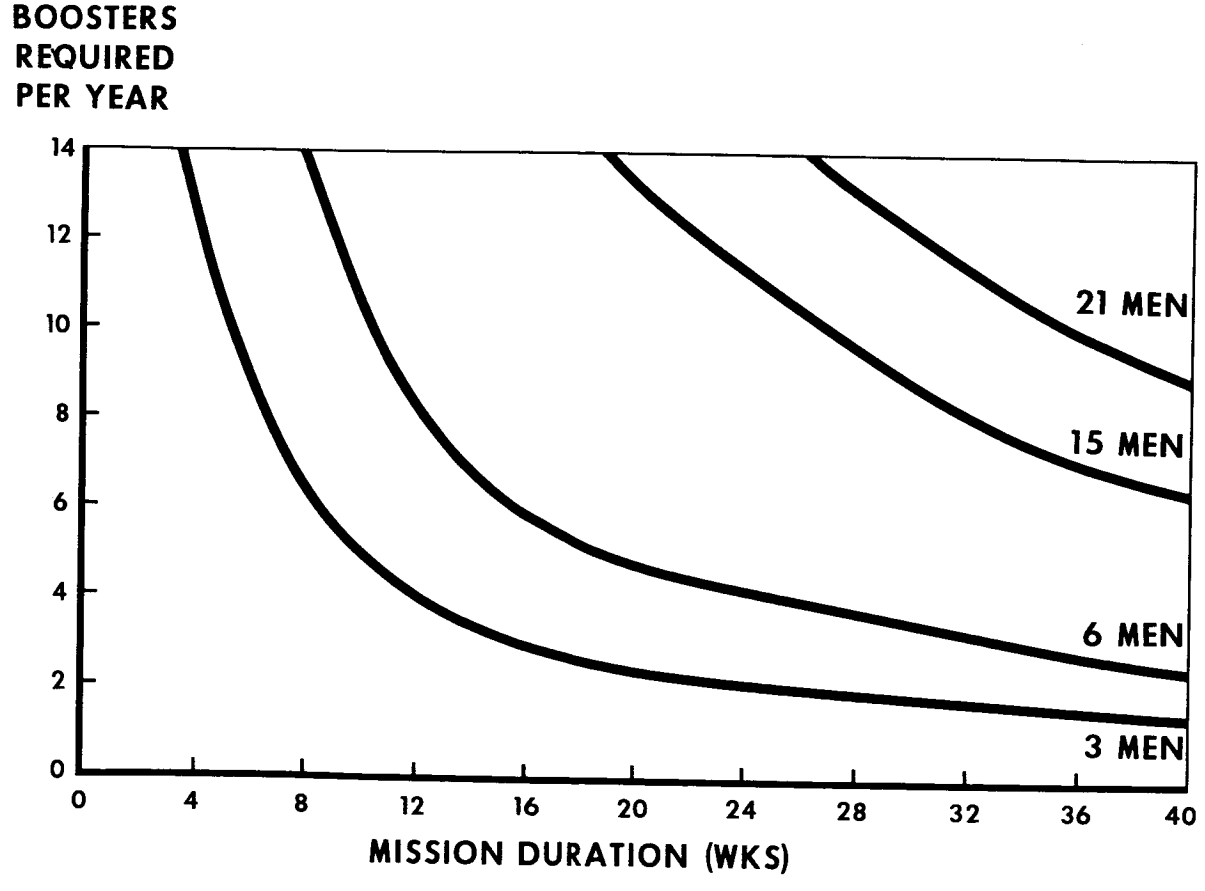

FIGURE 13. SATURN C-I BOOSTER REQUIREMENT

PROGRESS REPORT ON THE DEVELOPMENT OF PROTECTED CONSTRUCTION FOR HYPERSONIC VEHICLES

Wilfred H. Dukes
Asst Chief Engineer
Vehicle Structures
Bell Aerosystems Company

The structural problems of re-entry occasioned by aerodynamic heating are now generally well known. Typical of these heating problems is the environment experienced by the manned lifting vehicle re-entering from a low altitude orbit. Figure 1 shows typical curves of lower surface temperature as a function of time for a wing loading of 25 lbs/ft^2, and a lift-drag ratio of 2.5. The two curves cover a practical range of re-entry angles, the lower curve representing an ideal re-entry path with zero dive angle and the upper curve assuming a 2^o error in the re-entry angle. Maneuvers for course change or correction are also added to the upper curve.

Significant factors from this curve are the relationship between the maximum temperatures and the capabilities of available metallic material, and also the long re-entry time and its effect on total heat load. If a very shallow re-entry is made, maximum lower surface temperatures reach 2000^{o}F which is just within the range of conventional superalloys. To accommodate practical re-entry angles and maneuvers, however, the temperature capability must reach about 2500^{o}F which requires refractory metals. The re-entry time may be as high as 100 minutes, which gives total heat loads of approximately 40,000 BTU/ft^2. A heat load of this magnitude, with equilibrium surface temperatures of the values shown, suggests that a lighter airframe can be constructed by dissipating the heat by radiation from the surface, rather than by absorbing it with a heat sink, or surface cooling, or ablation.

Air Force programs to provide airframes for this type of environment have involved the parallel development of a number of different structural concepts. The development to be discussed here was carried out by Bell Aerosystems Company for the Fabrication Branch, Manufacturing Technology Laboratory, Directorate of Materials and Processes, Aeronautical Systems Division, Wright-Patterson Air Force Base, Ohio, under Contract AF33(600)-40100 (Double-Wall Cooled Structure).

The Bell concept involves the use of an aluminum alloy airframe which is of essentially conventional construction and which is protected from the effects of heating by an external insulation system and an integral cooling system. The insulation serves to keep the heat away from the aluminum airframe thereby generating surface temperatures sufficient to radiate almost all of the heat back to the atmosphere. This system is shown schematically in Figure 2.

The program to be discussed in this paper followed earlier Air Force and company-sponsored efforts to develop this type of construction and was directed particularly at the development of methods for manufacturing the various structural elements. It began in December 1959 and was completed in the Summer of 1961 with the strength and thermal testing conducted at Wright-Patterson Air Force Base of a typical full-scale airframe section. The work involved analysis development and testing, of the various components, the materials and the associated manufacturing techniques. Small assemblies were then built to check the concepts and develop additional data, and finally a full-scale specimen was designed, constructed and delivered to Wright Field for testing. Most of the program was devoted to development of the construction with a 2000^{o}F temperature capability. Initial steps to extend the capability to 2500^{o}F were also made, but since this part of the development is not yet complete it will not be discussed in this paper.

Referring to Figure 2 it will be seen that the insulating system which protects the aluminum airframe consists of a layer of insulating material, which is suitably packaged, and a series of external surface panels which are fabricated from high temperature materials. Because of the long flight times it is necessary to use very efficient insulating materials such as powders or fibers, and these have no structural capability. Accordingly, the surface panels provide the vehicle contour and resist aerodynamic forces. Panel construction is used rather than a complete shell in order to accommodate thermal expansion relative to the supporting internal structure, which is maintained at a temperature of approximately 200^{o}F. The insulation is sufficiently efficient to dissipate by radiation, approximately 98% of the convective heat. The remaining 2% of the heat, which does penetrate through the insulation, is more than can be accommodated by the internal structure, however, so that a low intensity liquid cooling system is integrated into this structure.

From this point it is convenient to discuss separately the development of the three principal components of the construction; the primary structure with its cooling system, the insulation material and its containing package, and the surface panels.

The cooling system consists of a closed loop circuit running through all elements of the primary structural skin and carrying a low freezing point propylene glycol coolant which is circulated by a small pump. The coolant picks up heat from the skin and transfers it to a heat exchanger which is also part of the circuit. Water is introduced into the open side of the heat exchanger, the heat is absorbed from the glycol mixture by evaporation of the water, and the resulting steam is expended overboard. A cooling system of this type is very efficient since the heat absorbing capability matches the heat input precisely at all points in the structure and at all times. Since it is essentially an active mechanical system, however, it requires consideration of reliability, and appropriate provisions in the design. In the present work such provisions include duplication of pumps, seals and certain elements of the heat exchanger.

A number of methods of integrating cooling passages into the aluminum load carrying skin have been investigated and two of these methods were developed extensively. The most promising is shown in Figure 3. The cooling passages, which are about 7/16" wide and .05" deep and spaced about 3" apart, are integrated into the structural skin and this has been accomplished by using inflated tubed sheet in which two thin sheets of material are metallurgically bonded together by hot rolling, except in the areas where cooling passages are required. These unbonded areas are then hydraulically inflated to the required passage shape. This type of material is commonly used in the refrigeration industry for which soft aluminum alloys suffice. For the airframe application, in which load carrying capability is required, it was necessary to develop the technique using the higher strength aluminum alloys. This work was carried out under subcontract by Reynolds Metals and was accomplished with 2024-clad material. The soft cladding served to form the metallurgical bond between the two sheets, and it also provided protection of the inside of the cooling passages against corrosion by the glycol.

Another aspect of the tubed sheet development program involved modifications of the inflation methods so that passages of different heights could be produced in an individual sheet. The large variations in passage area which were possible by adjusting both height and width permitted the incorporation of both cooling passages and distribution manifolds within the skin. In addition it was possible to incorporate various lengths of passage of restricted cross section in order to control the flow distribution. As a result of the work conducted by Reynolds these sheets have been made available in the high strength aluminum in sizes up to 8' long and 2' wide and with a minimum thickness of .040".

In addition to the tubed sheet, a method of brazing aluminum tubing to the structural skin was also developed using 6951 alloy. Elemental tests were made on small samples incorporating both cooling systems, and these included compression and shear tests on small stiffened specimens to study the effect of cooling passages on local buckling strength, acoustic tests, and coolant flow tests to measure pressure losses. The data obtained from these element tests were used to establish the basic structural sizes for the primary structure of the end item test specimen. Such details as skin thicknesses, stringer geometry and spacing, frame geometry and spacing, and cooling system circuitry were established, and then a more extensive mechanical test program was set up, on large panels of both fuselage and wing construction, to determine the effect of the cooling system on the load carrying characteristics of the structure, and the effect of structural loads, buckles and deformations on cooling system performance. The program consisted of a number of compression and shear panels each of which was 3' square, and both inflated tubed sheet samples and brazed tube-on-sheet samples were included. Control specimens involving the same structural stiffening but with plain skins were also included.

Figure 4 shows the results of these tests in terms of failure loading. From these results it will be apparent that the introduction of the tubed sheet material did not reduce the load carrying capacity by more than 5%. The brazed tube-on-sheet panels gave substantially reduced strength values principally due to brittleness resulting from the brazing operation. A typical shear panel under load is shown in Figure 5. Coolants were circulated through these specimens during the tests and pressure drops were determined. After several loadings to limit load in which the skins containing the integral passages were buckled, it was found that permanent reductions in coolant flow rates did not exceed 5%.

A larger specimen, as shown in Figure 6, was then constructed, principally to check coolant flow distributions and the methods to be used for designing the cooling system circuits. The specimen contained curved sheets typical of the proposed fuselage so that it served also to develop the manufacturing techniques for stretch-forming the inflated tubed sheet. This was accomplished on a Hufford stretch press and it was done after the cooling passage had been inflated. Hydraulic pressure was contained within the passages to prevent collapse during forming of the sheet.

The test specimen shown in Figure 6 was 6' long and 4' wide and contained primary structure skin with both inflated tubed-sheet and the brazed tube-on-sheet forms of cooling system. Typical structural stiffening was also added on the

underside of the specimen. The specimen was heated with radiant lamps at low intensity corresponding to the heat load that would normally penetrate through the insulation. It was also coupled to a pump, heat exchanger, and a propyleneglycol reservoir, and measurements were made of coolant flow rates, pressure drops and temperatures. From these tests it was found that aluminum skin temperatures were below 250°F and coolant flow rates and temperature increases were essentially as predicted. Accurate prediction of the coolant distribution in the various passages was not achieved, however, due to variations in the passage cross section and variations between laminar and turbulent flow in various parts of the circuit due to differences in passage shape, flow rate, viscosity, etc. Fortunately, with this type of cooling system, large safety factors can be applied to analytically determined flow rates at no cost in weight of coolant material and at negligible cost in pumping power. The coolant pumps for a complete aircraft, for instance, weigh only about 2 lbs. and require less than 1 HP so that overdesign in these areas is not critical.

The second phase of the program involved the development of insulating media to be used between the outer wall and the primary structure. The work proceeded in two parts; the development of insulating powder and the development of metal packages to contain the powder, both for 2200°F operation.

The powder development, which was carried out for Bell by Arthur D. Little, Inc., was based on the use of very fine powders to exploit the low pressures at altitude to achieve what is effectively a vacuum insulation. The work began with theoretical studies of the conduction of heat through fine powders and included such items as selection of material constituents and examination of material stability at various temperatures, pressures and densities. The principal material was aluminum oxide powder and other materials were added to reduce radiant heat transmission by absorption and scattering. Studies were made of powder settling under mechanical vibration to determine the minimum acceptable density, and conductivity measurements were made on the final mixture over a range of temperatures and pressures. Figure 7 shows the results of this work for a powder density of 12 lb/ft^3. A typical value of lower surface pressure experienced during lifting re-entry is 0.7 mm of mercury and an average surface temperature is about 1800°F. For these conditions the product of conductivity and density for this material is about one-third of the value attainable with typical commercial insulations for the same temperature range.

In order to contain the insulation powders, metal foil packages 24" sq. and about 3/4" thick were developed. Oxidation tests were conducted on potential foil materials using different alloys and thicknesses, and in conjunction with the insulating powder to check for chemical reactions. As a result of these tests .003" thick annealed Inconel material was selected.

Figure 8 shows a typical package in its final form. Holes are provided so that the clips which support the external surface panels can pass through the insulation. Special filters, which can be seen as elongated shapes in the figure, were developed and installed so that the package could be vented of pressure during vehicle boost to altitude. This was accomplished, after a number of experiments, without loss of the very fine powders and without the entry of moisture. Since the air diffuses only very slowly through the fine powder, it was necessary to use a relatively large number of filters and to arrange each one to penetrate the full thickness of insulating material. Methods were developed for welding the foil gauge material using special wheel type electrodes, and methods for filling the insulation package with the powder were also devised. The filling process was based on fluidizing the powder with an airjet, in conjunction with vibration of the package to cause powder settling. The required density of powder was determined by weighing.

Initial package concepts were based on the use of an unstiffened foil bag, but it was found that venting to achieve zero pressure differential between the inside and the outside of the package could not be accomplished. Accordingly, very light stiffening consisting of beads and hat-section stiffeners was incorporated into the side, or cool surface, of the package. This is the top surface in Figure 8. The hot side of the package is not stiffened but instead is maintained in contact with the inner surface of the external panels. This is done by utilizing springs to keep the packages pressed against the surface panels. The springs serve also as the package support and they accommodate fabrication tolerances and thermal distortions, and provide a long conduction path to minimize the leakage of heat into the aluminum structure.

The final item of development was concerned with the outer wall panels which form the exterior vehicle surface. A typical panel is shown in Figure 9. It is 12" sq. x 1/4" thick, of brazed honeycomb construction, with .0045" thick faces and a stepped edge so that adjacent panels can overlap. Each panel is supported from the aluminum primary structure by four sheetmetal clips spaced on 6" centers and which accommodate thermal expansions by flexing while still positively resisting

any applied loads. Adjacent panels are positioned with a .2" gap to accommodate thermal expansion due to the 2000°F surface temperature.

Brazed honeycomb construction was selected as the lightest form of panel construction on the basis of a number of design studies involving welded and riveted constructions, corrugation stiffening, etc. The brazed construction is believed lightest for a panel which must have bending strength in all directions. If the panel is supported continuously along two edges, so that bending strength is necessary only in one direction, then corrugation stiffening may be satisfactory but the continuous edge support permits an unacceptable amount of heat leakage through the insulation.

With emphasis on oxidation resistance rather than strength the materials selected for panel construction were Haynes 25, a cobalt base alloy, and Inconel 702, a nickel base alloy. Material testing was conducted to develop strength, oxidation, and embrittlement data at various temperatures and after various exposure cycles. Some typical results are shown in the following table which gives ultimate strength and elongation values for the two materials after a thermal exposure representative of total vehicle life. Oxidation, of these materials, is intergranular rather than surface scaling and the degree of oxidation is therefore expressed as a reduction in useful thickness of the materials, measured at the point of maximum oxidation penetration.

PROPERTIES OF INCONEL 702 & HAYNES 25
AFTER 5 HOURS AT 2000°F

	Inconel 702	Haynes 25
70°F		
F_{TU}(psi)	90,000	123,000
e(% in 2")	24.5	21.0
2000°F		
F_{TU}(psi)	6,100	12,000
e(% in 2")	13.0	3.5
% Intergranular Oxidation	2.0	42.0

The table shows the strength superiority of the Haynes 25 and the superior oxidation resistance and ductility after exposure of the Inconel 702.

Bending tests were conducted on elements of brazed sandwich material in order to select brazing alloys and to verify the brazing procedure, and on the basis of this work GE-J-8100 was selected for brazing of all panels. The bend specimens indicated that in a brazed sandwich element very little oxidation occurs at the inside faces of the material due to the inadequate supply of oxygen. As a result the inferior oxidation resistance of the Haynes 25 alloy, indicated in the above table, becomes less significant, and the Haynes 25 elements showed over twice the load carrying capability of the Inconel 702 elements.

Typical flat and curved outer wall panels were also fabricated and thermally tested as a final check of materials and fabrication processes. A special multistation brazing facility was constructed for this purpose. Four stations are provided for simultaneous assembly, purping, brazing and cooling so that four panels can be in operation simultaneously. A travelling furnace moves to each station when the panel is ready for brazing and the total panel fabrication cycle takes 30 minutes.

With the development of individual elements complete, the 6'x4' test specimen which was described earlier was modified by the addition of a complete set of insulation packages and outer wall panels and the complete assembly is shown in Figure 10. The second phase of testing with this assembly was conducted to check the overall conductance of the entire protection system with various constant temperatures applied to the external surface. The test program included surface temperatures of 1600, 1800 and 2000°F and heating was supplied by standard GE filament type quartz lamps mounted in water-cooled aluminum reflectors. The heat flux through the protection system into the aluminum was determined by circulating coolant through the cooling system in the aluminum skin, and measuring the coolant flow rates and temperature rise. The results expressed in terms of heat flux at various outer wall temperatures are shown by the appropriate curve in Figure 14 where a comparison is made with analytical predictions using the measured thermal conductivity for the insulation powder. The test results and the corresponding analytical curve are based on sea level thermal conductivity values.

Initially, the target temperature for the entire program was 2000°F and initial testing of the 6'x4' specimen was conducted to these temperatures. Excessive oxidation and warpage of many of the outer wall panels resulted from these tests. Extensive detailed investigations were conducted to determine the cause of these troubles. It was found that the oxidation was caused partly by overheating, due to faulty control of the heating elements, and partly by contamination of the panel material by residual brazing flux. The warpage was traced to a combination of excessive temperatures, nonuniform temperature distributions across the panel surface and braze softening and remelt temperatures which were lower than had been expected. These problems were

eventually resolved by instituting panel cleaning procedures to remove the residual brazing flux, and by reducing maximum test temperatures to 2000°F to avoid the remelt problem and to provide a tolerance for heater operation.

As was mentioned previously, the high temperature surface of the insulation package is unstiffened and after the tests on the 6'x4' specimen this surface of each package was found to be wrinkled. This was expected since provision was not made in the design for thermal expansion, apart from wrinkling of the metal. It was found, however, that these wrinkles creased sufficiently in limited areas to cause pin holes in the package material with corresponding loss of insulating powder. Modifications were introduced, therefore, to incorporate beads into the hot surface and along the package edges in order to accommodate thermal expansion. Considerable improvement was achieved but the problem was not completely resolved.

Using the data accumulated during the development programs described above, the final test component was designed and fabricated. This component is a full scale section of a typical glide re-entry vehicle, containing a portion of wing and fuselage. It is 15' in span, 8' in chord and approximately 5' high. It consists of an aluminum airframe, with skin stringer construction for the wing and frame stiffened skin and longeron construction for the fuselage. Inflated tubed sheet in 2024 alloy is used as the skin material. Figure 11 shows the primary structure under construction. One upper side of this specimen was covered with packaged insulation and external surface panels, fabricated from both the cobalt base and nickel base alloys. Eighty-six panels were used to cover the test section. The cooling system was connected to a pump, heat exchanger and reservoir assembly, and the specimen was instrumented with thermocouples, to measure surface panel temperatures and temperatures in the aluminum structure, and also with flow meters, pressure pick-ups and thermocouples to measure the performance of the cooling system. Figure 12 is a photograph of the complete specimen as it was shipped to Wright Field for testing.

The test program involved loading without heat, representative of the critical conditions experienced during the early stages of boost, with loads applied to fixtures attached to each wing tip and to each end of the fuselage. Load tests were followed by heating tests at various maximum temperatures to 2000°F, during which temperatures were held constant with time. These constant temperature tests served to check the oxidation and thermal expansion characteristics of the protection system, and the insulating capability of the system was also determined for comparison with predictions. This was done by measuring the coolant flow rates and the coolant temperature rise and making appropriate corrections for heat leakage around the edges of the specimen.

The constant temperature tests were followed by transient heating and loading representative of the conditions experienced during a complete flight. The heat and load cycles which were applied are shown in Figure 13 where it will be seen that the effects of pilot induced maneuvers have been included. Five such re-entry cycles were applied to the test specimen.

Results of the test were generally satisfactory although slight scaling type oxidation of some of the surface panels was experienced and very local areas of braze separation were noted in some of the surface panels. Local panel damage was also experienced at two places due to electrical shorts in the heating system and arcing to the test specimen surface. Maximum temperatures experienced in the aluminum structure were 234°F and no significant hot spots were found at the points where the surface panels are attached to the aluminum structure.

The performance of the heat protection system is summarized in Figure 14 which shows a comparison between the predicted heat flux into the aluminum structure at various surface temperatures, with measured values. It will be noted that the predictions agree well with measured values from the fuselage of the final test specimen and also with measurements made on the 6'x4' test specimen. Data taken from the wing of the final test specimen gives higher values of heat flux than the analytical predictions, and although many possible reasons for this discrepancy are being investigated no satisfactory answer has been found. Since all testing was done under sea level conditions and pressure has a significant effect on the insulation performance, the figure also shows the analytically predicted heat flux to the aluminum structure for a pressure of .5 mm of mercury, typical of that experienced on the lower wing surface during glide re-entry. This analytical curve is based on measured conductivity values.

The final measure of performance of the thermal protection system, which is being developed in the program under discussion, is the weight required for particular applications. Figure 15 shows weight values of the complete protection system for various constant surface temperatures and times of flight. The weight values include all elements of the protection system and assume a square wave heat pulse. For applications where the external heating is not constant with time, it is satisfactory for preliminary weight

estimates to use the maximum surface temperature that is expected and to use an equivalent time of flight which would give the same area under the temperature-time diagram.

Figure 15 is divided into two areas. Below the broken line the lightest weight is achieved if insulation is used alone, without the cooling system, while above the line the minimum total weight is achieved by using the optimum proportions of insulation and cooling. From this figure it will be apparent that typical protection system weights for lifting re-entry vehicles are about 2.5 lb/ft^2, which must be added to the weight of the load carrying aluminum primary structure.

Measured weights of the outer panels are .97 lb/ft^2 and the insulation package complete with powder weighed 1.04 lb/ft^2. Measured weights of the cooling system have no significance since many of the units were laboratory equipment and were not designed for aircraft applications. Design studies of the cooling system, however, show a weight of .46 lb/ft^2 of cool surface, a value which includes the heat exchanger, tanks, pumps, plumbing and the residual coolant in the system.

The program also involved initial development work of refractory metal surface panels as a step in the development of the concept for a 2500°F temperature capability. Other programs supporting such a development are presently under Air Force sponsorship while preliminary development work to increase the capability to 4000°F, using nonmetallic materials, is being carried out under Bell sponsorship.

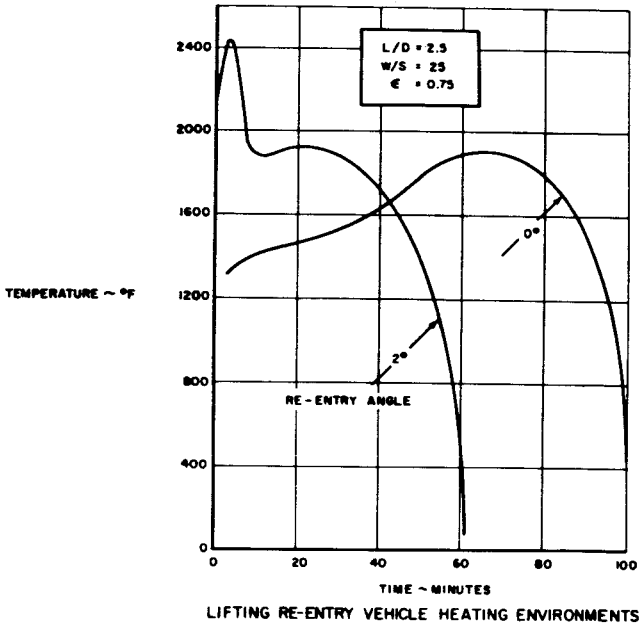

LIFTING RE-ENTRY VEHICLE HEATING ENVIRONMENTS

Figure 1

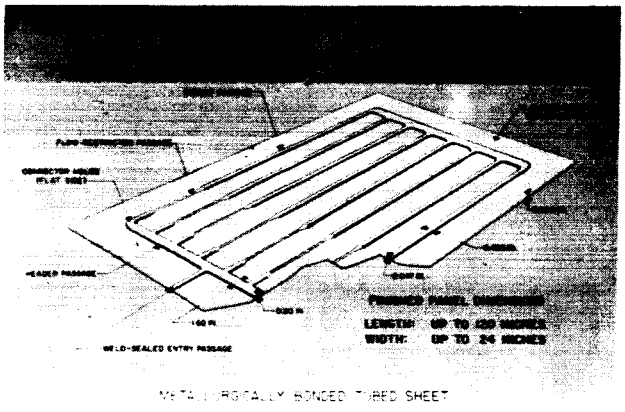

METALLURGICALLY BONDED TUBED SHEET

Figure 3

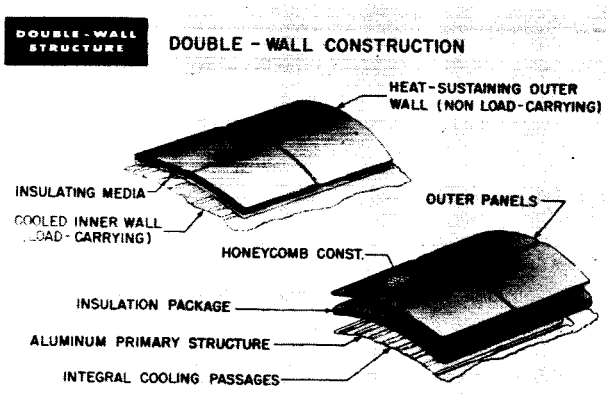

Figure 2

COMPRESSION AND SHEAR TEST RESULTS

DOUBLE-WALL STRUCTURE

Design Type and Design Strength	Type of Skin	Coolant Passage Orientation	Average Failing Stresses (lb/in^2)	Panel Loading at Failure (lb/in.)	Failure Comparisons With Plain Specimens
		3 X 3 - in. Specimens			
Shear Design Limit Loading - 230 lb/in. Design Ultimate Loading - 344 lb/in.	Reynolds 2024 Tubed Sheet	Plain Skin	23400	938	
		Parallel	23630	945	+0.5
		Normal	23000	920	-2.0
		Normal	22350	902	-4.6
	Brazed 6951 Tube-On-Sheet	Plain Skin	13750	631	
		Parallel	15640	501	-20.7
		Normal	17000	545	-13.7
		Normal	16430	527	-16.5
Wing Shear Design Limit Loading - 290 lb/in. Design Ultimate Loading - 420 lb/in.	Reynolds 2024 Tubed-Sheet	Plain Skin	24900	995	
		Normal	24400	976	-2.0
		Normal	24500	981	-1.7
	Brazed 6951 Tube-On-Sheet	Plain Skin	19040	610	
		Normal	13750	505	-17.3
		Normal	15260	489	-19.8
Wing Compression Design Limit Loading - 1054 lb/in Design Ultimate Loading - 1585 lb/in	Reynolds 2024 Tubed Sheet	Plain Skin	26000	2010	
		Parallel	24650	1910	-5.0
		Normal	24550	1900	-5.5
		Normal	25200	1931	-2.7
	Brazed 6951 Tube-On-Sheet	Plain Skin	26400	1840	
		Parallel	24100	1827	-0.7
		Normal	25000	1740	-5.5
		Normal	25300	1766	-4.2

Figure 4

BODY SHEAR SPECIMEN

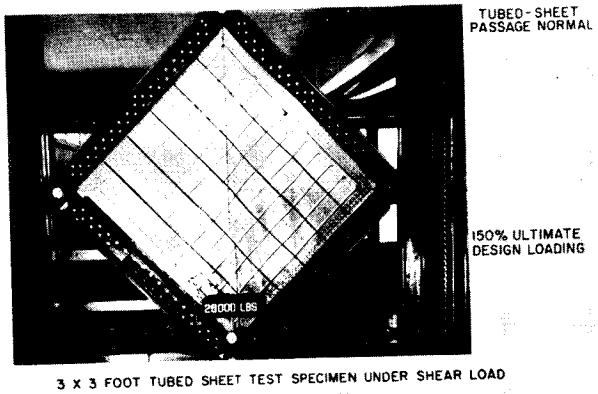

3 X 3 FOOT TUBED SHEET TEST SPECIMEN UNDER SHEAR LOAD

Figure 5

6 X 4 - FOOT COOLANT FLOW SPECIMEN

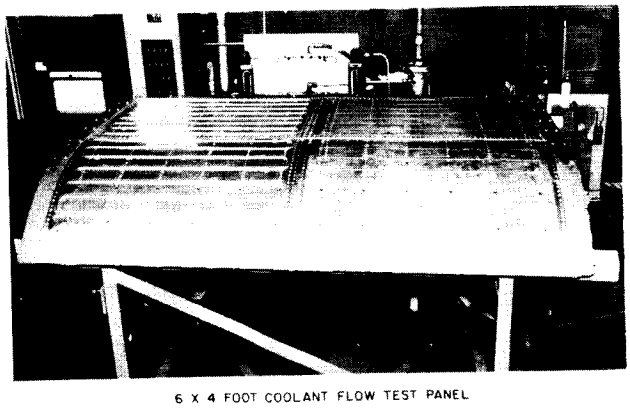

6 X 4 FOOT COOLANT FLOW TEST PANEL

Figure 6

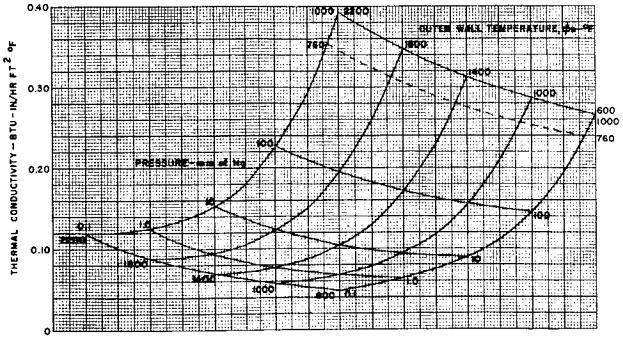

Figure 7. Effect of Temperature and Pressure on Thermal Conductivity of ADL-17 Powder (Density of Powder -- 12lb/cu ft)

INSULATION PACKAGE

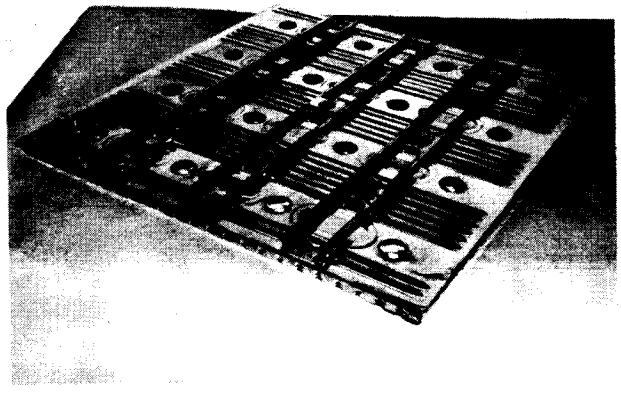

INSULATION PACKAGE CONTAINING ADL-17 POWDER

Figure 8

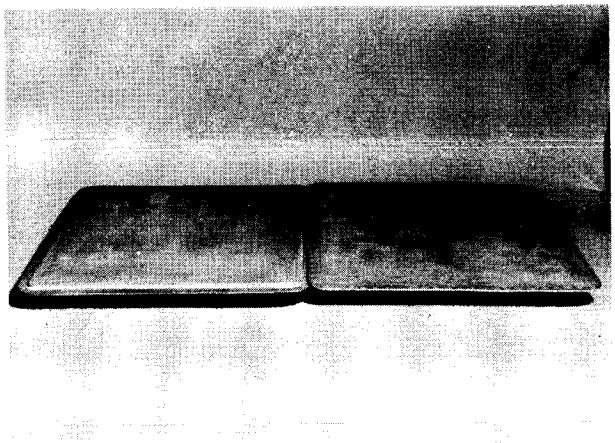

Figure 9. Flat Outer Wall Panels

This page is reproduced again at the back of this report by a different reproduction method so as to furnish the best possible detail to the user.

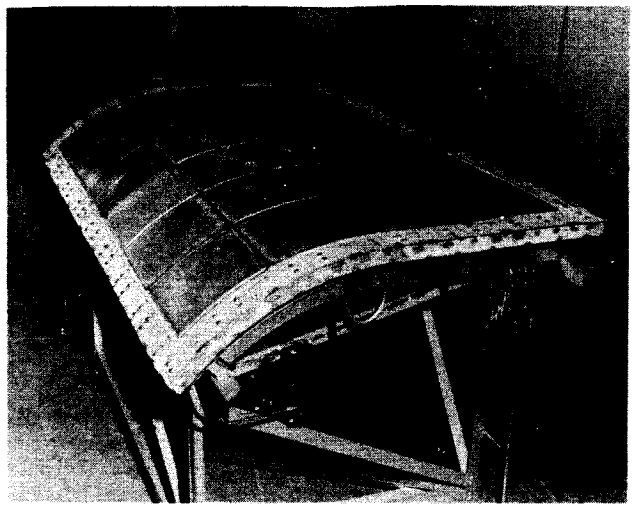

Figure 10. 6'X4' Protection System Test Specimen

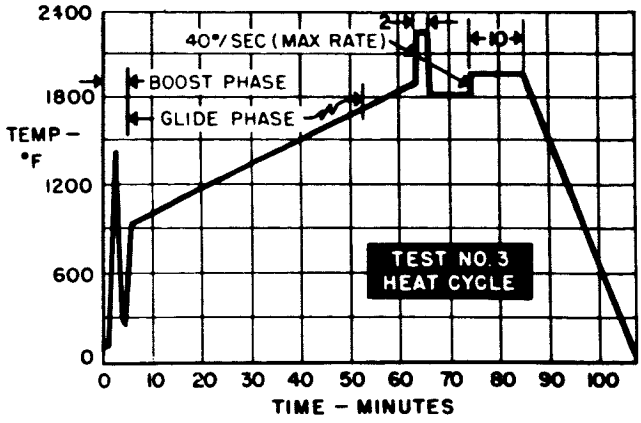

Figure 13. Test Program Heat Cycle

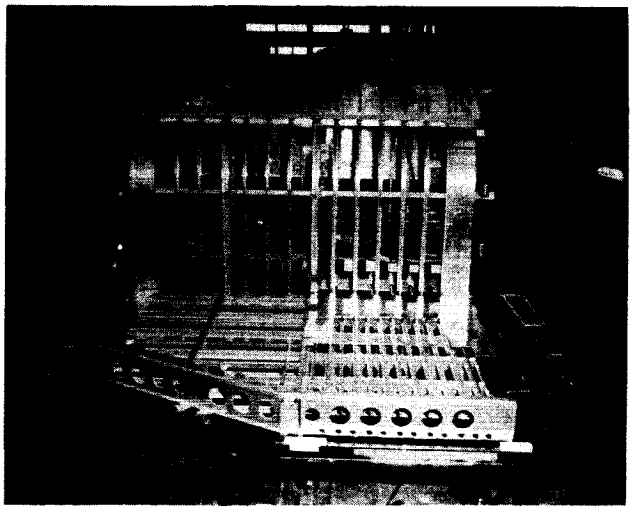

Figure 11. Full Scale Test Specimen Under Construction

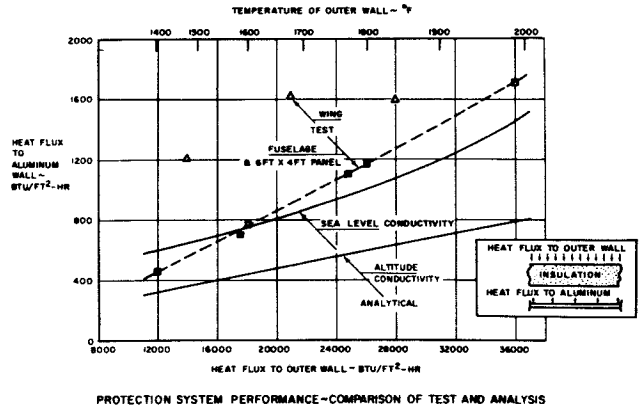

Figure 14

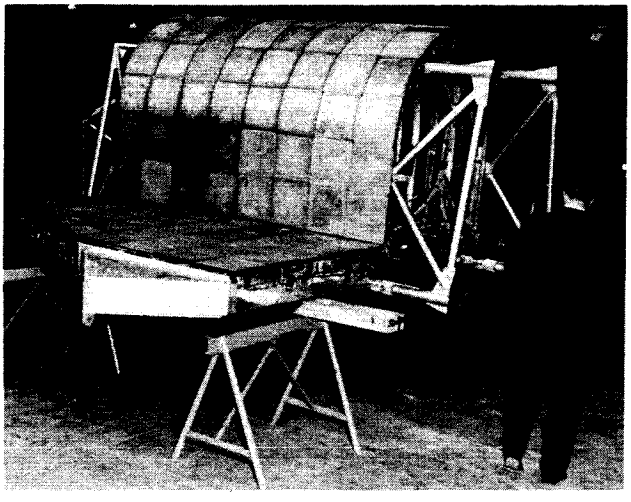

Figure 12. Full Scale Test Specimen Complete

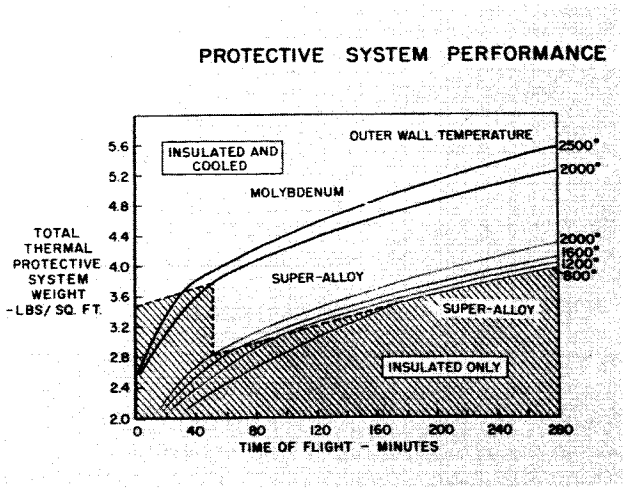

Figure 15

This page is reproduced again at the back of this report by a different reproduction method so as to furnish the best possible detail to the user.

RE-ENTRY MATERIALS

D. L. Kummer
Ceramic Group Engineer
McDonnell Aircraft Corporation

H. J. Siegel
Metallurgical Group Engineer
McDonnell Aircraft Corporation

Introduction

The major requirement for a re-entry material is that it protect the vehicle from the aerodynamic heating associated with re-entry. A relatively short time ago, the term re-entry brought to mind a ballistic type trajectory and its characteristic heat pulse. Today, however, a variety of thermal re-entry conditions are common due to the various types of vehicles currently of interest. Extremes of re-entry heating-time conditions vary from the relatively low heat flux-long time pulse associated with glide and shallow orbital re-entries through high flux-short time ballistic re-entry to the very high heat flux-moderate time pulse associated with super orbital re-entry. Materials for providing thermal protection, therefore, vary considerably depending upon the type of re-entry heat-time pulse. From a functional standpoint, thermal protection materials may be divided into two types; absorptive and radiative. The absorptive material dissipates heat by storage (heat sink) or mass transfer and chemical change (ablation, transpiration or sublimation).

Ablation materials have been fully investigated for ballistic re-entry conditions; however, much less effort has been expended on ablation materials for the low flux-long time heating condition associated with the glide and shallow orbital re-entry vehicles. The long time pulse increases the importance of the materials' resistance to heat transfer and at the low flux the relative ablation or heat dissipation efficiency of many materials is greatly affected. Considerable material development and testing is currently being conducted for this low flux-long time heating condition. Many of the materials, composites and techniques showing promise are considerably different from those utilized for ballistic re-entry; however, details cannot be discussed at this time.

With the radiative method of thermal protection, the re-entry heat is dissipated by radiation from the material's surface to the cooler surroundings such as the surface of the earth, clouds, etc. This is, in general, a very effective method of heat protection with high reliability and weight efficiency due to its simplicity and the fact that no mass is lost as with ablation. Also the materials can, in many cases, be reused for subsequent flights. Utilization of the radiative method is limited to the lower heat fluxes due to the maximum temperature resistance of available materials. At equilibrium, the material attains a temperature sufficient to radiate all the incident re-entry heat, less the small amount of heat which flows into the vehicle. Approximately 4200°F is currently the highest temperature at which any moderately proven flight material can operate

(Continued)

for relatively long times in an oxidizing atmosphere. Assuming a material emittance of 0.8, a flux of approximately 130 $BTU/Ft^2/Sec.$ will cause a well insulated material to attain this limit of 4200°F. Therefore, above this flux an absorptive or combination absorptive-radiative system is required. Many re-entry vehicles or portions of re-entry vehicles, particularly of the glide and shallow re-entry type, encounter fluxes below this limit; therefore, increased emphasis is being placed on the radiative method of thermal protection.

Materials for Radiative Protection Systems

The higher the temperature at which a radiator can operate the higher the flux at which it can be used. The basis for design of efficient, radiation cooled components must, therefore, be materials capable of operating at high temperatures. The cobalt and nickel base super alloys such as HS-25, Inconel X, Rene' 41, etc., provide the highest temperature resistant materials of the conventional alloy systems. The melting point of alloys of this type ranges from approximately 2350°F to 2550°F. The necessity for extending operating temperatures past this range has led to the commercial development, with considerable support from government agencies, of more refractory materials systems.

Consideration of materials systems which might provide the basis for the more refractory materials required was based initially upon melting point and availability. Some of the material systems fulfilling these criteria, their melting points and an estimate of their approximate maximum useful temperature are indicated in Figure 1. Development and utilization of these refractory materials for structural or semi-structural purposes is beset by many problems. These problems are being studied at the present time and there are indications that they will be resolved, at least in part. The present state of development of these materials, the problems involved in their application in structures and areas in which additional development is required will be described.

Molybdenum

Due to its abundance, particularly in this country, and its high melting temperature (4730°F), molybdenum was the first of the more refractory metals to which attention was directed. Structurally, alloys of molybdenum have many advantages; a high elastic modulus (approximately 45×10^6 psi at room temperature); reasonably high strength both at room and elevated temperature (Figure 2); moderate density, $0.369\ LB/IN^3$, at least compared to some of the other refractory materials; good thermal conductivity; and a low coefficient of thermal expansion. As the development of molybdenum base alloys proceeded, problems in applying these alloys to engineering structures were presented. Today, some ten years after many of the problems were defined they have not yet been resolved.

One major problem is that the ductile-to-brittle transition temperature of molybdenum and its alloys is near or above room temperature. A plot of impact strength, reduction of area and bend angle versus temperature is presented in Figure 3. This transition is characterized by a pronounced loss in ductility, a striking decrease in fracture strength and a change in mode of failure from a ductile shear rupture to a brittle cleavage or grain boundary fracture. This behavior imposes problems in handling and fabrication. To avoid brittle fracture during forming, all but the most simple operations must be performed at elevated temperature, significantly adding to the difficulty and cost of producing structural assemblies.

A second major limitation in the application of molybdenum alloys which is related to the mechanical behavior previously described is the brittle behavior of fusion welds. Inability to produce structurally acceptable welded joints severely limits design and almost invariably results in structures which are less efficient and more difficult to fabricate.

An additional problem area arises from the chemical activity of molybdenum. At temperatures above about 1200°F, molybdenum begins to oxidize at a significant rate. At approximately 1450°F the oxide melts and provides no protection to the metal. At temperatures above this, the oxide sublimes and oxidation proceeds at a catastrophic rate. In order to utilize this material at elevated temperature, oxidation protection must be provided.

A number of reasonably good protective coatings have been developed, all basically silicides, similar in nature and applied by somewhat similar processes. Unfortunately, the application of these protective coatings is not simple and requires careful preparation of the parts to be protected. Coating growth occurs normal to the surface and any abrupt changes in section or sharp corners or edges lead to development of cleavage planes in the coating in these areas and lack of protection as illustrated in Figure 4. To prevent this, all corners and edges must be rounded and in addition the parts and assemblies must be adequately cleaned and kept free of contamination prior to coating application.

Some of the protective coatings developed for molybdenum utilize the pack cementation process which involves packing around the part or assembly a powder containing the constituents required to form the silicide coating. The retort containing the powder and parts is then heated to the temperature required to produce the desired reaction. The throwing power of this coating method is limited. Complex assemblies such as corrugation stiffened panels containing internal openings whose ratio of length to cross-section is high cannot be adequately coated. Adequate protection of formed sheet assemblies of this type is best provided by coating all of the detail parts and fasteners, assembling the structure and then recoating to repair any areas of the brittle coating which may have been damaged during assembly.

At the present time, reliable protection by the silicide type coatings, which are the best thus far developed, is limited to temperatures of about 3100°F. This temperature is below that at which molybdenum alloys could presently be utilized.

Molybdenum alloy structural assemblies can be fabricated and used successfully if the limitations of the material are considered when the design is developed. A small molybdenum alloy assembly which was successfully tested at 2500°F under load is shown in Figure 5.

Columbium

The previously described problems which limit the use of molybdenum base alloys have caused materials engineers to investigate other of the refractory metals. Columbium, which has a slightly lower melting point than molybdenum (4475°F compared to 4730°F), is less dense (0.310 compared to 0.369 LB/IN^3), exhibits ductile behavior at sub-zero temperatures (Figure 6) and is oxidized more slowly, has for about the past five years received the attention of metallurgists.

A large number of columbium base alloys have been developed. These alloys generally can be divided into two classes, the moderate strength alloys which are being produced commercially and for which, in some cases, there are guaranteed properties and those alloys which appear to offer much higher strength but which cannot be purchased at present. These two classes of alloys might better be described as first and second generation; the second generation has not yet matured.

The available columbium base alloys have only moderate strength at room and elevated temperature as shown in Figure 7. However, these alloys are weldable, are formable at room temperature and in general are not difficult to produce.

The newer, higher strength alloys provide some indication of the growth potential of columbium. These alloys have two to two and one-half times the strength of the first generation alloys at elevated temperature (Figure 8). Unfortunately, this increased strength is not always achieved without loss of other properties. For example, F48, one of the earliest high strength alloys developed strength by sacrificing fusion weldability and room temperature formability. Also, preliminary tests indicate that fusion welds in the C-129 alloy are not ductile. A great deal of additional evaluation will be required before the high strength alloys can be applied to structures.

The mechanical behavior of the moderate strength columbium base alloys is superior to the molybdenum alloys in that the columbium alloys are weldable and easily formable, however, the strength of these alloys certainly leaves something to be desired. The high strength columbium alloys approach the structural efficiency and also reflect some of the poor fabrication characteristics of the molybdenum alloys.

The chemical activity of columbium, so far as oxidation is concerned, is lower than molybdenum, but columbium alloys are not sufficiently inert at elevated temperature to preclude the requirement for oxidation protective coating. The oxidation of columbium results in two different types of reactions. The first involves the formation of an oxide layer on the surface of the metal, gross oxidation. The second involves diffusion of oxygen into the base metal, internal oxidation, and results in significant hardening of the affected area and embrittlement. Any oxidation protective coating for columbium must provide protection against both types of oxidation.

Two basic types of high temperature resistant protective coatings have been developed for columbium base alloys to date; aluminide and silicide coatings. The aluminide coating is produced by applying an aluminum alloy slurry, somewhat like an aluminum paint, to the surface of the columbium, air drying and then diffusing at about 1900°F to develop the protective intermetallic coating. The silicide coatings are applied by the pack cementation process similar to that used for molybdenum alloys.

The aluminide coating at present is limited to maximum operating temperatures of about 2700°F, whereas the silicide coatings can be used at temperatures up to approximately 3100°F. The aluminide coating, as a result of the method of application can be used for protection of complex assemblies such as those shown in Figures 9, 10, 11 and 12. The silicide coatings have the advantage of producing a very uniform coating thickness, but current processes limit the complexity of components that can be reliably protected to relatively simple configurations. In applications requiring very close dimensional control such as threaded fasteners, the silicide coatings perform very well. Examples of the uniformity of this type of coating are shown in Figure 13.

As in the case of molybdenum, adequate oxidation protection of complex columbium assemblies starts with the design. All edges and corners must be rounded and the completed assembly must be clean at the time it is presented for protective coating. Due to their complexity, many components cannot be adequately recleaned after assembly, therefore, the detail parts are cleaned and must remain clean during assembly. This is by far the most difficult aspect of the problem.

Tantalum and Tungsten

The two remaining refractory metals, tantalum and tungsten, are of considerable interest because of their potentially higher useful operating temperatures, in the order of 4500°F and 5200°F respectively. Neither of these metals has received the attention previously afforded to molybdenum and columbium. Both materials have a relatively high density, 0.600 LB/IN^3 for tantalum and 0.697 LB/IN^3 for tungsten. This high density limits the structural efficiency of alloys developed from these bases.

The mechanical and chemical behavior of tungsten is similar to that of molybdenum. It has a very high ductile-to-brittle transition temperature as shown in Figure 14, welds in tungsten are brittle, it oxidizes rapidly at elevated temperature and has a high elastic modulus as shown in Figure 15. High strength, fabricable tungsten base alloys have not yet been developed nor have effective high temperature oxidation protective coatings been developed.

The mechanical and chemical behavior of tantalum is similar to columbium. It has a very low ductile-to-brittle transition temperature, lower than that of columbium, as shown in Figure 16; it is weldable; has a moderately high elastic modulus as was shown in Figure 15, and like columbium it suffers from gross and internal oxidation and must be protectively coated.

Recently some high strength tantalum base alloys with reduced density have been developed which, on a strength/weight basis, compare quite favorably with the higher strength columbium alloys. Preliminary properties for one of these alloys (Ta-30Cb-7.5V) and the older Ta-10W alloy are compared with a high strength columbium alloy in Figure 17. A present restriction in the use of tantalum alloys is the lack of protective coatings. Based upon its close chemical similarity to columbium, it is anticipated that the coatings developed for columbium will also be applicable to tantalum, but very little testing has been done thus far.

An aluminum-tin coating has been developed for application to tantalum base alloys, but only limited testing of this coating has been completed. This coating appears to be self-healing, however, this is accomplished by the presence of a liquid phase at high temperature which somewhat limits its use.

In general, the early stage of development of both tungsten and tantalum base alloys limits most present applications for radiation cooled structures.

Graphite

Graphite is a common material and has numerous industrial uses; however, it is also one of the most refractory of materials, being limited by its sublimation temperature of approximately 6600°F. Although a variety of graphites are available, high density, fine grained, conventionally formed; hot pressed; and pyrolytic are the three types of graphite of primary interest for aerospace use. Conventional graphite is currently being evaluated at MAC for nose tip and leading edge applications for hypersonic glide re-entry vehicles. Conventional graphite was selected over the pyrolytic and hot pressed types primarily due to cost, availability, and in the case of pyrolytic graphite, superior thermal shock resistance.

General characteristics of graphite are:

(a) Very high temperature resistance.

(b) Easily machined.

(c) High strength to weight ratio at high temperatures (strength increases with increasing temperature).

(d) Good thermal shock resistance.

(e) Brittle.

(f) Low strength.

(g) Must be used in thick sections.

(h) Must be protected from oxidation (oxidation at high temperatures, however, is not catastrophic).

(i) Parts must be machined from molded blocks or cylinders except in the case of pyrolytic where it is deposited on a mandrel.

The inherent brittleness and low strength of graphite can be accounted for in the design of the part, with the attachment provisions requiring particular attention. A graphite leading edge incorporating an effective attachment design is shown in Figure 18. This leaves oxidation protection as a primary problem to be overcome in order to effectively utilize the high temperature resistance of graphite. Silicon carbide, produced by siliconizing graphite, has proven to be an effective oxidation protective coating for graphite up to 3100°F with the oxidation product, silica, being the actual oxidation protective film. Means of increasing the temperature limit of silicon carbide coatings have been investigated at MAC and an overcoating of zirconia has proven to be effective. The zirconia interacts with the silica formed when the silicon carbide is heated in air and forms a mixture which is more refractory than the silica. This composit will resist removal by aerodynamic shearing stresses at temperatures well above the 3100°F softening point of silica. Based upon considerable testing, this composite coating will prevent oxidation of graphite at 4000°F for periods of at least 15 minutes, will satisfactorily withstand very high heating rates, high noise levels, at least two cycles of rapid heating to 4000°F and moderate surface erosion forces. However, in order to reliably withstand the above environment, the zirconia coating must be scored or applied to undercut graphite due to the appreciable differential expansion coefficient between graphite and zirconia. Figure 19 shows a typical nose tip specimen after testing at 3800°F. Although brittleness is one of the major disadvantages of graphite, a thermal shock or mechanical failure of a test part has yet to occur in the many tests conducted to date.

Oxide Ceramics

The oxide ceramics are very desirable for use at high temperatures due to their excellent chemical stability and temperature resistance; however, brittleness and lack of thermal shock

(Continued)

resistance greatly limits their usefulness. Various investigators are working on means of overcoming these two limitations and considerable advances have been made. Some of the approaches showing promise are very low expansion bodies, metal reinforced ceramics, modified foams and bodies made from controlled grain size powders. Continued advances in some of these areas should result in production of bodies satisfactory for use to 5000°F.

A method for utilizing currently available oxide ceramics for hypersonic glide re-entry vehicles nose tips has been investigated at MAC. This method utilizes adjacent, small diameter oxide ceramic rods held in a graphite or molybdenum retainer as shown in Figure 20. In this case, the ceramic rods are utilized at the area of maximum temperature, thus the retainer attains a somewhat lower temperature. By utilizing the oxide ceramic material in the form of individual small elements, the thermal shock problem is greatly alleviated. A coarse grained, relatively porous and partially stabilized zirconium oxide has proven to be the most satisfactory oxide ceramic investigated and is useful to at least 4200°F. Figure 21 shows a 6" diameter test specimen after rapid heating to 4100°F, exposure to 150db white noise at room temperature and reheating to 4100°F. Heating rates were approximately 50°F/Sec. in both cases and the test time was 15 minutes. This specimen contained some 300 zirconia rods 0.250" in diameter and four 1" cube zirconia blocks. The two primary functions of the blocks are to provide a lip over the retainer for added thermal protection and to form a hexagonal recess which is the best pattern for installing the rods. Normally the blocks would extend around the entire retainer periphery. A chemically bonded zirconia cement was used to fill the interstices between the rods in order to provide a smooth surface. The blocks, rods and retainer are mechanically locked together at the base by a complex method.

Summary

Present and future vehicle temperatures exceed those at which the nickel and cobalt base super alloys can be used for radiation cooling. It will be necessary to utilize more refractory materials in these applications. The use of these refractory materials is limited by the reliability and maximum operating temperatures of the available oxidation protective coatings. Development of protective coatings which can be applied to complex assemblies and which provide reliable protection at higher temperatures is the most pressing problem in the field of refractory materials at the present time.

Refractory materials are not generally off-the-shelf items, lead time for delivery is long and close coordination with the producers is required to obtain material with required properties.

Many hardware items normally taken for granted such as nuts, bolts and rivets are not available in these materials as standard products. These items must be designed and custom

(Continued)

made. Lead time for these products can be quite long.

Maintaining tight schedules in development programs utilizing refractory materials is difficult and can be accomplished only by working very closely with the material producers.

COMPARISON OF MELTING POINTS, USE TEMPERATURE LIMITS AND APPROXIMATE COST OF HIGH TEMPERATURE MATERIALS.

MATERIAL	DENSITY (LB/IN³)	MELTING POINT (°F)	PRESENT TEMPERATURE LIMIT (°F) IN AIR	POTENTIAL TEMPERATURE LIMIT (°F)	APPROXIMATE COST/POUND ($)
GRAPHITE	0.081	6600**	4000	5000	2-1000
TUNGSTEN	0.697	6170	3100	5200*	35-70
TANTALUM	0.600	5425	3000	4550*	50-120
ZIRCONIA (STABILIZED)	0.190	4800	4200	4300	3-10
MOLYBDENUM	0.369	4730	2900-3100	3950*	50-125
COLUMBIUM (NIOBIUM)	0.310	4475	2500-2700	3750*	75-150
SUPER ALLOYS	0.297 to 0.330	2350-2550	1800-2000	2000*	3-10

* Based upon 85% of absolute melting point.

**Sublimation temperature.

FIGURE 1. COMPARISON OF DENSITY, MELTING POINT, PRESENT AND POTENTIAL USE TEMPERATURE.

EFFECT OF SHARP AND ROUNDED EDGES UPON THE FORMATION OF PROTECTIVE COATINGS

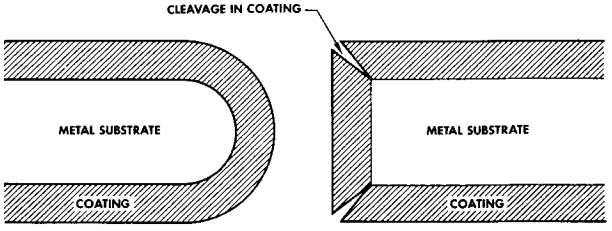

FIGURE 4. EFFECT OF SHARP AND ROUNDED EDGES UPON FORMATION OF PROTECTIVE COATINGS.

ULTIMATE TENSILE STRENGTH AND MODULUS OF MOLYBDENUM ALLOYS AS A FUNCTION OF TEMPERATURE

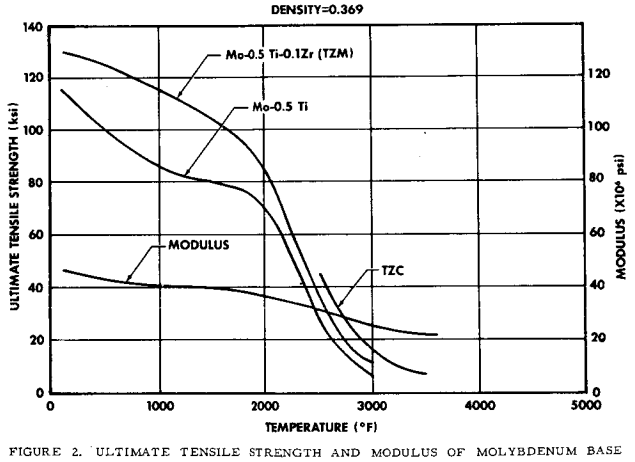

FIGURE 2. ULTIMATE TENSILE STRENGTH AND MODULUS OF MOLYBDENUM BASE ALLOYS AS A FUNCTION OF TEMPERATURE.

DUCTILE TO BRITTLE TRANSITION TEMPERATURE OF WROUGHT MOLYBDENUM

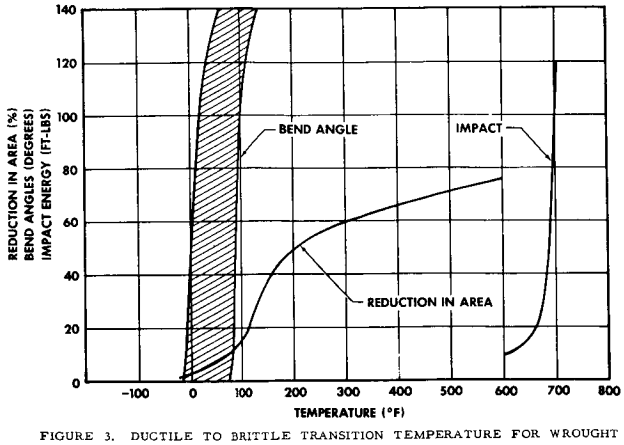

FIGURE 3. DUCTILE TO BRITTLE TRANSITION TEMPERATURE FOR WROUGHT MOLYBDENUM.

MOLYBDENUM TEST COMPONENT

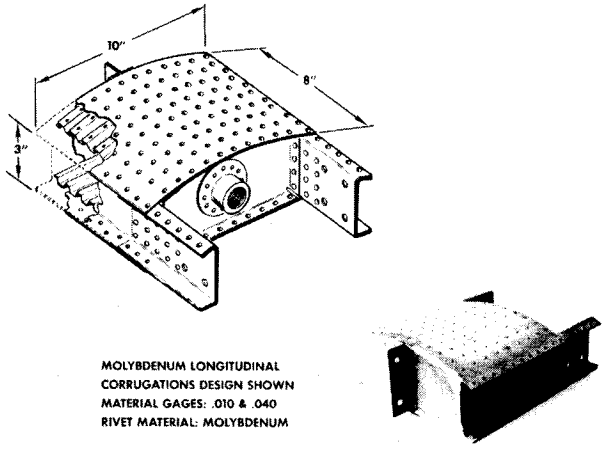

FIGURE 5. PROTECTIVELY COATED MOLYBDENUM ALLOY ASSEMBLY STRUCTURALLY TESTED AT 2500°F.

DUCTILE TO BRITTLE TRANSITION TEMPERATURE OF WROUGHT COLUMBIUM

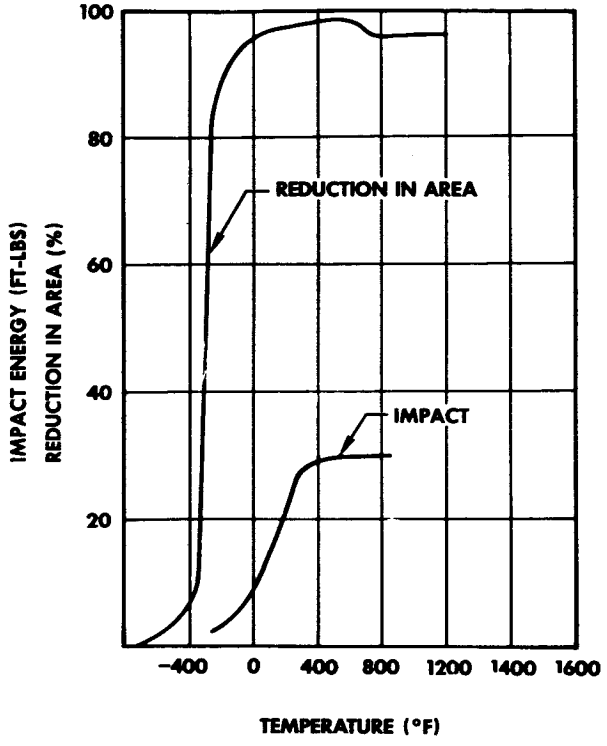

FIGURE 6.

ULTIMATE TENSILE STRENGTH (TYPICAL) OF HIGH STRENGTH COLUMBIUM BASE ALLOYS AS A FUNCTION OF TEMPERATURE

ALLOY IDENTIFICATION	COMPOSITION	DENSITY
SCb-291	Cb-10Ta-10w	0.355
C-129	Cb-10W-10Hf	0.365
Cb-74	Cb-10W-5Zr	0.346
F-48	Cb-15W-5Mo-1Zr	0.343

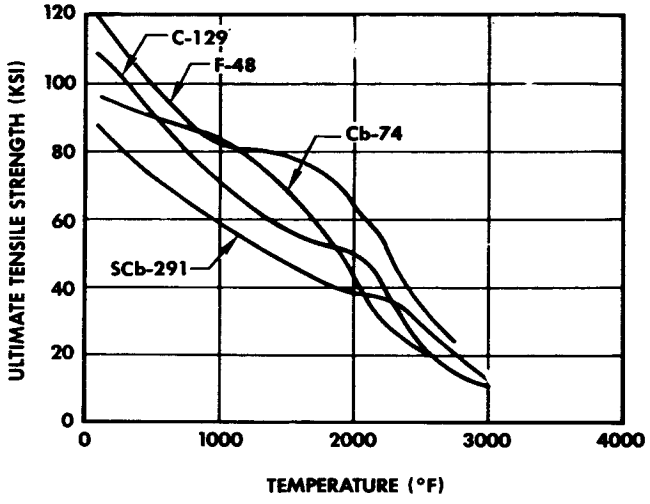

FIGURE 8. ULTIMATE TENSILE STRENGTH OF HIGH STRENGTH COLUMBIUM BASE ALLOYS AS A FUNCTION OF TEMPERATURE.

ULTIMATE TENSILE STRENGTH (GUARANTEED) OF MODERATE STRENGTH COLUMBIUM BASE ALLOYS AS A FUNCTION OF TEMPERATURE

ALLOY IDENTIFICATION	COMPOSITION	DENSITY
FS-82	Cb-33Ta-1Zr	0.370
D-14	Cb-5Zr	0.310
C-103	Cb-10Hf-1 Ti-.5Zr	0.319
B-33	Cb-5V	0.306

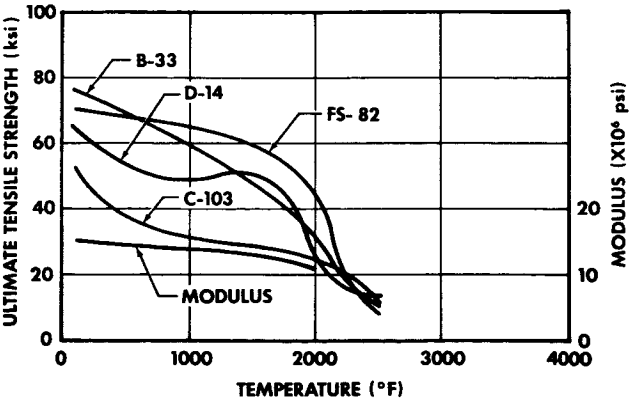

FIGURE 7. ULTIMATE TENSILE STRENGTH (GUARANTEED) AND MODULUS OF MODERATE STRENGTH COLUMBIUM BASE ALLOYS AS A FUNCTION OF TEMPERATURE.

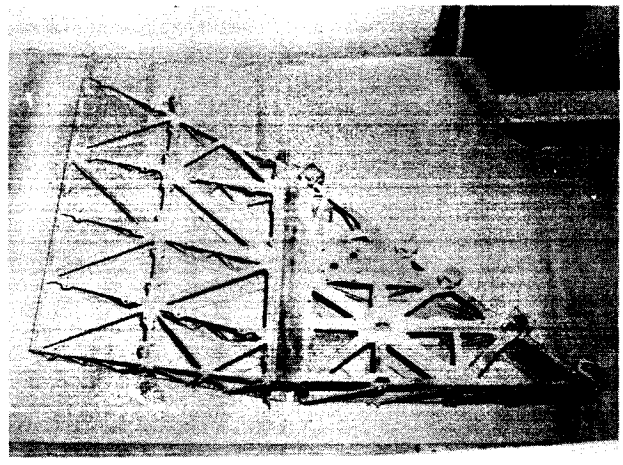

FIGURE 9. PROTECTIVELY COATED F48 COLUMBIUM ALLOY STRUCTURAL COMPONENT.

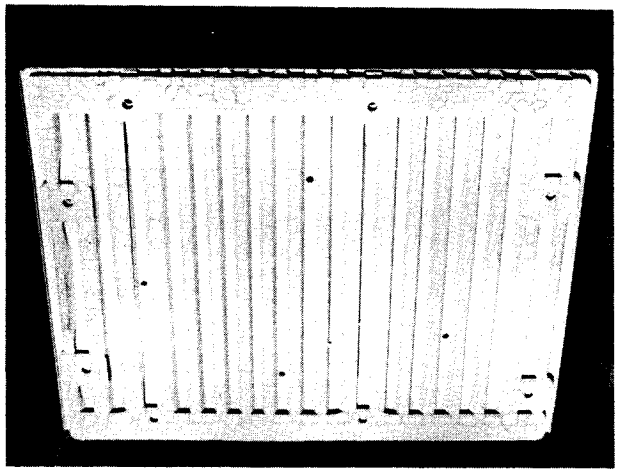

FIGURE 10. PROTECTIVELY COATED F48 COLUMBIUM ALLOY SKIN PANEL FOR STRUCTURAL COMPONENT (INTERNAL SURFACE).

FIGURE 11. F48 COLUMBIUM ALLOY COMPONENT DURING STRUCTURAL TEST AT 2500°F.

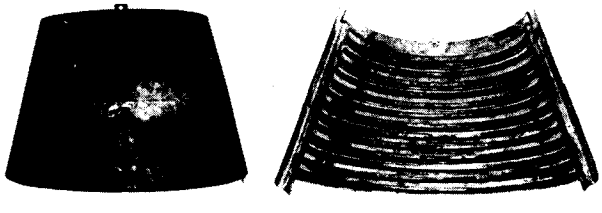

FIGURE 12. PROTECTIVELY COATED D-14 COLUMBIUM ALLOY COMPONENT AFTER EXPOSURE AT 1900° F.

FIGURE 13. **SILICIDE COATED COLUMBIUM ALLOY BOLT**

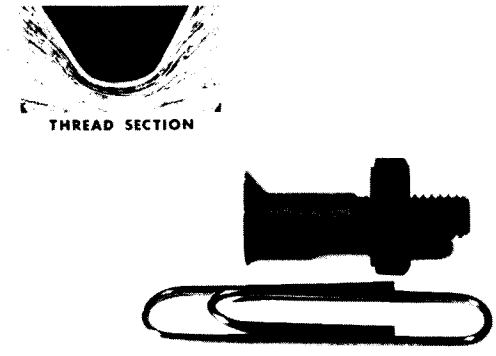

DUCTILE TO BRITTLE TRANSITION TEMPERATURE OF WROUGHT TANTALUM

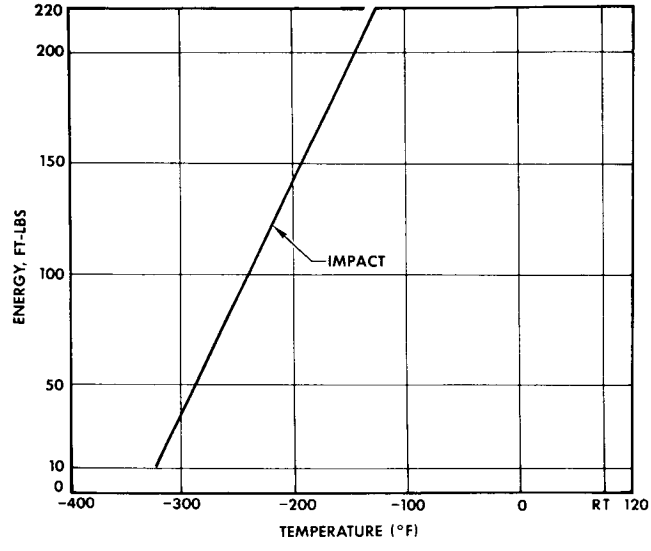

FIGURE 14.

MODULUS OF ELASTICITY OF TUNGSTEN AND TANTALUM AS A FUNCTION OF TEMPERATURE

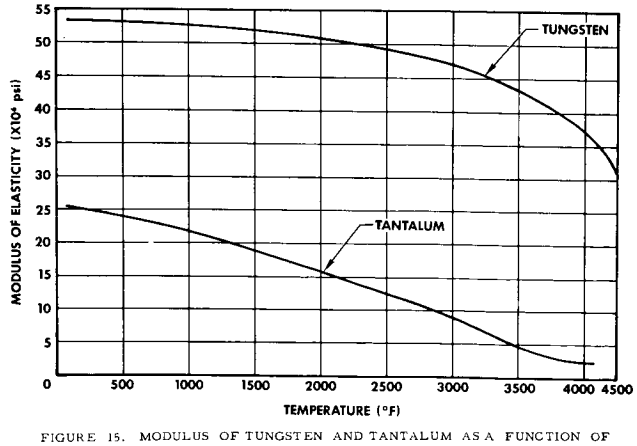

FIGURE 15. MODULUS OF TUNGSTEN AND TANTALUM AS A FUNCTION OF TEMPERATURE.

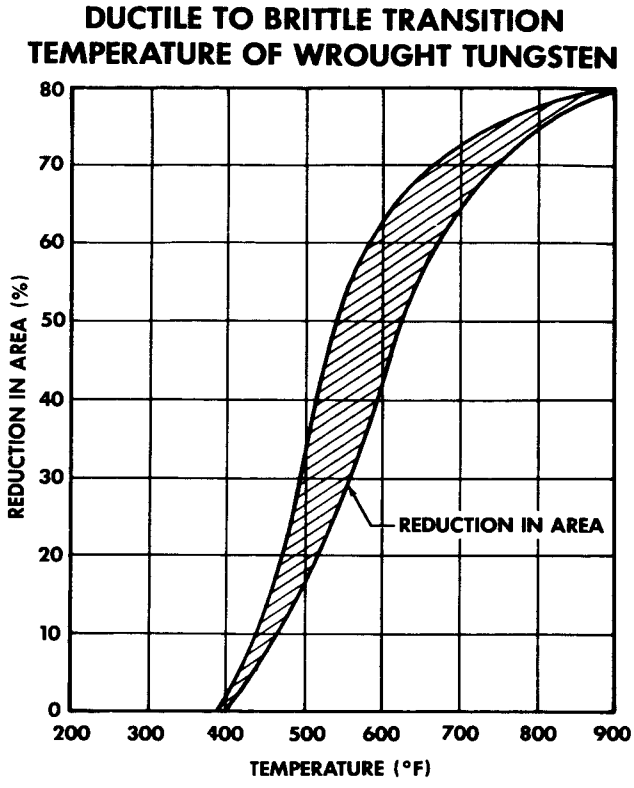

FIGURE 16. DUCTILE TO BRITTLE TRANSITION FOR WROUGHT TANTALUM.

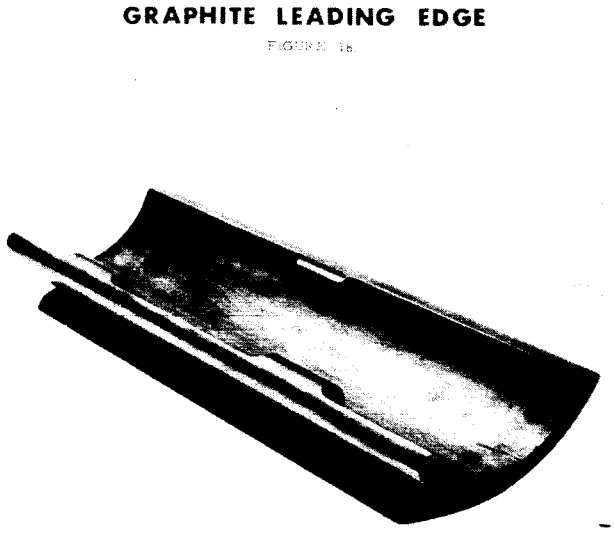

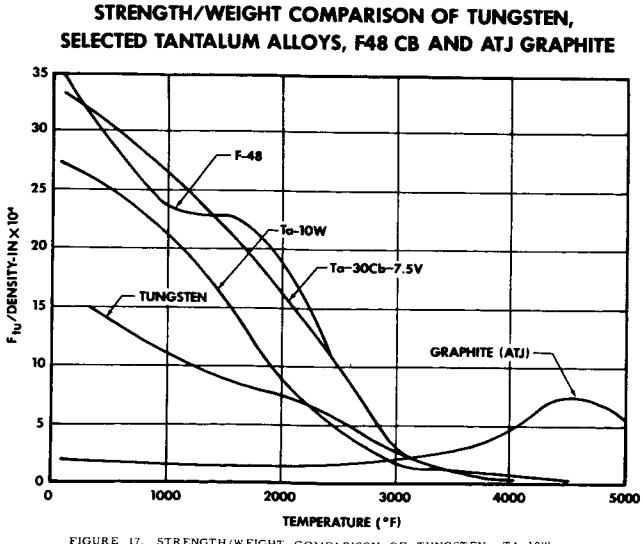

FIGURE 17. STRENGTH/WEIGHT COMPARISON OF TUNGSTEN, TA-10W, TA-30Cb-7.5V, F48 AND GRAPHITE AS A FUNCTION OF TEMPERATURE.

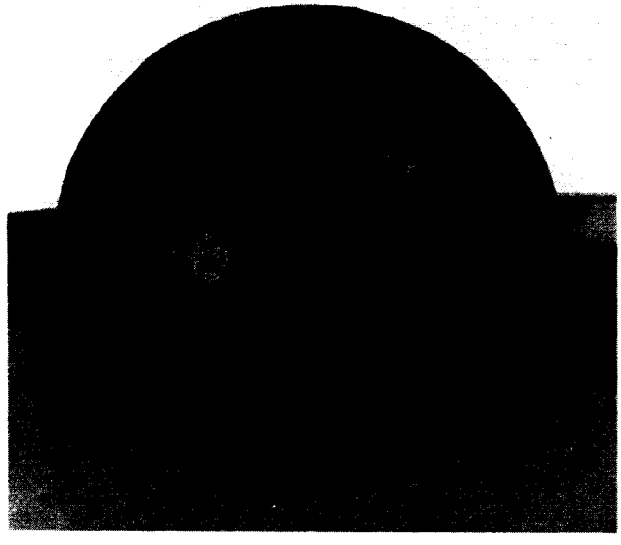

FIGURE 19. UNDERCUT SILICONIZED GRAPHITE TEST SPECIMEN COATED WITH ZIRCONIA AFTER TESTING AT 3800°F.

This page is reproduced again at the back of this report by a different reproduction method so as to furnish the best possible detail to the user.

This page is reproduced again at the back of this report by a different reproduction method so as to furnish the best possible detail to the user.

REFRACTORY OXIDE CERAMIC ROD NOSE CAP DESIGN

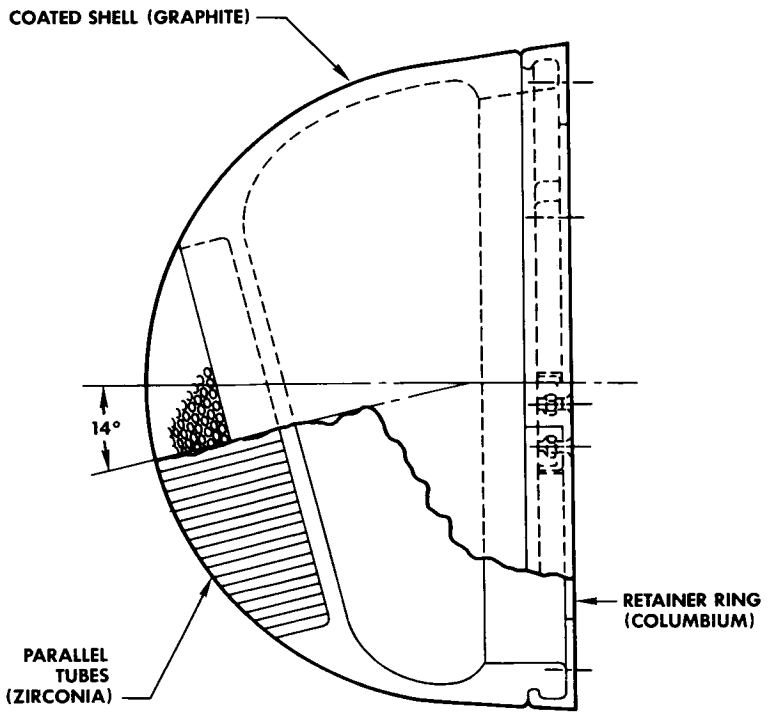

FIGURE 20.

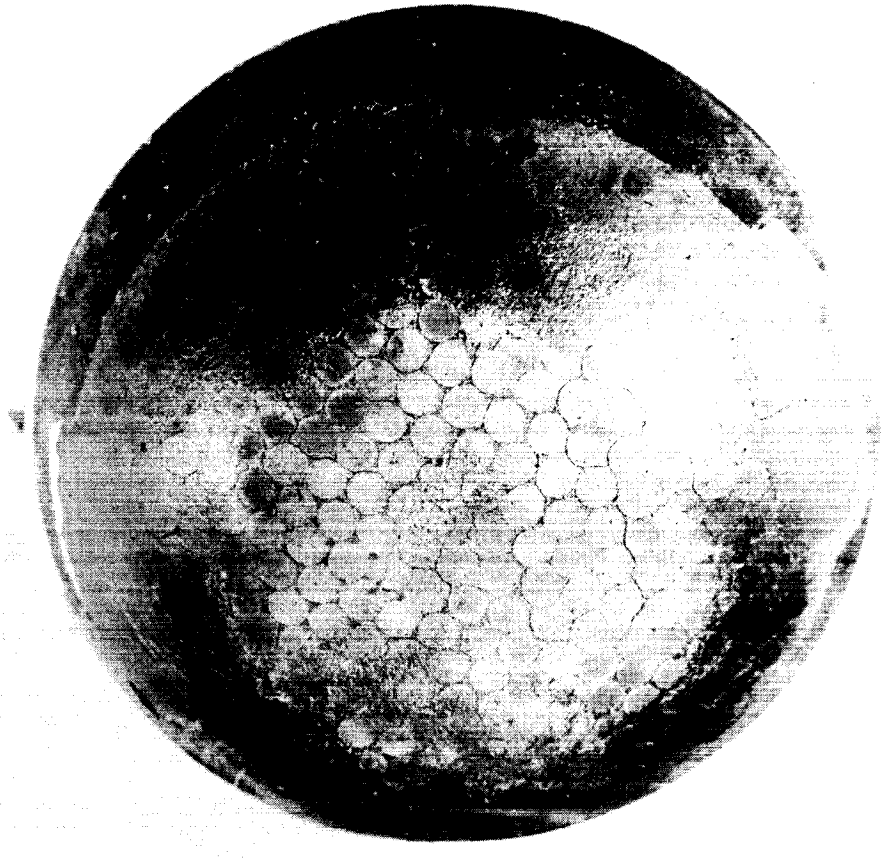

FIGURE 21. ZIRCONIA ROD TYPE NOSE TIP AFTER SECOND TEST AT 4100°F.

SOME ABORT TECHNIQUES AND PROCEDURES FOR MANNED SPACECRAFT

John M. Eggleston

Aerospace Technologist

Manned Spacecraft Center

National Aeronautics and Space Administration

Introduction

This paper is concerned with our present state of knowledge on the procedures and effectiveness of aborts from manned orbital and lunar missions. By abort is meant a deliberate or unintentional termination of the primary mission followed by an expedient return to earth of the payload (spacecraft and crew). A deliberate abort may be initiated if a critical component failed and thus impaired the probability of mission success or the crew's safety. Examples of this kind of abort are failure of the launch guidance system or the oxygen and cabin pressure system. Also, an unintentional abort may occur during the launch phase due to the complete or partial failure of one of the launch-vehicle stages to operate. For each mission every conceivable set of circumstances must be considered and evaluated to see if an abort of the mission is called for and to determine what sequence of events should occur to bring the spacecraft and crew safely back to earth with the highest probability of success. Factors which must be considered are: how to specify and sense an abort condition, how much fuel should be put onboard the vehicle for abort purposes, what size and kind of rocket engines are best suited for each mission, and what compromise is incurred due to other mission requirements? If an abort occurs, the optimum time of application as well as the magnitude and direction of the velocity changes must be determined beforehand and the crew must be clearly informed of what action is required or what the situation is so that they can decide the proper action.

It follows then, that mission abort considerations are not simply of academic interest, nor do they play a minor role in the overall requirements of the vehicle design. For example, in the Mercury program the mission analysis group spends four times as much effort on planning for abnormal missions as they do for the normal missions. From their experience we know that in the atmosphere the most critical factor is the lateral and negative accelerations that may occur if the spacecraft tumbles during abort at high dynamic pressure. Once outside the atmosphere, the reentry decelerations may be high but usually are not critical, and the more important consideration will be in landing the vehicle in a specified recovery area. Regardless of what happens, both the spacecraft and pilot must be conditioned to survive a wide spectrum of emergency conditions. While the people who obtain funding for space projects must optimistically point out what can be achieved if the mission succeeds, a group of pessimists must consider what to do to save the crew and the spacecraft if the mission fails.

In this paper some of the abort considerations applicable to manned missions such as Apollo and Gemini will be discussed with occasional reference made to the techniques used in the present Mercury program. It should be clearly understood, however, that the information to be presented represents research data obtained by many groups and does not necessarily represent any final decision on the abort techniques that may be used in these programs. A number of published reports on the subject of extra-atmospheric aborts are listed at the end of the paper[1] to 11. Many other papers not suitable for general publication (such as Mercury and Apollo Working Papers) have provided background material. While only a review of the subject is given herein, most of the details can be obtained from the referenced papers.

Atmospheric Abort

The atmospheric phase of launch will be treated only briefly since a great deal has already been written and said about procedures for the abort of a manned spacecraft at the two most critical conditions within the atmosphere: Off-the-pad and at high dynamic pressures. For the purpose of abort at these conditions, the Mercury spacecraft uses a set of tower-mounted solid rockets. The tower and rockets went through an extensive series of tests early in the development program and are now considered one of the most reliable systems connected with the Mercury spacecraft. However, two important changes have been considered for improving this system.

The question often arises as to whether an escape tower with rockets that pull the spacecraft off the launch-vehicle is the best way to do the job, or whether pusher-type rockets should be used. After investigating the various alternatives to the escape tower, the conclusion to date is that no better alternative exists for the contemplated Apollo configuration. However, the Gemini spacecraft will probably not use the escape tower but will use ejection seats for the crew in the event of an abort at altitudes below 20,000 to 40,000 feet.

One aspect of the present abort tower, however, will probably be improved. An illustration of this aspect is the case in which the launch-vehicle and spacecraft have reached a launch velocity of 2,000 or 3,000 ft/sec and an abort is required. The fuel flow to the launch-vehicle is shut off and by using the tower-mounted rockets, the spacecraft is separated from the launch-vehicle with an initial separation velocity of say 400 ft/sec. Immediately following separation then, the spacecraft is subjected to a dynamic pressure somewhat greater than that of the launch-vehicle while the weight or inertia of the launch-vehicle is about 100 times greater than that of the spacecraft. Even with a tumbling launch-vehicle, this difference in inertia and dynamic pressure would be enough to cause the launch-vehicle to overtake the spacecraft in 5 to 10 seconds. For this reason the "thrust line" of the escape rockets does not pass through the center of gravity (eccentricity), and thus a pitching moment is produced and the spacecraft is given a

component of velocity away from the trajectory of the launch-vehicle.

The present shortcoming with this arrangement is illustrated in figure 1. If the launch-vehicle is tumbling, then the pitching moment applied by the separation rocket ($\dot{\theta}_c$ of fig. 1) may be completely or partially cancelled by the pitching moment of the launch-vehicle—spacecraft combination $\dot{\theta}_b$ and the result will be a subsequent collision. On the other hand, if the spacecraft were able to sense the direction of rotation (pitching and yawing velocity) at the time of abort, and the rotational velocity imparted by the separation rocket were applied in approximately the same direction $\dot{\theta}_b + \dot{\theta}_c$, then sufficient clearance would be provided. This type of control would be a refinement to the atmospheric abort system and studies of such a system are now being made.

Suborbital Abort (Extra-Atmospheric)

Decelerations during entry.- One aspect of the Mercury launch program which may not be too well known is the fact that if an abort occurs at a launch velocity of 14,000 to 16,000 ft/sec, the spacecraft, without lift capability, will undergo as much as a 16g reentry. Although 16g is not critical for reentry from a launch abort, it may be of interest to examine how even lower values can be obtained.

An indication of the maximum entry decelerations following an extra-atmospheric abort is shown in figure 2. This figure, taken from[1] with some details deleted, shows the maximum deceleration that will be reached for a nonlifting entry when the trajectory conditions are measured at an altitude of 394,000 feet (120 km). Although the figure does not cover a sufficiently wide range of flight-path angles and applies only to nonlifting entries, it does illustrate the sensitivity of deceleration to flight-path angle over a wide range of velocities. (Similar curves are also given in[2] for flight-path angles up to 20° based on a reference altitude of 300,000 feet and for values of L/D from 0 to 2.) For most orbital or lunar launch trajectories, the critical area of this figure lies between velocities of 14,000 and 18,000 ft/sec for it is here that the combination of state variables (altitude, velocity, and flight-path angle) usually leads to the highest decelerations on entry following an abort. Exact values of deceleration will vary with different launch profiles, but for manned missions this is not a desirable region to undergo launch-vehicle staging if it can be avoided. Some considerations of problems of this type are discussed in[3,4].

Optimum time and direction for corrective thrust.- If an abort does occur outside of the atmosphere at suborbital velocities and the spacecraft is equipped with a rocket engine and fuel, then the decelerations at entry may be reduced by proper use of the fuel available. The proper time and direction for the thrusting maneuver can be illustrated with the aid of figures 3 to 5 taken from[5].

In figure 3 is shown a typical variation of altitude with time for a spacecraft following a suborbital abort. For this example, the spacecraft can produce a lift-to-drag ratio L/D of 0.5 once inside the atmosphere and, in addition, is equipped with a rocket engine capable of thrusting for 11.05 seconds and producing a velocity increment of 3,000 ft/sec. This ΔV may be applied in any direction, and at any time along the coast trajectory up until the time of entry. Seven possible positions are indicated on the figure where the rocket could be ignited. The last position coincides with the initial buildup in deceleration, which occurs at a relative low altitude due to the large flight-path angle (-20°) and low velocity (14,000 ft/sec) at entry.

The effect on the entry decelerations of applying the thrust at these various positions is shown on figure 4. On the left of figure 4 is the maximum deceleration measured during the entry plotted against the direction of thrust application for four of the seven positions considered in figure 3. The curves for positions 4, 5, and 7 lie in between those shown for positions 3 and 6 and have been left out for simplicity. The data show that the decelerations are minimized if the thrust is started at position 6 and applied at an angle of about 100° to the initial velocity vector. The results also show that applying the velocity change at the time of abort (position 1) is the least effective of the cases considered.

On the right of figure 4 a formula is given for the impulsive velocity change ΔV producing the maximum change in flight-path angle $\Delta\gamma$. The values of ζ obtained by this formula are shown with ticks on the curves of figure 4 and, as may be seen, give a good representation for the minimums of these curves.

The data of figure 4 indicate that the optimum time to apply this thrust is just prior to the buildup of dynamic pressure during the entry. However, sufficient time must be allowed for (1) the rocket to finish thrusting, (2) separating the rocket from the spacecraft (if required), and (3) to reorient the spacecraft for entry prior to an excessive buildup of dynamic pressure with the associated high rates of heating and deceleration. Therefore, it is necessary to know, among other things, how sensitive is this "optimum" condition and how do these results change with various sizes of rocket engines. In order to answer these questions, the data from figure 4 have been plotted in figure 5 showing maximum entry deceleration as a function of dynamic pressure at the time of rocket ignition. Figure 5 also shows similar data for several other thrust levels. In all cases the total velocity change was 3,000 ft/sec, the initial vehicle weight was 7,000 pounds, and an L/D of 0.5 (or 0) was used during the atmospheric pullout. Since the lower thrust levels require the longer burning times, the data indicate that low-thrust engines must be started at a higher altitude than the higher-thrust engine. The exact values will, of course, change somewhat with different entry conditions.

Vehicle attitude control.- If a set of assumptions are made as to the shape, etc., of the manned spacecraft, then a sequence or procedure for reorientation can be postulated for aborts at suborbital velocities, and a study can be made of some of the factors involved in the use of a rocket for maneuvering prior to entry.

Such a study was recently performed at the NASA Langley Research Center and will be reported in

more detail in[6]. For this study it was assumed that:

1. The manned vehicle was a blunt-faced spacecraft.

2. The rocket engine discussed in the preceding section was located on the face of the heat shield of the spacecraft similar to the retrorocket now used on the Mercury spacecraft.

3. The spacecraft center of gravity was offset so that, in the atmosphere, the spacecraft would trim at an angle α of 33° with respect to the relative wind. The resulting aerodynamic force would produce a ratio of lift-to-drag L/D of 0.5. The vehicle would be rolled to direct this lifting force in the proper direction for both side-force and for "negative" lift.

An instrument used in this study to describe the motions of the spacecraft to the pilot is shown in figure 6. The instrument is simply a two-needle synchro with an image of the spacecraft on one needle and a "velocity vector" on the other needle. This instrument gives information on the angle of attack α, the flight-path angle γ, and the angle of the spacecraft with respect to the local horizon θ and covers a range of 360° with a read-out accuracy of about 1° or 2°. Such an instrument supplements the normal flight instruments and is generally referred to as a "situation display." It is indicative of the feeling of many researchers in this field that new situations often require new instruments to describe adequately the flight conditions to the pilot.

A typical sequence of maneuvers following an abort at suborbital velocities is illustrated in figure 7. A typical trajectory profile is shown in the upper portion of the figure with the orientation of the capsule shown at several key positions on the trajectory. In the lower portion of the figure the pilot's display at these same positions is shown. If the pilot and crew are in an upright position* with respect to local horizons at the time of abort, then a positive pitch maneuver of about 100° is required in order to fire their rocket in the optimum direction. The pilot will normally have several minutes in which to make this maneuver while coasting well above the earth's atmosphere. During this time, the vehicle should also be rolled 180° (the sequence of pitch + roll or roll + pitch is optional) so that, following burnout of the maneuver rocket, only a pitching maneuver will be required to orient the spacecraft in the proper attitude for entry. This final pitching maneuver requires an angular change of about 67° (from an angle of attack of 100° to an angle of 33°) and may have to be done very rapidly. Since the available thrust is most effectively used just prior to entering the atmosphere, the elapsed time between the end of the thrust and the beginning of the high atmospheric heating rates may have to be kept necessarily small.

*During the boost phase and under "zero-gravity" conditions, there is nothing unique about an "upright" position. On the other hand, there does not appear to be any overpowering reason to change the position of the crew to any other position either.

The minimum time required to make these maneuvers is primarily a function of the control power of the spacecraft's attitude control system. In the simulation program of[6], it was found that when pilots were presented with the aforementioned reorientation problem, they used the maximum pitch rate capability of the spacecraft even when the spacecraft's automatic damping system was inoperative. A typical time history of one of these maneuvers is shown in figure 8. In the case shown, the spacecraft had a rate command system with a maximum pitching rate of 6.2 deg/sec. Similar results were also obtained with maximum rates of 12.4 and 18.6 deg/sec. In the example shown in figure 8, the heating rates would have already become extremely high by the time the maneuver was completed. However, in simulation programs, it is usually necessary to give the pilot an incentive for high performance. For this reason, the pilot was forced (in the simulation) to perform the maneuver very close to the atmosphere. If he failed to complete the pitch maneuver before the buildup in dynamic pressure, the spacecraft became aerodynamically unstable and uncontrollable. In actual flights the high heating rates would precede this condition of instability and would undoubtedly provide the same incentive.

Range after suborbital abort.- Exact values for the range traveled by the vehicle following the abort will depend on the launch trajectory and characteristics of the spacecraft L/D and W/C_DS. However, some results on a blunt-faced spacecraft with L/D of 0.5 are indicative of the general trends that can be expected. (See[6,7].) Figure 9 shows a typical launch trajectory with the trajectories that would be followed if aborts had occurred when the launch velocity was 12, 15, 18, 21, and 24 thousand feet per second. Associated with each abort trajectory, there is a footprint of available landing sites which can be reached by varying the L/D and the corrective thrust ΔV prior to entry. Only one such footprint is illustrated in figure 9. These footprints can be characterized by shape, width, length, and the down-range distance from the launch site to some reference point on the footprint. Taking these characteristics in their given order, some range and cross-range data are given in figures 10, 11, and 12. In figure 10 is shown the general shape of the available footprint obtained by a pilot using an L/D = 0.5 and restrained to not exceed entry decelerations of 10g. The difference between the maximum and minimum available longitudinal range L determines the length, the maximum lateral range B determines the width, and the longitudinal distance traveled while achieving maximum lateral range A determines the reference center of the footprint.

In the cases studied, corrective velocity changes of 0, 1,500, and 3,000 ft/sec were applied in the direction giving a maximum reduction in entry angles (see fig. 4) just prior to entry. It was found that the ratios of A/L and B/L were not affected by the thrust maneuver. Furthermore, the ratio of A/L remained constant at 0.67 ± 0.02 regardless of abort velocity and the ratio of B/L varied as shown in figure 10.

In figure 11, the variation of L with the velocity at abort and with ΔV is shown. Since each degree represents about 60 nautical miles, it can be seen that at 18,000 ft/sec the maximum footprint is 240 nautical miles long L and ±48 nautical miles wide B if a ΔV of 3,000 ft/sec is used and only 1/2 that size if no ΔV is used.

In figure 12, the maximum down-range distance obtained is plotted on a semilog scale against the velocity at abort. The curves with symbols are distances measured from the position at abort while the dashed curve gives the distance from the launch site to the position at abort. It can be seen that up to 24,000 ft/sec, we are concerned with recovery sites on the order of 80° to 90° down range from the launch site.

One useful application of these data could be made by plotting these footprints along the nominal ground track of the vehicle during launch to determine the desirable location of recovery sites for a lifting vehicle. A further study is also necessary to determine how much ΔV should be used by a pilot from range considerations since, as the figures show, both the entry decelerations and the range will be affected by the onboard propulsion. Of the two, range considerations and the simplicity of procedures will probably predominate over considerations of reducing the decelerations on entry.

It may be of interest to note that in the operational procedures for the Mercury spacecraft the retrorocket normally used for deorbit can also be used at suborbital abort to shorten the range. However, this rocket produces a velocity change of only 450 ft/sec and procedures call for its use in a retrograde direction from 30 to 250 seconds after abort. The proposed larger velocity capability of Gemini and Apollo offer considerable more choice in the field of range control. Complexity is, however, the price to be paid for this freedom of choice.

Superorbital Abort

General.- Probably the most difficult region in which to establish an ironclad abort procedure is the region between orbital and escape velocity. Depending upon the amount of fuel carried and the time required to use that fuel, an immediate return to earth can be executed only up to a certain point during the launch; beyond that point, an immediate return cannot be made and the procedure for using the available fuel becomes entirely different. Once superorbital velocities have been reached, the centrifugal acceleration due to velocity will exceed the acceleration due to gravity and the vehicle will move away from earth on a Keplarian ellipse even though the launch-vehicle is shut down. Because of this fact, any increase in velocity, altitude, flight-path angle, or time will also increase the velocity change required to deflect the vehicle's trajectory so that it intersects the atmosphere before apogee is reached. If sufficient fuel to accomplish this velocity change is not available, then the vehicle must continue to apogee, using the available fuel along the way to change the orbit so that perigee lies within the earth's atmosphere. These considerations are necessary both for direct launches and launches from orbit and we will not distinguish between the two in this paper. Some of these factors have been covered in[8] for impulse thrust applications. Also, a very comprehensive parametric study giving the impulsive thrust requirements for immediate return to earth from superorbital aborts is given in[2]. However, to the impulsive velocity requirements of[2,8] must be added the additional velocity cost due to the time required to reorient the vehicle and to apply the thrust. We will consider only these factors here.

Vehicle attitude control.- In figure 13, a typical reorientation procedure designed from an immediate atmospheric entry following an abort at superorbital velocities is illustrated. If the pilot is in an upright position at the time of abort, the sequence of figure 13 can be described as essentially that of a forward somersault. At the signal for an abort, the pilot (or automatic control sequencer) has several choices. If the abort is not caused by the launch-vehicle and the pilot can override the launch-vehicle control system, then he may use the launch-vehicle to change his trajectory back toward the atmosphere before separation. If the abort is caused by a failure of the launch-vehicle control system, a launch-vehicle thrust failure, or by an impending explosion, immediate separation must be made using an abort or separation rocket. If sufficient fuel is available for an immediate return to earth, the sequences shown in figure 13 are applicable. Upon separation, the pilot should immediately pitch down about $96^\circ \left(\text{according to the equation } \zeta = 180^\circ - \cos^{-1} \frac{\Delta V}{V_o} \right)$ and fire the maneuver rocket. This procedure will produce a maximum negative change in flight-path angle for the given available ΔV. Following the firing of the maneuver rocket the pilot will probably continue the pitch-down maneuver to an angle of attack of -33° in preparation for the atmospheric entry. This attitude will produce a negative L/D of 0.5 and should hold the spacecraft in the atmosphere until near orbital velocities are reached, at which time a roll-out of 90° to 180° can be made. Since the ΔV requirement for immediate earth return changes vary rapidly during the superorbital phase of the boost (see[8]), an excess of velocity may be available to the pilot and if this is the case then positive lift may be required at entry. This situation is similar to the undershoot and overshoot boundaries as described by Chapman[12] and others, and care must be taken at abort to stay within the accepted corridor for supercircular entries.

Pilot response times.- The maneuvers just described have been examined in[6] from a pilot response viewpoint, and a typical time history is shown in figure 14. A critical case was chosen in which atmospheric capture depended upon the pilot's response time following the abort signal. Allowing for the 3-second burning time of the separation rocket, the time τ required to hit the separation switch, reorient, and fire the maneuver rocket was evaluated for a number of test pilots. The results are shown in figure 15 along with results obtained from the suborbital aborts of figure 8. The data are presented as the probability of the pilot exceeding a given time τ for the maneuver where τ is given on the abscissa. The critical values of τ for the two flight conditions considered are given on the figure.

An indication of the additional velocity requirement imposed by the time to reorient and fire the maneuver rocket is given by figure 16. Taken from[5], the figure gives the ratio of propellant weight W_p to total initial weight W_o of the spacecraft as a function of delay time τ at two different abort conditions and for three different thrust levels. The reason for haste in making these maneuvers and using maximum available thrust levels is apparent in this figure.

The orientation time between the firing of the maneuver rocket and entry does not appear to be critical even for launches from low-altitude orbits. This fact can be illustrated by considering a case in which the spacecraft is in a capture condition, say $V = 30{,}000$ ft/sec, $\gamma = 0^{\circ}$, $h = 250{,}000$ ft, and $L/D = -0.5$. If we then compute backward in time, the trajectory leading up to this capture condition is obtained. Each position on this trajectory represents a possible condition of state following an abort and the firing of the maneuver rocket. The time required to go from each of these state conditions to the final capture condition is shown in figure 17. It may be seen, for instance, that it takes 150 seconds to go from 300,000 feet and 233 seconds to go from 400,000 feet to the final condition at 250,000 feet. When considering a maneuver requiring 10 to 20 seconds, sufficient time appears to be available for reorientation prior to entry.

Range available for energy management.- Due to the wide range of entry conditions following aborts between orbital and escape velocities, it would be a formidable task to establish the range capabilities of the spacecraft throughout this entire region. No such analysis is known to exist and may not be merited until more information on the launch trajectory, the available fuel, and the abort entry conditions are established. On the other hand, a less extensive study does appear to be warranted. Although it may be difficult to guide the space vehicle from a superorbital abort to a direct return to the atmosphere with a prespecified set of entry conditions, it should be possible to achieve these desired entry conditions accurately if the spacecraft is allowed to coast to apogee first. For this reason, it may be desirable at this time to investigate what the range envelope for the "middle-of-the-corridor" conditions at superorbital velocities might be.

Abort From Translunar Trajectories

Although not as probable as an abort from launch, it may be necessary on occasion to abort from the translunar trajectory. Penetration by a meteoroid, solar flares, or sudden illness may justify this type of an abort. Also, closely associated to this problem is the case (referred to in the preceding section) in which the vehicle is aborted at superorbital velocities, coasts to apogee and uses the available thrust to insure a safe return to earth on the next pass. Since it will take from 2 to 24 hours (or more) to return to earth from this type of an abort, the element of time is no longer as critical as in the preceding cases considered. Furthermore, the guidance logic for making the proper velocity correction for these types of aborts should dovetail with the procedures used for midcourse corrections for the nominal return trajectory from the moon.

The only published work in this field known to the author is given in9. The paper essentially describes a method of calculating positions on the nominal translunar trajectory where aborts may be made which lead to a return to earth at a predetermined landing site. The concept referred to as abort "way stations" appears to be particularly suited to guidance schemes which store influence coefficients derived from perturbations on a nominal trajectory. Such a scheme is now being seriously considered for the Apollo mission.

Aborts From Lunar Landings

An entirely new field of study has recently developed with the consideration of lunar landings and lunar rendezvous. Since there is very little difference between an abort from a lunar landing and the problem of launching a rendezvous operation from the surface of the moon, these two problems are currently being studied jointly. It is too premature to discuss any detailed results now but papers on these subjects may well become quite numerous in the very near future.

Concluding Remarks

To date the United States' only manned venture into space has been made with the relatively simple and reliable system of the Mercury spacecraft. Without lift control and with only a small fixed thrust rocket, the procedures for abort and recovery have not required a complex guidance and control system. The next generation of vehicles will have both lift control and considerably more maneuver thrust capability. Just how these capabilities will be used will depend on the continued desire to keep the procedures as simple and reliable as possible. It seems possible that atmospheric and suborbital aborts can be kept relatively simple. The computations for superorbital and translunar aborts appear to be complicated by the necessity of highly accurate velocity changes. However, even these types of abort can be kept simple by using stored programs such as the abort way stations. At the moon, it now appears that onboard computations of the optimum thrust maneuver will be a virtual necessity in the case of an abort during some phases of the lunar landing. However, since onboard computations will also be necessary for the basic landing maneuver, an abort may not place an undue burden on the guidance logic system. The lack of an atmosphere at the moon should, in some ways, greatly simplify the choices and the computations of the optimum course of action.

References

1. Hoelker, R. F., Teague, Roger, and Lisle, Ben J.: Studies of Pilot Abort From Saturn C-2 Trajectories. Marshall Space Flight Center Report, MTP - AERO - 61-22, March 21, 1961.

2. Slye, Robert E.: Velocity Requirements for Abort From the Boost Trajectory of a Manned Lunar Mission. NASA TN D-1038, 1961.

3. Carter, C. V., and Huff, W. W., Jr.: The Problem of Escape From Satellite Vehicles. NATO Report 242, May 1959. (Also IAS Paper 59-14.)

4. Carter, W., and Kramer, P. C.: Escape of Manned Vehicles From Lunar Mission Ascent Trajectories. AAS Paper, Preprint 61-20, January 16-18, 1961.

5. McGowan, William A., and Eggleston, John M.: A Preliminary Study of The Use of Finite-Thrust Engines for Abort During Launch of Space Vehicles. NASA TN D-713, 1961.

6. Young, John W., and Goode, Maxwell W.: Fixed-Based Simulation Studies of the Ability of the Human Pilot to Provide Energy Management Along Abort and Deep-Space Entry Trajectories. Paper to be Presented to the National Aerospace Electronics Conference, Dayton, Ohio, May 14-16, 1962.

7. Battey, Robert V.: Abort Considerations. NASA-Industry Apollo Technical Conference, Washington, D.C., July 18-20, 1961.

8. Eggleston, John M., and McGowan, William A.: A Preliminary Study of Some Abort Trajectories Initiated During Launch of a Lunar Mission Vehicle. NASA TM X-530, 1961.

9. Kelly, Thomas J., and Adornato, Rudolph J.: Determination of Abort Way-Stations on a Nominal Circumlunar Trajectory. ARS Paper 2085-61, October 9-15, 1961.

10. Gervais, R. L., and Johnson, M. C.: Abort During Manned Ascent Into Space. AAS Paper No. 62-36, January 1962.

11. Thompson, Robert F., and Cheatham, Donald C.: Considerations for Spacecraft Recovery From Lunar Missions. Aerospace Engineering, vol. 21, no. 1, January 1962.

12. Chapman, Dean R.: An Analysis of the Corridor and Guidance Requirements for Supercircular Entry Into Planetary Atmospheres. NASA TR R-55, 1959.

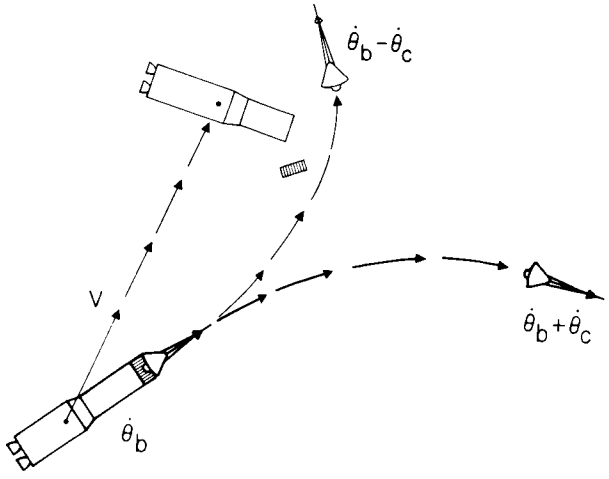

Figure 1.- Atmospheric abort anticollision control.

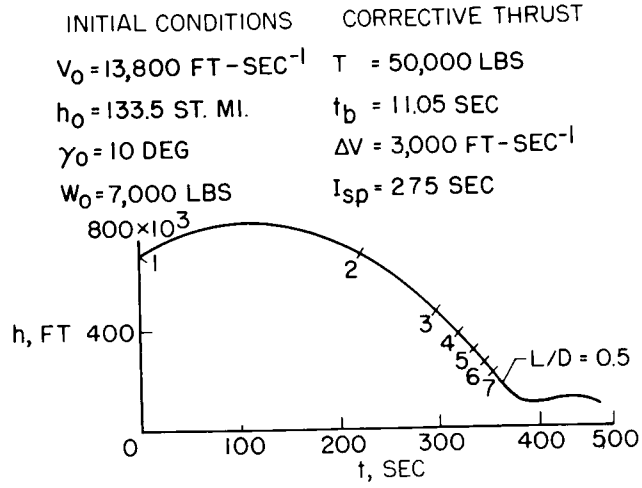

Figure 3.- Typical trajectory after abort.

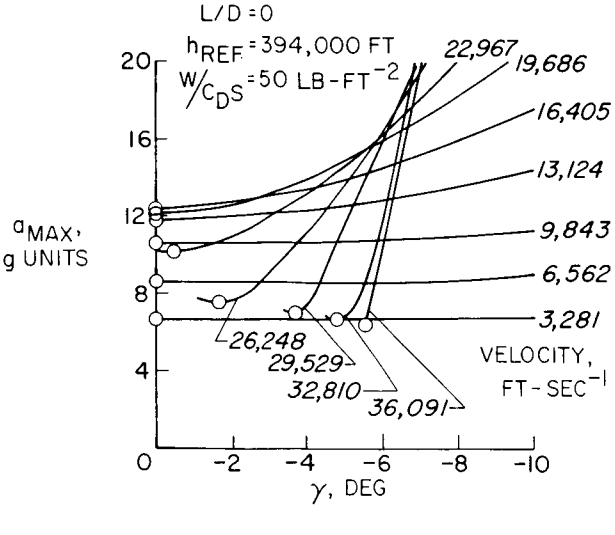

L/D = 0.

Figure 2.- Maximum deceleration at entry.

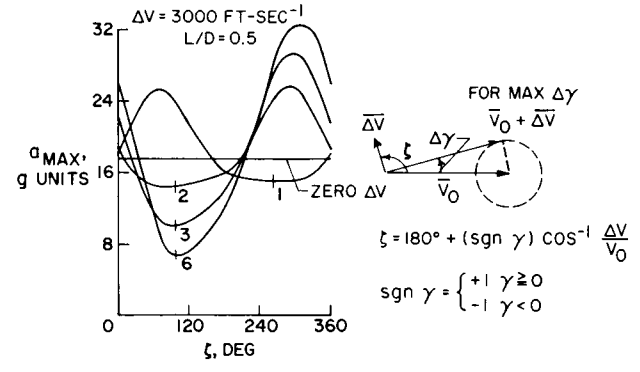

Figure 4.- Variation of maximum deceleration with direction of thrust.

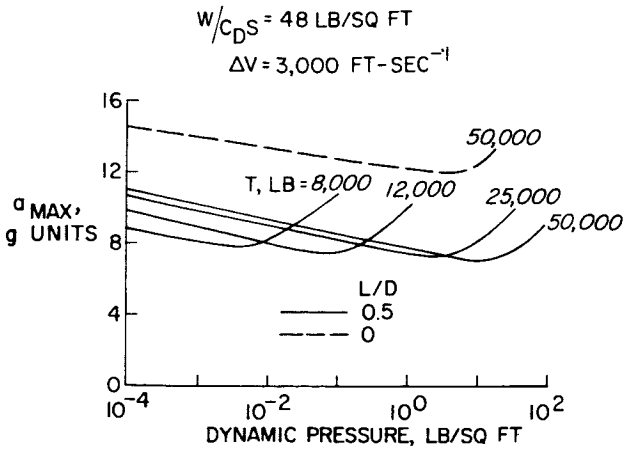

Figure 5.- Variation of maximum deceleration with time of thrust.

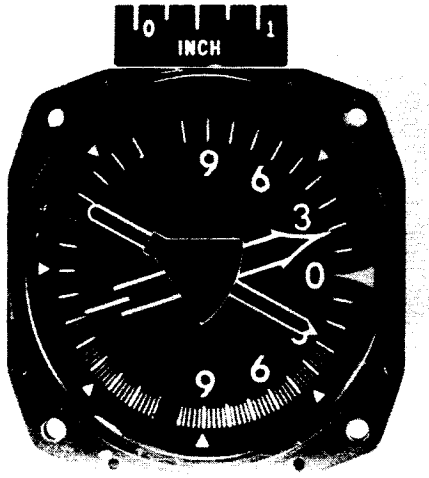

Figure 6.- Attitude-situation display.

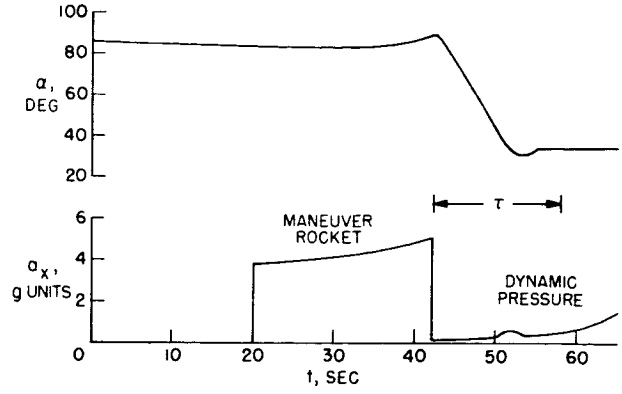

q_{max} = 6.2 deg-sec^{-1}.

Figure 8.- Typical suborbital final pitch maneuver.

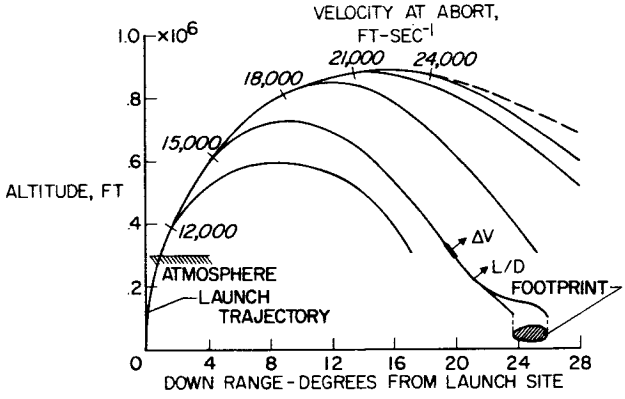

$(L/D)_{max}$ = 0.5.

Figure 9.- Range after suborbital abort.

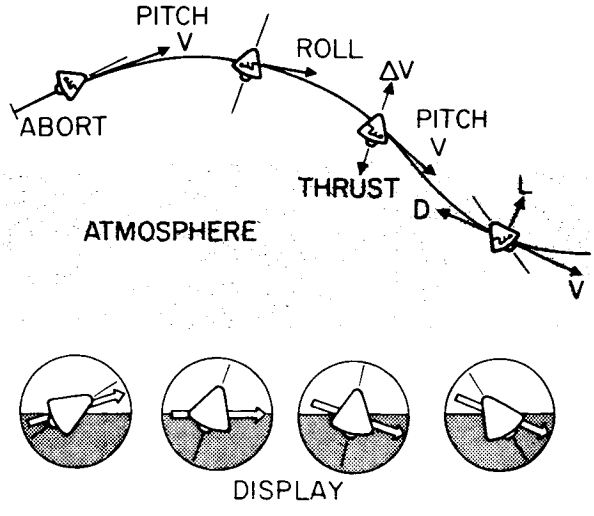

Figure 7.- Reorientation after suborbital abort.

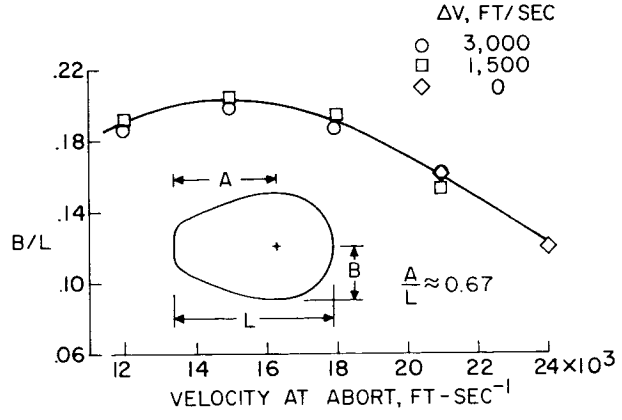

$(L/D)_{max}$ = 0.5.

Figure 10.- Ratio of maximum cross range to length of footprint.

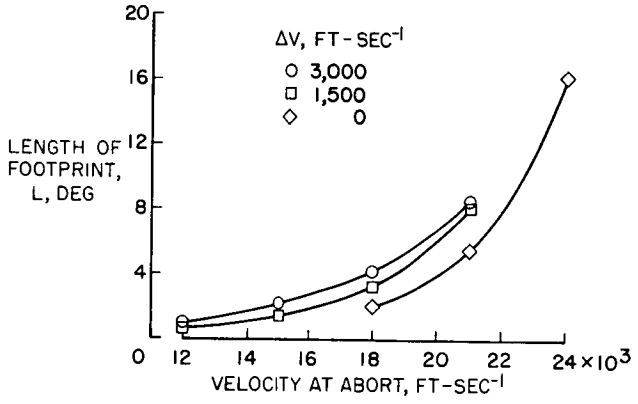

Figure 11.- Length of footprint.

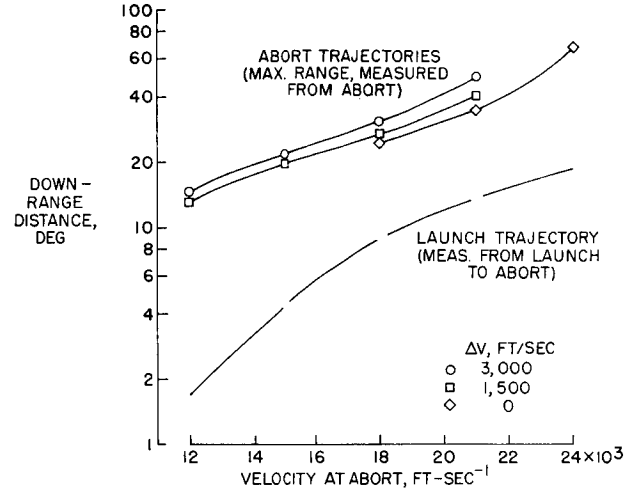

Figure 12.- Maximum down-range distance obtained following an abort.

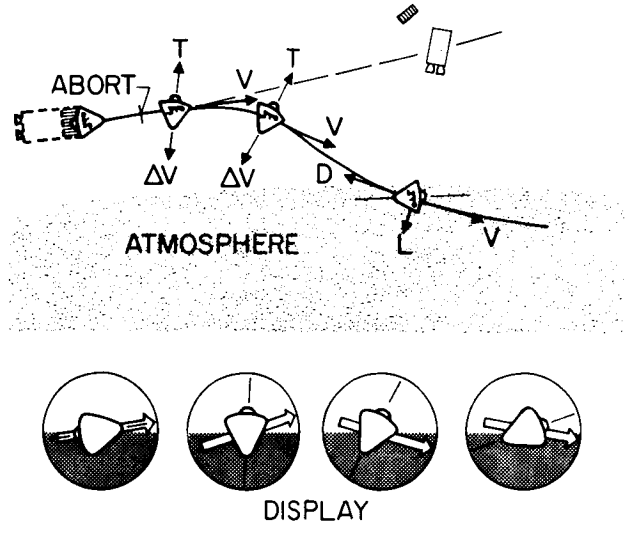

Figure 13.- Reorientation after superorbital abort.

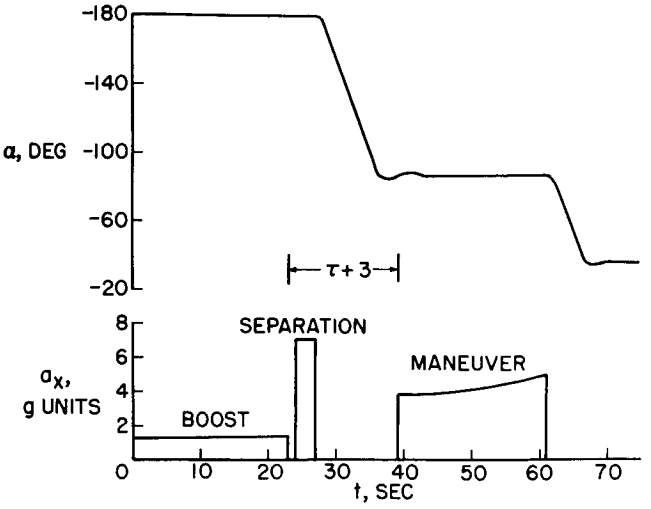

q_{max} = 12.4 deg/sec.

Figure 14.- Typical superorbital pitch maneuver.

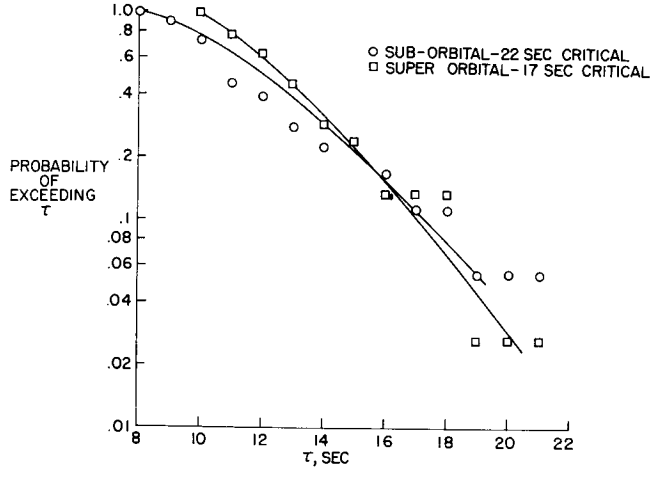

q_{max} = 12.4 deg-sec^{-1}.

Figure 15.- Time response of pilots.

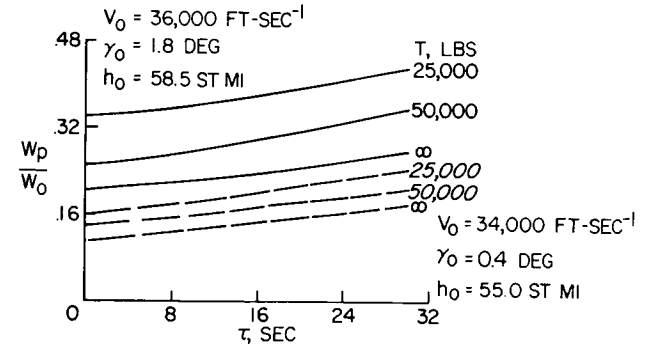

W_0 = 14,200 lb; I_{sp} = 420 sec.

Figure 16.- Abort fuel requirements with time delay.

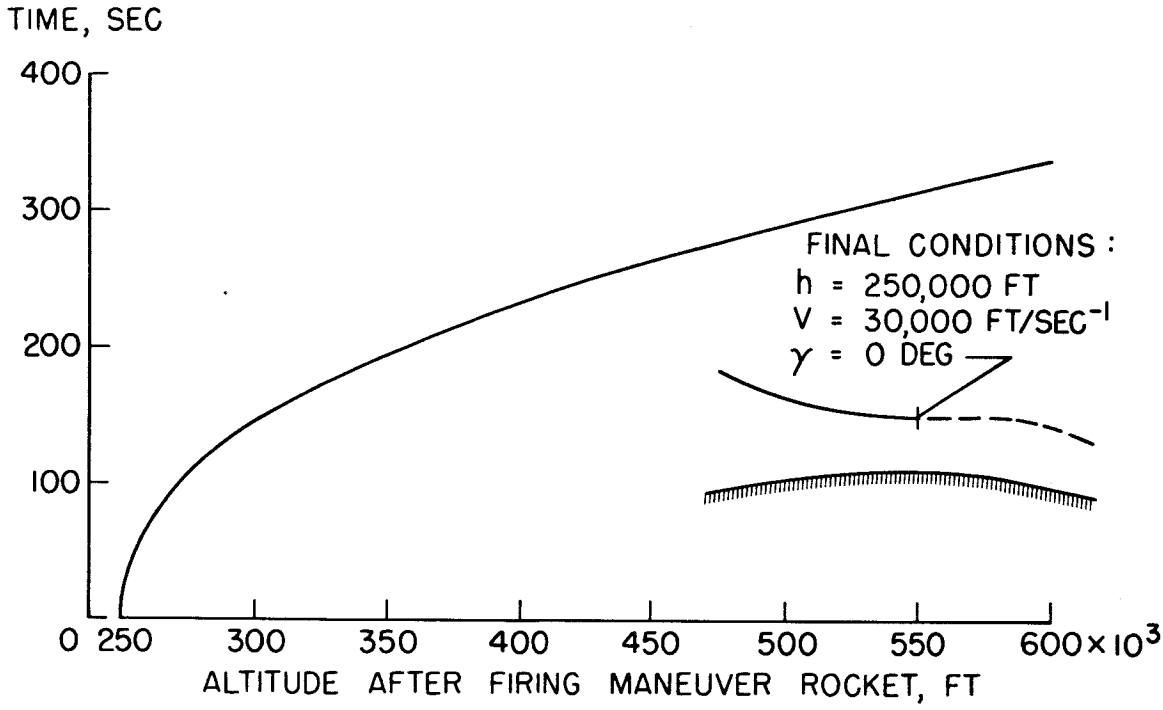

NASA

Figure 17.- Time to reach an altitude of 250,000 feet.

N66-14482

HUMAN CONTROL PERFORMANCE AND TOLERANCE UNDER SEVERE COMPLEX WAVE FORM VIBRATION, WITH A PRELIMINARY HISTORICAL REVIEW OF FLIGHT SIMULATION

by Carl C. Clark, Ph.D.
Manager, Life Sciences Department
Martin Company
Baltimore 3, Maryland

Introduction

As man travels, he vibrates. For as he travels, he generally experiences accelerations not perfectly uniform in magnitude nor direction, and these he feels as varying forces or vibrations. As he first travels faster, these vibrations become more severe, until he learns new ways to reduce them: the clearing of foot paths, the paving of roads, the welding of railroad tracks, the use of gust alleviation autopilot controls in aircraft, the improved spacecraft "adapter ring" attachment fairings to reduce trans-sonic buffet of multi-stage rocket vehicles. We will insure that the grandmothers, going to tea, booming across the oceans in rockets, will have smooth trips. But the pioneers, the pathfinders, will vibrate, while travelling faster on or near the earth, or penetrating through the atmosphere, or using thrust.

What can we do, preparing for these pioneers, to insure that these expected vibrations will not jeopardize their lives nor their missions? This paper will describe one approach, of attempting to simulate the expected and more than the expected complex wave form vibrations to determine tolerance and pilot control capabilities, to attempt to find solutions in simulation before the first flights in reality. The experimental work to be described was done in November, 1959, and June, 1960, on the Johnsville Navy human centrifuge, at the Aviation Medical Acceleration Laboratory, U.S. Naval Air Development Center, Johnsville, Pennsylvania, and in June, 1960, on the North American "G-seat", the vertical accelerator of the North American Aviation Co., Inc., Columbus, Ohio, while the author was Jostle Program Officer at the Aviation Medical Acceleration Laboratory. The experimental work was the subject of the confidential reports NADC-MA-L6005 and NADC-MA-6128, U.S. Naval Air Development Center, and NA60H-444, North American Aviation, Inc., Columbus. Unclassified aspects can now be reported.

Use of these large simulator facilities can only be made with the cooperation of many people. Particular acknowledgement is expressed for the efforts of Capt. F. K. Smith, MC, USN, and Mr. Robert Snyder, Aviation Medical Acceleration Laboratory, U.S. Naval Air Development Center, Harold Tremblay, Edward Loller, Tom Foley, and Harold Doerfel, Aeronautical Computer Laboratory, U.S. Naval Air Development Center, Dr. Robert Laidlaw, Mr. Charles Walli, Dr. Edward Marlowe, and Mr. Jack Willer, North American Aviation, Inc., and the pilots, Lt. James Willis, USN, Lt. Paul Weitz, USN, Lt. Charles Caricofe, USN, Lt. Paul Easton, USN, Lt. j.g. C. Garber, USN, Lt. David Glunt, USN, Capt. Robert Solliday, USMC, Lcdr. William Murphy, USN, Robert Smyth, Richard Wenzell, and Donovan Heinle.

Acceleration Terminology

In the first papers I know in which accelerations were measured in flight[10,11] a distinction was made between the accelerometer readings, called "accelerometer ratios", and the changes of velocity, which I call the displacement accelerations. In straight and level flight at constant speed, an accelerometer mass is deflected an amount which may be called 1G due to the gravitational attraction, but the displacement acceleration is zero. At other flight path angles as well, the gravitational components must be subtracted to determine the displacement accelerations. Unfortunately in the early United States papers measuring accelerations in flight[61-63,71,93] this distinction between gravitational attraction and displacement acceleration was not made, with the consequence that today it is the unusual rocket engineer who is quickly certain when you tell him that you have a 2g liftoff whether the velocity change is 32 or 64 feet/second^2.

In rocket vehicles, the crew are no longer necessarily in the typical airplane transverse seated position. Accelerations are no longer primarily along the transverse (Z) axis. Rotations may be more severe than with aircraft, and should be specified with more convenience than, for example, "2.0 radians per second squared about the Z axis". A physiological acceleration terminology[25] has therefore been established with recommendations for its adoption in the United States[49] and inclusion in a Table of Equivalents of Acceleration Terminologies[37] recommended for international use. This terminology has the following key points:

1. The unit for the physiological acceleration shall be G to distinguish this acceleration from the "true" displacement acceleration, generally designated by aerodynamicists with the unit g. The physiological acceleration represents the total reactive force divided by the body mass, and hence includes both displacement and resisted gravitational acceleration effects. Note that the physiological acceleration or total reactive load acceleration G rather than the displacement acceleration g is what is measured by accelerometers.

2. The physiological acceleration axes represent directions of the reactive displacements of organs and tissues with respect to the skeleton. The Z axis is down the spine, with $+G_z$ (unit vector) designations for accelerations causing the heart, etc., to displace downward (caudally). The X axis is front to back, with $+G_x$ designations for accelerations causing the heart to be displaced back toward the spine (dorsally). The Y axis is right to left, with $+G_y$ designations for accelerations causing the heart to be displaced to the left. For accelerations in which effects on the entire body are of concern, the origin of the axes

shall be half way between the anterior (rostral) surfaces of the iliac crests, with the Z axis passing through the midpoint between the suprasternal notch and the dorsal surface of the dorsal spine of the last cervical vertebra to this origin. The X and Y axes are mutually perpendicular to this Z axis.

For acceleration effects on the vestibular apparatus, the origin of the head axes shall be the midpoint between the external auditory meatuses (on the Y axis), with the X axis passing from the ventral medial margin of the nasal bones through this origin.

3. Angular accelerations which cause the heart to rotate (roll) to the left within the skeleton shall be specified by the $\dot{R}_X$ unit vector, representing radians/sec^2 about the X axis. Angular velocities in the same sense shall be specified by the $+R_X$ unit vector, representing radians/sec about the X axis. Similarly, $+\dot{R}_Y$ represents pitch down of the heart within the skeleton, and $+\dot{R}_Z$ represents yaw right of the heart within the skeleton.

4. Linear acceleration environments may be represented by the three acceleration components (along the G_X, G_Y and G_Z unit vectors) or by a resultant acceleration and the azimuth and altitude angles of the resultant with respect to the body axes. Azimuth is measured from the +X axis (to the back), with positive rotation clockwise as seen from above. Attitude is measured from the horizontal (XY) plane, with positive angles when in the hemisphere of the +Z axis (downward). Thus a man reclining in a chair tipped back 45° is experiencing 0.7 G_X and 0.7 G_Z, or 1G/0°, 45°.

5. Whenever rotations accompany linear accelerations, the reference point for the linear accelerations should be specified, and the time histories of the angular velocities and angular accelerations should accompany the time histories of the linear accelerations, to allow the computation of linear accelerations at other points. (Note: For complex motions, measurements vs. time of these 9 parameters (G_X, G_Y, G_Z, R_X, R_Y, R_Z, $\dot{R}_X$, $\dot{R}_Y$, and $\dot{R}_Z$) should be made. With improvements of instrumentation and the specifying of initial conditions, angular velocities may be adequately determined by the integration of angular accelerations, reducing the required channels to six, which may indeed be three pairs of linear accelerometers, with the accelerometers of each pair separated by a known distance. For the specification of vehicle flight paths and the determination of the displacement accelerations, the three Euler angles must also be determined, generally by integration of rate gyro signals.)

This physiological acceleration terminology is illustrated in figure 1. Figure 2 provides a comparison to the NASA vehicle acceleration terminology. It is suggested that the hybrid "normal load" terminology be dropped, to avoid the confusion possible, for example, when stating that a flight vehicle at constant velocity has a normal load of 1g. Let us restrict g to displacement acceleration, so that a vehicle at constant velocity is experiencing 0g. The crew then, if positioned transverse to the vehicle, would experience $1G_X$ if the vehicle is climbing vertically or $1G_Z$ if the vehicle is flying horizontally, and these would be the values read by accelerometers. An alternate name for the "physiological acceleration" G might be the "total reactive load," but the former term emphasizes that the pilot body axes are used, whatever his orientation to the vehicle.

It is necessary to here extend this terminology for the jostle acceleration situation. For aperiodic jostle motions of moderate duration, time histories of the nine linear accelerations, angular velocities, and angular accelerations should be given. Until more is known, allowing the use of body motion mathematical models,[42,67] empirical experience in the actual or simulated environment will be required to determine tolerance and control capabilities, if this environment is more severe than previously studied environments. For "stationary random" jostle motions, due for example to turbulence, six linear acceleration and angular acceleration power spectra, versus frequency, may in addition to the time histories be specified, summarized by "root mean squared" or RMS values. Note that the RMS values alone are not sufficient specification of the jostle; these must be accompanied by the power spectral frequency distributions. For vehicle responses and forcing functions of moderately similar frequency distributions, with acceleration power spectra peaks between 1 and 10 cycles per second, initial comparisons of the severity of jostle may be made on the basis of RMS values alone, but power spectra should be compared before final decisions of tolerability are made.

To emphasize the displacement aspects of the jostle environment, it is appropriate to represent the jostle by an RMS g, with the understanding that this is superimposed on a specified G, with a varying degree of transmission and phase shift into specific organs of the body, as represented by the mathematical models.

An Historical Review of Flight Simulation

The origins of flight simulation are obscure. Indeed, one of our anthropoid ancestors perhaps a million years ago probably ran about with his arms out - or jumped from a tree - and grunted, "Look, ma, I'm flying." The first pilots, having built their planes, sat in the seats and moved the controls, thinking through their flights - the beginning of "fixed base" or "static" flight simulation - then, as Stewart [81] puts it, "Men who had never been in the air in their lives before took their seat in the cockpit and opened the engine and took off to find out in a few desperate minutes whether they could fly or not." The Wright brothers (1903), J. C. Ellehamer (1906), Albert Santos-Dumont (1906), Charles Voisin (1907), Horatio Phillips (1907), Louis Blériot (1907), Robert Esnault-Pelterie (1907), Henri Farman (1907), L. Delagrange (1908), A. V. Roe (1908), Glenn Curtiss (1908), Samuel Cody (1908), Glenn Martin (1909) and others learned their flying in this way. In 1908, the first airplane flight with a passenger [40] was made by Wilbur Wright and Charles Furnas (May 14), and in 1908 the first airplane fatality[40] occurred during a training flight, with Orville Wright being seriously injured

and Lt. Thomas Selfridge killed (September 17). It is interesting to note that in April, 1962, we have yet to see our first two man rocket flight, now planned by the United States with the Gemini spacecraft and Titan launch vehicle for 1964.

In the summer of 1913, Adolphe Pégoud persuaded his employer, Louis Blériot, to allow him to attempt the first intentional upside-down airplane flight. He prepared by strengthening the airplane wings and tail, developing shoulder straps as an addition to the available lap belt, and trained by inverting the airplane on trestles and practicing operating the controls while experiencing the $-1G_z$, an early flight simulation with acceleration effects added. On September 1, 1913, Pégoud successfully flew upside down,[2,40,81] and subsequently (September 21) made full loops,[40] shortly after Nesterov looped in Kiev (August 20) an event much less widely known at the time. As Védrines said about Pégoud, "He taught the world how to fly" with his demonstrations of the maneuverability of aircraft.[81] We have yet to see the intentional looping of a rocket vehicle, that is, the demonstration of its full maneuver and emergency recovery capabilities, although I understand that an unmanned Atlas vehicle looped during thrust during an early development flight. This is quite analagous to the accidental inverted flight of H.R. Reynolds[48] in 1911 and of Pégoud's abandonned airplane following his parachute jump, which caused Pégoud to reason that with training, inverted flight could be treated as a recoverable rather than a "bailout" emergency flight condition. In the same way I look forward to the first intentional looping with thrust - not just tumbling with attitude control, although this should occur first - of the X-15 or Mercury or Gemini or Dyna-Soar, to break the bonds of viewpoint which still bind manned rocket flight to the precise dull mathematical non-adaptive essentially ballistic launch flight paths, and show that manned maneuvering rocket flight "design path" deviations are not a cause for aborting the flight.

In 1918, recognizing that many crashes were due to vestibular disorientation leading to "ear deaths"[52], the Ruggles Orienter was developed[3] to tumble pilots in all three rotational axes and introduce them to the range of their vestibular sensations, the anticedent of the "Multi-Axis Spin Test Inertia Facility" used to tumble the Mercury astronauts at rates up to 50 revolutions per minute about all three rotation axes and train them in the use of the Mercury attitude control equipment.[83] The Ruggles Orienter, with a covered cockpit, was used by William C. Ocker in early simulations of blind flight using the Sperry turn indicator, developed in 1917.[52] For more extensive field use, David Myers and William Ocker utilized the "turning chair with the instrument box", (fig.3), a Barany chair and a turn indicator, to train pilots in the distinction between their subjective feelings of rotation and their actual rotations.[52] The development of the Link trainer in the mid 1930's gave pilots a quite detailed "closed loop" pilot control moving base (or "dynamic") simulator, in which pilot control continuously modified cockpit instrument readings and simulator angular motions, limited in range in roll and pitch. In this same period, the first of the power driven human centrifuges were built[25], but their initial use was to provide pre-programmed rather than pilot controlled flight simulation accelerations. Further refinements in simulated vehicle characteristics awaited the development of the electronic computers following World War II.

The rocket flight pioneers, from Sanders (1928), von Opel (1929), and Warsitz (1939) to Milburn Apt (1956), who was killed in his first flight in the X-2 after reaching 2078 miles per hour, and indeed the rest of the proud line of test pilots in any new airplane up to this period, made their first flights in vehicles which could have quite different characteristics from any they had previously experienced. It was in this mid-1950 period that flight simulation began to catch up with the complexities of actual flight, so that now our X-15 pilots, our Mercury pilots, and apparently our Vostok pilots are intimately familiar with the handling qualities and flight loads of their vehicles under normal and emergency conditions before their first flights. Thus Robert White[89], after his X-15 flight to 217,000 feet, stated[89], "...the static simulations and the Johnsville centrifuge program contributed to very good training for these conditions so that the actual reentry did not result in a completely new or unexpected flight experience." Other moving base or dynamic flight simulators for the X-15 included a T-33 variable stability aircraft[7] and, of particular use, an F-104 landed with dive brakes extended to simulate the lift-drag characteristics of the X-15[30]

With the development of electronic analog computers after World War II, both computations of aircraft performance and the use of airborne electronic components to change control responses and improve auto-pilots were greatly expanded. An historic moving base, pilot controlled flight simulator of this period was the NACA Langley Aeronautical Laboratory "elevator seat", developed by William H. Phillips,[69,89] using an hydraulic analog of an aircraft response to control a seat moving vertically on rails in response to pilot control stick motions. By the mid-1950's, electronic control of aircraft responses was such that one airplane could have its responses modified to feel like another airplane, and the variable stability airplane was created, particularly by work at the NACA Ames Aeronautical Laboratory (for example, reference 58) and the Cornell Aeronautical Laboratory (for example, ref.55)

In 1948, William Phillips[68] had theoretically predicted the decreasing stability problem of short wing aircraft at higher speeds which came to be called the "roll coupling" problem. This and other stability problems associated with thrust misalignment and limited control effectiveness at high altitude were being faced by the rocket airplane pilots. Charles Yaeger vividly described[92] a flight on December 12, 1953: "You reach a maximum speed of 1650 miles an hour - twice the speed of sound! Your fuel exhausted then, you pull out through the same violent buffeting and shock into the transonic range again. Then suddenly you lose control of the ship....Your mind is half blank, your body suddenly useless, as the X-1A begins to tumble through the sky. There is something terrible about the helplessness with which you fall.

There's nothing to hold to and you have no strength. There is only your weight, knocked one way and another as the plane drops tumbling through the air. The whole inner lining of its pressurized cockpit is shattered as you're knocked around, and its skin where you touch is still scorching hot." Elsewhere[91], he added, "The airplane finally pulled about 11g's upward," (that is, $11G_z$)," tried to stabilize itself, and of course then started snapping and I was pretty well blacked out due to the high acceleration forces." The pilots were beginning to have flight experiences for which their previous training was inadequate.

The F-100 was the first production aircraft in which severe roll coupling was a problem, although the F-86 had a "pitch-up" characteristic under certain flight conditions[30]. First flown in May, 1953, the F-100 had already "become uncorked" and killed test pilot George Welch when in late 1954 it came to the NACA Flight Test Center, where the roll coupling problem was evaluated in flight[30].

At about the same time, a fixed base pilot controlled display simulator, with five degrees of freedom electronic analog flight mechanics computation was developed to seek solutions for the F-100 inertial coupling problem, under the direction of Leonard Sternfield at the NACA Langley Aeronautical Laboratory[80]. This simulator represented major refinements over the airplane procedures trainers of World War II in utilizing far more detailed computations of flight performance. Today we have many fixed base pilot controlled display flight simulators or procedures trainers, with electronic analog computation of detailed flight response and display changes as a consequence of pilot control motions. Many more "flights" can be made in the simulator than in the actual vehicle. Hazardous boundaries can be explored both from the safe and from the unsafe sides, to establish cockpit design, pilot technique, and training before confirmation of the data in actual flight. As a result of simulator and flight studies, a larger tail was put on the F-100, to reduce the inertial coupling problem.

Sir George Cayley had written in 1846 about the remaining problems of flight[40], "A hundred necks have to be broken before all the sources of accident can be ascertained and guarded against." Now pilot control simulation had reached a precision such that many sources of accidents could be identified and eliminated before the first flights. But the consequences of pilot motion could still not be adequately predicted. In the early 1950's, an autopilot was under development by the Bell Laboratories to allow automatic tail-chase tracking. This would subject the pilots to considerable jostle during which they might have to take over flight control. In 1952 the Navy Johnsville human centrifuge was dedicated. This centrifuge (figure 4) has a double gimbal system at the end of a 50 foot centrifuge arm, allowing three degrees of freedom of motion control. The first moving base flight simulation utilizing this gimballed centrifuge capability[34] determined that pilots experiencing the pre-programmed computed motion could tolerate the automatic interceptor control mode. Subsequently, computer refinements of the interceptor system were made[75], partly with the use of the U.S. Naval Air Development Center "Typhoon" analog computer, which had been developed in cooperation with the Moore School of the University of Pennsylvania.

On September 27, 1956, Milburn Apt was killed during his first flight of the X-2 rocket airplane, when he initiated a turn at too high a speed, and lost control[32]. He had not previously trained in this type of motion environment. In 1956, North American Aviation Inc. representatives, who had been awarded the development contract for the X-15 research airplane, approached the Navy to use the Johnsville centrifuge to determine the consequences of accelerations simulating those computed for the X-15 under certain extreme flight conditions (figure 5) on pilot control capabilities[16]. The first study, carried out in March, 1957[27,53], used pre-programmed cam control of the centrifuge. Pilot tolerance to the expected accelerations was confirmed, and aspects of cockpit design were studied. Fig. 5 shows one of the cam control runs.

But the consequences of pilot motion on vehicle control modifying subsequent motion and control could not be studied by pre-programmed centrifuge operation. A project was therefore initiated by John L. Brown and the author to control the centrifuge through the Typhoon analog computer, such that as the pilot moved his flight controls, the computer would continuously determine the changes of flight path, provide signals to the cockpit display instruments to show the changing flight conditions (as with the usual fixed base simulator), and at the same time provide drive signals to the centrifuge so that the pilot experienced the accelerations that he would have experienced if he had made the same control motions in actual flight.

With the active participation of the Aeronautical Computer Laboratory staff of the U.S. Naval Air Development Center, and of representatives from the Moore School, University of Pennsylvania, the first moving base pilot controlled motion and display flight simulation, with three degrees of freedom of centrifuge motion, was carried out in July, 1957[17,69] with the encouragement and participation of NACA, particularly of Leonard Sternfield and his stability and control group of the Langley Aeronautical Laboratory, this new technique was applied to two further studies of the X-15[27,90,19] with extensive participation by representatives of North American Aviation, Inc., in the final study. Over 600 centrifuge moving base flight simulations of the X-15 (and tens of thousands of fixed base simulations with the North American Aviation simulator) were made before the first actual flight. Fig. 6 shows one of the pilot-computer control runs.

With three X-15 aircraft, and over 50 flights, with altitude and speed advances made in small increments, centrifuge training at the beginning of the program, rather than on a flight by flight basis, has been adequate. With experienced pilots, with training maintained by periodic actual flights, detailed flight planning is adequately done using only the fixed base simulator. With vehicles going into orbit and beyond, initially one man will make less frequent flights. In this early "sling shot era"[23] of rocket travel in which most of the thrust is delivered in the first few minutes of

travel, design and emergency accelerations are high enough that training in the straining procedures [20], and in continuing control and display monitoring in spite of discomfort, should be maintained.

Over 1000 Navy centrifuge moving base flight simulations [18,83] of NASA project Mercury were carried out before the first flight, but it is not yet established what frequencies of the various moving base simulations should be used to maintain astronaut proficiency in this early period in which actual flights by a particular astronaut will be many months apart. Indeed, the actual flights will hopefully never involve the extreme emergency accelerations, for which training should also be maintained. Moving base flight simulation should remain a periodic task of this pioneering rocket era so that the astronauts, like their successful brothers of the pioneering airplane era, can step into their vehicles and fly them correctly the first time, and each time.

It is emphasized that the centrifuge cannot provide a perfect motion simulation of a flight vehicle, nor can any simulator which does not precisely follow the flight path of the vehicle of concern. Unconstrained flight, with six degrees of freedom of motion, may be analysed in terms of three linear acceleration and three angular acceleration time histories which must be matched for perfect motion flight simulation. The Johnsville centrifuge has independent controls for arm angular velocity (limited to 0 to 3.6 rad./sec., giving 20G, when the gimbals are used) and the inner (usually limited to +85° to -85°) and outer (limited to 0° to 90°) gimbal angle positions.

These limited range, three degrees of freedom of motion may be controlled to simulate the three linear accelerations (see for example figures 5 and 6) but at the expense of incorrect angular accelerations, although the position of the pilot can be regulated to at least provide critical angular accelerations in the same sense if not the same magnitude in comparing flight to centrifuge simulation [10]. Vehicle aerodynamics affects the simulation precision; with an approximate simulation of the linear accelerations, angular motions of the gondola exceeded those computed for the X-15 but were less than those computed for the Mercury vehicle.

For any moving base simulator, the importance of these "motion artifacts", or inaccurately simulated motions, must be judged, ideally by a growing body of "flight validation" experience [11, 89,78,45,41]. Under certain circumstances the artifact motion cues may provide an incorrect training experience or produce an artifact performance effect, leading to incorrect conclusions made on the basis of simulator experience alone. In the future, this validation experience should be used to establish psychophysiological equations representing reactions to motions. Computations of the six degrees of freedom accelerations of the flight vehicle can then be modified by these psychophysiological equations in controlling the limited degrees of freedom of the simulator, in order to minimize these artifact motion reactions and consequent artifact performance effects. This may involve a continuous change from linear acceleration to angular position or angular acceleration control, in order to provide the simulation which feels the most realistic within the capabilities of that simulator.

For certain aspects of training it may not be required to provide a precise simulation of the accelerations, so long as the simulated experience feels like - or the evoked performance is like or more than adequate for - the real flight experience. Thus after obtaining initial tolerance experience, repeated training for emergency conditions might be carried out for the most part at less than the emergency accelerations. Jostle control capabilities may be judged as adequate following demonstration of capabilities in a more severe albeit not precisely simulating jostle environment. It is just this capacity of the human to evaluate present experience in terms of remembered more stressful past experience that allows the greatest part of the training to be made on fixed base or very limited motion flight simulators. But the frequency that the moving base simulator or actual flight vehicle must be used in order to retain this "transfer" experience has not yet been evaluated.

The refinements and use in combination of other aspects of simulation, including low pressure [21], gas composition, temperature, [14] noise, out-the-window visual appearance, [13] prerun rest, food, and flight preparation activities, etc. must all be added to the cockpit configuration, control and display actions, and motions to minimize performance artifact due to simulator training. How soon will we be able to awaken an astronaut, transport him to a device, and "launch" him with such fidelity that he is unable to tell whether he is in real or simulated flight? With the costs of one manned rocket flight in this early period probably more than the costs of all pilot control simulation studies to date, simulation improvements which even slightly reduce the probability of real accidents are justified.

Moreover, now that we are developing refined simulation techniques, all future "environmental pioneering" [20] or the first entering by man of predicted new environments, should first be made in simulation so that consequences can be evaluated with help at hand. Many more people should study the effects of new environments in simulation than in an early period meet them in reality. Thus our "simulo-astronauts" [20], who only "go boom in black boxes" rather than in real flight, have a part to play in present day space pioneering. Today there are five people who have made five actual flights above 100 miles altitude; there are perhaps 50 people who have made perhaps 2000 "flights" in moving base simulators to a simulated orbital condition.

It is emphasized that this is a preliminary historical review of flight simulation, particularly of moving base flight simulation. The extensive development of pilot-computer controlled procedures trainers, and the increasing addition to these of at least some minimum cockpit motion, warrants a thorough documentation. Figure 7 diagrams the motion capabilities of a number of types of moving base simulation facilities. Reports of the Acceleration Panel [38,46,55] of the Armed Forces - National Research Council Committee on Bioastronautics, and of the informal international Acceleration Group continued under the

Chairmanship of Dr. James D. Hardy after the disbanding of the Committee on Bioastronautics, with one meeting[50] under the sponsorship of the National Academy of Science Space Science Board Man in Space Committee and the National Aeronautics and Space Administration, and with additional meetings under consideration, provide details about these facilities and programs.

In conclusion of this preliminary review it is suggested that at least the following aspects of a flight simulation should be specified when referring to it:

a) Identify the simulator used.

b) Is it a "fixed base" (stationary cockpit) or "moving base" (moving cockpit or pilot control area) simulation? The terms static or dynamic simulation should be dropped because of confusion by some as to whether these latter terms refer to the cockpit or display motions.

c) If it is a moving base simulation, give the number of degrees of freedom or independent control parameters of the motion.

d) Does it have pilot control? Does the pilot control (through the vehicle response equations) both the cockpit motion and the display changes, or does he ride a pre-programmed motion and control only the display? The previously used terms of closed loop and open loop simulation for these conditions should be dropped because of the confusion by some people, since in both cases display changes are in a closed loop relation to pilot control actions.

e) Give the number of degrees of freedom of the flight mechanics computation.

f) State additional aspects of the simulation, such as noise, low pressure, temperature effects, out-the-window display, pre-flight activities, etc.

Consider two examples: 1) The Martin-Baltimore fixed base pilot controlled display lunar landing simulator, with five degrees of freedom of flight mechanics computation, and 2) the Navy Johnsville centrifuge moving base three degrees of freedom of motion pilot controlled motion and display Mercury simulator, with six degrees of freedom of flight mechanics computation, and with pre-launch diet, rest, and preparation, flight noise, low pressure, and gas composition simulation.

Vibration Studies

No attempt will be made here to review the vibration literature[42,74], nor give the characteristics of vibration devices[85]. Early work with low amplitude (less than 1g RMS), moderate frequency (5-20 cps) devices with sine waveform vibrators is now being extended by devices capable of higher accelerations at lower frequences, having greater amplitudes of motion, and in some cases having complex waveform control systems. Vibration programs are particularly noted at the Naval Medical Research Institute, Bethesda[42]; the Aerospace Medical Laboratories, Dayton[42,94,73]; the Army Medical Research Laboratory, Fort Knox[74,72]; the Bostrom Research Laboratories, Milwaukee[51]; the Boeing Company, Wichita[65,66]; the Grumman Aircraft Engineering Co., Bethpage[54]; the Bell Helicopter Co., Fort Worth[50]; the U. S. Army Ordnance Tank Automotive Command, Detroit[70]; Ohio State University, Columbus[36]; and the RAF Institute of Aviation Medicine, Farnborough, England[47]; in addition to work at the U. S. Naval Air Development Center, Johnsville[59,88]; and the North American Aviation, Inc., Columbus[5], further described here. Russian[64,84,79], German[33], French[43] and Japanese[64] studies are noted.

Previous work has dealt primarily with effects of steady sine wave vibrations. For such vibrations of elastic (and biological) structures near resonance frequencies, large resonance amplitudes of the elastic structures can be built up for small amplitudes of the forcing structure. With "complex waveform" excitation, much of the vibrational energy will be at frequencies other than those of resonance, resulting in a lower amplitude of the elastic structure than if all of the energy were at a resonance frequency. On the other hand with complex waveform excitation, partial resonances of adjacent structures at different frequencies can occur simultaneously. With the expected non-linearities of biological interactions, excitation with complex waveform giving multiple resonances might produce more damage than sine wave excitation. In addition, with complex waveform excitation, individual acceleration peaks show a variation from the steady sine wave amplitude from much larger to much smaller, with the former possibly producing more damage.

Previous work with sine wave vibrations in the 1 to 10 cps region had indicated a considerable spread in peak accelerations which subjects refuse to tolerate, from about a 0.3 g_z peak[42] (or 0.2g_zRMS) for 5 to 20 minute exposures with moderate motivation to about a 2g_z peak[94] (1.4g_zRMS) in the frequency range of 4 to 8 cps for a few seconds exposure with greater motivation. Parks and Synder[66] report the "alarming" level of sine waveform vibrations as 0.4 to 0.9G (0.3 to 0.6g_z RMS) at 1 cps, and 0.3 to 1.05G (0.2 to 0.7g_z RMS) at 5 cps, for different subjects. On the other hand, single acceleration events of even 10G_z and higher at a frequency of 1 cps or higher are quite tolerable. How often could these larger amplitude events be repeated in a given time for the motion still to be acceptable, if they occurred with a complex waveform, hence with periods of rest between the high acceleration events? With the general increase in blood pressure and pulse rate following a moderate acceleration event, tolerance to a later acceleration event might for certain conditions of time and magnitude be increased by previous exposure to a "conditioning" acceleration event.

Vibration can produce damage. Riopelle et al[72] had one monkey die in one hour and two survive eight hours of 10 cps, 0.25 inches double amplitude sinusoidal motion, or 0.9 g_z RMS. At 0.5 inches double amplitude, one monkey died after 7 hours of vibration, one died the next day, and two survived 8 hours of vibration (1.8 g_zRMS measured at the seat). Severe chest pain[88] has developed in some humans after 25 seconds of sine waveform vibration at a double amplitude of about 0.15 inches in the frequency range of 10 cps (about 0.5 g_zRMS) and

and White himself[88], after 15 minutes without pain at 20-25 cps with a double amplitude of 0.17 inches (about 2.4 g_zRMS) later observed blood in the soft stools. Medical monitoring is recommended for environmental pioneering studies. It is emphasized that "tolerable" and "damaging" levels of vibration will vary depending on the nature of the body support-restraint system[73].

Performance is also affected by vibration. With a sine waveform motion of frequency below 10 cps., the pilot can anticipate or brace again the uniformly repeated changes of acceleration in making his control motions. With complex waveform motion on the other hand the phases and amplitudes of successive acceleration events are not uniformly repeated, and involuntary pilot control motions would expectedly increase.

Brief studies were therefore initiated on the Johnsville centrifuge and the North American Aviation "G seat" to determine the tolerance and performance decrement effects of the severe complex waveform vibrations of concern.

A "Chronological Bibliography on the Biological Effects of Vibration", by Carl Clark and Keith McCloskey[26], similar in format to the "Chronological Bibliography on the Biological Effects of Impact"[22,50], is in preparation.

Jostle with the Navy Johnsville Centrifuge

Centrifuge jostle is obtained by varying arm and gimbal angular velocities, using a "white noise" electrical source shaped electronically to give the desired G_z power spectrum. These variations must be precisely controlled[28] in amplitude and phase in order to simulate particular time histories of the three linear accelerations. The simulation may be described as follows: moving base Navy centrifuge jostle simulation, with three degrees of freedom of preprogrammed jostle motion and pilot controlled maneuver motion, with pilot controlled display and three degrees of freedom of flight mechanics computation.

As shown in figures 5 and 6, it is difficult to eliminate the G_x acceleration artifacts. For large and rapidly varying linear accelerations, the angular motions of the centrifuge gondola are also large, as illustrated in figures 8, 9, and 10, for a $5G_z$ haversine waveform of 10 second period. These angular motion artifacts can be nauseating, producing performance artifacts. The centrifuge is most useful for simulating flight accelerations above perhaps 3G, for variations at higher accelerations require smaller gimbal motions.

On the other hand, flight jostle generally involves angular as well as linear motions. Jostle with the three degrees of freedom of control of the centrifuge does indicate some of the restraint and control problems which might not be apparent on a vertical accelerator with only one degree of freedom of motion. If low amplitude jostle is considered acceptable on the centrifuge, it would probably also be acceptable in the less severe actual flight conditions.

Although $-G_z$ accelerations can be provided on the centrifuge by tipping the subject's head "outboard", rapid oscillations from $+G_z$ to $-G_z$, passing smoothly through 0G, can only be provided at points away from the center of the gondola, using rapid gondola rotations out from under the subject to give brief moments of true 0G or $-G_z$. The potential of this technique is illustrated in the bottom tracing of figure 11. Although the centrifuge arm begins to have amplitude loss near 1 cps., the gimbals can follow motions to about 5 cps.

Under usual conditions, when the computer commands a resultant acceleration of less than 1G, the centrifuge simply stops. In order to avoid this continual starting and stopping, a "bias acceleration" of 2 or 2.5G was utilized, a technique first suggested for use at the Johnsville centrifuge by the NASA Ames group (B. Creer, M. Sedoff, G. Rathert, R. Wingrove, et al.). Hence with a jostle or pilot maneuver input, the centrifuge would speed or slow about the 2G level. This provides acceptable simulation of low amplitude jostle, but at higher amplitudes the very important non-linear effects of lifting out of the restraint system when passing through 0G are not provided on the centrifuge except with the offset seat position[79]. A vertical accelerator provides a better simulation of flight jostle than the present Johnsville centrifuge.

A brief examination of tolerance to acceleration events repeated within seconds was made. Three subjects were used. One blacked out with a $4.2G_z$ haversine of 30 second period and the other two greyed out at a $4.0G_z$ peak. The first again experienced blackout with the first cycle of a $4.0G_z$ haversine of 15 seconds period but had clear vision for the second cycle. The other two, with dimmed vision on the first cycle, had clearer vision on the second. There is a conditioning effect of an acceleration event.

With a $4.0G_z$ haversine of 10 seconds period, the first subject had a visual dimming on the first and third cycles; a fatigue or decompensation effect may be setting in. The second subject had a dimming on the first cycle, but clear vision on the next two cycles. With a $4.8G_z$ haversine of 5 seconds period, the first subject had no visual dimming for 6 cycles, and the second subject had a similar experience with $4.5G_z$ peaks.

Centrifuge response capabilities limited study with higher haversine peaks of shorter periods, although the Johnsville centrifuge has been used to show human tolerance to a single $15G_z$ "spike" of 1.75 seconds width[4], with the gimbals prepositioned.

A curve showing RMS g tolerance versus frequency would therefore rise from the 2G peak for 24 hours point[24] toward the $4G_z$ peak blackout level to some higher G_z value for repeated acceleration spikes near about 1 cps (with the maximum tolerance expectedly - on a teleological basis - in the 0.5 to 1 cps range of walking) then falling again as the torso resonance frequency (4-8 cps) is approached, then rising again at higher frequencies of the seat motion. As specific points, the first subject, discussed about, experienced a $2.5G_z$ peak haversine waveform ($1.2g_z$RMS oscillating about $1.75G_z$) of 3 second period for 5 minutes with only moderate post-run nausea, and the second subject experienced a 1.6 G_z peak haversine waveform ($0.2g_z$ RMS

oscillating about 1.3G_z) of 2 second period for 5 minutes with only slight post-run nausea.

It is interesting to note that head motions in these multiple rotation jostle environments did not seem from brief observation to be as disorienting as head motions in a steady rotation situation. In the latter case[24], for a body rotation of 10 rad/sec (2G centrifugation) head motions such that the vector product of the head angular velocity and the body angular velocity exceeded 0.06 rad^2/sec^2 were discernible as a Coreolis illusion[44], and (in brief observations with one subject) if the vector product exceeded 0.6 rad^2/sec^2 nausea developed. In the jostle situation, perhaps the short duration of any particular rotation rate or perhaps the lack of distinguishability of a rotation illusion from an actual rotation a moment later seems to suppress the nausea level, although eventually centrifuge jostle becomes nauseating.

Jostle with the North American Aviation "G-Seat"

A moving base simulation of flight jostle was carried out in June, 1960, with the North American Aviation, Inc. "G-seat" (figure 12) with one degree of freedom (vertical acceleration) of preprogrammed jostle motion, pilot controlled maneuver motion in G_z, and pilot controlled display (roll and pitch changes), with three degrees of freedom of flight mechanics computation. Fig. 13 shows the frequency response capabilities of the G-seat, and Fig. 14 shows the power spectrum[31, 56] of the jostle motion of concern. The power spectral density ordinate of this figure is given in units of sec^{-1}, representing density in units of g^2 per cps normalized by the square of the RMS jostle, in g units, times a constant with the value of 20 sec. Dimensionally:

$$\frac{\Phi}{(KgRMS)^2} \qquad \frac{g^2\ sec}{(cycles)\ sec^2 g^2} = sec^{-1}$$

In actual flight[57], jostle level (represented by an RMS g level, and also possibly a changing power spectrum shape) will vary with time[31]. Indeed, if this change is too rapid (less than perhaps 20 sec. of fairly consistent jostle) the power spectrum description of jostle is not adequate, for this description assumes a "stationary random" process independent of phase relationship. In such cases, it is urged that the entire time histories (ideally of three linear accelerations, three angular accelerations, and three angular velocities) be given. Moreover, until the power spectrum description is more familiar to biologists, representative actual acceleration time histories should be presented even in cases in which the power spectrum description is adequate.

There are cases in flight in which the complex wave form jostle is not a "stationary random" process, with continuously ("randomly") varying amplitudes and phase relationships of the different frequency components, but is a true periodic complex waveform. It then has constant phase relationship and amplitudes of the different frequency components, suitably represented by a Fourier analysis of these amplitudes and phase relationships, often with narrow band resonances of particular vehicle structures clearly distinguishable.

As at Johnsville, the jostle command signal was generated by shaping a "white noise" electric source with a filter of proper transfer function. In addition, the pilot operated a usual center control stick in pitch and roll, with pitch commands affecting through the vehicle response equations both the G-seat motion and display changes, and roll commands affecting only the display.

Because of the limited travel of the G seat (± 5 feet for regular use), maneuver loads would initially be felt, but would be rapidly "washed out," with the G seat having a bias drift back to the center position. This can be seen in the lower part of Figure 15, in which the command channel shows maneuver loads, but the response channel does not. Indeed with large maneuver load commands it was possible to briefly bump the G-seat against its top or bottom limits, as shown in Figure 15.

The RMS g_z values used in this report are the expected response values. Unfortunately, equipment was not available to determine the actual RMS accelerations. The measured seat acceleration time histories are however quite reasonable for these expected response values, with peaks of 4 times the RMS g value every few seconds for example. The panel accelerometer values are means of many readings which, of course, represent maximum seat response maneuver plus jostle loads during an entire run. These maximum values may not be observed during a particular brief time period of an accelerometer recording (for example, Figures 15 and 16).

The pilot wore a Navy torso restraint system, with attachments at the shoulders and sides of the hips. His primary display was a five inch face oscilloscope. His task was to follow a command line moving in response to three sine waves with 44, 19, and 13 second periods with relative amplitudes of 6 to 4 to 2. Pilot anticipation of the task requirements were provided by two additional scope lines, of decreasing length, which indicated the task positions one and two seconds later. Vehicle roll was indicated by another line on the scope. The task was to track in pitch and hold roll 0, correcting for any involuntary or unintended inputs in roll.

A green light above the panel oscilloscope was on if the tracking error was less than a relative amplitude of 1 (i.e. 1/12th of the task range); the time this light was on during a typical 100 seconds of jostle was recorded. A red light came on if the tracking error exceeded about a relative amplitude of 10, i.e. 5/6 of the task range; the number of these events were counted. See the classified reports for further details of these tasks.

The pilots tracked without motion, then with maneuver loads only, then with increasing levels of jostle of 0.15, 0.35, 0.50, and 0.70 g_z RMS. Subsequent exposures with the same subject did not repeat this entire set. Fourteen subjects made 70 moving base runs; this can only be considered as a preliminary study. Three runs were of longer duration: 0.35g_z RMS for 15 minutes, 0.50g_z RMS for 5 minutes, and 0.35g_z RMS for 30 minutes (Solliday).

Complex Waveform Jostle Tolerance

For the acceleration power spectrum used (Figure 14), the jostle was not uncomfortable until the spinal axis load went below $0G_z$, and the pilots began to lift out of their seats. Table I summarizes the jostle levels used, and

Table 1: Jostle Conditions

Computed Jostle Accelerations	Measured Cockpit G Meter	Pilot Comment	Tolerance
0	0 to $2G_z$	Maneuver loads only.	A pleasure.
$0.15g_z$ RMS	0 to $2.5G_z$	Mild turbulence.	Not uncomfortable.
0.35	-1.2 to $4.0G_z$	Very severe turbulence.	Fatigue limiting in 30 minutes.
0.50	-2.5 to $5.0G_z$	Never more than one of these jolts in flight.	Not limiting in 5 minutes.
0.70	-3.0 to $5.5G_z$	Still flying.	Not limiting in 100 seconds.

their effects. Following $0.35g_z$ RMS, the panel accelerometer with maximum and minimum needles recorded -1.2 to $4.0G_z$. The torso restraint system was inadequate, even with very tight straps, to hold the subject in his seat. The pilot would therefore begin to "splint" in place, pushing on the rudder pedals to force the shoulders against the seat back and reduce body "slap" in the restraint. To the experienced pilots the $0.15g_z$ RMS level felt like flying a fighter aircraft in mild turbulence, and the $0.35g_z$ RMS level felt like flying in very severe turbulence. Higher levels, except for perhaps single jolts had not been experienced by the pilots in flight.

These higher levels could however be tolerated. The $0.5g_z$ RMS level, with accelerometer swings from -2.5 to $5.0G_z$, required vigorous splinting. Some subjects also forced their helmets against the seat back, to reduce head "slap" which would expose the head to far higher accelerations than the seat. Other subjects, by tipping their heads forward and with perhaps faster neck reflexes, did not attempt to lock their heads in position until the $0.7g_z$ RMS level.

For these highly motivated subjects doing a tracking task which held their entire attention, "tolerance" of these jostle levels seemed essentially fatigue limited. Even the $0.70g_z$ RMS level, with accelerometer swings from -3.0 to $5.5G_z$, had as its primary discomforts the head and body "slaps" due to motion with respect to the seat and the fatigue of trying to splint or lock the body in place, not limiting in 100 seconds. One pilot tolerated the $0.50g_z$ RMS level for 5 minutes and could have gone longer. Another subject tolerated $0.35g_z$ RMS for 15 minutes and could have gone longer. Another subject, after 30 minutes at $0.35g_z$ RMS, was glad to stop, and felt that this duration was close to his fatigue limit unless he had extreme motivation.

Two subjects experienced diarrhea during the experiment, attributed to other causes. One subject experienced a "pulling" sensation under the seventh rib on the left side from 30 minutes (delayed onset) to 5 hours after a set of jostle runs. Several subjects experienced brief headaches during their runs, attributed to helmet contact against the cockpit. The G-seat runs were neither nauseating nor disorienting (although the centrifuge jostle runs often were). Microscopic examination of the urine indicated no blood due to the jostling.

It was felt that tolerance could be extended by using an improved restraint, as has been shown[73], perhaps using inflated air bags[1,36] to allow rapid tightening of the restraint just prior to use. A foam restraint system (Figure 16) is also under development[37].

The tolerance observed in this experiment is commensurate with other experience[42,12] that above 0.3g humans are increasingly uncomfortable, with different "tolerance" values explainable perhaps in terms of differences of task complexity and motivation. Brief observation suggests that $0.3g_z$ RMS of complex waveform is less comfortable than $0.3g_z$ RMS of a low frequency sine waveform, because of body and head "slap" problems. A systematic comparison program would be appropriate.

Performance

Figure 17 summaries the tracking performance of the nine pilots. They experienced the low jostle levels first; they learned to splint in place, minimize involuntary control inputs, and not be startled or unduely distracted by the jostle experience. Learning "plateaus" were probably not reached however.

The pilot with the best tracking was able to stay within the loose error tolerance even at $0.5g_z$ RMS but his time within the tight error tolerance was cut from 54 to 26%. The mean scores on the other hand show, at $0.5g_z$ RMS, errors beyond the loose tolerance about every 5 seconds and time within the tight tolerance cut from 32 to 13%. The pilot, experiencing accelerations in the range of -2.5 to $5.0G_z$, could not be said to be flying with precision, as he experienced considerable involuntary control input in both roll and pitch.

The display, with its four moving lines on the scope face, was not always readily interpreted by the pilots, although "double vision" due to vibration[59] did not occur. Hence during severe jostle, decision delays expectly increased (although not directly measured) and voluntary control action in the wrong direction increased. The pilots found the panel lights indicating tight and loose tolerance error helpful in making control decisions.

It would be appropriate to develop this use of lights to reduce the requirement for clear vision by the pilot. In a severe motion environment the display should be useable even if the pilot is jouncing within the cockpit. An ideal display for a previously planned flight path would provide him with indications of the optimum control for him to make to follow the desired path, with a one to one relationship, without crosstalk, of the display parameter and the particular control parameter required.

The task used was severe, requiring constant attention by the pilot. In a number of cases, questions to the pilot during jostle, or statements to him such as "The movie camera is starting now" led to his developing large flight path deviations. Questions which required repeating back numbers in the answer were answered incorrectly (at 0.35g_z RMS), due to the necessary task concentration. Glances to other parts of the instrument panel or outside the simulator often preceded large flight path deviations. Pilot control during severe jostle is jeopardized, and requires his full attention.

Control

Figure 18 shows typical pilot pitch and roll controls. At 0.35g_z RMS, involuntary inputs are not obvious to the pilot. At 0.5g_z RMS involuntary inputs become obvious. In the lower part of Figure 18, involuntary pitch and particularly roll inputs are shown accompanying acceleration peaks. For G_z motions, involuntary roll control becomes especially troublesome when a jostle peak occurs during a roll input, and hence when the weight of the stick acts with a moment arm about its floor pivot. In the jostle environments particularly, abrupt control "pulses" are frequently terminated with overshoot in the opposite direction (Figure 19).

A side arm controller[15] would probably give less involuntary control input. A "digital control" (Figure 20) proposed by the author[18] could be used with even greater certainty of making definite control signals in the presence of jostle "noise". Push button operation generates a signal of precise magnitude precisely terminated without overshoot when the button is released (Figure 19). This digital or switch control is particularly useful when the pilot is providing stability augmentation, damping oscillations at 0.3 to 3 cps. Control gain is changed by a toggle switch on the controllers. One of these also has trim knobs for providing low frequency analog control.

Comparison of the Effects of Different Jostles

It would be desirable in specifying a random jostle for biologists to give not only the RMS g level and the acceleration power spectral density but also to give a more readily recognized distribution of acceleration peak heights, in the form of the standard deviation of peak heights, and some "relative jostle biological effectiveness" frequency weighting function to allow the comparison of the biological effects of jostles with different frequency components. This "relative jostle biological effectiveness" (RJBE) weighting function is analogous in concept to the "relative biological effectiveness" concept used in high energy radiation biology, and has analogous limitations that the effects with different jostle frequencies, or different radiations, may not be comparable. One must specify the effect, such as lethality, nausea, body core temperature elevation, tracking control performance, visual resolving power, etc.: the relative jostle biological effectiveness functions vs. frequency will presumably differ for these different effects. The "tolerability" RJBE function for a seated man with lap belt and shoulder straps would have the general dependence on frequency discussed in the Vibration Studies section, with a minimum at the body resonance frequency range of 4-8 cps.

For an acceleration power spectrum Φ_f, vs. frequency f,

$$\text{RMSg} = \left[\int \Phi_f \, df\right]^{\frac{1}{2}}$$

We may then define

biological effect RMSg $= \left[\int \Phi_f RJBE_f \, df\right]^{\frac{1}{2}}$

using the appropriate relative jostle biological effectiveness frequency function for the particular effect of concern, and

the biological effect power spectrum $= \Phi_f RJBE_f$

We may also define

total spectrum RJBE $= \int \Phi_f RJBE \, df / \int \Phi_f \, df$

which experiment may show is adequately represented by

$$\text{total spectrum RJBE} = \frac{\text{RMSg at 5 cps}}{\text{RMSg of the jostle}}$$

for those RMS g values required to give the same biological effect.

Note that for two different acceleration power spectral sources, when $\int \Phi_1 RJBE \, df = \int \Phi_2 RJBE \, df$, that is when the biological RMS g's are equal, the same biological effect should be observed. Equations of this form must be adjusted to give the most suitable relative jostle biological effectiveness functions; it is expected that the use of the 5 cps sine wave as a standard may not be adequate for many biological effects.

Until further information is available, a preliminary tolerability RJBE$_f$ function might be based on one tenth of the reciprocal of the vibration tolerance for military aircraft[39, 42], extended in frequency range, hence with the following values:

Table II

Frequency	Preliminary Relative Jostle Biological Effectiveness
0 - 0.2 cps	0.07
0.2 - 1.0 cps	0.07 increasing to 1.0*
1.0 to 20 cps	1
20 - 100 cps	1.0 decreasing to 0.07*
> 100 cps	0.07

*With linear RJBE changes when plotted as log RJBE vs. log frequency.

Further work must establish the improved form of this function. As noted above, in the 0.2 to 1.0 cps range, acceleration tolerance may actually show a peak, or RJBE may decrease below 0.07 before returning to 1. Between 1 and 20 cps a curve more accurately indicating body resonance may be required. Likewise at some frequency above 100 cps, the tolerance RJBE presumably further decreases, since transmissibility decreases, although skin damage rather than deeper internal discomfort becomes the basis of tolerance estimation.

Unfortunately we are still in an early period of acceleration measurement in which measurements must be analyzed with caution because of the frequency characteristics of the transducers. Certain accelerometers will not respond to frequencies above 20 cps, and others will not respond to frequencies above 30 cps, for example. One can conceive of a "biological acceleration" meter, with a relative jostle biological effectiveness weighting function filter. It can be seen that accelerometers recording the frequency range of 0-20 cps give a better measure of biological tolerance

than those recording just frequencies above 20 cps. Using the "biological acceleration" meter, one could then determine a biological RMS g and a standard deviation σ of this RMS g. Then 99.7% of the acceleration peaks important to the biological effect of a time history would fall within the range of the biological RMSg $\pm$ 3σ. This acceleration description may be used with greater ease than one which requires interpretation in terms of a power spectrum. However, until the more precise form of the relative jostle biological effectiveness function can be determined, RMS g values should be specified with an associated power spectrum.

A report by Parks[65] comparing tracking performance while experiencing complex waveform or sinusoidal vibrations suggests some of the ideas developed in this section. He says, "In summary, there is evidence that a transfer function can be found and that data derived with sinusoidal data may be extended to complex patterns of random vibration.....Results of this experiment show that the physical description which could serve this purpose may be a combination of frequency and some factor related to RMS." (i.e. RMS g). Buchmann[12] also reviews the problem of establishing a mathematical means to compare the biological effects of different jostle environments.

Conclusion

This preliminary study has indicated that pilots can tolerate for at least 100 seconds and carry out some useful control up to at least a jostle level of $0.7g_z$RMS. Training in these environments in techniques of bracing to reduce body and head "slap" and reducing involuntary control input is recommended for these expecting to enter such environments either during normal or emergency operations. Improvements of restraints, displays, and controls could extend man's usefulness in these environments.

Summary

Problems of terminology of acceleration and flight simulation are reviewed, with a preliminary historical review of particularly moving base flight simulation. The capabilities and limitations of the Navy Johnsville human centrifuge and the North American Aviation (Columbus) "G-seat" for jostle simulation are presented; the latter is more realistic.

For jostle acceleration power spectra peaking near 1 cps, limited flight control could be maintained at a jostle level of $0.35g_z$RMS, equivalent to aircraft response to very severe turbulence, with panel accelerometer readings between -1.2 and $4.0G_z$, maintained for 30 minutes. A jostle of $0.70g_z$RMS, with panel accelerometer readings between -3 and $5.5G_z$, could be tolerated for at least 100 seconds, although with severe but far from complete control loss. For these jostle conditions, tolerance was fatigue limited, due to muscular efforts to stay in place in the cockpit. The torso restraint is inadequate for jostle conditions considerably more severe than those experienced in present aircraft.

Potential developments of restraints, displays, and controls for use in severe jostle environments are noted. A "relative jostle biological effectiveness" concept is suggested for test as a means of comparing the biological effects of jostle environments with different frequency components.

Bibliography

1. Angel, Chester, Bloetscher, Fred, Kerber, Harold E., and Gold, Armand J.: Proposed program to develop techniques for simulation of physiological sensations of reentry and landing of boost-glide vehicles. Report TAP-8935, Goodyear Aircraft Corp., Akron, Ohio, 21 December 1959.

2. Anon: Turning somersaults with an aeroplane: The remarkable exploit of Adolphe Pégoud. Sci. Amer. 109:240, 1913.

3. Anon (but edited by Isaac Jones[52]): Air Service Medical Manual. War Department, Air Service Division of Military Aeronautics, Washington, D. C., 1918.

4. Beckman, Edward, Duane, Thomas, Ziegler, J.E., and Hunter, Howard: Human tolerance to high positive G applied at a rate of 5 to 10 G per second. Report NADC-MA-5302, U.S. Naval Air Development Center, Johnsville, Pa., June, 1953

5. Besco, Robert O.: The effect of cockpit vertical accelerations on a simple piloted tracking task. Report No. NA-61-47, North American Aviation, Inc., Columbus, Ohio, 13 April 1961.

6. Borshchevskiy, I.Ia., Koreshkov, A.A., Markaryan, S. S., Prebrazhenskiy, V. V., and Terent'yev, V. G.: Vliianie na organizm cheloveka vibratsii nekotorykh tipov sovremennykh i samoletov. (Effects of vibration of certain types of contemporary helicopters and airplanes on man. Voyenno Meditsinskiy Zhurnal 74-77, 1958. (Translation JPRS/NY-406/CSO-1374/4)

7. Breuhaus, W.O.: Simulation of the X-15 using the T-33 Variable Stability Airplane. Presented to the Panel on Acceleration Stress of the Armed Forces - Nation Research Council Committee on Bioastronautics, NASA Ames Research Center, March, 1961. Cornell Aeronautical Laboratory, Buffalo, N. Y., 1961.

8. Brown, B. Porter, Johnson, Harold I., and Mungall, Robert G.: Simulator motion effects on a pilot's ability to perform a precise longitudinal flying task. NASA Technical Note D-367, National Aeronautics and Space Administration, Washington, D. C., May 1960.

9. Brown, B. Porter, and Johnson, Harold I.: Moving cockpit simulator investigation of the minimum tolerable longitudinal maneuvering stability. NASA Technical Note D-26, National Aeronautics and Space Administration, Washington, D. C., September, 1959. See also NASA Memorandum L-405, of the same title.

10. Brown, John L.: Subjective preference among different modes of closed loop operation of the centrifuge for flight simulation. NADC Letter Report NM 11 02 12.6, serial 9535, U.S. Naval Air Development Center, Johnsville, Pa., 9 December 1957.

11. Brown, John L., Kuehnel, Helmut (NASA), Nicholson, Francis T., and Futterweit, Adolf: Comparison of tracking performance in the TV-2 aircraft and the ACL computer/AMAL Human Centrifuge simulation of this aircraft. Report NADC-MA-6016/NADC-AC-6008, U. S. Naval Air Development Center, Johnsville, Pa., 7 November 1960.

12. Buchmann, E.: Criteria for human reaction to environmental vibration on Naval ships. Proceedings of the 1962 Meeting, p. 119-128, Institute of Environmental Sciences, Mt. Prospect, Ill., April 1962.

13. Buddenhagen, T. F., and Wolpin, M.P.: A study of visual simulation techniques for astronautical flight training. (Bell Aerosystems Company, Buffalo, N.Y.) WADD Technical Report 60-756, Aerospace Medical Laboratory, Wright-Patterson Air Force Base, Ohio, March, 1961.

14. Burgess, Benjamin F.: The effect of temperature on tolerance to positive acceleration. Aerospace Med. 30:567-571, 1959.

15. Chambers, Randall M.: Control performance under acceleration with side-arm attitude controllers. Report NADC-MA-6110, U. S. Naval Air Development Center, Johnsville, Pa., 27 November 1961.

16. Clark, Carl C.: Acceleration problems associated with projected research aircraft. Project TED ADC AE-1406, Letter Report Serial 1589, U. S. Naval Air Development Center, Johnsville, Pa., February, 1957.

17. Clark, Carl C.: Centrifuge simulation of flight: Open loop computer control and closed loop subject-computer control of the human centrifuge accelerations. Letter Report, Project TED ADC AE 1410, U. S. Naval Air Development Center, Johnsville, Pa., September, 1957.

18. Clark, Carl C.: Navy Centrifuge Simulation of the NASA Project Mercury Vehicle, Program 1, August, 1959. Report Serial 0890, U. S. Naval Air Development Center, Johnsville, Pa., October, 1959. See also Clark, Carl C.: Technical Film Report Med 5-60 on Navy Centrifuge Studies for NASA Project Mercury, Program 1, August 1959. Report NADC-MA-16014, U. S. Naval Air Development Center, Johnsville, Pa., 1961. (Dr. Randall Chambers became Project Officer for the three subsequent Navy centrifuge-Mercury programs.)

19. Clark, Carl C.: Motion pictures, scene descriptions, and safety procedures of Navy centrifuge simulations of the X-15 research aircraft. Report NADC-MA-16126, U. S. Naval Air Development Center, Johnsville, Pa., July, 1961.

20. Clark, Carl C.: Acceleration and Body Distortion. Engineering Report 12138, Martin Company, Baltimore, Md., November 1961.

21. Clark, Carl, and Augerson, William: Human acceleration tolerance while breathing 100 per cent oxygen at 5 psia pressure (Abstract). Aerospace Med. 32:226, 1961.

22. Clark, Carl, Faubert, Denis, and Cooper, Bruce: A chronological bibliography on the biological effects of impact. Engineering Report 11953 (Revised), Martin Company, Baltimore 3, Md., April, 1962. This extends ER 11953 (27 September 1961) and ER 11953 Appendix (22 November 1961).

23. Clark, Carl C., and Gray, R. F.: A discussion of the restraint and protection of the human experiencing the smooth and oscillating accelerations of proposed space vehicles. In Bergeret, P., editor: Bio-Assay Techniques for Human Centrifuges and Physiological Effects of Acceleration, AGARDograph 48, Pergamon Press, New York, 1961. See also Report NADC-MA-5914, U. S. Naval Air Development Center, Johnsville, Pa., 29 Dec., 1959.

24. Clark, Carl, and Hardy, James D.: Gravity problems in manned space stations. Proceedings of the Symposium on Manned Space Stations. Institute of Aerospace Sciences, New York, April, 1960. See also Report NADC-MA-6033, U. S. Naval Air Development Center, Johnsville, Pa., March, 1961.

25. Clark, Carl C., Hardy, James D., and Crosbie, Richard J.: A proposed physiological acceleration terminology, with an historical review. In Human Acceleration Studies, Publication 913, National Academy of Sciences, Washington, D. C., 1961.

26. Clark, Carl, and McCloskey, Keith: A Chronological bibliography on the biological effects of vibration. Engineering Report 12402, Martin Company, Baltimore 3, Md., in preparation, 1962.

27. Clark, Carl C., and Woodling, C. H.: Centrifuge simulation of the X-15 research aircraft. Report NADC-MA-5916, U. S. Naval Air Development Center, Johnsville, Pa., December, 1959. This summarizes the three X-15 centrifuge programs and includes the references to interim reports.

28. Crosbie, Richard: Utilization of a system of gimbals on the human centrifuge for the control of direction of acceleration with respect to the subject. Report NADC-MA-5608, U. S. Naval Air Development Center, Johnsville, Pa., August 1956.

29. Crosbie, Richard, and Hall, Robert: Explicit expressions for the angular accelerations and linear accelerations developed at a point off center in a gondola mounted within a three gimbal system on the end of a moving centrifuge arm. Report NADC-MA-6034, U. S. Naval Air Development Center, Johnsville, Pa., October, 1960.

30. Crossfield, A. Scott, and Blair, Jr., Clay: Always Another Dawn: The Story of a Rocket Test Pilot. The World Publishing Co., Cleveland, 1960. See also the Research Airplane Committee Report on the Conference on the Progress of the X-15 Project. National Aeronautics and Space Administration, Washington, D. C., November, 1961.

31. Curtis, Allen J.: Concepts in vibration data analysis. Chapter 22, Volume 2, in Harris, Cyril M.; and Crede, Charles E., editors: Shock and Vibration Handbook. McGraw-Hill Book Co., New York, 1961. See also many other chapters of this excellent work.

32. Day, Richard, and Reisert, D.: Flight behavior of the X-2 research aircraft. Technical Memorandum X177. National Advisory Committee for Aeronautics, Washington, D. C.

33. Dieckmann, D.: Ein mechanisches Modell für das schwingungserregte Hand-Arm System des Menschen. (A mechanical model for the human hand-arm system during vibration). Zeitschrift angew. Physiol 17:125, 1958.

34. Ecker, P., Hunter, Howard N., and Crosbie, Richard J.: The effect of acceleration forces on a pilot during automatic interceptor attack. Report TED-ADC EL-43018, Serial 0919, U. S. Naval Air Development Center, Johnsville, Pa., 2 June 1953.

35. Fournier, E.: Effets pathologiques des sons, ultra-sons, bruits, et vibrations industrielles. (Pathological effects of sounds, ultra-sounds, noise, and industrial vibrations. Bull. méd. Paris 71:ii, 1957.

36. Fraser, T. M., Hoover, G. N., and Ashe, W. F.: Tracking performance during low frequency vibration. (Ohio State University, Columbus) Aerospace Medicine 32:829-835, 1962.

37. Gell, C. F., Chairman: A Table of Equivalents of Acceleration Terminologies, Recommended for general international use by the Acceleration Committee of the Aerospace Medical Panel, Advisory Group for Aeronautical Research and Development, North Atlantic Treaty Organization, 1961.

38. Gerathewohl, Siegfried: Zero-G Devices and Weightlessness Simulators. Publication 781, National Academy of Sciences - National Research Council, Washington, D. C., 1961.

39. Getline, G. L.: Vibration tolerance levels in military aircraft. Supplement to 22nd. Shock and Vibration Bulletin, p. 24-27, Office of the Secretary of Defense, Washington, D. C., 1955.

40. Gibbs-Smith, Charles H.: The Aeroplane: An Historical Survey of Its Origins and Development. Her Majesty's Stationery Office, London, 1960.

41. Glenn, Jr., John H.: in Results of the First United States Manned Orbital Space Flight, February 20, 1962. National Aeronautics and Space Administration, Washington, D. C., 1962.

42. Goldman, David, and von Gierke, Henning: The Effects of Shock and Vibration on Man. Lecture and Review Series No. 60-3, Naval Medical Research Institute, Bethesda, Maryland, January, 1960. See also Chapter 44, Volume 3, of Harris, Cyril M., and Crede, Charles E., editors: Shock and Vibration Handbook, McGraw-Hill Book Co., New York, 1961.

43. Grandpierre, R., and Grognot, P.: Effets physiopathologiques des vibrations transmises par l'air en aviation; les moyens de protection. (Physiopathological effects of vibration transmitted by air in aviation; means of protection.) Méd. aéronaut. 10:309-344, 1955.

44. Gray, R. F., Crosbie, R. J., Hall, R. A., Weaver, J. A., and Clark, Carl C.: The presence or absence of visual Coreolis illusions at various combined angular velocities. Report NADC-MA-6131, U. S. Naval Air Development Center, Johnsville, Pa., June, 1961.

45. Grissom, Virgil: in Results of the Second U. S. Manned Suborbital Space Flight, July 21, 1961. National Aeronautics and Space Administration, Washington, D. C., 1961.

46. Guedry, Frederick E., and Graybiel, Ashton: Rotation Devices Other than Centrifuges and Motion Simulators. Publication 902, National Academy of Sciences-National Research Council, Washington, D. C., 1961.

47. Guignard, J. C., and Travers, P.: Physiological effects of mechanical vibration. (RAF Institute of Aviation Medicine, Farnborough, England). Proc. Royal Soc. Med. 53:92-96, 1960.

48. Hamel, Gustav, and Turner, Charles C.: Flying: Some Practical Experiences. Longmans, Green, and Co., London, 1914.

49. Hardy, James D., Chairman: Recommendations of the Acceleration Group, National Academy of Sciences Symposium on Impact Acceleration Stress, San Antonio, Texas, November, 1961.

50. Hardy, James D. (Chairman): Proceedings of the Symposium on Impact Acceleration Stress, San Antonio, November, 1961. In press, National Academy of Sciences - National Research Council, Washington, D. C., 1962.

51. Hornick, Richard J., Boetcher, Charles A., and Simons, Allison K.: The effect of low frequency, high amplitude, whole body, longitudinal and transverse vibration upon human performance. Final Report, Project No. TE1-1000, U. S. Army Ordnance Corps and U. S. Army Transportation Corps, Bostrom Research Laboratories, Milwaukee, Wisconsin, July 1961.

52. Jones, Isaac: Flying Vistas: The Human Being as Seen Through the Eyes of the Flight Surgeon. J. B. Lippincott Co., Philadelphia, 1937. See also Ocker, William C., and Crane, Carl J.: Blind Flight, in Theory and Practice. Naylor Printing Co., San Antonio, Texas, 1932.

53. Kaehler, Richard C.: X-15 centrifuge simulation program. Final Report No. 57-829; and Individual data sheets and pilot's comments, Report No. 57-830, North American Aviation, Inc., Los Angeles, Cal., July, 1957.

54. Kennelly, E. J.: Development of a multi-purpose research simulator. Grumman Research Brochure, Grumman Aircraft Engineering Co., Bethpage, L. I., N. Y., February, 1959.

55. Kidd, E. A.: Artificial stability installations in B-26 and F-94 aircraft. Report No. TB-757-F-9, Cornell Aeronautical Laboratory, Buffalo, N. Y., September, 1954, and Technical Report 54-441, Wright Air Development Division, Wright-Patterson Air Force Base, Ohio, September, 1954.

56. Lebedev, V. L.: Sluchainye Protesessy V Elektricheskikh I Mekhanicheskikh Sistemakh (Random Processes in Electrical and Mechanical Systems, The State Publishing House of Physical and Mathematical Literature, Moscow, 1958. Translated by J. Flancreich and M. Segal, Office of Technical Services PST Cat. No. 200, Washington, D. C., 1961.

57. Magrath, H. A., Rogers, O. R., and Grimes, C. K.: Shock and vibration in aircraft and missiles. Chapter 47, volume 3, in Harris, Cyril M., and Crede, Charles E., editors, Shock and Vibration Handbook, McGraw-Hill Book Company, New York, 1961.

58. McNeill, Walter E., and Creer, Brent Y.: A summary of results obtained during flight simulation of several aircraft prototypes with variable stability airplanes. Research Memorandum RM A56C08. National Advisory Committee for Aeronautics, Washington, D. C., May, 1956.

59. Mozell, M. M., and White, D. C.: Behavioral effects of whole body vibration. Project NM 18 01 12.4, Report No. 1, U. S. Naval Air Development Center, Johnsville, Pa., January, 1958. See also J. Aviation Med. 29:716-724, 1958.

60. Nicholson, F. T.: Aircraft simulation for the human centrifuge. ACL Technical Note 57-44-03, U. S. Naval Air Development Center, Johnsville, Pa., 11 July 1957.

61. Norton, F. H., and Allen, E. T.: Accelerations in flight. Report No. 99, National Advisory Committee for Aeronautics, Washington, D. C., 1921.

62. Norton, F. H., and Carroll, T.: The vertical longitudinal, and lateral accelerations experienced by an S.E. 5A airplane while maneuvering. Report No. 163, National Advisory Committee for Aeronautics, Washington, D. C., 1923.

63. Norton, F. H., and Warner, F. P.: Accelerometer design. Report No. 100, National Advisory Committee for Aeronautics, Washington, D. C., 1921.

64. Oshima, Masamitsu: (Vibration and the human body). Tekko Rodo Eisei (Hygiene for the Steel Workers) 2-1, 2, 3, 4, 39 pages, 1953. Translation No. MCL-803/1 & 2, Technical Documents Liaison Office, ASTIA No. AD529593, 25 April 1961.

65. Parks, Donald L.: A comparison of sinusoidal and random vibration effects on human performance. Report D3-3512-2, The Boeing Company, Wichita, Kansas, 28 July 1961.

66. Parks, Donald L., and Snyder, F. W.: Human reaction to low frequency vibration. Report D3-3512-1, The Boeing Company, Wichita, Kansas, 24 July 1961.

67. Payne, Peter R.: The Dynamics of Human Restraint Systems. National Academy of Sciences Symposium on Impact Acceleration Stress, San Antonio, Texas. Also Frost Engineering Development Corp., Denver, Colorado, November, 1961.

68. Phillips, William H.: Effect of Steady Rolling on Longitudinal and Directional Stability. Technical Note 1627, National Advisory Committee for Aeronautics, Washington, D. C., June, 1948.

69. Phillips, William H., and Cheatham, Donald C.: Ability of pilots to control simulated short period yawing oscillations. Research Memorandum L50D06, National Advisory Committee for Aeronautics, Washington, D. C., November, 1950.

70. Pradko, F.: Dynamic simulator. Proceedings of the 1962 Meeting, pl29-135, Institute of Environmental Sciences, Mt. Prospect, Ill., April, 1962.

71. Reid, H.J.E.: The NACA three component accelerometer. Technical Note 112, National Advisory Committee for Aeronautics, Washington, D. C., 1922.

72. Riopelle, A. J., Hines, Marion, and Lawrence, Merle: The effects of intense vibration. Report No. 358, U. S. Army Medical Research Laboratory, Fort Knox, Kentucky, October, 1958.

73. Roman, James: Effects of severe whole body vibration on mice and methods of protection from vibration injury. WADC Technical Report 58-107, ASTIA No. AD 151070, Aerospace Medical Laboratory, Wright-Patterson Air Force Base, Ohio, April 1958.

74. Schaefer, V. H., and Ulmer, R. G.: A representative bibliography of research in low frequency mechanical vibration. Report No. 405, U. S. Army Medical Research Laboratory, Fort Knox, Kentucky, November, 1959.

75. Schy, Albert A., Gates, Ordway B., and Woodling, C. H.: Part I; Preliminary studies of the lateral and longitudinal control systems; Sherman, Windsor L., and Sternfield, Leonard: Part II, Some results of a study performed on the Typhoon computer; of the report, "Simulator studies of the attack phase of an automatically controlled interceptor." Research Memorandum L55E27a, National Advisory Committee for Aeronautics, Washington, D. C., August, 1955.

76. Searle, G.F.C., and Cullimore, W.: Report on measurement of accelerations on aeroplanes in flight. Advisory Committee for Aeronautics Reports and Memoranda No. 469, London, June, 1918.

77. Searle, G.F.C., and Lindeman, F.A.: Preliminary report on the measurement of accelerations of aeroplanes in flight. Advisory Committee for Aeronautics Reports and Memoranda No. 376, London, September, 1917.

78. Shepard, Jr., Alan: in Results of the First U. S. Manned Suborbital Space Flight, May 5, 1961. National Aeronautics and Space Administration, Washington, D. C., June 1961.

79. Shevi, I., and Kuz'mina, N. G.: Izmeneniia v kletkakh nekotoryhh organov khdodnokrovnykh zhivotnyhh pod deistviem vibratsii. (Changes in the cells of some organs of cold blooded animals under the effects of vibration. Gig. san 21:37-40, 1956.

80. Sternfield, Leonard: A simplified method for approximating the transient motion in angles of attack and sideslip during constant rolling maneuvers. NACA Research Memorandum L56F06, 1956. This was superseded by NACA Report 1344, 1958, National Advisory Committee for Aeronautics, Washington, D. C. See also the Conference on Inertial Coupling for Aircraft, Aircraft Laboratory, Wright Air Development Center, Dayton, Ohio, 1956.

81. Stewart, Oliver: First Flights. Pitman Publishing Corp., New York, 1958.

82. Taylor, John W. R.: Picture History of Flight. Pitman Publishing Corp., New York, Revised, 1959.

83. Voas, Robert: Project Mercury Astronaut Training Program. In Grether, Walter, editor: The Training of Astronauts. Publication 873, National Academy of Sciences, Washington, D.C., 1961. See also in Flaherty, Bernard E., editor: Psychophysiological Aspects of Space Flight. Columbia University Press, New York, 1961. See also Voas, Robert B.: Manual control of the Mercury spacecraft. Astronautics 7:18-20, 34-38, 1962.

84. Volkov, A.M., and Chirkov, V. Ya.: (Vibration of the human body). Gigiyena truda i professional'nyye zabokvaniya, No. 5, 8-11, 1960.

85. von Gierke, Henning, and Steinmetz, Eugene: Motion Devices for Linar and Angular Oscillation and for Abrupt Acceleration Studies on Human Subjects (Impact): A Description of Facilities in Use and Proposed. Publication 903, National Academy of Sciences - National Research Council, Washington, D. C., 1961.

86. Vykukal, H. C., Stinnett, G. W., and Gallant, R. P.: Performance of an interchangeable mobile pilot restraint system designed for use in a moderately high acceleration field. Presented at the Aerospace Medical Association Meeting, Chicago, April 26, 1961. To be published in Aerospace Medicine. See also Aviation Week 75(1): 57-59, July 3, 1961.

87. Weaver, John, Rubenstein, M., Clark, C. C., and Gray, R. F.: Direct casting of a human in rigid polyurethane foam for use as a restraint system in high acceleration environments. Report, U. S. Naval Air Development Center, Johnsville, Pa., 1962.

88. White, D. C., and Mozell, M.M.: Whole body oscillation, preliminary report. Project NM 001 111 304, Serial 2683, U. S. Naval Air Development Center, Johnsville, Pa., April, 1957.

89. White, Robert M., Robinson, Glenn H., and Matranga, Gene J.: Résumé of X-15 Handling Qualities. Research Airplane Committee Report on the Conference on the Progress of the X-15 Project. National Aeronautics and Space Administration, Washington, D. C., November, 1961.

90. Woodling, C. H., Whitten, J. B., Champine, R. A., and Andrews, R.: Simulation study of a high performance aircraft including the effect on pilot control of large accelerations during exit and reentry flight. Research Memorandum L58E08a, National Advisory Committee for Aeronautics, Washington, D. C., 1958.

91. Yaeger, Charles: Quoted in Duke, Neville, and Lanchbery, Edward: The Saga of Flight. The John Day Company, New York, 1961.

92. Yaeger, Charles: Quoted in Lundgren, William R.: Across the High Frontier: The Story of a Test Pilot - Major Charles E. Yaeger, USAF. William Morrow and Co., Inc., New York, 1955. See also reference 91.

93. Zahn, A.F.: Development of an airplane shock recorder. J. Franklin Institute 188:237,1919.

94. Ziegenruecker, G., and Magid, E.B.: Short time human tolerance to sinusoidal vibration. WADC Tech. Report 59-39, Aerospace Medical Laboratory, Wright-Patterson Air Force Base, Ohio, July, 1959. See also Magid, Edward B., Coermann, Rolf R., and Ziegenruecker, Gerd H.: Human tolerance to whole body sinusoidal vibration. Aerospace Med. 31:915-924, 1960.

Addendum

Another pre-World War I moving base flight simulator has come to my attention: the "oscillator", an airplane like devise pivoting on the ground with large control surfaces moved by the pilot in a strong wind, to give him the feel for airplane responses (at small angles of attack). See figure 121 of reference 82.

In the historical vein, it is appropriate to name those instrumental in the first controlling of the Johnsville human centrifuge through a computer, the first high acceleration moving base pilot controlled motion and display flight simulation[17,60] for which the author was "project officer". Aviation Medical Acceleration Laboratory: Dr. John L. Brown, Richard Crosbie, Carter Collins, Dr. Carl Clark. Aeronautical Computer Laboratory: Morris Plotkin, Jay Rabb, Cdr. C. Fink Fischer, Harold Tremblay, Victor Doesch, Harold Doerfel, Edward Loller, Dr. Edward Knobelaugh. Moore School, University of Pennsylvania: Frank Nicholson, William Wachter, Elizabeth Schoff, Dr. Emil Grosswald.

- End -

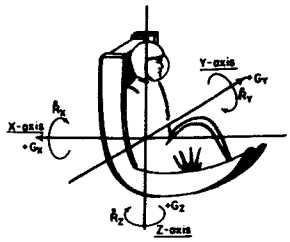

(Directions Are Those of Heart Displacement, With Respect to the Skeleton)

Linear Acceleration Modes

Description of Heart Motion

ACTUAL	OTHER DESCRIPTION		UNIT VECTOR
Towards spine	Eye-balls-in	Chest-to-back	$+G_x$
Towards sternum	Eye-balls-out	Back-to-chest	$-G_x$
Towards feet	Eye-balls-down	Head-to-foot	$+G_z$
Towards head	Eye-balls-up	Foot-to-head	$-G_z$
Towards left	Eye-balls-left	———	$+G_y$
Towards right	Eye-balls-right	———	$-G_y$

$$NG = \frac{a}{g} = N_1 G_x + N_2 G_y + N_3 G_z$$

$$N^2 = N_1^2 + N_2^2 + N_3^2$$

Angular Acceleration Modes

Acceleration about X-axis (The heart rolls left in the chest)	$+\dot{R}_x$
Acceleration about Y-axis (The heart pitches down)	$+\dot{R}_y$
Acceleration about Z-axis (The heart yaws left)	$+\dot{R}_z$

Figure 1: The physiological acceleration terminology. (Official U. S. Navy photograph)

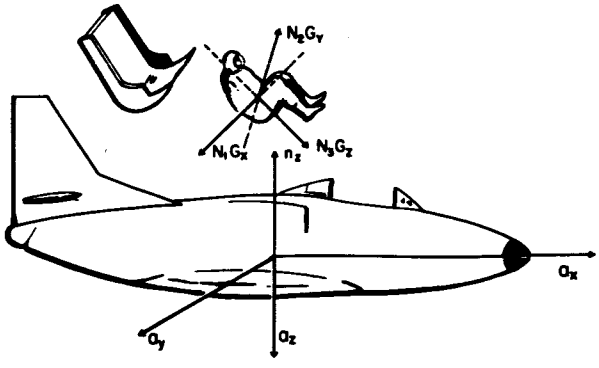

Linear Acceleration Modes

Description		Symbol	
Aircraft	Physiological	Aircraft	Physiological
Forward	Supine G	$+a_x$	$+N_1 G_x$
Backward	Prone G	$-a_x$	$-N_1 G_x$
Upward	Positive G	$-a_z$	$+N_3 G_z$
Downward	Negative G	$+a_z$	$-N_3 G_z$
Straight and level flight at constant speed		$a_z = 0$; $n_z = 1g$	$N_3 G_z = 1 G_z$
To right	Lateral G	$+a_y$	$+N_2 G_y$
To left	Lateral G	$-a_y$	$-N_2 G_y$

Angular Acceleration Modes

Roll right	The heart rolls left	$+\dot{p}$	$+N_4 \dot{R}_x$
Pitch up	The heart pitches down	$+\dot{q}$	$+N_5 \dot{R}_y$
Yaw right	The heart yaws left	$+\dot{r}$	$-N_6 \dot{R}_z$

Figure 2: A comparison of the physiological and NASA aircraft acceleration techniques. (Official U. S. Navy photograph)

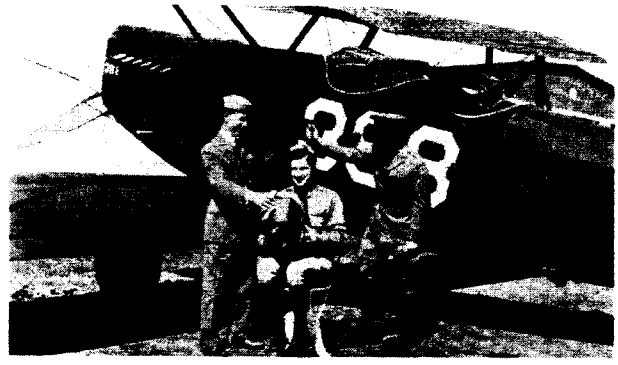

Figure 3: The "instrument box on the turning chair", and airplane with hood for blind flight. (From Isaac Jones: Flying Vistas: The Human Being as Seen Through the Eyes of the Flight Surgeon. J. B. Lippincott Co., Philadelphia, 1937, by permission.

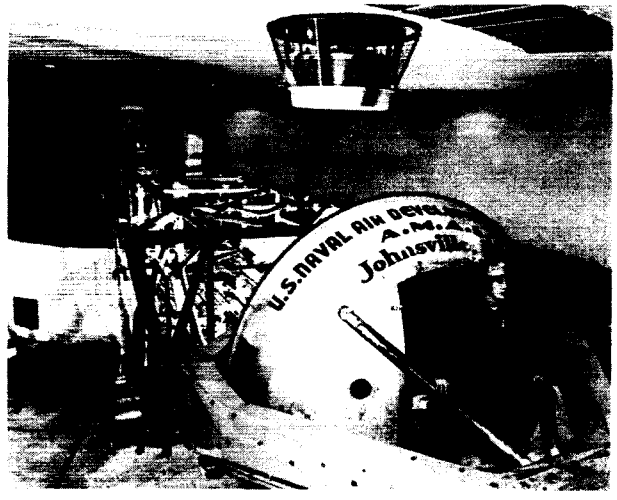

Figure 4: The Navy Johnsville Human Centrifuge. (Official U. S. Navy photograph)

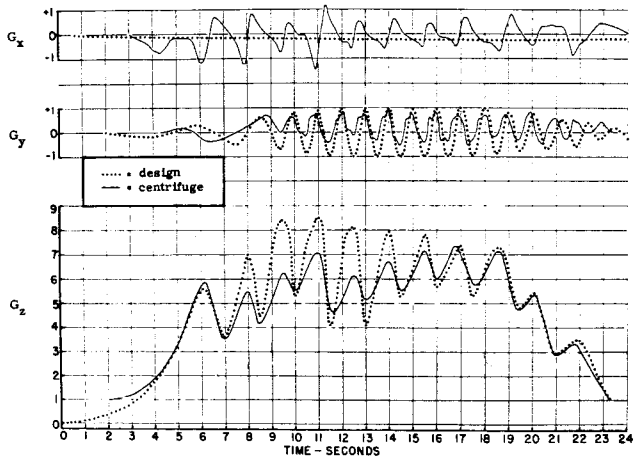

Figure 5: Accelerations computed for an X-15 re-entry with speed brakes closed and pitch damper off, and Navy centrifuge simulation by cam control. (Official U.S. Navy photograph)

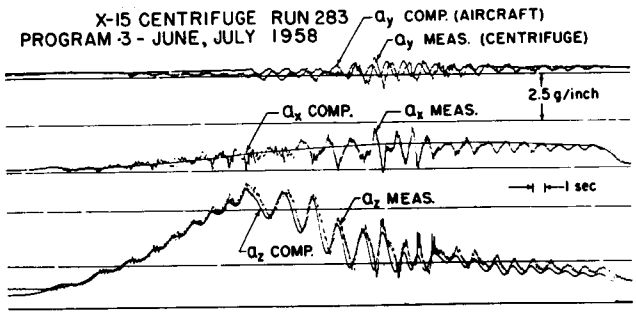

Figure 6: Accelerations computed for an X-15 reentry with dampers off, and Navy centrifuge simulation by pilot-computer control. (Official U. S. Navy photograph).

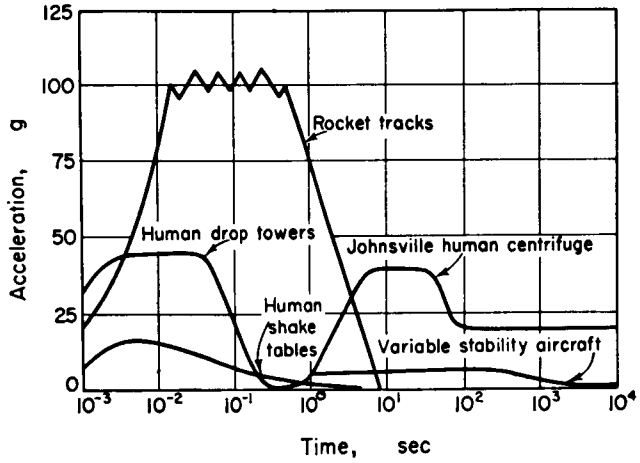

Figure 7: Acceleration vs. time capabilities of various motion simulation devices. (Official U. S. Navy photograph).

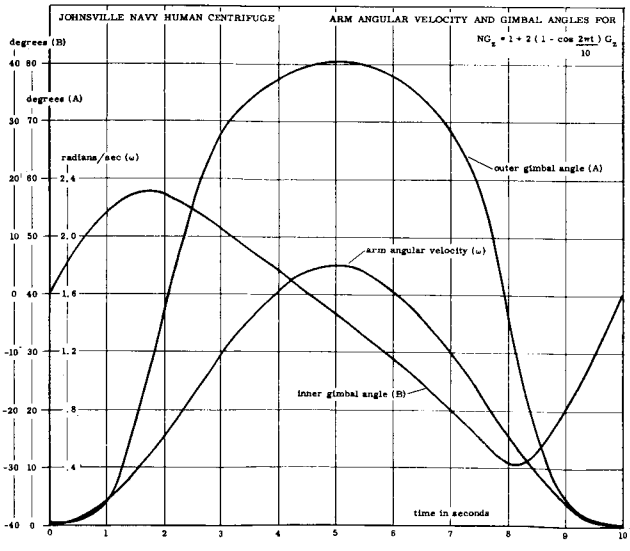

Figure 8: Navy centrifuge gimbal responses for a $5G_z$ peak haversine waveform.

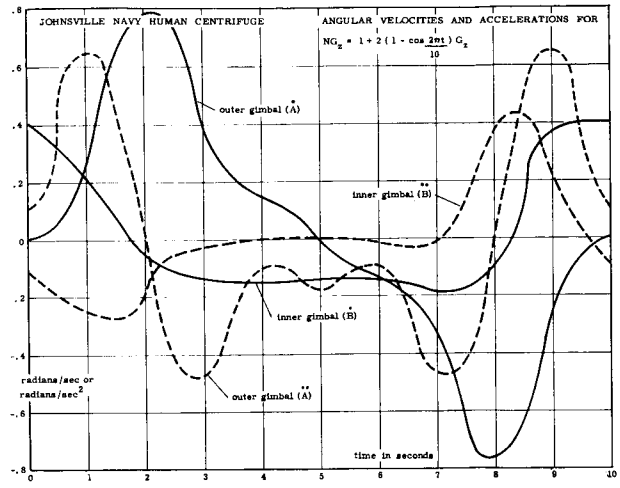

Figure 9: Navy centrifuge gimbal velocities and accelerations for a $5G_z$ peak haversine waveform.

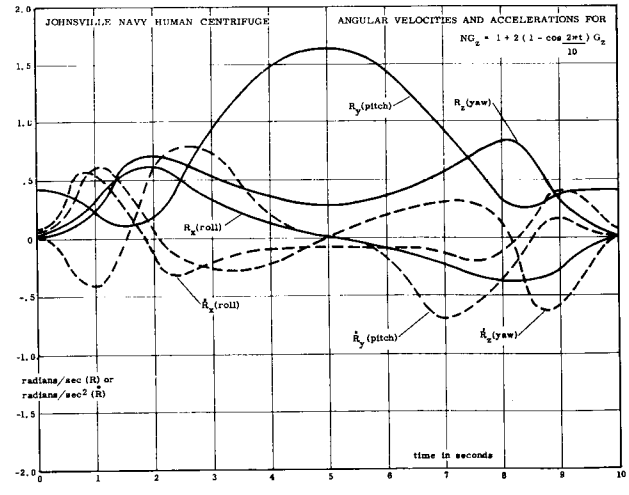

Figure 10: Physiological angular velocities (R) and angular accelerations ($\dot{R}$) for a $5G_z$ peak haversine waveform on the Navy centrifuge.

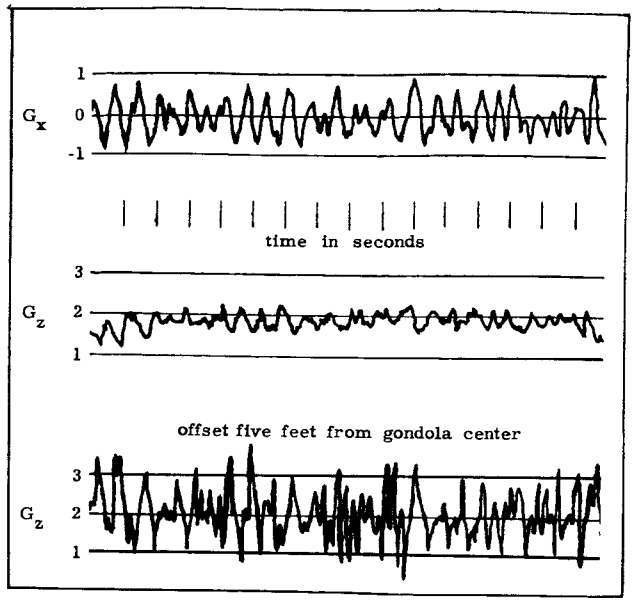

Figure 11: Jostle accelerations with the Navy centrifuge.

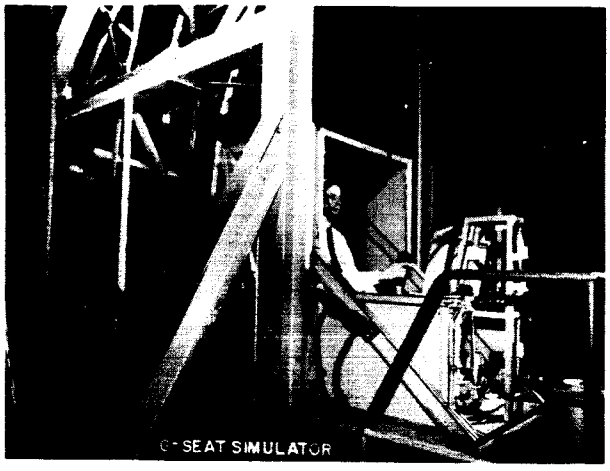

Figure 12. The North American Aviation (Columbus) "G-seat." (Courtesy of North American Aviation, Inc.).

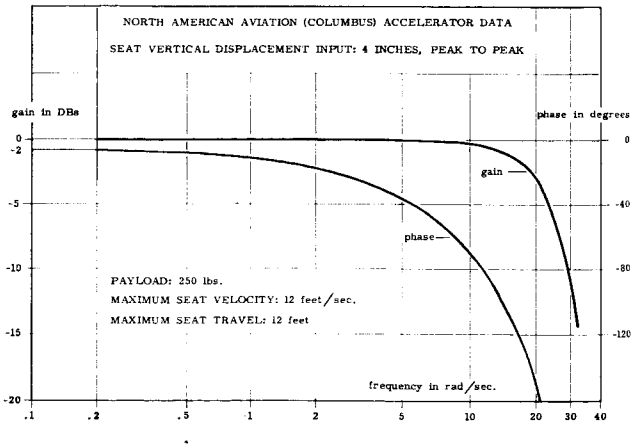

Figure 13: Response capabilities of the G-seat. (Courtesy of North American Aviation, Inc.).

...p ... ...gn at the back of ... ...duction method so as to furnish the best possible detail to the user.

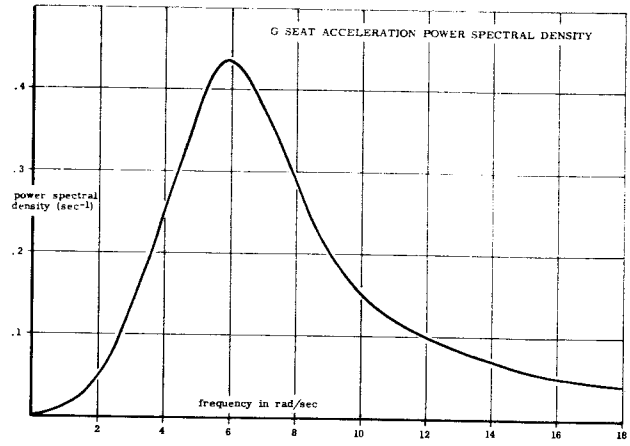

Figure 14: The acceleration power spectral density of this study. (Courtesy of North Amer. Aviation, Inc.)

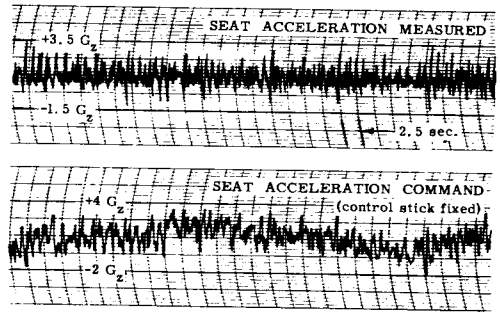

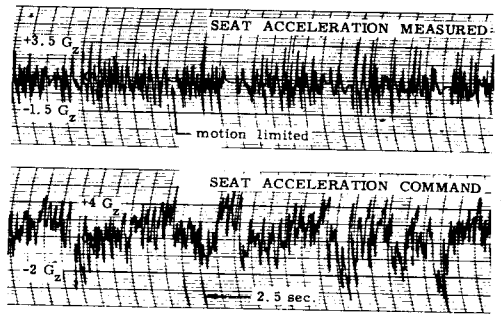

Figure 15: Jostle time histories with the G-seat.

Figure 16: The Navy polyurethane foam restraint. (Official U. S. Navy photograph).

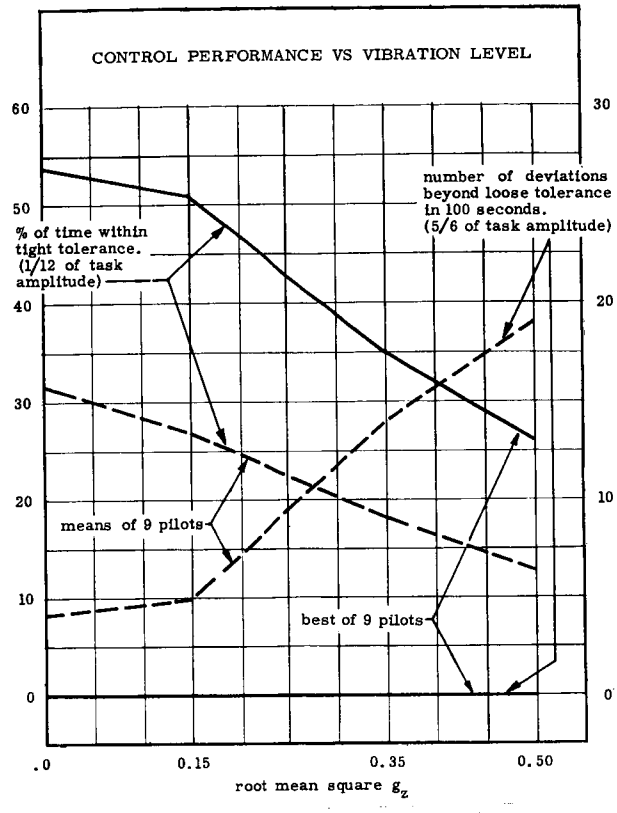

Figure 17: Tracking performance on the G-seat.

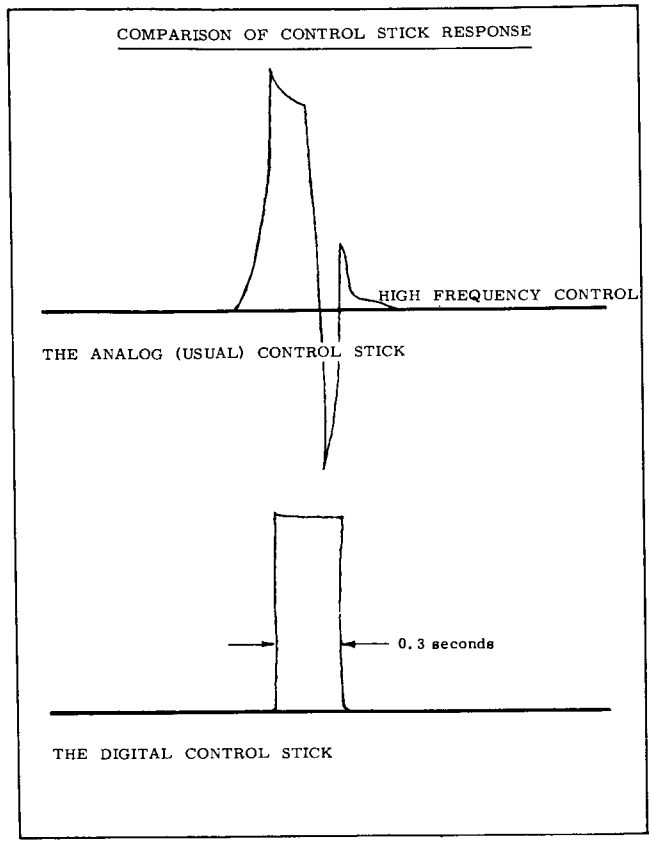

Figure 19: Typical control pulses for the analog and digital controllers.

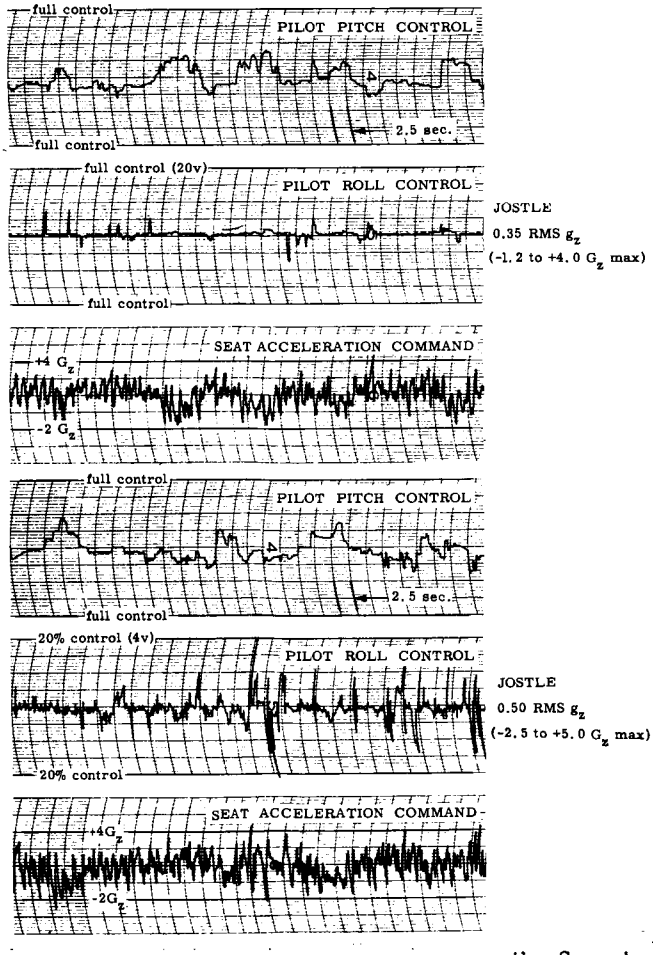

Figure 18: Pilot control responses on the G-seat.

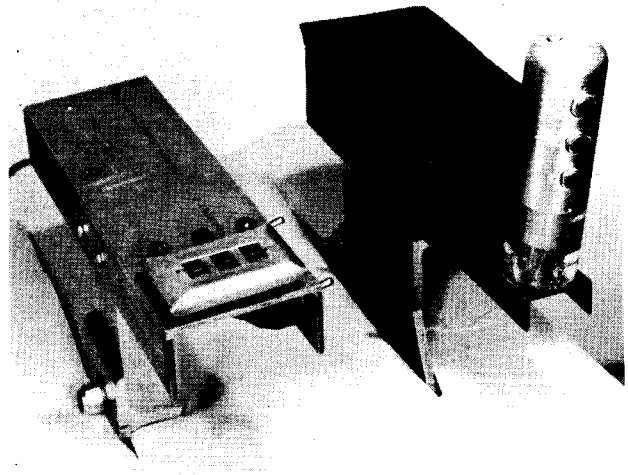

Figure 20: Two early designs of digital (push button) controllers.

This page is reproduced again at the back of this report by a different reproduction method so as to furnish the best possible detail to the user.

CREW SAFETY AND SURVIVAL ASPECTS OF THE LUNAR-LANDING MISSION

Hubert M. Drake
Chief of Programs
NASA Flight Research Center
Edwards, California

Abstract

Some of the safety and survival aspects of the manned lunar-landing mission are examined. The conditions requiring abort to the earth, lunar orbit, and lunar surface are determined. Some of the possible design requirements to permit abort to lunar orbit or surface are indicated. Lunar orbital and surface survival kits are described, and the stationing of such kits in lunar orbit and at the intended landing site is proposed.

Introduction

A manned lunar-landing mission includes all of the safety and survival problems of earth orbital and lunar orbital missions, plus problems that arise from flight phases peculiar to the lunar landing. For example, the lunar landing involves several additional powered phases and the danger of landing accidents on the moon, with resulting problems of survival. Phases common to other missions, such as boost, earth orbit, translunar flight, lunar orbit, and earth recovery are not considered in this paper, since these areas are covered adequately in other investigations. The lunar-landing mission is considered from the standpoint of the initial exploratory missions; that is, no permanent lunar base is assumed to have been established.

In this paper, the term "safety" refers to the escape and survival of the crew should an emergency or accident occur. The term "survival" refers to the long-term aspects of the crew existence after an emergency. Rescue would be included in the survival area.

An indication of the extent of the problem and the flight phases to be considered is given in figure 1. A small sector of the moon is shown, and the trajectory of a vehicle landing from lunar orbit, then taking off to return to earth is indicated. In general, the four flight phases are, as indicated: phase 1, the lunar deorbit and approach; phase 2, the actual lunar landing; phase 3, lunar residence, which includes all the time spent on the moon; and phase 4, the lunar take-off which extends from the firing of the take-off engines to injection into lunar orbit.

Also included in figure 1 is a list of pertinent items such as the altitude, the characteristic velocity increment involved in each of the four flight phases, and the approximate duration, in minutes, of the flight phase. Phases 1, 2, and 4 are characterized by the operation of the main propulsion system, maneuvering, and possibly staging. Phase 3 is primarily characterized by long duration, while phase 2 has the added problem of lunar impact.

Obviously, any number of emergencies and accidents could occur during a mission such as that illustrated in figure 1 which would result in safety and survival problems. The presence of man in the lunar-landing vehicle both complicates and simplifies the problem because, although the requirements for provision of safety and survival are much more severe, the man can be relied upon to take a personal and active interest in the matter.

Safety

Considerations of safety are limited to phases 1, 2, and 4, inasmuch as these phases involve powered flight. Phase 3 is discussed in the following section on survival.

System Failures

Some of the critical system failures that might occur in phases 1, 2, and 4 are shown in figure 2. A general safety requirement might be to always provide a way out following one failure (preferably two in series). Figure 2 lists how this requirement might be met for several systems. Emergencies are presented in order of increasing urgency: those requiring no immediate abort; those which may require immediate abort, depending on the conditions prevailing at the time of the failure; and, finally, one which requires immediate abort. These, of course, are not all of the systems in the spacecraft, but are representative of the various types. It might be noted that under safety provisions, redundancy and repair are the most important factors for all systems except structure and propulsion, for which repair is the primary provision. Redundancy is generally the only acceptable safety provision for failures occurring during power-on operations such as in phases 1, 2, and 4, but when conditions provide adequate time, it is possible for the crew to take action to perform repairs. Thus, on the surface of the moon or in lunar orbit, the original capability and reliability of the systems may be regained if suitable equipment, parts, and skills are available.

Abort Requirements and Goals

Abort requirements and the goals of abort should also be considered in a discussion of safety, inasmuch as abort is the last resort following emergency. Figure 3 shows the characteristic velocity requirements for abort to each of three possible target areas: the earth, lunar orbit, or the moon. These three locations, of course, have different levels of desirability and attainability, depending on the flight phase when the emergency occurs. For example, if an emergency occurs just as deorbiting is initiated, it is obviously possible to return to the earth or to the lunar orbit with much less expenditure of energy than is required by an abort to the moon. Conversely, if an emergency occurs during the final phases of landing, aborting to the moon involves much less energy than to the earth or lunar orbit. Omitting the earth, the choice between abort to the lunar orbit or surface is dependent upon design, supply, and survival considerations to be discussed.

It might be noted in figure 2 that only failures of the propulsion system require immediate abort. Various propulsion configurations can be utilized to obtain the 17,000 ft/sec velocity potential required to land on the moon from lunar orbit and return to earth. Figure 4 shows examples of some of these configurations, with comments on the results of propulsion failures. The first configuration consists, essentially, of a single stage for lunar landing and earth return. With this configuration, any failure in phase 1 and 2 results in a crash on the moon. In phase 4, if a failure occurs below orbital velocity, a crash results; whereas, at velocities above orbital speed, the vehicle can remain in lunar orbit. With the second configuration, a separate stage is indicated for earth return and lunar landing. Failure of the lunar-landing stage in phase 1 or 2 permits the use of stage B to abort to the earth, lunar orbit, or the moon, since sufficient velocity potential exists in this stage. If stage B fails subsequent to a stage A failure, there is still a possibility that the vehicle will remain in orbit rather than crashing on the moon. Phase 4, in this instance, is the same as phase 4 for the single-stage vehicle. The third configuration has three stages: lunar landing, lunar take-off, and earth return. In each phase there are two propulsion systems that can fail without a resulting crash. It might be noted that for all three configurations, failures in phase 4 preclude abort to the earth.

Safety considerations of another possible operational technique and group of propulsion configurations for the lunar landing are shown in figure 5. A small vehicle is assumed to leave a mother vehicle in lunar orbit, make a landing on the moon, then take off from the moon to rendezvous with the mother vehicle which will be used for earth return. Three configurations are also shown in this figure. The first again consists of a single propulsion system capable of the 14,000 ft/sec requirement for this mission. Any propulsion failure in phase 1, 2, or 4 with this configuration will cause the vehicle to crash on the moon. In the second configuration, two parallel, independent propulsion systems are utilized which operate throughout the flight. The propellant supply systems can be interconnected at the pilot's discretion, as required. If either propulsion system fails, the mission can be completed or an abort can be made to the moon or to lunar orbit in all flight phases. The third configuration is similar to the second, in that two independent propulsion systems are used. In addition, a second stage is provided having a capability of approximately 3,000 ft/sec, for a total capability of 17,000 ft/sec. Both A and B propulsion systems can fail, and system C will still permit an abort to either the moon or to lunar orbit. If desired, the lander can be designed for a 14,000 ft/sec total capability and lunar surface refueling used to provide the required redundancy.

Considering the various possible configurations and operational techniques presented in figures 4 and 5, selection of the best balance between complexity, reliability, safety, and efficiency is dependent, of course, upon the hardware involved. It would seem that the first configuration in each figure could not be considered because of safety requirements. A choice between the second and third configurations would probably depend upon the relative reliability of the propulsion systems. It would appear that serious consideration might be given to the third configuration in the direct lunar landing and to the second configuration for the lunar rendezvous.

Effects on Design

In all of the foregoing, a tacit assumption has been made that abort to the lunar orbit or the moon is preferable to the emergency being experienced at the given time. However, the effect of such an abort requirement on the design of the actual lunar vehicle must be considered. Some effects have been indicated, such as the additional staging or parallel staging. Again, the possibility of aborting to the moon with a stage that is not the primary lunar-landing stage introduces the necessity of having two lunar-landing gears on successive stages, or a single landing gear capable of two landings mounted on the lunar take-off stage. Although it might also be possible to build sufficient shock-attenuation capability into the capsule itself to withstand lunar-landing impact, this capability does not appear to be a solution because of the danger of fire and explosion. Safety considerations would appear to require that the lunar take-off engines not only be extremely reliable but also be throttleable or otherwise capable of performing emergency lunar landings. The capability of emergency landing, of course, would be inherent in the parallel propulsion configurations mentioned previously.

Survival and Rescue

In speaking of survival, it is assumed that the crew have escaped the immediate emergency and have been able to attain a place of relative safety. In this paper, this safety area is considered to be lunar orbit or the surface of the moon. Each of these survival locations offers a number of survival supply and rescue possibilities, as shown in figure 6. Each survival area has different requirements in regard to launch rates, vehicle development problems, and operational feasibility. Some of the particular problems and operational considerations are discussed in the following sections.

Lunar Orbit

The lunar orbit might be considered desirable as a location for long-term survival because less expenditure of energy is required for rescue; that is, a vehicle in lunar orbit is in a much more shallow energy well than it would be on the lunar surface. Also, as indicated in figures 4 and 5, it is frequently the only survival area available.

If it is assumed that a survival type of emergency has occurred, that is, the living module of the vehicle is essentially undamaged but cannot leave lunar orbit, the basic problem is that life must be sustained until a successful rescue attempt can be mounted. As indicated in figure 6, rescue may be by a vehicle already in orbit, which would present no supply problem, or by a vehicle from earth, which would require sufficient supplies on the lunar lander or a lunar orbital supply ship. It is, of course, preferable that sufficient supplies be contained in the lunar lander, if possible, thereby avoiding the necessity of providing a second vehicle; however, the amount of

supplies required depends upon the time for rescue and may be excessive for the lunar lander.

Consideration of the supplies required indicates, as discussed in reference 1, that the provision of atmosphere is most critical for survival, because the crew can survive from 30 to 40 days on the supplies of food and water carried on a 14-day lunar mission, but can survive only a few minutes without breathing. Thus, from a survival standpoint, any excess payload capability should be used for atmospheric supplies: oxygen and CO_2 absorbent. A minimum of about 110 pounds of oxygen and lithium hydroxide (plus container weight) per man would be required to match the total survival period possible with the food and water carried on a 14-day lunar-landing mission. This weight does not appear to be too great a penalty to pay for the increase in survival potential.

Another hazard, however, precludes reliance solely upon supplies stored in the lunar lander. This is the high probability of encountering a major solar flare. Normally, insufficient shielding would be carried on the lunar mission for solar-flare protection, reliance being placed, instead, on prediction and statistics. Thus, lunar-orbit survival will require the provision of additional shielding by a supply ship or rescue in a very short time. The improbability of being able to launch a rescue ship in a short time makes the provision of a supply ship in lunar orbit quite attractive. Such a supply ship would be capable of carrying sufficient shielding and supplies to permit survival in lunar orbit for a period of several months until a rescue ship from earth could arrive. This orbiting supply ship is discussed further in the next section.

Rescue can be performed by providing a manned or unmanned rescue ship in lunar orbit (fig. 6); however, it appears that the manned ship is undesirable because its duration on station is limited. An unmanned ship, it is believed, would be much less reliable than the simpler supply ship discussed above. Therefore, it is felt that the provision of a supply ship in a permanent lunar orbit is to be preferred to the orbiting rescue ship.

The third rescue possibility, that of using a lunar-launched rescue vehicle, will not be practical until a permanent base with sufficient facilities exists on the moon. At that time, it may be the preferred base for rescue operations because a velocity of only 10,000 ft/sec will be required to perform the rescue and proceed to earth, or 14,000 ft/sec to rescue and return to the moon. An earth-based rescue would require about 41,000 ft/sec velocity.

It might be noted that all of these procedures for rescue in lunar orbit involve the assumption that the problems of orbital rendezvous have been solved and that rendezvous is essentially a normal operational technique. It is believed that this capability will probably have been achieved during the time period under consideration.

One final point might be mentioned with regard to rescue in lunar orbit by an orbiting rescue vehicle. This is the normal procedure of operation if the lunar landing has been made by means of a special vehicle, as discussed previously (fig. 5); thus, a special rescue vehicle is not required, since the mother vehicle fulfills this role.

Lunar Survival

Problems resulting from an accident or emergency late in the lunar landing, during the lunar residence, or immediately after lunar take-off (phases 2, 3, and 4 of fig. 1) could eliminate the possibility of attaining a lunar-orbit condition. Therefore, survival on the moon itself must be considered.

The high level of energy expenditure required for a lunar landing creates complex supply and rescue operation problems; therefore, it might be well to regard survival on the moon operationally in the same light as survival during polar expeditions. In the past, it was not considered catastrophic or even unexpected if the return of an arctic or antarctic expedition was delayed 6 months to a year by their ships being frozen into the ice. Similarly, it would seem that if adequate preparation were made, a lunar accident which prevented immediate return of the crew should not be considered a catastrophe or cause extreme concern. Six months' survival potential would probably be adequate if the planned second lunar-landing mission had rescue capabilities. This second mission would probably be scheduled for launch 2 months after the first. Thus, allowing for failure of this mission, 2 months to launch a third, and a 50-percent safety margin, a 6-month survival time should probably be provided.

Two general survival areas must then be considered, as shown in figure 6: the intended landing site, and a remote site. First, consider survival following accident or emergency at the intended landing site. Accidents and emergencies are most likely to occur in this area, since it is here that landing impact is made and the long-duration lunar residence occurs. As indicated in figure 6, there are four possibilities for supply at the lunar-landing site. In this instance, it would appear to be advantageous to place the supply vehicle at the landing site before the lunar landing was attempted. This can be done during vehicle development just prior to the landing attempt. Although, as will be discussed later, supply by a ship in lunar orbit is also attractive, it offers somewhat less assurance of success. The supply ship could fail to operate properly when called down, then reliance would have to be placed on supply from earth.

The first requirement for long-term survival on the moon is adequate shelter for protection from radiation, micrometeorites, temperature extremes, and vacuum. Since the stay on the moon is to be possibly as long as 6 months, there is a virtual certainty of encountering multiple solar flares of sufficient intensity to be hazardous. Similarly, micrometeorites of appreciable size can be expected. Although no detail design has been made, a possible form of shelter to provide adequate protection against these hazards is shown in figure 7. This shelter would be buried under 8 to 10 feet of lunar rock for protection from radiation and extremes of temperature. At this depth, the rock is estimated to have a constant temperature of -40° F. With proper insulation, the internal heat generated by the occupants and

equipment will maintain a comfortable temperature. Burial of a lunar shelter of this type would be performed by blasting out a hole, installing the shelter, then mounding the lunar debris over the shelter. It is possible that good fortune would provide a crevice or cave in the vicinity of the landing and thus greatly reduce the effort required. In figure 7 the astronauts have been fortunate to find sufficient loose soil to bury the shelter without an excavation. The shelter illustrated has two air locks; one is normally used for a sanitary facility, but provides also an emergency air-lock capability. The general dimensions are: length, 22 feet; width, 9 feet; height, 7 feet; and volume, 1,070 cubic feet. It might be of interest to compare these dimensions with those of the hut in which Admiral Byrd spent 6 months alone in the antarctic. This hut[2] was 9 by 13 by 8 feet high, was designed for three men, and was similarly buried for protection from the environment.

The supplies and systems required for the proposed shelter are listed in the following table:

Supplies for Lunar-Landing "Survival Kit"
(Six-month duration, three-man crew, pressure - 7.5 psia)

	Weight, lb
Breathing atmosphere:	
Oxygen (2 lb/man/day, 10 shelter cycles, 500 air-lock cycles, 10 percent leakage, 400 lb for space suits)	2,050
O_2 storage	1,280
Nitrogen (10 shelter cycles, 500 air-lock cycles, 10 percent leakage)	900
N_2 storage	680
CO_2 absorption (LiOH)	2,040
Atmosphere decontamination (catalyst burner, charcoal, fuel)	430
Food (2 lb/man/day)	1,100
Water	300
Water reclamation (condenser, 2 stills, filters, etc.)	320
Sanitary facilities (fixtures, storage, etc.)	200
Electric power 1 kw (2 fuel cells, 1 photo voltaic system, battery)	500
Hydrogen	216
Hydrogen storage and system	200
Oxygen	1,944
Oxygen storage	1,200
Shelter	1,560
Miscellaneous supplies (suits, communications, tools, recreational equipment, etc.)	3,000
Total	18,900

No attempt has been made to optimize this "survival kit;" therefore, considerable weight reduction would probably be possible, particularly in the electrical power system. A heat-engine system operating on the temperature difference between the lunar surface and subsurface might replace the fuel cell required for night-time power with a considerable saving in weight. Similarly, the life-support system assumes no regeneration of oxygen, but future developments will probably make this feasible. Only a small water reserve is supplied because regeneration of waste water and the additional water resulting from the fuel cell will insure an adequate supply. The total payload weight of the shelter and all supplies would thus be about 20,000 pounds. Most of these supplies would not be stored within the shelter, but, instead, would be stored above ground in a shelter provided by the nose cone of the supply ship.

The survival shelter would be shipped to the moon in two parts for ease of assembling and handling. As mentioned previously, it would probably be best to land the supply vehicle on the moon prior to the manned landing so that the supplies would be available for use at that time. If the supplies were not required by the lunar-landing party, they would be available for the next landing crew in the same manner in which supplies have been left by antarctic expeditions for use by later expeditions.

Survival in a landing away from the primary landing site, that is, immediately after take-off in phase 4, poses special problems. The distance may be too great to permit the crew to return to the landing site and use the stored supplies at that point. Although this is, perhaps, the most difficult of all lunar survival problems, the probability of an emergency in this area requiring survival provisions is fairly remote. Most malfunctions requiring abort can be expected to occur in the first few seconds of powered operation when the ship is still very close to the base. For example, if the emergency occurs at less than 1,000 ft/sec, the landing will be made within about 20 miles of the base, probably within walking distance. An emergency occurring at a later point requires that a survival kit be provided at the emergency landing site within the time during which survival is possible with the stored atmosphere on board the lunar-landing vessel. Survival, in this case, is critically dependent upon having a supply vessel ready for launch on earth, or in orbit about the moon to be called down to the proper landing site. It would probably be preferable to have a survival supply ship in lunar orbit for call down to the emergency landing site. This vehicle would contain essentially the same "survival kit" described previously and would thus serve as a backup for the normal landing site. The vehicle would probably be most accurately and favorably positioned if it were landed by radio control from the lunar lander. Thus, it could be landed at a location near suitable shelter locations and still sufficiently remote from the lunar lander to avoid damage from flying rocks and other debris dislodged by the supply ship landing rockets.

Proper design of this survival vehicle would enable its use as the supply ship for aborts to lunar orbit. To perform this function, it would be necessary for the survival vehicle to incorporate adequate rendezvous capability and the addition of the large amount of shielding for solar-flare protection. As indicated in references 3 and 4, water shielding weights on the order of 5,000 pounds to 10,000 pounds may be required for protection. This shielding could be provided in an auxiliary compartment which could be jettisoned if the "survival kit" is to be landed on the moon, thus not interfering with the lunar-landing performance. Having the kit already in orbit rather than on the earth would greatly increase the chances of successful supply as well as reduce the time required for supply.

The orbiting supply ship might be used for emergencies occurring at the normal landing site

and remote sites, thus requiring only one survival vehicle rather than two. However, it would appear to be much more effective to have the supplies on the moon at the intended landing site as discussed previously, particularly when the probability of a malfunction at this location is considered.

One final point that might be discussed is the possibility of a form of lunar-surface rendezvous being utilized to improve the safety and survival potential of the mission. A rendezvous of this type could take the form of a duplicate mission vehicle landed automatically at the intended landing site prior to the mission. This is particularly attractive if the lunar-orbit rendezvous technique is employed because of the extremely small vehicle required and the fact that the mother ship is already waiting in lunar orbit. Similar possibilities exist to provide propellants to avoid marginal fuel conditions at lunar take-off. The best combination of facilities, supplies, and equipment in the survival kit will vary greatly, depending on the chosen lunar-mission flight procedure and will require extensive study and evaluation.

Concluding Remarks

This study of the lunar-landing mission indicates that abort to lunar orbit and the lunar surface is probable as a result of emergencies in various phases of the mission. These emergencies may result in considerably longer orbital or lunar residence time than originally planned for the mission. Consequently, external supplies and assistance will be required for survival and ultimate rescue.

It appears that the most practical supply vehicle combination for all the conditions discussed would consist of:

a. An unmanned supply ship at the planned primary landing site and

b. An unmanned supply ship in orbit capable of orbital rendezvous for orbital supply and capable of lunar landing for supply of unplanned remote landings.

In each of these cases rescue would be performed by a rescue ship sent from earth.

Provisions of increased safety potential may place unusual requirements on various spacecraft systems, particularly for the propulsion system and the landing gear where safety requires some form of redundancy. Additional important design requirements are the provision of rescue capability in the basic lunar lander and extension of automatic lunar-landing capabilities to large payloads.

References

1. Celentano, J. T., and Copping, D. G.: Emergency Survival in Space. Proc. of the Aerospace Support and Operations Meeting, IAS, Dec. 4-6, 1961, pp. 187-190.

2. Byrd, Richard E.: Alone. G. P. Putnam's Sons, Inc., (New York), 1938.

3. Wallner, Lewis E., and Kaufman, Harold R.: Radiation Shielding for Manned Space Flight. NASA TN D-681, 1961.

4. Foelsch, T.: Radiation Hazards in Space. AIEE paper no. CP 61-1143. Presented at Fall General Meeting of American Institute of Electrical Engineers, Detroit, Mich., Oct. 15-20, 1961.

PHASES OF LUNAR-LANDING MISSION

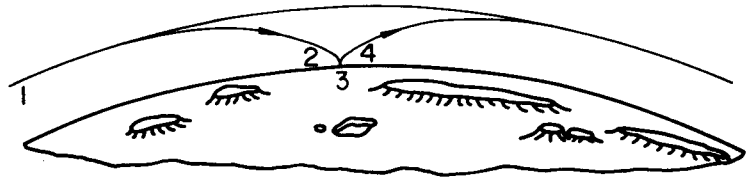

FLIGHT PHASE	ALTITUDE, FT	CHARACTERISTIC VELOCITY INCREMENT,* FT/SEC	DURATION, MINUTES
1. LUNAR DE-ORBIT AND APPROACH	50,000 TO 1,000	6,400	7 TO 20
2. LUNAR LANDING	1,000 TO 0	400	1
3. LUNAR RESIDENCE	0	0	1 TO 10,000
4. LUNAR TAKEOFF TO LUNAR ORBIT	0 TO 50,000	6,500	5 TO 6

*INCLUDES 10° ORBITAL-PLANE CHANGE AND 1 MINUTE OF HOVERING

FIGURE 1

SYSTEM FAILURES AND SAFETY PROVISIONS

SYSTEM	SAFETY PROVISIONS	REQUIRED ACTION
GUIDANCE	REDUNDANCY, REPAIR	
ENVIRONMENT CONTROL	REDUNDANCY, REPAIR	NO IMMEDIATE ABORT
COMMUNICATIONS	REDUNDANCY, REPAIR	
CONTROL SYSTEM	REDUNDANCY, REPAIR	MAY REQUIRE IMMEDIATE ABORT
AUXILIARY POWER	REDUNDANCY, REPAIR	
STRUCTURE	REPAIR	
PROPULSION	PARTIAL REDUNDANCY, REPAIR	IMMEDIATE ABORT

FIGURE 2

CHARACTERISTIC VELOCITY REQUIREMENTS FOR ABORT

FLIGHT PHASE	VELOCITY, FT/SEC		
	ABORT TO –		
	EARTH	LUNAR ORBIT	MOON
DE-ORBIT	3,500 TO 10,500	0 TO 7,000	6,500 TO 100
LANDING	10,500	7,000	100
RESIDENCE	10,500	7,000	0
TAKE-OFF	10,500 TO 4,000	6,500 TO 0	0 TO 6,500

FIGURE 3

PROPULSION CONFIGURATION EFFECTS ON SAFETY FOR DIRECT EARTH RETURN TECHNIQUE

CONFIGURATION	PHASE 1	PHASE 2	PHASE 4
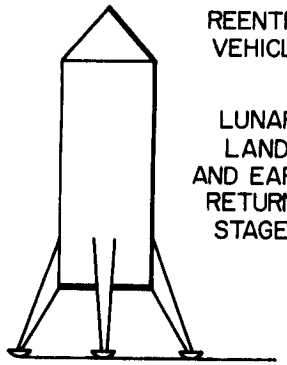 REENTRY VEHICLE LUNAR LAND AND EARTH RETURN STAGE	FAILURE–CRASH	SAME AS PHASE 1	FAIL AT $V<V_C$–CRASH FAIL AT $V>V_C$–REMAIN IN ORBIT (V = VELOCITY, V_C = LUNAR ORBITAL VELOCITY)
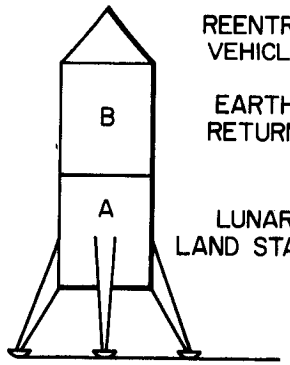 REENTRY VEHICLE B EARTH RETURN A LUNAR LAND STAGE	A FAILS—ABORT TO EARTH, ORBIT, OR MOON B FAILS–$V>V_C$–REMAIN IN ORBIT $V<V_C$–CRASH	SAME AS PHASE 1	B FAILS–$V<V_C$–CRASH $V>V_C$ REMAIN IN ORBIT
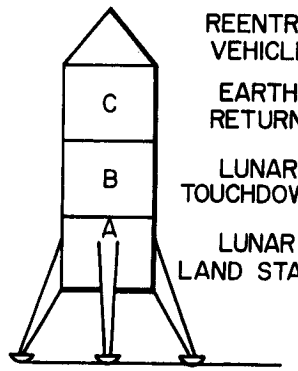 REENTRY VEHICLE C EARTH RETURN B LUNAR TOUCHDOWN A LUNAR LAND STAGE	A FAILS—ABORT TO EARTH, A AND B FAIL –V>3500 FT/SEC ABORT TO ORBIT V<3500 FT/SEC ABORT TO MOON	SAME AS PHASE 1	B FAILS–V<3500 FT/SEC ABORT TO MOON V>3500 FT/SEC ABORT TO LUNAR ORBIT C FAILS–REMAIN IN ORBIT

FIGURE 4

PROPULSION CONFIGURATION EFFECTS ON SAFETY USING LUNAR RENDEZVOUS TECHNIQUE

CONFIGURATION	PHASE I	PHASE 2	PHASE 4
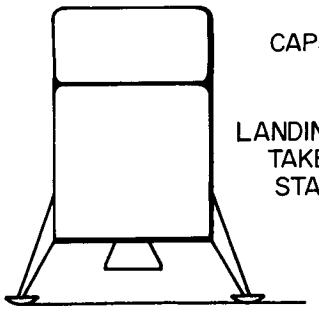 CAPSULE LANDING AND TAKEOFF STAGES	FAILURE—CRASH	SAME AS PHASE I	FAILURE—CRASH
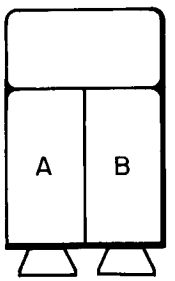 CAPSULE LANDING AND TAKEOFF STAGES	A OR B FAILS—COMPLETE MISSION OR ABORT TO ORBIT OR ABORT TO MOON A AND B FAIL —CRASH	SAME AS PHASE I	A OR B FAILS—COMPLETE MISSION A AND B FAIL—CRASH
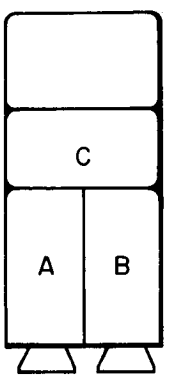 CAPSULE ORBIT STAGE LANDING AND TAKEOFF STAGES	A OR B FAILS—COMPLETE MISSION OR ABORT TO ORBIT OR ABORT TO MOON A AND B FAIL —ABORT TO MOON OR ABORT TO ORBIT	A OR B FAILS—SAME AS PHASE I A AND B FAIL—ABORT TO MOON	A OR B FAILS—COMPLETE MISSION A AND B FAIL—ABORT TO MOON

FIGURE 5

SURVIVAL AND RESCUE POSSIBILITIES

SURVIVAL LOCATION	SOURCE OF SURVIVAL SUPPLIES	SOURCE OF RESCUE VEHICLE
LUNAR ORBIT	LUNAR ORBIT LANDER (STORED) EARTH	LUNAR ORBIT EARTH MOON
MOON (LANDING SITE)	LUNAR ORBIT LANDER (STORED) EARTH LANDING SITE	LUNAR ORBIT EARTH MOON
MOON (REMOTE SITE)	LUNAR ORBIT LANDER (STORED) EARTH	LUNAR ORBIT EARTH MOON

FIGURE 6

LUNAR SHELTER AND SUPPLY SHIP

FIGURE 7

EFFECTS OF HIGH G CONDITIONS ON PILOT PERFORMANCE

Randall M. Chambers, Ph.D. and Lloyd Hitchcock, Jr., Ph.D.
Aviation Medical Acceleration Laboratory, U. S. Naval Air Development Center, Johnsville, Pa.

The general development trend in space vehicle design suggests the desirability of maximally using the occupant to both control capsule attitude and to monitor vehicle systems during the boost (and reentry) acceleration phases, as well as during orbital flight. Consequently, much more information is needed concerning man's ability to perform certain control functions under conditions in which he is exposed to accelerations which approach not only his physiological tolerance limits, but also his performance tolerance limits. In addition to the need for more data concerning the acceleration stress that man can endure and still retain the ability to perform control functions, there is a need to know specifically the nature of performance errors which can arise, not only as the direct result of acceleration, but also as secondary effects of acceleration interacting with other conditions such as the type of control task, the type of control device, the damping and stability parameters, and the pilot's physiological endurance[8]. Current concern over the performance capabilities of the human pilot immersed in certain acceleration environments is well founded since there are very few experimental reports describing the effects of these conditions on performance. The present paper attempts to summarize some of the results of recent studies conducted at the Aviation Medical Acceleration Laboratory (AMAL) in which specific pilot performance capabilities were studied under several conditions of acceleration stress.

General Experimental Method

The primary apparatus was the human centrifuge, located at AMAL, Johnsville, Pennsylvania (Figure 1). By applying suitable signal inputs to the servo systems controlling the radial velocity of the centrifuge arm and the motion and position of the two gimbals, the centrifuge provides the capability for exposing a pilot positioned in the gondola to acceleration fields which may vary along the dimensions of direction (vector), amplitude, duration, rate of onset, and complexity. Equations of motion and related vehicle characteristics, stored in a computer system, also may be programmed to present acceleration and control display conditions to the pilot as he "flies" realistic flight problems using a display panel such as that shown in Figure 2. The accelerations and displays thus received are functions of the pilot's performance interacting with the aerodynamic equations and vehicle characteristics stored in the computer. A relatively large variety of studies have been conducted utilizing this facility and general approach. Some of the studies have been concerned with basic human abilities within certain specified acceleration environments. These types of studies are to be contrasted with the vehicle simulation studies which were more oriented towards studying man's interactions with specified flight tasks and predicted vehicle conditions.

Linear acceleration is simulated on the centrifuge by using angular velocity. Three linear acceleration components may be simulated and emphasis is placed upon these. So far as the pilot is concerned, it is convenient to consider the acceleration environment in terms of the three components (Figure 3). These components are G_x (acceleration along the pilot's dorsal-ventral axis), G_y (acceleration along the pilot's side-to-side axis), and G_z (acceleration along the pilot's longitudinal body axis). Since the relative orientation of the pilot with respect to the resultant acceleration vector can be continuously controlled, any given vector may be positive, negative, or zero, depending upon the pilot's position with reference to the primary acceleration vectors. The acceleration nomenclature used in this report is the physiological-heart-displacement system[5, 16]. Regardless of whether the subject is in the seated position, the supine position, or the prone position, this nomenclature system refers to the physiological displacement of the heart within the chest when a particular acceleration force is applied. In the current report, we are concerned primarily with positive G_x (heart displaced towards the spinal column), minus G_x (heart displaced away from the spinal column), and plus G_z (heart displaced downward). Sometimes these vectors are referred to as eye-balls-in, eye-balls-out, and eye-balls-down, respectively.

To date, a consistent terminology for representing acceleration and its various components has not been adopted for univeral use by engineering, biological, physiological, and psychological groups. There is much variation in nomenclature, even within the same laboratory. More detailed discussion of the problems of acceleration nomenclature may be found in Dixon and Patterson[18], Gauer[22], Clark, et al[16], and Chambers[5].

For this report, the G system of units proposed by Dixon and Patterson[18] is used throughout, as the measure of acceleration force, although it is recognized that there is much confusion in the field regarding this terminology. In practice, therefore, G is considered as a unit of force and observed accelerations are expressed as so many "G's". For example, terms such as "6 G units" or "a force of 6 G" are frequently used to represent a force magnitude six times the weight of the body in question. It is important to note that the symbol g is used only for the

acceleration due to gravity, while G is used in aviation medicine to represent the unit of reactive force [23].

Physiological Tolerance and Performance Tolerance

One of the most important concepts in acceleration research is that of physiological tolerance, or the ability of the human subject to physiologically withstand acceleration stress. Physiological tolerance is a complex concept and encompasses a wide variety of both physiological functions and environmental factors. In reviewing the ability of man to perform a task within an acceleration environment and to maintain control over his perceptual, intellectual, and emotional faculties, it is essential that the general physiological stamina of man be considered as defining the upper limit of acceleration force within which he may be required to perform a piloting task. The concept of physiological tolerance includes all of the common physiological responses which are functions of the intensity and duration of a stress stimulus. Theoretically, therefore, the point of response may be separated from the point of no-response by a simple stimulus strength-duration curve. Figure 4 presents a summary of the authors' survey of the scientific literature and presents the current accepted physiological tolerances defined as functions of duration and G load. It should be pointed out that the points on this curve do not necessarily reflect the maximum exposures which have been experienced by human subjects.

There are some excellent reviews on physiological problems within acceleration fields in the scientific literature and the reader is referred to these for a more detailed consideration of the problem of physiological tolerance of acceleration [19, 28, 12, 14, 1, 23, 27, 4].

As pointed out in the early part of this section, the upper limits of acceleration loadings under which a given person may perform a piloting task are primarily determined by the limits of physiological tolerance. However, in addition to these physiological tolerance limits which define the maximal endpoints for safe exposure of a particular physiological system to acceleration stress, there are also performance tolerance limits which define the upper limits of reliable functioning of a particular performance-ability system under comparable acceleration exposure. Although physiological and performance tolerance limits are often functionally related, they need not be of the same magnitude since each is dependent upon its defining criteria. Performance tolerance limits are of major importance in the allocation of man-machine functions.

Prior research has indicated that as G increases, there may be an initial improvement in performance of the piloting task, followed by a gradual decline, until a performance tolerance limit is reached. Beyond this point, performance deteriorates extremely rapidly. The point of maximum efficiency is usually at a lower G than the upper performance tolerance limit; however, to date, this point has not been specified directly. Under conditions of moderate acceleration, experienced pilots may utilize motion and acceleration cues in performing their tasks and these cues, along with reasonably high concentration and motivation, may enable the pilot to do better under moderately high acceleration than under static conditions. At high G, performance proficiency deteriorates markedly. This deterioration generally reflects impairment of vision and the ability to breathe, physically strain, or a reduction of the pilot's ability to resist the physiological effects of acceleration. Summaries of the effects of acceleration upon performance may be found in Brown [2] and Chambers [4, 5].

G tolerance may be expressed as a function of at least five primary acceleration variables: (a) the direction of the primary of resultant G force with respect to the axes of the human body, (b) the rate of onset and the decline of G, (c) the magnitude of peak G, (d) the duration of peak G, and (e) the total duration of acceleration from time of onset to termination. There are also other auxillary conditions which influence a human subject's tolerance. Among these are: (a) the types of endpoints used in determining tolerance, (b) the types of G protection devices and body restraints, (c) the type of environment in which a subject is tested, such as temperature, ambient pressure, noise and lighting, (d) age, (e) psychological factors such as fear and anxiety, competitive attitude, and willingness to tolerate discomfort and pain, (f) previous acceleration training and exposed accumulated effects, (g) the type of acceleration device used for exposing the subject to acceleration, and (h) muscular tensing and effort [23].

Effects of Acceleration on Vision

During exposure to high positive, negative, and transverse acceleration, visual disturbances occur. During positive acceleration, these disturbances result primarily from ischemia; however, mechanical distortion of the eye may also occur in severe cases. Generally, a period of grayout exists before blackout occurs. Grayout is characterized by general dimming and blurring. Total visual disturbance occurs approximately one G unit below the level at which blackout occurs. During exposure to high transverse acceleration, the effects on the visual system depend largely on whether the acceleration force is $+G_x$ (eye-balls-in) or $-G_x$ (eye-balls-out). When the acceleration is $+G_x$, no major visual disturbances have been reported up to loads of + 14 G_x for 5 seconds at peak G. At levels between plus 6 and plus 12 G_x, however, there may be some tearing, apparant loss of peripheral vision, and difficulty in keeping the eyes open. For $-G_x$ (eye-balls-out acceleration), some pain may be experienced and small

petechiae may occur on the lower surface of the eyelids. Vision may be temporarily impaired, although to date, no internal damage has been reported for accelerations as high as +15 G_x. For -G_x acceleration, however, the kind of restraints provided for the anterior surface of the body is a major consideration.

The problem of seeing under transverse acceleration appears to be largely a mechanical problem, due partially to mechanical pressures on the eyes and the accumulation of tears. In addition to G amplitude and the direction of the primary G vector, the duration of peak G is of major importance. Total time in which a human subject can endure exposure to acceleration stress and maintain good vision depends largely on the system of G protection. Using a system of G protection developed by Smedal, et al[25], ithas been possible to achieve the following record runs by transverse and positive G on the AMAL centrifuge: 90 seconds at +7 G_z, 127 seconds at +14 G_x, and 71 seconds at -10 G_x. These record runs were conducted on the AMAL centrifuge using the advanced restraint system developed by the Ames Research Center. They do not necessarily establish limits of visual performance, however, since the relationship between amplitude of G and duration at peak G has not been established. For example, in an earlier experiment at AMAL, one subject, using a contour couch restraint system developed at AMAL, was able to performa visual task during an extremely high G run which took him to +25 G_x for 5 seconds.

Visual acuity decreases as the magnitude of G increases[20, 29]. This occurs during exposure to both positive and transverse acceleration. As G increases, a given level of visual acuity may be maintained by increasing the size of the target or the amount of luminance. White and Jorve[29], for example, found that at +7 G_x the target had to be twice as large as it was at one G in order to be seen. In another study, White[30] observed that a test light had to be nearly three times as bright at 4 G_z as at 1 G_z in order to be seen. Thus, a pilot's ability to read his instruments is influenced by acceleration. However, the magnitude of this effect is a partial function of the level of illumination. At high luminance, the impairment due to G is not as great as it is for the same G at lower levels of luminance. White[30] has shown that at moderate tolerance limits, increasing the amplitude of positive acceleration increases the absolute foveal visual thresholds. In most situations in which a pilot is going to be exposed to acceleration, it is important to know the amount of contrast required by the pilot in order to insure visual discrimination. As acceleration increases, an increase in contrast is required to detect a target. This has been shown in a recent study by the authors and Drs. Braunstein and White at AMAL. In this study, it was demonstrated that the minimally acceptable (threshold) contrast was greater for positive acceleration than for transverse acceleration. For example, a 16 percent contrast between the target and its background was required at +5 G_z and a 12 percent contrast was required at +7 G_x. For static conditions, an average luminance differential between target and background of approximately 8.5 percent was required for discrimination. In this particular experiment, visual brightness discrimination was studied at four levels of background luminance, at four levels of positive acceleration, and at five levels of transverse acceleration. For this study, a stimulus display generator (see Figure 5) was mounted in the gondola. This generator presented a circular test patch against a diffuse background. The display was viewed monocularly through an aperture which was 17 1/2 inches from the eye. The visual angles subtended by the circular test patch and its background were 1 degree and 28 minutes, and 8 degrees and 4 minutes, respectively. The background was generated by eight 25 watt light bulbs behind two sheets of flashed opal by a 500 watt slide projector. A frontal view of the display is shown in Figure 6. Voltage to the projector bulb was controlled by a motor-driven variac which altered the operating voltage at the rate of volts per second. A neutral density filter was placed behind the viewing aperture to produce the desired background luminance. A response button, provided to the subject, was used to indicate the appearance or disappearance of the test patch. Figure 7 shows the installation of this visual response button. After activation of the response button by the subject, the direction of rotation of the motor driving the variac which controlled test patch luminance was automatically reversed with the time between subject response and motor reversal programmed to range from 1.25 to 3.75 seconds in a random delay order. At the instant of the subject's response, the voltage across the projection bulb was stored and displayed upon a digital volt meter located at the experimenter's station. Approximately 15 responses were made during the peak G of each run. With this apparatus, it was possible to repeatedly measure a subject's ascending and descending visual discrimination thresholds. Using 6 healthy adult males with 20/20 vision, brightness discrimination thresholds were determined at transverse acceleration levels of + 1, 2, 3, 5, and 7 G_x and positive acceleration levels of + 1, 2, 3, and 5 G_z. Determinations were made at each G level with background luminance of .03, .29, 2.9 and 31.2 foot-lamberts. Figure 8 shows the observed relationship between brightness discrimination threshold and background luminance for each of the four levels of positive acceleration. Similarly, Figure 9 shows the obtained relationship between brightness discrimination threshold and background luminance for each of the 5 levels of transverse acceleration.Figure 10 shows the effects of positive acceleration (+ G_z) on brightness discrimination thresholds for perceiving the circular target against each of the four background levels. These figures show that for each of four positive acceleration conditions, the mean required contrast

increased as the background luminance decreased. Also, for any given background luminance level, the higher acceleration levels required more brightness contrast. Similar results were shown for the transverse G exposures as may be seen in the figures although the differences due to background luminance were more than those due to acceleration levels. As previously mentioned, positive acceleration stress consistently imposed higher contrast requirements than did transverse acceleration. These data clearly show that marked increases in the brightness contrast required for discrimination as G increased in both the positive and transverse axes.

It is important to indicate that the physiological conditions under which the pilot performs a task such as this greatly influences the data which are obtained. For example, some of the subjects in the above study also served in an experiment to determine whether or not positive pressure breathing of 100 percent oxygen facilitates brightness discrimination at the upper G levels [9]. The subjects performed under three breathing conditions; breathing normal air, 100 percent oxygen, and 100 percent oxygen under positive pressure. Given a background luminance of .03 foot-lamberts, the subjects were required to repetitively operate a switch (see Figure 7) to maintain the target (Figure 6) at the minimally discriminable brightness contrast level. The results obtained under positive (G_z) acceleration exposures of 90 seconds duration each under acceleration loads of +1, +3, +4, and +5 G_z are shown in Figure 11. These data suggest that at the +3, +4, and +5 G_z levels, the positive pressure plus 100 percent oxygen required less visual contrast than was required under the other experimental conditions. Similar results were found for the transverse G. The contrast required for discrimination appeared to be the same for both the 100 percent oxygen and 100 percent oxygen plus positive pressure breathing conditions. Oxygen would appear to play an important role, since subjects breathing normal air under positive pressure required increasing amounts of contrast for discrimination as G increased.

The two investigations just described were presented primarily to illustrate the sort of investigations which are conducted using the AMAL human centrifuge in w hich basic sensory capacities are being studied. Similar investigations have been concerned with the effects of high accelleration upon pilot ability in such areas as discrimination reaction time, complex psychomotor performance, and higher mental abilities.

Discrimination Reaction Time Performance

In addition to influencing the pilot's ability to perceive stimuli, acceleration modifies his ability to respond to them as well. Many maneuvers which pilots must perform frequently require not only the discrimination of but the reaction to visual stimuli. In this section, we present the results of some recent work in which this latter aspect of performance was studied in some detail.

Many investigators have studied discrimination reaction time behavior on human pilots during exposure to acceleration stress. Although it is generally agreed that some acceleration environments do influence discrimination reaction time behavior, thus far it has been impossible to designate all of the underlying mechanisms which mediate these effects. During acceleration, the changes observed in reaction time could be associated with pilot impairment in a variety of physical loci. Acceleration might well reduce the capacity of the peripheral system to receive the stimulus, or of the central nervous system to process already received stimuli and to initiate discriminatory choice, as well as reduce the ability of the neuromuscular system to coordinate the motor components which translate the response into the manipulation of the appropriate control device. In addition, some studies have indicated that discrimination time under G is indirectly affected by the protective equipment and related components present in the situation in which the tests are conducted. There were also several types of discrimination reaction times, depending on the stimuli, responses, and the types of tests.

Frankenhauser[21], using red, green, and white light signals, measured complex choice reaction time during exposure to +3 G_z and found the subject took significantly longer to respond under acceleration than under normal (+1 G_z) conditions. This was true for exposures of both two minutes and five minutes duration. Her conclusion was that visual choice reaction time was increased by positive acceleration. Similarly, Brown and Burke[3] found highly significant effects of positive acceleration upon discrimination reaction time.

In contrast, relatively little information is available concerning the effects of transverse acceleration on discrimination reaction time. At our laboratory, a discrimination reaction time test apparatus was developed which consisted of four small stimulus lights, a small response handle containing four small response buttons, and a programmer device which could present a large variety of random sequences to subjects on the centrifuge[11]. Tests conducted on discrimination reaction time behavior of subjects statically and while submerged in water showed that subjects could respond steadily and reliably on this device. A typical example of data from this experiment is shown in Figure 12. However, mounting the device upon the centrifuge revealed that transverse acceleration exposures significantly influenced performance of the discrimination reaction time tasks. Figure 13 shows the installation of this apparatus in the centrifuge. As each of the lights came on, the subject was required to press the associated finger button with his right hand as fast as he could. Both the automatic program which activated

the stimulus lights and the subject's responses were fed to an analog computer where initial data reduction was accomplished. Following pre-acceleration training to a stable baseline performance level, each subject received three blocks of twenty-five trials each while exposed to 6 G_x for five minutes. Each subject received three such acceleration trials. Since speed and accuracy are both involved in this type of response behavior, times and errors were normalized and added. The results are shown in Figure 14. This figure shows that during the first block of twenty-five trials, the average response scores were slower than the overall average. During the second series of trials, the response scores were even slower than for the first block of trials. For the third block of trials under G, however, performance was significantly improved over that exhibited during the earlier trials. The results of this study suggest that acceleration initially impaired performance during the first and second series of acceleration trials but that by the third series of trials, the subjects had learned to maintain their physiology and performance under acceleration stress and, consequently, their discrimination reaction time scores improve, suggesting that learning how to perform during exposure to acceleration stress is a primary factor in determining pilot performance ability. It may well be that the process of learning could account for some of the differences in findings which have been reported by earlier investigators who contrasted static and dynamic conditions with taking into account the possibility of rapid adaptation to the experimental conditions.

Another approach to reaction time investigation involves the use of an auditory rather than a visual stimulus in order to avoid the problem of visual interference which is known to accompany acceleration. One such task[17] required the subject to add pairs of numbers which he heard via an auditory magnetic tape system and then to describe the sum by pressing the small odd and even response buttons which were mounted upon his left and right hand grips, respectively. Primarily, work with this apparatus during positive G_z exposures to grayout levels indicated that the time required to make these responses increased during exposure to positive acceleration.

Complex Psychomotor Performance

The ability to perform a complex psychomotor test is impaired in most cases by acceleration. A typical example of a relatively simple case is shown in Figure 15 in which the skill with which six subjects performed the horizontal and vertical components of a tracking task response at one minute intervals during each of two +8 G_x trials is plotted as a function of acceleration. The acceleration profile is dotted at the bottom of the graph. During these test runs, the subjects operated a control device in response to the coordinated pitch and roll tracking maneuvers which were pre-programmed and presented to the subject by means of the oscilloscope. The apparatus and the contour couch on which the subject was accelerated is shown in Figure 16. The graph shows steady performance levels for the horizontal and vertical components of the tracking tasks prior to exposure to acceleration. When peak G was reached, decrements in both components were obtained but as acceleration receded to normal, both performance components rapidly returned to the normal skill level. Figure 15 also shows the effects of acceleration following submersion in water to the neck level for 12 hours[11]. These subjects showed approximately the same performance curves, even after an unusual and prolonged intervening experience, suggesting the relative stability of the control decrement associated with acceleration stress.

In other recent work at our laboratory the authors, in cooperation with Mr. Creer and Dr. Smedal of NASA, used the centrifuge to simulate sustained reentry tracking control problems. It was demonstrated that well trained test pilots could successfully perform a moderately complex tracking task while being subjected to a relatively high and varied acceleration for prolonged periods of time. A special restraint system[25] was used to minimize physiological discomfort during this particular study. Tracking efficiency was calculated in percentage units based on the accumulated tracking error divided by the accumulated excursion of the target in this study. Pitch and roll control inputs were made with a small two axes pencil controller and the yaw inputs were made with the toe pedal which was operated by flexion and extension of the foot about the transverse axes of the ankle joints. The restraint equipment used in this study is shown in Figure 17. In this particular study the rate of onset for all the accelerations was approximately .1 G per second. Each tolerance run was preceded by a static run which was intended to serve as the baseline for the prediction of performance under acceleration. Tracking performance was impaired at the high G levels; however, the pilots were able to maintain proficiency above the minimum levels considered necessary to continue the run, as determined from a percentage scale of -100 to +100 percent derived from the division of actual control output by required output. Smedal, et al[26] have published some of the results from this experiment and have related these performance boundaries to the accelerations anticipated during reentry from both circular and parabolic (lunar return) orbits. They concluded that a man properly restrained can withstand the acceleration stress imposed by reentry from minimal circular orbits. The subjective findings obtained during this study emphasized the visual, cardiovascular, and respiratory effects accompanying acceleration. One major advantage of $-G_x$ acceleration over $+G_x$ was indicated by this study, namely that during $-G_x$ acceleration, the forces of acceleration assist in breathing by increasing the interior and posterior diameter of

the chest, the normal functions of inspiration, whereas during $+G_x$ these same forces impede inspiration through chest compression.

In a more recent study with NASA/Ames, conducted at the AMAL centrifuge, Chambers and Smedal tested pilots able to reach phenomenal transverse acceleration endurance records and still maintain a relatively high level of performance proficiency on a complex tracking task. The most striking centrifuge runs for $+G_x$ steady state acceleration was +14 G_x for 127 seconds. The outstanding run for $-G_x$ steady state was -10 G_x for 71 seconds. This was accomplished by using the special restraint system shown in Figure 18.

In another AMAL study, test pilots who had performed a complex tracking test at transverse acceleration levels of 1, 3, 5, 7, 9, 12 and 15 G_x were asked to estimate the amount of performance decrement which occurred under each acceleration load. In making their estimations, the pilots used their performance at 1 G as the base referant and attempted to contrast their performance at other levels against their own 1 G performance. The average estimates for performance decrement are shown in Figure 19. At the 12 and 15 G_x levels, the outstanding problems which the pilots reported they encountered were impairments of vision, difficulty in breathing, as well as difficulty in operating the control device used.

To study the effects of acceleration on the ability of pilots to perform control tasks during simulated boost accelerations, Chambers and Holloman exposed pilots to staging acceleration profiles characteristic of both a two-stage launch vehicle and a four-stage launch vehicle. The analog computer facility used generated and converted into vehicle dynamics the pilot's display and control problem as well as the commands for driving the centrifuge. In this particular series of runs, the longitudinal mode (pitch) required almost continuous control whereas the yaw control required only monitoring and correcting for disturbances. Figure 20 summarizes some of the findings and provides an example of pilot performance in which some features of the piloting task were greatly affected by acceleration while others were not. In this particular study, the pilots indicated that they were unable to concentrate on more than one or two things at the same time at high G. Thus, they found it necessary to neglect some parts of the four dimensional tasks shown here while under acceleration. Subjective ratings made by the pilots showed that under low accelerations, only normal physical effort was required to perform the launch control task. However, at the highest acceleration tested, 100 percent effort was required. The 100 percent effort rating was applied to a series of special runs which sampled abilities to perform under acceleration loads extending up to as high as 15 G. Such limit testing only augmented the primary portion of this investigation which involved a computer controlled simulation of a hypothetical four-stage launch vehicle. Figure 21 shows a typical launch curve for this simulated condition. The pilot's task was to fly the vehicle through the orbital injection "window". At the acceleration level studied (all below 7 G_x), there appeared to be little effect of the acceleration on the control task as determined by the pilot's ability to manage the primary control quantities. These results are shown in Figure 22.

Effects of Varying the Type of Control Device Used

In addition to both the direct effects of acceleration upon human performance and the less obvious interactions between performance and acceleration already mentioned, there is a growing body of information pertaining to the somewhat secondary role that other flight conditions play in determining a pilot's performance during exposure to acceleration[7,8]. An important example of this is the contribution made by the type of control device that the subject is using. Control devices have many characteristics which may influence performance under acceleration conditions. Some of the variables found to be important are: (a) the relationship between the axes of controller motion and the acceleration vectors imposed upon the pilot's hand, (b) the number of axes of motion, (c) the stick force gradient along each mode of control, (d) the centering characteristics along each mode of control, (e) the basic location of the control device, (f) controller breakout forces, (g) control device friction, (h) damping characteristics, (i) the magnitude of control throw, (j) control response time, (k) control harmony, (l) cross coupling, (m) the amount of kinetic feedback provided by the controller, (n) controller shape and size, and (0) the dynamic and static balancing of the control device. The combination and interactions of these characteristics requires a very complex and extended discussion. Therefore, the present report will cover only those aspects found to contribute most to controllability.

In the course of early simulations of proposed space vehicles, several types of right hand side controllers have been tested. Figure 23 presents a diagram of four of these controllers: a three axis balanced controller with all three axes intersecting; a three axis controller (unbalanced) having none of these three axes intersecting; a three axis balanced controller; a finger tip controller having two intersecting axes with yaw operating via toe pedals; and a two axis controller with axes that do not intersect, coupled with toe pedals for yaw control. In Figure 24, the effects of two specific acceleration fields upon pilot performance during the pitch and roll maneuvers involved in a tracking task are shown for each of the four types of controllers. While the pilots performed in one acceleration field, their error performance on all four controllers was essentially the same. However, when these same pilots flew

the same problem under a different acceleration vector, performance on Type II controller greatly increased while performance on the other two controllers remained essentially unchanged. A simular change in G field resulted in an increment in error for Types II and III controllers and reduction in error for Type IV, resulting in a shift in rank order of the controllers. The differential effects upon performance induced by different types of acceleration controllers are shown in Figure 25. Here, the mean tracking efficiency scores for test pilots who perform the same tracking tasks using each of the four different t ypes of side arm controllers within given acceleration fields and under varying amounts of cross coupling and damping are shown. This figure shows not only the effect of using different specific G fields on particular tracking tasks but also illustrates the effects of damping and cross coupling when the effects of acceleration are held constant.

In studying the effects of acceleration, one must also consider the complexity of the task to be performed by the pilot since t ask complexity is magnified under G^2. Basic research upon the effects of high G upon complex task performance is frequently complicated by the need to control the numerous variables associated with task difficulty. Aerodynamic stability, damping frequency, time constant, and other vehicle response characteristics strongly interact with acceleration to determine pilot performance at high G. If the simulated vehicle is highly stable and well damped within the desired frequency ranges, the pilot may find performance under high G relatively easy. However, the same general piloting task may be impossible at lower G levels with a simulated vehicle having less desirable aerodynamic characteristics.

Effects of Acceleration on Higher Mental Abilities

To date, there is a severe lack of reliable and valid tests of higher mental activities which can be administered within the basically restrictive and time-limited conditions encountered in centrifuge operation and still retain the measurement sensitivity required. A way to monitor the intellectual functioning of the subject while he is being exposed to acceleration conditions is sorely needed. Several reviews of this problem have been presented [5, 6, 7, 24]. It is a generally accepted fact that exposure to high or prolonged acceleration may produce confusion, unconsciousness, disorientation, memory lapse, loss of control of voluntary movements, or prolonged vertigo. However, the tolerance limits of basic intellectual functions are unknown, and there is very little quantitative information which would indicate which of the specific higher mental skills may suffer impairment.

An astronaut or scientific observer during some phases of flight may be required to perform tasks such as monitoring, reporting, flight guidance, and other tasks which require immediate memory and the processing of information. To date, there is no conclusive information available regarding the effects of acceleration upon the basic intellectual abilities required for such functions, i.e., immediate memory and the ability to process information.

Using the human centrifuge at AMAL, Ross and Chambers conducted a study on the effects of both positive and transverse acceleration upon the ability to perform a task which placed demands upon these psychological abilities. A continuous memory testing apparatus was developed which could be used under both static and acceleration conditions. This test required the continuous and repetitive memorization of a portion of a sequency of random symbols. As each symbol occurred, the subject was required to compare it with his memory of the s ymbol which had been presented to him two, three, or four presentations previously. New symbols appeared continuously so that the subject continuously had to f orget earlier symbols as he added the new ones. Basically, this task involved both the immediate memory and the facility for handling an "information load" of symbols under conditions in which opportunity for symbol interference was at a high level. The "running matching memory" task used was simple to grasp and administer but difficult to perform without error. The subject was presented with a plus or a minus sign by means of a digital display tube mounted in front of him and was required to judge whether the sign he saw was the "same" as "or different from" the sign he had seen either 2, 3, or 4 presentations previously. These three memory spans were interspersed throughout a test series and were known as the 2-back, 3-back, and 4-back condition, respectively. Simultaneous with the presentation of the plus or minus sign, the subject saw the numeral 2, 3, or 4 in another tube, indicating whether a 2-back, 3-back, or 4-back match was to be performed. The subject made the required matches for each sign as it appeared. Each sign was presented for four seconds with a one-second interval between presentation. A series of fifty signs was presented within any given run. The G-level selected for investigation was 5 transverse G for 5 minutes.

Data analysis indicated no significant differences in percentage of correct memory matches between static and G conditions. Twenty-four subjects completed the required series of four 5 G runs of five minutes each, however, there was an increase in the latency betweenpresentation and time of response. Also, the subjective comments concerning performance on this task did not correlate well with the actual quantitative measures (Figure 26). The number correct for each series was converted into a percentage since the number of matching responses made were not quite the same for each condition — 48 matches for a 2-back condition, 47 matches for a 3-back condition and 46 matches for a 4-back condition. Subjects reported that their performance deteriorated under G and they regarded this exposure as an extremely stressful experience.

Related research has suggested that the previously discussed measures of discrimination reaction time reflect intellectual performance, and that one may use such measures as a general indicator of higher mental functioning. The results of some studies at AMAL suggested not only that discrimination time was impaired under G, but also for some time after the termination of G. Figure 27 summarizes the results of one such study. In this figure, the abscissa is quantified in standard-error-of-mean units. Using a one tailed t-test, it was shown that performance was significantly impaired not only under +6 G_x acceleration but that this decrement persisted after the centrifuge run was completed and the pilot returned to the normal (+1 G_x) acceleration field.

In a more recent study conducted at AMAL, a second attempt was made to explore higher mental functioning of human subjects exposed to acceleration stress. The task required the subject to monitor two small display tubes which were located directly in front of his normal line of vision. The left-side tube presented numbers, and the right-side tube presented plus and minus symbols. The task was to continuously make matches for these two presentations simultaneously as the runs proceeded and to select one of two buttons to indicate whether both the number and symbol which were then appearing were the same as or different from those which had occurred a specified number of trials previously. Nineteen male subjects volunteered to perform this running matching task while sustaining transverse accelerations of 1, 3, 5, 7, and 9 G's. Each test was 2 minutes 18 seconds long. The results of the experiment suggested that proficiency in immediate memory was maintained at least through 5 transverse G. However, at 7 G and 9 G, some impairment in immediate memory was observed.

During prolonged exposure to acceleration, the continuous concentration necessary for performance maintenance is difficult, fatiguing, and boring. For example, during an extended 2 G centrifuge run which lasted for 24 hours, the subject started out with a somewhat detailed set of procedures to follow in making medical observations upon himself, recording his subject comments, and writing and typing [13, 15]. However, the subject found that, in spite of his initial high resolves, he took naps and listened to the radio instead and suffered primarily from boredom and fatigue. Areas of contact with the chair in which he was seated were the sources of the greatest localized discomfort. At 16 hours elapsed time, the subject reported the onset of aesthenia of the ring and little finger and outer edge of the palm of the left hand. The subject found it impossible to maintain his originally prescribed maintenance and observation schedules.

In an attempt to obtain specific information concerning the effects of extended, moderate acceleration upon higher mental abilities, a shorter study (+2 G_x for 4 hours) was performed. The subject was secured in a contour couch and required to perform the two-symbols running matching memory task previously described every 10 minutes. The subject was able to perform this task throughout the entire period with only minor performance impairment. Furthermore, task performance during the 4-hour acceleration exposure was not significantly different from performance either before or after the centrifuge run. Throughout the test period, task performance was highly correlated with the pilot's subjective estimations of his proficiency.

The Effects of Acceleration Upon Specific Mission Tasks

The performance measurements described thus far have emphasized the effects of acceleration(s) upon the expression of rather general psychological and/or psychomotor abilities. Recent data indicate that even highly specific and well practiced skills are not immune to the effects of acceleration. For example, performance measures collected during a recent astronaut training program, Mercury Centrifuge IV, conducted jointly by NASA and AMAL, revealed several significant effects of dynamic simulation upon pilot performance and response.

Two primary modes of centrifuge control may be used during such a dynamic simulation of the accelerations associated with space vehicles and high-speed aircraft: (1) open-loop and (2), closed-loop centrifuge command systems. In open-loop control, the centrifuge commands are preprogrammed either on punched tape or within the computer proper. These programmed commands are not subject to pilot control short of termination of the simulation by activation of the abort switch. In closed-loop centrifuge control, the pilot overlays the effects of his control actions upon the preprogrammed acceleration profile. The actual accelerations imposed upon the pilot thus reflect not only expected system characteristics but pilot performance as well.

By combining the control motion outputs with the preprogrammed acceleration commands, the computer's coordinate converter system presents drive signals to the centrifuge which directly reflect the pilot control outputs.

During both modes of operation, the pilot's instruments and panel displays, particularly those concerned with the vehicle's rates and attitudes, are usually controlled by a closed-loop system to provide the pilot with immediate and continuous feedback regarding his control activities. However, certain displays such as event-times and/or sequences are often controlled in an open-loop manual or preprogrammed fashion. Figure 28 is a schematic presentation of the centrifuge/computer interface during open-loop acceleration command (solid lines) and closed-loop panel display (open lines).

For the simulation to be discussed here, a punched-tape program was used to drive the centrifuge in an open-loop command fashion. The side-arm controller, the computer, the instrument panel, and the pilot formed a closed-loop system of display activation. The acceleration profile (Figure 29) was a real-time approximation of the accelerations predicted for the orbital mission. For the runs to be discussed here, the orbital time was collapsed with retrofire closely following the completion of the boost phases and capsule turnaround. During static simulations, only the closed-loop display system was activated, thus providing a real-time simulation of the control tasks with their associated panel displays and telepanel sequence indications. The dynamic simulations used the same displays and controller tasks but were accompanied by the open-loop driving commands to the centrifuge which superimposed the acceleration profile upon these piloting tasks.

The data to be discussed here are based upon a series of twelve simulations (four static and eight dynamic) which were flown by each of the seven astronauts. These twelve simulations sampled performance under most of the possible combinations of acceleration, suit, and cabin pressurization conditions.

During such simulation programs, pilot performance is continuously monitored and evaluated. The facility primarily responsible for this phase of simulation assessment, the Engineering Psychology Laboratory, is equipped with an analog computer and associated equipment including graphic plotting, digital print out, and FM-tape recording capabilities. The primary unit of measurement is the analog error as represented by the voltage differential between inputs representing the existing controller and/or vehicle positions and the preprogrammed inputs representing the appropriate or desired attitudes. Figure 30 graphically summarizes the techniques of analysis and summarization available within this facility. This figure also portrays the capability for discrete task and event recording as well as for recording the latency of pilot response to displayed event indications.

In the course of an orbital mission of the Mercury type, in addition to his other duties the astronaut is required to monitor the telelight portion of the capsule instrument panel and to confirm booster and/or capsule response(s) to a programmed sequence of flight events. If an event is not performed at the scheduled time, the telelight panel displays a RED-LIGHT condition (indicating capsule receipt of the event command not accompanied by internal confirmation of the required operations) or a NO-LIGHT condition (indicating panel and/or internal telemetry system failure). It may then be necessary for the pilot to manually initiate (over-ride) the operation(s) normally instigated by the automatic, programmed circuitry. During training simulations such as the recent Mercury IV program, an externally mounted control panel (Figure 31) is used to monitor and control the inputs to the telelight display which is along the left side of the pilot's control panel (Figure 2). When RED-LIGHT or NO-LIGHT indications were given, a .01-second timer recorded the time between normal automatic instigation and its associated telepanel warning and the performance of the required over-ride by the pilot.

It should be noted that only one of the required telepanel over-rides, manual operation of the Escape Tower Jettison ring, occurred under G. Even this over-ride involved only moderate acceleration loads of approximately 2 G. However, for purposes of the following discussion, telepanel responses which were made in the course of simulations involving centrifuge acceleration are classed as Dynamic responses even though little or no acceleration loads were present at the actual moment of response.

The following three general categories of acceleration effects were among those noted during the course of this program:

1. Acceleration resulted in the insertion of specific control inputs of which the pilots were often unaware.

2. Acceleration generally disrupted the timing and precision of pilot control.

3. Discrete task functions such as an operation over-ride were affected by accelerations which preceded and/or followed them though the operations themselves were performed under minimal acceleration loads.

These three effects of acceleration have been treated generally elsewhere [5, 10]. The purpose of the following discussion is to show how these general effects are expressed within a specific system configuration.

Inadvertent Control Inputs

At rest, a side-arm controller such as that used in the Mercury capsule is adjusted to maintain the central position in all axes and is balanced to retain this inactive, central position under acceleration. Any displacement of the controller, in excess of the central inactive range or "dead-band", serves to activate the capsule's control jets (nozzles) which impose reorientation accelerations upon the capsule. Dynamic conditions are not infrequently accompanied by controller deflections of which the pilot is unaware. Any control deflections occurring without the knowledge and intent of the pilot can seriously complicate the control task. Such inadvertent control inputs can even result in complete loss of control, since the limitations upon nozzle velocity are such that inadvertent inputs can easily reach sufficient magnitudes and/or durations to impose reorientation rates beyond those which can be damped within the time limits established by the mission profile. These inadvertent inputs often mirror the acceleration profile under which the

control tasks are performed. Figures 32, 33, and 34 are representative examples taken from actual records, which display such inputs in the roll, yaw, and pitch axes respectively. As illustrated by these sample records, these involuntary control deflections generally appear in a single axis though Figure 35 illustrates the less frequently observed simultaneous appearance of inadvertent inputs in two axes: roll and yaw. The fact that the pilots are often unaware of such inputs is illustrated by the fact that the excessive fuel utilization associated with such sustained deflections was interpreted upon several occasions as a simulated fuel leakage problem and not as the result of controller activation.

General Control Effects

In addition to inadvertent inputs which accompany acceleration, other more general effects of dynamic conditions may be observed. Acceleration appears to generally reduce the sensitivity and timing of all controller movements. Figures 36 and 37 are sample portions of the recorded static and dynamic performance of the same pilot taken within twenty minutes of each other. These records serve to illustrate the general effects of acceleraupon the frequency and amplitude of control movements. Certainly no one should be surprised to learn that the task of flight control is made more difficult by the imposition of acceleration forces. However, the authors are willing to risk the accusation of pedantry in order to emphasize the extent of such effects as well as the need to assess such effects by dynamic simulation before attempting to estimate actual flight performance parameters. The fact that dynamic conditions do affect pilot effectiveness is amply illustrated by the percentage of simulated reentries in which the rates of capsule oscillation were kept within the limits of control capability under static and under dynamic conditions (Figure 38). Since the simulations upon which these percentages are based imposed pitch and yaw oscillation rates drawn from the upper extreme of the range of expected values, and insofar as Friendship 7 successfully reentered even though the oscillations were quite large, these percentages do not represent the probability of success of an actual Mercury flight or similar missions. However, these figures may be considered representative of the general effects of acceleration upon the ability of pilots to dynamically perform control tasks which they perform easily under static conditions.

As previously mentioned, the tendency to use less discrete, more frequent control inputs (Figure 37) under dynamic conditions is associated with an overall increase in fuel utilization. A most important aspect of this relationship rests upon the fact that differential rates of fuel usage were observed even when no significant differences in adequacy of control as measured by integrated attitude error were present. As previously indicated, pilot ability to damp the reentry oscillations in pitch and yaw was reduced under dynamic simulation. In contrast, control capability in the roll axis was not significantly affected by dynamic reentry accelerations. Therefore, roll control during reentry can be used to illustrate this dynamic effect under conditions of equivalent error. Figure 39 illustrates not only the correlation between incurred roll rate error and compensatory fuel usage [fuel used/lbs. = k·(.00012·Integrated Roll Rate Error in Degree seconds/sec.)]but also that fuel utilization was approximately 33 percent greater under dynamic (k = 1.328)than under static conditions (k=1.00) though integrated error was of the same approximate magnitude under both conditions. It is highly unlikely that the additional fuel usage predictable from these results would interfere in any way with a mission such as the Mercury three orbital flight sinceadequate fuel reserves were available. However, it is conceivable that the failure to take into account a potential increment in fuel expenditure in excess of 30 percent could have serious consequences in future missions of longer duration. Data of this nature emphasize the advisability of obtaining both dynamic and static performance evaluations for any system configuration before placing estimated values upon such design parameters as required fuel reserves.

Other aspects of pilot performance also confirm the value of dynamic performance evaluations. As may be seen in Figure 40, the hard suit (5 psi differential pressure) conditions resulted in a reduction in relative piloting performance as measured by the percentage of the reentry simulations in which capsule oscillations were successfully damped during static simulation of the reentry control task, but appeared to assist performance under dynamic conditions. The performance values presented in this figure are not absolute but represent relative performance using the conditions of STATIC/SOFT-SUIT, under which control most often retained throughout the reentry profile, as a base-line referent. The additional forearm support provided by the pressurized suit appeared to reduce the frequency and/or magnitude of the previously described inadvertent inputs which accompanied dynamic simulation. As the tendency to insert such inputs was reduced through practice, the stabilization provided by the inflated suit appeared to become less and less of an advantage and the interaction between suit and run conditions was markedly less during the latter stages of training. Verbal reports obtained toward the end of the training program indicated that the pilots considered SUIT-HARD conditions more uncomfortable and perhaps even less effective.

Discrete-Task Responses

As can be seen in Figure 41, the overall mean response time to telepanel indications was not affected by acceleration. However, dynamic simulation did significantly increase response variability ($F = 2.9$, $p < .05$). This latter finding could be of operational significance in system configurations requiring precise manual sequencing on the part of the pilot. Also, of interest, is the observation, implied by the large variance in the response times obtained under acceleration, that individual pilots

react differentially to the stress(es) of dynamic acceleration conditions. Table 1, which summarizes the performance of the five astronauts for whom complete data were available, serves to demonstrate the extent of this differential reaction. As shown in this table, pilots No. 1 and No. 4 displayed shorter reaction times under dynamic conditions to all but one malfunction indication. At the other extreme, the response times of pilot No. 2 to all indications were retarded during dynamic simulation. Under acceleration, the other two pilots exhibited consistent but mixed response time alterations as a function of the indication involved.

Table 2 summarizes the relative response times to the NO-LIGHT and RED-LIGHT panel indications under both static and dynamic conditions. As can be seen, response time was considerably longer when no indication was given than when improper sequencing was displayed to the pilot by the RED-LIGHT panel indication. Response variability was significantly ($F = 88.53$ $p<.01$) greater under the NO-LIGHT condition. There was some tendency for acceleration to increase reaction time to the NO-LIGHT condition more than for RED-LIGHT presentations though response variability was such that this interaction was not found to be statistically significant. However, additional evidence of an interaction between type of indication and acceleration is available from a tabulation of totally missed telepanel indications. Upon only seven occasions did the pilots fail to make any response whatever that would indicate recognition of an existing sequencing problem. All seven of these response failures occurred under the NO-LIGHT and Dynamic conditions.

Average response times were not significantly affected by the change in altitude simulated by gondola evacuation (Figure 42). Average override latency was 3.64 seconds at sea level pressure (14.7 psi) and 4.68 seconds when gondola pressure was reduced to 5 psi. As shown in Figure 43, the pressurization of the suit did not significantly alter response time. Average latency was 4.28 under SUIT-HARD conditions and of 3.68 seconds with the soft suit.

Summary and Conclusions

This report attempts to consolidate the findings of both prior and recent research in the area of acceleration effects upon performance and to relate these findings to basic piloting behaviors. The decrements in the visual, psychomotor response, and intellectual processes which have been found to accompany acceleration stress are quantified where possible. Both transverse and positive accelerations have been shown to raise the level of contrast required for visual brightness and to reduce general acuity at acceleration loads well below those which result in gross visual impairment. Similar impairments in discrimination response rates are also discussed. The techniques thus far used to assess higher mental ability under acceleration are presented as are some of the problems which complicate such measurements. Data from such studies are presented to illustrate the reduction in immediate memory and information processing capabilities of pilots experiencing both high-level, short term and moderate, extended accelerations.

The known effects of acceleration upon the ability of pilots to "fly" both simple and whole-system simulations are cataloged with special attention given to the ways in which such variables as system complexity, controller construction, restraint and life-support equipments, and subject learning serve to augment or reduce these effects.

Brief introductions describing the relevant nomenclature, simulation techniques, and data handling processes precede the discussion of research findings.

References

1. Bondurant, S. Transverse G. Prolonged Forward, Backward, and Lateral Acceleration. In Gauer, O. H. and Zuidema, G.D. (Eds). Gravitational Stress in Aerospace Medicine, pages 150-159, Boston: Little, Brown & Co. 1961.
2. Brown, J.L. The Physiology of Acceleration - Performance. In Gauer, O.H. and Zuidema, G.D. (Eds). Gravitational Stress in Aerospace Medicine, pages 90-114, Boston: Little, Brown & Co., 1961.
3. Brown, J.L. and Burke, R.E. The effect of positive acceleration on visual reaction time. J. Av. Med. 29: 48-58, 1958.
4. Chambers, R.M. Control Performance under Acceleration with Side-Arm Attitude Controllers. Aviation Medical Acceleration Laboratory, U.S. Naval Air Development Center, Johnsville, Pa., Report NADC-MA-6110, 27 Nov 1961.
5. Chambers, R.M. Human Performance in Acceleration Environments. In Burns, N.M., Chambers, R.M., and Hendler, E. (Eds). Human Behavior in Unusual Environments. Chicago, Ill.: Free Press, 1962. In press.
6. Chambers, R.M. Dynamic Simulation for Space Flight. In Chambers, R.M. and Smith, B.J. (Eds). What Needs Doing About Man-in-Space? A discussion at the 1959 American Psychological Association Convention, Phila., Pa., The General Electric Co., 1959.
7. Chambers, R.M. Problems and Research in Space Psychology. Aviation Medical Acceleration Laboratory, U.S. Naval Air Development Center, Johnsville, Pa. Report NADC-MA-6145, 24 Apr 1962.

8. Chambers, R.M. and Nelson, J.G. Pilot Performance Capabilities during Centrifuge Simulations of Boost and Reentry. American Rocket Society Journal 31 (11): 1534-1541, 1961.

9. Chambers, R.M., Augerson, W.S., Kerr, R., and Morway, D. Effects of Positive Pressure Breathing on Performance and Physiology during Acceleration. Aerospace Med. 33: 1962.

10. Chambers, R.M. and Lathrop, R.G. Considerations in Testing for Intellectual Impairment due to Acceleration. Paper presented at the Annual Meeting of the American Medical Association, Military Medicine Division, New York, June 1961.

11. Chambers, R.M., Morway, D.A., Beckman, E. L., DeForest, R. and Coburn, K.R. The Effects of Water Immersion on Performance Proficiency. Aviation Medical Acceleration Laboratory, U. S. Naval Air Development Center, Johnsville, Pa. Report NADC-MA-6133, 22 Aug 1961.

12. Clark, C. C. Acceleration and Body Distortion. The Martin Company, Baltimore, Md. (Life Sciences Department), Nov 1961, Report ER 12138.

13. Clark, C.C. and Gray, R.F. A Discussion of Restraint and Protection of the Human Experiencing the Smooth and Oscillating Accellerations of Proposed Space Vehicles. Aviation Medical Acceleration Laboratory, U. S. Naval Air Development Center, Johnsville, Pa. Report NADC-MA-5914, Oct 1959.

14. Clark, C.C. and Faubert, D. A Chronological Bibliography on the Biological Effects of Impact. The Martin Company, Life Sciences Department, Baltimore, Md. Report ER 11953, 27 Sep 1961.

15. Clark, C.C. and Hardy, J.D. Preparing Man for Space Flight. Astronautics 18-21 and 88-90, Feb 1959.

16. Clark, C.C., Hardy, J.D. and Crosbie, R.J. A Proposed Physiological Acceleration Terminology with an Historical Review. In Human Acceleration Studies, Publication 913, pages 7-65. National Academy of Sciences, National Research Council, Washington, D.C., Panel on Acceleration Stress for the Armed Forces-NRC Comm. on Bio-Astronautics, 1961.

17. Cope, F.W. and Jensen, R. Preliminary Report on an Automated System for the Study of Higher Mental Function in the Human Subjected to Acceleration Stress. Aviation Medical Acceleration Laboratory, U.S.Naval Air Development Center, Johnsville, Pa. Report NADC-MA-6113, 8 Sep 1961.

18. Dixon, F. and Patterson, J.L., Jr. Determination of Accelerative Forces Acting on Man in Flight and in the Human Centrifuge. In Gauer, O.H. and Zuidema, G.D. (Eds.) Gravitational Stress in Aerospace Medicine, pages 243-256, Boston: Little, Brown & Co., 1961.

19. Eiband, A.M. Human Tolerance to Rapidly Applied Accelerations. NASA Memorandum 5-19-59E, June 1959.

20. Frankenhauser, M. Effects of Prolonged Radial Acceleration on Performance. Reports from the Psychological Laboratory, University of Stockholm, No. 48, pages 1-10, 1957.

21. Frankenhauser, M. Effects of Prolonged Gravitational Stress on Performance. Acta. Psychologica 14: 92-108, 1958.

22. Gauer, O.H. Definitions: Magnitude, Direction, and Time Course of Accelerative Forces. In Gauer, O.H. and Zuidema, G.D. (Eds.) Gravitational Stress in Aerospace Medicine, pages 10-15, Boston: Little, Brown & Co., 1961.

23. Gauer, O.H. and Zuidema, G.D. Gravitational Stress in Aerospace Medicine. Boston: Little, Brown & Co., 1961.

24. Galambos, R. Psychological Testing of Subjects undergoing Acceleration Stress. In Reports on Human Acceleration, Publication 901, pages 13-54. National Academy of Sciences, National Research Council, Wash., D. C., 1961.

25. Smedal, H.A., Stinnett, G.W. and Innes, R.C. A Restraint System Enabling Pilot Control under Moderately High Acceleration in a Varied Acceleration Field. NASA Tech. Note D-91: 1-19, May 1960.

26. Smedal, H.A., Creer, B.Y. and Wingrove, R.C. Physiological Effects of Acceleration Observed during a Centrifuge Study of Pilot Performance. NASA Tech. Note.D-345, Dec 1960.

27. Stapp, J.P. Human Tolerance to Severe, Abrupt, Acceleration. In Gauer, O.H. and Zuidema, G.D. (Eds) Gravitational Stress in Aerospace Medicine, Pages 165-188, Boston: Little, Brown & Co., 1961.

28. Swearingen, J.J., McFadden, E.B., Garner, J.D. and Blethrow, J.G. Human Voluntary Tolerance to Vertical Impact. Aerospace Med. 31: 989-998, 1960.

29. White, W.J. and Jorve, W. R. The Effects of Gravitational Stress upon Visual Acuity. USAF, WADC-TR-56-247.

30. White, W.J. Variations in Absolute Visual Thresholds during Accelerative Stress. Wright Air Development Center, Wright-Patterson AFB, Ohio, WADC-TR 58-334, 1958.

Table 1

Malfunction Indication

Pilot Number	Jett. Tower	Sep. Cap.	Jett. Retros	Ret. Scope	.05 G	Main Chute
1	-	+	+	+	+	+
2	-	-	-	-	-	-
3	-	-	+	-	-	+
4	+	+	+	-	+	+
5	-	-	+	-	+	+

(+) = Pilot took longer to respond under STATIC than DYNAMIC conditions.

Table 2

Average Response Times as a Function of Indication Mode and Acceleration

	RED-LIGHT	NO-LIGHT	TOTAL
STATIC	2.102	5.126	3.383
DYNAMIC	2.236	6.683	3.537
TOTAL	2.733	5.988	

This page is reproduced again at the back of this report by a different reproduction method so as to furnish the best possible detail to the user.

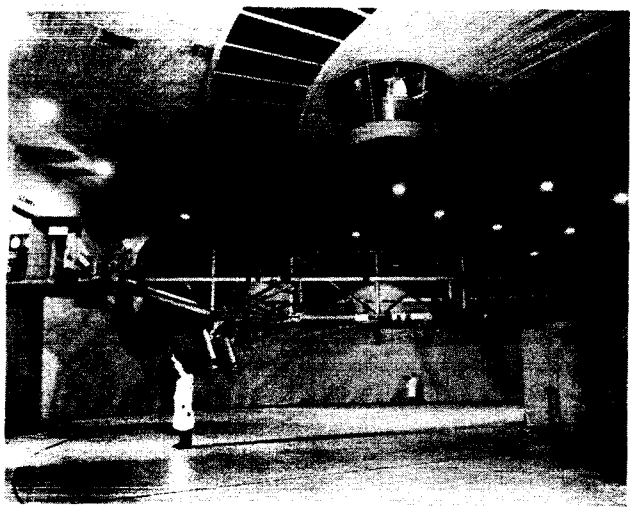

FIGURE 1. The AMAL centrifuge chamber showing the 50-foot arm, the gimbal mounted gondola, the control blister, and the loading platform.

PHYSIOLOGICAL DESCRIPTION OF ACCELERATION

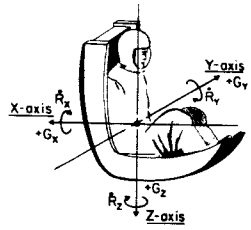

(Body Fluids, Heart Displacement, With Respect to Skeleton)
Linear Acceleration Modes

Description of Heart Motion

Actual	Other Descriptions			Symbol	Unit
Towards spine	Eye-balls-in	Chest-to-back	Backward facing	$+G_x$	g
Towards sternum	Eye-balls-out	Back-to-chest	Forward facing	$-G_x$	g
Towards feet	Eye-balls-down	Head-to-foot	Headward	$+G_z$	g
Towards head	Eye-balls-up	Foot-to-head	Footward	$-G_z$	g
Towards left	Eye-balls-left	——	Rightward	$+G_y$	g
Towards right	Eye-balls-right	——	Leftward	$-G_y$	g

$$NG = \frac{a}{g} = N_1 G_x + N_2 G_y + N_3 G_z$$

$$N^2 = N_1^2 + N_2^2 + N_3^2$$

Angular Acceleration Modes

Acceleration about X-axis (roll axis)	$\ddot{R}_x$	rad/sec²
Acceleration about Y-axis (pitch axis)	$\ddot{R}_y$	rad/sec²
Acceleration about Z-axis (yaw axis)	$\ddot{R}_z$	rad/sec²

(Angular acceleration is positive or negative by right hand rule)

FIGURE 3. Physiological displacement nomenclature used in describing the physiological effects of acceleration.

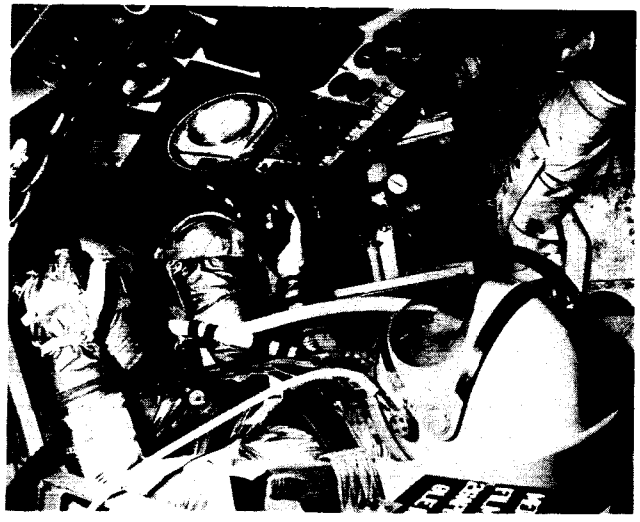

FIGURE 2. Mercury Astronaut in AMAL centrifuge gondola during training and simulation in preparation for Mercury Redstone and Mercury Atlas space flights.

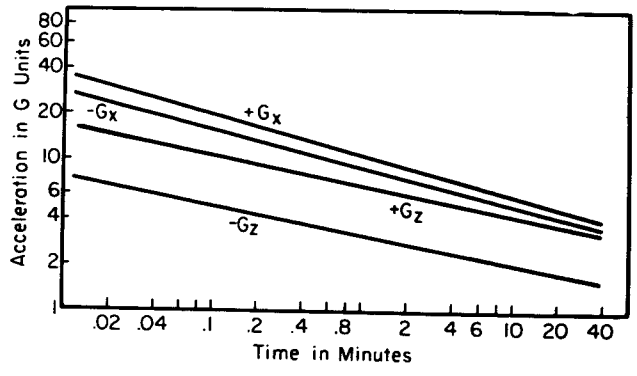

FIGURE 4. Average acceleration tolerances for positive acceleration ($+G_z$), negative acceleration ($-G_z$), transverse supine acceleration ($+G_x$), and transverse prone acceleration ($-G_x$).

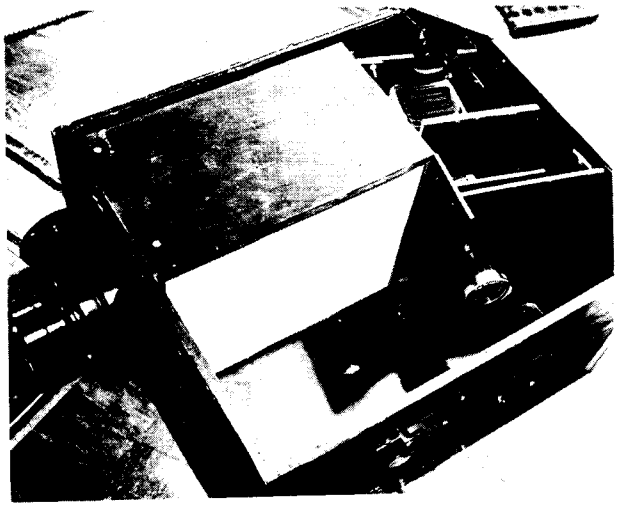

FIGURE 5. Stimulus Display Generator.

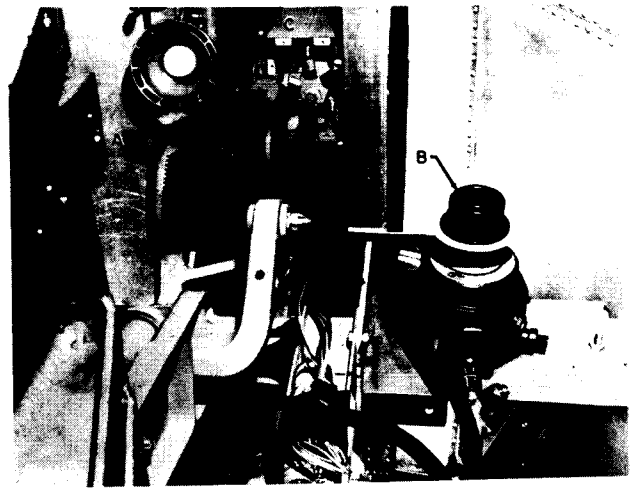

A. Mercury Type Control Handle
B. Oxygen Regulator
C. Visual Response Button

FIGURE 7. Pressure Breathing Oxygen Regulator

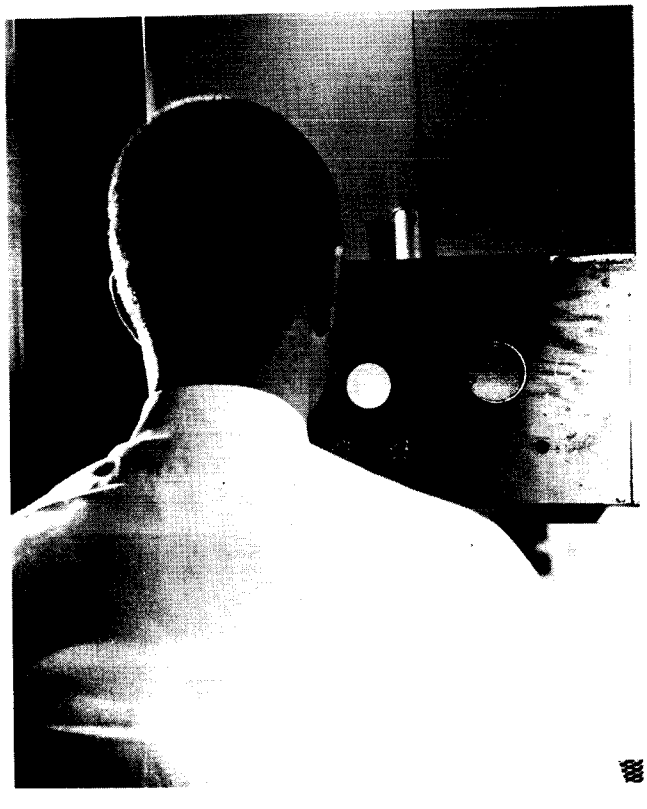

FIGURE 6. Subject shown viewing the stimulus display generator.

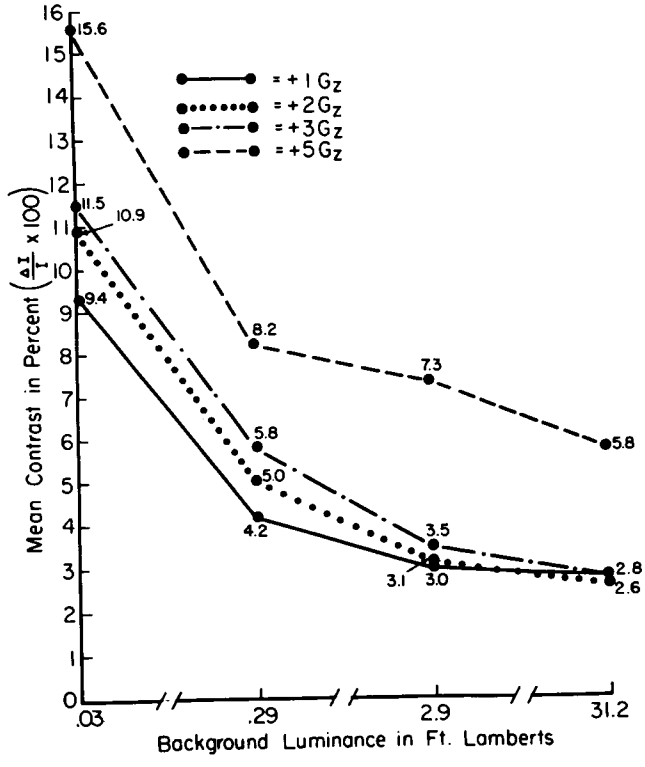

FIGURE 8. Results of experiment showing the relationship between brightness discrimination threshold and background luminance for each of four levels of positive acceleration.

This page is reproduced again at the back of this report by a different reproduction method so as to furnish the best possible detail to the user.

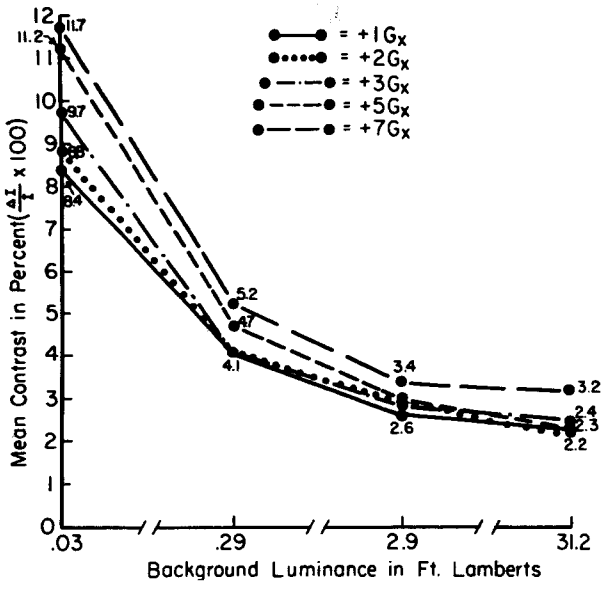

FIGURE 9. Results of experiment showing relationship between brightness discrimination threshold and background luminance for each of five levels of transverse acceleration.

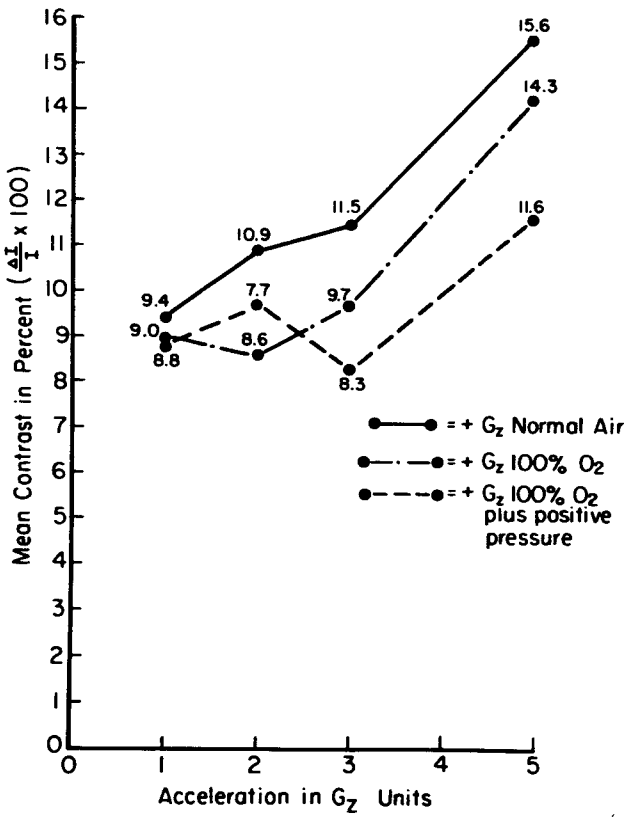

FIGURE 11a. Comparison of the effects of breathing normal air, 100% oxygen, and 100% oxygen plus positive pressure. The comparison is in terms of mean brightness contrast requirements during exposure to three positive accleration levels.

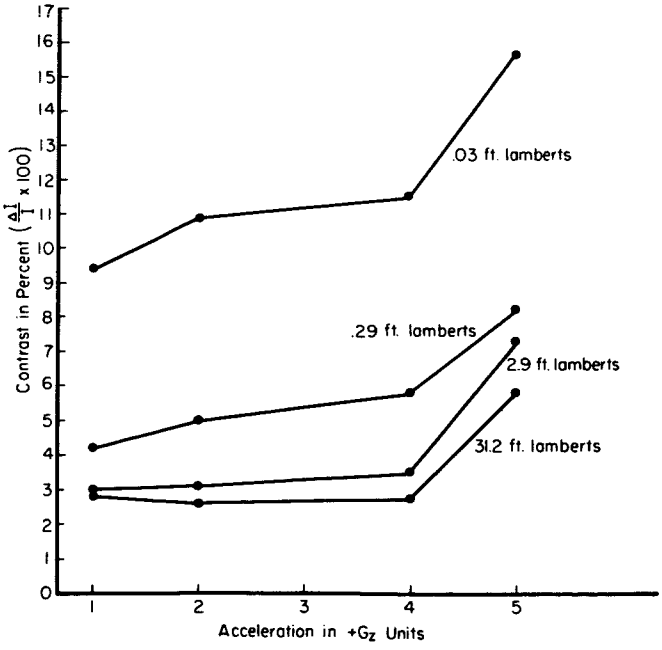

FIGURE 10. Effects of positive acceleration (+G_z) on brightness discrimination thresholds for perceiving an achromatic circular target against each of four background luminances.

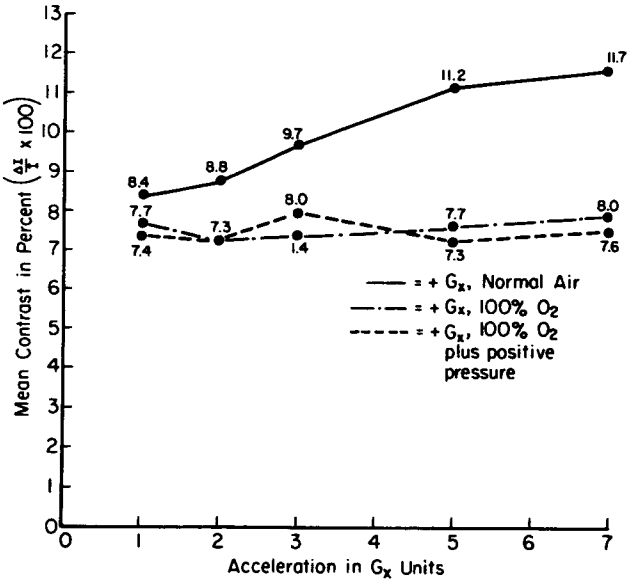

FIGURE 11b. Comparison of the effects of breathing normal air, 100% oxygen, and 100% oxygen plus positive pressure. The comparison is in terms of mean brightness contrast requirements during exposure to three transverse acceleration levels.

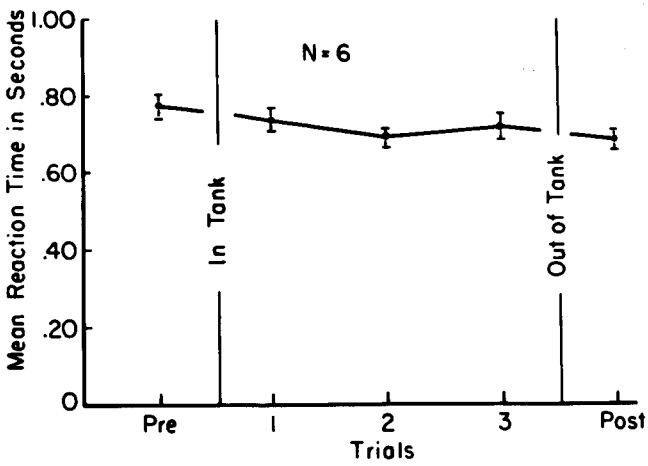

FIGURE 12. Discrimination under static and static-immersed conditions.

FIGURE 13. Centrifuge installation used in study of discrimination reaction time during exposure to acceleration. The subject responds continuously to each of four randomly presented lights by operating 4 small buttons on his right-hand control stick.

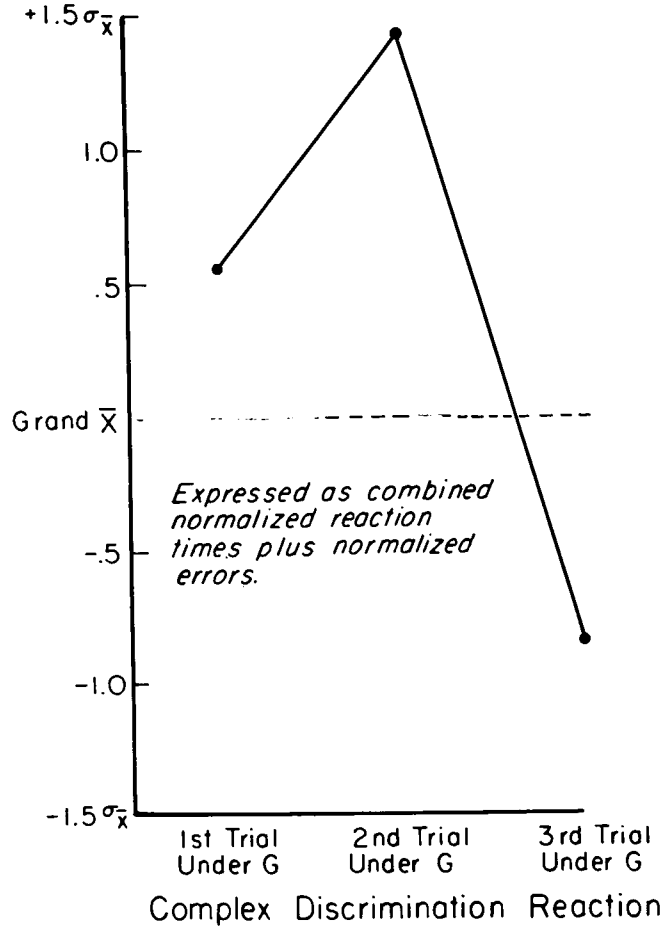

FIGURE 14. Discrimination reaction time performance during exposure to 6 G_X for 5 minutes per run.

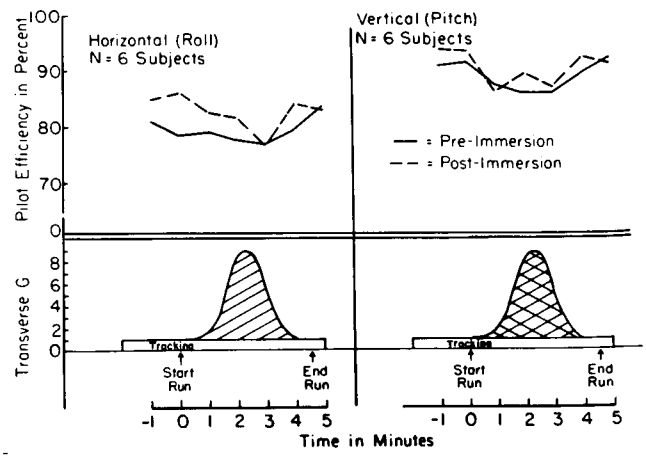

FIGURE 15. Mean pilot efficiency scores in tracking pitch and roll components during exposure to a transverse G reentry acceleration profile.

This page is reproduced again at the back of this report by a different reproduction method so as to furnish the best possible detail to the user.

This page is reproduced again at the back of this report by a different reproduction method so as to furnish the best possible detail to the user.

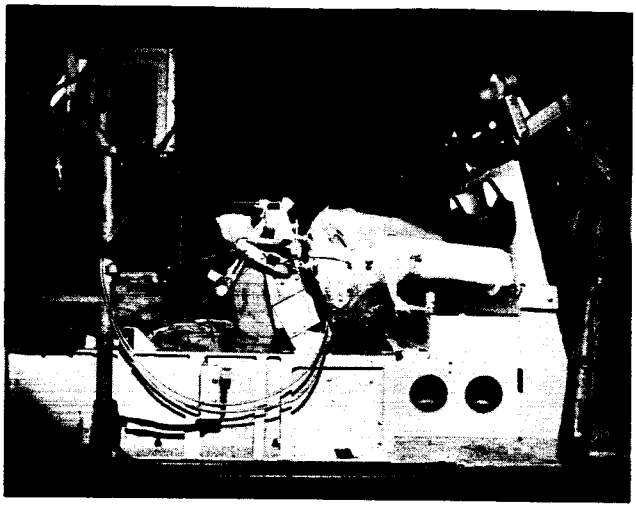

FIGURE 16. Subject positioned in contour couch, suspended from the centrifuge arm, and operating a control device during a tracking trial.

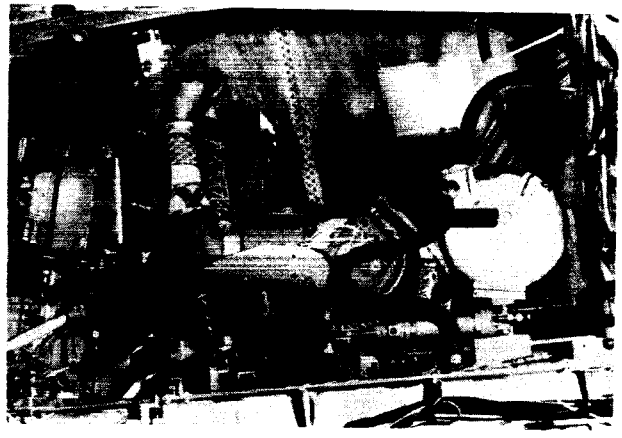

FIGURE 18. Pilot in advanced G-protection system, developed by NASA and tested at the AMAL Human Centrifuge. This system was designed to provide protection for $+G_x$ $-G_x$ and $+G_z$ accelerations.

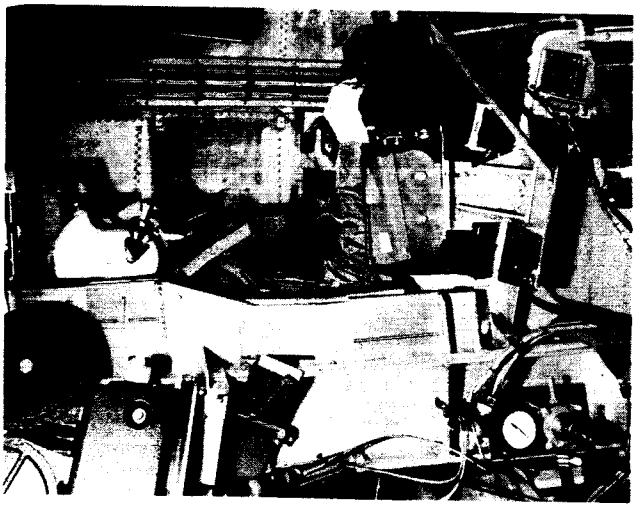

FIGURE 17. Pilot restrained in contour couch, with associated shoulder, arm, head, and face restraints performing a tracking task in the AMAL Centrifuge.

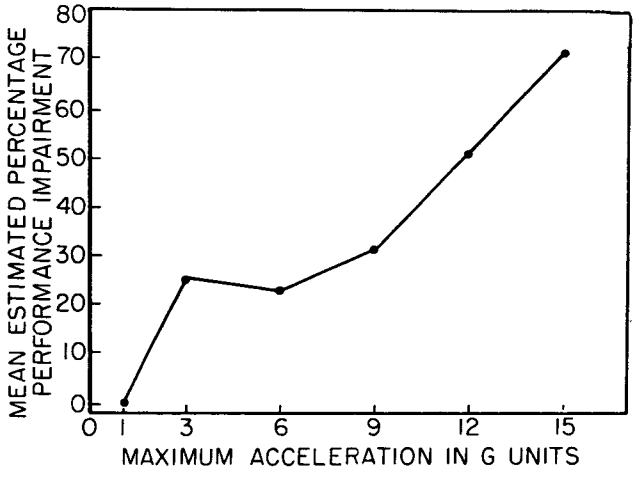

FIGURE 19. Average estimated performance decrements by pilots who performed complex launch and insertion maneuvers through peak accelerations of 1, 3, 6, 9, 12, and 15 G_x.

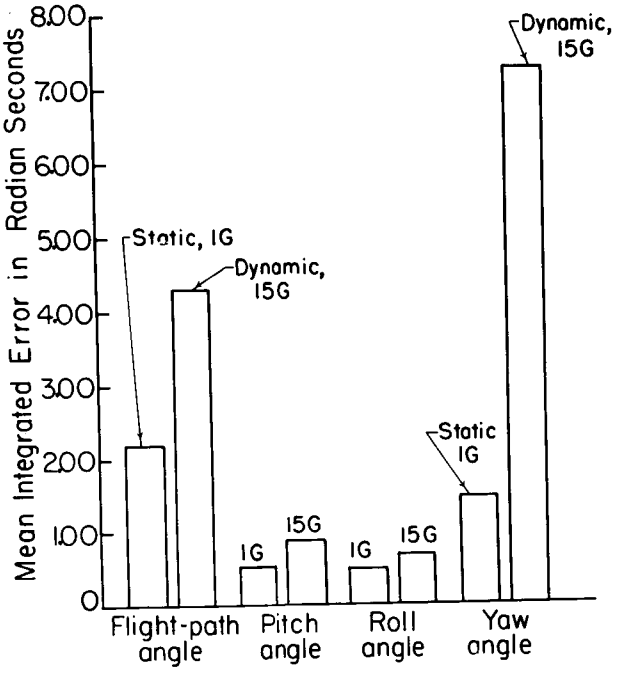

FIGURE 20. Pilot error performance on each of four task components during exposures to static (1G) and dynamic (15G) acceleration conditions.

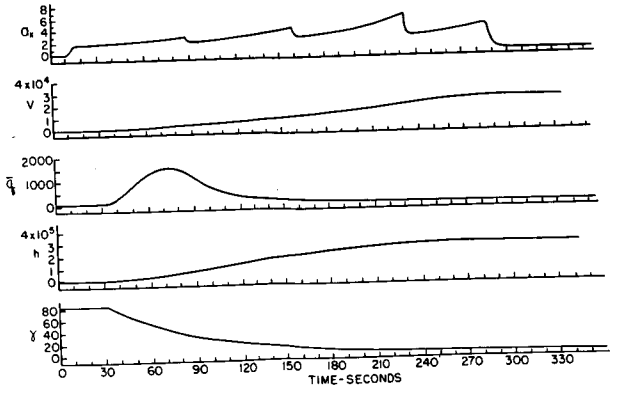

FIGURE 21. Acceleration profile used to simulate a 4-stage launch vehicle on the AMAL Human Centrifuge.

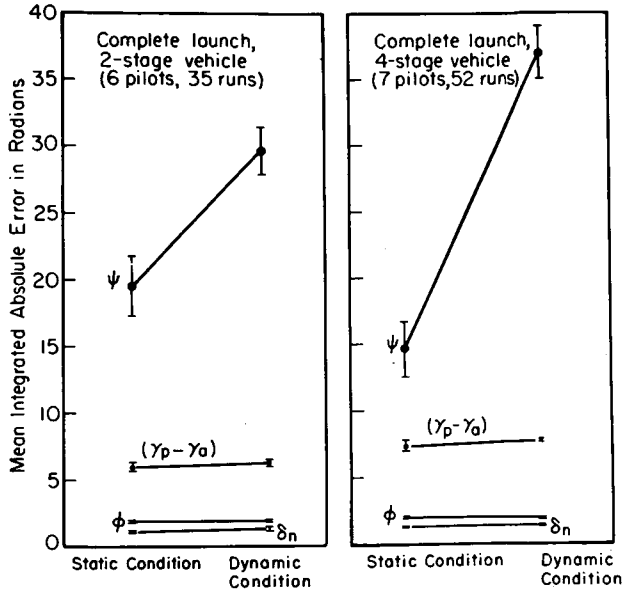

FIGURE 22. Performance scores for pilots performing a control task during the launch to insertion phases of a proposed boost four-stage vehicle.

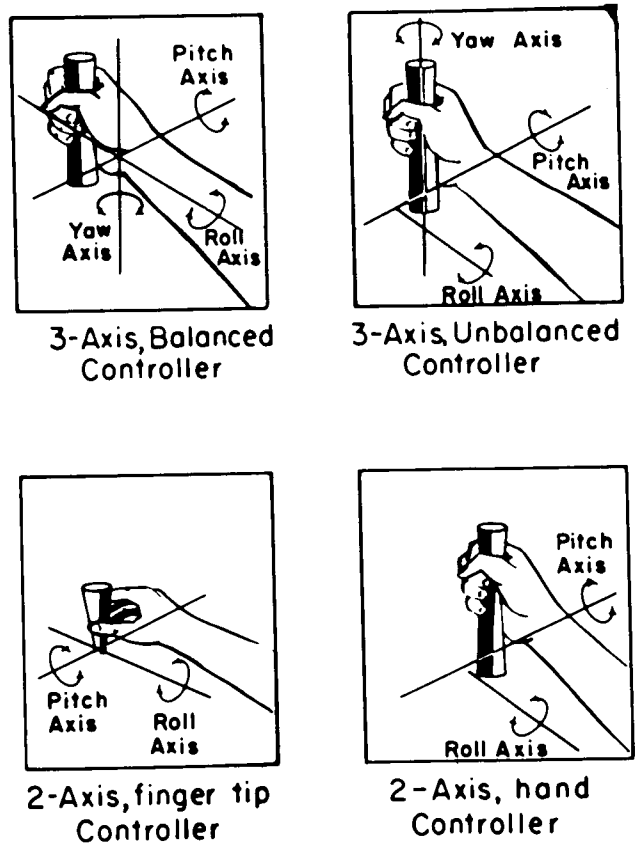

FIGURE 23. Four types of right-hand side arm controllers used in high-G sustained acceleration studies on the Human Centrifuge.

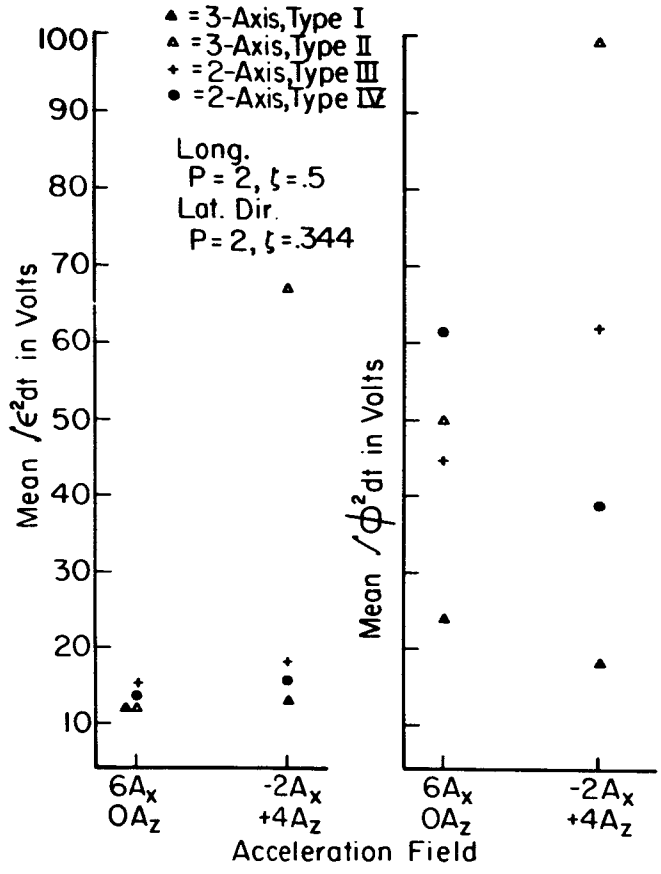

FIGURE 24. Mean error scores for pitch error and for roll error components of a tracking task in which the same pilots flew the same problem in each of 2 G-fields using each of four side-arm controllers.

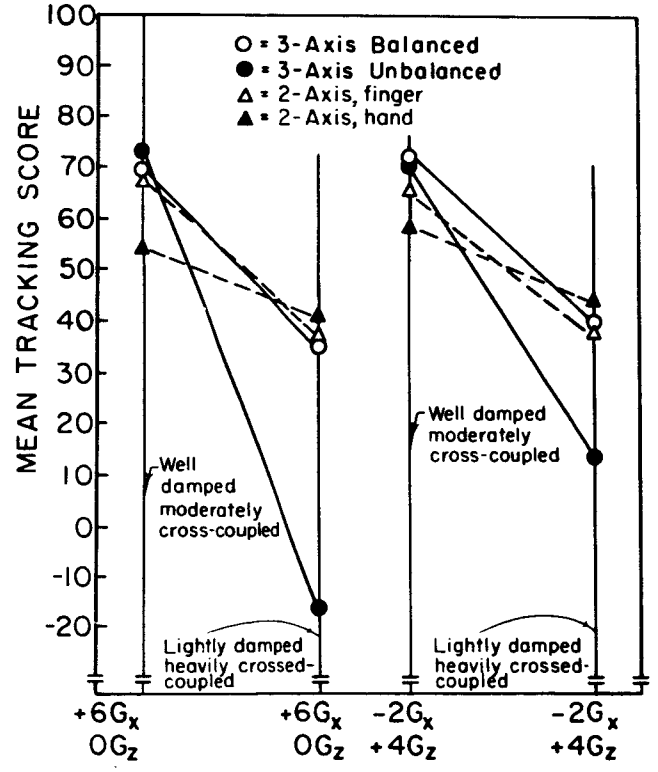

FIGURE 25. Mean tracking efficiency scores for pilots who performed the same tracking task with each of 4 different types of side-arm controllers within given acceleration fields.

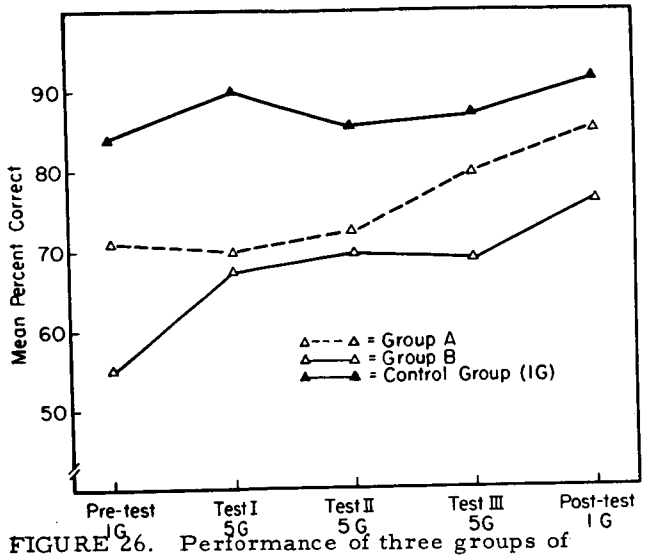

FIGURE 26. Performance of three groups of subjects on a 4-back running matching memory test. Group A was a sample of students from Rutgers University. Group B was a sample from AMAL, and Group C was a control group which performed the task only under static (IG) conditions.

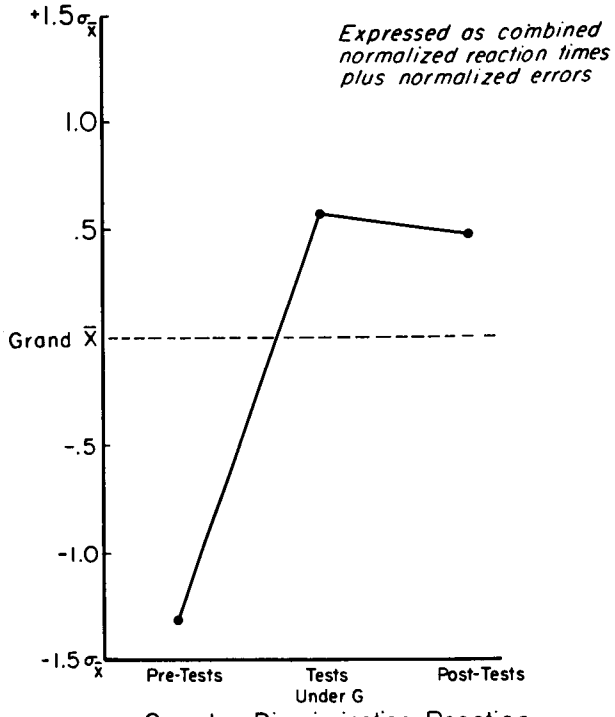

FIGURE 27. Results of administering a complex discrimination reaction time task before, during, and following exposure to 6 G_x. for 5 minutes per run. In order to account for both error and time decrement, reaction times and errors were normalized and then added in this experiment.

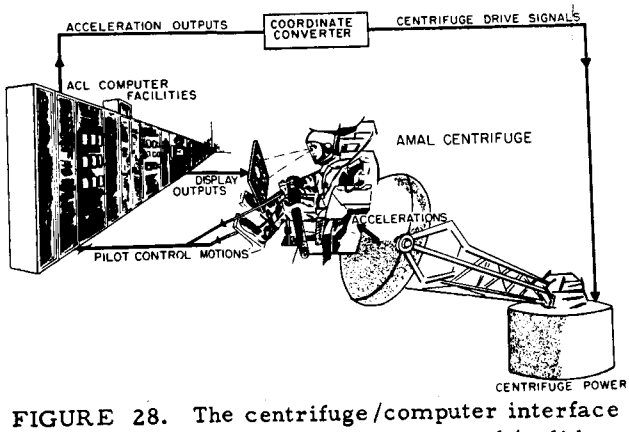

FIGURE 28. The centrifuge/computer interface during open-loop acceleration command (solid lines) and closed-loop panel display (open line).

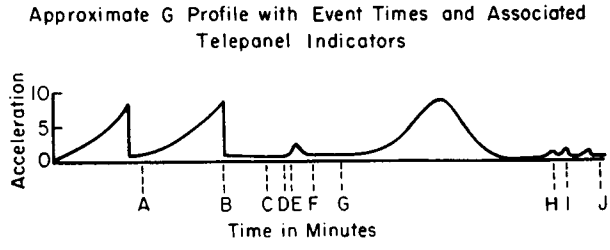

A. Escape tower jettison
B. Capsule separation
C. Retro sequencing and Initiated
D. Retro attitude confirmed (or denied) by telemetry
E. Retro fire
F. Retro pack jettison
G. Retract scope
H. Snorkel
I. Drogue chute
J. Main chute

FIGURE 29

FIGURE 30 EPL Data Reduction Facility – Bldg. No. 85

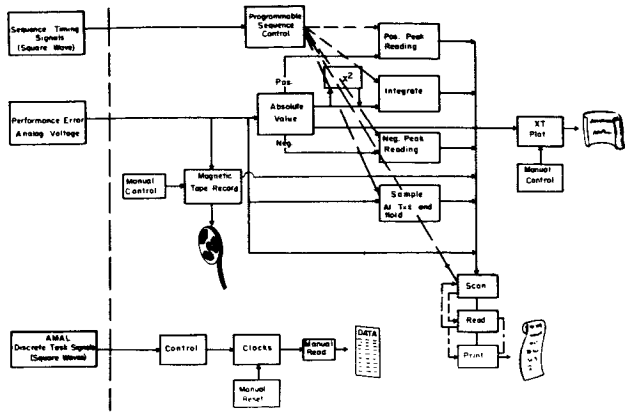

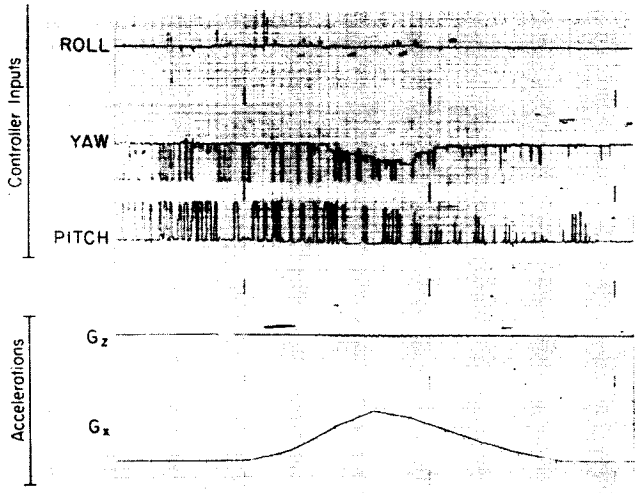

FIGURE 33 Inadvertant Control Input in the Yaw Axis

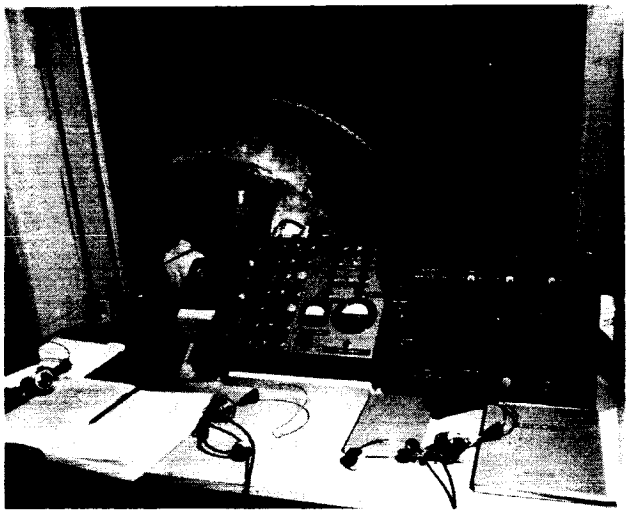

FIGURE 31. Externally mounted control panel.

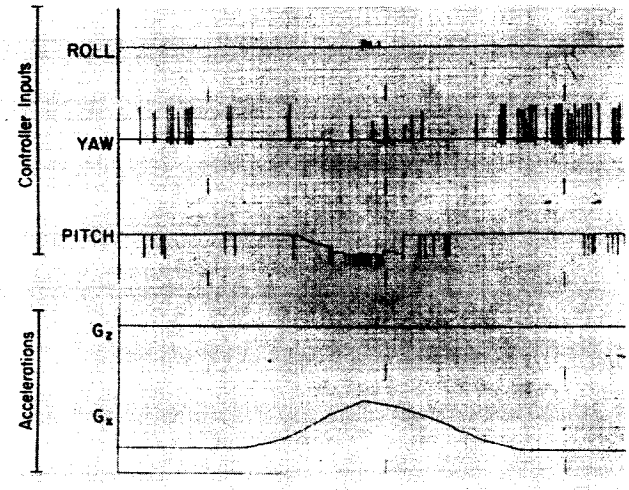

FIGURE 34 Inadvertant Control Input in the Pitch Axis

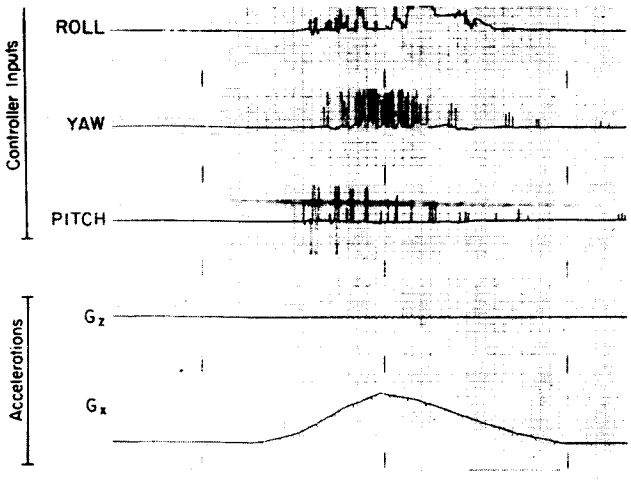

FIGURE 32 Inadvertant Control Input in the Roll Axis

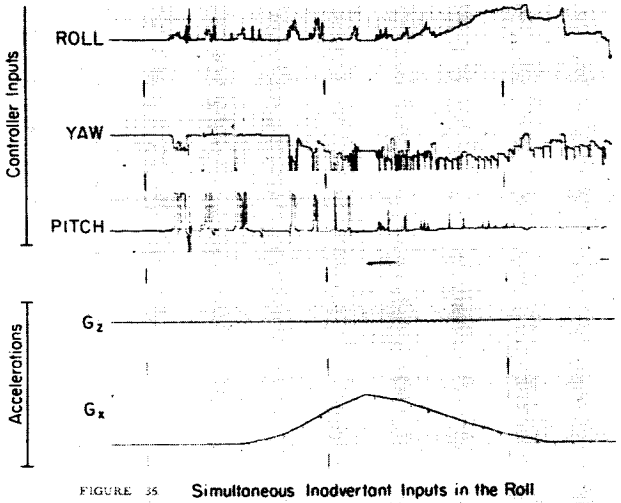

FIGURE 35 Simultaneous Inadvertant Inputs in the Roll and Yaw Axes

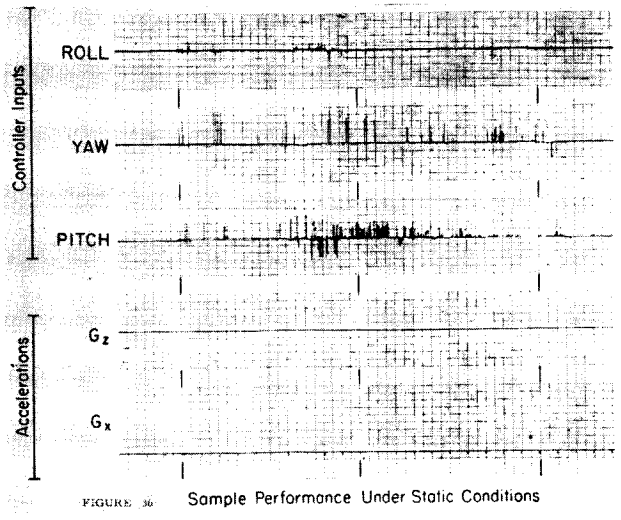

FIGURE 36 Sample Performance Under Static Conditions

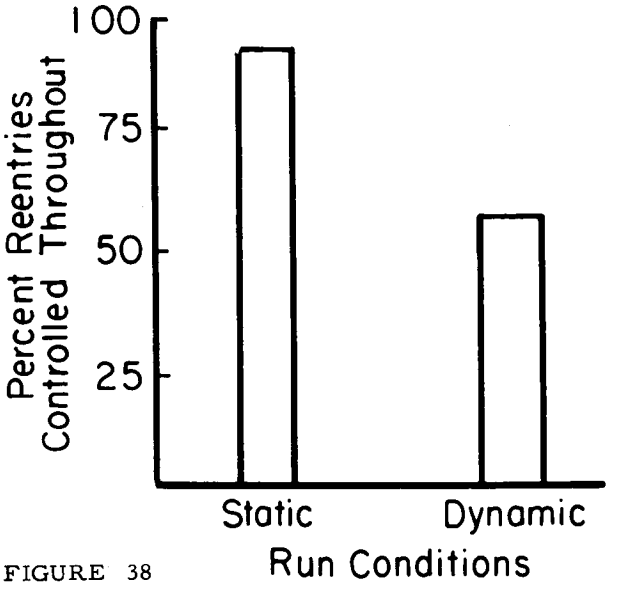

FIGURE 38

Reentry Control Under Static and Dynamic Conditions

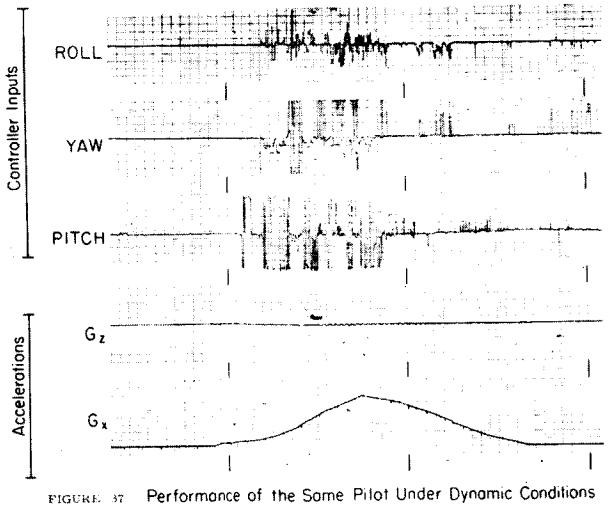

FIGURE 37 Performance of the Same Pilot Under Dynamic Conditions

FIGURE 39

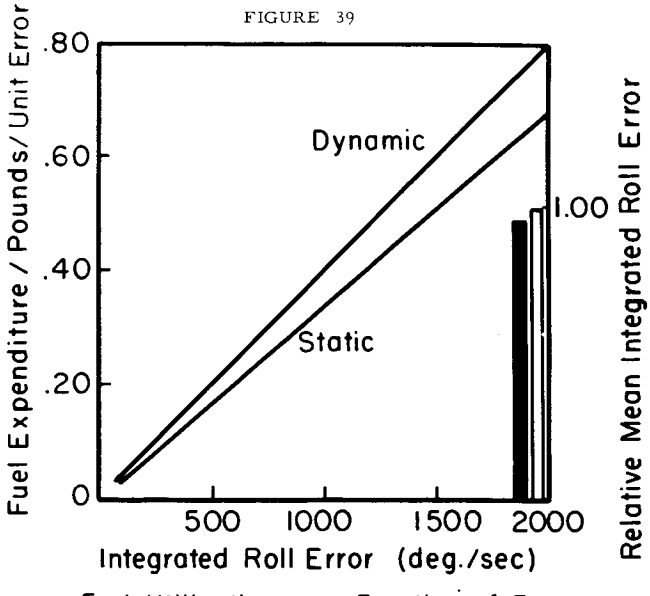

Fuel Utilization as a Function of Error Magnitude and Acceleration

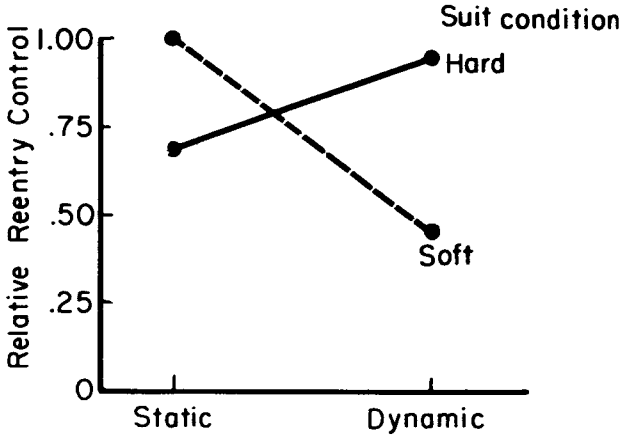

FIGURE 40 Run Condition

Relative Reentry Control as a Function of Suit Pressurization and Acceleration

FIGURE 42

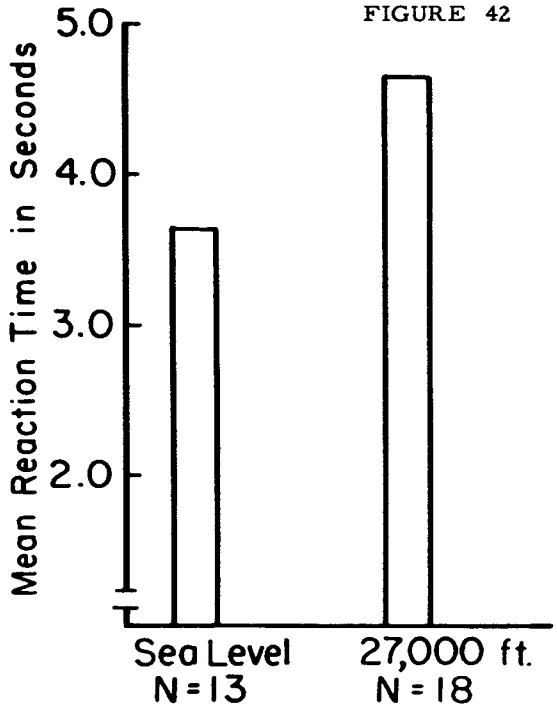

Cabin Pressurization

Telepanel Response Time as a Function of Cabin Pressure

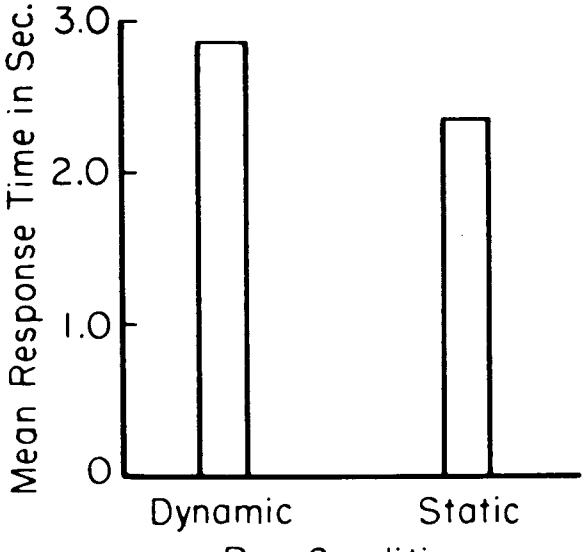

FIGURE 41 Run Condition

Telepanel Response Time Under Static and Dynamic Conditions

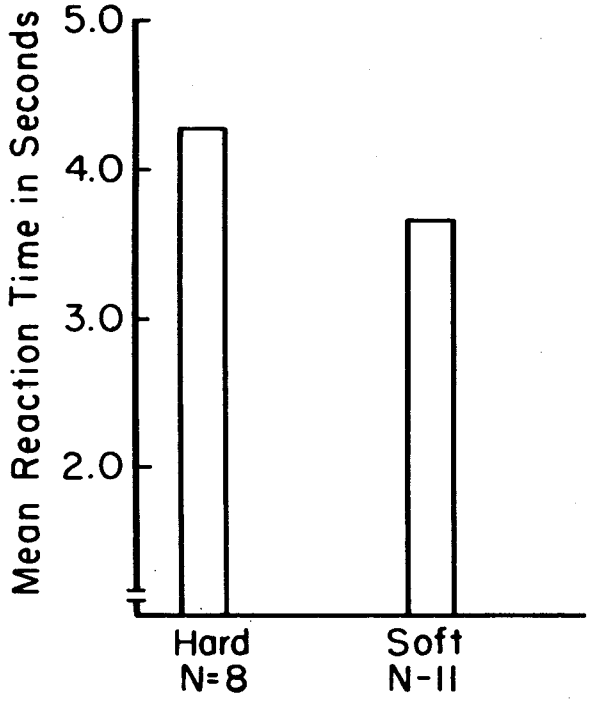

FIGURE 43

Suit Pressurization

Telepanel Response Time as a Function of Suit Pressure

The Mercury Capsule Attitude Control System

J. W. Twombly
Section Manager, Guidance and Control Mechanics
McDonnell Aircraft Corporation

In accordance with the basic design concepts of the Mercury Capsule, the manual and automatic control systems were developed to provide a redundant and integrated method of controlling the capsule attitude. The systems were designed to meet the requirements of ballistic and orbital flight, for normal and abort missions. Since the orbital mission includes all modes of control, it will serve as a basis for the system description. This mission profile is shown in Figure (1), and its attitude control system requirements are summarized as follows:

A. Provide a 180 degree yaw maneuver following separation from the booster, and achieve a zero-roll, minus 34 degree pitch attitude. In this attitude, the retro-rockets are properly aligned and beacon transmission from the cylindrical portion of the capsule is not blocked by the heat shield.

B. Maintain attitude with $\pm$ 10 degree accuracy until time of retrograde rocket firing.

C. Maintain attitude with $\pm$ 5 degree accuracy during retrorocket firing.

D. Achieve re-entry attitude of + 1.5 degrees pitch, then maintain it until 0.05g deceleration is experienced.

E. Provide re-entry roll rate of 10 degrees per second to minimize touchdown dispersion, and limit pitch and yaw rate oscillation to 2 degrees per second during re-entry.

The control system may be divided into automatic, semi-automatic, and manual subsystems all of which utilize the decomposition of hydrogen peroxide for generation of thrust necessary for rotation of the capsule.

As shown in Figure (2), two completely separate and independent fuel supplies are provided. One is primarily for the automatic control system and the other for the manual control system, although each may be used by auxiliary means.

The automatic control system, which has the capability of meeting all attitude control requirements throughout the mission, consists of an attitude reference utilizing two horizon scanners and two attitude gyros, three rate-sensing gyros, and control logic, which commands on-off operation of reaction control thrust. On pitch and yaw axes, 1-pound and 24-pound thrusters provide angular accelerations of 0.5 deg./sec.^{2} and 12 deg./sec.^{2}, respectively. On the roll axis, 1-pound and 6-pound thrusters provide 0.5 and 3 deg./sec.^{2} respectively.

The reaction control system is supplied by Bell Aerosystems; the horizon scanners are manufactured by Barnes Engineering; and the remainder of the electronics, the Automatic Stabilization and Control System (ASCS), is supplied by the Minneapolis-Honeywell Regulator Company.

The manual control system consists of a three-axis hand controller, which is connected by mechanical linkage to throttling valves. These valves provide fuel flow such that output thrust is essentially proportional to controller deflection and has a maximum value of 24 pounds for pitch and yaw control and 6 pounds for roll control. Several sources of attitude information are available to the astronaut. A 360-degree view of the horizon may be seen through the periscope and a window gives direct but more limited view of the earth. In addition, a more quantitative display is provided by the rate and attitude indicator. The displayed attitude information is derived from the ASCS attitude gyros, and the rate signals are taken from a separate set of rate gyros. These same rate gyros are a part of the Rate Stabilization and Control System (RSCS). This semi-automatic system will, if selected by the astronaut, provide angular rates proportional to controller deflection, and in the absence of rate commands provides rate damping about all three axes. Like the ASCS, the RSCS is an on-off system which actuates solenoid-controlled valves, but it uses fuel from the manual system supply.

One other manual system, known as "Fly-By-Wire" (FBW), is also available to the astronaut as a means of utilizing the automatic fuel supply in case of a malfunction of the ASCS. Microswitches actuated by the hand controller linkage energize low and high level solenoid valves of the automatic fuel system. Low level thrust is obtained at approximately 1/3 of total controller travel; high level thrust is obtained at 3/4 total deflection.

It can be seen, therefore, that each of the independent hydrogen peroxide fuel supplies may be used by two separate systems of attitude control.

The physical locations of major systems, including the control system components, are shown in Figure (3). Gyros and ASCS electronic equipment are mounted on shelves which are located on each side of the astronaut. The RSCS electronics package is located under the astronaut's right arm; the hand controller and linkage are also displayed. The pitch and yaw thrusters are located in the cylindrical section of the capsule, and the roll thrusters are located on the sides of the capsule near the maximum diameter. The horizon scanners are also mounted in the cylindrical section of the capsule.

The astronaut's instrument panel is shown in Figure (4). At the top is the rate and attitude indicator. This instrument was designed to minimize eye motion byplacing rate and attitude needles for each axis in close proximity. The instrument is located so that the rate indicator can be used in conjunction with either the window or periscope display. The ASCS/RSCS selector switches and reaction control fuel supply valves are on the left console. Automatic, semi-automatic, and manual control modes may be selected on any or all of the three axes, and super-position of manual and automatic control is possible.

Despite the control capability of the astronaut, normal attitude control is provided by the ASCS, and of course in unmanned flights, it must operate unassisted. This system, therefore, will be described more extensively and some early flight test results will be presented.

Figure (5), a block diagram of the ASCS, shows it to consist of a set of rate gyros, having outputs at discrete rates rather than proportional rates, a set of two, two-degree-of-freedom attitude gyros, an 0.05g accelerometer switch and a major electronics unit, known as the amplifier-calibrator. Within the "amp-cal" are four major sections, mode logic, control logic, gyro slaving loops and attitude repeater servos. The amplifiers and logic systems use solid state devices throughout; approximately 500 diodes and transistors are required. The mode logic responds to commands from capsule wiring and places the ASCS in an appropriate mode of control. The control logic maintains attitude control in one of several modes: orientation, orbit, retro-fire, or rate damping. The attitude repeater servos take the attitude gyro output synchro signals representing pitch, roll and yaw angles and drive multiple outputs; attitude sector switches for control logic, potentiometers for telemetry, and synchros for attitude indication to the astronaut. It is by biasing the pitch axis repeater that pitch attitude is changed from orbit to re-entry attitude.

As shown in Figure (6), the slaving loops are used to slave the vertical gyro gimbals to the roll and pitch horizon scanners, to slave the directional gyro roll gimbal to the vertical gyro roll gimbal, and to slave the yaw gimbal of the directional gyro to a yaw reference signal derived from the vertical gyro slaving loop. This yaw reference signal is taken from the input to the roll (inner) gimbal torquer, since the average torquing rate of this gimbal is proportional to the yaw angle of the capsule. This may be more readily visualized from the vertical gyro gimbal diagram of Figure (7).

In its normal, or zero yaw angle condition, which is shown in Figure (7a), the vertical gyro inner gimbal requires no torquing rate to maintain the spin axis vertical. For a 90-degree yaw angle of the capsule, as shown in Figure (7b), the horizon scanner slaves the inner gimbal at the orbital rate in order to maintain a vertical spin axis. At any intermediate yaw angle, the torquing rate is proportional to the sine of the angle. For small yaw angles, therefore, the roll gimbal torquing signal, when multiplied by $(1/\Omega)$, is approximately equal to the capsule yaw angle and is the yaw reference to which the directional gyro is slaved. For economy of electrical power, the slaving loops are energized approximately 8 minutes of every half-hour in orbit.

The control logic, which is made up of transistor and diode circuits not critically dependent on voltage, receives the step function outputs of the attitude repeaters and the discrete rate signals from the ASCS rate gyros. Using these stepwise indications of attitude and rate conditions, along with the output of the mode switching section defining the current phase of the mission, "decisions" are made which result in the actuation of appropriate reaction control valves.

Two examples of the control logic are shown by the phase plane diagrams of Figure (8). In the upper portion of the figure, the "retrograde attitude hold" mode is displayed. The control logic applies high positive or negative torque depending upon the combination of existing rates and attitudes. In this example, the positive disturbance torque initially adds to the control torque to reduce the negative rate. Following a period of zero control torque, negative torque is applied. The phase plane trajectory then continues to converge toward zero rate and attitude, but may reach an equilibrium point at 3-degrees of error if the disturbance torque is sufficiently great.

In the lower portion of Figure (8) is shown the orbit mode of control. In this mode, only attitude error signals are used to develop a series of torque pulses which increase in width as attitude error increases. These pulses produce sufficient impulse to damp original rates of 0.5 degree per second and provide a convergent limit cycle oscillation, which will normally exceed the $\pm$ 3-degree boundaries only intermittently. The typical steady state oscillation shown has a period of approximately four minutes and requires less than 0.4 pound of fuel per hour. As a precaution, however, the ASCS is programmed to revert to the maneuvering or "orientation mode" of control if attitude errors continue to increase beyond the values corresponding to the outer orbit mode pulses.

Other control modes are the orientation mode, which utilizes both high and low thrust and is employed during the capsule maneuvers, such as the 180-degree yaw rotation after separation, and the rate damping mode, used for re-entry. In the latter mode, both high and low torques are used, in response to rate gyro output signals.

Flight testing to date has consisted of five ballistic trajectory flights and three orbital missions. In general, the control systems have performed as designed, that is, satisfactory attitude control has been provided despite the occurrence of reaction control malfunctions. Figure (9) illustrates the system performance during the first manned ballistic flight, with Commander Shepard at the controls. A portion of the yaw axis flight test data is shown in Figure (9). Following capsule separation, the ASCS provides 5 seconds of rate damping, then the 180-degree yaw maneuver. The ASCS then drops into the orbit mode of control for a short period. In accordance with the flight plan, manual control is achieved by turning off the automatic fuel supply in a pitch, yaw, roll sequence.

Manual yaw control is observed at t=331 seconds, and thereafter yaw rates are manually controlled to less than three degrees per second, even during the retro-rocket firing period. Average yaw error during the rocket firing period is approximately six degrees, a satisfactory value for an orbital mission since the resultant down range error would have been less than 10 nautical miles. This error had no appreciable effect on the ballistic trajectory of Capsule No. 7 however.

Captain Grissom's flight was equally successful, and he was the first to make use of the RSCS.

There followed the three orbital flights of one-orbit unmanned, two-orbit, with Enos aboard, and the three-orbit mission of Col. Glenn's. In all of these orbital flights the systems have operated satisfactorily, but their performance has been marred by one recurring malfunction. In every case, during the first or second orbit there has occurred an apparent orifice blockage of one or more of the one-pound thrust chambers. When this occurs in the orbit mode, the capsule continues to deviate from the desired attitude until it reaches, in the case of the yaw axis, a value of thirty degrees. At this point the ASCS returns automatically to the orientation mode and utilizes the 24-pound thrusters to reduce the error to zero. The system then continues to cycle in and out of the orbit mode and consumes fuel at the rate of about eight pounds per hour. After a number of such cycles were noted in Enos' flight, the decision was made to terminate the mission at the end of the second orbit. In the case of Col. Glenn, however, attitude control could be maintained somewhat more efficiently by use of the Fly-By-Wire and Manual Proportional modes of control so that he was able to complete the 3-orbit mission. During the retro-rocket firing period, Col. Glenn did employ the ASCS as the primary means of maintaining attitude while also applying manual proportional control.

In addition to the continuing emphasis on system cleanliness, modifications to the orifice plate and to the thrust chamber catalyst bed are expected to overcome the thruster problem; tests of these modifications are currently underway.

In summary, it can be concluded that the Mercury control systems have provided both automatic and manual attitude control of the capsule. With respect to the solid-state electronics system, it can be said that a high degree of reliability has been achieved; there has been no in-flight failure of any of the control system electronics components.

Based upon Col. Glenn's flight, it is apparent that future spacecraft can dispense with the "fully automatic" design of the Mercury Capsule and revert to the concepts of providing effective manual control modes for astronaut control, and of including pilot-selectable automatic modes which provide pilot relief or precision control when they are required.

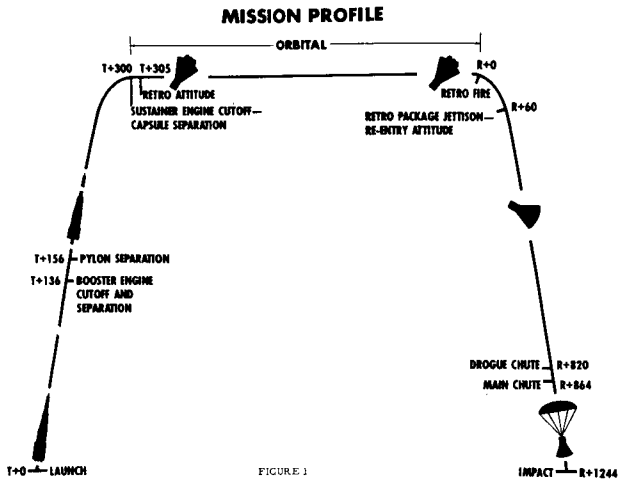

FIGURE 1

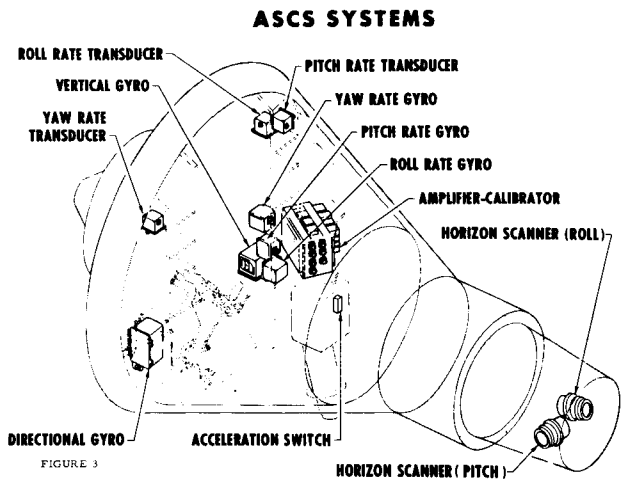

FIGURE 3

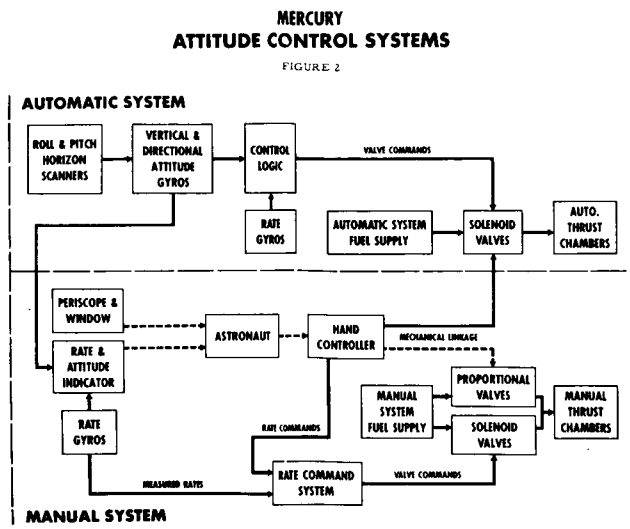

FIGURE 2

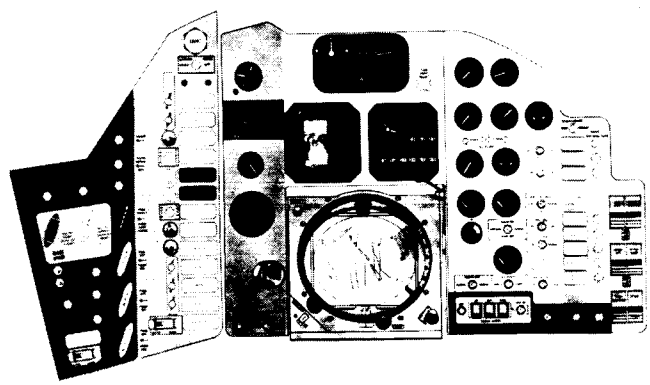
FIGURE 4

FUNCTIONAL BLOCK DIAGRAM ASCS

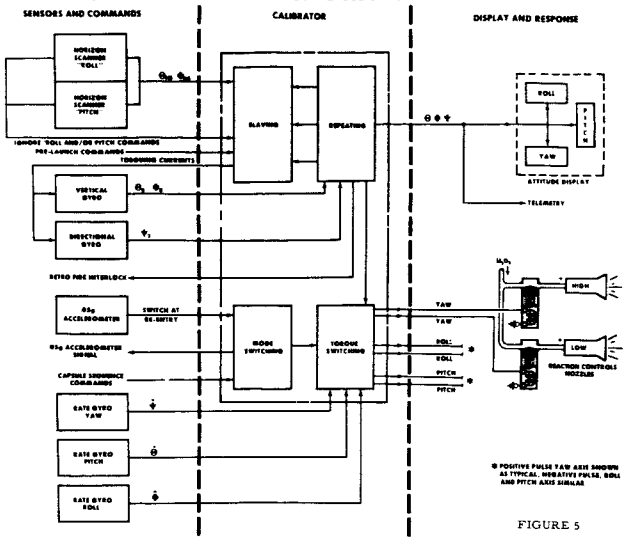

FIGURE 5

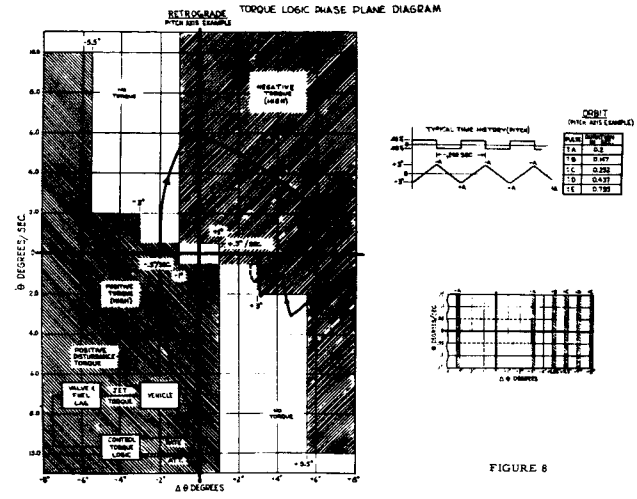

FIGURE 8

MERCURY YAW REFERENCE SYSTEM

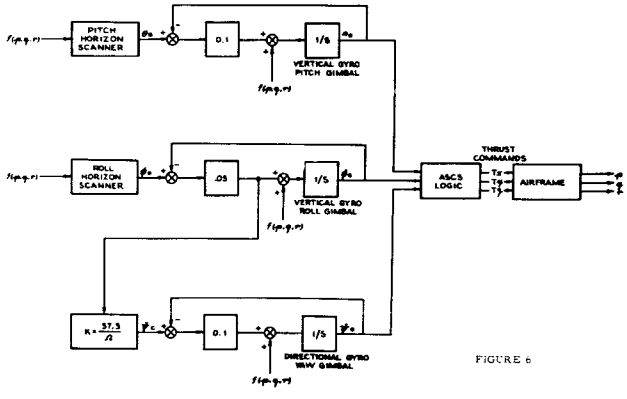

FIGURE 6

MERCURY
VERTICAL GYRO ORIENTATION

FIGURE 7

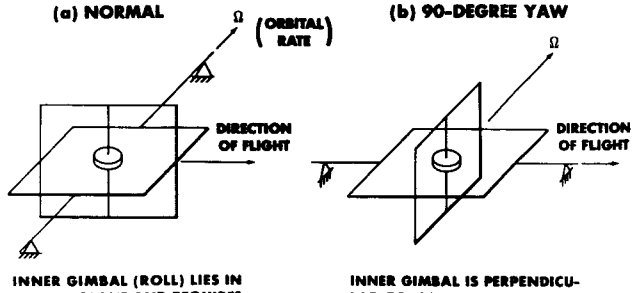

INNER GIMBAL (ROLL) LIES IN ORBITAL PLANE AND REQUIRES NO TORQUING TO MAINTAIN SPIN AXIS VERTICAL.

INNER GIMBAL IS PERPENDICULAR TO ORBITAL PLANE AND MUST BE TORQUED AT ORBITAL RATE, Ω, TO MAINTAIN SPIN AXIS VERTICAL.

AT INTERMEDIATE YAW ANGLES, THE ROLL GIMBAL TORQUING RATE, $\dot{\phi}_V = \Omega \sin \Psi$

MERCURY
CAPSULE 7 FLIGHT TEST DATA
YAW AXIS

FIGURE 9

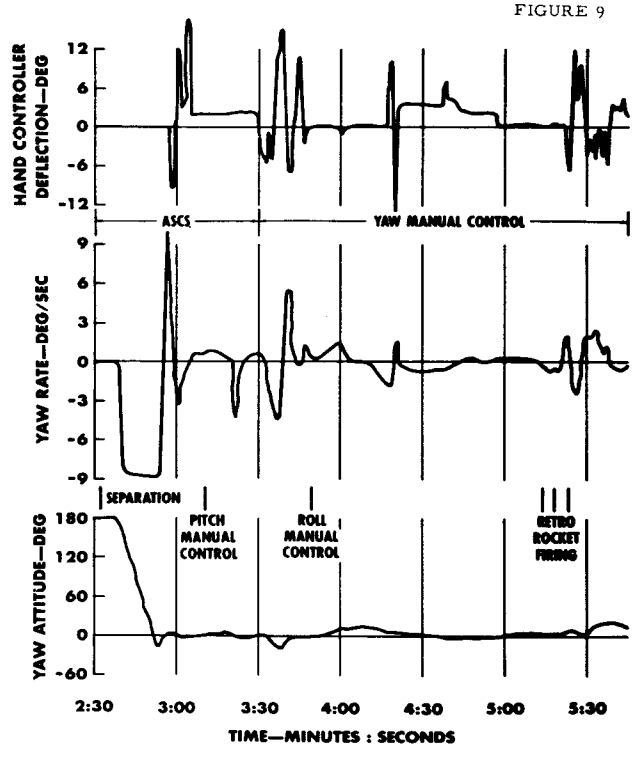

N62-14485

SIMULATION EQUIPMENT USED IN THE TRAINING OF ASTRONAUTS AND FLIGHT CONTROL CREWS IN PROJECT MERCURY

Stanley Faber
Head, Flight Simulation Section
NASA - Manned Spacecraft Center

At the beginning of the Mercury Program it was realized that the entire preparation of the man for piloting the spacecraft would have to be done by use of simulation techniques. It was also realized that no single all-inclusive flight simulator could provide the astronaut with practice in all phases of the mission in a sufficiently realistic environment. To determine the simulation needs, the Mercury-Atlas flight was broken down into areas of astronaut mission responsibility and into areas of physiological and psychological factors affecting the astronaut. A study was made of existing and proposed devices to determine requirements, suitability, feasibility, and availability of these devices. The simulators and devices finally selected are listed in Figure 1. Omitted from this list are several devices that are not actually simulators, such as mockups and visual devices, disorientation devices such as the one at Pensacola, and airplane 0 g familiarization flights. The listings in Figure 1 are not by order of importance or time availability but rather in groupings of fixed-based and dynamic or moving-based simulators.

The first two devices, Control Simulators No. 1 and No. 2, were part-task trainers consisting of a pilot support, a hand controller, a simplified display panel, and an analog computer programmed with six-degree-of-freedom equations of motion. In Trainer No. 1, the pilot was upright in a chair and used a research type three-axis hand controller. In Trainer No. 2, the pilot used a couch support and a Mercury type hand controller. Both of these training devices were used for initial indoctrination and training in the manual control of the spacecraft attitudes during orbit, retrofire, and reentry. Control techniques, display configurations, and manual control with inflated pressure suit were all evaluated on these devices. The devices were retired upon receipt of the Mercury Procedures Trainers.

The Mercury Procedures Trainers are complete flight trainers that allow practice and evaluation of all procedural and inflight tasks. Figure 2 shows the trainer, the instructor's station in the foreground and the capsule in the background. Two trainers were produced by the McDonnell Aircraft Corporation, one for Langley and one for Cape Canaveral. The trainers are nearly identical with the exception of the computing equipment used to define the vehicle motions. The Langley equipment is capable of solving for all motions including those caused by the aerodynamic effects during reentry. The Cape equipment, however, can only reproduce the vehicle rotary motions of space flight. The trainers are relatively high-fidelity simulators of the operation of most of the onboard systems, especially those that involve direct astronaut activity. The major items not simulated are the spacecraft noises and the view out of the capsule through the window and the periscope. The periscope display in the Langley Trainer has been animated to allow some attitude control practice using this reference system. The instructor from his station can introudce directly approximately 275 separate vehicle failures and indirectly, countless more.

The design of these trainers follows that of most airplane flight trainers in the limited use of actual vehicle hardware and to the use of electronic techniques to animate all displays. The use of actual or pseudo-actual vehicle hardware is limited to that required to produce the physical environment, that is, the enclosure, the panel, the hand controller and associated linkages, the couch, the switches, and so forth. System hardware such as for the Automatic Stabilization and Control System or for the Life Support System is not used. The operation of these systems is duplicated through techniques making use of timers and diode function generators and analog computing amplifiers, integrators, and servos.

The next group of devices listed in Figure 1 are those in which physical motion is involved. These motions were used either to subject the astronaut to an inhospitable environment, reference the centrifuge or Multiple-Axis Spin Test Inertial Facility; or where motion cues are considered to be important; or where a moving base was the simplest method of generating satisfactory displays.

The first of these moving-based devices was the Pilot Egress Trainer. This trainer is a boiler-plate mockup of the spacecraft with similar hydrodynamic characteristics and similar escape path obstructions. The trainer was used in both tanks and open seas to develop the preferred recovery and egress procedures. Procedures were formulated for egress from all probable vehicle conditions including very rough seas and a completely submerged spacecraft. The trainer is also used to train ground teams supporting the flight. Helicoptor and ship retrievals were made in which the communications and recovery procedures were practiced.

The next device is the MASTIF (Multiple-Axis Spin Test Inertia Facility). This NASA-Lewis built simulator is shown in Figure 3. Very briefly it consists of three gimbals individually powered by compressed nitrogen gas thrusters. Angular rates from near zero to over 60 revolutions can readily be generated. The astronauts were whirled to rotational speeds above those where disorientation occurs to become familiar with this disorientation and to practice stopping the motions by use of the Mercury hand controller and angular rate instrument displays. The tests served mainly to build confidence that in the event of a gross Automatic Control System failure, the astronaut could regain control of the vehicle and stop all tumbling.

Next on our list of simulation devices is a facility considered one of the most important for the program. The Centrifuge at Johnsville has been used in astronaut training and in engineering evaluations of man and equipment. The gondola of the centrifuge was equipped with as much vehicle hardware as was required to support the astronaut in the launch and reentry phases of the mission. This vehicle equipment included the support couch, display panel, hand controller and linkages, Environment Control System, pressure suit, and the biomedical instrumentation. To further duplicate flight conditions, the gondola was evacuated to reduced cabin air pressure of the actual flight. Six-degree-of-freedom equations of motion were used to animate the display panel however the acceleration profiles were predefined. In the final training sessions man, equipment, and procedures were evaluated by simulation of the complete three-orbit mission starting with the preflight physical examination through countdown, launch, three orbits reentry, recovery, post mission debriefings and physicals. Base line medical data for comparison with the flight data was a very important byproduct of these astronaut training periods.

The last of the devices listed is the ALFA Trainer. Figure 4 shows the present form of this trainer. It is basically a pseudo-Mercury spacecraft mounted on a spherical air bearing. This nearly frictionless support coupled with a combined astronaut-plus-trainer center of gravity at the center of the ball, produces an almost perfect simulation of spaceflight, as far as attitude control is concerned. The structural support system and the effects of the 1 g field on the trainee limit the yaw and pitch motions to plus and minus 35 degrees. Roll is unlimited. All three attitude reference systems are available to the astronaut including the periscope, panel instruments, and the window. For the periscope display, a 10-foot diameter screen is viewed through optics simulating the wide-angle view of the vehicle periscope. A moving earth scene of the orbital track is back projected onto the screen . This display is relatively accurate for deviation angles up to 25 degrees. For the panel displays, actual vehicle hardware is used to measure the attitudes and rates and to display these to the astronaut. For the view through the window, a lighted horizon and a generalized star field are provided. Motion of the trainer is controlled by astronaut use of compressed air jets. Either the manual proportional jets or the manual low-level fly-by-wire jets can be used. Disturbances which can be produced by misalinment of the retrorockets are also simulated by compressed air jets.

This paper has thus far described the simulators developed for astronaut training. The astronaut, however, is but one member of the flight team. The operational plan for Project Mercury includes a network of telemetry, command, and tracking stations around the world directed by the Mercury Control Center at Cape Canaveral. As the design and construction of the network proceeded, it became evident that procedures to operate the network and facilities to test these procedures were required. This was especially true for the Control Center with its large staff who monitor many varied inputs. At the same time, it was evident that a need existed for verification of the readiness of the network to support a particular flight. The techniques of mission simulation were developed in order to supply the required facilities to exercise procedures and to verify readiness.

As in astronaut training, no one device or technique could supply all the required training and indoctrination to bring the Flight Controllers, the astronaut, and the entire Mercury Network into a well-integrated team. To accomplish this integration, two simulation facilities were constructed and a technique of world-wide simulation developed.

The first of these facilities, and by far the simpler, was constructed at Langley and was used to give the remote site Flight Controllers their initial familiarization with the displays and with the team aspects of flight monitoring. The facility consists of the procedures trainer and the displays typical of a remote site. Figure 5 shows a schematic of the facility. Vehicle data is obtained from the trainer, conditioned, and sent directly to the Flight Controller displays. All intra and intersite communications are simulated. Before each Mercury mission, exercises are run to evaluate site procedures and to exercise the Flight Controller-astronaut interface in both normal and abnormal situations.

The second facility, the mission simulator, was constructed at the Control Center and consists of the Procedures Trainer, interface equipment, and of course the Control Center facilities. When operated to animate Control Center displays only, the simulation is considered to be operating closed loop. This means that any real time astronaut or Flight Controller action will affect the simulated mission exactly as it would an actual mission. The complex is also operated in an open loop mode in connection with world-wide simulations.

Figure 6 is a photograph of the simulation area and shows the data conditioning equipment, the data control panels, the trajectory displays, and controls in the foreground. The procedures trainer instructor's station, the trainer capsule, and the trainer analog computer are in the background. Figure 7 is a schematic detailing the simulation equipment and the tie-in to the Control Center. Spacecraft data, approximately 50 functions, are taken from the trainer, conditioned to look like telemetry, and transmitted to the operational telemetry receiving equipment in the form of the telemetry composite before conversion to radio frequency. The reverse path, commands to the spacecraft, are simulated be sensing switch closures in the Control Center and using these closures to effect changes in trainer operation. The UHF and HF air-ground voice communications are also simulated. The intermediary equipment can modify, interrupt, or cause false readings on any of the channels. This equipment also generates the remaining 40 telemetry parameters (including the biomedical parameters) which come from the vehicle during flight.

The voice aspects of the vehicle countdown and the range operations are simulated so that prelaunch and launch procedures involving these communications paths could be exercised.

The trajectory--and at this time we will speak only of the powered flight phase--was generated by either of two methods. Both methods make use of the high speed operational data transmission

systems and the Goddard Computing Complex. The first method which utilizes the "B" Simulator was used during most of the simulations. This machine uses magnetic tapes containing all necessary data to simulate the launch area tracking. These data include the outputs of the Atlas Guidance System, the outputs of the Impact Predictor Computer, and raw radar data. Also on the tapes are the discrete commands of booster and sustainer burnout which control the procedures trainer operation. The tapes used on the "B" Simulator can and have been made to produce both normal and problem launches and orbits. A typical problem might be an overspeed cutoff which restricts the possible landing areas.

The second method of powered flight trajectory simulation is used on launch day to verify the complete launch area trajectory data flow subsystem. Taped inputs to the guidance and to the impact computers are used to exercise the computers, the launch area data conversion and transmission system, as well as the high speed data lines to Goddard. With this second system, the discrete launch events can only be sent to the trainer via manual action of the trainer operators.

Simulation of radar tracking after capsule separation was not necessary from the flight control procedures standpoint as the operational programs of the Goddard Computer can define the entire flight path and generate all Control Center displays from just the insertion vector. Remote site radar tracking was simulated however to exercise the teletype system which is used to transmit this data to Goddard. The teletype tapes were generated by Goddard for replay at the remote sites during simulations.

The above system details the closed loop mission simulation capability at the Control Center. However one of the requirements of true mission simulation was to simulate world wide. To extend the capability to the remote sites, a method of animating the site displays was needed. Referring to Figure 7, it can be seen that the simulated vehicle data was displayed at the Control Center via operational ground station telemetry equipment, equipment that is an integral part of every remote site. Therefore all that was required was to record the data from the trainer on magnetic tapes and play these tapes at the remote sites. The tapes are made prior to each mission so that the format and calibration of the data would be relatively similar to the flight configuration. The other spacecraft data input to a site, the astronaut's voice, was simulated on the site by an individual scripted to make the standard reports and answer any expected querries from the Flight Control Teams. Both individual site exercises and integrated network mission simulations were conducted using this technique.

To conduct an integrated network simulation, special telemetry tapes and astronaut scripts were supplied to each site. Detailed instructions as to when to play the tapes (in terms of time from liftoff) and as to the setup of the telemetry receiving station were also sent to all sites.

Preparation of these simulations required careful and thorough planning and coordination. Since the simulations are basically open loop, the actions of the astronaut and the Flight Controllers had to be anticipated and these effects included in the prerecorded tapes. The missions were based on the flight plan and on the existing mission rules. A number of abnormalities or faults were included to exercise the astronaut and flight control procedures and to test the mission rules.

The special telemetry tapes were prepared by having an astronaut fly a complete mission with the trainer personnel simulating all ground stations. A master telemetry tape was recorded and the site tapes were prepared from this master by copying data for only those periods the spacecraft would be over that particular site. The recorded data was reviewed to evaluate the suitability of the data from the standpoints of calibration accuracy, conformity to last minute vehicle modifications, and adherence to the mission rules. If any of the data was not suitable, the telemetry ground station decommutators were repatched so that the flight control displays would be close to the desired readings. Repatchings were also used to produce further spacecraft failures. The use of this repatching technique allowed one telemetry tape to serve as the basis for several simulated missions. The scripts for the simulation of the air-to-ground voice were based on the astronaut's voice reports as recorded and on the objectives of the mission. As with telemetry repatchings, the voice scripts allowed considerable flexibility of operation.

Mission simulations are conducted in a manner similar to the actual launch. The entire network goes through a three-to six-hour countdown actually performing the equipment, communications, and data flow checkouts. At the Cape, most of the launch area checkouts such as the spacecraft and booster are only simulated; however, where tie-in to the network exists, the actual checkout is performed. After liftoff each site receives contact with the spacecraft in turn and transacts its voice and data collection tasks. As a standard mission operation, each site reports to the Control Center a summary of the telemetry readouts and a synopsis of the Flight Controller's opinions of the vehicle and astronaut status. These teletype messages are carefully monitored by the simulation group to insure that the desired displays and data were received by the site and that the anticipated actions were taken. If deviations are noted, the simulation group teletypes new instructions to the subsequent sites to attempt to get the "mission" back on track. The simulations normally terminate with splash; however recovery aspects have been exercised. Not to be forgotten in the simulations are the debriefings conducted by the Flight Director. These debriefings can and have lasted almost as long as the simulated flight itself and have lead to many improvements in procedures and equipment usage.

As may be evident from the preceding paragraphs, mission simulation is more "technique" than equipment. These paragraphs just brush the surface as to the many varied duties required before and during simulations to effect a successful world-wide simulated mission.

In conclusion, I might summarize the training routine that leads up to each flight. Sometime in the months preceding his flight, the flight astronaut participates in a centrifuge program. He re-acquaints himself with the techniques of

increasing his acceleration tolerance and with the acceleration profile as it affects his mission sequencing. Approximately three months before a flight, he starts intensive use of the procedures trainer and the ALFA Trainer to plan the flight and to become proficient in the inflight duties.

The network schedule is somewhat more abridged. About three weeks before the flight, exercises are held on the remote site trainer with the flight astronaut participating if possible. After deployment to the remote sites, approximately F -7 days, the Control Center with an assist from Bermuda conducts launch abort exercises. The flight astronaut participates in these drills as much as possible. The closed loop mode of Control Center simulation is used so that the total effect of any decision can be evaluated. Between F -4 and F -2 days, full integrated network simulations are conducted around the world. The astronaut has already "flown" these missions and participates mostly as an interested spectator.

The above routine, in fact the entire simulation and training effort was developed by a process of evolution and continues to develop as the needs of the program grow.

MERCURY ASTRONAUT TRAINING DEVICES

FIGURE 1

1. CONTROLS SIMULATORS NOS. 1 & 2 } FIXED BASE
2. MERCURY PROCEDURES TRAINER
3. PILOT EGRESS TRAINER
4. MASTIF SIMULATOR
5. JOHNSVILLE CENTRIFUGE } MOVING BASE
6. ALFA TRAINER

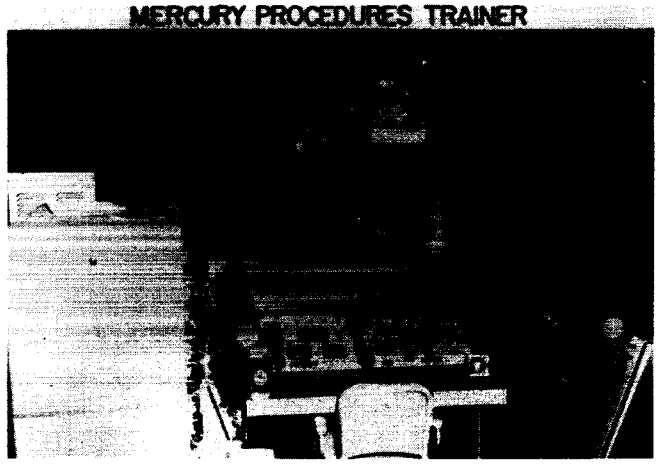

FIGURE 2

FIGURE 3

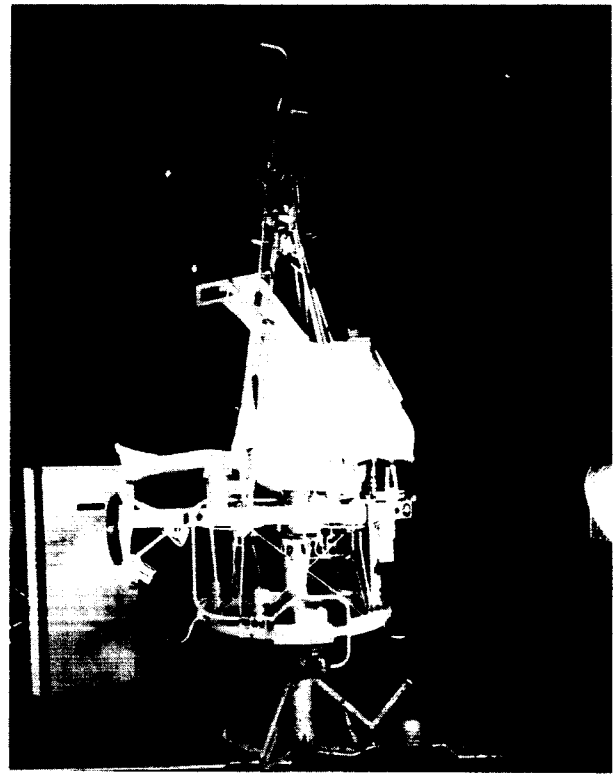

FIGURE 4 ALFA TRAINER

REMOTE SITE SIMULATOR, LANGLEY FIELD

FIGURE 5

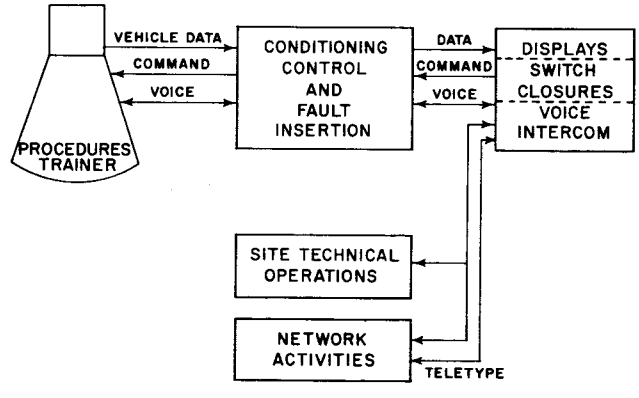

This page is reproduced again at the back of this report by a different reproduction method so as to furnish the best possible detail to the user.

SIMULATION AREA, CAPE CANAVERAL

FIGURE 6

MISSION SIMULATOR, CAPE CANAVERAL

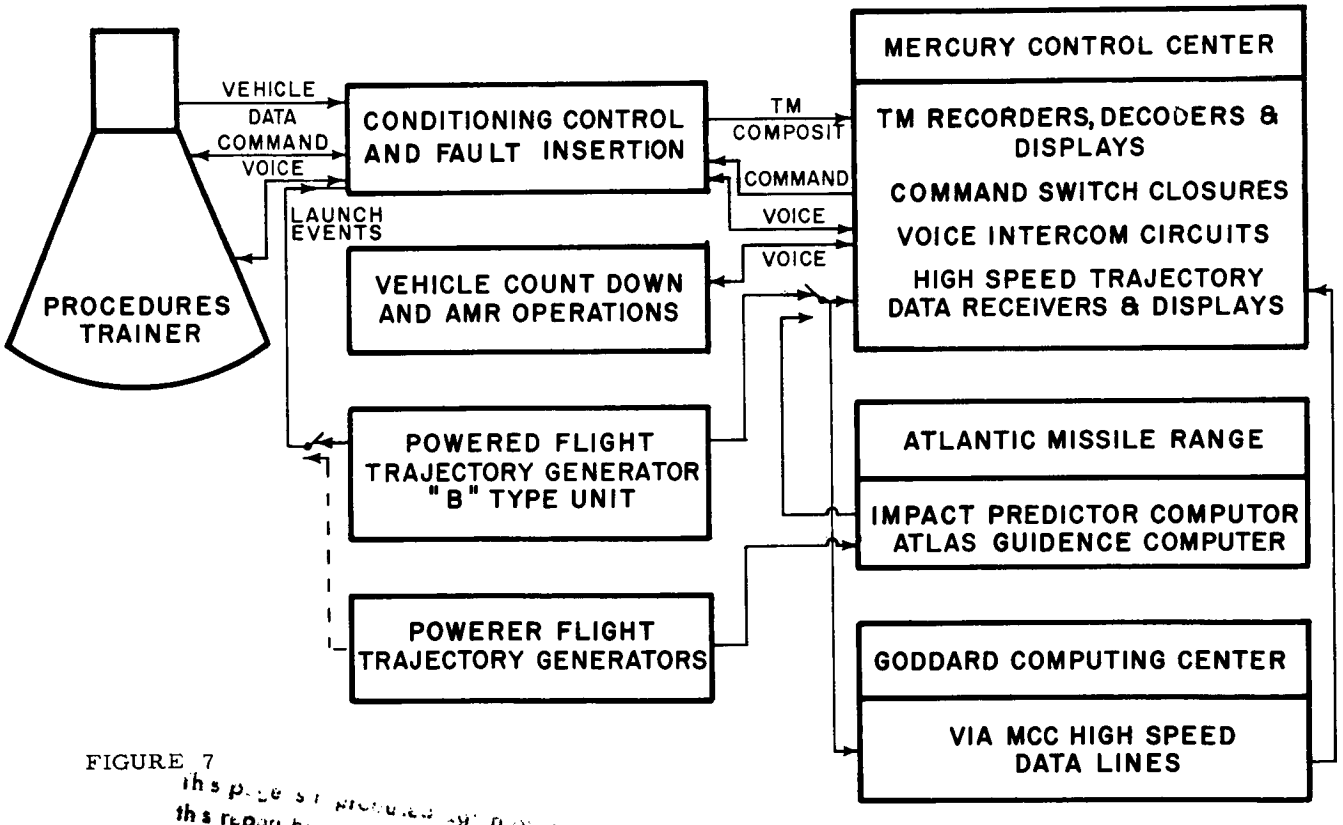

FIGURE 7

This page is produced ... from the best copy furnished for this report by the author. Reproduction may have been limited so as to furnish the best possible detail to the user.

PARAGLIDER RECOVERY SYSTEMS

By Francis M. Rogallo
Aerospace Technologist
NASA Langley Research Center

The flexible-wing concept, which may be as old as the pterodactyl and was given serious consideration by Leonardo Da Vinci, was apparently ignored by the Wright Brothers, Glen Curtiss, and others whose rigid-wing structures followed established bridge and roof-truss design. Today's airplanes have evolved from these early rigid-wing designs. The thin cantilever wings of modern high-speed airplanes are not completely rigid, but they are elastic rather than flexible. They can not be folded up like a balloon or parachute.

In 1945 it occurred to the writer that if we could discover how to make flexible wings that could be packaged and deployed somewhat like a parachute, such wings would have many new applications as well as replacing some parachutes and rigid wings. Previous uses of flexible materials in aerodynamic surfaces - parachutes, kites, boat sails, and wind mills - were reviewed, and some crude experiments were performed with gliders and kites. Before the end of 1948, the device now generally called a paraglider was evolved and developed sufficiently to merit a patent application[1]. The study was continued privately as time permitted, and in 1954 a short paper on the subject[2] was presented to an audience of about 50 Reserve Air Force Officers. This paper was given rather wide distribution, although it suffers from lack of the many kite and glider demonstrations of the original presentation. Little serious interest was shown by the aeronautical community, however, until about a year after Sputnik I. In December 1958 the flexible-wing concept was presented to the Langley Committee on General Aerodynamics with the aid of the hurriedly prepared charts shown in figure 1, faithfully reproduced here for historical purposes.

Of the many configurations and applications shown in figure 1, it was decided that the two-lobe, single-curvature, suspended-load design that had already shown much promise[1,2] should be investigated as a possible reentry glider. While preliminary work of this nature, which is reported in references 3 to 7, was in progress, information pertaining to other applications was requested. The parawing was shown to be a very effective high-lift device for aircraft[8]. It was demonstrated as a wing for a powered aircraft and an air-drop glider, both radio controlled[9]. It was considered for the recovery of rocket boosters[10], and for the terminal glide and landing of manned space capsules[11]. And to support such applications, basic information on pressure distribution was obtained[12,13]. The aerospace industry, particularly Ryan, North American, and Goodyear, has also contributed paraglider information and has made feasibility studies of the recovery of boosters and space vehicles by paraglider. These studies indicated that such recoveries were feasible.

Because NASA work on flexible wings prior to 1961, including Langley Film L-593, was well received at the January 1961 New York IAS Meeting, it was thought that a brief mention of NASA work done since then and continuing, in addition to that listed in the references, might be of interest. Langley Film L-688 shows some of this work.

A wide range of wing geometric variables is being investigated with static wind-tunnel setups such as those shown in figure 2. Line loads and complete glider static forces and moments are determined by the setup of figure 3. Stability and control characteristics of gliders in flight are determined by tests of remote-control models, such as are shown in figures 4 and 5. Space capsule (fig. 4) and booster (fig. 5) models were flown in the full-scale tunnel and also by radio control after being dropped from a helicopter. Deployment of the folded wings after dropping was an important part of the investigation by the Outdoor Test Unit of the Recovery Systems Branch at Langley.

In figure 6 is shown a propeller-powered model being flown in the full-scale tunnel, and in figure 7 is a roughly similar gas-powered radio-controlled model with which some impressive flight demonstrations were made. Figure 8 is a static wind-tunnel model for force test in the 7- by 10-foot wind tunnel, and figure 9 is the Ryan Aircraft being statically tested in the Langley full-scale tunnel.

The glider shown in figure 10 just after lift-off by a helicopter is 50 feet long and has 32-inch-diameter inflated fabric tubes at the leading edges and keel. It has been towed to an altitude of several hundred feet and released for free glide with weights of about 700, 1,300, and 1,900 pounds with the small capsule shown. A standard sized Mercury Capsule will be used next, and weight progressively increased.

In figure 11 is shown a glider built and flown by the NASA Flight Center at Edwards Air Force Base, California. This glider has been towed to altitude and then released for glide and landing.

References

1. United States Patent Office, Patented March 20, 1951, no. 2,546,078. Flexible Kite, Gertrude Sugden Rogallo and Francis Melvin Rogallo, Hampton, Virginia.

2. Rogallo, Francis M.: Introduction to Aeroflexibility. Presented April 21, 1954 to ARDC Reserve Unit at Langley Field, Virginia.

3. Rogallo, Francis M., and Lowry, John G.: Flexible Reentry Gliders. For Presentation at the Society of Automotive Engineers, 485 Lexington Ave., New York 17, New York. April 4-8, 1960. Preprint no. 175C.

4. Rogallo, Francis M., Lowry, John G., Croom, Delwin R., and Taylor, Robert T.: Preliminary Investigation of a Paraglider. NASA TN D-443, 1960.

5. Taylor, Robert T., Judd, Joseph H., and Hewes, Donald E.: Flexible Gliders. Joint Conference on Lifting Manned Hypervelocity and Reentry Vehicles. April 11-14, 1960, p. 215, N-82529.

6. Taylor, Robert T.: Wind-Tunnel Investigation of Paraglider Models at Supersonic Speeds. NASA TN D-985, 1961.

7. Penland, Jim A.: A Study of the Aerodynamic Characteristics of a Fixed Geometry Paraglider Configuration and Three Canopies With Simulated Variable Canopy Inflation at a Mach Number of 6.6. NASA TN D-1022, 1961.

8. Naeseth, Rodger L.: An Exploratory Study of a Parawing as a High-Lift Device for Aircraft. NASA TN D-629, 1960.

9. Hewes, Donald E.: Free-Flight Investigation of Radio-Controlled Models With Parawings. NASA TN D-927, 1961.

10. Hatch, Howard G., Jr., and McGowan, William A.: An Analytical Investigation of the Loads, Temperatures, and Ranges Obtained During the Recovery of Rocket Boosters by Means of a Parawing. NASA TN D-1003, 1961.

11. Hewes, Donald E., Taylor, Robert T., and Croom, Delwin R.: Aerodynamic Characteristics of Parawings. NASA-Industry Apollo Technical Conference, Washington, D.C., July 18, 19, 20, 1961. Part I, p. 423.

12. Fournier, Paul G., and Bell, B. Ann: Low Subsonic Pressure Distributions on Three Rigid Wings Simulating Paragliders With Varied Canopy Curvature and Leading-Edge Sweep. NASA TN D-983, 1961.

13. Fournier, Paul G., and Bell, B. Ann: Transonic Pressure Distributions on Three Rigid Wings Simulating Paragliders With Varied Canopy Curvature and Leading-Edge Sweep. NASA TN D-1009, 1961.

This page is reproduced again at the back of this report by a different reproduction method so as to furnish the best possible detail to the user.

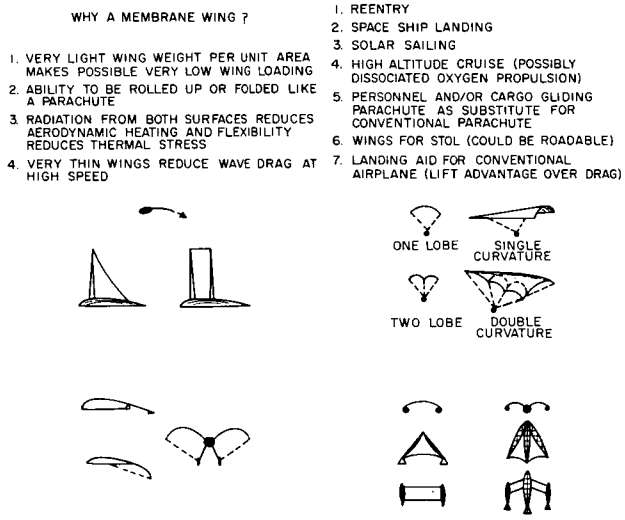

Figure 1.- Flexible-wing concept as presented to Langley Committee on General Aerodynamics, December 19, 1958.

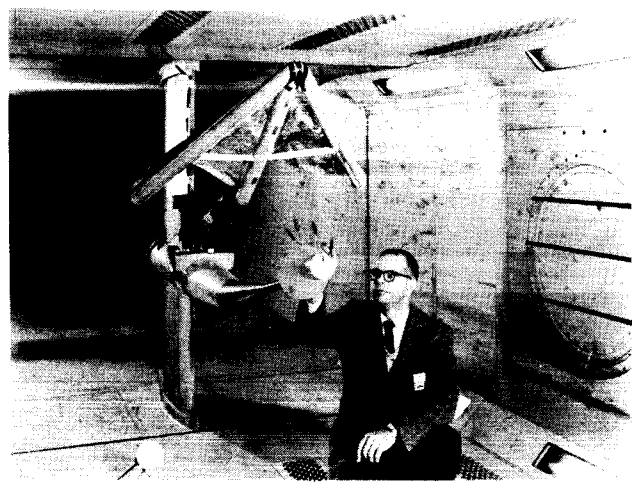

Figure 3.- Wind-tunnel setup for determination of line loads and complete glider statis aerodynamic characteristics.

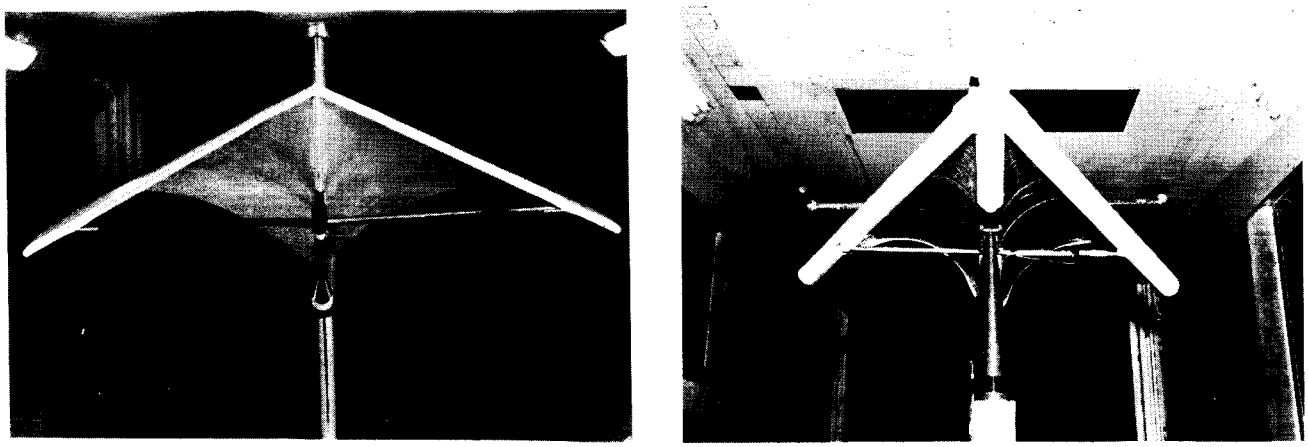

Figure 2.- Typical wind-tunnel setup for systematic investigation of the effect of wing geometry on the static aerodynamic characteristics of flexible wings.

This page is reproduced again at the back of this report by a different reproduction method so as to furnish the best possible detail.

Figure 4. - Remote-controlled model of a paraglider recovery system for space capsules, shown flying in the Langley full-scale wind tunnel.

Figure 7. - Radio-controlled gas-powered model of a manned flexible-wing vehicle being prepared for flight by the Langley Recovery Systems Branch.

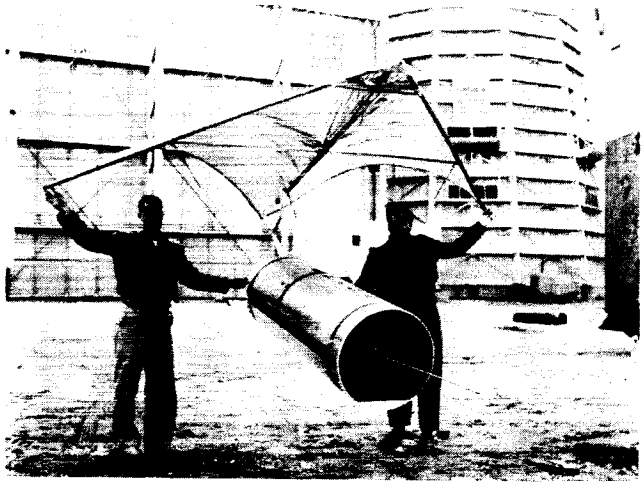

Figure 5. - Paraglider booster-recovery model that was radio-controlled after drop from a helicopter by the Langley Recovery Systems Branch.

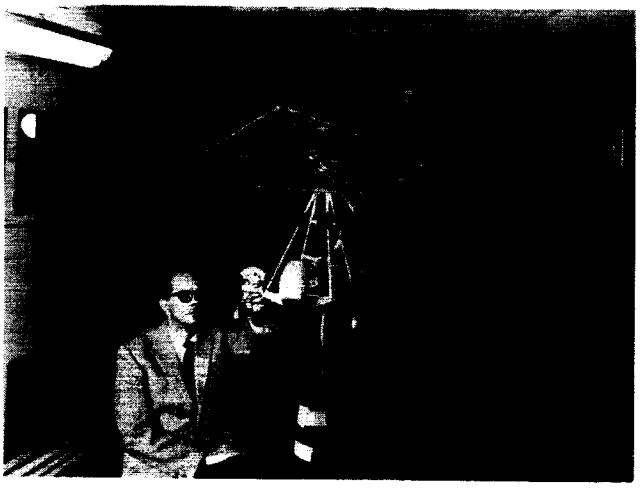

Figure 8. - Static wind-tunnel model of a manned flexible-wing vehicle in a Langley 7- by 10-foot tunnel.

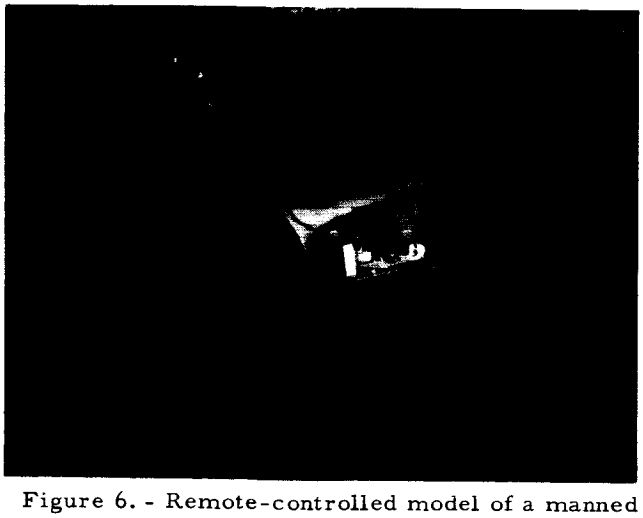

Figure 6. - Remote-controlled model of a manned flexible-wing vehicle flying the Langley full-scale wind tunnel.

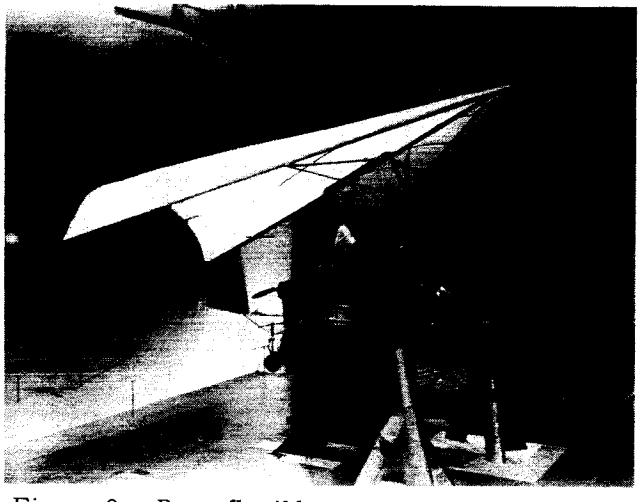

Figure 9. - Ryan flexible-wing vehicle setup for force tests in the Langley full-scale wind tunnel.

This page is reproduced again at the back of this report by a different reproduction method so as to furnish the best possible detail to the user.

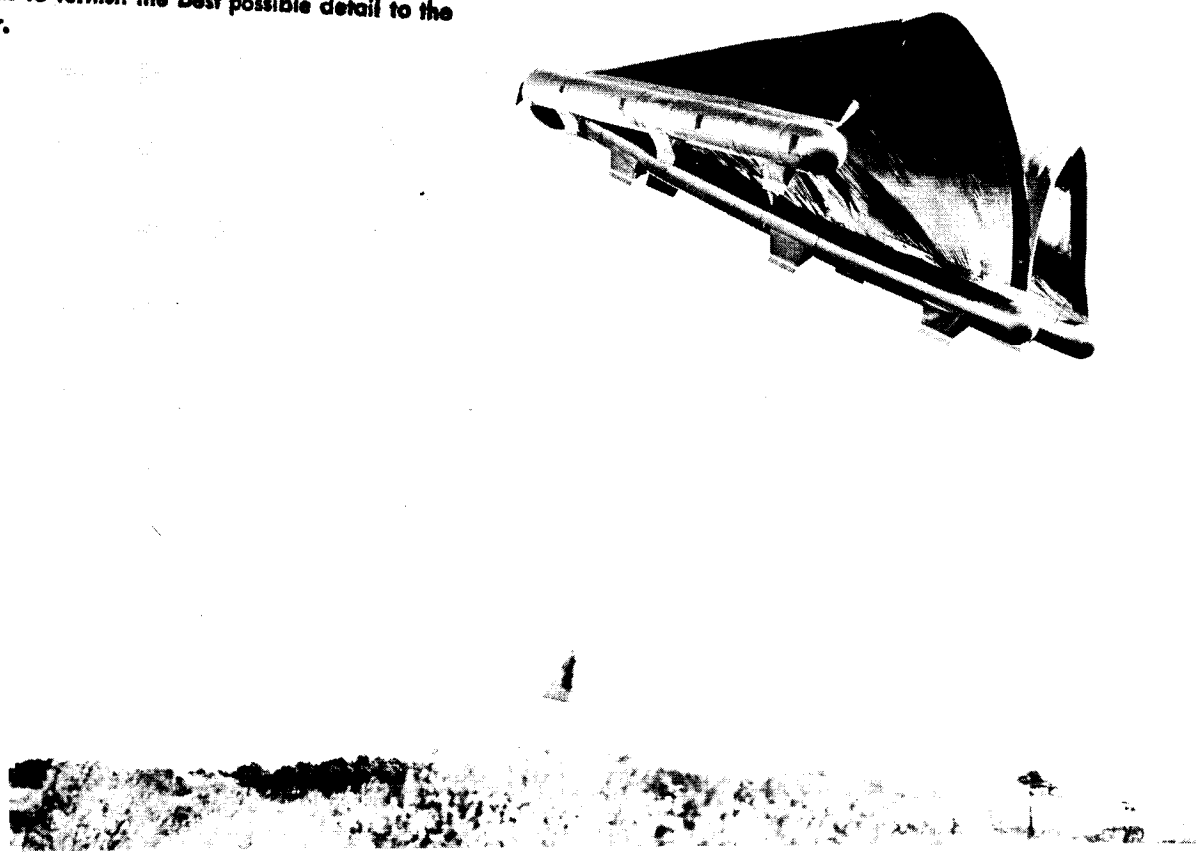

Figure 10. - Fifty-foot inflated-frame paraglider immediately after lift-off by a helicopter.

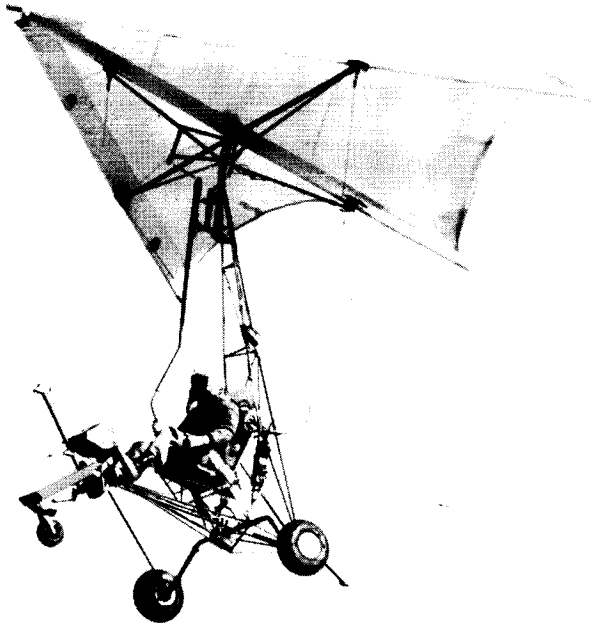

Figure 11. - Paraglider research vehicle built and flown at NASA Flight Research Center, Edwards, Calif.

IMPACT ATTENUATION METHODS FOR MANNED SPACECRAFT

Harold W. Bixby

Chief, Advance Engineering Group,
Paradynamics Systems Section

Northrop Corporation, Ventura Division

Introduction

One of the major concerns in the preliminary design of manned spacecraft is the selection of the impact attenuation system. From a designer's point of view this involves determining a reliable system of minimum weight and size to limit the forces generated in the final phase of landing. These forces should not exceed prescribed deceleration levels compatible with crew tolerance and vehicle integrity; e.g., a gentle touchdown almost comfortable to the astronaut and non-damaging to the space cabin will assure the highest survival probability. Other prime criteria affecting the design are the manner of approach and surface conditions to be encountered.

The landing approach parameters for earth let down systems applicable to manned spacecraft are shown graphically in Figure 1. They divide into two distinct velocity direction categories; those having primarily horizontal velocity, in which sinking speed is countered by the lift capability of the horizontally approaching system, and those having a predominantly vertical landing mode. The horizontal landing is exemplified by the Dynasoar spacecraft at relatively high ground speeds and requires substantial runout distance. The normal landing mode for a vehicle descending with paraglider is also horizontal, but at more moderate ground speeds. A prime example of vertical landing is the parachute descent system. So called vertical landings are often complicated by substantial horizontal velocity due to wind.

Present generation spacecraft must land the crew safely under as wide a variety of terrain, sea-state and weather conditions as possible because an aborted deep-space mission may require return to earth almost anywhere. Systems capable of landing in the vertical mode satisfy more completely such an emergency landing requirement. Horizontal landings and especially high-speed landings are a particular problem because they require a hard surface prepared runway. Use of an ejection seat for emergency escape may be considered an adequate compromise measure for crew survival with spacecraft unable to achieve satisfactory horizontal landings. The ensuing landing gear simplicity is a recognizable advantage to be gained from such a design and operational philosophy. Horizontal landing system requirements appear to be adequately satisfied by impact attenuation gear such as that employed by the X-15.

This paper is concerned with a review of available energy absorbing materials and devices, and the results of an example evaluation of specific techniques applied to a vertical landing system. Many of the energy absorbers discussed have been investigated by Northrop Ventura for use in lunar as well as earth landing systems.

Design Considerations

The problem of achieving an efficient highly reliable impact attenuation system for a vertically landing manned spacecraft is complicated by the many design conditions which must be satisfied. The principle of solution lies in the application of a controlled impulse to oppose vertical momentum, or a controlled dissipation of vertical energy, until only horizontal motion remains to be taken out by the friction.

In determining impact attenuator system size, the vertical velocity, of course, is the most critical factor to consider since energy varies as the square of the velocity. Since descent system weight reduces with increased rate of descent, and impact attenuation system weight increases, a vertical velocity should be selected that will provide a minimum combined systems weight unless impractical stroke or reduced reliability dictate otherwise. Minimum weight vertical landing systems have been theoretically optimized at rates of descent of from 35 feet per second for parachutes and airbags, to 70 feet per second for parachutes and retro-rockets[1]. Size of individual energy absorbers will be affected when friction due to horizontal velocity introduces unequal loadings. Horizontal energy dissipation is simpler to deal with than vertical energy dissipation since translational friction is all that is involved. The vehicle attitude at initial contact is important, and in a

vertical landing system is determined by the selected parachute suspension angle. Direction of the vehicle should be such that the vehicle plane of symmetry coincides with the direction of the wind to favor an antitoppling position with vehicle attitude.

Several factors peculiar to the spacecraft need to be integrated into the impact attenuator design. The spacecraft shape which is determined principally by launch and re-entry considerations may be of concern in the region of the contacting and bearing surface. The weight at landing defines another factor in the momentum or energy to be overcome. The mass distribution and inertia of the vehicle influence the response in motion to eccentrically applied forces. The position of the center of gravity with respect to reacting forces by the energy absorbers determines the magnitude of overturning or restoring moments that may occur. The structural strength and rigidity of the vehicle influence the attachment points of the energy absorbers and mode of reaction forces which result from dynamic application. Adequate stowage space should be immediately adjacent to the operating position of the energy absorbers with suitable access provided for check-out and servicing. The environments in the stowed area will determine the materials to be used. Ease and reliability of deployment are of major concern in the system design.

Crew survival based on human tolerance to accelerations is the primary purpose of the impact attenuation system, although redundant cushioning is provided in the structure of the astronaut's couch and suspension system. Crew position, direction of force, rate of onset and force duration must be considered in the design and application of energy absorbers. Crew participation prior to impact should be utilized to assess the landing situation, orient the spacecraft, and if possible maneuver and position spacecraft over the best achievable impact site. System design should consider wind velocity and direction, and altitude for its effect on vertical velocity.

Surface conditions at impact must be carefully considered in the design of the impact attenuator system. A requirement for suitable touchdown on land or water presents a wide variety of possible and probable situations to a non-controllable vertically descending system. A small degree of maneuver capability would permit avoidance of minor obstacles, a reduction of horizontal velocity due to wind, and the selection of a clear area of moderate to zero slope. Surface hardness and smoothness, (low sliding friction) as stated before, are favorable to horizontal runout. Surface roughness (high sliding friction) and softness cause greater resistance to horizontal runout and increase pitching moments inducive to toppling.

Energy Absorbers

The candidates for working components of attenuator systems include a wide variety of energy absorbers: pneumatic bags, various forms of fabricated metallic and non-metallic honeycomb structures, balsa wood, numerous foamed plastics, combinations of these materials, hydraulic cylinders, pneumatic cylinders, metal deforming devices and rocket motors.

Pneumatic bags have been successfully employed as energy absorbers in a number of applications including Mercury. Development of the airbag technique continues to reveal advantages and improved potential efficiencies. These bags are constructed of high strength fabric, coated with rubber-like material to create an air tight flexible envelope of desired shape. Bags are capable of being folded and tightly contained in a small and even shallow compartment. They are normally deployed and inflated during final descent just prior to impact. Bags are equipped with exhaust orifices which are sealed by burst diaphragms designed to rupture at a preselected pressure level as the gas in the bag is compressed under impact loading. A typical force versus stroke curve is shown in Figure 2 for an airbag using a fixed area orifice. The curve shows an adiabatic rise until burst of diaphragms occurs; then the curve continues upward at a reduced rate until the exhaust flow matches the compression rate, then falls rapidly as vertical velocity is overcome. Bag efficiency has been improved slightly by the use of simple variable orifices which level the pressure curve by retarding the escape of air over the latter part of the stroke. A theoretical optimum has been determined[2] which shows that a properly controlled variable area orifice could achieve at least a 15 percent improvement of efficiency in an airbag.

Aluminum honeycomb has been used effectively as an energy absorber. This material is available in a range of cell sizes and foil thicknesses in different alloys, and provides a wide variety of crushing strengths for attenuator structures. This material compressed in the direction parallel to the cell axis develops an excellent and uniform resistance force by a characteristic buckling and collapsing action as crushing progresses. A force peak occurs at the beginning of the stroke representing a start of crushing action. This peak may be eliminated by a slight precrush or modification in shape of the material. Usable crush distance is approximately 70% of uncrushed height before the characteristic bottoming out force-rise starts at the limit of usable stroke for the material. Reduced crushing strength at loads applied at angles other than parallel to the cell axis must be considered in the impact attenuator design.

Honeycombs constructed of other materials display similar characteristics at

different crushing pressure limits depending upon modulus and density of the material.

Plastic foams provide a generally homogeneous structure which performs with uniform resistance in all directions. Bottom out force rise is a function of the density of the foamed structure. Styrofoam is more effective as an energy absorber than other foams. Polyurethane, which may be foamed in place, is more easily adapted to a system.

Balsa wood is an especially efficient energy absorber and behaves in a manner similar to honeycomb. Its crushing stress changes with angle of force from the grain direction, and best grades satisfy a limited range of crush pressure. Various in-between energy absorbing characteristics can be achieved by using either foamed plastic or balsa wood as filler in the honeycomb cells.

Deformable metal tubes offer another efficient means of absorbing energy. Such a technique lends itself to strut arrangements in which the metal tube of known flexural characteristics is forced over a die which deforms the metal and causes flexural failure in a controlled manner. Frangible metal tubes have been investigated[3] for energy absorption performance employed in much the same manner and found to produce consistent results. Proper design can result in close to ideal force stroke patterns.

Pneumatic cylinders provide good energy absorption, properly applied in landing strut arrangements. The principles of control of force and stroke are similar to other mechanisms which employ a variable orifice. Hydraulic cylinders, oleo-struts and liquid springs commonly used in aircraft landing systems may be employed if rebound is properly controlled.

Both solid and liquid propellant rocket motors possess the high specific impulse characteristics required to efficiently perform impact attenuation of a spacecraft. Landing rocket thrust initiation and performance are not so positive as the contact and compression of energy absorbers physically positioned between approaching load and landing surface.

Analysis

One method of evaluating various energy absorption materials and devices compares their performance efficiencies by relating energy capacity to an ideal unit represented by a rectangular force-stroke curve. The area under the curve equals the required kinetic energy, dissipated at a maximum allowable force level throughout the deceleration stroke. Figure 3 shows the relative efficiency by area ratio for several typical energy absorbers. Such a comparison implies that the material or device with the shortest stroke is necessarily the most efficient. Performance efficiency obtained by this method, although useful where minimum stroke is a critical factor, is not suitable for comparative evaluation of energy absorbers widely different in nature.

A more useful evaluation comes from a comparison of materials and devices based on energy absorbed per pound of absorber weight. Such a comparison is shown in Figure 4. On the basis of weight, balsa wood has the greatest energy capacity per pound of any investigated crushable material; nearly double that of the best rated aluminum honeycomb.

An evaluation on the basis of energy absorbed per unit volume of absorber serves to indicate packageability and light weight in overall design. Figure 5 shows specifically that although the weight efficient items generally hold good bulk efficiency, two devices, liquid spring and airbag show special advantage as to stowed volume. The fact that the airbag is a low pressure energy absorber makes it suitable for large bearing area applications.

It is apparent that a minimum weight impact attenuator system cannot be selected based on the preceding evaluation methods without a knowledge of the load bearing structure of the spacecraft involved, or of the environments to which materials will be exposed. Many efficient absorbers are devices which present a high concentrated load to the structure, and require additional weight in reinforcement to satisfy the impact attenuation function. Balsa wood and plastic foams deteriorate at high temperature. Other factors which will influence the utility, size and weight of the impact attenuation subsystem will show up in the application to a specific spacecraft design.

Applied Techniques

A preliminary analysis and design study aimed at the selection of a most suitable impact attenuation subsystem for the Apollo Command Module* considered a number of techniques. Design was based on requirements which affected all methods alike. Evaluation on a basis of minimum weight, minimum volume, relative cost, reliability and overall system complexity revealed very close competition between the applied techniques examined.

Following a review of many methods, only those techniques employing airbags, crushable materials, frangible metal tubes, springs with hydraulic struts and retrorockets were examined in close detail.

---

* Results are taken from a study performed for North American Aviation, S&ID (Contract No. M2H43X-406003)

The Apollo Command Module presently prescribes a state-of-the-art landing system consisting of three large parachutes in a cluster, supporting the spacecraft at 15 degrees toe-down during final descent. The impact point will be subject to drift due to wind, but direction of the vehicle plane of symmetry may be controlled to present a most favorable landing attitude either on land or water. The edge down attitude plus the ability to direct the vehicle, permits a concentration of maximum energy absorption in a smaller portion of the landing structure than would be feasible without directional control. Space available for stowage of the impact attenuation subsystem was limited to two inches between heat shield and crew compartment, plus reasonable volume in an annular space inside the maximum diameter. Heat shield removal is required before the impact attenuator can be deployed. Hence, the shield provides deployment force, positioning control, a bearing structure and sliding surface for taking horizontal run out. These advantages to the landing system are considered more desirable than the weight difference resulting from reduced parachute size for the same rate of descent without shield.

An airbag system of six self-inflating cylindrical envelopes between crew compartment and suspended heat shield also included an arrangement of restraint cables to control shield deployment and lateral motion. Bags were designed for unequal loading under most severe conditions of low leading edge impact into a 15 degree rising ground slope.

Several strut arrangements were examined using different devices for energy absorption. Weight of the released heat shield is used to deploy the system into operating position. Figure 6 shows three types of struts and their manner of energy absorption. A cluster of leaf and liquid springs provided heat shield support and lateral restraint in a 4 group strut arrangement. A series of 20 struts employing the frangible tube around the outer edge of the crew compartment represent another concept. An arrangement of six struts employing aluminum honeycomb was also considered a likely application. All systems were designed to take out the total energy in the forward struts, or on all struts equally without exceeding allowable acceleration limits. The deforming devices provided a two-area profile, a small area for low force and a larger area for high force in those struts required to accept extra energy. This two stage strut technique properly applied will automatically compensate for unbalance of forces which may be introduced by lateral drift, sloping surface or high friction.

Several landing rocket arrangements were considered. One shown in Figure 7 in which four solid propellant motors were arranged around the lower periphery of the crew compartment employed two telescoping probes to serve as surface distance detectors and initiators for the system. A principal difficulty associated with this method is landing distance error, due to initiation means, propellant grain temperature variation and accurate rocket ignition timing. Openings were created through the heat shield for rocket thrust and probe extension. An error analysis showed that by controlling grain temperature and the use of an adjustable probe plus blow-out thrust alleviators, a suitable impact velocity could be achieved. The number of series events required resulted in a low potential reliability for this technique.

Shown also in Figure 7 is a new concept by Northrop Ventura in landing rocket design which employs a peripheral "skirt jet" principle to produce retro thrust plus an air cushion between the spacecraft and the ground on close approach. Features of this method include better adaptability, lighter weight and improved reliability. The torus form of the combustion chamber and continuous circular nozzle may be readily supported in the annular space around the crew compartment. Heat shield removal and a probe initiator or other accurate distance sensing device will be required as with the four rocket technique. Because the peripheral jet generates a strong curtain wall and a region of augmented pressure between the vehicle and the landing surface, the total rocket impulse is substantially reduced, and very little jet thrust is required to arrest the vehicle completely on the air cushion just before contact. This action automatically adjusts the effective decelerating impulse to variations in descent velocity, rocket burning time, the height at which the reaction is initiated and other significant variables.

A weight evaluation of the various applied techniques is shown in Figure 8. A minimum weight impact attenuation system using a landing rocket is indicated. However, the low potential reliability of either of the two rocket configurations described would certainly not be acceptable for Apollo without extensive development to increase this reliability. Two of the strut techniques and the airbag technique are essentially equal in weight value, making a selection difficult except on a basis other than weight.

A comparison of the energy capacity in absorber material with the energy per pound of an example system using that material, reveals that less than 10 percent of the system weight does the work. This would indicate that in the example cited, weight penalty for heat shield release, restraint suspension, attachment fittings and reinforcement of structure is very high. Refinement of a design can overcome some of this difference in efficiency potential.

An installation of low pressure crushing material in the bottom structure would appear to be an alternate technique which would not suffer from the high dead weight penalty. Were it not for the length of deceleration stroke needed, and the inherent resistance to crushing in the heat shield, such a method would be attractive. The addition to the landing face of a spacecraft of low density material of required stroke depth, seriously affects center of gravity position, hence aerodynamic stability, and valuable space needed for crew.

Conclusions

Some aspects of the problem of selecting an impact attenuation technique for manned spacecraft applications have been presented herein. The study shows that the materials and devices used for energy absorption have inherent properties which make it possible to predict their relative efficiencies in applied systems without a specific knowledge of the details of the application. On the other hand, it is shown that sample impact subsystems may become involved with the detail characteristics of the application resulting in a reduced overall efficiency. A principal determinant of the effect produced by the application is the nature of the basic structure related to impact load concentration. A similar interaction exists between the structure and the crew system which was not considered here. A method of interrelating these factors in a more exact numerical solution is needed which can be useful in evaluating and selecting optimum subsystem components.

There has been no intent here to present the complete picture of the final aspects of actual selection of an impact attenuation system for the Apollo Command Module. Examples described were a part of a preliminary design study and are used only to point out the evolution of selection factors. Techniques described, although developed for vertical descent systems using parachutes in clusters or gliding parachutes, are not limited to strict vertical landing applications, but may be adapted to predictable conditions possible with rotary wing or paraglider flare out. With proper design allowance for vacuum environment, most of these techniques will provide suitable attenuation of the terminal impact phase of a spacecraft making a vertical landing on the moon.

References

1. Ewing, E.G., "A Minimum Weight Landing System for Interplanetary Spacecraft", Symposium on Recovery of Space Vehicles, Los Angeles, September 1960.

2. Simonson, J.R., "Study of Design Criteria for Landing Shock Absorption Devices for Recoverable Flight Vehicles", ASD-TR-61-583, January 1962.

3. Fisher, Lloyd J. Jr., "Landing-Impact Dissipation Systems" Paper in NASA-Industry Apollo Technical Conference, Part I, Confidential, July 1961.

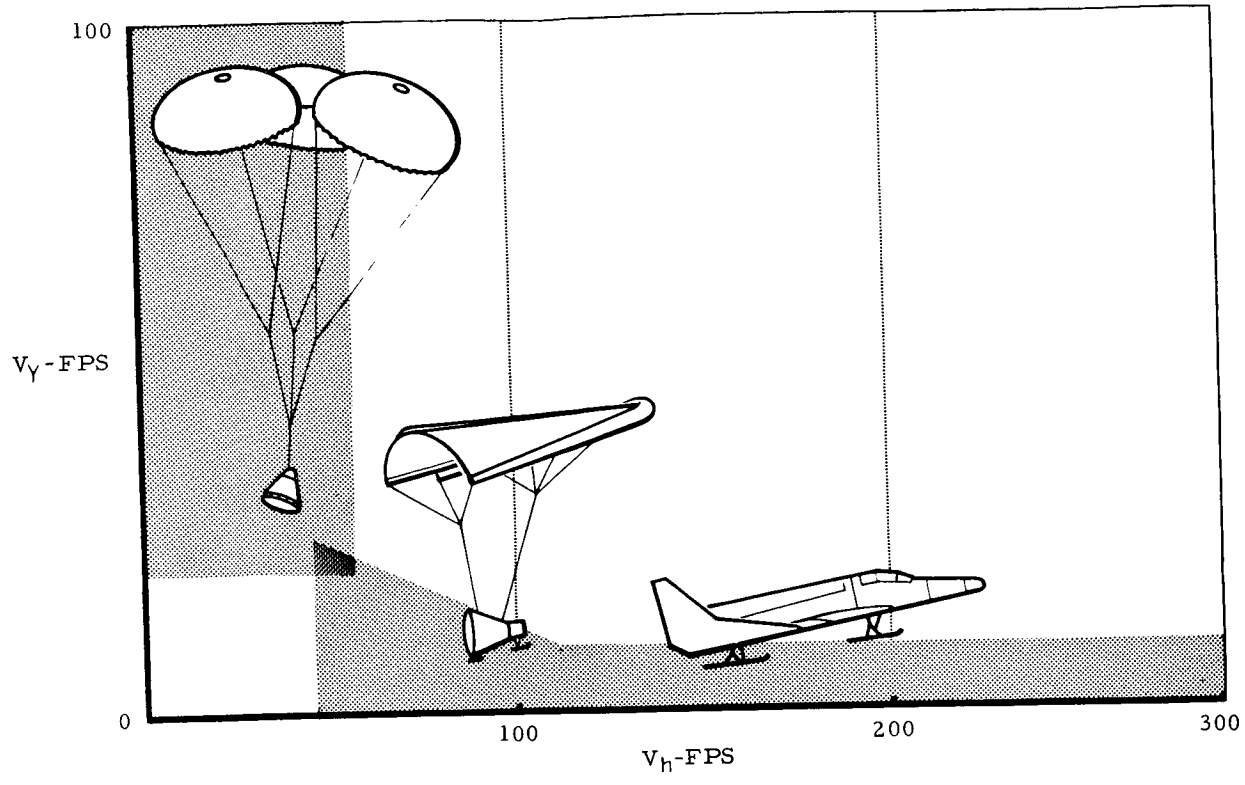

FIGURE 1 - LANDING VELOCITY REGIMES

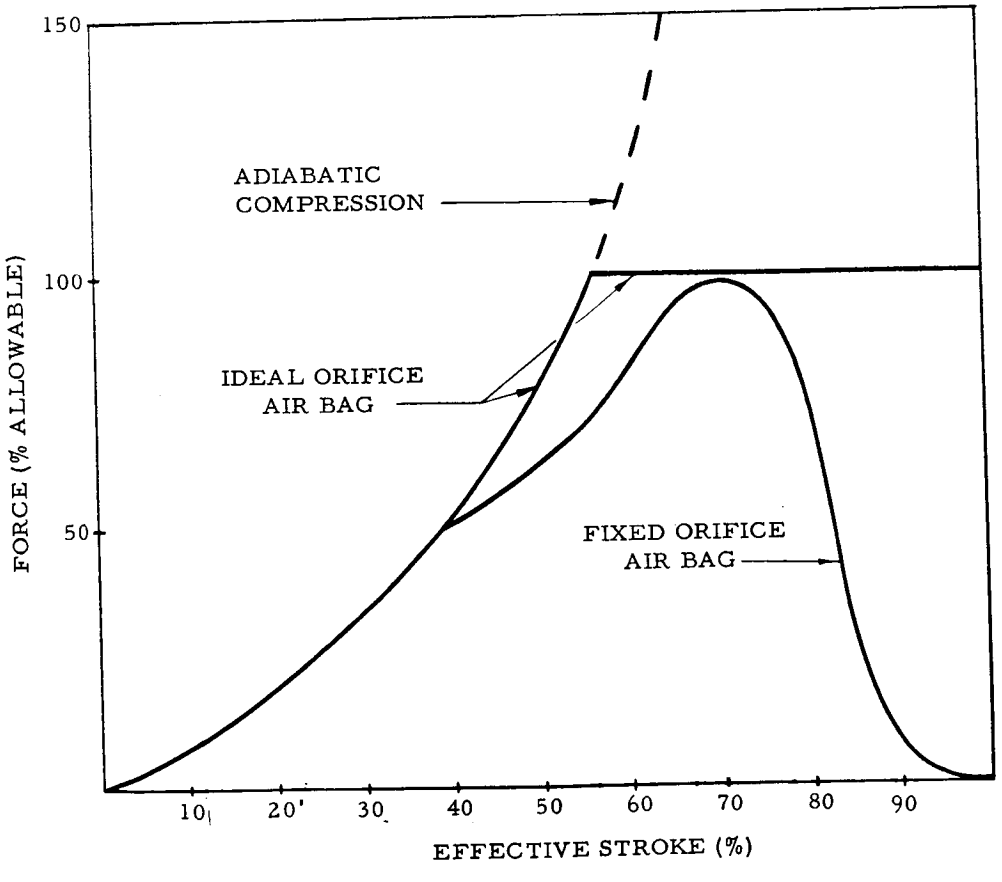

FIGURE 2 - AIR BAG FORCE VS DEFLECTION CHARACTERISTICS

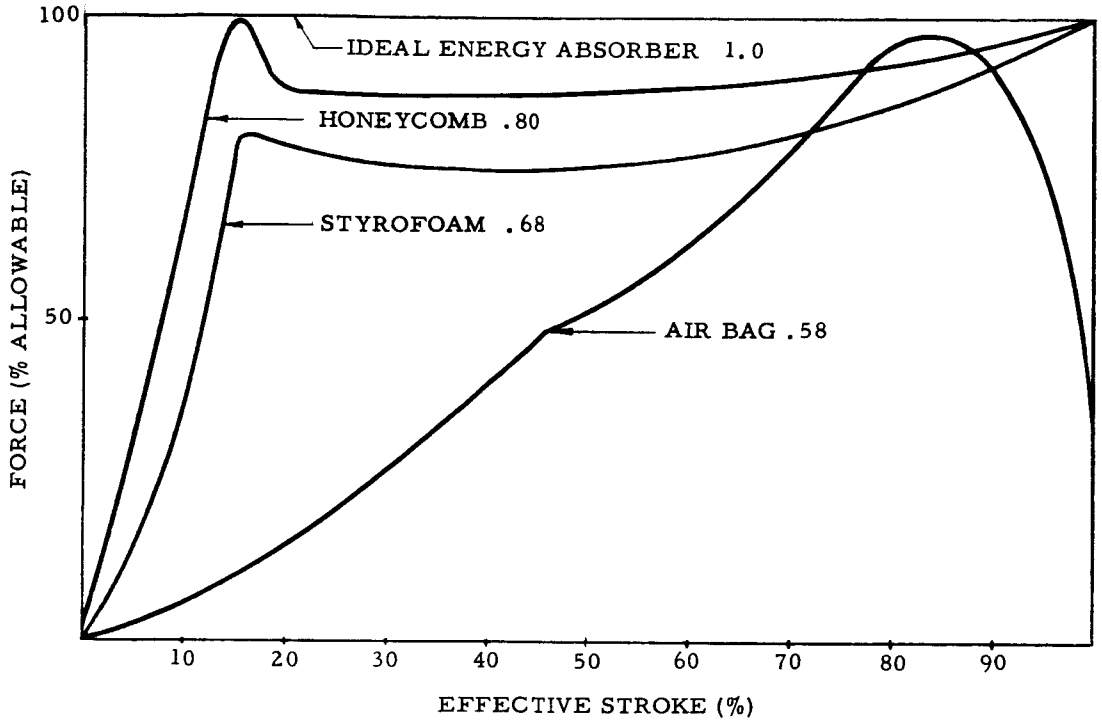

FIGURE 3 - PERFORMANCE EFFICIENCY

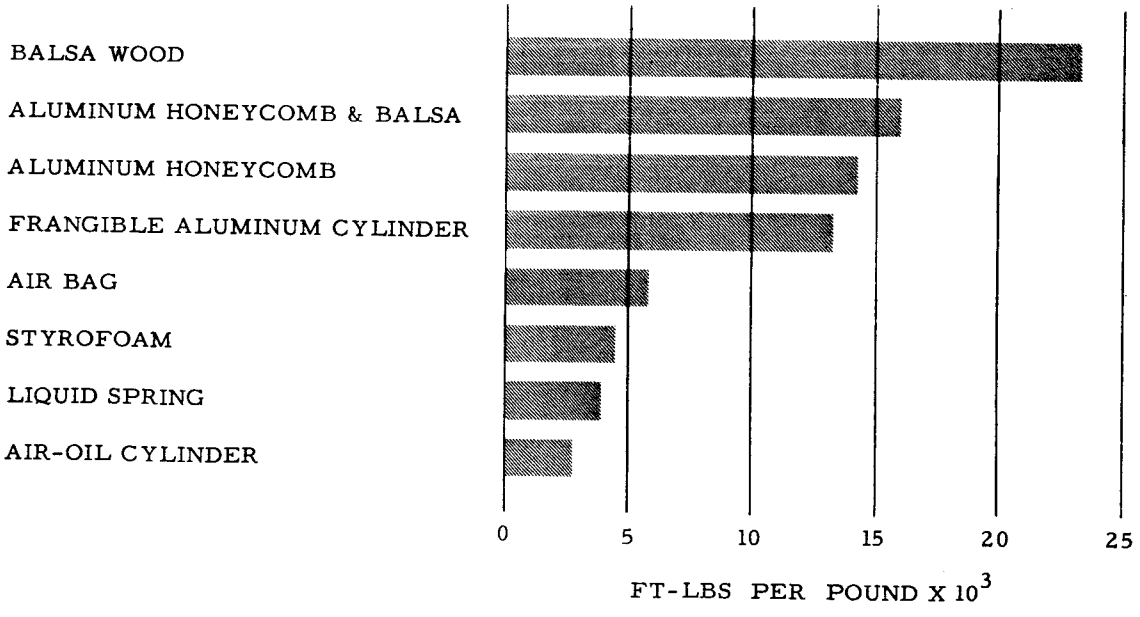

FIGURE 4 - ENERGY PER POUND OF ABSORBER

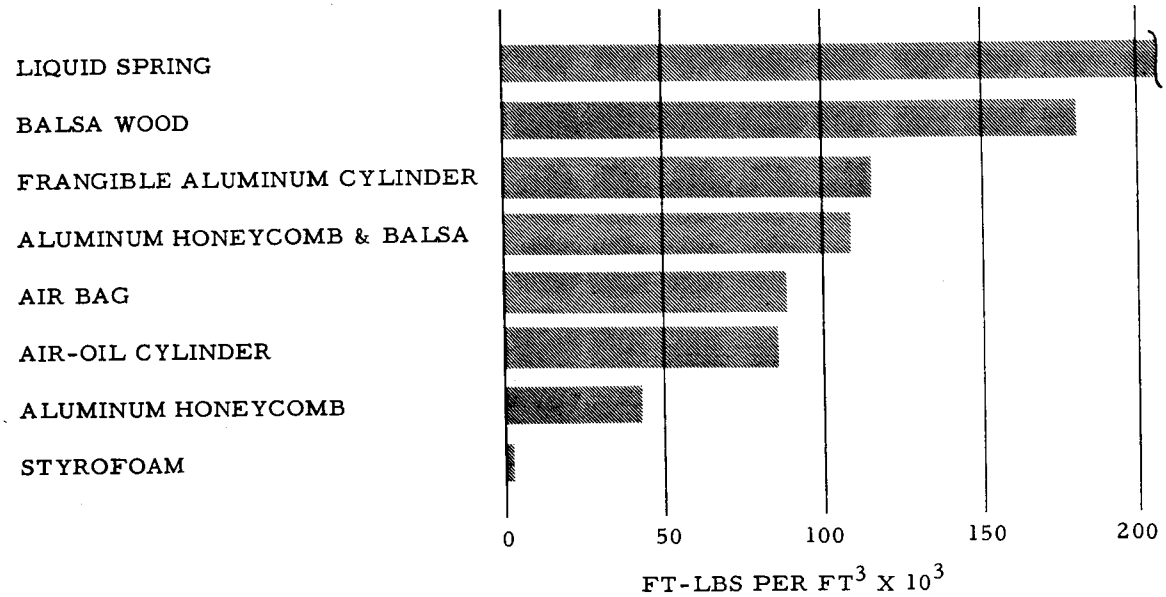

FIGURE 5 - ENERGY PER CUBIC FOOT OF ABSORBER

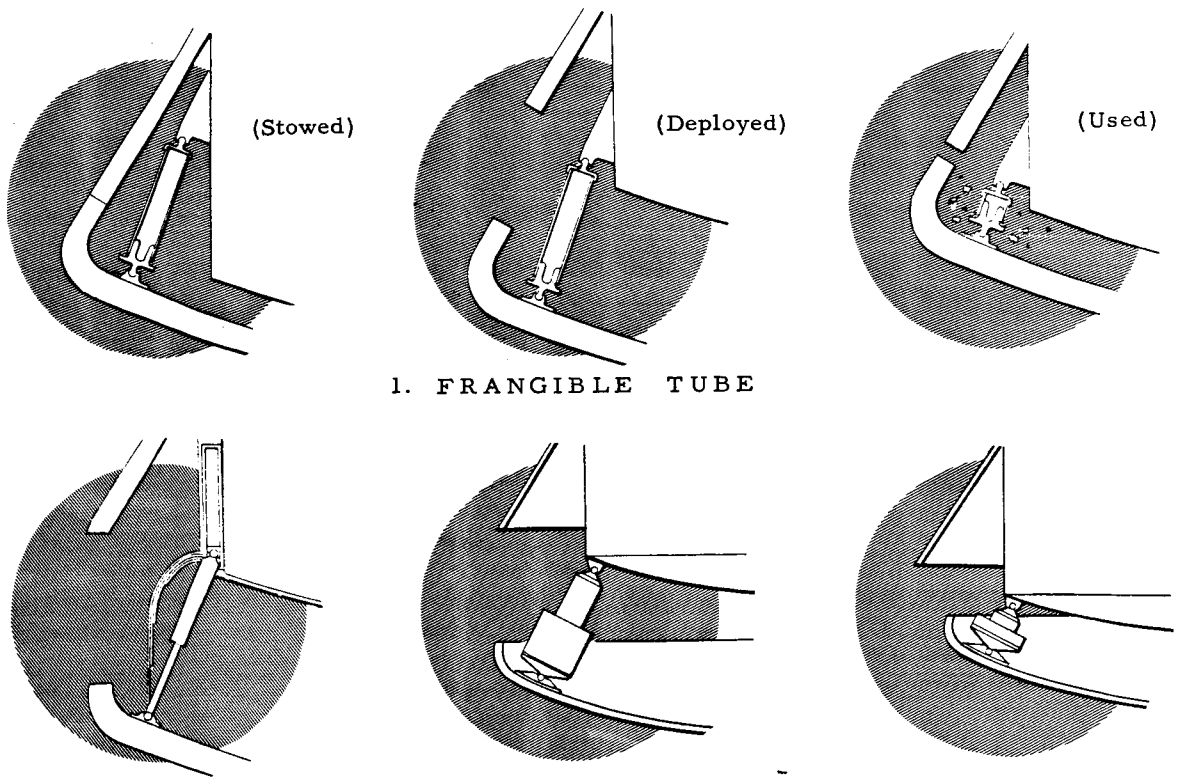

FIGURE 6 - DETAILS OF THREE STRUT METHODS

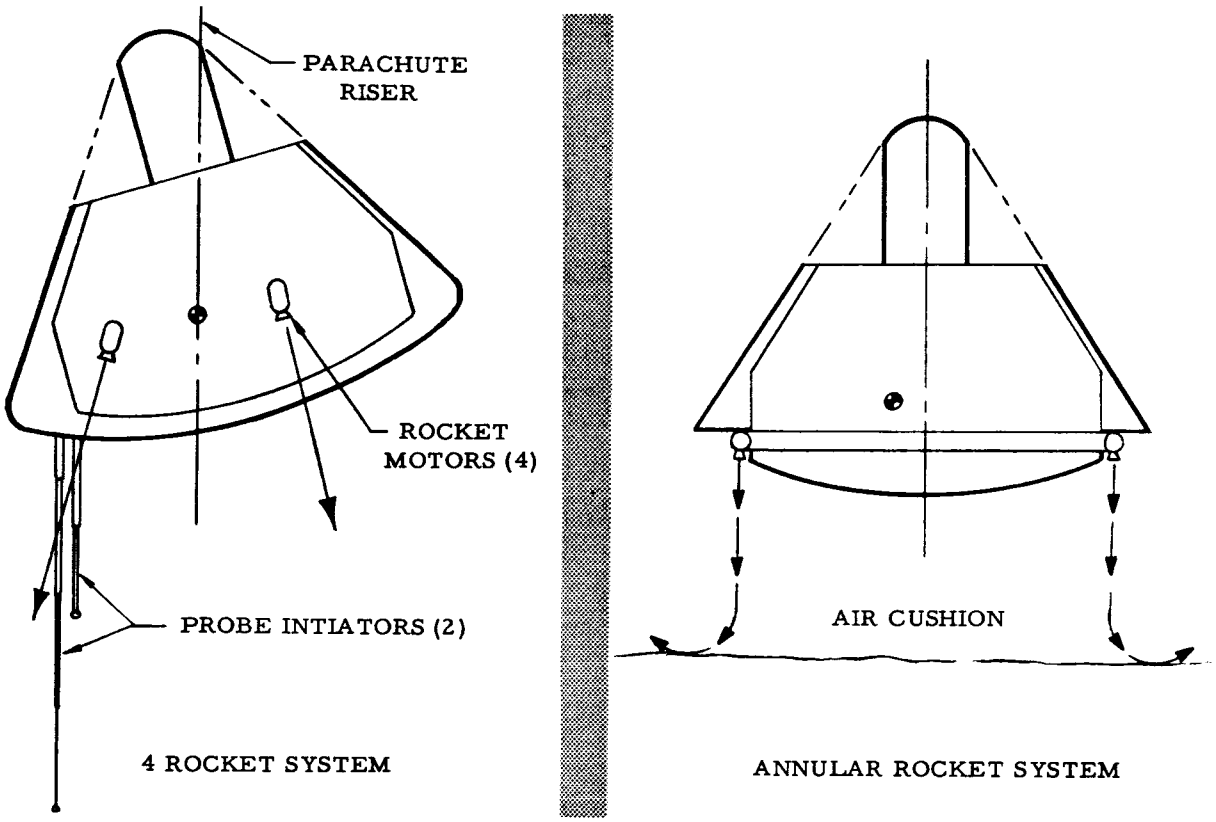

FIGURE 7 - LANDING ROCKET ARRANGEMENTS

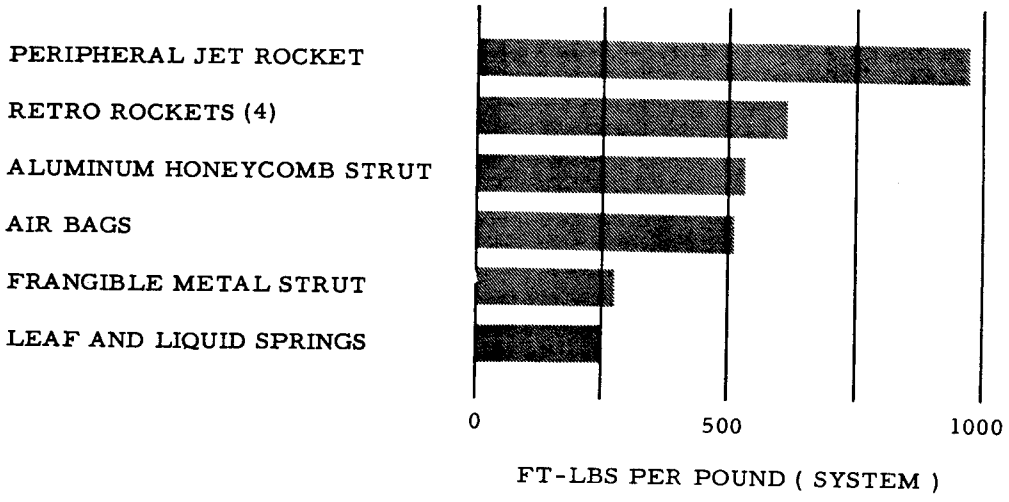

FIGURE 8 - ENERGY PER POUND OF ATTENUATION SYSTEM

EFFECT OF STERILIZATION IN SPACECRAFT DESIGN

Albin M. Nowitzky
Head, Spacecraft Sterilization Systems
Lockheed Missiles and Space Company
Lockheed Aircraft Corporation

I. INTRODUCTION

Modern spacecraft design no longer involves only the Engineering Sciences. To get "the bugs" out of a system must now be taken literally to signify erradication of actual free-living micro-organisms. A severe impact of a non-sterilized space vehicle could result in overt, reckless contamination, virtually eliminating a celestial body as a scientific base for the exobiological phases of space exploration.

Recognizing the potentially damaging effects of septic launchs, the National Aeronautics and Space Administration in December, 1960 authorized spacecraft sterilization and decontamination as National policy, thereby elevating the space effort onto a higher scientific plane. In the NASA directive, the basic reasons for sterilization were established, viz.,

> to preserve clues to the origin of life and of the universe, which may be hidden beneath the lunar strata or under the atmospheres of strange planets,
>
> to prevent inadvertent seeding of extraterrestrial surfaces by earth-life cultures, and
>
> to protect the earth from mutual contamination.

In light of the foregoing, spacecraft sterilization should be regarded as the most significant single mission as well as design requirement of planetary space exploration --- especially if our objectives are primarily scientific.

II. STERILIZATION AND THE PLANNED SPACE PROGRAMS

The projected timetable of U. S. space exploration is illustrated in Figure 1. The missions shown, both manned and unmanned, are those which would involve sterilization techniques to various degrees, depending on the nature of the particular mission. Of these projects, the bulk of practical experience has been obtained during the current Ranger series of moonshots.

In the Ranger hard-lunar-impact program, all present concepts of the broad spectrum of spacecraft sterilization were initially established. Spacecraft and spacecraft compartment designers and manufacturers were introduced to the subject, and personnel at the launch site received preliminary indoctrination. Results of research into the various techniques, materials, and apparatus required to effect sterilization were implemented, and Qualified Products Lists were initiated.

Project Surveyor and Prospector, involving soft lunar landings of unmanned scientific equipment, will of course benefit immensely from the pioneering Ranger experience. The sterilization confidence level, discussed later, will be markedly increased, and influence during countdown will be reduced.

The Mariner and Voyager unmanned planetary flybys, with planet-orbit capability, present a reasonable possibility of extraterrestrial impact. Sterilization of this type of spacecraft is therefore notably important, and knowledge of a nonsterile condition constitutes special justification for an automatic hold or flight cancellation.

Quarantine inspection and aseptic retrieval procedures, hopefully established through unmanned probes and samplers before manned-mission escape velocity, will form part of the routine modus operandi of the manned missions as will aseptic personnel movement.

III. RANGER AND THE SCOPE OF STERILIZATION

The Ranger program afforded an advanced opportunity to establish and investigate the techniques required to achieve the ultimately sterile spacecraft. In Figure 2, the scope of these techniques is shown. Final sterility depends primarily upon precise adherence to previously established standard operating procedures, involved in performance of each sterilization phase.

In brief, all components, sub-assemblies, assemblies, adhesives, lubricants, sealants, and any other constituent of which the complete spacecraft is composed, are internally sterilized. The internally-sterilized parts are then aseptically assembled. The aseptically-assembled spacecraft is enclosed in a sealed spacecraft compartment. Sterilant gas is introduced into the sealed compartment which is subsequently purged following a previously-established sterilization soak period. Aseptic removal of the sterilant gas transfer system is effected and sterile conditions mechanically maintained until the spacecraft has left the earth atmosphere.

In the case of Ranger, the spacecraft compartment is the Lockheed Agena nose-cone illustrated in Figure 3, incorporating special filler valves for aseptic introduction and purge of sterilant gas, and installation and removal of the gas transfer lines. Further provided are a biological breather-filter for pressure equalization caused by ambient thermal changes during ground handling, and a biologically-tight, out-only relief valve for venting during boost. The valve and filter are installed in a fibre-glass diaphragm which together with a special o-ring, seals and protects the spacecraft compartment from atmospheric contamination.

Before being placed in the sealed compartment, the Ranger spacecraft, manufactured by NASA's Jet Propulsion Laboratory, was subjected to aseptic final-assembly by JPL personnel. Previously, the

spacecraft sub-assemblies and components had been internally heat-sterilized or aseptically-assembled, to the best extent possible, as had the impact-limited capsule furnished by Aeronutronic Division of Ford. The equipment required for aseptic assembly, shown in Figures 4, 5, and 6, is similar to ordinary hospital-type glove-box apparatus but of course is more rugged, designed to sustain rigorous assembly operations involving heavy, bulky spacecraft equipment. In isolated cases, lack of compatibility information prohibited prolonged thermal exposure at the heat level required for internal sterilization. The affected parts were installed regardless, and the level of sterility confidence became principally a function of natural internal contamination during manufacture and efficacy of the surface terminal sterilization, conducted during countdown.

Sterile conditions were maintained by the combined action of the seal between the Agena nose-cone and forward equipment rack, the out-only relief valve, and the breather-filter.

Returning to Figure 2, to establish standard operating procedures for internal sterilization, aseptic assembly, terminal surface sterilization and sterility maintenance, it was necessary to continuously monitor the effect of each procedure and media on the associated material or component. Compatibility testing became routine in the Ranger program, including all Agena nose-cone materials, and essentially all of the Ranger spacecraft components and sub-assemblies. Spacecraft sterilization is a natural, second generation follow-on of aerospace quality assurance. Sterilization compatibility assurance is a must for spacecraft constituents of the future and will constitute a basic requirement for placement on the qualified products lists established for each affected project.

Integration of terminal surface sterilization into the otherwise normal countdown procedure is not particularly difficult. When combined with pre-launch ground cooling and other spacecraft conditioning procedures, surface sterilization is conducted with minimum influence on other mission requirements.

Sampling of near and far space for base information concerning cosmic contamination has thus far been ignored in current space program planning. Such valuable information as possibility of ice crystals and organic fraction in micrometeorites, and the knowledge of bacteriological debris of panspermia outside the sensible earth atmosphere has yet to be obtained. Such information would serve to establish requirements for extraterrestrial sterilization activity as well as providing information of value to manned space travel and space medicine. Aseptic retrieval of a living, reproducible organism from space would be a vital step in determination of the origin of life.

Terminal Surface Sterilization

The internally-sterilized spacecraft, having been placed in the confines of a sealed spacecraft compartment, must be surface sterilized with a germicide which must demonstrate a combination of:

- previously proven lethal sporicidal activity,
- maximum compatibility with materials,
- suitability for countdown usage by launch-site personnel.

A mixture which best fulfilled these requirements is the presently established sterilant, a non-combustible, blend of the monopropellant ethylene-oxide and the solvent Freon -12. This gas standard was established by the Army Chemical Corps at Ft. Detrick, Maryland and is currently the accepted mixture for prelaunch usage at AMR. Gaseous surface sterilization using the ethylene-oxide base sterilant was systemized as shown in the flow diagram, Figure 7. Pressurized, bottled sterilant is released through a regulation into a gas generator which supplies gaseous flow through a humidifying group. A required level of humidity is introduced into the gas, with the resulting end-mixture analyzed for concentration, temperature, and water-vapor, and subsequently directed into the nose-cone sealed cavity. After a suitable sterilization soak period, previously established in the biological laboratory, the cavity is purged with inert nitrogen gas. The nitrogen is passed through a filter system before displacing the sterilant from the spacecraft compartment and into the disposal system. The disposal consists of a water supply containing an acid or salt catalyst, which converts the ethylene-oxide/freon -12 mixture into freon gas and ethylene glycol (anti-freeze). In Figure 8, the system illustrated by the flow diagram in Figure 7 is shown as a mobile gas transfer system, currently in use at Cape Canaveral. Readout consists of sterilant and purge-gas flow rates; temperature and pressure in the test plenum; and temperature and pressure in the sealed compartment. Gas concentration and relative humidity are monitored by sampling small amounts of gas at convenience points in the flow cycle.

A more refined system is envisioned for the soft-lunar-landing Surveyor program. Relative humidity and gas concentration will be directly read on the control panel, and the gas cycle will include aseptic temperature control combined with pre-launch terminal sterilization, illustrated in Figure 9. Utilization of such an approach would be a major step in minimizing effect of sterilization on the countdown procedure.

IV. SPACECRAFT DESIGN EFFECTS

The requirement of sterilization has an effect on ordinary spacecraft design philosophy in five major areas as outlined in Figure 10.

Product Qualification

To be truly qualified for use on an extraterrestrial spacecraft, components must demonstrate compatibility with such liquid wipe-on sterilants as ethylenimine, beta-propionolactone and peracetic acid. Component performance must remain unaltered after exposure to sterilizing heat loads and radiation cycles. Structural materials, surface coatings, cements, sealants, and lubricants must be capable of withstanding prolonged contact with sterilant gases.

Many hundreds of components and material samples have been compatibility-tested by J.P.L., Fort Detrick, Brooks Air Force School of Aerospace medicine and by industry participants. Results for the most part indicate no major problems in product qualification for spacecraft use.

Component Manufacture

A number of sealed spacecraft parts, especially hermetically-sealed electronic components,

present a unique sterilization problem in that they may not be capable of sustaining the internally-sterilizing heat or radiation without subsequent malfunction. The questions of course arise,

a - are the components naturally contaminated during manufacture?

b - are the materials used in manufacture sufficiently sporicidal to yield sterile end-products?

c - do normal manufacturing heat cycles yield sterile end-products?

d - are the components compatible with chemical additives and changes in manufacturing procedures which may result in internal sterility?

Answers to these and other questions are presently being sought under various existing government contracts.

Non-sterile components, before being installed, should be either subjected to post-manufacture sterilization techniques, aseptically-assembled, or eliminated from the system.

Vehicle Assembly

Aseptic final and sub-assembly of the previously internally-sterilized components can be simplified if maintainability and fabrication sequence are considered in light of the sterilization requirement early in design. Steps should be taken during initial design phases to minimize assembly procedure steps. Further, reduction of captive pockets and cells, accidental weldments, and enjoining incasements will naturally enhance the terminal surface sterilization phase, thereby increasing the sterility confidence level.

Compatibility with sterilization techniques and media again plays an important role in vehicle assembly, especially in areas requiring sterile sealants and lubricants.

Launch Adaptability

The sterilization requirement necessitates aseptic ground handling and pre-launch conditioning in order that the sterile condition, once achieved, is maintained. Biologically-tight, out-only pressure relief must be afforded the sealed compartment. Filtration must be provided to enable thermal breathing during ground handling to be accomplished without recontamination. Ground cooling media must be introduced through a suitable filter system and possibly maintained in a closed, sterile cycle. The ports for installation and removal of terminal sterilization and purge gas lines must be such that asepsis prevails.

Crew Accessibility

Design of manned spacecraft must be such that ingress and egress transfer of personnel into and out of the command capsule or living quarters can be aseptic. Procedures for such operations have been routine for years at University of Notre Dame and at Ft. Detrick Army Chemical Corps headquarters. An ideal approach appears to be combine sterilization with the escape lock or decompression lock. Filtration of course would be integral with any pressure-equalization valve system between the outside environment and the entrance lock system.

With respect to filters and filtration systems involved in spacecraft sterilization, the screening of all forms of earth life, regardless of infinitesimal size, presents an imposing task. Referring to Figure 11, the pore size requirement for absolute filtration could result in an excessive filter flow cross-sectional area unless certain rules are followed in selecting the filter, viz.,

a - pre-filter the flowing media,

b - provide minimum pore-size and maximum flow area by combining unique packaging techniques with efficient filter materials,

c - use filter material of highest dielectric constant, and provide moisture control to maintain the electric charge.

Worthy of note in Figure 11 is the existance of free-living bacteria smaller than many viruses. The result is pronounced dependence on a highly reliable, highly efficient filter system.

V. MANNED RELATIONSHIPS

The relationship of sterilization to manned space flight and manned spacecraft design is far more critical than that for the unmanned missions. Not only must the new environment be protected from contamination by earth-life, but the reverse precaution must now be considered. The unknowns are indeed appreciatively increased.

Sterilization for manned missions depends to a great extent on requirements established by biomedical results obtained from unmanned space probes. Involved are effects on earth-human tissue of exposure to unknown life forms and, of course, the reverse effects.

In the main, however, the same general requirements for sterilization of space missions and vehicle design apply similarly to manned and unmanned programs, with the following exceptions:

a - The living quarters (command capsule) is not subject to sterilization.

b - The entrance lock should incorporate sterilization apparatus to the extent required for aseptic crew and equipment transfer.

c - Compatibility of space-suits, man-operated sampling equipment, and life support hardware must be considered.

As outlined in Figure 12, in addition to the above, important consideration must be afforded logistics associated with extended parking orbits, for quarantine inspection preceding aseptic retrieval of manned vehicles, and of course, the associated unmanned probes.

VI. CONCLUDING REMARKS

Experience on the Ranger program has borne out

two important facts which should govern future spacecraft design:

- emphasis should be placed on use of maximum number of qualified spacecraft components compatible with internal sterilization by heat.
- sterilization should be included as a design concept in the earliest possible design phase, in order to minimize downstream effects.

The desire to implement such an approach was at the heart of the Ranger design philosophy. However, being a new requirement, sterilization was implemented mostly after-the-fact, to be emphasized to a much greater extent on future programs. The Ranger decontamination confidence level; that is, the confidence of obtaining complete sterility, was not maximized on the first Ranger lunar impact, since some hermetically-sealed components had not been checked for contamination before installation. However, the level of possible contamination was held to a minimum by aseptic assembly, surface terminal sterilization and maintenance of the decontamination level.

Although there is a strong inclination to place a much higher level of importance on planetary sterilization activity than that related to lunar exploration, it should be noted that clues to the origin of life could be hidden beneath the lunar strata, indigenous or foreign, impregnating what is apparently, but not positively igneous matter. Reckless contamination could destroy these vital secrets, or render invalid, results of biological samples.

For millions of years, the moon has been a vulnerable target in the path of extraterrestrial debris; possibly organic, bacterial, and living; almost certainly, if existent, in the lyophilized state, and therefore, preserved in a state highly acclimated to unfavorable environmental extremes. If these forms do exist and are in any way dangerous or destructive, their early detection would prove vital to man's future planetary exploration and to the protection of earth from mutual contamination.

The returning space probe or vehicle, unmanned or manned, possibly highly contaminated by exposure to exobiology, should be subjected to quarantine parking orbit and biomedical inspection, before being reentered through the earth atmosphere. Final retrieval, in addition, must be an aseptic, biomedically monitored, and closely controlled operation.

In conclusion, if our objectives in exploring space are primarily scientific, then we should take the scientific approach. If they are not, then we should still feel obliged to take the approach least likely to upset the biological balance of life on earth.

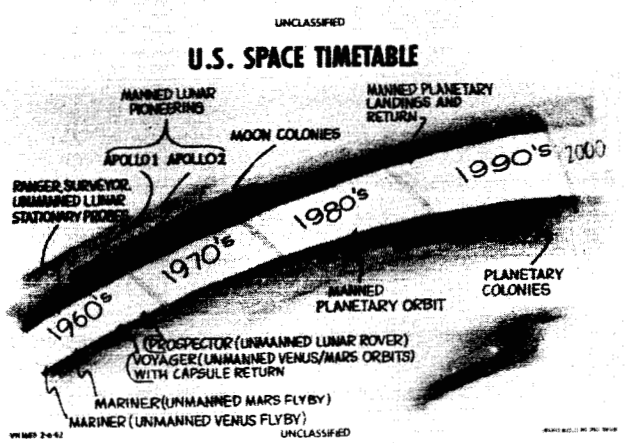

FIGURE 1

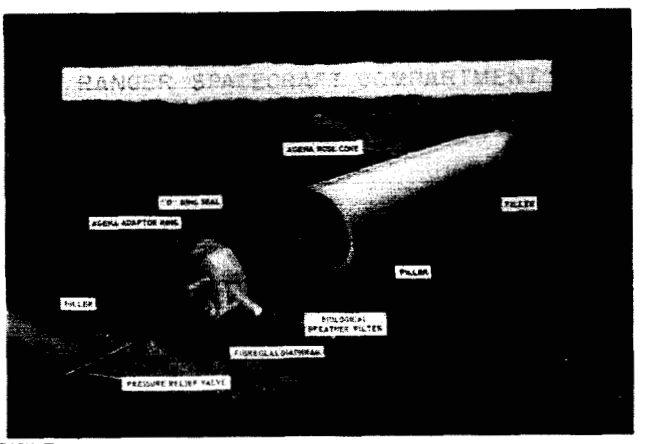

FIGURE 3

SCOPE OF SPACECRAFT

STERILIZATION

• Internal Sterilization	Supported by:
• Aseptic Assembly	• • Compatibility Assurance
• Terminal Sterilization	• • Countdown Integration
• Sterility Maintenance	• • Space Sampling

FIGURE 2

SPACECRAFT STERILIZATION SCOPE

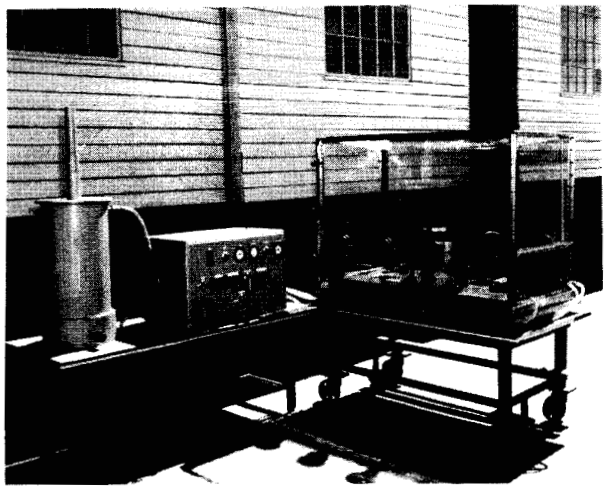

FIGURE 4 RANGER ASEPTIC ASSEMBLY EQUIPMENT

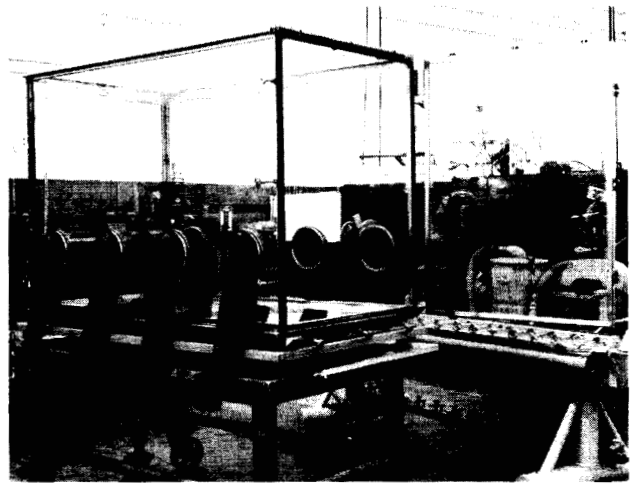

FIGURE 5 RANGER ASEPTIC ASSEMBLY GLOVE BOX

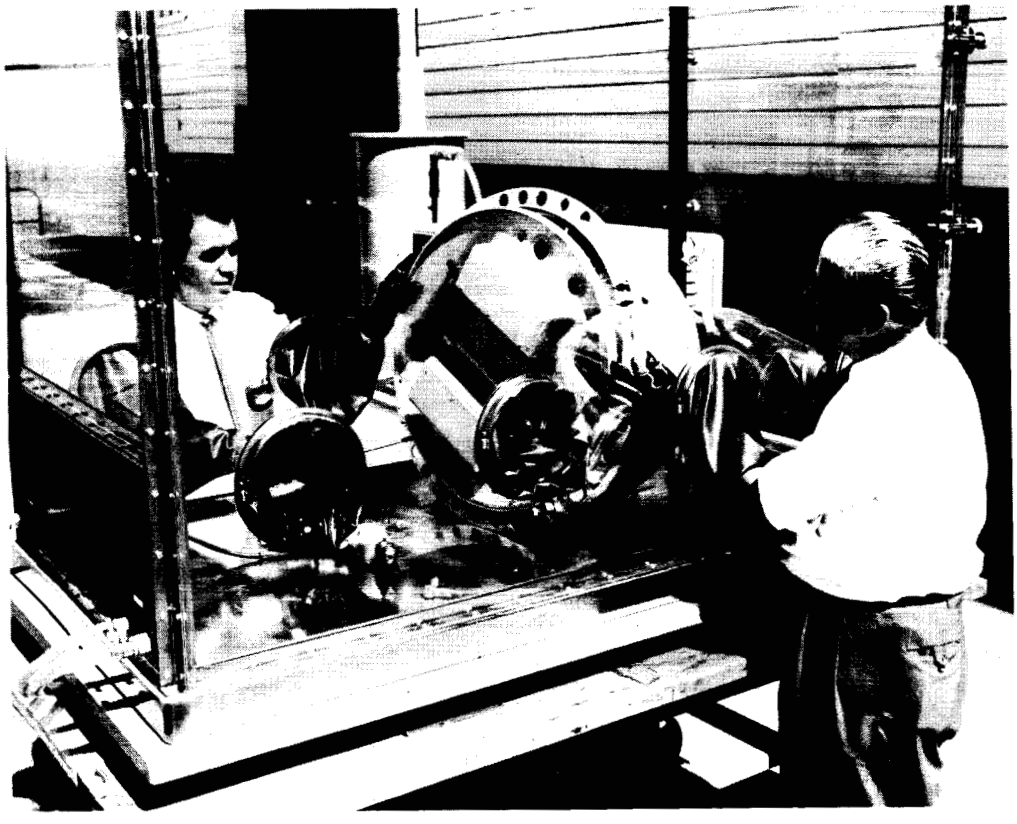

FIGURE 6 ASEPTIC ASSEMBLY OPERATION

This page is reproduced again at the back of this report by a different reproduction method so as to furnish the best possible detail to the user.

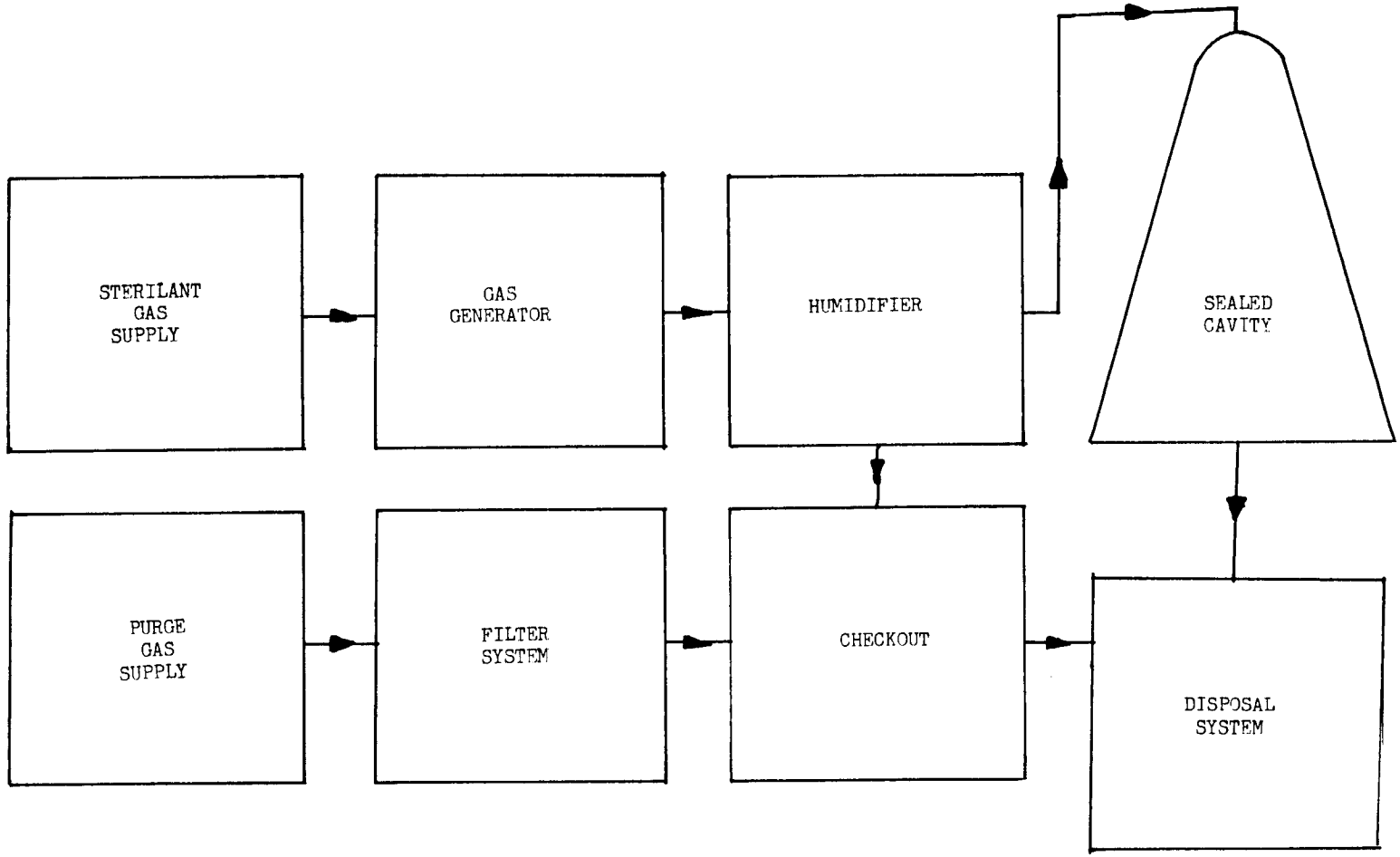

FIGURE 7 - FLOW DIAGRAM FOR
TERMINAL GASEOUS STERILIZATION

FIGURE 8 RANGER MOBILE STERILIZATION GAS TRANSFER SYSTEM

TERMINAL STERILIZATION OPERATION

PROJECT SURVEYOR

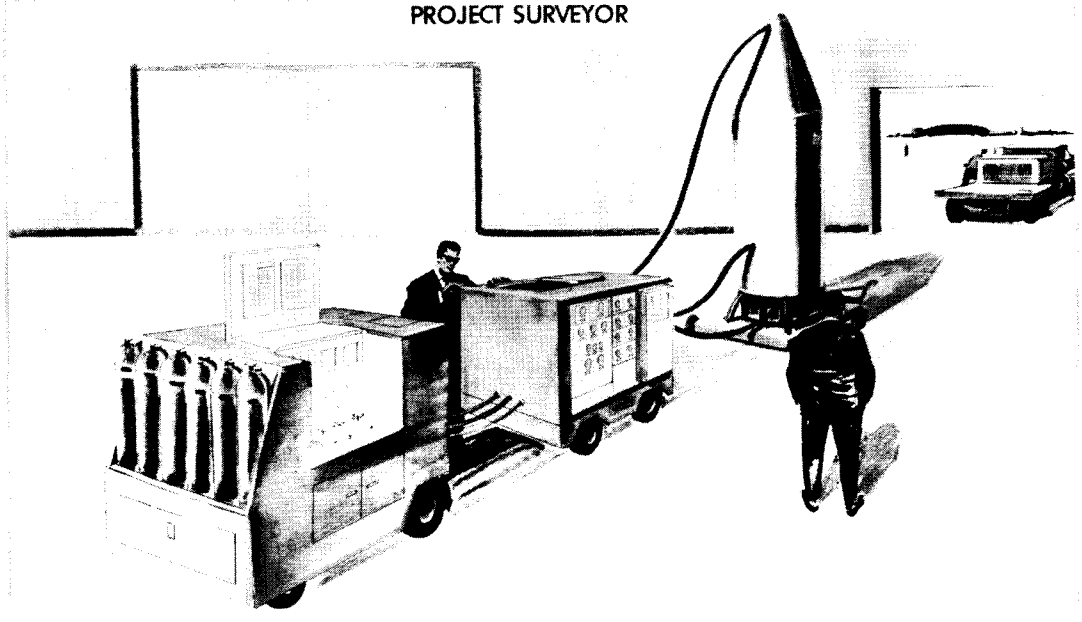

FIGURE 9 SURVEYOR-TYPE TERMINAL STERILIZATION OPERATION

This page is reproduced again at the back of this report by a different reproduction method so as to furnish the best possible detail to the user.

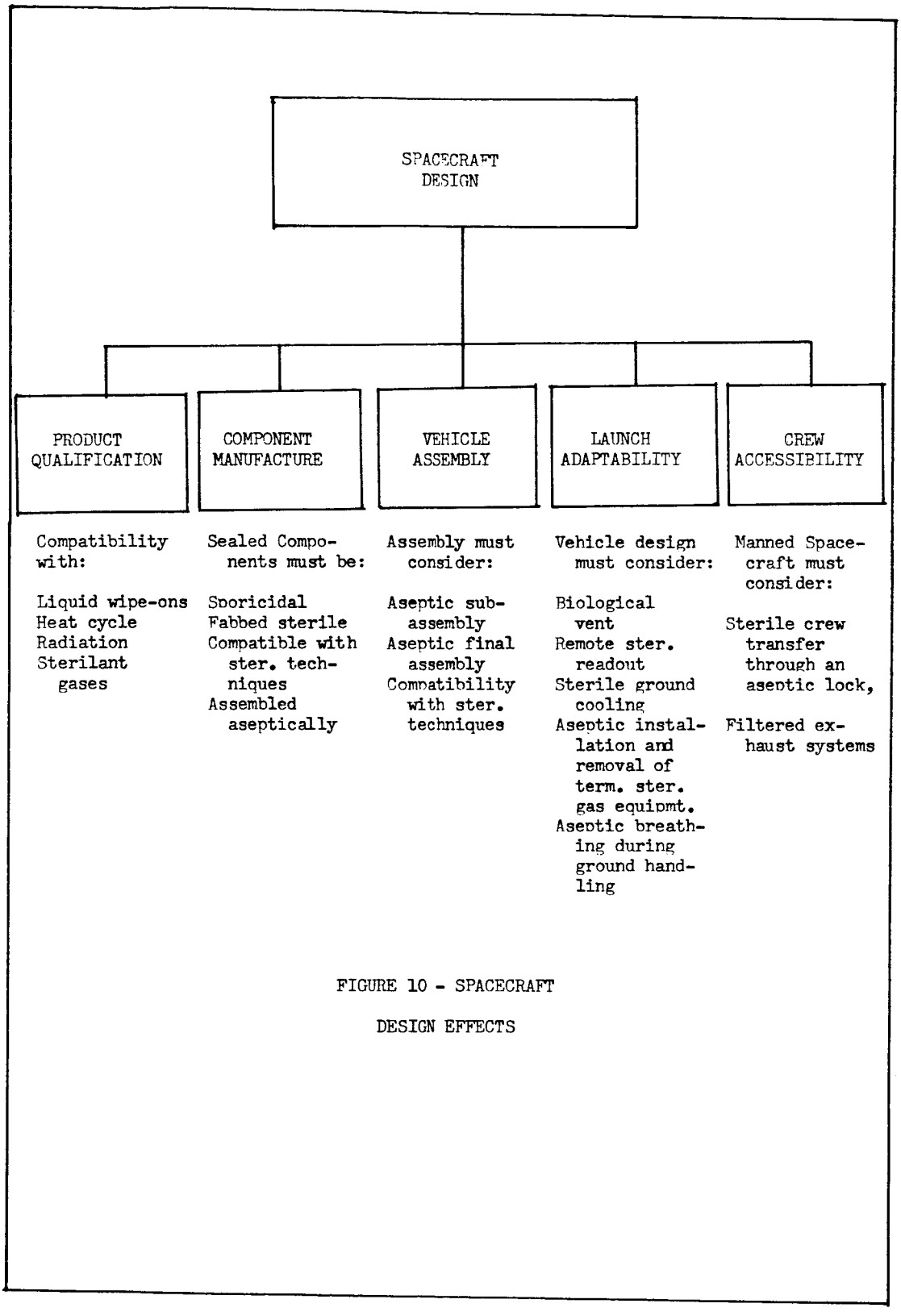

FIGURE 10 - SPACECRAFT

DESIGN EFFECTS

FILTER PORE SIZE REQUIREMENTS

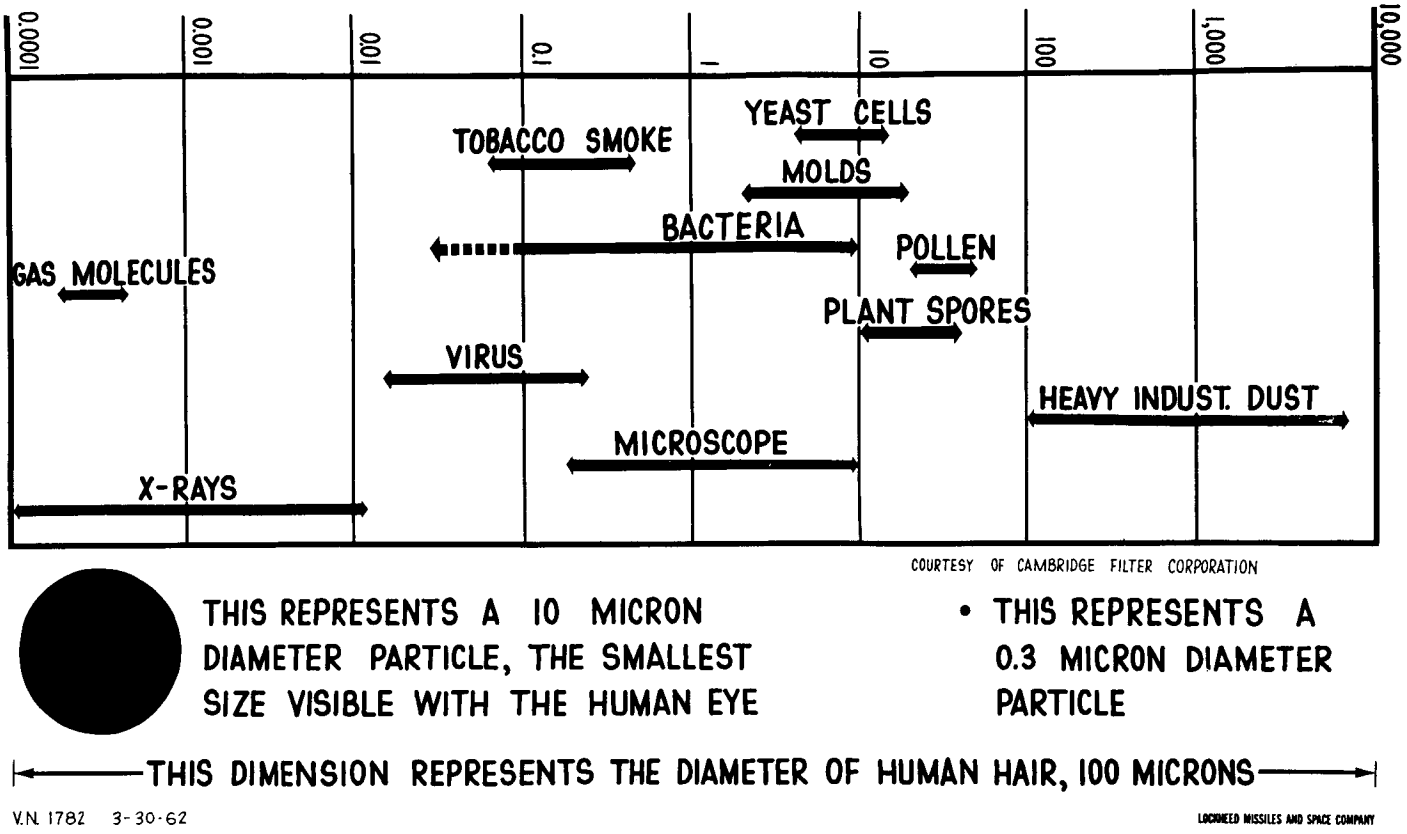

FIGURE 11 FILTER PORE SIZE REQUIREMENTS

STERILIZATION RELATIONSHIP

TO

MANNED SPACEFLIGHT

1. Same General Requirements as Unmanned
2. Compatibility of Space Suits
3. Sterile Transfer of Personnel
4. Quarantine Orbit
5. Aseptic Retrieval

FIGURE 12

MANNED RELATIONSHIPS

LIQUID PROPELLANT LAUNCH VEHICLES FOR MANNED SPACE FLIGHT

by

Wilson B. Schramm
Chief, Advanced Flight Systems Branch
Propulsion and Vehicle Engineering Division
National Aeronautics and Space Administration
George C. Marshall Space Flight Center

Introduction

Launch vehicle technology has probably been the most controversial aspect of the manned space flight program as it has developed during the past twelve months. This paper is a hopefully concise exposition of the present lunar flight system concept, and necessarily represents the concerted efforts of numerous individuals within government and industry who are engaged in the Apollo/Saturn program, and whose substantial contributions must be acknowledged at the outset.

In the midst of confusing and complex issues, we have seen through the year 1961 a period of resolution, reassessment and realignment of the national goals in space flight. This has been a period of great expectations, great impatience, intense debate, and concentrated technical effort. The decisions that have been made are emerging in broad outline in the contract structure. It is my purpose here to provide some insight into the assessment and decision phase that has led to our present position and course of action.

From the many conceivable lunar mission profiles, NASA has selected the rendezvous approach for the early Apollo manned lunar flights, based on the Saturn C-5 launch vehicle. Evaluation and selection of flight systems for lunar missions have proved a most intricate and demanding task. That which is technically feasible is not necessarily desirable in the broader sense of achieving a national objective. One must move far afield in systems engineering and operations research to associate mission concepts with the means of accomplishment for specific tasks within a given time frame. Selection of the present mode has been made in full recognition that we are stuck with these basic decisions for many years to come.

Lunar Flight Systems

The C-5 rendezvous approach for early manned lunar missions was identified and selected during the course of a series of in-house NASA studies that culminated in the recent NASA-DOD Golovin Committee. This concept has withstood the rigors of many months of critical examination. Although it has only recently been revealed as an integrated flight system, the various concepts consolidated in this plan existed in 1960, and in prior years.

Eventual full development of manned space flight requires a broad spectrum of mission capabilities extending from early spacecraft qualification flights in earth orbit through lunar logistics and planetary exploration. The principal flight systems considered for the lunar mission are indicated in FIG 1, along with mission phases.

Launch vehicles in three principal performance classes are required in sequence. The Saturn C-1 is aimed at a growth capability of 25,000 lb in earth orbit. The initial concept and objective of the booster was to demonstrate operational feasibility of clustered engine systems, to which has been added the development of large hydrogen-oxygen upper stage technology. Its principal mission in the manned space flight program is to develop the Apollo spacecraft. The second and larger vehicle, Saturn C-5, is aimed at initial manned lunar landing capability. The projected lunar orbit rendezvous mode provides approximately 90,000 lb to lunar transfer injection. The earth orbit rendezvous mode provides 400,000 lb assembled in earth orbit with a capability to inject approximately 150,000 lb to lunar transfer. The Saturn C-5 launch vehicle is utilized in qualification of the entire Apollo flight system, projected unmanned lunar logistics support, development of earth orbital operations technology, development of advanced nuclear propulsion technology, and the Apollo manned lunar circumnavigation and initial manned lunar landing. The Nova is generally conceived to be a direct mode vehicle, having a 400,000-lb earth orbit capability and a 150,000-lb injection capability to lunar transfer. Its applications include the Apollo lunar exploration phases following initial lunar landings, manned lunar logistics support of the lunar base, and development and application of both rendezvous and nuclear propulsion technology for initial planetary exploration.

In outlining such a program it is only natural to place reliance on the most accessible technology. Basic elements more or less in hand at the outset of this evaluation, which began in earnest one year ago, included the basic Saturn launch vehicle technology as we know it today, a substantial investment in the F-1 engine development, and a substantial investment in hydrogen-oxygen upper stage technology with the Centaur, the RL-10 engine, the Douglas S-IV stage, and the J-2 propulsion system development. At each step in the decision-making process, we have moved forward from an established position in launch vehicle technology.

To place events in perspective, consider the status of the national large launch vehicle program one year ago. FIG 2 shows the original Saturn building block concept in which the S-IV stage of C-1 moves to the third stage of C-2 and a new large hydrogen-oxygen stage known as S-II, powered by the J-2 propulsion system, is brought in to achieve maximum utilization of the 1.5 M lb thrust S-I stage. Indicated orbital capabilities for these systems were in the range of 20,000 lb for C-1 and 45,000 lb for C-2. The proposed prime mission for C-2 at this time was manned lunar circumnavigation with a forerunner of the Apollo spacecraft.

As illustrated in FIG 3, detailed conceptual design of the S-II stage was well underway with a 260-inch diameter and a propellant load of approximately 330,000 lb. Concurrently, the J-2 propulsion system was being developed, specifically

tailored to this stage concept.

Moving out from this base line into an evaluation of the lunar program, investigation of many alternate proposals in this performance class has shown conclusively that no newly conceived launch vehicle system would likely become available at a more rapid pace. The Saturn C-1 booster, as presently conceived, has moved on into the flight test phase. FIG 4 graphically depicts SA-1 at the instant of lift-off in its successful first-stage test flight in October 1961. The Saturn C-1, in its growth versions, is well on the way to becoming the "DC-3" of manned earth orbital space flight.

Evaluations of the lunar flight systems summarized in FIG 1 have indicated certain general fundamentals. It is clear that substantially larger flight systems are necessary; it is also substantially true that we cannot reach the moon without mastering liquid-hydrogen technology, regardless of booster configuration. This technology paces the program, and is in fact an awesome development as those familiar with it can readily testify.

Prime Approach

A very broad range of possibilities has been suggested for launch vehicle configurations to accomplish manned lunar missions. In establishing the present concept, all facets of advanced propulsion technology have been examined. The booster stage investigations range from all-liquid systems, through hybrid liquid-solid systems, to all-solid systems. Myriad combinations of high-energy upper stage systems have been utilized, each matched in its performance class to specific booster stages and mission profiles.

A starting point for establishing the concept is the projection of mission profiles such as lunar and earth orbit rendezvous, and the direct profile. Mission development projection establishes performance requirements, and determines the essential tasks for each mode and the flight sequence and number of flights to qualification. Conceptual design of approximately 50 launch vehicle systems was undertaken to match the performance requirements. The launch vehicle development projection then determines the flight sequence and number of flights for stage and vehicle systems qualification. The full mission model is then employed to integrate mission and vehicle qualification programs, to develop a master flight plan for each specific launch vehicle configuration, in which the expected flight history is projected on the basis of detailed failure modes analysis of the primary propulsion and related vehicle subsystems. With detailed PERT networks, operations analysis can proceed, incorporating manufacturing and test facilities, logistics, funding, schedules for engine stage and vehicle development, to assess the total system cost and capability on an operational basis in achieving the mission objective. Following initial screening of likely prospects, the assessment is recycled in greater depth in all areas of detailed preliminary design in the launch vehicle, and its primary subsystems, to establish technical feasibility and performance capability. In conjunction with operations analysis, the expected probability of mission success must be substantiated within expected funding levels and within the specified time frame. In successive iterations we move from the feasible to the desirable.

Many novel proposals offered to accomplish early manned lunar missions have not withstood critical examination. In development of the broad outline for projected lunar flight systems the contention is not primarily among launch vehicle concepts; it is between Nova class direct flight and C-5 class rendezvous modes. Studies indicate that whether we use liquid or solid booster stages is a relatively minor factor in achieving the desired performance capabilities. The large solid booster concept has been amply tested, and upon the most careful projections appears deficient as a prime approach. Its main attractiveness is contingent upon adoption of Nova concepts. If solid motor development and facilities concepts are aimed at growth capability for Nova class vehicles, the projected schedules for motor development and stage and vehicle integration become incompatible with lunar mission objectives in a C-5 class vehicle.

The Nova concept itself has also been amply tested. It has long been recognized that it is only the logistic support of a permanent manned lunar base, coupled with manned planetary exploration, that demands a booster of this capability. Only in view of a multibillion dollar national commitment for such a sustained and ambitious level of manned space flight activity does a decision to undertake Nova class booster development early make sense.

With rendezvous, the Saturn C-5 is large enough to do the initial mission; with all factors considered, it potentially provides the capability for the earliest manned lunar circumnavigation and manned lunar landing. The major advances in technology required for this concept are the development of hydrogen-oxygen systems and rendezvous techniques. This conclusion represents the end product of thousands of man-hours of homework and the integrated technical judgment of hundreds of individuals. Confidence in the validity of this approach is high.

The conceptual phases of the assessment and decision tasks have been concluded and implementation of the lunar flight program is well advanced, as indicated by the commitments represented in FIG 5. The Apollo spacecraft system is being developed by North American Aviation. The Saturn C-1, S-I stage is being developed by Chrysler Corporation Missile Division, and the S-IV stage by Douglas Aircraft Company. The Saturn C-5 is being designed and developed with Boeing on the S-IC stage, North American on the S-II stage, and Douglas on the S-IVB stage which also has application into Saturn C-1. The C-5 S-IC stage major assemblies will be fabricated at the newly acquired plant in Michoud, Louisiana; the S-II stage will be fabricated at Seal Beach; and the S-IV and S-IVB stages will be fabricated at contractor facilities on the West Coast. C-5 stages will be tested at MSFC, during the early phases of the program, and later at the newly acquired Mississippi Test Facility. The entire launch vehicle system will be flown from Cape Canaveral out of a newly acquired 80,000-acre site now being developed.

Evolution Of C-5 Concepts

Exposition of lunar mission profiles with the Saturn/Apollo flight system has been ably set forth in many previous papers and recent publications. The review of rendezvous modes herein is limited to those aspects of the flight system that reflect directly in launch vehicle systems engineering, which is approximately to the point of lunar transfer injection.

The present Saturn C-5 launch vehicle concept evolved in detail from conceptual design studies of the earlier Saturn C-4. Just as the Saturn C-1 program started with a well established H-1 engine program, the advanced Saturn concept starts with the F-1 engine depicted in FIG 6. This F-1 engine is expected to approximately equal in thrust the combined output of the eight H-1 engines of the present Saturn C-1 booster. Conceptual designs of a four-F-1 engine booster began at MSFC late in 1960, utilizing an expanded version of the four-J-2 engine S-II stage already in detailed preliminary design for the earlier C-2. This configuration was affectionally known as "Nova Junior" at the time, and evolved into the Saturn C-5 concept, shown in FIG 7, concurrently with the development of rendezvous concepts for the manned lunar mission.

It is important to note that this launch vehicle configuration is not optimized for a specific application. Rather it represents a careful balance of design choice decisions aimed at preserving mission flexibility throughout the range of applications in the rendezvous modes.

Rendezvous is largely a matter of staging technique and logistics in its effects on launch vehicle size and development phasing relative to the mission profile. The Saturn C-5 is capable of two general mission profiles based on rendezvous in lunar orbit and rendezvous in earth orbit. In earth orbit mode (EOR), rendezvous defers the commitment of men until flight readiness in orbit is verified; thus it is essentially a fail-safe technique. In lunar orbit mode (LOR) man is committed prior to rendezvous; thus a relatively higher degree of exposure is anticipated.

Rendezvous in earth orbit comes at a price in cost, complexity, and performance capability of the total launch vehicle system. A rather trite but fundamental equation can be stated as follows: 2 X C-5 is not equal to Nova. Depreciation to approximately 80 per cent of combined vehicle escape capability of 2 X C-5 results from the orbital mechanics and weight budgets associated with EOR.

In a very crude illustration, the logistics of earth orbit rendezvous can be summarized as follows: a plush manned lunar mission can be provided with a flight system based on ten F-1 engines. Now, this capability can be cut in a number of ways: one flight with ten F-1's (a Nova class vehicle), two flights with five F-1's, or five flights with two F-1's. Performance and cost optimization indicate the optimum solution to be two flights with five F-1's.

As it is presently conceived, the C-5 flight system has a flexible capability for lunar transfer injection payloads ranging from 90 to 150,000 lb, depending on the mode selected, and the time phasing in which the mission capability is required.

Two operating modes utilizing earth orbital operations with the Saturn C-5 are illustrated in FIG 8. In the tanking mode the tanker is parked in orbit with the full load of oxygen required for the orbital departure stage. The R-1 and R-2 stages plus the Apollo spacecraft system are mated and checked out on the ground, and launched as an integral unit by the second Saturn C-5 to the high departure orbit illustrated in FIG 9. Economics of the weight budget are such that the tanker represents a full load for one C-5, and the orbit launch vehicle with its LOX tank empty represents a full load for the second C-5. Following transfer of LOX from the tanker to the escape stage of the orbit launch vehicle, separation occurs at the designated station (FIG 8) in which case all equipment associated with rendezvous and propellant transfer are left behind in orbit. This arrangement has the obvious advantages of permitting staging to occur at lunar transfer injection so that the R-2 lunar braking and landing stage remains sealed until the lunar braking phase is initiated. This arrangement also provides the minimum orbital staytime for liquid hydrogen in the R-1 stage, and permits flexibility in loading because the liquid oxygen is most easily ballasted across the docking interface to equalize the launch load place on the two C-5 vehicles.

In the connecting mode, also illustrated in FIG 8, similar maneuvers are executed with the R-1 escape stage injected to orbit fully fueled. However, the staging ratio of the lunar transfer injection stage and the lunar braking and landing stage cannot be maintained as favorably. The injection maneuver has the disadvantage that the parasitic weight of the docking structure and auxiliary maneuvering propulsion systems must be carried part way to the transfer velocity, and the larger R-2 stage must provide a portion of the initial transfer injection. This stage thus arrives at the lunar braking maneuver with partially expended tanks and a used propulsion system having unpredictable leakage. In this mode an additional restart of the propulsion system is required on the braking and terminal stage, and the expected reliability deteriorates. Our present attention is focused on the tanking mode. The C-5 launch vehicle configurations employed in the tanking mode are illustrated in FIG 10. The C-5 launch vehicle configuration utilized here as a two-stage orbital carrier has an approximately equal payload for the unmanned first launch and the manned second launch.

As mentioned previously, the Saturn C-5 launch vehicle system is not an optimized system. The S-IC and S-II stages are basically designed for maximum orbital capability without sacrifice of the many other requirements placed on the design. Propellant optimization of the S-II stage is a compromise between the full five-engine burning case and the engine-out optimization. In the three-stage-escape configuration illustrated in FIG 7, design studies were undertaken specifically to assess constraints and compromises in stage configuration and vehicle performance associated with application of the "building block" S-IVB stage, which is utilized as an escape stage on C-5, an orbit launch stage for the tanking mode, and as a

second stage of the C-1 launch vehicle system. In all cases, designs were made for the maximum flight loads encountered in the limit loads case, e.g., the S-IVB when flown on Saturn C-1 is designed structurally to accommodate the three-stage-escape trajectory flight loads in the C-5 application. The S-II tankage is sized for the two-stage-orbit mission, and designed structurally for a three-stage-escape mission which imposes the highest aerodynamic and structural loads. The S-IC stage is designed substantially by ground windload and longitudinal accelerations, including the rebound dynamic loads in the tail section associated with approximately a three-second holddown during the F-1 engine ignition period. Alternate missions with the Saturn C-5 are flown off-loaded as required, with consequent performance deterioration. But with careful design choices, payload penalties can be limited to about one to three thousand lb in escape missions, which is acceptable in the interest of retaining mission flexibility without altering the basic stage geometries.

To summarize the C-5 applications, this launch vehicle is conceived as a flexible system to accomplish, in a two-stage orbit configuration, either of the earth orbit rendezvous modes illustrated; or in a three-stage escape configuration to accommodate the manned lunar orbit rendezvous mode as well as direct lunar logistics support; or in a two-stage escape configuration to accommodate the early Apollo lunar circumnavigation flights; or as a two-stage booster, to accommodate the NERVA nuclear third stage for escape missions; and to provide in the S-IVB a "building block" upper stage for the present Saturn S-I in the C-1 program.

To complete the picture of the Saturn C-5 as a basic launch vehicle, the booster stage, shown in FIG 11, will be approximately 140 feet long, 33 feet in diameter, and powered by five F-1 engines, using liquid oxygen and RP-1 fuel as propellants to deliver a sea level thrust of about 7,500,000 lb. The propellant containers will have a combined capacity of about 4,600,000 lb.

The basic propellant container design will feature a cylindrical structure that has separate bulkheads for the propellant containers, with the liquid oxygen tank forward and the RP-1 tank aft. Each container will have slosh suppression devices. The launcher holddown loads are distributed to the thrust structure by the launcher, or holddown, posts. Thrust loads introduced by the center engine are carried out to the ring frame of the thrust structure by a crossbeam system.

The four outboard engines are to be mounted on a diameter of 364 inches with an aerodynamic fairing located over each. Thrust loads are sheared out by four vertical posts over the engines. A separate liquid oxygen suction line, connecting each engine to the liquid oxygen container, will run through insulated tunnels in the fuel container. Two fuel suction lines connect each engine to the fuel container. Fuel container pressurization will be accomplished with helium. Gaseous oxygen generated in the engine mounted heat exchangers may be used for pressurizing the liquid oxygen tank; however, this scheme may be replaced by a helium system similar to that used by the fuel tanks, if weight and reliability advantages are realized. Engine gimbaling for flight control is accomplished by double-acting piston gimbal actuators using the RP-1 fuel, bled from the high pressure propellant feed system, as the hydraulic fluid. A staggered engine start and shutdown sequence is to be used.

The S-II stage, illustrated in FIG 12, will be approximately 80 feet long, 33 feet in diameter, and equipped with five J-2 rocket engines that operate on liquid oxygen and liquid hydrogen. The five engines will develop a total thrust of about 1,000,000 lb. Four of the engines will be mounted on a diameter of 210 inches, with the fifth engine mounted in the center of the conical thrust structure. The propellant containers will be designed for a capacity of about 900,000 lb.

The basic propellant tank structure is of a conventional semimonocoque design with a common, insulated, double walled bulkhead separating the liquid oxygen container from the liquid hydrogen container. The liquid hydrogen, as shown, is to be located above the liquid oxygen.

Control of the S-II stage will be achieved by gimbaling the four outboard engines. The center engine will be fixed. All five engines will be aligned parallel to the centerline of the vehicle.

The S-IVB stage employs similar technology to the S-II except for certain accommodations for adaptation to orbital launch operations. The propellant container design will be cylindrical with a diameter of 220 inches, with propellant capacity of approximately 230,000 lb. As in the S-II stage, a common insulated, double walled bulkhead will separate the propellant containers. The liquid hydrogen is above the liquid oxygen. This stage is conceived to be equipped with a single J-2 engine.

Operational Considerations

Returning again to the broad outline of projected lunar flight systems summarized in FIG 1, it has been shown that the principal dependence for the early manned lunar landing attempts is placed on the Saturn C-5/Apollo system. It appears likely that there will be substantial pressure to fly operationally early in the vehicle R&D program, which places a premium on the initial reliability growth history rather than the inherent or operational probability of mission success. The launched cost of these very large systems is indeed substantial and it is obvious that opportunities to fly will necessarily be limited by the available dollars, facilities, and launch crews. Also as vehicle capability moves into the 100-ton range, it is obvious that the investment committed in spacecraft systems and upper stages with each launch is tremendous even when a substantial portion of this weight is represented by propellants available in orbit.

The desire for high probability of mission success is evident. Very general statements have been made to the effect that "new design philosophy" must be adopted to achieve an order of magnitude increase in stage and subsystems reliability. Realistically, we are stuck with the technology rather as it exists today. The basic items of propulsion, structure and flight control that will be utilized in the first manned lunar

landing attempt are in hand. Figuratively speaking, the keel has been laid. In the area of propulsion, H-1 engine experience can be extrapolated but it is doubtful that this much experience can be gained on F-1 and J-2 engines prior to the point of commitment. Major portions of the engine system hardware, such as the F-1 prevalves, are being exercised on the test stands today, and vital items of this nature are not going to look much different when the C-5 first flies.

The flight history of past programs based on ballistic missile practice is hopefully not typical of expectations for the man-rated advanced flight systems utilized in the lunar landing program. Recent experience with Minuteman, Titan II, and Saturn C-1 offers encouragement that technology is improving more rapidly than the complexity of the flight systems. Holding on to these gains necessitates a rather conservative design philosophy for manned flight systems, leading hopefully to an inherently high tolerance for malfunctions, and a high confidence of early success. It is felt that the present Saturn C-5 concept represents a very substantial advance in launch vehicle technology that will stretch both our capabilities and our courage to accomplish. To place this development in perspective, FIG 13 presents a comparison of the present state-of-the-art in Mercury-Atlas with projections for Apollo flight systems. The intermediate launch vehicle is the Saturn C-1 configuration utilized for the Apollo earth orbital spacecraft qualification. The large model represents our present concept of the Saturn C-5. It appears that a substantial task lies ahead to achieve manned lunar landing within this decade.

LUNAR FLIGHT SYSTEMS

FIGURE 1

SATURN C-1

- EARTH ORBITAL LOGISTICS - GROWTH TO 25,000 POUNDS
- OPERATIONAL FEASIBILITY OF CLUSTERED ENGINE SYSTEMS
- DEVELOPMENT OF HYDROGEN OXYGEN STAGE TECHNOLOGY
- APOLLO EARTH ORBITAL SPACECRAFT QUALIFICATION FLIGHTS

SATURN C-5

- LOR MODE - 90,000 POUNDS TO LUNAR TRANSFER
- EOR MODE - 400,000 POUNDS ASSEMBLED IN EARTH ORBIT - 150,000 POUNDS TO LUNAR TRANSFER
- APOLLO FLIGHT SYSTEMS QUALIFICATION
- UNMANNED LUNAR LOGISTIC SUPPORT
- DEVELOPMENT OF ORBITAL OPERATIONS TECHNOLOGY
- DEVELOPMENT OF ADVANCED NUCLEAR PROPULSION TECHNOLOGY
- MANNED LUNAR CIRCUMNAVIGATION AND INITIAL MANNED LUNAR LANDING

NOVA

- DIRECT MODE - 400,000 POUNDS IN EARTH ORBIT - 150,000 POUNDS TO LUNAR TRANSFER
- APOLLO LUNAR EXPLORATION
- MANNED LUNAR LOGISTIC SUPPORT - LUNAR BASE
- DEVELOPMENT OF RENDEZVOUS AND NUCLEAR PROPULSION - PLANETARY EXPLORATION

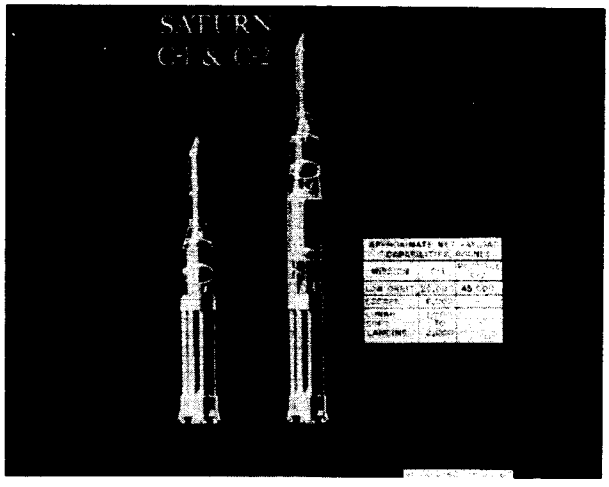

FIGURE 2

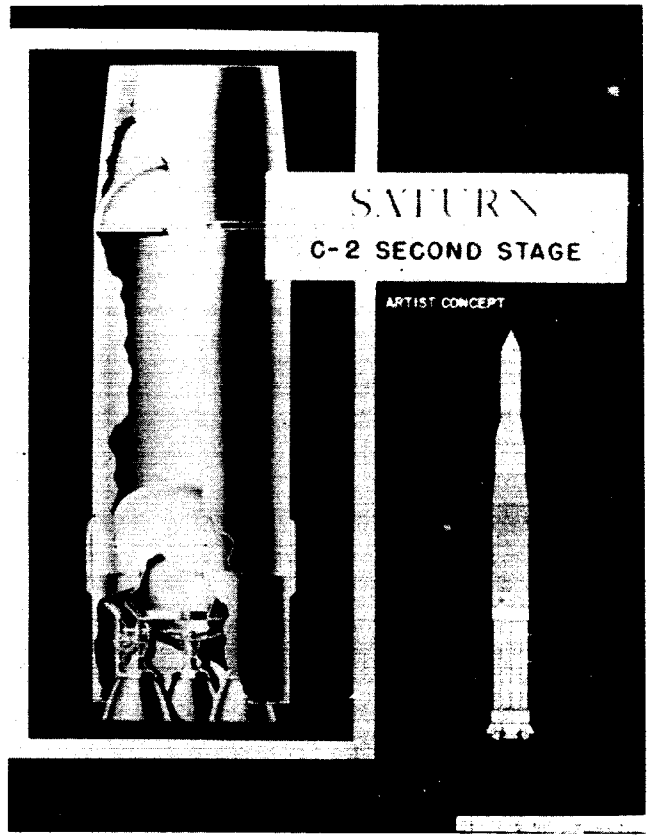

FIGURE 3

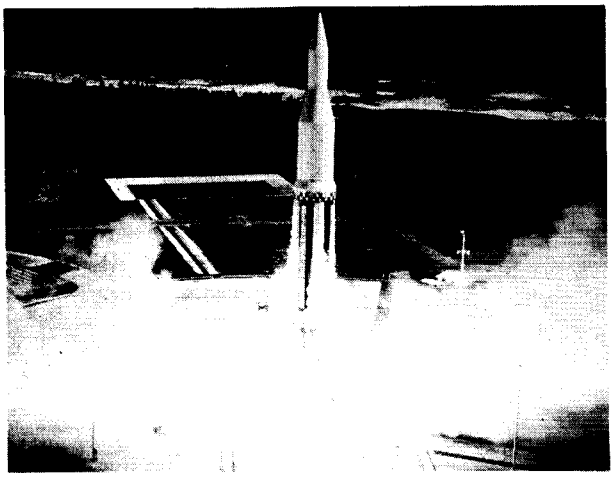

FIGURE 4 SA-1 AT INSTANT OF LIFT-OFF

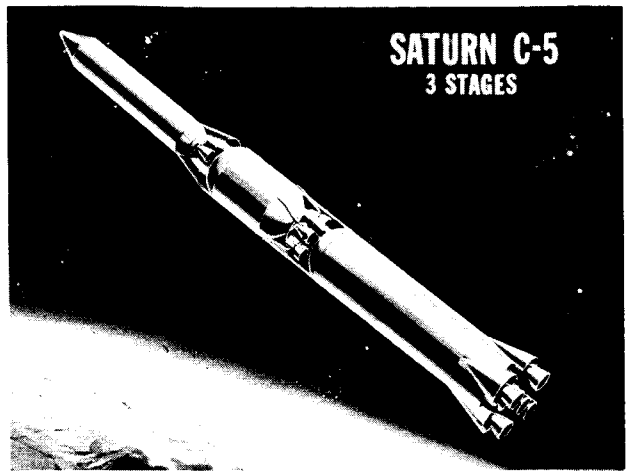

FIGURE 7

FLIGHT SYSTEMS
IMPLEMENTATION

- SPACECRAFT SYSTEMS
  APOLLO - NORTH AMERICAN
  GEMINI - McDONNELL
- BASIC PROPULSION
  H-1 F-1 J-2 ROCKETDYNE
  RL10 PRATT AND WHITNEY
- LAUNCH VEHICLE SYSTEMS

SATURN C-1

S-I STAGE DEVELOPMENT - CHRYSLER/MSFC
S-IV STAGE DEVELOPMENT - DOUGLAS

SATURN C-5

DESIGNED AND DEVELOPED

S-IC STAGE - BOEING
S-II STAGE - NORTH AMERICAN
S-IVB STAGE - DOUGLAS

FABRICATED
MICHOUD
SEAL BEACH
WEST COAST FACILITIES

TESTED
MSFC
MISSISSIPPI TEST FACILITY
WEST COAST FACILITIES

LAUNCHED
AMR - CAPE CANAVERAL
80,000 ACRES

M-1 ENGINE - AEROJET

FIGURE 5

ORBITAL LAUNCH VEHICLES // MODE COMPARISON

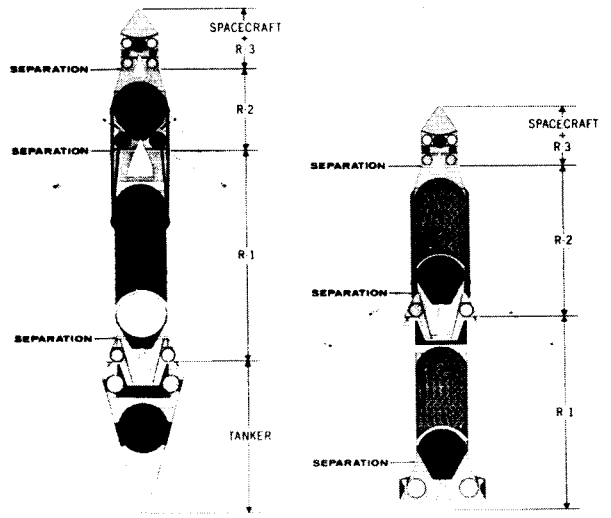

TANKING MODE CONNECTING MODE

FIGURE 8

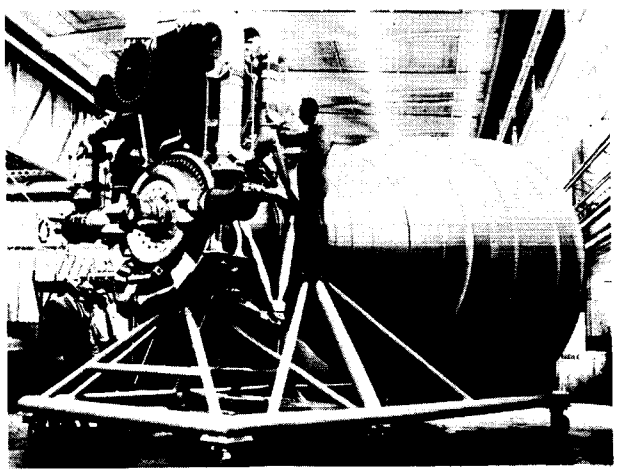

FIGURE 6 F-1 ENGINE

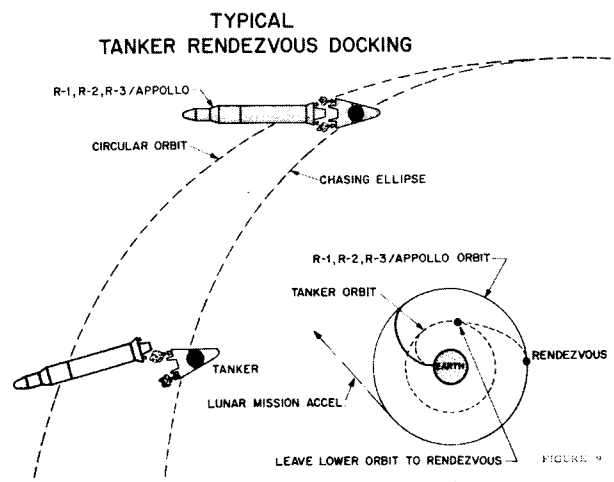

FIGURE 9

This page is reproduced again at the back of this report by a different reproduction method so as to furnish the best possible detail to the user.

This page is reproduced again at the back of this report by a different reproduction method so as to furnish the best possible detail to the user.

(TYPICAL) C-5 FOR ORBITAL OPERATIONS
TANKING MODE

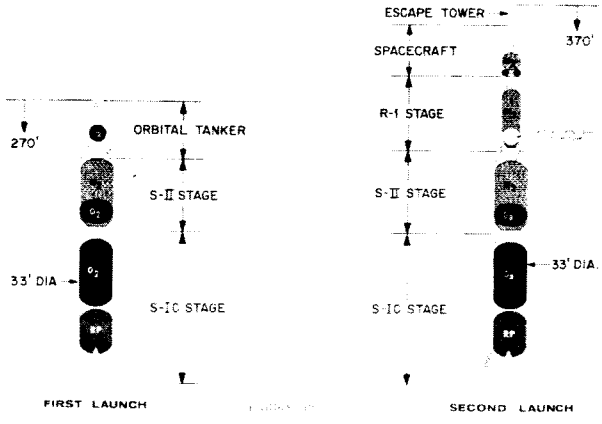

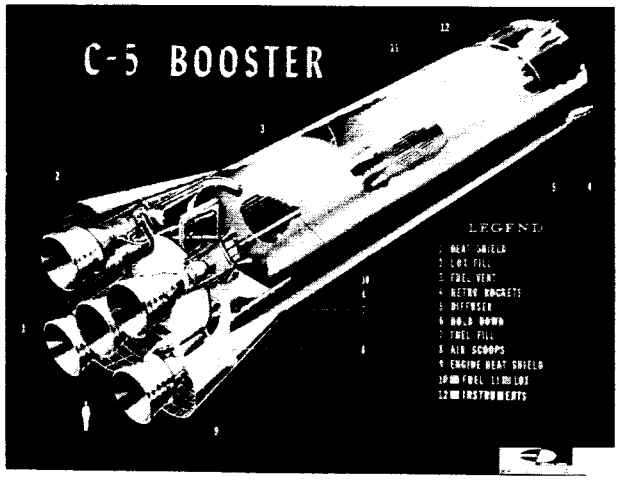

FIGURE 11

S-II STAGE

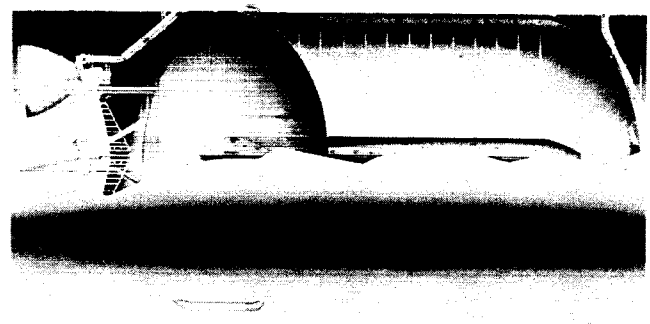

FIGURE 12

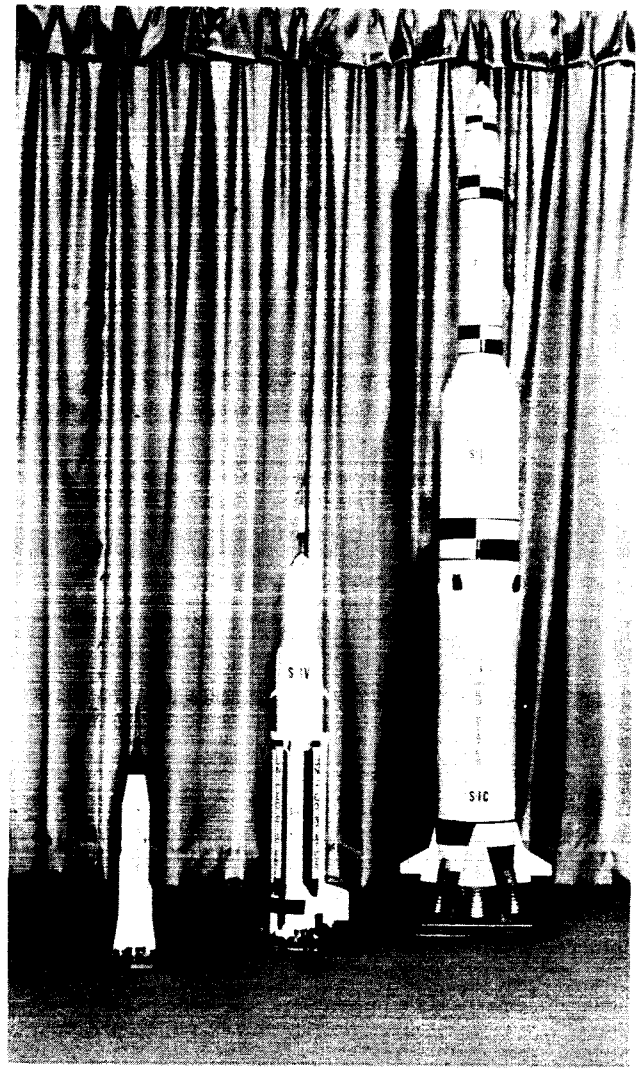

FIGURE 13 COMPARISON OF THE PRESENT STATE-OF-THE-ART IN MERCURY-ATLAS

SOLID PROPELLANT BOOSTERS FOR MANNED SPACE FLIGHT

Colonel Langdon F. Ayres
Director, Large Solid Motor Program
Space Systems Division
Air Force Systems Command

Introduction

Within the past year, large solid propellant rocket motors have become very prominent in discussions of possible launch vehicles for manned space flight. This is partly due to active promotion by the solid propellant rocket industry. The role that large solid rockets may play in space launching vehicles is also indicated, however, by the results of numerous analyses and vehicle studies that have been made in the past two years by government and other unbiased agencies. The promise of the large solid rocket motor has been further substantiated by major development accomplishments which have been achieved in the past year.

The purpose of this paper is to review some of the reasons for the dramatic entry of large solid propellant boosters into the manned space flight field, to assess their present position, and to discuss some areas where need for further work is indicated.

It is an historical fact that in many engineering developments all of the basic technology on which a development rested was available for a considerable time before recognition of both capability and need stimulated the development of useful products. A comprehensive study has been made of the circumstances wherein turbojet engine development occurred simultaneously (and independently) in both England and Germany in the early part of World War II but not in the United States[1]. The necessary state-of-the-art in metallurgy, fluid mechanics, and machine design seems to have been present about equally in all three countries. There are numerous other developments, on the other hand, where the desirability of creating something could be fairly well established on the basis of induction from theoretical principles, but a breakthrough was required in some branch of technology before the dream could become a practical reality. The idea of using nuclear rocket propulsion for large space vehicles has probably received serious study for a longer period than large solid rockets have, but the road ahead for the nuclear rocket is still long and arduous. With these thoughts in mind, it is interesting to regard the situation in the large solid propellant rocket and space launch vehicle fields in the recent past.

General Characteristics of Solid Rockets As They Relate To Space Launch Vehicle Requirements

The purpose of the primary propulsion system in any launching vehicle stage is to impart a velocity gain to the vehicle. Therefore, the relative merits of propulsion systems are usually judged on the basis of minimizing vehicle gross weight or cost for a given velocity increment. Other factors including reliability, safety and servicing requirements may be considered in the selection. Finally, the flexibility of design afforded by a particular type of propulsion system may influence its selection. For example, constraints on the vehicle flight path such as maximum acceleration and dynamic pressure may be more compatible with one type of propulsion system than another.

Consider first the ability of a propulsion system to impart velocity. The magnitude of this velocity gain for a simplified vertical trajectory (neglecting atmospheric drag) is given by the following equation:

$$V_f = g_e \, I_{sp} \ln \left[\frac{1}{1 - \lambda_p} \right] - \bar{g} t_b$$

where

g_e - gravitational acceleration at earth's surface. (ft/sec^2)

$\bar{g}$ - gravitational acceleration averaged over powered trajectory. (ft/sec^2)

I_{sp} - specific impulse $\left(\frac{lbf - sec}{lbm}\right)$

λ_p - propellant mass fraction

t_b - time of burning (sec)

It is obvious that specific impulse and mass fraction are of direct concern. The history of the improvement of specific impulse of solid propellants is shown in Figure 1. Steady improvements have been made with the development of more energetic fuel binders. Improvements in fuel binder physical properties have also made higher oxidizer content and more nearly stoichiometric oxidizer to fuel mixture ratios practical. The largest single increase in I_{sp} of solid propellants in recent years, however, has come about through the introduction of the aluminized propellants about 1955. Presently available, well proven propellants deliver approximately 245 sec I_{sp} at standard conditions of comparison (1000 psi. p_c expanded to S.L. pressure). When operated at chamber pressures optimized for overall system design and with nozzle expansion ratios likewise near optimum from a system design standpoint, delivered I_{sp} of 230 sec. at sea level and 261 sec. at altitude have been available for several years.

Along with increase in I_{sp} has come a steady improvement in propellant physical properties. Tensile strength of 150 psi. is commonly obtained in propellants of 245 sec. I_{sp} against a value of about 80 to 100 psi. 7 years ago. Even greater improvements have come about in reducing the temperature coefficient of tensile strength.

Elastic modulus has been reduced, and up to 30% elongation is possible over a wide temperature range. Advancements in stress analysis methods and laboratory tests devised to evaluate the most significant physical properties of propellants have given designers the ability to proceed beyond previous limits with greater assurance. A program is now under way to conduct a thermal grain structural analysis for the purpose of determining environmental limitations and modes of failure of large propellant grains. Suitable experiments will be conducted to confirm the theoretical studies and the analysis methods will be reduced to engineering practice.

Considering next the problem of obtaining favorable mass fraction, some significant advancements have been made in recent years in reducing the weight of inert parts. For cases, both steel and fibreglass have afforded about equal gains and remain competitive with titanium also in the picture. When reviewing developments in this field, it is well to keep in mind that for years the primary application of solid propellants was to JATO and armament type rockets, so little stimulus existed to strive for improved mass fraction in large size motors. The solution of other problems such as TVC and thrust termination opened the way to the application of solid rockets to ballistic missiles, creating the immediate need for mass fractions of about 0.86 or better. This need was met satisfactorily in a variety of ways. In the Minuteman program, the Stage I engine has a case fabricated from ring forged and machined components of D 6 AC alloy (without longitudinal welds) treated to an ultimate tensile strength of 215,000 psi. The second stage engine is now being produced in titanium alloy, 6 Al 4 V. The third stage engine has a fibreglass wrapped case. Case designs do not tell the whole story, of course, as the four movable nozzles, thrust termination devices, etc., are also involved on Minuteman. For certain final stage applications, very efficient rocket and case designs have been produced having a mass fraction exceeding 0.95. It is thus evident that very favorable mass fractions can be obtained in solid propellant rockets, at least for selected applications. Examination of the possibility of application of large solid motors to space launch vehicles must, therefore, seek to establish what the trend of mass fraction will be as sizes grow larger. Increasing vehicle size generally makes possible more favorable mass fraction in pump fed liquid propellant rocket vehicles.

Consider a solid rocket motor as shown in Figure 2. Assume for the purpose of this analysis that as the size of the motor is varied, the following are held constant: L/D, p_c, case stress level, grain configuration, and web fraction.

$$\text{Mass fraction} = \frac{W_{prop}}{W_{case} + W_{insul} + W_{nozzle} + W_{prop}}$$

To determine the probable influence of size on mass fraction, an approximation of how each of the terms is likely to vary with size can be made:

$W_{prop} = K_1 (D^3)$ under the assumption of constant L/D and web fraction.

Taking into consideration the influence of motor diameter on case wall thickness

$$W_{case} = K_2 (D^3)$$

Since the insulation over most of the inside surface of the case is exposed to the flame only at the moment of propellant burnout, the required thickness can be considered to be relatively independent of size. The weight required will then be a function of the surface area to be protected, or

$$W_{insul} = K_3 (D^2)$$

The area of the nozzle throat must be proportional to the area of propellant burning surface if the assumption of constant p_c is to be maintained. The weight of the structural parts of the nozzle may be expected to vary with diameter in approximately the same manner as the case does. The weight of throat inserts and parts exposed to high temperature gases will be dependent upon the duration of exposure. As will be seen later, the duration is likely to become longer as size increases, so it seems reasonable to assume as a first approximation that the thickness of non-structural heat resistant parts will also vary about as the cube of the diameter.

$$W_{nozzle} = K_4 (D^3)$$

Roughly, then for the assumed relationships

$$\text{Mass fraction} = \frac{K_1 (D^3)}{K_2 (D^3) + K_3 (D^2) + K_4 (D^3) + K_1 (D^3)}$$

$$= \frac{K_1}{K_2 + K_3 \left(\frac{1}{D}\right) + K_4 + K_1}$$

In a typical rocket in the 100-inch class the value of the constants in the above equation are approximately

$$K_1 = 0.190 \text{ lbm/in}^3$$

$$K_2 = 0.015 \text{ lbm/in}^3$$

$$K_3 = 0.470 \text{ lbm/in}^2$$

$$K_4 = 0.003 \text{ lbm/in}^3$$

So that for the type of rocket pictured in Figure 2 the mass fraction may be expected to vary with diameter according to the relationship

$$\text{Mass fraction} = \frac{0.190}{0.208 + \frac{0.470}{D}}$$

This trend is illustrated on the curve in Figure 3. It is obvious that for a given state of art in case material, charge design, and nozzle technology, little improvement in mass fraction will be associated with increased size. This

observation ignores, of course, the influence that optimizing other parameters such as p_c may have on mass fraction. Requirements for additional inert hardware peculiar to a given system, such as thrust termination ports, skirts, etc., usually result in actual mass fractions slightly lower than shown in Figure 3.

The burning rate of propellants otherwise suitable for large rockets may be rather readily varied from about 0.3 in/sec. to about 0.7 in/sec. by changes in oxidizer grind, use of catalysts, and other techniques.

The constraints on web thickness as a function of diameter are grain stresses and erosive burning as the port becomes too small. A small port area is desirable to achieve high volumetric loading. Typical practice limits the web thickness to about 55% of the radius. The approximate range of durations readily obtainable in rockets of from 100" to 300" diameter is shown in the shaded zone of Figure 4. This fairly well brackets the burning times most frequently required for individual stages in multi stage vehicles.

In some recent rocket motor developments, notably Minuteman, nozzle development became a major problem. The circumstances of this problem must be examined to see if the nozzle may become a major obstacle to further exploitation of large solid rockets.

The development problems with Minuteman nozzles stemmed from two requirements. These were an essentially non-eroding throat to maintain almost constant chamber pressure and motor performance, and a swiveled nozzle for thrust vector control (TVC). The requirement for a non-eroding throat was met through use of tungsten or tungsten alloy throat inserts. These refactory metal throats easily provided the necessary erosion resistance, but the retention of the throat inserts in the surrounding graphite parts proved troublesome. This difficulty was partly related to the requirements to swivel the nozzle. The geometry of the movable joint limited both the space available and the path through which the loads could be taken out. The other part of the swiveling problem was associated with sealing the joint against gas leakage while keeping actuating torques to acceptable limits, and protecting the seal from the hot gases.

The advent of fluid injection TVC, where used, will obviate the need for movable nozzles. This is fortuitous for as nozzles become larger, it might be expected that increasing difficulty would be encountered in maintaining satisfactory seals. "O" Rings have proven satisfactory in present applications but the close control of tolerances necessary to insure proper compression might be more difficult to achieve, and the thermal expansion over the diameter would be more difficult to cope with.

If it could be assumed that the rate of ablative type materials is constant for a given gas temperature and velocity, the percentage increase in nozzle throat area with time is approximately inversely proportional to the throat diameter, i.e., the larger the throat, the smaller the fractional area increase. The success achieved with large nozzles to date indicates that another factor working in favor of the larger sizes may be a thickening of the boundary layer as the exposed surface is extended in the direction of flow, thus effectively reducing the ablation rate at the throat.

One of the development hazards in liquid rocket development has been combustion instability. Analysis of the causes and conditions under which combustion instability will occur has not led to successful techniques for scaling satisfactory small chamber designs to large size. Baffled injectors presently are the only satisfactory way of preventing the propagation of combustion disturbances leading to standing waves of destructive amplitude. Combustion vibration has been encountered in small solid motors in the past, but since the advent of aluminized composite propellants instances of combustion vibration have not been reported with this type propellant. Initial tests of large motors have not indicated the presence of any problems.

Summing up what might be reasonable to expect of solid propellant motors scaled to very large size using today's component technology, we see a specific impulse of about 245 sec. in the propellant, a mass fraction not significantly different than that being obtained in today's test motors, burning times tending to want to get longer as sizes get larger, this tendency not posing a critical problem in nozzle design. There appear to be no fundamental problems attendant to large size.

The facts on which this assessment rest have been in existence or ascertainable for several years, with the exception of fluid injection TVC, which has been reduced to practice only recently. The development of very large solid motors then awaited acceptance of feasibility engendered by successful conclusion of development of Minuteman and Polaris size motors, or the indication of a requirement, or both.

Let us turn next to the question of where such rocket motors might be useful.

Results of Launch Vehicle Analyses

Since 1957, scores of studies have been made of space launch vehicle possibilities. Every study has its particular objective. The objective may be to find an expedient way of launching a certain payload at the earliest possible time; a study may seek to show the variety of uses possible for an existing system; it may show attractive applications for a particular type of equipment. Many studies have endeavored to establish a relation between the probable trend of future requirements and the expected advancements in the state-of-the-art, with the view toward identifying the direction toward which new developments should be pushed. The Air Force Space Systems Division and its closely associated contractor, the Aerospace Corporation, have made many such studies.

Among the SSD/Aerospace studies pertinent to the present subject was a study -- or really a related series of studies -- begun by the Space Technology Laboratories in early 1960 and recently concluded by the Aerospace Corporation. This effort is known as the Phoenix Study[2]. It was undertaken as the result of a review of the course of events in aeronautics and science over the last 60 years in broad historical perspective, to seek the answer to what really needs to be done to make space travel -- particularly military space operations -- more practical. The answer seemed to be that the cost of putting objects into space needs to be reduced by one or two orders of magnitude, in terms of dollars per pound of payload. The purpose of the Phoenix Study, therefore, was to explore possible ways of accomplishing this objective. Much of the work is just now being formally reported, and undoubtedly many of the interesting aspects will be published in the future by the various authors. Suffice here to summarize a few conclusions significant to the use of solid propellant rockets in manned space vehicles.

The relative cost effectiveness of liquid and solid propellant multi-stage vehicles is shown in Figure 5. The position and shape of the curves have been exaggerated slightly to clarify the trends. A single solid propulsion stage is simple, reliable, readily serviced, and is indicated to be the lowest cost method for low velocities. For a given state-of-the-art in propellants (Isp) and motor design (mass fraction) a glance back at the equation for velocity gain and the discussion of the influence of size on mass fraction shows that there is an upper limit to the velocity obtainable with a single stage no matter how large the size (and, therefore, cost). Use of additional stages has the effect of increasing the mass fraction so that higher velocities can be achieved, but the vehicle size (and hence cost) to launch a pound of payload still becomes enormous at velocity increments of practical interest. The oxygen-hydrogen stage cost effectiveness is shaped by the same considerations, differing in degree. The complexity of the system is the main factor underlying the estimate of somewhat higher cost effectiveness for stages (or multistage vehicles) where low total velocity gains are required. The considerable spread in cost effectivensss at higher velocities is attributable almost entirely to the superior specific impulse of the oxygen-hydrogen combination.

The trends illustrated in Figure 5 led to consideration of the possibility of employing both types of stages in the same vehicle. When parametric studies were made of optimum staging ratios to minimize gross weight, it was found that when the performance of the first stage is appreciably lower than the upper stages, the highest value of payload ratio is obtained in a three stage vehicle at a first stage ratio of 1.0, that is, the first stage disappears and the vehicle becomes a high performance vehicle of two stages. For two stage liquid and solid combinations the maximum payload ratio occurs at a first stage ratio of about 1.5. These trends are illustrated in Figure 6.

When a cost analysis was made it indicated that the most favorable first stage ratio for a two stage vehicle occurs at about 2.0, when the ratio of cost per pound of the first stage is half the cost per pound of the second stage. For the three stage case, it was found that a preferred first stage ratio does exist when the vehicle stage ratios are optimized on a cost effectiveness basis. This ratio is around 2.0 also. These trends are illustrated in Figure 7.

The conclusions of these studies were that two and three stage solid and liquid "hybrid" vehicles have optimum stage proportions resulting in minimum costs. These stage proportions for minimum cost differ from the stage proportions for best performance, sometimes significantly. Costs for the cost optimum two stage vehicle were estimated to be lower than costs for the all-liquid two-stage vehicle.

While the studies just mentioned show that solid motors of themselves do not provide the order of magnitude cost reductions sought, they do give one indication of the potential usefulness of large solid motors for space launch vehicles. Other factors which could significantly influence the choice of propulsion systems to put into development are development time, desire to provide alternate approaches in areas of development risk, and the way proposed motors or stages fit into some larger scheme of things as space "building blocks."

Present Program on Large Solid Rockets

The present program on large solid rockets is the outgrowth of feasibility experiments initiated two years ago and the more recent recognition of possible requirements.

Following its established policy of pursuing applied research, technical development and feasibility demonstrations in fields where military usage of the results of such work are foreseeable but sometimes speculative, the Air Force began the study of larger solid propellant rockets as soon as the feasibility of the size rocket used in the Minuteman first stage was accepted as a reality. First recommendations for experiments in the million pound thrust class were made in late 1957. Proposals were obtained from industry for the demonstration of a 20 million lb.-sec. motor in December 58. After much review of the principal requirements of the specification and various possible program plans, a contract for a feasibility demonstration program on 100" diameter segmented motors was awarded the Aerojet-General Corporation in July 1960. The first firing of a single center segment motor delivering over 400,000 lbs. thrust for nearly 50 sec. took place in June 1961. The test was successful in every respect. The original program plan called for demonstration of additional one segment motors, but after the success of the first test, it was decided to proceed directly to a two segment motor, which was successfully fired on 29 August 1961. This motor delivered about 440,000 lbs. of thrust and operated over 60 sec.

In the spring of 1961 inquiries into ways of augmenting the nation's space effort by an advisory committee appointed by the President afforded the solid rocket industry the opportunity to present the case for the large solid rocket booster. The necessary impetus was given by the President's Special Message to Congress on 25 May 1961 in which he urged a greatly expanded space program, one objective being to attempt to put a man on the moon in this decade. Noting that much larger rocket boosters would be required, the President recommended that both liquid and solid approaches be taken. Acting on this recommendation, the Congress appropriated $50 million in FY 62 to support the solid motor development effort.

By agreement between the Secretary of Defense and the Administrator of the NASA, the Air Force was assigned responsibility for the program. Planning commenced immediately to organize and conduct the program on a high priority basis.

When it became apparent in mid-summer 1961 that the detailed and exhaustive studies which were necessary to define explicit space launching vehicle requirements would consume several months, during which no specification would be possible of the requirements for large solid motors, the Air Force recommended that the existing technology program be immediately expanded and diversified to provide as substantial a base as possible on which to build when the launch vehicle requirements crystallized. This recommendation was followed.

The most urgent need was for more firings of large size motors to further prove out basic design practice. Additionally, development work was needed on various components and materials to explore alternative design approaches. Prominent in this area were nozzle design techniques and materials. A very substantial effort was needed to investigate fluid injection thrust vector control as applied to large size motors.

The bulk of the work was undertaken by three companies who had large motor case hardware available or in an advanced stage of fabrication. These firms were Aerojet-General Corporation, The United Technology Corporation, and the Lockheed Propulsion Company (then Grand Central Rocket).

The United Technology Corporation (UTC) began privately financed work on large solid motors in the summer of 1960. Some NASA support was obtained and a one segment tapered motor, 96" in diameter at the largest end, was fired in August 1961. It was highly successful. A second motor containing two center segments was successfully fired in December, this firing being partially financed under the Air Force's expanded technology program (See Figure 8). Preparations are currently being made by UTC to fire two single segment motors on which will be performed a variety of TVC experiments. Different nozzle materials and ignition techniques will be investigated also. The program at UTC will culminate in July 1962 with the firing of a two segment motor which will incorporate the more promising results of the current work.

The original Aerojet feasibility demonstration program was modified and expanded under the present technology program. The earlier firings had been so successful that it was decided to modify the three segment motor to provide the longer burning time and regressivity which were emerging as requirements for booster motors. The 3-segment firing was made on February 17, 1962. It burned for about 90 seconds, produced a maximum thrust of slightly over 600,000 pounds, and incorporated a TVC experiment. Again, it was highly successful. This motor is pictured in Figure 9 and the firing is shown in Figure 10. The Aerojet 100" technology program will be completed in June with the firing of a 5-segment motor containing over 300,000 pounds of propellant and delivering about 700,000 pounds of thrust. This motor approximates in size and general characteristics the motor envisioned for use with the Titan III space launch vehicle.

The Lockheed Propulsion Company was awarded a contract for the development of a tapered pin clevis joint design under the original Air Force feasibility program, the design to be proven by a full scale hydrostatic test of a 120" diameter joint. Under the expanded technology program, the decision was made to load and fire the complete motor, the completion of the case having been privately financed. The firing is scheduled for May 1962.

Throughout the series of firings described, as many TVC experiments as possible are being performed. These experiments are being supported by extensive analytical and subscale work. The scope of investigation includes a variety of fluids, location of ports, the limits of side forces obtainable, and the efficiency of injection. It appears that for first stage booster application, the dominant factor in the design may be the maximum side force required.

A premise of the whole program has been that very large solid boosters having acceptable performance are feasible using existing state-of-the-art in the various fields which are pertinent. The principal problem foreseen is reducing this state-of-the-art to practice in the sizes required.

Considerations in Development Programs for Manned Space Launch Vehicles

In planning a development program for solid boosters for manned space launch vehicles, the characteristics required of the motor may have an important influence on the schedule and cost, to the extent that they present difficult design, manufacturing, or test problems. A motor which adequately demonstrates its feasibility may fail to meet exacting vehicle requirements in a number of respects.

The preliminary design of a launch vehicle will represent a number of design compromises, hopefully made to permit the solid motor design to stay comfortably within the limits of burning

time and thrust inherently available in a given size motor as discussed in a previous section. Beyond the parameters of total impulse and burning time, the motor specification must take into account numerous constraints and special requirements. Important among these are the maximum acceleration and dynamic pressure which the vehicle will withstand. These may considerably influence the distribution of impulse over the burning time, or in other words, the thrust time curve. In order to allow the motor designer as much latitude as possible in devising suitable charge configurations, the method of specifying the impulse-time relationships shown in Figure 11 has been devised. Limits are established for maximum acceleration, maximum dynamic pressure, and the degree of regressivity thought prudent to permit without exceeding the state-of-the-art. The enclosed area represents the possible ratios of impulse delivered during the first half of burning to the total impulse which do not result in the established limits being exceeded. It should be noted that the limits are valid only for the burning time stipulated.

While the exact shape of the thrust time curve is thus allowed considerable freedom, the motor-to-motor deviation allowed from an established thrust-time curve may be rather precisely specified in order to assure satisfactory vehicle operation when motors are employed in parallel or clusters. Other parameters likely to require establishment of limits in the specification are ignition delay, rate of onset of thrust, rate of thrust decay, and tail-off residual impulse.

Thrust termination is required on the final stage of both Minuteman and Polaris for velocity control. The devices are fairly simple and are proving quite reliable. The need for thrust termination capability on first stage motors has been widely debated. Two possible requirements are to insure simultaneous cessation of forward thrust of two or more motors, and to terminate thrust in an abort situation to permit the manned component of the vehicle to be separated. The latter requirement dictates that the thrust termination feature be operable on command any time after ignition.

Ignition of large motors has not been a problem in the sizes fired so far. Conventional techniques -- both pyrotechnic and small rocket type -- have been successfully used. Other methods are under investigation. These include hypergolic fluids and devices inserted through the nozzle. It is felt that with a launcher mounted ignition system a higher degree of ignition reliability might be more readily achieved using more redundancy. A special study of the problems of igniting clusters of large rockets is being made.

In the manufacture of large segmented motors, it has already been shown that all components can be successfully made up to 120" size. Processing has been demonstrated. The same techniques and processes appear satisfactory for motors up to the 156" in size. The principal problem foreseen in the manufacture of 156" size segmented motors is the fabrication of the steel case. Existing heat treatment furnaces having the capability of processing the types of alloys expected to be used are limited to a working diameter of about 140". Undoubtedly, larger furnaces will become available as the requirement becomes firm. As the size of the part increases, the problem of maintaining dimensional stability during heat treatment may be expected to increase.

Graphite in one of its various forms is the presently preferred material for nozzle throats. In some grades blocks of sufficient size to yield one-piece rings for 120" motors are not yet available. Orders have been placed for experimental blocks in the required size. Investigations are being conducted on other throat materials, in particular, ablating graphite cloth phenolic compositions. This type of material and also asbestos-phenolic moldings are used for the nozzle expansion cone. A question exists over the molding pressures that will be required. Various techniques have been discussed including matched die molding, hydroclaves, and some rather novel schemes. Although sufficient evidence on erosion rates and structural integrity is not in hand to definitely state a requirement, some manufacturers are placing themselves in a position to furnish higher pressure moldings should the need be confirmed.

Discussions of solid propellant motors for manned space launch vehicles always bring up the subject of "man rating." People have different interpretations of this term, but in general it seems to reflect agreement that special consideration must be given to the matter of crew safety. Requirements for man rating might include higher reliability, increased factors of safety, malfunction detection, and explosive classification.

The impressive reliability records of solid propellant JATO rockets used to assist "launch" of piloted aircraft was achieved after extensive development programs culminating in large numbers of firings of production units to statistically demonstrate the reliability of the motor. The enormous cost of giant solid motors for space launch vehicles makes the same development approach impractical. Instead there will have to be more emphasis on rigorous analysis, ample safety margins, and intensive reliability effort through manufacture and prepration for firing.

Studies are presently under way to identify the parameters which should be monitored to provide the first indication of operating malfunction. Preliminary results lead to the belief that a number of dangerous conditions can be sensed in sufficient time for an escape system to react.

The question of man-rating solid motors was first faced years ago with the JATO rockets. The largest solid motor presently used for launching manned vehicles (F-100's) is the Rocketdyne M-34 ZEL. There is no reason to believe that as motors get larger, the problems of man-rating change in any fundamental way.

The explosive classification of solid propellant motors is a factor affecting manufacturing and test facility layout probably more than safety of manned flight. Safety people require

proof by actual test of the explosive behavior and detonability of large motors. The initiating charge requirement is becoming so large as to raise a question about the realism of the situation being simulated. The prediction of the critical diameter for a given propellant or the criticality of a given grain geometry appears impossible or at least unconvincing with available analytical techniques. Additional theoretical and experimental work on this subject is desirable.

Future Prospects

The role of solid propellant boosters in the manned space flight picture is now emerging as plans for the various manned space flight programs take shape.

About a year ago the conviction was growing that a degree of standardization was essential for space launching vehicles. The wide variety of combinations that had come into being and were being suggested multiplied development costs and flight test problems. The reliability growth that should come with repeated use of identical equipment was impossible to achieve. Independent studies by the Air Force and the Institute of Defense Analysis concluded that a significant degree of standardization is feasible for basic components of space launching systems. These components might be regarded as "building blocks" which might be "stacked" in suitable combinations permitting the flexibility to perform a wide variety of missions. The studies further indicated that the Titan II missile had characteristics which made a good "core" around which to associate other building blocks. Accordingly, studies were initiated to confirm the technical feasibility of this approach and to develop an improved management approach to the enormous problems of bringing such programs to timely fruition in an orderly and economical manner. Recognition is growing that in the space age the problems of management of the complex undertakings transcend the numerous and often formidable technical problems.

The study and program planning phase for a standardized space launch vehicle employing a modification of the Titan II missile in conjunction with two large solid booster rockets is nearing completion. Among the many missions for which this launching system can be used are at least one involving manned space flight. If the result of the final evaluation is favorable, this would become the nation's first space launch vehicle employing large solid boosters which could be used for manned space flight.

The motors for the Titan III, as it is now being called, will be the segmented type approximately 120" in diameter. Loaded weight of the motor will be almost 400,000 lbs. and the thrust will be in the million pound class. Burning time will exceed by a very modest amount times that have been achieved in experimental motors. About 40% regressivity is required. Following the philosophy of the program an effort was made in drawing up the specifications to equalize the technical risks in development of various parts of the system.

The conclusions and recommendations of the studies and reviews of large launch vehicle requirements for the lunar landing and other missions, point to an important role for even larger solid rockets in the nation's most ambitious manned space flight program. The objectives and schedules which can be reasonably expected to be achieved are being developed in light of critical milestones in the lunar landing program. Planning for prototype motor development in the largest size that appears practical for segmented motors (about 156" because of transportation limitations) is well along, as are plans for demonstration of the feasibility of various steps in the development and operational use of very large (240 - 260 inch) non-segmented solid rockets. In formulating the plans for these programs, the Air Force is fully responsive through the Department of Defense to the stated views and indicated requirements of the NASA.

The approach and immediate goals of these two efforts are being set in accordance with the accepted feeling about the uncertainties involved. The feasibility of the 156" size segmented motor is generally conceded, hence the expectation of proceeding directly to a prototype which represents as nearly as possible a flyable model based on available information on requirements. The larger monolithic motor, on the other hand, while expected to be designed using existing state-of-the-art in propellants, metallurgy, plastics, and proposed to be handled by methods which appear possible, represents such a departure from present experience that the feasibility is less certain. Probably there will be some difference of opinion over the definition of feasibility. As it has been employed in connection with the very large motor, the term means the capability of reducing to practice that which on paper appears possible.

Conclusion

In summing up the discussion of solid rocket boosters for manned space flight, it appears correct to say that for all, except the largest sizes, the technology exists to satisfy immediate needs. The attractiveness of large solid propellant rockets as first stage boosters has been shown from an overall cost effectiveness standpoint. The role that solid motors ultimately will play in the nation's manned space flight endeavors will depend on events and decisions still in the future. Certainly the ability of both the liquid and solid rocket industry to meet their commitments with regard to performance, cost, and schedule will have an important bearing on the outcome.

References

1. Schlaifer, R.O., "Development of Aircraft Engines" and Heron, S.D., "Development of Aviation Fuels," Harvard University Division of Research, 1950.

2. Phoenix Space Launching System Study," Phase I Final Report Volume III, Aerospace Corporation, 28 Jan 1962 (Confidential).

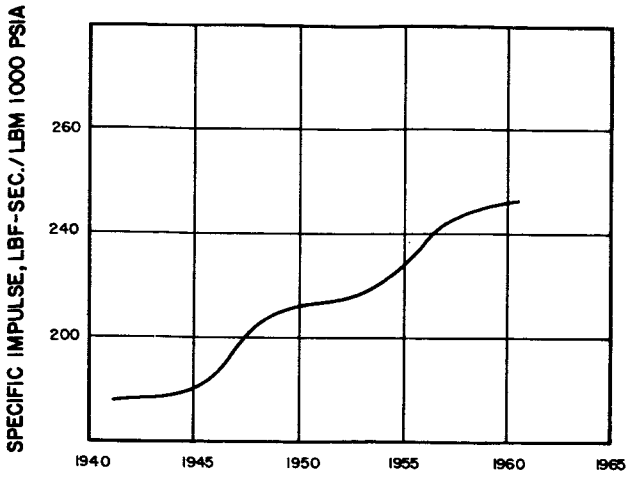

FIG. 1 SPECIFIC IMPULSE OF SOLID PROPELLANTS VS. TIME

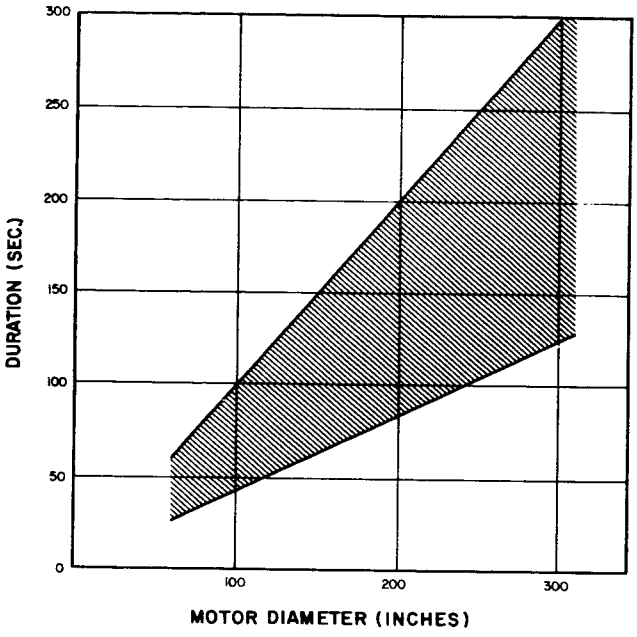

FIG. 4 RANGE OF PRACTICAL BURNING TIME VS. MOTOR DIAMETER

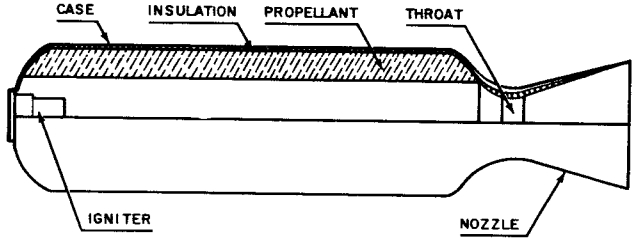

FIG. 2 TYPICAL SOLID PROPELLANT ROCKET MOTOR

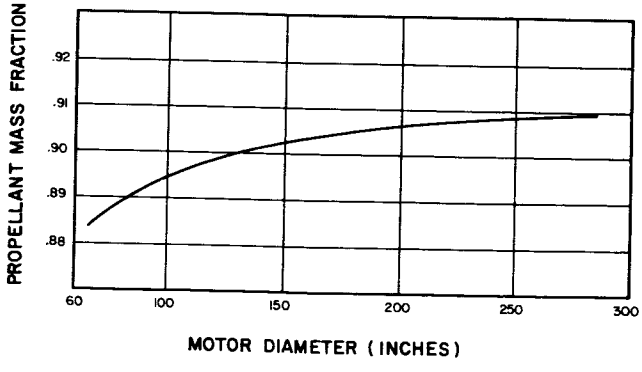

FIG. 3 SOLID PROPELLANT MOTOR MASS FRACTION VS. MOTOR DIAMETER

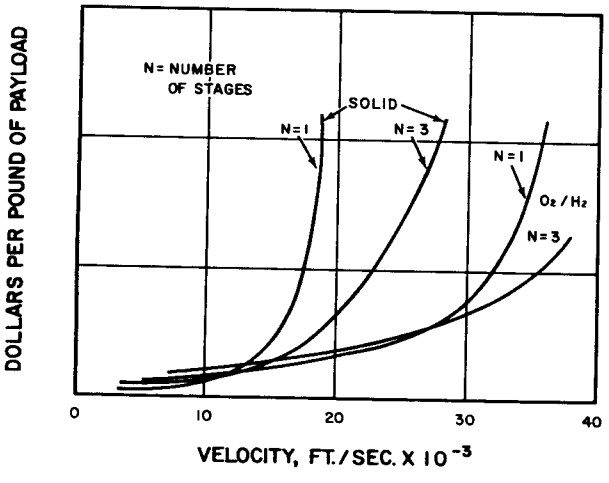

FIG. 5 RELATIVE COST EFFECTIVENESS OF LIQUID AND SOLID PROPELLANT MULTISTAGE VEHICLES

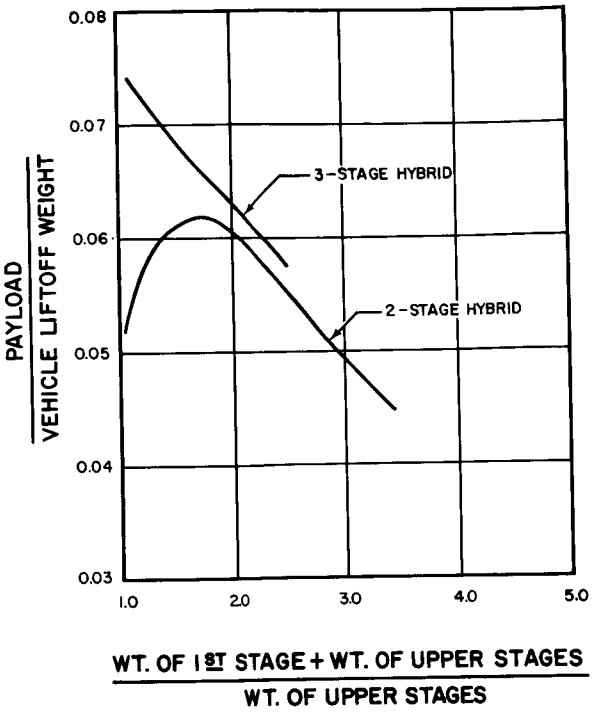

FIG.6. PAYLOAD RATIO VS. STAGE RATIO FOR HYBRID LIQUID/SOLID VEHICLES

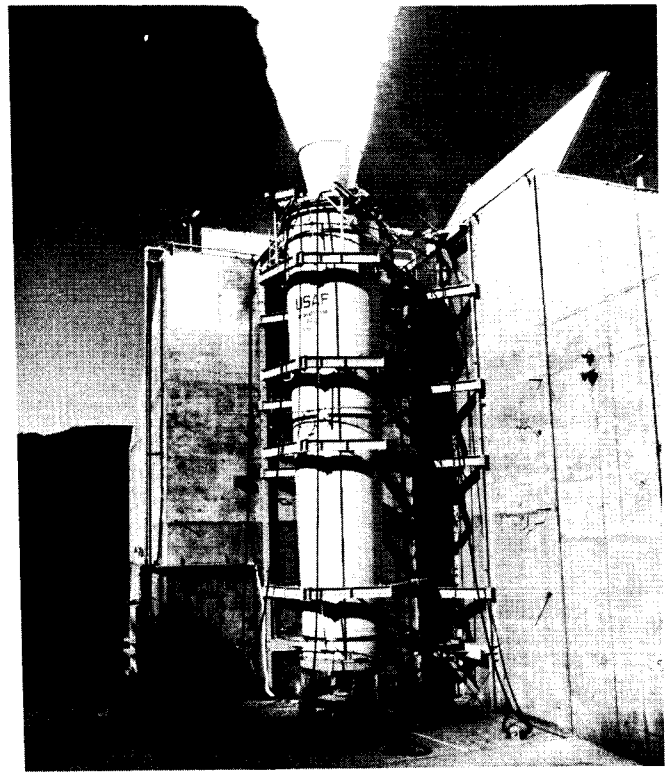

FIGURE 8. UTC TEST OF 2-SEGMENT MOTOR

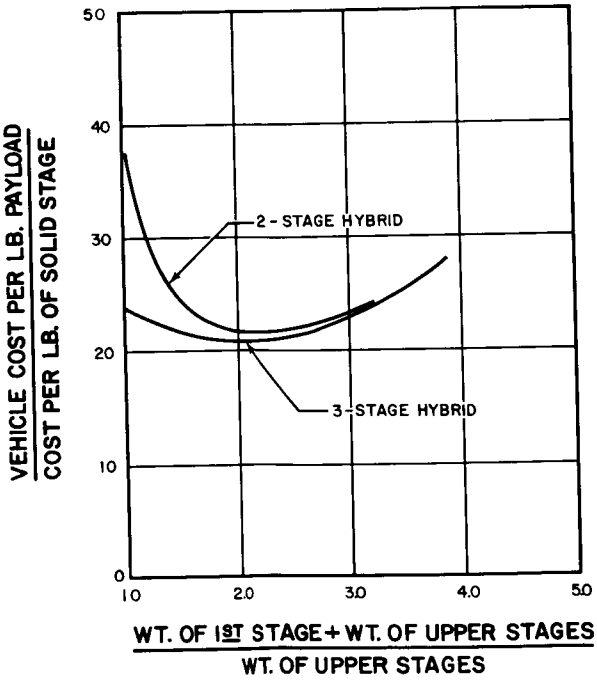

FIG.7 COST EFFECTIVENESS VS. STAGE RATIO FOR HYBRID LIQUID / SOLID VEHICLES

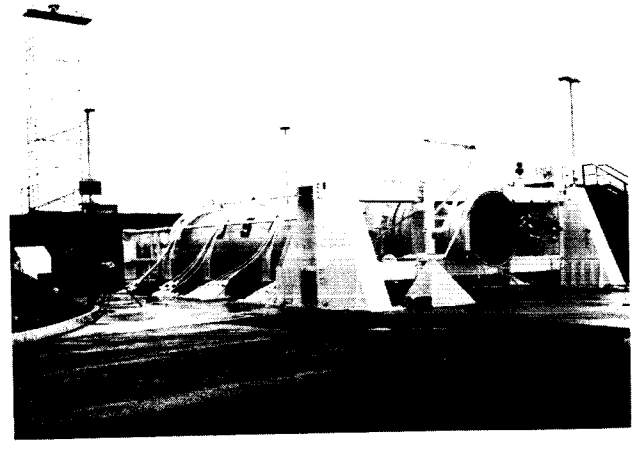

FIGURE 9 AEROJET 3-SEGMENT 100 INCH MOTOR

This page is reproduced again at the back of this report by a different reproduction method so as to furnish the best possible detail to the user.

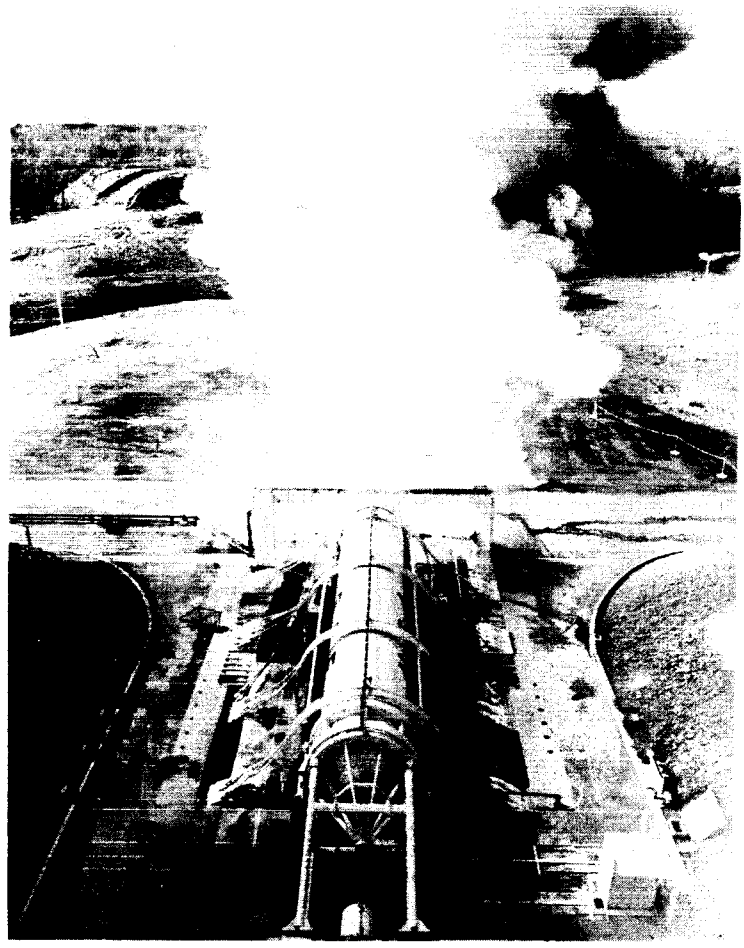

FIGURE 10 TEST FIRING AEROJET 3-SEGMENT MOTOR

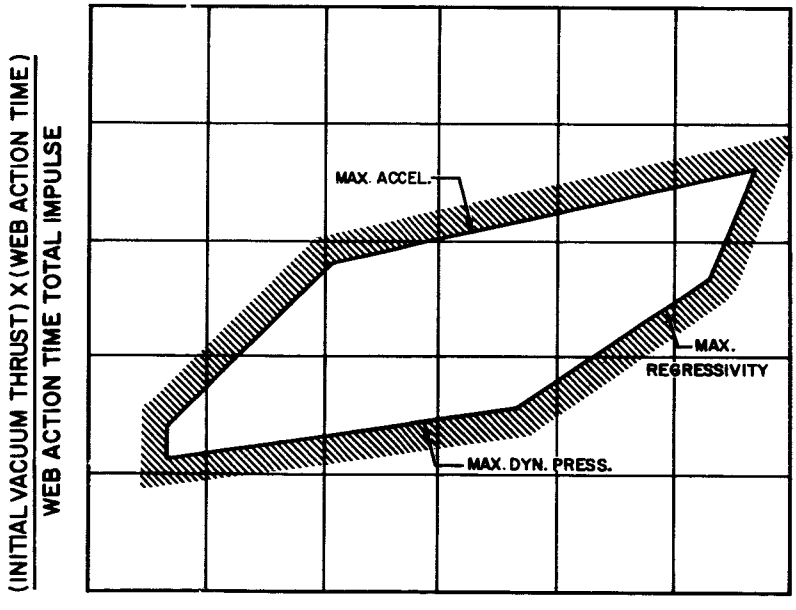

FIG.11 METHOD OF SPECIFYING THRUST – TIME RELATIONSHIP.

This page is reproduced again at the back of this report by a different reproduction method so as to furnish the best possible detail to the user.

THE POTENTIAL FOR NUCLEAR PROPULSION FOR MANNED SPACEFLIGHTS

Maxwell W. Hunter, Jr.
Member, Professional Staff
National Aeronautics and Space Council
Washington, D. C.

INTRODUCTION

Nuclear propulsion for rocket application can be separated into several categories. Probably the most obvious approach to utilizing nuclear energy is a nuclear thermal rocket consisting of a reactor made of solid material used to heat a propellant which is expelled in a hot jet to give useful thrust. Unfortunately, high specific impulse in a thermal rocket requires a high temperature in the exhaust stream. Therefore, fundamental performance limitations appear which are high temperature reactor material problems rather than limitations on the amount of nuclear energy available. It is well known that these limitations tend to give the order of magnitude of twice the specific impulse of high energy chemical systems, even when hydrogen, with its low molecular weight, is utilized as the propellant in order to yield the lowest possible temperatures. The Rover Project is developing a modest-sized rocket of this type. A doubling of the specific impulse is a very substantial performance gain, and the use of upper stages powered with these rockets, combined with conventional chemical lower stages substantially increases performance. Such stages would tend to double the earth orbital payloads of large chemical rockets such as Saturn, and decrease the size of interplanetary orbit-to-orbit shuttle vehicles by one order of magnitude[1].

Those performance improvements are worthwhile goals, and it is important that they be pursued with vigor. The situation is, however, still very frustrating on two counts. First, the cost of deploying people and equipment throughout space is still extremely high, and it would be most desirable to make a really fundamental reduction in this important basic quantity. Second, the energy potential of nuclear reactions is far higher than that which can be released in solid core fission rockets with current material limitations, so that vastly greater performance improvements are latent in the nuclear process. Attempts to get around this second frustration of "fundamental" performance limitations have, so far, split into two families. The first family utilizes a nuclear thermal rocket modified so that part or all of the energy release takes place in a gas so that no fundamental temperature restriction exists. Two sub-groups of this family are: (a) The use of nuclear bombs which detonate behind the ship and throw debris against a cunningly mounted striker plate as a method of obtaining thrust (Project Orion); and (b) The running of a contained reaction in a thrust chamber with the energy release actually occurring in the gaseous phase, the so-called gaseous fission reactor. The second family utilizes electrical methods of accelerating the propellant to avoid completely the need for high temperatures. This family has spawned a fair amount of research on various electrical propulsion schemes and, as a by-product, a large number of mission performance analyses.

A one-sentence-each summary of the recent state of such advanced propulsion follows. The present version of Orion is limited to huge payloads, and certainly was impossible to test adequately while a nuclear test ban was in effect. Electrical rockets have extremely low thrust-weight ratios due to the weight of power conversion equipment required, and their performance is consequently severely attenuated in spite of yeoman efforts in mission performance analysis. No one has yet come forth in a convincing fashion with a constructive idea for making the gaseous fission rocket work at all.

This paper will first review certain lines of reasoning which led to a possible scheme for greatly reducing the cost of space travel, even if only solid fission rockets were available. An attempt will then be made to expand the same line of reasoning to the utilization of gaseous fission rockets, an approach inspired by a number of new suggestions which have materialized recently with respect to gaseous fission reactors. Reference to Orion, nuclear electrical rockets, and fusion rockets will be made occasionally, if appropriate, but no attempt to present a completely comprehensive treatment of all types will be made. The discussion will be limited to solar system transportation requirements.

SOLID CORE FISSION ROCKETS

If one examines the reasons for the high cost of space travel, he is usually impressed with the apparent fact that everything seems hopeless. Large installations such as Cape Canaveral are evidently necessary, and expensive pieces of hardware are effectively placed almost beyond recovery on each flight, particularly after being spread around the planet and throughout local space during the operation. The very high velocities required in space flight would seem intuitively to involve such tremendous energies that it is natural to expect everything to be fantastically expensive anyway, so that the hopeless feeling tends to increase.

A really high performance rocket is capable of making fundamental improvements in this picture. If performance can be made high enough so that single-stage rockets have adequate capability, it becomes possible to re-use equipment exactly as in transport airplane practice. Although a single-stage, re-usable, high-energy chemical rocket can almost certainly be developed for earth orbital operations, nuclear energy is required for virtually all deep space missions. Except possibly for safety provisions surrounding the engine, there is no reason why a single-stage nuclear rocket should be any more complicated than a standard transport airplane, and no reason why it should be much more expensive in production, except for the price of the nuclear inventory which it must carry on board for reactor criticality requirements. True, the temperature inside the reactor (and in the exhaust jet) will be substantially higher than that to be found anywhere near a normal transport aircraft. On the other hand, the rocket accelerates out through the atmosphere slowly, and hence, is never subjected to severe external environmental factors such as supersonic transport aircraft face. In space, conditions are mild, although sometimes too radiantly beautiful. Should aerothermodynamic loads on unpowered re-entry prove too distressing, a really high performance rocket could reenter the atmosphere on jet thrust. The high reactor core temperature, hence, is really the only major vehicle difference, and if that problem can be solved, all else settles into a normal pattern which could well be an easier environment than most modern aircraft encounter.

It is felt by the author that most people tragically underrate this point. Five-stage rockets of the large man-and-cargo variety tend to spawn large, complicated launching systems, fantastic numbers and types of engines, vast real estate developments, and similar complicating phenomena. As a matter of fact, one of Hunter's additions to Parkinson's laws is: "The management structure (total number of companies and agencies) involved in large manned rocket programs is at least directly proportional to the gross weight times the number of stages of the vehicle." Most of us intuitively, if not always consciously, understand that Parkinson would certainly have discovered his laws in the space launch vehicle business if the British Admiralty and Foreign Service had not already provided his source of inspiration. We are duty-bound to keep a stiff upper lip, however, and should not be blind to the fact that it never takes more than one adequate propulsion system to give a simple, reliable vehicle which might be no more difficult to prepare for the next flight than the average, equally complicated, transport plane (regardless of the exhaust temperature when the throttle is opened).

It is clear from the above discussion that sufficiently high rocket performance capabilities might well yield tremendous cost reductions in both hardware and overhead costs. One of the more startling aspects of nuclear rocketry is that, in addition, the energy costs turn out to be relatively reasonable. At first thought it would seem that the energy expended in generating 60,000 fps total velocity for a lunar expedition would be far greater than any normal transportation requirement. The total velocity is almost twice earth escape speed, and even earth escape speed had not been obtained with any appreciable payload only 5 years ago. It turns out, however, that this is about the same amount of energy which a transport airplane utilizes in suspending itself in the air long enough to make a flight from Los Angeles to New York. If one assumes a jet transport to be cruising for 6 hours at an L/D of 12, this means that the engines were applying 1/12 of the weight of the airplane for the six hour period. If somehow this could have been applied in field-free space, the airframe would have accelerated at 1/12 of a g for 6 hours and would have generated 58,000 fps, essentially the total velocity required for a lunar transport. Thus normal cruising aircraft utilize the same order of magnitude of energy as required for a modest space transport system, essentially because they fight gravity incessantly during their whole flight. In space, transports fight gravity quickly and efficiently in the early part of their flight and coast through space to their destinations. Looking at it another way, a Nova-type vehicle would use about 10^7 pounds of chemical fuel to give 2×10^4 pounds of payload a lunar round trip. This is 500 pounds of propellant per pound of payload and, at an average energy of 3000 KCAL/KG, is approximately 1000 KW-HR of energy per pound of payload. Since the current rates for commercial electrical energy (in Washington, D.C.) are about 1¢ per KW-HR, $10 is the terrestrial price of the energy per pound of payload. Hence, space flight is expensive not because the energy required is high, but because no way has yet been found to package and utilize these energies out in space. Only the nuclear rocket achieves high enough exhaust velocity to create the necessary performance in a single-stage vehicle. If it were possible to build a nuclear rocket with perfect fuel containment, the price of uranium burned to generate the required energy would be only a fraction of a cent per pound of payload. This is much lower than the chemical rocket example quoted, since not as much energy must be expended accelerating inefficient fuel to high kinetic energies. The difference becomes even more pronounced at higher velocities.

These various points have been explored, various ways of presenting them have been given, and analyses have been made as to velocity requirements for various future space missions[2-6] Perhaps the most concise way to summarize this data is shown in Figure 1, where dollars per pound of cargo delivered is shown vs velocity of mission for chemical rockets, solid fission rockets, and two examples of gaseous fission

rockets. Figure 1 assumes values of hardware costs consistent with current airframe practice, weight ratios of vehicles consistent with current rocket practice, and the achievement of re-use consistent with transport aircraft experience[6]. Chemical rockets can be used as orbital trucks without causing more than a few dollars per pound increase in operating cost for the missions. The only effective way to keep costs in bounds for high velocity flights, however, is with high performance nuclear rockets. The additional assumptions in the gaseous fission cases are rather difficult to meet since they presume perfect containment of the reacting fuel and high thrust-weight ratios, regardless of the specific impulse obtained. The difficulty of meeting either of these assumptions explains why gaseous core rocket development to date has been confined to theoretical and some experimental detailed investigations, rather than any large scale development. It can be seen that even if only the lower performance gaseous fission rocket is achieved, interesting additional missions are feasible compared to solid fission systems. Therefore, the state of gaseous fission rockets will be investigated.

One other point should be elaborated from Figure 1 before proceeding. One cannot operate in the high velocity regions by the simple pyramiding of chemical rockets in any reasonable fashion. This is due to the logarithmic nature of propellant weight requirements. This effect is shown by the example in Figure 2, where number of launches required for 60,000 fps, 120,000 fps, and 180,000 fps missions are shown for chemical rockets, solid fission rockets and gaseous fission rockets. Figure 2 assumes all higher performance missions to be achieved by refueling rather than staging. If staging were used, the values shown represent roughly the total weight to be launched, rather than number of launches.

GASEOUS FISSION ROCKETS

Most of the earlier ideas for ways of utilizing gaseous fission cavity reactors for propulsion involved diffusion of the propellant through the gaseous fuel so that heating occurred by direct conduction and convection. It was then necessary to separate the two gases and hopefully retain virtually all of the fuel on board while exiting all of the propellant. Hydrogen was normally assumed as propellant since low temperatures are always comforting, even in non-temperature limited cases. Schemes such as magnetic field containment or the use of centrifugal separation in some form of vortex, were considered. Weight of magnetic equipment was, as always, a problem, and the details of vortex stability and containment with any substantial diffusion rate have remained vexing.

Another family of systems has orignated from these investigations. Although deceptively similar in appearance, they operate on a basically different principle. These are systems which heat the propellant by means of radiation from the fission plasma, rather than direct intermixing. The containment problem, therefore, is not one of separation but rather one of the prevention of mixing. This is a fundamentally different containment problem. Vortex stabilization criteria will certainly differ when hydrogen is not diffusing through the core. If magnetic forces are used in any of the schemes, they become of the intensity required to prevent boundary layer mixing, almost obviously a much smaller field requirement than that for containment of a fission plasma in the face of hydrogen diffusion. A coaxial flow reactor has been suggested where a central, slow-moving, stream of fission fuel heats an annular, fast-moving stream of hydrogen solely by radiation, with separation obtained by velocity differential[7]. The scheme has even been suggested, in the "glow plug" reactor, that the fission plasma be contained in a quartz (or similar material) bottle[8]. It is possible to cool the bottle to reasonable temperatures while still heating the propellant to high temperature by radiation, if the bottle transmits most of the radiant energy. This system would yield perfect containment, and is hence a very exciting thought. New ideas are afield in the gaseous fission reactor arena, and an attempt will be made to catalogue the limitations and capabilities of some of these schemes.

The specific impulses theoretically achievable with fission rockets are basically very high, but extremely difficult to achieve in practice since very high temperatures are required. Economy is a problem, since separation (ratio of mass flow rates of unburned fuel to propellant in the exhaust) must be of the order of 10^{-4} to reduce fuel cost to a value comparable to propellant cost, Figure 3. Separation ratio as lax as 1.0, however, does not strongly deteriorate specific impulse. The propellant costs in Figure 3 are for a hydrogen/uranium mixture, assuming a hydrogen price of 25¢ per pound, and a uranium price of $5,000 per pound. It can be seen that for very high performance, fuel costs become very high even with perfect containment. Hence, a fusion rocket would be very desirable due to low fuel costs as well as lack of fission product production.

An analysis was previously performed by making use of the data of Figure 3, and assuming that it would be possible to create fission rocket propulsion systems with thrust-weight ratios comparable to solid fission systems over the entire performance spectrum[6]. This was a very great assumption indeed, for high temperatures not only force gaseous phase heating which complicates containment, they also generate such intense thermal energies that any spurious fluxes may be of large magnitude, and their consequent dissipation may create basic performance limitations. The reason for such a theoretical

exploit was to see if a limit on desirable performance existed for solar system transportation, regardless of engineering difficulties. The results were that even for relatively fast transits as far as the planet Pluto (less than two years), specific impulses of much beyond 20,000 seconds were not desirable. This was the reason for showing 20,000 seconds as the highest specific impulse in Figure 1. It can be seen from Figure 3 that this result could have been anticipated, considering the rapid increase in fuel cost which occurs at higher specific impulses. Figure 4, reproduced from Reference 6, shows that optimum operating costs (with high re-use assumptions) were achieved with single-stage vehicles with fuel to gross weight ratio varying from 20% at low velocities to 60% at high velocities.

The problem of achieving even 20,000 seconds with high thrust-weight ratio is still difficult. Even if perfect containment, either with some new vortex configuration or with a glow plug concept, were obtained, the problem of handling the energies involved still tends to limit engine performance seriously, as previously indicated. The portions of the rocket system which must remain solid have to be cooled in some way, even though no fission energy release takes place there. These thermal balances have been treated in generalized fashion by Meghreblian [9, 10]. The thermal loads are intense, and are determined by whether or not any fissioning takes place in the solid material, the fraction of energy that appears in nuclear radiations which will heat the solid surfaces, and by the question of whether the hydrogen propellant is transparent or opaque to thermal radiation. If the solid surfaces are cooled by regenerative cooling only, there is a limit to the amount of cooling capacity in the propellant at the temperature of the solid elements, and, therefore, there is a limit to the amount of specific impulse achievable with regenerative cooling. Even if no thermal load is radiated to the structure from the gas stream, the nuclear radiation tends to limit the specific impulse to about three times that obtainable with a solid core reactor. The actual limit is shown in Figure 5 related to the fraction of energy release (ζ) which appears as thermally effective nuclear radiation. This fraction is assumed to be 10% in Meghreblian's work, but it is a strong factor, and the possibility of going to smaller fractions by means of thinner reflectors and/or relatively gamma transparent shells should not be neglected. Only the neutrons must be reflected, and hence their energy absorbed in the reflector, in order to contribute to reactor criticality. It is logical to balance the neutron reflective properties of materials with their relative gamma transparencies and thermal cooling properties to give optimum reflectors for these applications. The use of a deliberately thinner reflector would require a modest increase in nuclear inventory for criticality, but would yield both higher thrust-weight ratio and higher basic performance. Any fission products which escape in the exhaust no longer contribute their share of nuclear radiation, again yielding increases in performance. As indicated previously, this is very likely to occur in gaseous fission systems. These latter two effects are illustrated in Figure 6.

If engine performance is extended beyond the values achievable with regenerative cooling, a radiator must be added to reject the excess heat, and the thrust-weight ratio immediately suffers as a result of radiator weight. This tends to be a severe penalty, since the desirable specific impulse is of the order of 10 or 20 times that achievable in a solid core reactor, and, consequently, huge quantities of energy must be rejected through the radiator system. The specific impulse ratio achievable for the case of all fission occurring in the gaseous phase (f=o), both for the case of no thermal radiation from the gas (β_s=o), and for the case of representative values of thermal radiation from an opaque gas, is shown in Figure 7, reproduced from Reference 10. The opaque gas assumption is used as being appropriate to systems where the propellant is heated by radiation rather than diffusion. The radiator power fraction (γ) is the energy which must be rejected from the radiator system compared to that handled by regenerative cooling. It can be seen that this value must be 10 to 100 if specific impulse improvements of 10 to 20 times that achievable in solid core reactors are to be generated.

Attempts have been made by various authors to estimate the thrust-weight ratio achievable with such systems. A typical example is shown in Figure 8 as the lowest curve[9]. Specific impulse ratio is defined as the as the ratio of specific impulse achieved to that of the propellant operating at the temperature assumed for the solid portions of the reactor. This curve clearly indicates that very low thrust-weight ratios are to be expected. Two justified changes in assumptions to this curve yield, however, startling results. The curve presented assumed a thrust-weight ratio of about one to be achievable with a solid core system, and also assumed a radiator temperature of 1000°K. A value of "Rover-equivalent" thrust-weight ratio of 5 was used for the remaining curves of Figure 8. Although this value can be assumed as high as 20, such estimates make no allowance for pump weights or pressure shells[11]. Such items were considered in the analyses of Reference 12, and the assumptions used here amount to adjusting the generalized expressions of Reference 9 to match the more elaborate single point of Reference 12.

Changing the "Rover-equivalent" thrust-weight ratio to 5 still indicates very low thrust-weight ratios at high specific impulse values as shown in the next-to-lowest curve in Figure 8. A review of radiator assumptions was therefore thought to be in order. All analyses of radiator

configurations for nuclear propulsion known to the author have centered around the requirements for nuclear electric systems for either propulsion or auxiliary power. In at least two respects these requirements are totally different from those for gaseous fission rockets. The first point is that nuclear electric systems must be designed for long operating times (of the order of years) so that such problems as meteoroid penetration of the radiator surface must be considered in terms of long-time probabilities. This point strongly influences radiator weight. A high-thrust gaseous fission system would only operate for periods of minutes at a time and, therefore, an investigation of short-life radiators is pertinent. It is true that the radiator must survive for the total flight duration, not simply the engine burning period, since the engine must be used for braking at the terminal. However, total flight times will be much shorter than for electrical systems, the radiators might be protected while not radiating, and the loss of a radiator segment would not be very crippling to mission performance. Secondly, and considerably more important, the radiator temperature of the gaseous fission system can be as high as it is possible to build radiators. In a nuclear electric system, a balance must be struck between the efficiency of the conversion process, which requires the rejection of heat at a low temperature, and the decrease of radiator weight which, in general, occurs at high temperature. As a result, radiators usually want to operate at a temperature on the order of three-quarters of the maximum cycle temperature, and the maximum cycle temperature is determined by the ability of either rotating machinery or thermionic systems to operate for periods of years. Therefore, radiators for gaseous fission rocket cooling systems should be operated at much higher temperatures than those for nuclear electric systems, and might be easier to design because of the vastly shorter operating time requirements.

The upper curves of Figure 8 compare the thrust-weight ratios of systems with radiators of 1000, 2000, and 3000°K temperature and, for comparison, a zero area case ($T_R \rightarrow \infty$). The radiator weight per unit area may well increase step-wise as temperatures increase due to the need to utilize different materials which are usually heavier at higher temperatures. A constant value was assumed here, and although Reference 11 used a 5 LB/FT^2 radiator system weight, the value of 1 LB/FT^2 of Reference 9 is felt more appropriate in light of the short operating times. It can be seen that even at specific impulse ratios of 20, a thrust-weight ratio of over one is achievable with only a 2000°K (3140°F) radiator temperature. Thus, if the radiator loop were operated in the same temperature region as the primary heat exchanger loops being considered for advanced power systems, high thrust-weight ratios result for gaseous fission rockets. Clearly, special radiator designs appropriate for gaseous fission reactors should be the subject of intensive investigation.

The ability to reject heat through a radiator and still keep a high thrust-weight ratio, leads to other interesting viewpoints on desirable propulsion systems. If a vortex containment system is used, although the containment may be very good, it is doubtful that it can be made perfect. As indicated, imperfect containment will adversely affect fuel costs. If a "glow plug" system can be made to work, it will have essentially perfect containment. It will have a lower peak performance, however, since the material in the plug itself will be heated by nuclear radiation, and, hence, the fraction of energy dissipated in solid heating will be higher than if no glow plug were used. If in a vortex system, 10% of the energy were dissipated in heating the solid elements, perhaps an additional 3% would be dissipated in the glow plug. The two cases are shown in Figure 9, which indicates only a modest degradation of the glow plug with respect to the vortex system. Utilization of the high temperature radiator obviously strongly influences this conclusion. Note that Figure 9 is plotted vs specific impulse with 2000°K material temperatures rather than specific impulse ratio as in Figure 8.

The utilization of either system at the higher specific impulses involves more than simply the provision of high temperature radiators. In general, hydrogen must be seeded with some other material in order to increase its absorptivity sufficiently to make radiant heat transfer practical. The amount and type of such material would be expected to vary with radiating temperature. In the glow plug, in addition, higher temperatures may shift the radiation spectrum so far toward the ultra-violet that it is moved essentially out of the region of transparency of the plug material. Internal seeding to shift the spectrum may solve this problem. The plug material may have to be at a lower temperature than other solid elements to maintain transparency, and, consequently, the assumed additional 3% loss may be optimistic. It is evident that all detailed problems of these systems have not yet been solved. The essential point is that as they are solved, high thrust-weight systems will be available with high specific impulse.

The curves of thrust-weight ratio presented so far have shown performance limitations for the idealized assumption of no energy deposited in the structure by thermal radiation from the gas stream. The radiators included were required to reject the energy deposited in the structure by the nuclear radiation, and the decreased thrust-weight ratio at high specific impulse was caused both by the inclusion of these radiator weights, and by the fact that more energy is required to generate higher specific impulses. For a constant

value of thrust, the energy required is directly proportional to specific impulse, and, consequently, the weight of the basic reactor increases with specific impulse due to the assumption of constant energy density in the solid portions of the reactor. With this simplified assumption, the thrust-weight ratio for the case of no radiator decreases exactly inversely with specific impulse as shown in Figure 8. The thermal load deposited in the structure from the gas stream is strongly dependent upon whether the gas is transparent or opaque to nuclear radiation. Since only systems which transmit energy from the nuclear plasma to the propellant by radiation are being considered here, it is implied that virtually all such radiation is absorbed in the gas stream and, consequently, the opaque gas assumption is logical. The effect of inclusion of thermal loads is shown in Figure 10. The assumed value of the radiation parameter ρ_s of 10^{-2} is representative of a gaseous fission system which has all fissioning plasma elements at least two optical thicknesses within the propellant mass. It can be seen that although thermal radiation becomes increasingly important at large values of specific impulse, thrust-weight ratios of about one are still possible throughout the regions of interest for interplanetary transportation.

GASEOUS FISSION PROPULSION APPLICATIONS

The previous section has indicated that gaseous fission reactors are capable of yielding thrust-weight ratios of about one up to a specific impulse as high as 20,000 seconds, if appropriately high temperature radiators are utilized. Radiator temperatures as well as the temperatures of all solid structure portions of the propulsion system can be held as low as 2000°K, and still achieve this performance. The containment problem must, of course, be adequately solved.

Many uses can be envisioned for such propulsion systems. The remaining discussion will be limited, however, to the examination of the possibility of the provision of a single highly effective versatile, space transportation system to handle all reasonable solar system missions. Space exploration (and competition) will spread as far away from the earth as technical and economic factors permit. If one is to keep from drastically revising his large vehicle program every year, he must anticipate, with vigor, the performance regions of interest. For manned exploration, interest centers around relatively large payloads, perhaps on the order of 50 tons. Although this is a small payload as far as sea transports are concerned, it is nonetheless representative of a fully loaded C-133 airplane. In terms of the feats of air transport logistics to date, it is perfectly clear that the ability to place 50 tons at predetermined locations in the solar system on a reliable and convenient schedule, would constitute a very commendable early space logistics capability. The velocity requirements for various missions of interest are shown in Figure 11, along with typical payload vs velocity curves for chemical rockets and the various classes of nuclear rockets discussed. It is clear that versatility demands the payload to be delivered over a very wide velocity region; tremendously large payload weights which are limited to low velocities should only be of interest to civil engineers. Many missions of extreme interest in planetary exploration occur in the velocity regions of several hundred thousand feet per second. If a spaceship were available which could deliver a 50 ton payload to these speeds, it would have the desired tremendous utility, and would be a very tough competitor, indeed. It is interesting to note that single-stage gaseous fission rockets of 5000 seconds specific impulse are capable of effectively penetrating these speed regions. (Even at only 2500 seconds, very interesting performance is possible.) Note in Figure 11 that different gross weights were assumed for the different classes of propulsion. The velocity shown for inner planet transportation is that which gives one-way travel times of about 3 months to Mars or Venus even at the most adverse time of the synodic period. A propellant supply (but not fuel) is required on each terminal planet for such operations. It is clear that the missions which gaseous fission rockets can perform span the whole solar arena at a quite reasonable operating cost, with travel times at least to the inner planets no worse than typical "windjammer" times of last century, and with the convenience of year-round operation to all points. A possible analogy between the frigates and galleons of old comes to mind. If slow, clumsy ships were the way to conquer the sea, this paper would be written in Spanish. Of all nations, the one most famous for "clipper ships" should be the first to grasp the many intrinsic advantages of short travel times in space. Historically, these advantages have invariably been overpowering.

A common complaint unites all people involved in space programs, be they technical, military, or political. The complaint is that programs are never sufficiently stable to permit the development of useful, reliable equipment in any reasonable time scale. It is usually felt, furthermore, that our competition is always doing a better job of such programming, and this is inevitably excused by reference to his non-democratic decision processes. It is submitted that this excuse is badly overworked, and that at best it is indeed a poor replacement for inspired advance planning. The problem can be seen at a glance in Figure 11. There are many missions to be performed in space. It is possible to foresee them, and it is possible to build one class of ship to do them. Unstable programs result from not facing the reality of the exotic missions as soon as they become feasible. If the lesson inherent in Figure 11 is not learned, our fate is to be driven violently

about by our competition. The question is not only what nuclear spaceships can do for you, but what nuclear spaceships might do to you.

THE DESIGN OF SPACESHIPS

In the opinion of the author, too many words have been written about the design of aircraft and the design of guided missiles, and too few about the design of spaceships. Manned space flight is the subject of this paper, and therefore, speculation on manned spaceship design is appropriate. Guided missiles have grown up in the the throw-away-everything atmosphere of bullets. Recovery and re-use has been looked upon as something mysterious, and achievable only at great expense and low reliability, partly because very little effort has been put into it. A difficult component development problem occurs since the equipment is rarely available for examination afterwards. It is hard to get enthusiastic about recovery, when it is not part of the operational scheme. Redundancy of design has usually been held to a minimum. High acceleration loads are tolerated both on launch and re-entry, sometimes because the equipment can take them, sometimes because they cannot be avoided, and sometimes because they are very desirable for trajectory efficiency. Aircraft, on the other hand, are re-used constantly, contain many redundant items so that missions are almost always completed, and, fortunately, constantly utilize almost perfect recovery reliability. This creates a tendency to feel that anything which breathes air and has wings is always economical to operate. This thought, if extended blindly into regions of poor payload carrying ability, will lead to uneconomical operation, regardless of past history.

The true spaceship will be neither missile nor airplane. It must have the extremely high performance of the missile, in fact, much higher than any built today. It will probably be single stage. Wings and/or air breathing engines, which can only aid in the first 5% of the mission, will not be tolerated if they should unduly deteriorate the performance of the other 95% of the mission. The spaceship will be as redundant and reliable as a transport aircraft, and there is no reason why it cannot land as reliably and safely as an aircraft. Since it will carry soft cargo and normal people, it will throttle its engines after take-off, and use lifting entries at landing in such a way as never to place more than perhaps 2g acceleration on the passengers except in emergencies. It will be able to operate at variable specific impulse levels for optimum economy with different missions. Typical design fuel weight and specific impulse as a function of velocity of the mission are shown in Figure 12.

It should be possible to make spaceship operation as safe as any other form of transportation. Since the fissionable material is always in the gaseous phase, if it should have to be jettisoned in case of emergency, it already is prevaporized for safe deposit in space or in an atmosphere. Assuming that calculations on gaseous fission reactors for booster propulsion give a reasonable estimate of reactor characteristics for spaceships, the nuclear inventory on board would be less than 10 kilograms for a BeO moderated system[13]. Thus, atmospheric contamination either in normal operation or during emergencies is truly negligible. A solid core fission rocket accumulates fission products during use, and hence is quite radioactive on return and difficult to leave, approach, unload, or maintain. A fundamental advantage to the gaseous core is that the fission products can be safely disposed in space, or the atmosphere, and the vehicle landed by aerodynamic means (auxiliary chemical propulsion would be needed on atmosphereless bodies). It is, consequently, safe to approach and work around essentially immediately after landing. A glow plug reactor would have perfect containment at launch, but retain fission products at landing, unless the plug were jettisoned. A vortex containment reactor would not be as perfect at launch, although it has the same inherent nuclear safety once aloft. Thus, the gaseous fission rocket has the potential to meet the most stringent safety requirements devised.

Landing Gear Design

In spite of a fundamentally safe operation, it is conceivable that for emotional reasons, such ships would not be permitted to take off directly from the earth on nuclear thrust. Auxiliary propulsion might, therefore, be required. If so, it could be one of three categories; namely, liquid chemical rocket, solid chemical rocket, or air breathing engines and wings. In view of the tremendous performance potential of nuclear rockets, it is perfectly clear that only minimum auxiliary chemical propulsion should be tolerated. The proper perspective is maintained if it is realized that these auxiliary chemical systems correspond, in a good spaceship, to landing gear design in a transport airplane. It should also be pointed out that the spaceship is primarily a vacuum-dwelling rocket-thrust vehicle which is, however, interested in periodic return to planetary bodies. If the proper shape and construction of propellant tanks and other structure can give better re-entry conditions, without severe weight penalties, it would be desirable. This is analogous to wing flap design in aircraft, another auxiliary function. In actual operation, this may be only a desirable emergency provision, since the extra price of fuel involved in a power letdown is not great. True spaceship designers will start to come forth whenever the potential for handling these auxiliary requirements without appreciably crippling basic spaceship performance becomes evident.

Shielding

Shielding of biological payloads from both the propulsion system and the natural environment is of extreme importance. Fairly extensive shielding analyses have been made which indicate that if multiple materials are used as appropriate, and clever use is made of propellant, food supplies, and equipment to aid in shielding, shield weight penalties are not overburdening in terms of nuclear rocket payloads[2, 14, 15]. The shield weights for nuclear space transports are reasonable even though shield weights have been one of the major problems of the nuclear aircraft program. Although the reactor power of an aircraft is several hundred times lower than that of a spaceship, shield weight is a function of power times operating time. The purpose in building nuclear aircraft is to obtain long duration flights so that the operating time is days or weeks. The nuclear spaceship, however, uses its main propulsion system for perhaps only 10 minutes at the beginning and end of each voyage. If we compare typical values of power times time, the nuclear spaceship is characterized by a value only one-quarter of that for the aircraft. Furthermore, the aircraft by definition must always operate in the earth's atmosphere, and hence is continually subject to the radiation scattered back from the earth's atmosphere. This scattered radiation accounts for the largest contribution to the shield weight. The spaceship, on the other hand, climbs quickly out of the atmosphere. Estimates of the equivalent power times time that each device would experience operating at sea level (a measure of the total scattered radiation) indicate a factor of 25 in favor of the nuclear spaceship. It is not surprising, therefore, that the shield weights required for the nuclear spaceship are an order of magnitude smaller than those for nuclear aircraft. As indicated previously, the use of gaseous fission reactors greatly reduces shielding requirements after landing. The higher performance ship thus would almost certainly be easier to handle and require less extensive ground facilities than either a solid core nuclear rocket or a nuclear aircraft.

An extensive shielding analysis will not be presented here, but a few remarks based on the References (which did not consider gaseous fission reactors in detail) are appropriate. A cursory analysis of the effects of the greater energies inherent in higher specific impulses and high velocity increments indicates no substantial effect on shield weight. This is primarily due to the logarithmic effects of shield thickness; a little more shield thickness gives a lot more protection if the shield was already thick enough to have reduced the flux by many orders of magnitude. If this were not so, the shield weights on electrical propulsion systems would be completely prohibitive since such systems use much more energy to achieve equivalent performance[16]. The effects of major solar bursts are confused at the present time. If they do remain a problem (there is some evidence that even major bursts may not be), then the very short flight times or out-of-ecliptic capabilities possible with high performance gaseous fission ships becomes even more desirable.

Other Propulsion System Considerations

The propulsion system thrust-weight ratios of Figures 8 through 10 are still somewhat tentative. Even though these curves are approximate, it does appear firm that high temperature radiators are fundamentally important. The thrust-weight ratio will decrease at the higher specific impulses, but perhaps not as much as indicated due to two strong compensating effects not included. These are the decrease in pump weight due to the lower fuel flow rates required at high specific impulses, and the decrease in reactor size due to the smaller radiant plasma area required to generate the necessary power at high temperatures. An interesting sidelight of the latter point is that the throttling of gaseous fission rockets may involve unusual design techniques since the power per unit plasma radiant area is constant at a given temperature, and hence some area must be removed from effective radiation in order to throttle at a constant specific impulse. Unless these effects cause the thrust-weight ratio to become almost independent of specific impulse, however, there will be an interest in multiple use engines which carry both the radiator required for high specific impulse and the pumps required for higher thrust at low specific impulse. Such ships can then take off on the highest thrust mode, and switch to the high specific impulse mode after orbital speed is attained. One example of the effect of carrying such extra radiator area, compared to designing an optimum engine for each specific impulse, is shown in Figure 13. It is practical to consider such two-phase engines. Figures 12 and 13 are not consistent. Figure 12 was derived assuming substantially higher thrust-weight ratios than even the peak values of Figure 13, and no attempt was made to analyze two-phase engine operation. A more accurate derivation of Figure 13, followed by a re-derivation of Figure 12, would yield more accurate spaceship design parameters.

One other interesting fact arises from the gaseous fission thrust-weight values presented. It is normally considered that such rockets would use hydrogen as a propellant. As long as radiators could not be used to improve gaseous fission reactor specific impulse due to their weight, it was still important to use hydrogen, both because of the relatively high specific impulse it provides for a given structural temperature, and also the high heat capacity, and, therefore, degree of regenerative cooling which it permits for a given structural temperature. It is clear that these restrictions do not apply for high temperature

radiators. It is thus interesting to look at more suitable propellants from the point of view of cost, density, and space storability. Many substances come to mind, such as diborane, ammonia, or the most convenient of all, water. Availability on other planets might well become the single governing item on propellant selection. The performance of a gaseous fission reactor operating on water, compared to operating on hydrogen, is shown approximately in Figure 14. This curve does not utilize an accurate estimate of enthalpy of water at high temperatures, but is probably a lower limit since complicated dissociation modes at high temperatures were ignored. In addition, allowance was not made for the fact that water pumps would be of considerably lighter weight than hydrogen pumps for these systems. It is clear that the water rocket should be actively pursued.

CONCLUSIONS

The capabilities of nuclear rockets are such that they possess great potential for future manned space flights.

Utilization of solid core nuclear fission rockets of the Rover type as upper stages on chemical vehicles gives substantial performance improvements. This development is justified.

Total velocities of several hundred thousand feet per second, with payloads sufficiently large for manned operations, will be required for future solar system exploration. Gaseous fission rockets possess the theoretical capability of achieving this performance economically.

The single-stage vehicles of high performance potentially achievable with gaseous fission rockets should be eminently suitable for manned exploration, due to overall vehicle simplicity, economy of operation, and versatility. Emphasis on very high speed capability is a better way to assure long useful life than emphasis on very large payload capability.

Relatively new concepts in gaseous fission reactor design involving the heating of the propellant by radiation from the fission plasma show promise as reactor design concepts. High temperature radiators appear to be the key to the achievement of high thrust-weight ratios at high specific impulses with these systems. Appropriate research is desirable in these areas.

The improvement in thrust-weight ratio with high temperature radiators re-opens the question of propellants other than hydrogen. Water, in particular, should be investigated.

Research and development efforts should, in general, be concentrated where the potential pay-off is greatest. Single stage, very high velocity spaceships are almost the toughest competitors imaginable in the solar arena. To be unprepared for their advent could be somewhat more than disadvantageous.

REFERENCES

1. Finger, Harold B., Nuclear Rockets and the Space Challenge. Astronautics, July 1961. Based on a talk presented at the ARS Space-Nuclear Conference. Oak Ridge National Laboratory, Gatlinburg, Tennessee, May 3, 1961.

2. Hallet, R. W., Jr., Matheson, W. E., Trapp, R. F. RITA, The Reusable Interplanetary Transport Approach to Space Travel. Douglas Aircraft Engineering Paper No. 1198, ARS Preprint 2042-61, Space Flight Report to the Nation, New York City, October 1961.

3. Hunter, M. W., Matheson, W.E., Trapp, R. F. The Potential of Nuclear Space Transport Systems. Douglas Aircraft Report SM-37427, March 1960.

4. Hunter, M. W. The Cost of Lunar Travel. Douglas Aircraft Engineering Paper No. 1122. Presented at International Congress and Exposition of Automotive Engineering, Detroit, Michigan, January 9 - 13, 1961.

5. Hunter, M. W., Trapp, R. F. Early Interplanetary Exploration with Nuclear Rockets. Douglas Aircraft Engineering Paper No. 1247. Presented at Japanese Rocket Society, Tokyo, Japan, August 28 - September 1, 1961.

6. Hunter, M. W., Matheson, W.E., Trapp, R. F. Direct Operating Cost Analysis of a Class of Nuclear Spaceships. Douglas Aircraft Engineering Paper No. 1016. Presented at the 11th Congress, International Astronautical Federation, Stockholm, Sweden, August 15 - 20, 1960.

7. Weinstein,H. and Ragsdale, R. G. A Coaxial Flow Reactor - A Gaseous Nuclear-Rocket Concept. ARS Preprint 1518-60. Presented at 15th Annual American Rocket Society Meeting, Washington, D.C., December 5 - 8, 1960.

8. McKee, J.W. The Glow-Plug Gas-Core Reactor. Presented at Symposium on Gaseous Fission Reactors, Jet Propulsion Laboratory, California Institute of Technology, Pasadena, California, April 26 - 27, 1962.

9. Meghreblian, Robert V. Gaseous Fission Reactors for Spacecraft Propulsion - Technical Report No. 32-42. Jet Propulsion Laboratory, California Institute of Technology, Pasadena, California, July 6, 1960.

10. Meghreblian, Robert V. Thermal Radiation in Gaseous Fission Reactors for Propulsion-Technical Report No. 32-139. Jet Propulsion Laboratory, California Institute of Technology, Pasadena, California, July 24, 1961.

11. Meghreblian, R. V. Prospects for Advanced Nuclear Systems. Volume VII, Astronautica Acta, 1961.

12. Hallet, R. W., Jr., McKee, J. W., Faller, R. J. Operational Use of Gase Core Nuclear Reactor Propulsion Systems in Large, Manned, High-thrust Spacecraft. Douglas Aircraft Engineering Paper No. 1200. Presented at 10th Annual Meeting of the German Rocket Society, Bremen, West Germany, September 23 - 25, 1961.

13. Meghreblian, Robert V. Gaseous Fission Reactors for Booster Propulsion. Journal of the American Rocket Society, Volume 32, No. 1, January 1962.

14. Konecci, E. B., and Trapp, R. F. Calculations of the Radiobiologic Risk Factors in Nuclear-Powered Space Vehicles, Aerospace Medicine, July 30, 1959. Also Douglas Aircraft Engineering Paper No. 711.

15. Trapp, R. F., and Konecci, E. B. Shielding and Nuclear Propulsion. Presented at American Astronautical Society Western Meeting, Los Angeles, California, August 1959. Also Douglas Aircraft Engineering Paper No. 808.

16. Hunter, M. W., and Tschirgi, J. M. Advantages of High-Thrust Space Vehicles. Astronautics, February 1960. Presented at 14th Annual Meeting, American Rocket Society, Washington, D. C., November 15 - 19, 1959. Also Douglas Aircraft Engineering Paper No. 912.

FIGURE 1

CARGO TRANSPORT COST
(SINGLE STAGE VEHICLES)

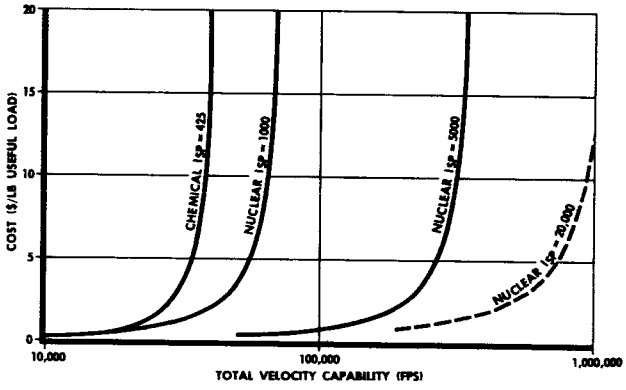

FIGURE 2

FUTURE VEHICLE REQUIREMENTS

PROPULSION TYPE	SPECIFIC IMPULSE	VELOCITY PER STAGE	NO. LAUNCHES TO ACHIEVE 60K FPS	120K FPS	180K FPS
CHEMICAL	425	30,000	18	324	5832
SOLID CORE NUCLEAR	1000	60,000	1	15	225
GASEOUS CORE NUCLEAR	5000	300,000	1	1	1

FIGURE 3

COST OF PROPELLANT FOR FISSION REACTOR ROCKET

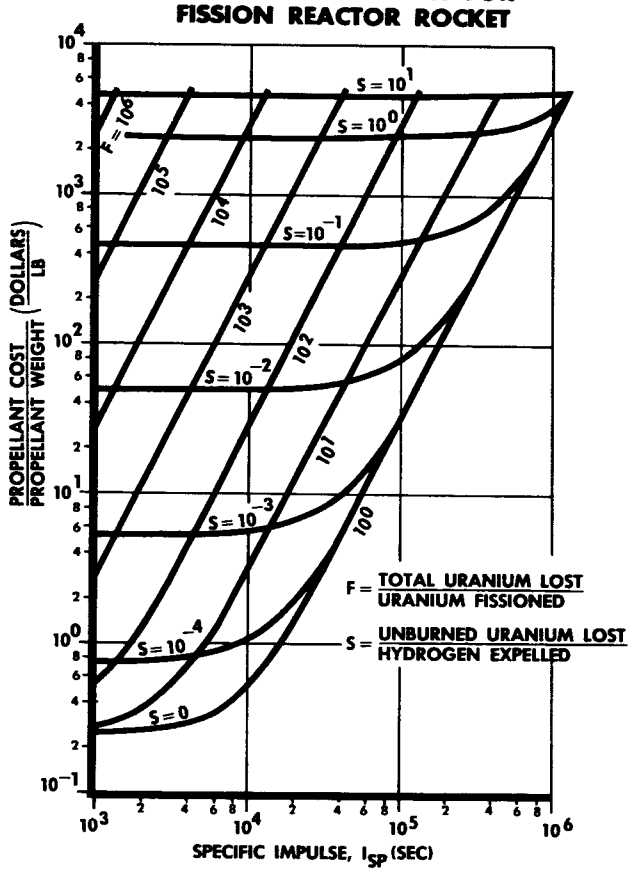

FIGURE 4

USEFUL LOAD FRACTION

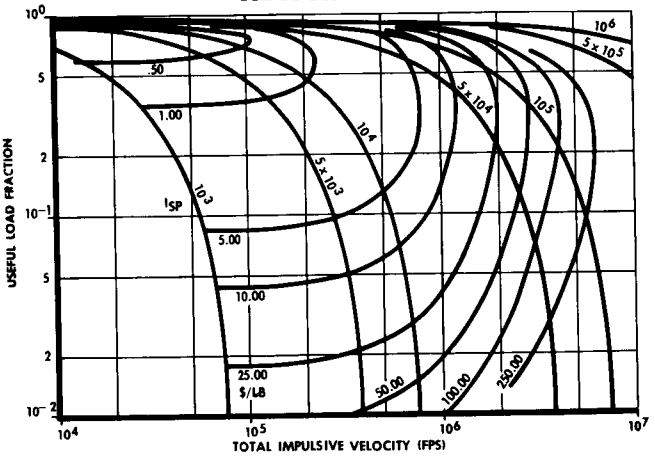

FIGURE 5

SPECIFIC IMPULSE VARIATION WITH REGENERATIVE COOLING ONLY

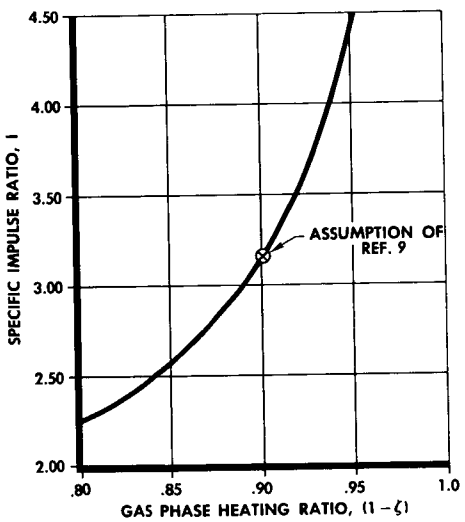

FIGURE 6

EFFECT OF REFLECTOR THICKNESS ON REACTOR PERFORMANCE

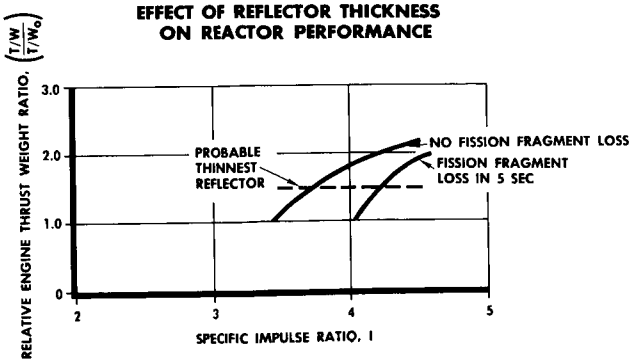

FIGURE 7

INFLUENCE OF RADIATOR POWER ON SPECIFIC IMPULSE

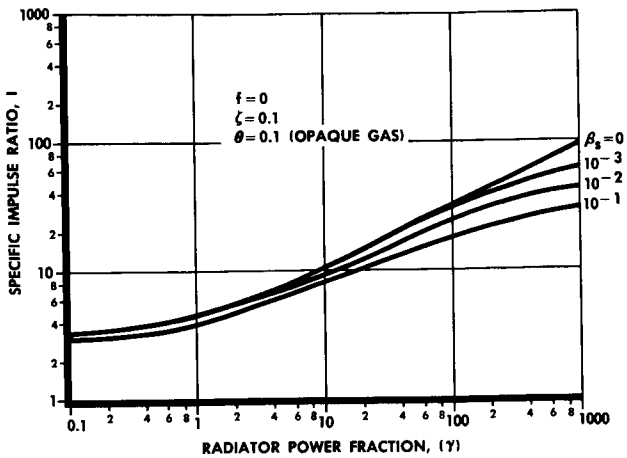

EFFECT OF RADIATOR TEMPERATURE ON ENGINE THRUST TO WEIGHT RATIO

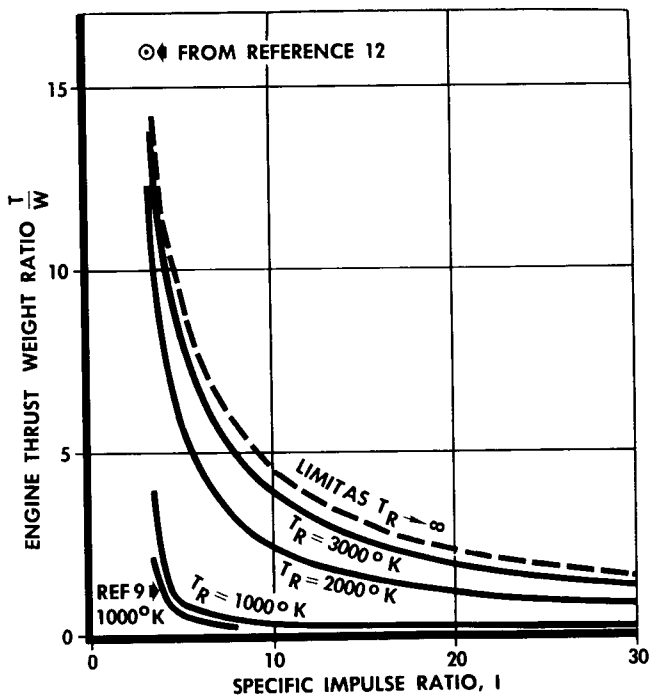

FIGURE 9

COMPARISON OF TWO REACTOR CONCEPTS

(RADIATOR AND REFLECTOR TEMPERATURE = 2000 °K)

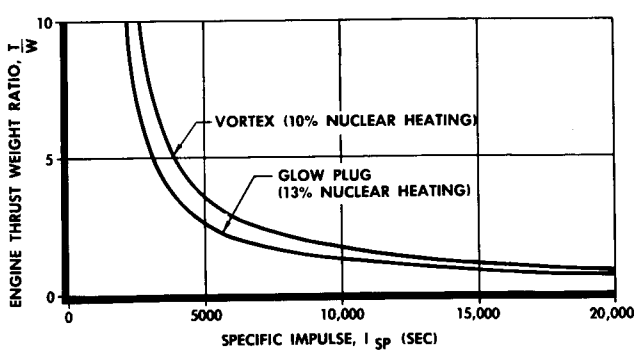

FIGURE 10

EFFECT OF THERMAL RADIATION LOAD TO SOLID ELEMENTS

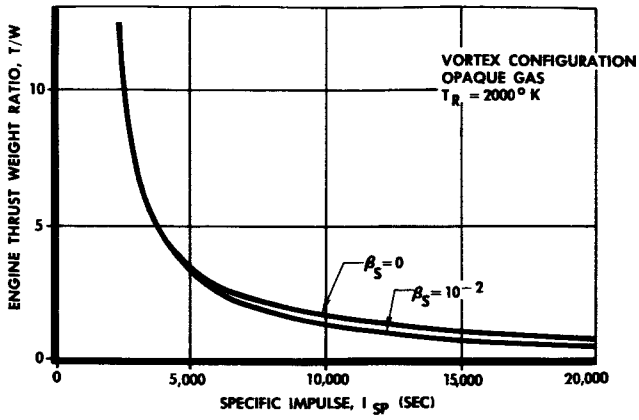

FIGURE 11

PAYLOAD VELOCITY CAPABILITIES CHEMICAL & NUCLEAR VEHICLES

(PRACTICAL STAGING)

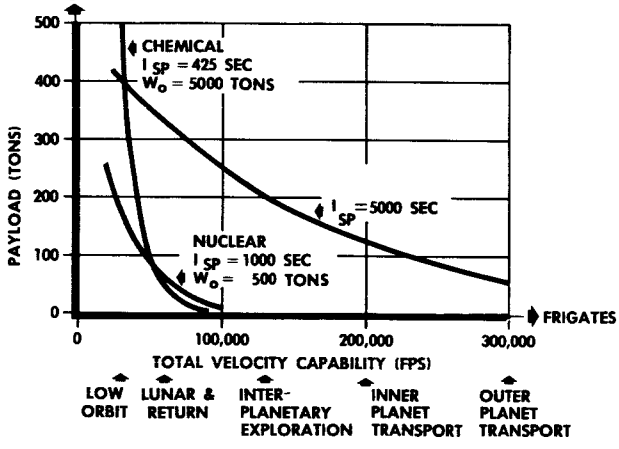

FIGURE 12

SPACESHIP DESIGN PARAMETERS

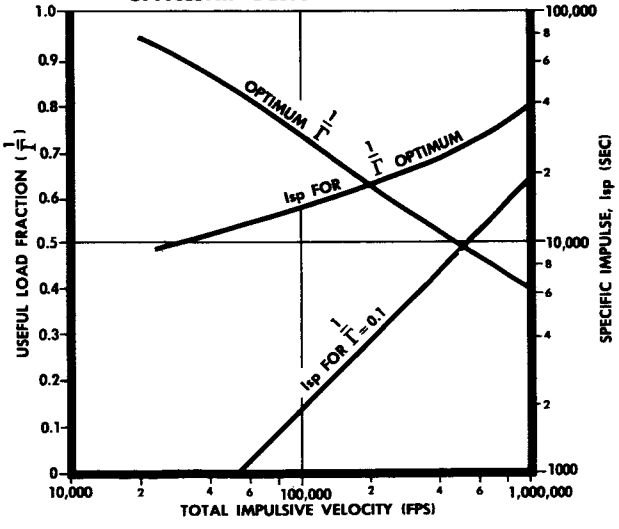

FIGURE 13

EFFECT OF TWO PHASE OPERATION ON ENGINE THRUST WEIGHT RATIO

T_R = 2000° K

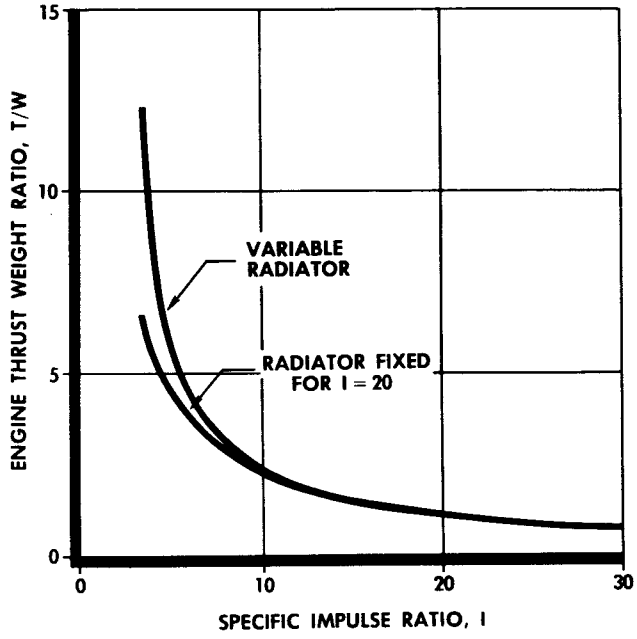

FIGURE 14

ENGINE PERFORMANCE FOR HYDROGEN AND WATER PROPELLANTS

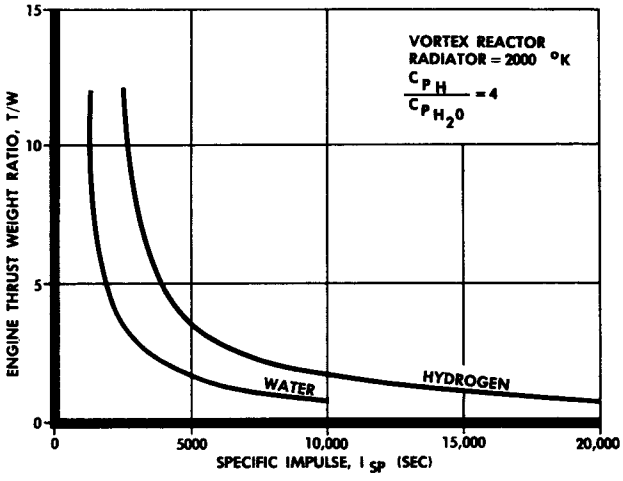

MANNED LUNAR LANDING VIA RENDEZVOUS

Fred E. Digesu
Chief, Advanced Studies Branch
Astrionics Division
George C. Marshall Space Flight Center

In any mission description, the vehicles, the flight profiles, and the astrionics hardware to implement the mission are all tightly interwoven things. A final result evolves only after many iterations to the solution are made. This paper will describe one of these iterations in the Saturn C-5 Earth Orbit Rendezvous approach to the Manned Lunar Landing Program. Since the iteration to be described in an n^{th} one, there exists some basis for the hope that the perturbation from the final solution is small.

This paper is not concerned with the landing itself, but only with those operations leading to injection of the space craft into the lunar transfer trajectory. However, as is to be expected, it is the target conditions which set the pace for the overall operation. The entire operation must be sized to culminate at a time and place which places the lunar target in an attainable position. The procedure would call for a burst of activity lasting over a relatively short time as compared to the long and extensive preparations leading up to it.

The activity must be aimed at the opening of the lunar "launch window". Figure 1 illustrates the variation in the velocity increment required to launch a vehicle into a lunar transfer trajectory from a 485 kilometer earth orbit. The minima are at irregularly spaced intervals and are a function of the inclination of the lunar and the earth satellite planes and of the position of the moon in its orbit around the earth (i.e., the day of the month). In an operations analysis these spacings will influence the number of vehicles on the launch pad (primary and back-up), their state of readiness, the firing rate, and also the flight profile to be chosen. Whether it is decided to go by "connecting" or by "tanking" mode, the objective must be to get the spacecraft in the launch ready state at the opening of one of these launch windows. It may be desired that the first vehicle be capable of remaining in a functionally capable state even after bridging one or more of the gaps between the windows. This consideration will influence the design of the vehicles as well as the operational modes to be designed into the flight control hardware. For example, a sleep switch may be desirable from the standpoint of savings in battery weight.

The Flight Profile

With the end objective in mind, let us start to define the flight profile.

First it can be established that the "parking orbit" technique is the desired approach. This is dictated by the possible lift-off delay of the chaser vehicle. If launch from other than the equator is considered, there is a two fold constraint upon the lift-off time. These are:

1. The chaser and target orbits are coplanar ("dog-leg" requirement).

2. That chaser and target meet at the same point in space and time.

(Phase Requirement)

It is possible to meet both of these requirements (even when launch is not in the equatorial plane) by so called "Rendezvous Compatible Orbits". These are orbits whose periods are an integral division of the earth sideral period. Thus, they can be designed such that, for instance, once a day the satellite target will appear over a given earth subpoint. Since, however, this condition holds for only an instant of time, a "direct ascent" rendezvous would presume zero launch delay time. The velocity penalty for lift-off delay can be placed into two categories.

1. That required to "dog-leg back into the target plane".

2. That required to "catch up" with the target.

The "dog-leg" requirement versus time (plotted in terms of velocity increment, ΔV) for a chaser launched at 90 degrees azimuth from Cape Canaveral into a 225 kilometer orbit inclined at 28.3 degrees to the equator is shown in Figure 2. If a variable azimuth launch for the second vehicle is presumed, the curve takes the shape indicated in Figure 3.

In the second category, the "catch up" maneuver manifests itself in essentially an off optimum ascent trajectory for the second vehicle. The ΔV penalty versus time for launch delay of a vehicle to meet the target depends on the ability to optimally guide to the desired end conditions. For one minute launch delay the cost can be of the order of 80 m/sec to meet a target in a 250 n. mi. orbit.

It can be seen that the second constraint poses a stiff requirement upon lift-off delay, while the first is a much more lenient restriction.

Since lift off delays are inevitable (the present best estimate for Saturn is that launch delays up to fifteen minutes are possible, even in the operational version, not considering the manned aspect) it is clear that launch into the plane of the first vehicle be the designing criterion and that other less expensive means be found for the phasing problem.

It turns out that a parking orbit for the chaser meets the requirements. If the orbits of the two vehicles are of different altitudes, the period difference automatically causes a catch up in phase. When the proper constellation is reached (Figure 4) the chaser can be injected into a Hohmann transfer ellipse to rendezvous with the target. Of course launch delays can occur even here, but these can be shown to be much less severe. Consider Figure 5. The ΔV required for transfer of the chaser from the lower to the upper orbit can be shown as a function of the central angle traversed (from perigee) by the chaser. This can be translated into "lead angle" deviation from nominal by the target, which in turn (due to the difference in angular velocity of the two vehicles) can be plotted as ΔV penalty versus chaser launch delay time, as is shown in Figure 5.

A parking orbit for the chaser can therefore be established as a requirement.

The next consideration concerns the sequence of launchings, manned first or second? This has ramifications in tracking requirements as well as abort precautions for the manned vehicle, since a variable azimuth launch will be mandatory for the second vehicle.

There are, however, two primary factors to be considered.

1. That man should not be committed until as late as possible in the operation, and

2. The first vehicle may have a prolonged orbit stay time. This means that (a) it must be penalized with heavy insulation and micrometeorite protection, and (b) the possibility must exist for turning off all equipment so that weight savings in the primary power source can be attained. Thus, the unmanned vehicle should go first.

The question as to which vehicle (the manned or the unmanned) should do the orbital maneuvering would tend to indicate a profit in propellant if the lighter of the two were the chaser. Since the maneuvering will probably be done with auxiliary propulsion systems with lower specific impulse than the primary propulsion, and since the chaser will be required to take the penalty of the reserve ΔV's in the velocity budget, it would seem expedient not to thus burden the manned vehicle.

The desirability of the tanker being the chaser in the Tanking Mode can be established; while evidence seems to favor the R-1 vehicle being the chaser in the Connecting Mode, it is not quite so conclusive as in the Tanker case.

The point of view taken here is that the unmanned vehicle does the maneuvering and that this maneuvering in the terminal (that is, the actual rendezvous phase) is done under close radio and radar supervision of the manned vehicle. It is quite likely that the actual docking (that is, from the last few feet up to mating of the vehicles) will be done by "man across the loop".

We are now in a position to establish the operational flight profile.

The unmanned vehicle is launched into the lower parking orbit. The lead time over the opening of the Lunar Launch window will be determined by the nominal time required to ready and launch the second (manned) vehicle. The stay time in the parking orbit can vary from as little as an hour or two, to as much as ten days. This is, of course, a direct function of the firing rate at the cape, lift-off delay of the second vehicle (and thus the phasing which must be done) and the opening of the first and subsequent (if necessary) lunar launch window.

Provision will be made for a chaser "midcourse" maneuver. This midcourse correction is defined as that impulse which either (1) injects the chaser into the perigee of a Hohmann transfer up to target acquisition point, or (2) corrects the existing chasing ellipse so that chaser will come into nominal target acquisition conditions. Thus, it can be seen that the question of a circular versus elliptical parking orbit looses significance as far as guidance is concerned.

The manned vehicle will be placed into the higher orbit by a launch phase which injects it into the perigee of a transfer ellipse with a subsequent circularizing apogee kick. Ground tracking will establish the two ephemerides and ground computation will determine the time, magnitude, and the direction of the chaser midcourse impulse.

The chaser ascent ellipse is so designed that at nominal acquisition range of 40 kilometers the relative closing velocity is 63 m/s and the angular rate of the line of sight in inertial space is zero. See Figure 6. The guidance logic is to hold the line of sight rate zero (thus maintaining a collision course) while breaking the closing velocity to essentially zero at some small distance ahead of the target. It is to be noted that this breaking thrust is in actuality boosting the chaser into the higher energy orbit and for the normal case is essentially nothing but a well timed apogee kick.

Docking can be accomplished by allowing a small closing velocity to remain after the rendezvous thrust. Alternately, the chaser can be

brought to a virtual stop and the vehicles guided together under the close supervision of the man across the loop. In either case the touching velocities and the docking dynamics will be very much determined by the close in accuracy of the sensors and it is quite likely that some form of optical sensor, perhaps TV, will have to be used for this phase.

After docking, and loxing in the case of the tanking mode, the space craft must be checked out and counted down for orbital launch. Although a given lunar launch window may be open for several hours, the actual orbital launch point will be optimum at only one place in the orbit. Specifically this means that inside of the larger launch window are smaller windows (in the order of several minutes) which occur once each orbit. The actual launch must take place inside these smaller launch windows, and since these windows appear at about one and a half hours intervals, provision for extended launch ready standby as well as updating of the guidance system must be made. This will be required if holds are encountered which cause misses of these windows.

Velocity Budgets and Error Analysis

Earlier in this paper, mention was made of the propellant contingency which must be designed into the chaser. This section will point out those places where tolerances must be designed in and will indicate the propellant contingency requirement in the form of a velocity budget. A detailed description of the analyses made is beyond the intent of this paper. However, it is felt that a description of the overall approach which was taken to establish the maneuver velocity budget would be informative. The impact of the analysis upon vehicle design can be felt when it is realized that the chaser burns about 100 lbs. of propellant per meter per second velocity increment.

Error sources which contribute to the velocity budget must be analyzed in detail and in themselves are an interplay between operational analyses, guidance scheme and hardware inaccuracy, navigational uncertainties, and the influence of physical phenomena upon the flight profile.

Under the heading of operational analysis we have the earth and orbital launch window influence. The effect of launch delay in the required velocity has already been shown. It remains that a figure of merit for the launch operation be established. This in itself requires a detailed evaluation of checkout and countdown procedures. The degree to which automation is involved in the countdown must be evaluated, among other things against the number of operations to be done, the number of checks which are to be made, and the length of time the various subsystems can be expected to reliably remain in the launch ready state. As has been already mentioned, the tolerance upon Saturn launch is established (at least for purposes of mission analysis) as 15 minutes. The probability of liftoff is a constant over the 15 minute interval.

A mitigating circumstance is that the Saturn ascending burn is long enough (that is, the central angle traversed is large enough) so that the maneuver of doglegging on the way up begins to pay off. In other words, the turning is done at the relatively lower velocities and, as is indicated in Figure 7, an overall saving in ΔV can be made. This is being investigated within the framework of the Saturn path adaptive guidance concept and thus the notion of variable azimuth launch begins to include the idea of some variation in the azimuth during Saturn boost to injection.

Two things come immediately to mind under the heading of the influence of physical phenomena. These are (1) the effect of atmospheric drag upon the lower vehicle, and (2) the difference in the nodal regression rates of the orbital planes of the upper and the lower vehicles.

The lower orbital altitude is a compromise between vehicle performance, remaining atmospheric drag, and the desirable difference in period between the upper and the lower venicles (i.e, the "stalking" rate). At the lower orbits considered, the air density is appreciable but its magnitude is unknown to the extent that calculations of orbit lifetime must be given a tolerance of 50%. This is an error source which must be accounted for in the velocity budget.

The regression of the nodes of satellite is, as is well known, due to anomalies in the attracting body's gravitational field. For the earth these regression rates are a function of the inclination of the satellite and earth equatorial plane and of the orbital altitude of the satellite, and can be fairly well predicted. Figure 8 shows the nodal regression rate as a function of altitude for an orbital inclination of 28.3 degrees to the equator. This shows that the difference in rates can lead to an inclination of 1.1 degrees between Target and Chaser orbital planes for a stay time of one day. This, of course, translates into a dogleg requirement for the chaser which must be budgeted.

The velocity budget for hardware and scheme errors can be determined by the following approach.

An analysis of the accuracy with which the target and chaser can be injected into their respective orbits is made after error distributions of the guidance components and of the guidance schemes have been established. This will indicate what must be added to the nominal ΔV for transfer between the nominal orbits.

Next an error analysis is made of the accuracy with which ground tracking can establish the ephemerides of the two vehicles. A correlation of the accuracy with which the chaser

hardware can deliver the midcourse maneuver impulse is then made to establish the accuracy with which the chaser can be injected into its transfer ellipse. This is in turn reflected into the deviation of the chaser from its nominal at the target radar acquisition point. Error in target orbit determination can be analyzed as being deviation of the chaser state variables from nominal at the acquisition point.

Having now established an error space at radar acquisition point, the error analysis proceeds to establish the velocity budget for the terminal phase. These errors fall into the two categories of hardware and scheme. Since the rendezvous guidance is basically a homing technique, the errors are convergent and the attainable end conditions (docking velocity zero at a given relative range) are directly functions of the close up sensor accuracy. Accuracy at the longer ranges (as well as dispersions from nominal conditions at acquisition) can be visualized as causing extraneous maneuvering which results in over expenditure of velocity increments.

The accuracy required of the sensors close up can be analyzed in a docking dynamics study as shown in Figure 9.

Let it be hypothesized that the conditions necessary for docking are that the cone tip and velocity vector of the chaser enter the cone of the target. (These are, of course, not sufficient conditions since relative closing velocity, cone angle, and friction coefficients will determine the cone penetration and thus the actual docking and latching).

The hypothesized necessary conditions can be thought of as guidance criteria which can be used to define the sensor inaccuracies (as well as the minimum controllable impulse and cutoff dispersion) as illustrated in Figure 10.

Hardware Instrumentation

This section will discuss the various items of the Saturn instrumentation package and their functional use in the given flight profile.

Consider the tanking mode and the unmanned tanker first launch. The instrumentation package is contained in the instrument unit shown in Figure 11. A typical component layout is shown in block diagram form in Figure 12, where the basic Saturn inertial guidance and control system is enclosed by a dotted line.

The inertial unit is a four gimbal, full angular freedom, platform stabilized in inertial space by three air bearing gyros. Three mutually orthogonal pendulum integrating gyro accelerometers are mounted on this stabilized reference frame.

The guidance computer will be an all solid state, core memory type, general purpose computer. Triple redundancy with voting circuitry will be employed in order to ensure reliability of operation. In addition to the guidance computation, one of the major functions of the computer will be its role in the orbital checkout procedure.

The Guidance Signal Processor is the input/output box for the computer. The computer communicates with this device only. It contains resolvers to transform the Euler angles computed in the computer into direction cosines which the platform gimbal resolvers translate to the missile body axes. In addition it can be seen that the GSP accepts and distributes the intelligence commands generated on board or externally. It thus can be thought of as the central distribution point for the guidance and control signal flow.

The control computer contains the servo electronics which position the control elements (engine throw angle, attitude control jets, etc.) in pitch, yaw, and roll in accordance with the guidance commands and the error signals resolved from the platform gimbal angles. The control computer also contains the electrical shaping networks required for rigid and flexual mode stability.

Injection of the tanker into the lower parking orbit is done by the basic Saturn Guidance and Control system just described.

In order to save power in the parking orbit, all subsystems except a command receiver and a tracking beacon are de-energized and the vehicle is permitted to tumble randomly. Should the required orbit stay time turn out to last for several days, a check is maintained on the operational hardware by subjecting the vehicle to an orbital checkout at least once a day. The orbital checkout will be initiated by ground request through the digital radio command link. See Figure 13.

The inputs to the high capacity solid state multiplexer contain all the analog channels to be used in the checkout. The multiplexer samples each channel at preselected rates. An analog to digital converter in the Vehicle PCM Telemetry System digitizes each analog data sample and formating and logic circuitry interlaces other data that originated in digital form in the vehicle. Thus, each channel of data in the vehicle becomes available for analysis by the spaceborne computer, transmission over the telemetry system and/or recording in the vehicle for later playback.

The spaceborne computer is programmed with sub-routines for total vehicle checkout, stored conditions for channel analysis, and self checking sub-routines. The checkout sub-routines would perform such test as, for example, "static" tests (tank pressures, temperatures, vehicle

voltages, etc.) "dynamic" tests (such as hardware response to test stimuli) and tests of the control and guidance systems (torquing of rate gyros, accelerometer readouts, etc.). The computer would analyze the results for a go-no-go decision. In case of a "no-go", some fault isolation could be done by prestored analytical subroutines. In other cases these analytical programs will have to be transmitted up from the ground and into the computer through the radio command link.

The manned vehicle is now launched into orbit. Again the primary launch guidance will be the inertial system. Injection will be into a "coast up" ellipse which has an apogee at the operational orbit attitude. The inertial system will compute and direct the velocity increment for the circularizing kick in the apogee. This will be verified for the astronauts by ground tracking and command prior to execution.

Once in orbit, the ephermis of the manned vehicle will be established by ground tracking. The time, direction, and magnitude of the velocity increment required for chaser midcourse will be computed on the ground.

A command to reactivate subsystems is transmitted to the chaser via its radio command link. The chaser goes into a search mode until its horizon sensors acquire earth. Once this is done the platform is re-erected by the gyro compassing technique and the ground computed impulse is transmitted into the chaser guidance computer through the radio command link. Thus, at the proper time the inertial equipment on the chaser supervises and measures the required impulse which will place the chaser at the acquisition point.

The target radar acquires the approaching chaser near the acquisition point. The radar measures the relative range, range rate, and bearing angle of the chaser. This information is displayed in the capsule, while at the same time it is processed in the target computer where the stored guidance logic transforms it into velocity increment commands for the chaser. These commands are sent to the chaser where they are executed in much the same manner as was the midcourse maneuver. Since the capsule control the command link, guidance override and preemption of the command function will be at the descretion of the astronaut.

The docking maneuver has so far been, of necessity, studied by analog computer and scale models. In this way the impact loading on the docking structures, mating mismatches, and vehicle dynamics can be studied in terms of the threshold inaccuracies of the docking sensors. Undoubtedly for the first times in orbit the astronauts will have available much more information than will actually be needed. Radar, optics, TV, even a window or a periscope! The instrumentation and actual techniques as well as man's effect across the loop can evolve only after actual docking experimentation in orbit.

Finally it might be mentioned that by and large the job of earth orbital rendezvous can be done with relatively conventional approaches to the guidance and control hardware. Only modest (at most) advances are called upon. More exotic implementations like cryogenic gyros and computers can be left for later developmental effort. Such exotic systems, while quite attractive for talking purposes, are not considered safe risks for hard planning purposes as yet.

It is considered that the overriding philosophy for the on board instrumentation will be a requirement for reliability and long life. The greatest advances will be required in these areas and it is expected that design and testing of components will be geared to this goal.

References

1. E. D. Geissler and W. Haeussermann, "Saturn Guidance and Control", Missiles and Rockets Magazine, dated February, 1962.

2. Lockheed/STL, "Orbital Docking Test Study", Contract Number NAS-8-864, dated July, 1961.

3. J. Jensen, G. Townsen, J. Kraft, J. Kork, "Design Guide to Orbital Flight", McGraw Hill Book Company, Inc., dated 1962.

4. W. E. Minor and D. H. Schmeider, "The Path-Adaptive Mode for Guiding Space Flight Vehicles", ARS Guidance, Control and Navigation Conference, Stanford University, August 7-9, 1961.

5. W. G. Thornton, "The Simulation of Docking Dynamics", MSFC Inter Office Memo, dated April 9, 1962.

6. J. Harden, Jr., "Minimization of the Angle Between Target and Chaser Orbital Planes with Reference to Chaser Launch Time Variations", MSFC Technical Memo, MTP-ASTR-A-62-3, dated January 30, 1962.

7. R. Weber, W. Pauson, and R. Burley, "Lunar Trajectories", NASA Technical Note D-866, dated August 1961.

8. J. Ladner and F. Speer, "Orbital Lifetimes of Tanker and R-Vehicles", MSFC Internal Memoranda data February 15, 1962, March 6, 1962, and March 26, 1962.

9. P. J. deFries, "Saturn C-5 Flight Profile for Rendezvous", Astronautics Magazine, dated April, 1962.

10. Georg von Tiesenhausen, "Engineering Problems of Orbital Operations", Astronautics Magazine, dated April 1962.

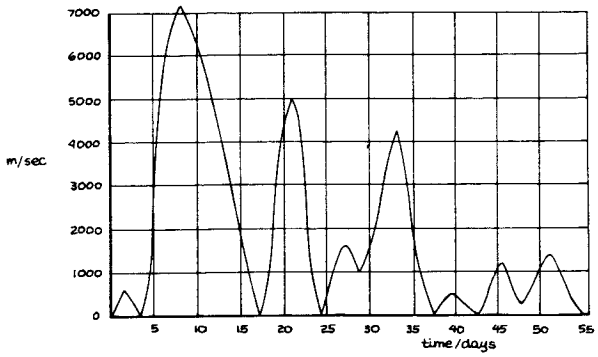

FIGURE 1

VELOCITY REQUIREMENT OVER NOMINAL FOR DEPARTURE FROM EARTH ORBIT TO MOON. LUNAR ORBIT INCLINATION 18.50°, EARTH ORBIT ALTITUDE 485 KM. EARTH ORBIT INCLINATION 30°

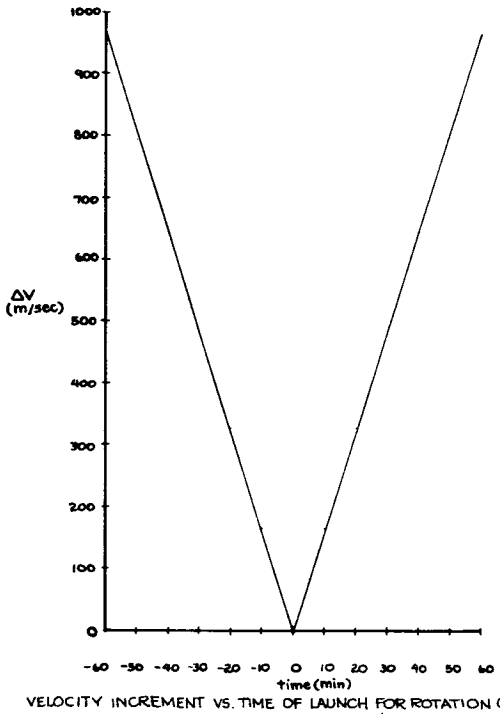

FIGURE 2

VELOCITY INCREMENT VS. TIME OF LAUNCH FOR ROTATION OF A 225 KM ORBIT INTO THE DESIRED ORBITAL PLANE (NON VARIABLE LAUNCH AZIMUTH)

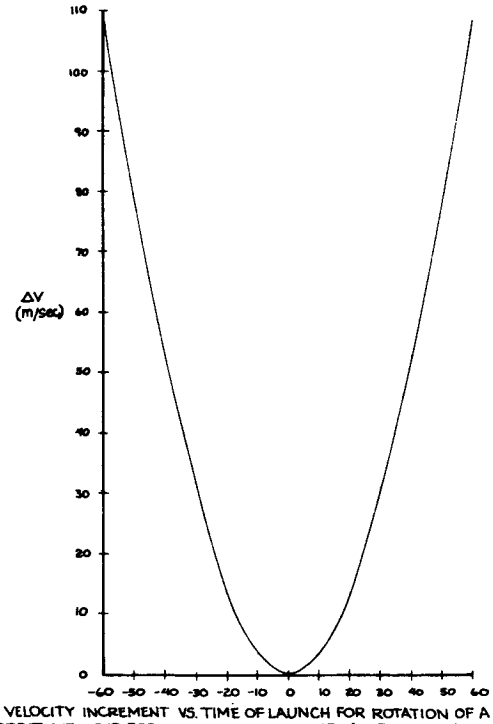

VELOCITY INCREMENT VS. TIME OF LAUNCH FOR ROTATION OF A 225 KM ORBIT INTO THE DESIRED ORBITAL PLANE (VARIABLE LAUNCH AZIMUTH)

FIGURE 3

ORBIT TRANSFER CONSTELLATION

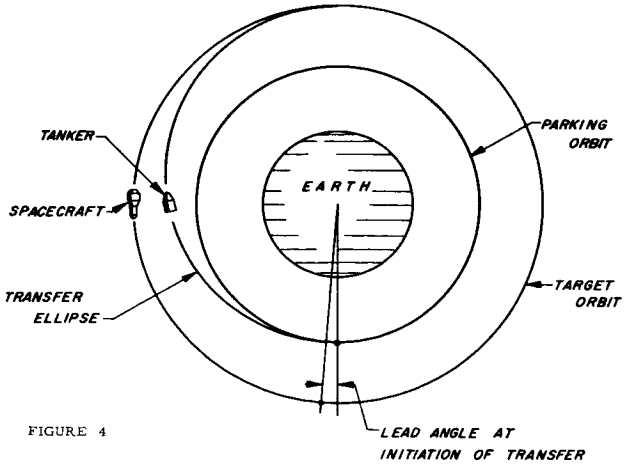

FIGURE 4

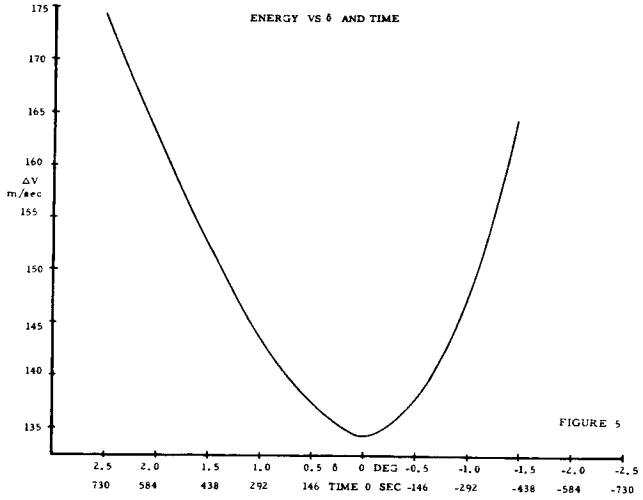

FIGURE 5

RENDEZVOUS MANEUVER

FIGURE 6

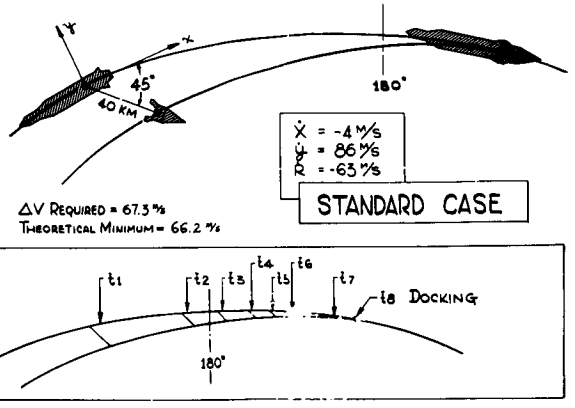

ACQUISITION CONDITION (t-0)

-.06 °/SEC. $< \omega_p <$ +.06 °/SEC.

-.06°/SEC $< \omega_y <$ +.06 °/SEC.

20 KM $< R <$ 60 KM

-100 M/S $< \dot{R} <$ -45 M/S

t	SEC	EVENT	$\dot{R}$ (M/S)
t_0	C	ACQUISITION	-63
t_1	600	BRAKING PHASE BEGINS	-67
t_2	626	FIRST ω_p CORRECTION BEGINS	-34
t_3	637	FIRST ω_p CORRECTION ENDS	-20
t_4	650	BRAKING PHASE ENDS	-.50
t_5	652	SECOND ω_p CORRECTION BEGINS	-.50
t_6	656	SECOND ω_p CORRECTION ENDS	-.49
t_7	760	ω_p CORRECTION FOR < 1 SEC	-.50
t_8	769	DOCKING	-.51

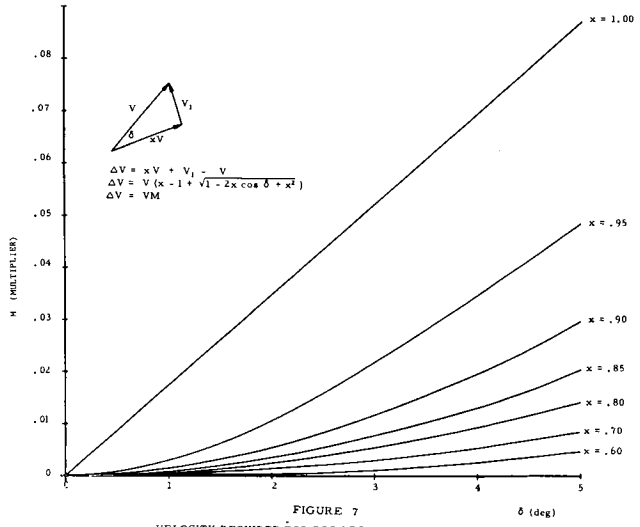

FIGURE 7

VELOCITY REQUIRED FOR DOG LEG DURING ASCENT

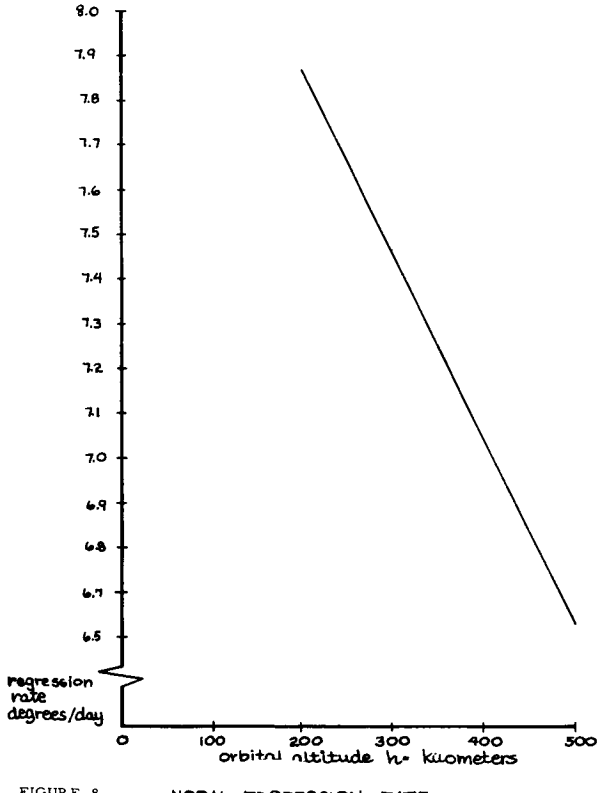

FIGURE 8

NODAL REGRESSION RATE VS. ORBITAL ALTITUDE (i = 28.3°)

DOCKING GUIDANCE ANALYSIS

FIGURE 9

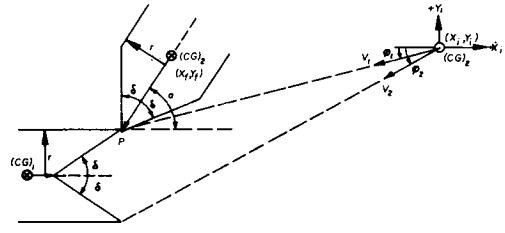

I DOCKING CRITERIA

A. POINT P LIES WITHIN DOCKING CONE AT INITIAL CONTACT

B. EXTENDED VELOCITY VECTOR OF CHASER $(CG)_2$ PENETRATES CONE

II ANALYSIS

$$\left.\begin{aligned} X_f &= X_i + (Y_f - Y_i)\frac{\dot{X}_i}{\dot{Y}_i} \\ Y_f &= Y_i + (X_f - X_i)\frac{\dot{Y}_i}{\dot{X}_i} \end{aligned}\right\} \quad (1)$$

$$\tan\varphi = \frac{\dot{Y}_i}{\dot{X}_i} \qquad (2)$$

III APPLYING CRITERIA

A. LIMITING POSITION OF (X_f, Y_f) IS ALONG ANGLE $\alpha = 90 - \delta$ WITH P WITHIN THE CONE

B. $\tan\varphi_1 = \frac{Y_{f1} - r}{X_i} = \frac{\dot{Y}_{f1}}{\dot{X}_i}$

$\tan\varphi_2 = \frac{Y_{f2} + r}{X_i} = \frac{\dot{Y}_{f2}}{\dot{X}_i}$

WHERE $\dot{Y}_{f1} \leq \dot{Y}_i \leq \dot{Y}_{f2}$ AND $\frac{\dot{X}}{X_i}(Y_i - r) \leq \dot{Y}_i \leq (Y_i + r)(\frac{\dot{X}_i}{X_i})$

$\dot{Y}_{f1} = (\frac{\dot{X}_i}{X_i})(Y_i - r)$

$\dot{Y}_{f2} = (\frac{\dot{X}_i}{X_i})(Y_i + r)$

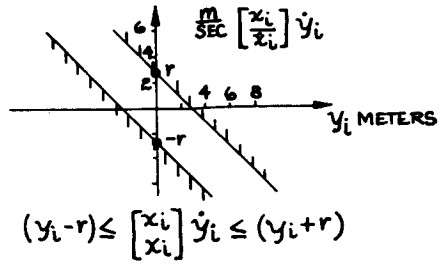

Example:

$r = 3$ meters
$\dot{x}_i = 0.5$ m/s
$y_i = 2$ meters

then if $x_i = 50$ meters
$\dot{y}_i$ can have 2 values
$\frac{1}{100} \leq \dot{y}_i$ (m/s) $\leq \frac{5}{100}$

FIGURE 10

PERMISSIBLE LATERAL VELOCITIES AND POSITIONS AS FUNCTIONS OF CLOSING VELOCITY AND POSITION

INSTRUMENTATION PACKAGE

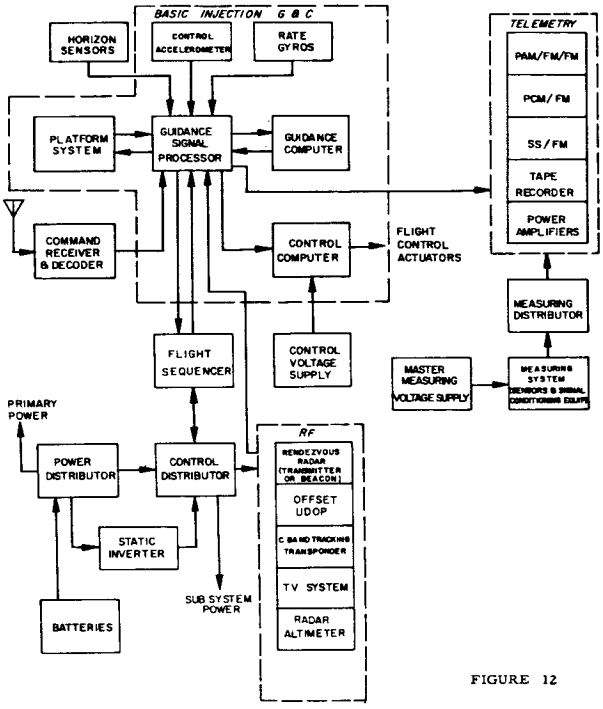

FIGURE 12

INSTRUMENT UNIT LOCATION

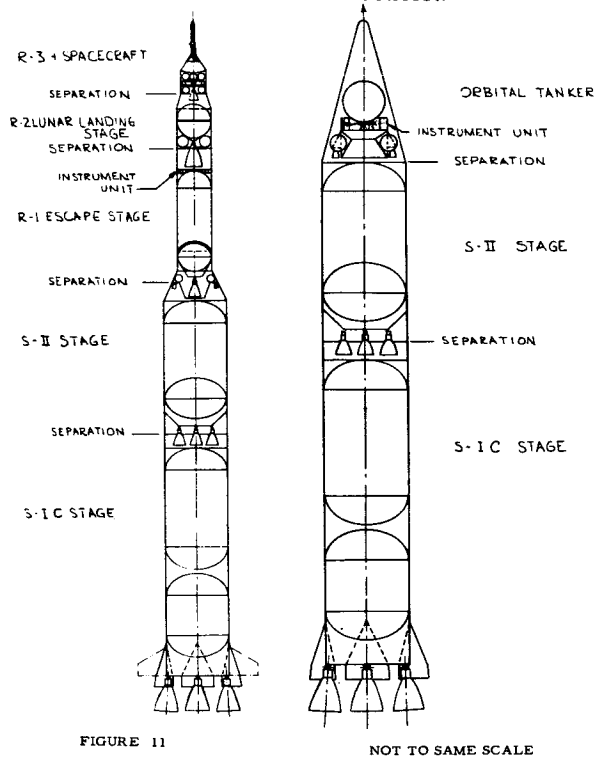

FIGURE 11

NOT TO SCALE

ORBITAL CHECKOUT

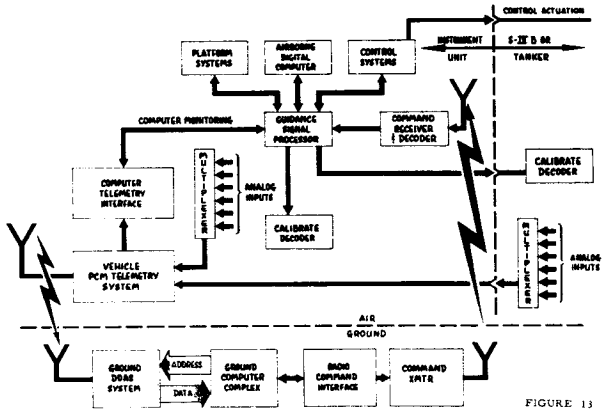

FIGURE 13

PILOT'S FLIGHT REPORT

by

John H. Glenn, Jr.
Astronaut

Manned Spacecraft Center
National Aeronautics and Space Administration

Introduction

The test objectives for the MA-6 mission of Friendship 7, as quoted from the Mission Directive, were as follows:

(1) Evaluate the performance of a man-spacecraft system in a three-orbit mission
(2) Evaluate the effects of space flight on the astronaut
(3) Obtain the astronaut's opinions on the operational suitability of the spacecraft and supporting systems for manned space flight

These are obviously broad objectives. Previous papers have described in some detail the operation of the spacecraft systems and, to a degree, man's integration with these systems.

My report is concerned mainly with those items in all three objectives where man's observation capabilities provided information not attained by other means. It is in this type of reporting that a manned vehicle provides a great advantage over an unmanned vehicle, which is often deaf and blind to the new and the unexpected. My report, then, will stress what I heard, saw, and felt during the orbital flight.

Preparation and Countdown

Preparation, transfer to the launch pad, and insertion into the spacecraft went as planned. The technicians and I had been through the entry to the spacecraft many times.

As with every countdown, short delays were encountered when problems arose. The support for the microphone in the helmet, an item that had been moved and adjusted literally thousands of times, broke and had to be replaced. While the spacecraft hatch was being secured, a bolt was broken and had to be repaired. During this time I was busy going over my checklist and monitoring the spacecraft instruments.

Many people were concerned about my mental state during this and earlier delays, which are a part of preparation for a manned space flight. People have repeatedly asked whether I was afraid before the mission. Humans always have fear of an unknown situation - this is normal. The important thing is what we do about it. If fear is permitted to become a paralyzing thing that interferes with proper action, then it is harmful. The best antidote to fear is to know all we can about a situation. It is lack of knowledge which often misleads people when they try to imagine the feelings of a astronaut about to launch. During the years of preparation for Project Mercury, the unknown areas have been shrunk, we feel, to an acceptable level. For those who have not had the advantage of this training, the unknowns appear huge and insurmountable, and the level of confidence of the uninformed is lowered by an appropriate amount.

All the members of the Mercury team have been working towards this space flight opportunity for a long time. We have not dreaded it; we have looked forward to it. After 3 years we cannot be unduly concerned by a few delays. The important consideration is that everything be ready, that nothing be jeopardized by haste which can be preserved by prudent action.

The initial unusual experience of the mission is that of being on top of the Atlas launch vehicle after the gantry has been pulled back. Through the periscope, much of Cape Canaveral can be seen. If you move back and forth in the couch, you can feel the entire vehicle moving very slightly. When the engines are gimbaled, you can feel the vibration. When the tank is filled with liquid oxygen, the spacecraft vibrates and shudders as the metal skin flexes. Through the window and periscope the white plume of the lox (liquid oxygen) venting is visible.

Launch

When the countdown reached zero, I could feel the engines start. The spacecraft shook, not violently but very solidly. There was no doubt when lift-off occurred. When the Atlas was released there was an immediate gentle surge that let you know you were on your way. The roll to the correct azimuth was noticeable after lift-off. I had preset the little window mirror to watch the ground. I glanced up after lift-off and could see the horizon turning. Some vibration occurred immediately after lift-off. It smoothed out after about 10 to 15 seconds of flight but never completely stopped. There was still a noticeable amount of vibration that continued up to the time the spacecraft passed through the maximum aerodynamic pressure or maximum q, at approximately T+ 1 minute. The approach of maximum q is signaled by more intense vibrations. Force on the outside of the spacecraft was calculated at 982 pounds per square foot at this time. During this period, I was conscious of a dull

muffled roar from the engines. Beyond the high q area the vibration smoothed out noticeably. However, the spacecraft never became completely vibration free during powered flight.

The acceleration buildup was noticeable but not bothersome. Before the flight my backup pilot, Astronaut Scott Carpenter, had said he thought it would feel good to go in a straight-line acceleration rather than just in circles as we had in the centrifuge and he was right. Booster engine cut-off occurred at 2 minutes 9.6 seconds after lift-off. As the two outboard engines shut down and were detached, the acceleration dropped but not as sharply as I had anticipated. Instead, it decayed over approximately 1/2 second. There is a change in noise level and vibration when these engines are jettisoned. I saw a flash of smoke out the window and thought at first that the escape tower had jettisoned early and so reported. However, this flash was apparently deflected smoke coming up around the spacecraft from the booster engines which had just separated. The tower was jettisoned at 2 minutes, 33.3 seconds, and I corrected my earlier report. I was ready to back up the automatic sequencing system if it did not perform correctly and counted down the seconds to the time for tower jettisoning. I was looking at the nozzles of the tower rockets when they fired. A large cloud of smoke came out but little flame. The tower accelerated rapidly from the spacecraft in a straight line. I watched it to a distance of approximately 1/2 mile. The spacecraft was programmed to pitch down slowly just prior to jettisoning the tower and this maneuver provided my first real view of the horizon and clouds. I could just see clouds and the horizon behind the tower as it jettisoned.

After the tower fired, the spacecraft pitched slowly up again and I lost sight of the horizon. I remember making a comment at about this time that the sky was very black. The accerelation built up again, but as before, acceleration was not a major problem. I could communicate well, up to the maximum of 7.7g at insertion when the sustainer-engine thrust terminates.

Just before the end of powered flight, there was one experience I was not expecting. At this time the fuel and lox tanks were getting empty and apparently the Atlas becomes considerably more flexible than when filled. I had the sensation of being out on the end of a springboard and could feel oscillating motions as if the nose of the launch vehicle were waving back and forth slightly.

Insertion into Orbit

The noise also increased as the vehicle approached SECO (sustainer engine cutoff). When the sustainer engine cutoff at 5 minutes, 1.4 seconds and the acceleration dropped to zero, I had a slight sensation of tumbling forward. The astronauts have often had a similar sensation during training on the centrifuge. The sensation was much less during the flight, and since the spacecraft did pitch down at this point it may have been a result of actual movement rather than an illusion.

There was no doubt when the clamp ring between the Atlas and the Mercury spacecraft fired. There was a loud report and I immediately felt the force of the posigrade rockets which separate the spacecraft from the launch vehicle. Prior to the flight I had imagined that the acceleration from these three small rockets would be insignificant and that we might fail to sense them entirely, but there is no doubt when they fire.

Immediately after separation from the Atlas, the autopilot started to turn the spacecraft around. As the spacecraft came around to its normal aft viewing attitude, I could see the Atlas through the window. At the time I estimated that it was "a couple of hundred yards away." After the flight an analysis of the trajectory data showed that the distance between the launch vehicle and the spacecraft should, at this point, be 600 feet. Close enough for a rough estimate. I do not claim that I can normally judge distance so close. There was a large sized luck factor in the estimate; nevertheless the facts do give an indication that man can make an adequate judgment at least of short distances to a known object in space. This capability will be important in future missions in which man will want to achieve rendezvous, since the pilot will be counted on to perform the final closing maneuver.

I was able to keep the Atlas in sight for 6 or 7 minutes while it traveled across the Atlantic. The last time I reported seeing it the Atlas was approximately 2 miles behind and 1 mile below the spacecraft. It could be seen easily as a bright object against the black background of space and later against the background of earth.

Orbit

The autopilot turned the spacecraft around and put it into the proper attitude. After my initial contact with Bermuda I received the times for firing the retrorockets and started the check of the controls. This is a test of the control systems aboard the spacecraft. I had practiced it many times on the ground in the Mercury procedures trainer and the test went just as it had in the trainer. I was elated by the precision with which the test progressed. It is quite an intricate check. With your right hand you move the control stick, operating the hydrogen peroxide thrusters to move the spacecraft in roll, pitch, and yaw. With your left hand you switch from one control system to another as the spacecraft is manually controlled to a number of precise rates and attitudes.

This experience was the first time I had been in complete manual control, and it was very reassuring to see not only the spacecraft react as ex-

pected, but also to see that my own ability to control was as we had hoped.

Following this controls check I went back to autopilot control and the spacecraft operated properly on autopilot throughout the first orbit.

Thruster Problem

Because of a malfunction in a low-torque thruster at the end of the first orbit, it was necessary to control the spacecraft manually for the last two orbits. This requirement introduced no serious problems, and actually provided me with an opportunity to demonstrate what a man can do in controlling a spacecraft. However, it limited the time that could be spent on many of the experiments I had hoped to carry out during the flight.

Flight Plan

The Mercury flight plan during the first orbit was to maintain optimum spacecraft attitude for radar tracking and communication checks. This plan would provide good trajectory information as early as possible and would give me a chance to adapt to these new conditions if such was necessary. Other observations and tasks were to be accomplished mainly on the second and third orbits. Since the thruster problem made it necessary for me to control manually during most of the second and third orbits, several of the planned observations and experiments were not accomplished.

Attitude Reference

A number of questions have been raised over the ability of a man to use the earth's horizon as a reference for controlling the attitude of the space vehicle.

Throughout this flight no trouble in seeing the horizon was encountered. During the day the earth is bright and the background of space is dark. The horizon is vividly marked. At night, before the moon is up, the horizon can still be seen against the background of stars. After the moon rises (during this flight the moon was full), the earth is well enough lighted so that the horizon can be clearly seen.

With this horizon as a reference, the pitch and roll attitudes of the spacecraft can easily be controlled. The window can be positioned where you want it. Yaw, or heading reference, however, is not so good. I believe that there was a learning period during the flight regarding my ability to determine yaw. Use of the view through the window and periscope gradually improved.

To determine yaw in the spacecraft, advantage must be taken of the speed of the spacecraft over the earth which produces an apparent drift of the ground below the spacecraft. When the spacecraft is properly oriented, facing along the plane of the orbit, the ground appears to move parallel to the spacecraft longitudinal axis. During the flight I developed a procedure which seemed to help me use this terrain drift as a yaw reference. I would pitch the small end of the spacecraft down to about -60° from the normal attitude where a fairly good vertical view was available. In this attitude, clouds and land moving out from under me had more apparent motion than when the spacecraft was in its normal orbit attitude and I looked off toward the horizon.

At night with the full moon illuminating the clouds below, I could still determine yaw through the window but not as rapidly as in the daytime. At night I could also use the drift of the stars to determine heading but this took longer and was less accurate.

Throughout the flight I preferred the window to the periscope as an attitude reference system. It seemed to take longer to adjust yaw by using the periscope on the day side. At night, the cloud illumination by the moon is too dim to be seen well through the periscope.

Three times during the flight I turned the spacecraft approximately 180° in yaw and faced forward in the direction of flight. I liked this attitude-seeing where I was going rather than where I had been-much better. As a result of these maneuvers my instrument reference system gave me an inaccurate attitude indication. It was easy to determine the proper attitude, however, from reference to the horizon through the window or to the periscope. Maintaining orientation was no problem, but I believe that the pilot automatically relies much more completely on vision in sapce than he does in an airplane, where gravity cues are available. The success with which I was able to control the spacecraft at all times was, to me, one of the most significant features of the flight.

Weightlessness

Weightlessness was a pleasant experience. I reported I felt fine as soon as the spacecraft separated from the launch vehicle, and throughout the flight this feeling continued to be the same.

Approximately every 30 minutes throughout the flight I went through a series of exercises to determine whether weightlessness was effecting me in any way. To see if head movement in a zero g environment produced any symptoms of nausea or vertigo, I tried first moving, then shaking my head from side to side, up and down, and tilting it from shoulder to shoulder. In other words, moving my head in roll, pitch, and yaw. I began slowly, but as the flight progressed, I moved my head more rapidly and vigorously until at the end of the flight I was moving as rapidly as my pressure suit would allow. In figure 12-1 the camera has caught me in the middle of this test, and this photograph shows the extent to which I was moving my head.

In another test, using only eye motions, I tracked a rapidly moving spot of light generated by my finger-tip lights. I had no problem watching the spot and once again no sensations of dizziness or nausea. A small eye chart was included on the instrument panel, with letters of varying size and with a "spoked wheel" pattern to check both general vision and any tendency toward astigmatism. No change from normal was apparent.

An "oculogyric test" was made in which turning rates of the spacecraft were correlated with sensations and eye movements. Results were normal. Preflight experience in this test and a calibration had been made at the Naval School of Aviation Medicine, Pensacola, Fla., with Dr. Ashton Graybiel, so that I was thoroughly familiar with my reactions to these same movements at 1 g.

To provide medical data on the Cardiovascular system, at intervals, I did an exercise which consisted of pulling on a bungee cord once a second for 30 seconds. This exercise provided a known workload to compare with previous similar tests made on the ground. The flight surgeons have reported the effect that this had on my pulse and blood pressure. The effect that it had on me during the flight was the same effect that is had on the ground--it made me tired.

Another experiment related to the possible medical effects of weightlessness was eating in orbit. (See fig. 12-2.) On the relatively short flight of Friendship 7, eating was not a necessity, but rather an attempt to determine whether there would be any problem in consuming and digesting food in a weightless state. At no time did I have any difficulty eating. I believe that any type of food can be eaten as long as it does not come apart easily or make crumbs. Prior to the flight, we joked about taking along some normal food such as a ham sandwich. I think this would be practical and should be tried.

Sitting in the spacecraft under zero g is more pleasant than under 1 g on the ground, since you are not subject to any pressure points. I felt that I adapted very rapidly to weightlessness. I had no tendency to overreach nor did I experience any other sign of lack of coordination, even on the first movements after separation. I found myself unconsciously taking advantage of the weightless condition, as when I would leave a camera or some other object floating in space while I attended to other matters. This was not done as a preplanned maneuver but as a spur-of-the-moment thing when another system needed my attention. I thought later about how I had done this as naturally as if I were laying the camera on a table in a 1 g field. It pointedly illustrates how rapidly adaptable the human is, even to something as foreign as weightlessness. (See fig. 12-3.)

We discovered from this flight that some problems are still to be solved in properly determining how to stow and secure equipment that is used in a space vehicle. I had brought along a number of instruments, such as, cameras, binoculars, and a photometer, with which to make observations from the spacecraft. All of these were stowed in a ditty bag by my right arm. Each piece of equipment had a 3-foot piece of line attached to it. By the time I had started using items of the equipment, these lines became tangled. Although these lines got in the way, it was still important to have some way of securing the equipment, as I found out when I attempted to change film. The small canisters of film were not tied to the ditty bag by lines. I left one floating in midair while working with the camera, and when I reached for it, I accidentally hit it and it floated out of sight behind the instrument panel.

Color and Light

As I looked back at the earth from space, colors and light intensities were much the same as I had observed when flying at high altitude in an airplane. The colors observed when looking down at the ground appeard similar to those seen from 50,000 feet. When looking toward the horizon, however, the view is completely different, for then the blackness of space contrasts vividly with the brightness of the earth. The horizon itself is a brilliant, brilliant blue and white.

It was surprising how much of the earth's surface was covered by clouds. The clouds can be seen very clearly on the daylight side. The different types of clouds--vertical developments, stratus clouds, and cumulus clouds--are readily distinguished. There is little problem identifying them or in seeing the weather patterns. You can estimate the relative heights of the cloud layers from your knowledge of the types or from the shadows the high clouds cast on those lower down. These observations are representative of information which the scientists of the U. S. Weather Bureau Meteorological Satellite Laboratory had asked Project Mercury to determine. They are interested in improving the optical equipment in their Tiros and Nimbus satellites and would like to know if they could determine the altitude of cloud layers with better optical resolution. From my flight I would say it is quite possible to determine cloud heights from this orbital altitude. (See figs. 12-4 to 12-8.)

Only a few land areas were visible during the flight because of the cloud cover. Clouds were over much of the Atlantic, but the western (Sahara Desert) part of Africa was clear. As I passed over it the first time I took the picture shown in figure 12-9. In this desert region I could plainly see dust storms. By the time I got to the east coast of Africa where I might have been able to see towns, the land was covered by clouds. The Indian Ocean was the same.

Western Australia was clear, but the eastern half was overcast. Most of the area across Mexico and nearly to New Orleans was covered with high

cirrus clouds. As I came across the United States I could see New Orleans, Charleston and Savannah very clearly. I could also see rivers and lakes. I think the best view I had of any land area during the flight was the clear desert region around El Paso on the second pass across the United States. I could see the colors of the desert and the irrigated area north of El Paso. As I passed off the east coast of the United States I could see across Florida and far back along the Gulf Coast. (See figs. 12-10 and 12-11.)

Over the Atlantic I saw what I assume was the Gulf Stream. The different colors of the water are clearly visible.

I also observed what was probably the wake of a ship. As I was passing over the recovery area at the end of the second orbit, I looked down at the water and saw a little "V". I checked the map. I was over recovery area G at the time, so I think it was probably the wake from a recovery ship. When I looked again the little "V" was under a cloud. The change in light reflections caused by the wake of a ship are sometimes visible for long distances from an airplane and will linger for miles behind a ship. This wake was probably what was visible.

I believe, however, that most people have an erroneous conception that from orbital altitude, little detail can be seen. In clear desert air, it is common to see a mountain range 100 or so miles away very clearly, and all that vision is through atmosphere. From orbital altitude, atmospheric light attenuation is only through approximately 100,000 feet of atmosphere so it is even more clear. An interesting experiment for future flights can be to determine visibility of objects of different sizes, colors, and shapes.

Obviously, on the night side of the earth, much less was visible. This may have been due not only to the reduced light, but also partly to the fact that I was never fully dark adapted. In the bright light of the full moon, the clouds are visible. I could see vertical development at night. Most of the cloudy areas, however, appeared to be stratoform.

The lights of the city of Perth, in Western Australia, were on and I could see them well. The view was similar to that seen when flying at high altitude at night over a small town. South of Perth there was a small group of lights, but they were much brighter in intensity. Inland there was a series of four or five towns lying in a line running from east to west. Knowing that Perth was on the coast, I was just barely able to see the coastline of Australia. Clouds covered the area of eastern Australia around Woomera, and I saw nothing but clouds from there across the Pacific until I was east of Hawaii. There appeared to be almost solid cloud cover all the way.

Just off the east coast of Africa were two large storm areas. Weather Bureau scientists had wondered whether lightning could be seen on the night side, and it certainly can. A large storm was visible just north of my track over the Indian Ocean and a smaller one to the south. Lightning could be seen flashing back and forth between the clouds but most prominent were lightning flashes within thunderheads illuminating them like light bulbs.

Some of the most spectacular sights during the flight were sunsets. The sunsets always occurred slightly to my left, and I turned the spacecraft to get a better view. The sunlight coming in the window was very brilliant, with an intense clear white light that reminded me of the arc lights while the spacecraft was on the launching pad.

I watched the first sunset through the photometer (fig. 12-12) which had a polarizing filter on the front so that the intensity of the sun could be reduced to a comfortable level for viewing. Later I found that by squinting, I could look directly at the sun with no ill effects, just as I can from the surface of the earth. This accomplished little of value but does give an idea of intensity.

The sun is perfectly round as it approaches the horizon. It retains most of its symmetry until just the last sliver is visible. The horizon on each side of the sun is extremely bright, and when the sun has gone down to the level of this bright band of the horizon, it seems to spread out to each side of the point where it is setting. With the camera I caught the flattening of the sun just before it set (fig. 12-13 (b)). This is a phenomenon of some interest to the astronomers.

As the sun moves toward the horizon, a black shadow of darkness moves across the earth until the whole surface, except for the bright band at the horizon, is dark. This band is extremely bright just as the sun sets, but as time passes the bottom layer becomes a bright orange and fades into reds, then on into the darker colors, and finally off into the blues and blacks. One thing that surprised me was the distance the light extends on the horizon on each side of the point of the sunset. The series of pictures shown in figures 12-13 and 12-14 illustrates the sequence of this orbital twilight. I think that the eye can see a little more of the sunset color band than the camera captures. One point of interest was the length of time during which the orbital twilight persisted. Light was visible along the horizon for 4 to 5 minutes after the sunset, a long time when you consider that sunset occurred 18 times faster than normal.

The period immediately following sunset was of special interest to the astronomers. Because of atmospheric light scattering, it is not possible to study the region close to the sun except at the time of a solar eclipse. It had been hoped that from above the atmosphere the area close to the

sun could be observed. However, this would require a period of dark adaptation prior to sunset. An eye patch had been developed for this purpose, which was to be held in place by special tape. This patch was expected to permit one eye to be night adapted prior to sunset. Unfortunately, the tape proved unsatisfactory and I could not use the eyepatch. Observations of the sun's corona and zodiacal light must await future flights when the pilot may have an opportunity to get more fully dark adapted prior to sunset.

Another experiment suggested by our advisors in astronomy was to obtain ultraviolet spectrographs of the stars in the belt and sword of Orion. The ozone layer of the earth's atmosphere will not pass ultraviolet light below 3,000 angstroms. The spacecraft window will pass light down to 2,000 angstroms. It is possible, therefore, to get pictures of the stars from the Mercury spacecraft which cannot be duplicated by the largest telescopes on the ground. Several ultraviolet spectrographs were taken of the stars in the belt of Orion. They are being studied at the present time to see whether useful information was obtained.

The biggest surprise of the flight occurred at dawn. Coming out of the night on the first orbit, at the first glint of sunlight on the spacecraft, I was looking inside the spacecraft checking instruments for perhaps 15 to 20 seconds. When I glanced back through the window my initial reaction was that the spacecraft had tumbled and that I could see nothing but stars through the window. I realized, however, that I was still in the normal attitude. The spacecraft was surrounded by luminous particles.

These particles were a light yellowish green color. It was as if the spacecraft were moving through a field of fireflies. They were about the brightness of a first magnitude star and appeared to vary in size from a pinhead up to possibly 3/8 inch. They were about 8 to 10 feet apart and evenly distributed through the space around the spacecraft. Occasionally, one or two of them would move slowly up around the spacecraft and across the window, drifting very, very slowly, and would then gradually move off, back in the direction I was looking. I observed these luminous objects for approximately 4 minutes each time the sun came up.

During the third sunrise I turned the spacecraft around and faced forward to see if I could determine where the particles were coming from. Facing forwards I could see only about 10 percent as many particles as I had when my back was to the sun. Still, they seemed to be coming towards me from some distance so that they appeared not to be coming from the spacecraft. Just what these particles are is still subject to debate and awaits further clarification. Dr. John O'Keefe at the NASA Goddard Space Flight Center is making a study in an attempt to determine what these particles might be.

Other Planned Observations

As mentioned earlier, a number of other observations and measurements during orbit had to be canceled because of the control system problems. Equipment carried was not highly sophisticated scientific equipment. We believed, however, that it would show the feasibility of making more comprehensive measurements on later missions.

Some of these areas of investigation that we planned but did not have an opportunity to check are as follows:

(a) Weather Bureau observations:
  (1) Pictures of weather areas and cloud formations to match against map forecasts and Tiros pictures
  (2) Filter mosaic pictures of major weather centers
  (3) Observation of green air glow from air and weather centers in 5,577-angstrom band with air glow filter
  (4) Albedo intensities-measure reflected light intensities on both day and night side

(b) Astronomical observations:
  (1) Light polarization from area of sun
  (2) Comets close to sun
  (3) Zodiacal light
  (4) Sunlight intensity
  (5) Lunar clouds
  (6) Gegenschein
  (7) Starlight intensity measurements

(c) Test for otolith balance disturbance and autokynesis phenomena

(d) Vision tests:
  (1) Night vision adaptation
  (2) Phorometer eye measurements

(e) Drinking

Reentry

After having turned around on the last orbit to see the particles, I maneuvered into the correct attitude for firing the retrorockets and stowed the equipment in the ditty bag.

This last dawn found my attitude indicators still slightly in error. However, before it was time to fire the retrorockets the horizon-scanner slaving mechanism had brought the gyros back to orbit attitude. I crosschecked repeatedly between the instruments, periscope presentation, and the attitude through the window.

Although there were variations in the instrument presentations during the flight, there was never any difficulty in determining my true attitude by reference to the window or periscope. I received a countdown from the ground and the retrorockets were fired on schedule just off the California coast.

I could hear each rocket fire and could feel the surge as the rockets slowed the spacecraft. Coming out of zero-g condition, the retrorocket firing produced the sensation that I was accelerating back toward Hawaii (fig. 12-15). This sensation, of course, was an illusion.

Following retrofire the decision was made to have me reenter with the retro package still on because of the uncertainty as to whether the landing bag had been extended. This decision required me to perform manually a number of the operations which are normally automatically programed during the reentry. These maneuvers I accomplished. I brought the spacecraft to the proper attitude for reentry under manual control. The periscope was retracted by pumping the manual retraction lever.

As deceleration began to increase I could hear a hissing noise that sounded like small particles brushing against the spacecraft.

Due to ionization around the spacecraft, communications were lost. This had occurred on earlier missions and was experienced now on the predicted schedule. As the heat pulse started there was a noise and a bump on the spacecraft. I saw one of the straps that holds the retrorocket package swing in front of the window.

The heat pulse increased until I could see a glowing orange color through the window. Flaming pieces were breaking off and flying past the spacecraft window. (See fig. 12-16.) At the time, these observations were of some concern to me because I was not sure what they were. I had assumed that the retropack had been jettisoned when I saw the strap in front of the window. I thought these flaming pieces might be parts of the heat shield breaking off. We know now, of course, that the pieces were from the retropack.

There was no doubt when the heat pulse occurred during reentry but it takes time for the heat to soak into the spacecraft and heat the air. I did not feel particularly hot until we were getting down to about 75,000 to 80,000 feet. From there on down I was uncomfortably warm, and by the time the main parachute was out I was perspiring profusely.

The reentry deceleration of 7.7g was as expected and was similar to that experienced in centrifuge runs. There had been some question as to whether our ability to tolerate acceleration might be worse because of the 4 1/2 hours of weightlessness, but I could note no difference between my feeling of deceleration on this flight and my training sessions in the centrifuge.

After peak deceleration, the amplitude of the spacecraft oscillations began to build. I kept them under control on the manual and fly-by-wire systems until I ran out of manual fuel. After that point, I was unknowingly left with only the fly-by-wire system and the oscillations increased; so I switched to auxiliary damping, which controlled the spacecraft until the automatic fuel was also expended. I was reaching for the switch to deploy the drogue parachute early in order to reduce these reentry oscillations, when it was deployed automatically. The drogue parachute stabilized the spacecraft rapidly.

At 10,800 feet the main parachute was deployed. I could see it stream out behind me, fill partially, and then as the reefing line cutters were actuated it filled completely. The opening of the parachute caused a jolt, but perhaps less than I had expected.

The landing deceleration was sharper than I had expected. Prior to impact I had disconnected all the extra leads to my suit, and was ready for rapid egress, but there was no need for this. I had a message that the destroyer Noa would pick me up within 20 minutes. I lay quietly in the spacecraft trying to keep as cool as possible. The temperature inside the spacecraft did not seem to diminish. This, combined with the high humidity of the air being drawn into the spacecraft kept me uncomfortably warm and perspiring heavily. Once the Noa was alongside the spacecraft, there was little delay in starting the hoisting operation. The spacecraft was pulled part way out of the water to let the water drain from the landing bag.

During the spacecraft pickup, I received one good bump. It was probably the most solid jolt of the whole trip as the spacecraft swung against the side of the ship. Shortly afterwards the spacecraft was on the deck.

I had initially planned egress out through the top, but by this time I had been perspiring heavily for nearly 45 minutes. I decided to come out the side hatch instead.

General Remarks

Many things were learned from the flight of Friendship 7. Concerning spacecraft systems alone, you have heard many reports today that have verified previous design concepts or have shown weak spots that need remedial action.

Now, what can be said of man in the system?

Reliability

Of major significance is the probability that much more dependence can be placed on the man as a reliably operating portion of the man-spacecraft combination. In many areas his safe return can be made dependent on his own intelligent actions. Although a design philosophy could not be followed up to this time, Project Mercury never considered the astronaut as merely a passive passenger.

These areas must be assessed carefully, for man is not infallible, as we are all acutely aware. As an inflight example, some of you may have noticed a slight discrepancy between launch photographs of the pilot and similar reentry views. The face plate on the helmet was open during the reentry phase. Had cabin pressure started to drop, I could have closed the face plate in sufficient time to prevent decompression, but nevertheless a face-plate-open reentry was not planned.

On the ground, some things would also be done differently. As an example, I feel it more advisable in the event of suspected malfunctions, such as the heat-shield-retropack difficulties, that require extensive discussion among gound personnel to keep the pilot updated on each bit of information rather than waiting for a final clearcut recommendation from the ground. This keeps the pilot fully informed if there would happen to be any communication difficulty and it became necessary for him to make all decisions from onboard information.

Many things would be done differently if this flight could be flown over again, but we learn from our mistakes. I never flew a test flight on an airplane that I didn't return wishing I had done some things differently.

Even where automatic systems are still necessary, mission reliability is tremendously increased by having the man as a backup. The flight of Friendship 7 is a good example. This mission would almost certainly not have completed its three orbits, and might not have come back at all, if a man had not been aboard.

Adaptability

The flight of the Friendship 7 Mercury spacecraft has proved that man can adapt very rapidly to this new environment. His senses and capabilities are little changed in space. At least for the 4.5-hour duration of this mission, weightlessness was no problem.

Man's adaptability is most evident in his powers of observation. He can accomplish many more and varied experiments per mission than can be obtained from an unmanned vehicle. When the unexpected arises, as happened with the luminous particles and layer observations on this flight, he can make observations that will permit more rapid evaluation of these phenomena on future flights. Indeed, on an unmanned flight there likely would have been no such observations.

Future Plans

Most important, however, the future will not always find us as power limited as we are now. We will progress to the point where missions will not be totally preplanned. There will be choices of action in space, and man's intelligence and decision-making capability will be mandatory.

Our recent space efforts can be likened to the first flights at Kitty Hawk. They were first unmanned but were followed by manned flights, completely preplanned and of a few seconds duration. Their experiments were, again, power limited, but they soon progressed beyond that point.

Space exploration is now at the same stage of development.

I am sure you will agree with me that some big steps have been taken toward accomplishing the mission objectives expressed at the beginning of this paper.

Fig. 12-1. -- Pilot looks to his right. Note the distance his head can be turned in the pressure suit.

Fig. 12-2. --Pilot opens visor to eat.

(Note: All the originals of these photographs are in color and some detail is lost in the black and white reproduction of these photographs.)

Fig. 12-3. --After his snack of applesauce, the pilot leaves his expended tube hanging in air momentarily.

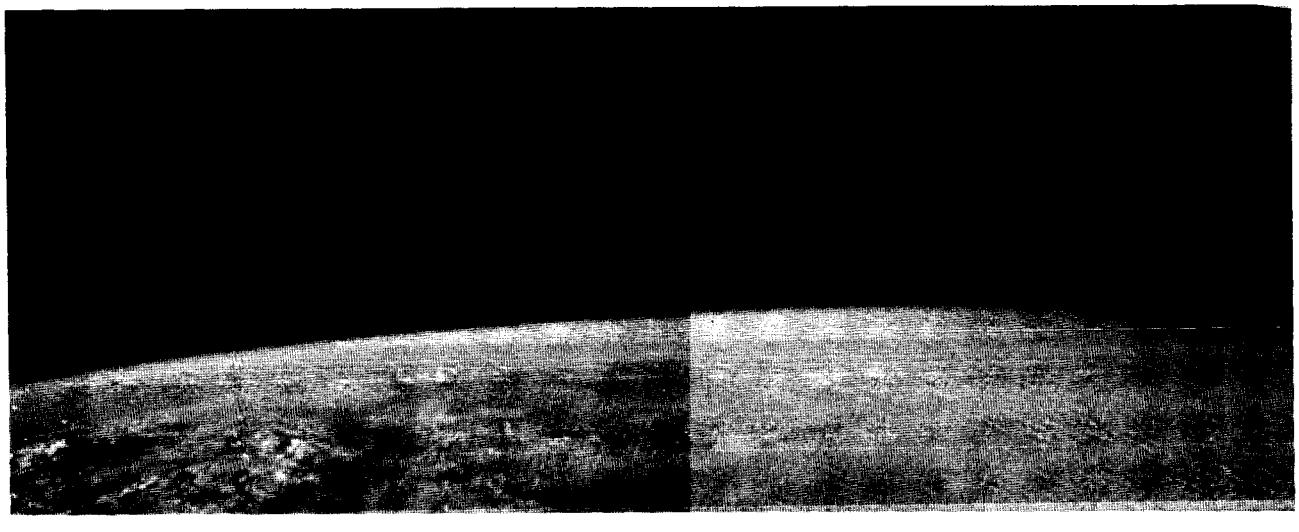

Fig. 12-4. --Photograph taken over the Pacific Ocean at the end of the first orbit. The cloud panorama illustrates the visibility of different cloud types and weather patterns. Shadows produced by the rising sun aid in the determination of relative cloud heights.

Fig. 12-5. --Just before sunset on the first orbit, the pilot's camera catches the darkening earth. The photograph shows how the shadows help to indicate cloud heights.

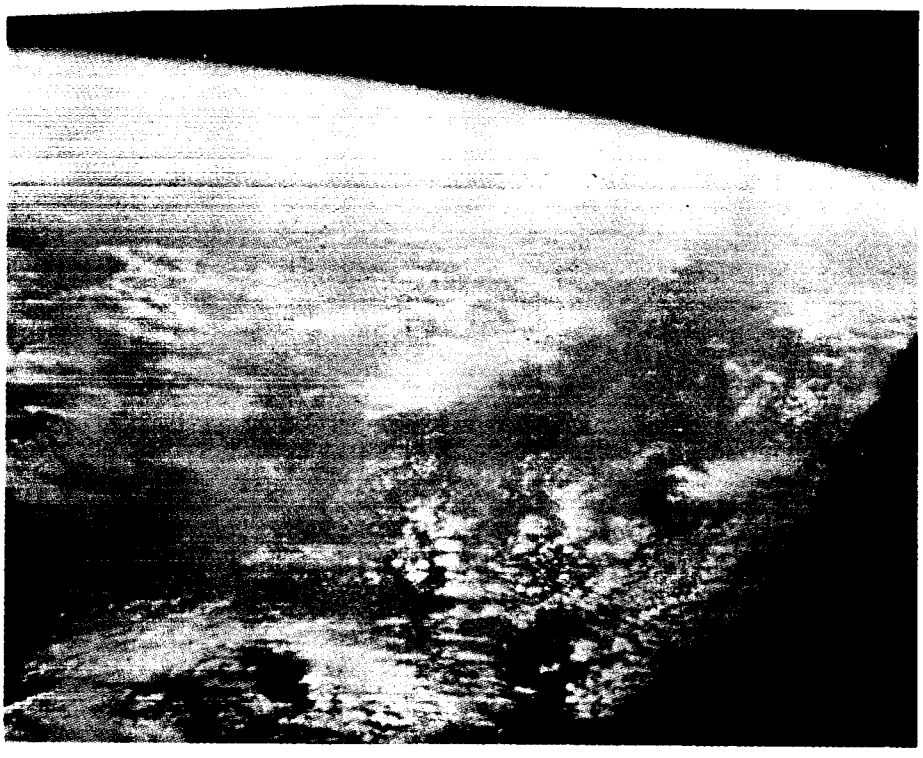

Fig. 12-6. --Over the Atlantic on the third orbit, the pilot's camera shows an overcast region to the northwest and patterns of scattered clouds in the foreground.

Fig. 12-7. --View from Tiros IV of approximately the same area in the Western Atlantic as that in figure 12-6. This view shows the appearance of the cloud as televised from a height of about 440 miles. Actual time of the photograph was 1428 G. c. t. Photograph is of the general vicinity of latitude 30° N., longitude 60° W. (U.S. Weather Bureau photograph).

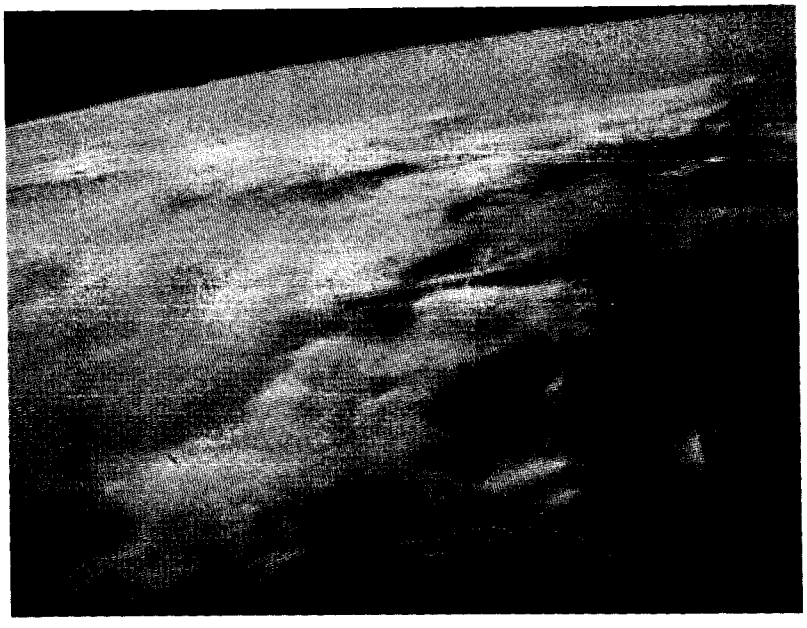

(a)

(b)

(a) First orbit. (b) Second orbit.

Fig. 12-8. --The Western Indian Ocean was overcast on the first and second orbits. The relative heights of the cirrus and the cumulus clouds can clearly be seen.

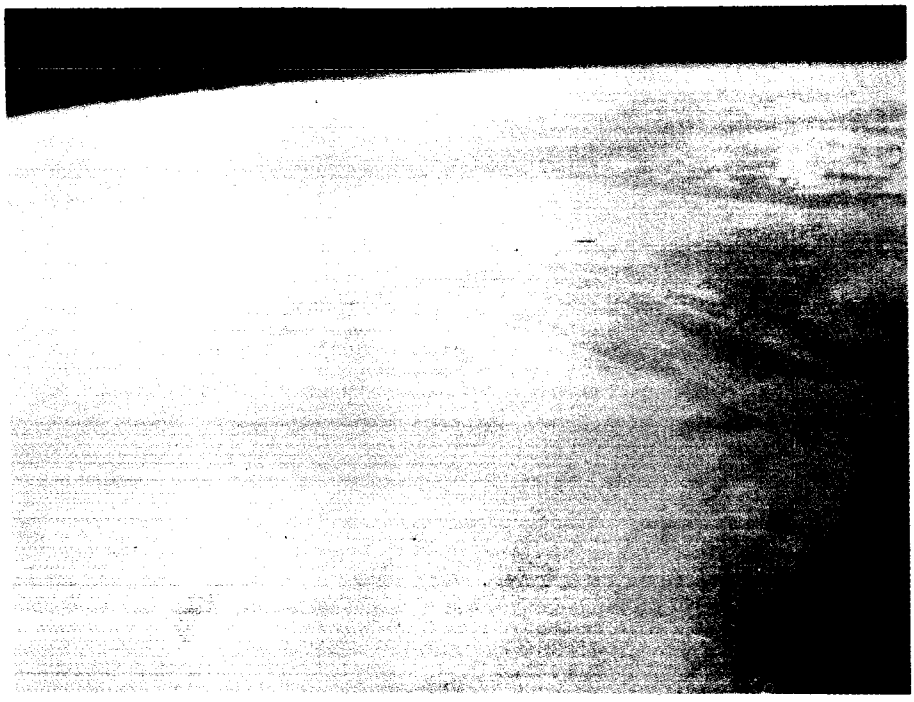

Fig. 12-9. --View looking back toward the African coast on the first orbit. The photograph from the pilot's camera shows the desert with blowing sand in the foreground.

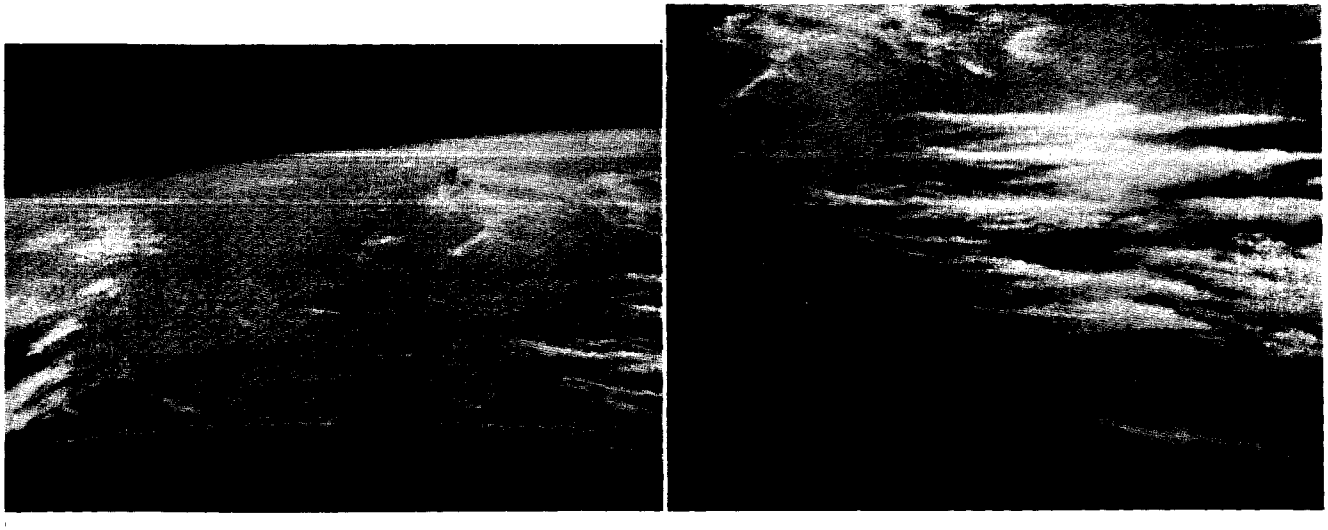

Fig. 12-10. --At the beginning of the third orbit, the pilot catches a panoramic view of the Florida coast, from the cloud covered Georgia border to just above Cape Canaveral.

Fig. 12-11. --View of the Florida area from Tiros IV taken at 1610 G. c. t. on Feb. 20, 1962. This photograph shows the bank of clouds (across Southern Florida) which had moved away from Cape Canaveral earlier that morning. The clouds just north of Florida are apparently the ones plainly visible in fig. 12-10. (U. S. Weather Bureau photograph; major land masses are outlined in white ink.)

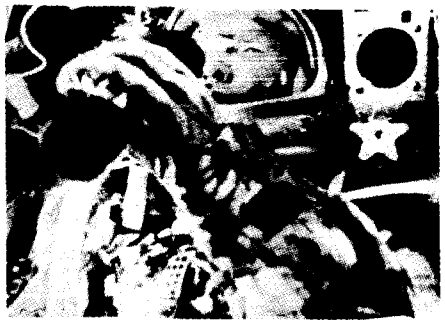

Fig. 12-12. --During sunset, the pilot used the photometer to view the sun.

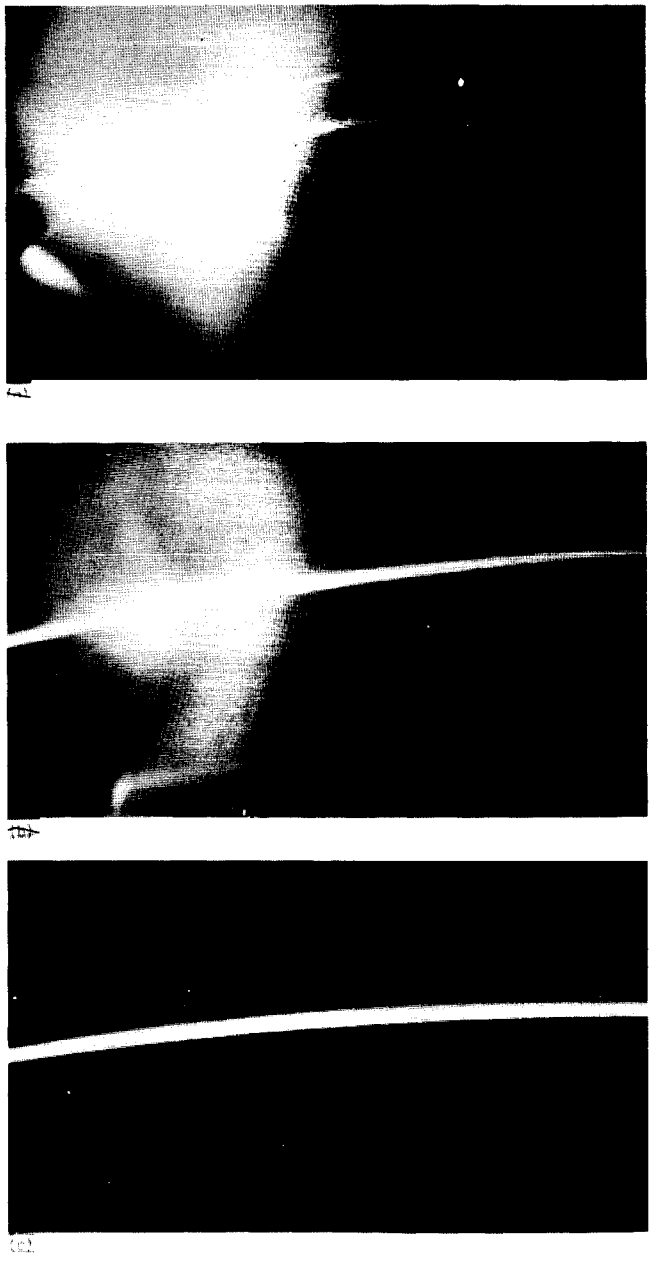

Fig. 12-13. --The third orbital sunset as shown by a series of three photographs. The camera catches the flattening of the solar disk just before the sun disappears below the horizon.

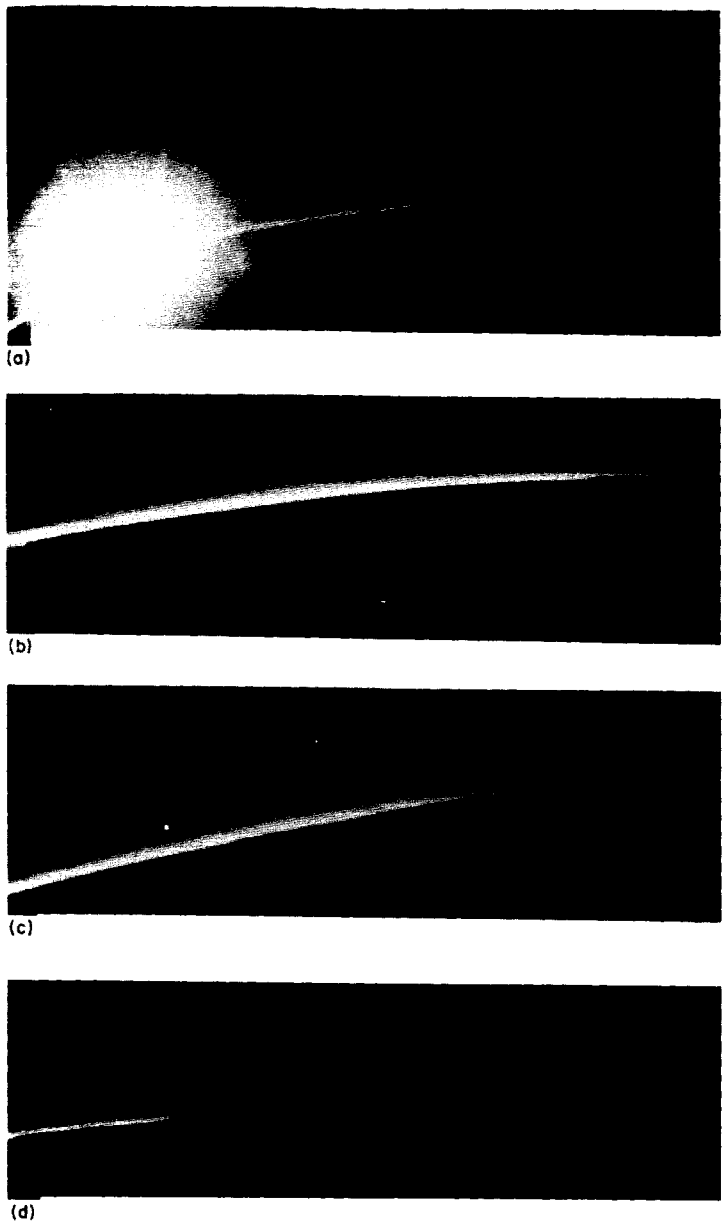

Fig. 12-14. -- The first orbital sunset is recorded in a series of four photographs. Patches of high clouds glow orange as the sun's light is diffracted by the atmosphere. The bright band of space twilight grows dimmer and shrinks in length with passing time.

Fig. 12-15. --Pilot concentrates on instruments while controlling attitude during retrofire.

Fig. 12-16. --Pilot looks out of window at fireball during maximum reentry heating.

METEOROID EFFECTS ON SPACE EXPLORATION

by

Maurice Dubin

National Aeronautics & Space Administration

Washington, D. C.

ABSTRACT

Although the meteoroid hazard has not been adequately evaluated for proper design of spacecraft for missions through cislunar and interplanetary space, the extent of meteoroid interactions on space exploration may be estimated. The available information about meteoroids and cosmic dust obtained from ground-based observations and satellite measurements is reviewed. This data is presently limited to meteoroids and cosmic dust with heliocentric orbits intersecting the plane of the ecliptic at one astronomical unit and interacting with the earth-moon system. From such information the expectation of the number of impacts with interplanetary matter as a function of exposed spacecraft surface area, exposure time, and meteoroid mass is presented. An estimate of the hazard has been made using appropriate hypervelocity cratering criteria. Some results of other authors are compared with the expectation of meteoroid interaction effects herein presented. The probability of damage to spacecraft is apparently considerably different and a bit less than some earlier estimates.

INTRODUCTION

Interplanetary space is populated by debris in heliocentric orbits known generally as "meteoroids". It is quite evident that a meteoroid impact with a space vehicle is a catastrophic event. The dynamic conditions of such an impact allow for impacting velocities ranging from a few kilometers per second to about 75 km sec $^{-1}$. The effects of the interactions of meteoroid impacts on space vehicles are a matter of concern in the design of spacecraft for various cislunar and interplanetary missions.

The hazard from meteoroid impacts may be evaluated from (a) knowledge of the distribution of interplanetary matter in the solar system, and (b) knowledge of the characteristics of impact cratering and penetration from meteoroid impacts on spacecraft structures. The distribution of interplanetary matter in the solar system may be described by a mapping function, Π, where

$$\Pi = \sum_i \pi_i$$

and $$\pi_i = \pi_i (m, \rho_m, S_m, a, e, i, \Omega, \omega, t)$$

where Π is the ensemble of the all small π_i. π_i is a description of the individual meteoroid structure and position in the solar system at any time. "m" is the mass, ρ_m the density, and Sm is a parameter defining the structural makeup of the meteoroid. a, e, i, Ω and ω define the meteoroid orbit, and the time, t, defines its actual position. "a" is the semi-major axis of the elliptical orbit, e the eccentricity, "i" is the inclination angle of the plane of the orbit with the plane of the ecliptic. "Ω", the ascending node, is the point where meteoroid crosses the ecliptic traveling north, and "ω", the argument of the perihelion, is the angle from "Ω" to the perihelion measured in the orbital plane of the meteoroid. The magnitude of the velocity of the meteoroid depends on the radial distance "r" of the meteoroid from the sun and is given by:

$$V = \left[G_o \left(\frac{2}{r} - \frac{1}{a} \right)\right]^{1/2}$$

where G_o is the solar gravitational constant. Thus, if the mapping function were known, the probability of a spacecraft impacting with a meteoroid anywhere in interplanetary space would be known. In fact, if the mapping function Π were sufficiently accurately known catastrophic impacts with meteoroids could be avoided.

A great deal is known about the mapping function, Π, for the ascending node, Ω equal to one astronomical unit. Π at 1 a.u. is not well enough known to give discrete predictions for encountering a micrometeoroid. However, statistical data from encounters of meteoroids with the atmosphere and spacecraft sensors have been sufficient to define a distribution function, I(m), which is mainly dependent on the mass of the meteoroid. I(m) is given in terms of the number of impacts by meteoroids of mass m and larger per unit area and time at 1 a.u. in the plane of the ecliptic and near the earth. That is to say, that I(m) near the earth may be derived from the mapping parameter Π. Actually, Π is practically an unknown function except for about 2000 known asteroids in orbit between Mars and Jupiter, several score known comets, and meteor showers usually associated with known comets.

The specific gravity or density, ρ_m, of meteoroids may vary considerably. Meteorites, meteoroids recovered on earth and apparently of asteroidal origin, are solid bodies made of stone or iron. The great majority of meteorites are

stones with density of about 3.5 gm cm^{-3}, while less than 10% are iron or iron nickel with densities of 8 gm cm^{-3} or slightly less. Most of the meteors detected by visual, optical or radio methods have characteristics defining a fragile and possibly fluffy structure. The orbits of the meteors vary considerably from the asteroid orbits. Hence, meteors in general probably have a cometary origin. The densities, ρ_m of the meteoroids observed in the earth's atmosphere as meteors are probably less than that of meteorites and probably between 0.3 and 3 gm cm^{-3}. Although the structure of comet material has been hypothesized from various comet models, this structure is practically unknown and difficult to simulate.

To assess the effects of meteoroids on space vehicles at 1 a.u. the distribution function I(m) has been derived from available knowledge and data. I(m) defines the expectation of an impact per unit area and time at 1 a.u. The function I(m) combined with cratering and penetration conditions defines the meteoroid hazard. The depth of penetration, p, depends upon the structural parameters m, ρ_m, and S of the meteoroid, the target material S_t and density ρ_t, and the relative velocity v of the impact (as well as the angle). Thus penetration depth is a function, $p(m, \rho_m, S_m, S_t, \rho_t, v)$. The penetrating flux may be derived from the combination of the function of penetration depth p, and the expectation of impact, I(m).

A number of papers have been written on the subject of penetration of spacecraft by meteoroids. Several papers are listed in reference 1 through 6. These and other references are considered in reveiwing the expected meteoroid effects. Some parts of references 2 to 6 will be compared critically below.

RATE OF METEOROID IMPACTS

The rate of meteoroid impacts upon the earth or per unit area and time, I(m) has been obtained from a variety of measurements of meteors and micrometeorites. Reference 7 reviews the derivation of I(m) from data obtained from visual, optical, and radio-observations of meteors, from accretion measurements in the atmosphere and on the earth's surface, and from direct measurements using satellites.

The cumulative mass distribution, I(m), for the omnidirectional flux of dust particles and meteoroids is plotted from reference 7 in figure 1. I(m), the cumulative influx rate in particles per square meter per second on the earth is plotted as a segmented function of the particle mass in grams using a log-log plot. The cumulative influx rate is plotted also in equivalent visual magnitude, Mv. The visual magnitude is an astronomical scale for comparing the light intensity of stars and meteor trails. It is a logarithomic scale of brightness, with 5 magnitudes representing a factor of 100. From optical and visual observations the number of meteors as a function of visual magnitude against a star background is almost directly obtained. Radar methods have been used to measure distribution and number of meteors as a function of the electrons density per unit length of the meteor trail. The electron line density is also related to the visual magnitude and particle mass of the meteor. Some solar radiation pressure limits for several densities are also included on the abscissae. For ρ_m of 1 gm cm^{-3}, particles of mass less than 10^{-12} gm would be subjected to a solar radiation pressure force greater than the solar gravitational attraction. The fact that dust particles of mass less than 10^{-12} gm have been detected, indicates that the dust particles have densities which are generally greater than 1 gm cm^{-3}.

The accretion rates represented by the curve labeled "Watson (1941)" were plotted from reference 8 as a function of particle mass. The dashed curve labeled "Whipple (1957)" is plotted as a function of visual magnitude and was obtained from reference 3. This method of plotting the two distributions serves to illustrate the kind of uncertainty involved in displaying the impact rates as a mass distribution. This uncertainty will be discussed later.

The curve labeled "Millman and Burland (1956)" obtained from reference 9, is presented in three segments and covers the range from $-10 \lesssim Mv \lesssim 10$. This curve is representative of meteor observations from optical, telescopic, and radar methods. In reference 10 the cumulative influx rate of photographic meteors in the range of visual magnitude $0 \lesssim Mv \lesssim 5$ was determined using a sample of over 300 meteor photographs. The naked-eye visual meteors and photographic meteors number several tens of thousands. The number of radio meteors observed is greater still by at least another order of magnitude.

In the range of visual magnitudes of $20 \lesssim Mv \lesssim 10$, or particles masses of $10^{-7}\,gm \lesssim m \lesssim 10^{-3}\,gm$, almost no data exists to define a distribution function. This range of particle mass is too small to interact with the earth's atmosphere and form meteors large enough to be detected by ground-based radio techniques and telescopes. A small amount of radar data has been reported in reference 11 out to visual magnitude 14. This same range of particle mass populates interplanetary space quite sparsely; so much so that the exposure times and exposure areas of sensors on satellites have so far been inadequate to obtain any measurements. This same range of mass is of importance in the penetration and damage of space craft structures.

On the other hand, particles of mass smaller than 10^{-8} gm are relatively more numerous and have been detected with probes and satellites. The curve labeled "McCracken et al (1961)" is based on experimental data by direct measure-

ments as described in references 7 and 12. The curve was obtained with sensors which were calibrated to measure particle mass rather than visual magnitude. This segment of the curve was obtained from experimental data from rocket probes, and satellite measurements as plotted in figure 2. For the interval of particle mass $10^{-10}\text{gm} \lesssim m \lesssim 10^{-6}\text{gm}$, the cumulative distribution curve of influx rate of dust particles as a function of particle mass may be described by the equation:

$$\log I = -17.0 - \log m$$

where I is in particles M^{-2} sec^{-1}. The function I(m), however, cannot be correctly described by a single first degree equation with logarithomic parameters.

The two segments for visual magnitude $30 \; M_V \lesssim 40$ in figure 1 were obtained in the analysis of reference 13, while the segment marked "Soberman and Hemenway (1961)" was obtained by collecting dust with an Aerobee rocket trapping device as described in reference 14.

The interpolated region between visual magnitudes 10 and 20 represent a region of concern for spacecraft design as particles of mass between 10^{-3} gm and 10^{-7} gm may penetrate surface materials used on spacecraft. The cumulative distribution function I(m), in figure 1 may be analyzed with greater ease if $dI(m)/dm$, the incremental mass distribution as a function of particle mass or visual magnitude $dI(m)/dm \cdot dm/dM_V$ is plotted. Figure 3 is the incremental mass distribution curve derived from figure 1. The rate of accretion by the earth per day in grams per visual magnitude per day (when divided by 1.3×10^{-19} this becomes the influx in particles M^{-2} sec^{-1} per visual magnitude) is plotted as a function of Mv and particle mass in grams. The curve has been smoothed to remove the effects of using a segmented cumulative mass distribution curve. The uncertainty of spread in mass influx per visual magnitude in the range of visual magnitudes from +10 to 0 is bordered between the curves marked "Whipple (1957)" and "Watson (1941)". The value of 25 grams for a meteoroid of zero visual magnitude and 28 km sec^{-1} average velocity (reference 3) was used in relating visual magnitude to particle mass.

The accretion of interplanetary material on the earth is shown in figure 3 to be dominated by dust particles with masses less than about 10^{-6} grams. The accretion rate of interplanetary dust particles is about 5×10^4 tons per day. A conservative estimate of 10^4 tons per day should probably be used until improved satellite measurements giving particle orbits are obtained. The accretion rate derived from direct measurements is in fair agreement with the estimate (reference 14) of 4×10^4 tons per day based on mountain top collections and an earlier estimate of 4×10^{-3} tons per day based on deep sea sediments. Reference 16 gives an influx of 10^{-13} gm cm^{-2} sec^{-1} (5×10^4 tons per day) for particles of radii greater than 1μ based upon observations of the earth's shadow during lunar eclipses.

The curves figure 1 and figure 3 are averaged in time. The character of all meteor and interplanetary dust measurements has been defined mostly from ground-based observations. The influx rate of particles usually undergo temporal variations; the major variations are often associated with meteor streams and showers. These showers are well described in the literature, references 9, 17, 18, 19 and 20. During short periods of time, a few hours to several days, the influx rate may increase by one to two orders of magnitude above the average rate. The observations of very faint radar meteors ($M_V \approx 14$), reference 11, have shown that a large fraction of meteors occur in streams or "sporadic showers". The large fluctuations in influx rates of faint radar meteors with mass $\approx 10^{-5}$ gm have also been observed from dust particle measurements from probes and satellites (references 7, 21 and 22). The distributions of showers and "sporadic showers" in interplanetary space are probably very similar to the distribution near the earth. The orbits of showers and sporadic meteors have been described in references 17, 18, 20 and 23. From these and other observations, nearly all the meteoroids observed as meteors appear to be of cometary origin and are travelling in direct heliocentric orbits. Although it had been apparent that nearly all meteors in the visual and radar range have only small inclinations angles with the plane of the ecliptic, a "toroidal" group discovered at the Jodrell Bank Experimental Station, England, has been confirmed (reference 23) to represent an important fraction of meteors with $M_V \approx 10$; the toroidal group is represented by short period orbits and inclination angles i, as high as 60°.

EXPECTATION OF IMPACT BY METEOROIDS AS A FUNCTION OF MASS

The expected impact rate of meteoroids as a function of mass may be obtained from figures 1 and 3. These figures are derived from experimental data averaged to smooth effects from large fluctuations and showers. The expectation of impact and penetration of surfaces could be estimated from such a curve. However, the variations appear excessively large in the range of visual magnitudes from $0 \lesssim M_V \lesssim 10$, because of the large spread in the influx rate bounded by the curves labeled "Whipple (1957)" and "Watson (1941)". Actually, there is no discrepancy or spread in the influx rate as a function of visual magnitude. Both photographic and visual data of the numbers of meteors M^{-2} sec^{-1} as a function of visual magnitude give indentical results except for a small correction factor of 1.8 visual magnitudes concerned with the photographic process.

The major discrepancy shown in figure 3 results from the estimates of the mass of a meteor resulting in a trail of given visual magnitude. The curve labeled "Watson (1941)", a zero visual magnitude meteor, was estimated to have a mass of 0.25 grams and a velocity of 55 km sec^{-1}. ρ_m of the meteor was assumed to be about 3 gm cm^{-3}. The curve labeled "Whipple (1957)" is based upon the same distribution with ρ_m of 0.05 gm cm^{-3} and an average velocity of 28 km sec^{-1}. In this case, a zero visual magnitude meteor would have an average mass of 25 grams. The discrepancy is dependent upon the luminous efficiency and assumptions relating to the specific gravity of the meteoroid. Recently measurements of luminous efficiency have been made (reference 25), which would support a higher ρ_m than given in reference 3. The reference 3 value of was recently reconsidered by the same author (reference 26) as possibly being too low; an average ρ_m of 0.3 gm cm^{-3} instead of 0.05 gm cm^{-3} was given.

From reference 9 the values given by various authors of the mass of a zero magnitude meteor may be compared as in Table I based on several references. Except for the change to 0.05 gm cm^{-1} by Whipple (reference 3, 17) the mass of a zero magnitude meteor has been estimated between 0.05 and 1.3 grams. This mass range is more than a factor of 20 less than the mass of 25 grams given in reference 3. The value of 25 grams for a zero magnitude meteor was derived from the assumption that the ρ_m of meteors generally had a value of 0.05 gm cm^{-3}. Although, it is well confirmed that the structure of meteoric bodies is weak and fragile, only a single (hence not significant) measurement of such a low ρ_m has been reported. A ρ_m close to 1 gm cm^{-3} is to be preferred. Thus, the expected impact rate by a meteoroid as a function of mass per unit time and area is really fairly well known.

Both figures 1 and 3 should be considered as plots of impact rate as a function of particle mass rather than visual magnitude. Since there is evidence (reference 27) that penetration depth is a function also of ρ_m (as will be discussed later) the cumulative influx rate as a function of particle mass in grams should be a curve consisting of the curves labeled "McCracken et al (1961)" and "Watson (1941)" and with an interpolation between the two distributions, figure 4. The effective ρ_m to be used should be 1 or 2 gm cm^{-3}. This is the curve and the ρ_m to be used to determine the expectation of impact by a meteoroid.

One may not in any case realistically use the curve labeled "Whipple (1957)" with a ρ_m other than 0.05 gm cm^{-3}. If ρ_m for this curve were assumed to be 3 gm cm^{-3}, then the curve would become the "Watson (1941)" curve. The deceleration as well as visual magnitude of meteors has been accurately measured by photographic methods; such an assumption in the change of area to mass ratio by assuming a ρ_m change without the attendant change of the mass of the meteoroid would be quite inconsistent with observations. The distributions from reference 9 and 10 were derived with a similar assumption relating to the mass of a meteoroid as a function of visual magnitude.

There is some indirect evidence from measurements of the F component of the solar corona and the zodiacal light that the satellite distribution curve may change in interplanetary space. The influx rate might drop by two or three orders of magnitude as discussed in reference 7. Hence, the expected mass distribution curve might be approximated in interplanetary space by the curve labeled "Watson (1941)" together with the curve labeled "McCracken et al (1961)" lowered by two to three orders of magnitude in the range of particle mass from 10^{-10} to 10^{-12} gm.

Thus, in designing spacecraft for journeys in satellite orbits and heliocentric orbits at 1 a.u. the hazard from meteoroid impacts should be evaluated based on the expectation of impact by a meteoroid of a given mass or larger using the available data as described in figure 4. It is doubtful that this curve is greatly in error. The influx rates as a function of mass would probably never be more than an order of magnitude greater than the natural influx rates except during periods of recognizable sporadic showers and several of the known meteor streams.

PENETRATION AND DAMAGE FROM MICROMETEOROID IMPACTS

The mechanism of crater formation is essentially one of cavitation, resulting from an intensive plastic deformation wave formed during the impact. The size of the crater and its shape are determined by the properties of the wave and the target material. The initial conditions of occurring during the early stages of the impact determine the amplitude and shape of the deformation wave. Eichelberger (reference 32) further describes the initial stage of the impact or primary penetration as characterized by a very rapid plastic deformation of the target and impacting projectile. If the impact velocity is very high, the surface pressure so far exceeds the yield strength of the material that a hydrodynamic treatment is quite accurate.

The shape of the plastic deformation is determined during a time proportional to

$$\sim \frac{m^{1/3}}{v}\left[1+\left(\frac{\rho_m}{\rho_t}\right)^{1/2}\right]$$

in the initial stage of crater formation. This time defines the width of the deformation wave. The amplitude of the deformation may be estimated from Bernoulli's equation as

$$\sim \tfrac{1}{2} v^2 \rho_m \rho_t \left[(\rho_m)^{1/2} + (\rho_t)^{1/2} \right]^{-2}$$

The deformation wave propagates into the target, displacing material as it disperses. Hence the effects in the target depends upon the properties of the target material as described by the equation-of-state of the material. The crater dimensions will be determined by the distance of travel of the deformation wave while its intensity is greater than the strength of the target material. The model described is essentially the same as that used by Bjork (reference 33) in his theoretical treatment of cratering.

The effect of a meteoroid impact at velocities between 10 km sec^{-1} and 75 km sec^{-1} may be determined theoretically. Some experimental studies have been made at low velocities; in some cases up to about 15 km sec^{-1}. Bjork has shown that the impacts at meteoroid velocities behave hydrodynamically. Using the equation of state, Bjork solved the impact equations for cylinders on semi-infinite iron (references 4 and 33). Calculations were made for impact velocities of 5.5, 20 and 72 km sec^{-1}. The impact forces exceed the strength of the materials impacted by a large factor, so that material strength was neglected in the calculations. Viscous effects and heat transfer were also neglected. The calculations agreed for craters produced in aluminum at 6.3 km sec^{-1} and iron at 6.8 km sec^{-1} with experimentally determined crater sizes and shapes.

The penetration depths p in cm may be described by the equations:

$$p = 1.09 (mv)^{1/3} \quad \text{for Al on Al}$$

and

$$p = 0.606 (mv)^{1/3} \quad \text{for Fe on Fe}$$

where m is the meteoroid mass in gm and v the velocity in km sec^{-1}. Experimental data for impacts on lead results in a similar equation (reference 34)

$$p = 1.3 (mv)^{1/3}$$

The calculated craters were hemispherical with radius p. Craters formed by impacts at oblique incidence were also hemispherical.

Although calculations were made for thick targets, enough information was obtained that if a meteoroid penetrated a depth p in a thick target, it would just penetrate a sheet of the same target material which was $1.5p$ thick.

Experimental impact data have been obtained from which the dependence of depth of penetration on projectile density was determined (reference 35). A series of impacts were made on the same target material with a constant projectile mass and a constant impact velocity of about 2 km sec^{-1}. A range of densities of projectiles from 1.5 gm cm^{-3} to 17.2 gm cm^{-3} was tested by using different metals. The dependence on ρ_m was described by the equation

$$p = 2.28 \left(\frac{v}{v_s}\right)^{2/3} \left(\frac{\rho_m}{\rho_t}\right)^{2/3} d$$

where v_s is the speed of sound in the target, d is the diameter of the projectile. The penetration depth probably depends upon the density ratio between the meteoroid and the target material at the higher velocities of impact, also. For this reason, the cumulative distribution of meteoroids as a function of mass given in reference 3 must be used with consideration for proper dependence of penetration depth on the density of the meteoroid.

The penetration depth to projectile diameter ratio has been plotted as a function of velocity in figure 5 (reference 36) to indicate how the theoretical analysis of Bjork compares with extrapolations of experimental results obtained by Summers and Charters (reference 35), Collins and Kinard, and Atkins. It is noteworthy that such extrapolations leads to very large errors in penetration depth which cannot be correct because of energy and momentum conservation requirements.

Another condition resulting from the deformation wave following the impulsive loading by the meteoroid impact is spallation. The intensive compressive shocks from the impact may rupture and eject material over an extended region around the crater as well as the far surface of the impacted sheet. The diameter of the section spalled is usually several times the sheet thickness, and the spall thickness, may be a tenth to a half the thickness of the sheet. In reference 5, an analytical derivation is used to indicate an energy rather than a momentum dependence for the volume of spalled material. For alloy aluminum a characteristic distance D in cm for spalling is given by

$$D = 7.6 \times 10^{-4} E^{1/3}$$

and for steel,

$$D = 5 \times 10^{-4} E^{1/3}$$

where E is the kinetic energy of the meteoroid in ergs. Spallation can occur in sheet thicknesses two or three times greater than necessary to prevent perforation.

DISCUSSIONS AND CONCLUSIONS

The estimation of meteoroid effects on space exploration at 1 a.u. and particularly near the earth depends on the expectation of impact by meteoroids larger than some critical mass so that penetration of the skin of a spacecraft occurs, and

it depends on the understanding of the extent of damage resulting from one or an ensemble of such impacts. The expectation of a meteoroid impact per unit area and time may be determined from the cumulative mass distribution curve, figure 4, consisting of the section derived from satellite measurements, the section derived from ground-based measurements approximately represented by the curve labeled "Watson (1941): and on the interpolation between the two curves (Figure 1). The density, which may be used with this distribution for determining penetration rates and spallation effects, ρ_m is 2 gm cm^{-3}. A nominal velocity for such impacts should be 30 km sec^{-1} For short exposure times to the space environment, adverse effects may be present during known or sporadic meteor showers. However, for long exposure times this distribution curve should be an effective expectation of the impact frequency. The impact rate at 1 a.u. but away from the neighborhood of the earth may be different, but only for particles of mass less than 10^{-6} gm. In the vicinity of Mars, radial distances from the sun between 1.5 a.u. and 5 a.u. the collision hazard from asteroidal debris may be greater than at 1 a.u. For distances less than 1 a. u. the concentration of meteoroids should increase with a decrease in solar distance. Although most of the meteoroids are moving in direct heliocentric orbits, a retrograde component is known to exist. Radiation pressure forces leading to the Poynting-Robertson effect, the Yarkovski-Radzievski effect (reference 20) and other effects should decrease the eccentricity of the meteoroid orbits and gradually cause the particles to spiral into the sun. The inclination angles of the orbits, particularly the toroidal orbits, are indicative of a substantial component of the meteoroid population with orbit planes intersecting the plane of the ecliptic at considerable angles; hence, the meteoroid impact velocities with a spacecraft in interplanetary space should be considered out to 30 km sec^{-1} and higher.

A good representation of the penetrating power of meteoroids is given by the theoretical solution of Bjork. So far, from the limited data available from direct experiments (reference 13) on satellites, Bjork's penetration condition with the expected cumulative distribution as a function of mass, figure 4, has been supported by experiment. Penetration and fracture experiments have been flown on Explorers I, III, XIII, Vanguard III, Midas II, and Samos II.

Comparison of several reference (references 3, 4, 5, 6) which treat the hazard from meteoroid impacts may be made. Whipple (reference 3) uses a ρ_m of 0.05 gm cm^{-3}, a value which must be used to determine penetration depth. Whipple's penetration formula is considerably less to be preferred than Bjork's (reference 4). Bjork's treatment of the problem is generally good. However, there is not sufficient reason for him to use the Whipple distribution (reference 3) while at the same time over estimating the meteoroid density. In fact, the correction for the mass of zero magnitude meteoroid, a factor of a hundred, would decrease the required armor thickness by a factor of 5!

Jaffe and Rittenhouse (reference 5) have used the Bjork penetration condition. However, the selected curves of cumulative mass distribution for low satellite altitudes and far from the earth are not recommended. Davison and Winslow (reference 6) have considered an upper and lower limit, curves I and II, (their figure 8) in their estimates of rates of penetration of stainless steel. The cumulative distribution curve used in deriving curve II is recommended (their figure 5). They used the Summers' penetration criteria rather than Bjork's with an impact velocity of 15 km sec^{-1} and ρ_m of 1 gm cm^{-3}. In deriving their curve I they also used the Whipple distribution (reference 3) but with a ρ_m of 2.7 gm cm^{-3}. They concluded that their curve II may be reasonable and that curve I represents a high estimate of the penetration rates of the material investigated.

Thus, there appears to be a preferred approach to the prediction of the rate of penetration of the skins of a spacecraft from meteoroid impacts. It is evident that theory and available experimental data support this singular method of computing the meteoroid hazard. The estimated rates of penetration determined by combining (a) the expected cumulative distribution as a function of mass, figure 4; (b) the Bjork penetration criteria together, with a ρ_m of 2 gm cm^{-3} and an average impact velocity of 30 km sec^{-1} is recommended for design purposes. The meteoroid penetration rates computed in this manner represent a consistent estimate based on available knowledge. The conservative designer may incorporate his own safety factors to establish the required reliability. Additional measurements from satellites to confirm the predicted penetration rates are certainly desirable. The extent of the hazard appears to be considerably less than some earlier estimates, hence experimental data in the space environment will require relatively long exposure times over extended surface areas.

ACKNOWLEDGEMENTS

The many discussions with W. M. Alexander and C. W. McCracken are gratefully acknowledged in the preparation of this paper, as well as permission to use some figures.

REFERENCES

1. Grimminger, G. - "Probability that a Meteorite Will Hit or Penetrate a Body Situated in the Vicinity of the Earth", Journal of Applied Physics, Vol. 19, pgs. 947, 1948.

2. Whipple, F. L. - "Meteoritic Phenomena and Meteorites", Physics and Medicine of the Upper Atmosphere, ed. by C. S. White and

O. Benson, Univ. of Mexico Press, p. 137, 1952.

3. Whipple, F. L. - "The Meteoritic Risk to Space Vehicles" Proc. VIII International Astronautical Congress, Springer Verlag, Vienna, 1957, also Vistas in Astronautics, Pergamon Press, 1958.

4. Bjork, R. L. - "Meteoroids vs. Space Vehicles", ARS Journal, Vol. 31, pp 803-807, June 1961.

5. Jaffe, L. D. and Rittenhouse, J. B. - "Behavior of Materials in Space Environments, ARS Journal, Vol. 32. No. 3, pp. 320-346, March, 1962.

6. Davison, E. H. and Winslow, P. C. - "Direct Evaluation of Meteoroid Hazard", Prepared for IAS, Jan. 1962.

7. Dubin, M. and McCracken, C.W. - "Measurements of Distributions of Interplanetary Dust", Astronomical Journal, Vol. 67. June, 1962. (to be published)

8. Watson, F. G. - Between the Planets, Harvard Univ. Press, 1956.

9. McKinley, D.W.R. - Meteor Science and Engineering, McGrawHill Book Company, Inc., N. Y. 1961.

10. Hawkins, G. S. and Upton, E. K. L. - "The Influx Rate of Meteors in the Earth's Atmosphere", Astrophysics Journal, Vol. 128, pp. 727-735, 1958.

11. Eshelman, V. R. - "Radar Rate Measurements on Very Small Meteors", Astronomical Journal, Vol. 67, June, 1962 (to be published).

12. McCracken, C.W., Alexander, W. M., and Dubin, M. - "Direct Measurements of Interplanetary Dust Particles on the Vicinity of the Earth", Nature, Vol. 192, No. 4801, pp. 441-442, Nov. 4, 1961.

13. Alexander, W. M., McCracken, C. W., Secretan, L. and Berg, O. E. - "Review of Direct Measurements of Interplanetary Dust from Satellites and Probes", Space Research, Vol. III (to be published) 1962.

14. Soberman, R.S., Hemenway, C. L. et al - "Micrometeorite Collection from a Recoverable Sounding Rocket" (three pages) GRD Res. Note, No. 71, AFCRL, Bedford, Mass. 1961

15. Pettersson, H. - Nature Vol. 18 p. 330, 1958, with Rotschi, H. "Nickel Content of Deep-Sea Ocean Deposits", Nature, Vol. 166, p. 308, 1950.

16. Link. F. - "Memoires Soc. Roy. Sci de Liege, Vol. 15, p. 39, 1955.

17. Whipple, F. L. and Hawkins, G. S. - "Meteors" Handbuch der Physik, Vol. 52, pp. 519-564, 1959.

18. Lovell, A.C. B. - Meteor Astronomy, Oxford University Press, Oxford, 1954.

19. Hawkins, G. S. - "Variations in the Occurrence Rate of Meteors", Astronomical Journal, Vol. 61, pp. 386-391, 1956.

20. Jacchia, L. G. - "Meteors, Meteorites and Comets: Interrelations", (to be published).

21. Dubin, M., Alexander, W. M., and Berg, O. E. - "Cosmic Dust Showers by Direct Measurements", Proc. International Symposium on Astronomy and Physics of Meteors, Cambridge, Mass., Aug. 28-Sept. 1, 1961 (to be published).

22. McCracken, C. W. and Alexander, W. M. and Labow, H. E. - "Interplanetary Dust Particles of Micron-Size Probably Associated with the Leonid Meteor Stream", Journal Geophys. Res., Vol. 66, No. 11, pp. 3970-3973, Nov., 1961.

23. Hawkins, G. S. - "A Radio Echo Survey of Sporadic Meteor Radiants", Royal Astronomical Soc. Mon. Not., Vol. 116, pp. 92-104, 1956.

24. Hawkins, G. R. - "Radar Measurements of Meteor Orbits", Astronomical Journal, Vol. 67, June, 1962. (to be published)

25. McCrosky, R. E. - "Results from an Artificial Iron Meteoroid at 10 km sec^{-1}", Proc. Symposium on the Astronomy and Physics of Meteors, Cambridge, Mass., Aug. 28-Sept. 1, 1961, (to be published).

26. Whipple, F. L. - "Meteoritic Erosion in Space", Space Research, Vol. III, Proc. of COSPAR, 1962 (to be published).

27. Summers, J. L. and Charters, A. C. - "High Speed Impact of Metal Projectiles in Targets of Various Materials" - Proc. of the Third Symposium on Hypervelocity Impact, ed. F. Genevese, Vol. I, pg. 101, Armour Res. Found., Chicago, 1959.

28. Whipple, F. L. - "Meteoric Phenomena and Meteorites", Physics and Medicine of the Upper Atmosphere, pp. 137-170, Univ. of New Mexico Press, Albuquerque, 1952.

29. Levin, B. J. - The Physical Theory of Meteors and Meteoric Matter, Izd. Akad. Nauk SSSR, Moscow, 1956. Three chap-

ters ASTIA, Doc. 40, AD 110091.

30. Whipple, F. L. and Hawkins, G. S. - "On Meteors and Rainfall", Jour. Meteorology, Vol. 13, pp. 236-240, 1956.

31. Opik, E. - Physics of Meteor Flight in the Astmosphere, Interscience Publishers, Inc., New York, 1958.

32. Eichelberger, R. J. "Discussion and Summary", Proc. Third Symposium on Hypervelocity Impact, F. Genevese ed., pp. 565-570, Armour Res. Found., Chicago, 1959.

33. Bjork, R. L. - "Effects of a Meteoroid Impact on Steel and Aluminum in Space", Proc. 10th International Astronautical Congress, Vol. 2, pp. 505-514, Springer-Verlag, Vienna, 1960.

34. Vanfleet, H. B., Partridge, W. S., and Cannon, E. T. - "Anomolous Behavior of Lead to Lead Impact", F. Genevese ed, pp. 115-139, Armour Res. Found., Chicago 1959, Proc. Third Symposium on Hypervelocity Impact.

35. Summers, J. L. and Charters, A. C. - "High Speed Impact of Metal Projectiles in Targets of Various Materials", Proc. Third Symposium of Hypervelocity Impact, Vol. 1, F. Genevese ed., pp. 101, Armour Res. Found., Chicago, 1959.

36. Davison, E. H. and Winslow, P. C., Jr. - "Space Debris Hazard Evaluation", NASA Technical Note D-1105, Dec. 1961.

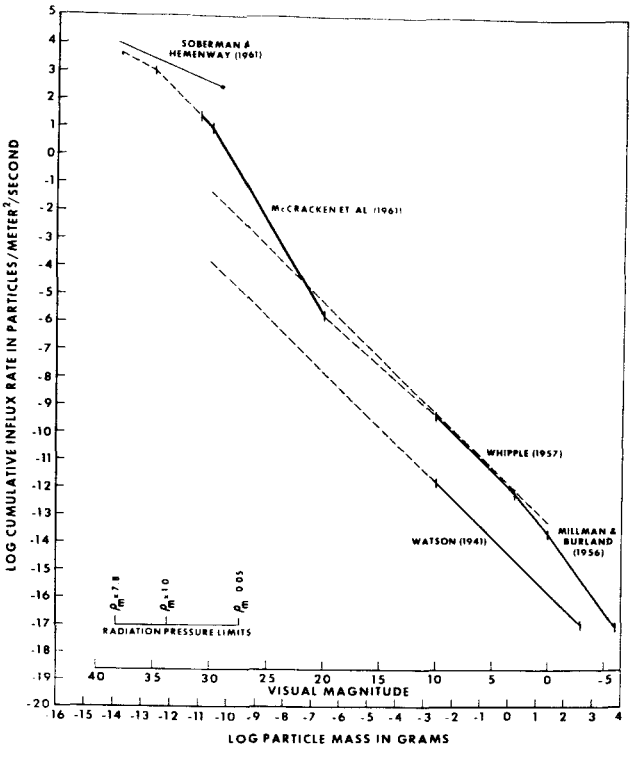

Figure 1 Segmented cumulative mass distribution for omnidirectional influx rates of meteoroids and dust particles.

Table I

MASS ON GRAMS OF A METEOROID OF ZERO VISUAL MAGNITUDE

Mv	Mass in grams	Velocity in Km sec^{-1}	Author	Reference
0	0.25	55	Watson (1941)	8
0	1.25	40	Whipple (1952)	28
0	0.055	40	Levin (1956)	29
0	25. (dustball)	28	Whipple (1957)	3
0	0.15	30	Whipple & Hawkins (1956)	30
0	0.29 1.29 (dustball)	42	Opik (1958) by McKinley	31 & 9

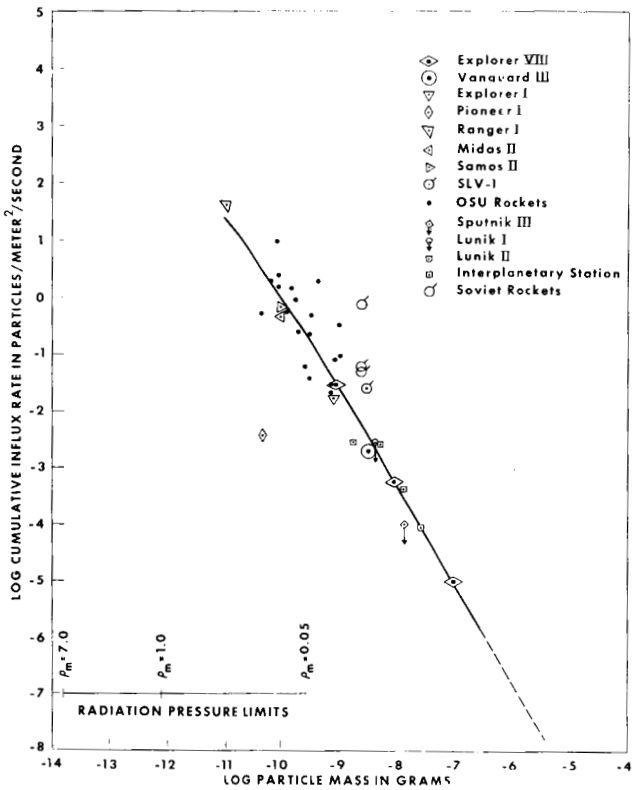

Figure 2 Average cumulative mass distributions of interplanetary dust particles derived from satellite and rocket probe measurements.

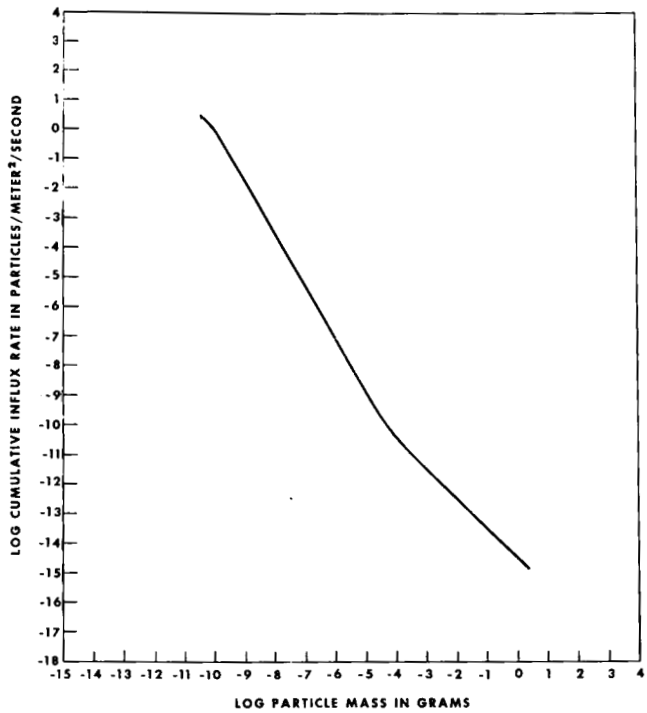

Figure 4 Expected average cumulative distribution of influx rate as a function of meteoroid mass in the vicinity of the earth. Specific gravity of the meteoroids assumed to be approximately two.

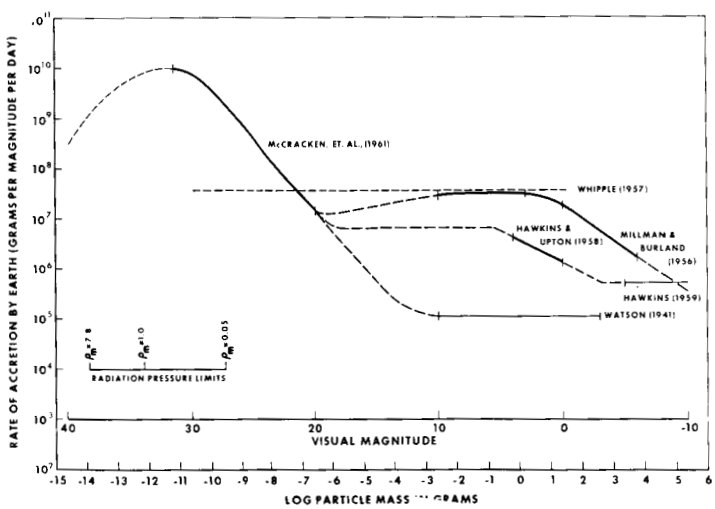

Figure 3 Incremental mass distribution curve for interplanetary material accreted by the earth.

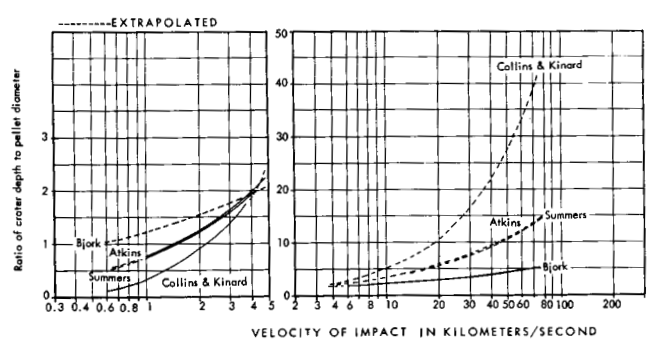

Figure 5 Velocity dependence of the penetration-depth-to-pellet-diameter ratio for aluminum impacting aluminum, based on theory and extrapolated experimental data.